Berichte
zur Polar-
und Meeresforschung

632
2011

Reports
on Polar and Marine Research

# The Expedition of the Research Vessel "Polarstern" to the polar South Pacific in 2009/2010 (ANT-XXVI/2 - BIPOMAC)

Edited by
Rainer Gersonde
with contributions of the participants

HELMHOLTZ GEMEINSCHAFT

ALFRED-WEGENER-INSTITUT FÜR
POLAR- UND MEERESFORSCHUNG
in der Helmholtz-Gemeinschaft
D-27570 BREMERHAVEN
Bundesrepublik Deutschland

ISSN 1866-3192

# Hinweis

Die Berichte zur Polar- und Meeresforschung werden vom Alfred-Wegener-Institut für Polar-und Meeresforschung in Bremerhaven* in unregelmäßiger Abfolge herausgegeben.

Sie enthalten Beschreibungen und Ergebnisse der vom Institut (AWI) oder mit seiner Unterstützung durchgeführten Forschungsarbeiten in den Polargebieten und in den Meeren.

Es werden veröffentlicht:

— Expeditionsberichte (inkl. Stationslisten und Routenkarten)
— Expeditionsergebnisse (inkl. Dissertationen)
— wissenschaftliche Ergebnisse der Antarktis-Stationen und anderer Forschungs-Stationen des AWI
— Berichte wissenschaftlicher Tagungen

Die Beiträge geben nicht notwendigerweise die Auffassung des Instituts wieder.

# Notice

The Reports on Polar and Marine Research are issued by the Alfred Wegener Institute for Polar and Marine Research in Bremerhaven*, Federal Republic of Germany. They appear in irregular intervals.

They contain descriptions and results of investigations in polar regions and in the seas either conducted by the Institute (AWI) or with its support.

The following items are published:

— expedition reports (incl. station lists and route maps)
— expedition results (incl. Ph.D. theses)
— scientific results of the Antarctic stations and of other AWI research stations
— reports on scientific meetings

The papers contained in the Reports do not necessarily reflect the opinion of the Institute.

The „Berichte zur Polar- und Meeresforschung” continue the former „Berichte zur Polarforschung”

* Anschrift / Address
Alfred-Wegener-Institut
für Polar- und Meeresforschung
D-27570 Bremerhaven
Germany
www.awi.de

Editor in charge:
Dr. Horst Bornemann

Assistant editor:
Birgit Chiaventone

Die "Berichte zur Polar- und Meeresforschung" (ISSN 1866-3192) werden ab 2008 ausschließlich als Open-Access-Publikation herausgegeben (URL: http://epic.awi.de).

Since 2008 the "Reports on Polar and Marine Research" (ISSN 1866-3192) are only available as web-based open-access publications (URL: http://epic.awi.de)

# The Expedition of the Research Vessel "Polarstern" to the polar South Pacific in 2009/2010 (ANT-XXVI/2 - BIPOMAC)

---

**Edited by**
**Rainer Gersonde**
**with contributions of the participants**

**Please cite or link this publication using the identifier**
**hdl:10013/epic.37910 or http://hdl.handle.net/10013/epic.37910**

**ISSN 1866-3192**

# ANT-XXVI/2

**27 November 2009 - 27 January 2010**

**Punta Arenas - Wellington**

**Chief Scientist**

**Rainer Gersonde**

**Coordinator**

**Eberhard Fahrbach**

# INHALT

# 1. FAHRTVERLAUF UND ZUSAMMENFASSUNG

## Fahrtverlauf

Am 27.11.2009 gegen 22:30 Ortszeit lief *Polarstern* von der Bunkerpier Cabo Negro unweit der chilenischen Hafenstadt Punta Arenas zur Expedition ANT-XXVI/2 aus. Vor Auslaufen hatte *Polarstern* den Tag über 1.400 $m^3$ Marine Diesel für die lange Reise bis nach Neuseeland gebunkert. An Bord befanden sich 45 Besatzungsmitglieder sowie 43 Wissenschaftler, Techniker und Hubschrauberpersonal. Die wissenschaftlichen Teilnehmer, darunter 17 Frauen, kommen aus Chile, Deutschland, Frankreich, Indien, Italien, Korea, Malaysia, Österreich, Schweiz, Spanien und den USA. Wegen des um fast 5 Stunden verspäteten Auslaufens wurde auf dem Weg zum Pazifischen Ozean die engste Passage der Magellanstraße im Morgenlicht des 28.11. gequert. Leider war die Sicht auf die umgebende Berglandschaft und Gletscher wegen des regnerischen Wetters getrübt.

Nach Verlassen der Magellanstraße wurde Kurs auf den südlichen Freeden Seamount (ca. 57°30´S, 90°30´W) zwischen Mornington und Bellingshausenbecken gesetzt (Abb. 1.1). Nach Verlassen der chilenischen Hoheitsgewässer am 29.1.09 um 14:30 UTC (52°49.3´S, 79°53.1´W) wurden die Geräte zur akustischen Vermessung der Meeresbodentopographie (Fächerecholot HYDROSWEEP) und der Sedimentverteilung (PARASOUND-Sedimentecholot) sowie das Seegravimeter in Aufzeichnungsbetrieb gesetzt und die erste Beprobungsstation (PS75/034) durchgeführt. Dabei wurden Multicorer, 20 m-Kolbenlot und CTD+Rosette erfolgreich eingesetzt. Technische Probleme, die den Einsatz des Fluorometers an der CTD und des Multinetzes verhindert haben, konnten am folgenden Tag behoben werden. Bereits 24 Stunden nach Ende der ersten Station wurde das Gebiet des Freeden Seamounts erreicht. Hier ist vor ca. 2,5 Millionen Jahre der kilometergroße Eltanin-Asteroid eingeschlagen. Dieses Ereignis ist bislang das einzig bekannte Beispiel eines Einschlages eines großen Asteroiden in den tiefen Ozean. Bisherige geowissenschaftliche Untersuchungen und daraus abgeleitete numerische Modellierungen haben ergeben, dass bei dem Einschlag ein über 20 km großer Wasserkrater geschlagen worden ist, der bis zum Tiefseeboden bei 5.000 m reichte und aus dem mit Überschall bis zu 100 Kubikkilometer Wasser zusammen mit Tiefseesediment und Meteoritenbruchstücken in die hohe Atmosphäre geschleudert wurde. Eine 200 - 300 m dicke Sedimentschicht, die sich in 40 Millionen Jahren auf dem Freeden Seamount abgelagert hatte, wurde zerstört und der Meeresboden weiträumig umgepflügt. Am Rande des Wasserkraters muss ein kilometerhoher Wellenring aufgestiegen sein, aus dem sich ein Tsunami mit weltweiter Ausbreitung entwickelt hat. Diese Befunde sollten insbesondere im südlichen Bereich des Freeden Seamounts komplettiert und dabei der noch unbekannte genaue Einschlagort („ground-zero“) des Asteroiden gefunden werden. Modellierungen des Einschlagereignisses hatten

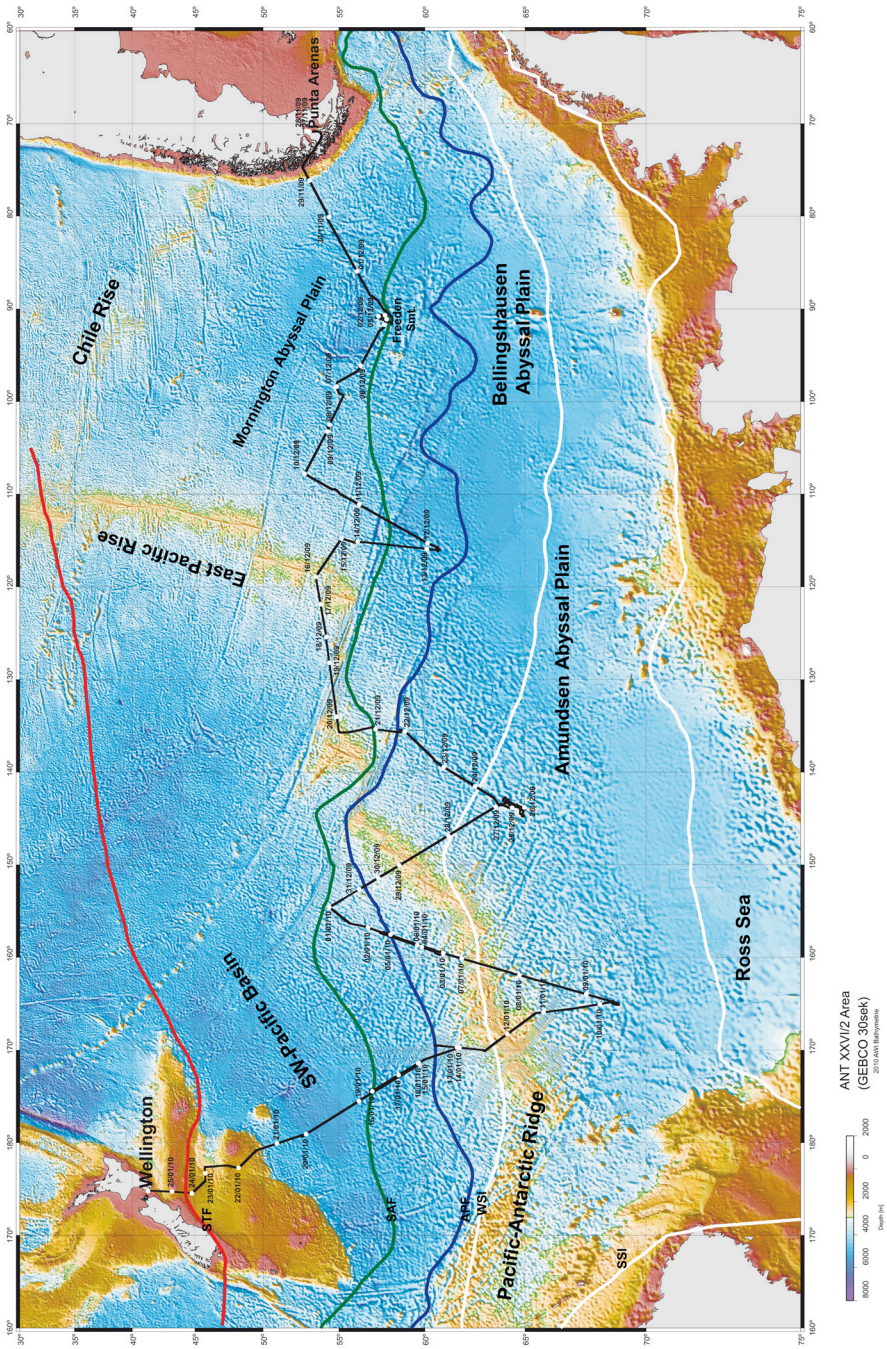


*Abb. 1.1: Kurskarte der Expedition ANT-XXVI/2 mit jeweiligem Datum. APF: Antarktische Polarfront, SAF: Subantarktische Front, STF: Subantarktische Front, nach Orsi (1995). SSI: Sommermeereisgrenze, WSI: Wintermeereisgrenze, nach Comiso (2003)*

*Fig. 1.1: Cruise track of Polarstern during ANT-XXVI/2 with dates. APF: Antarctic Polar Front, SAF: Subantarctic Front, STF: Subtropical Front, according to Orsi (1995). SSI: summer sea ice extent, WSI: winter sea ice extent, according to Comiso (2003)*

Hinweise auf diesen Ort gegeben, an dem große Mengen an Meteoritenmaterial zu erwarten sind.

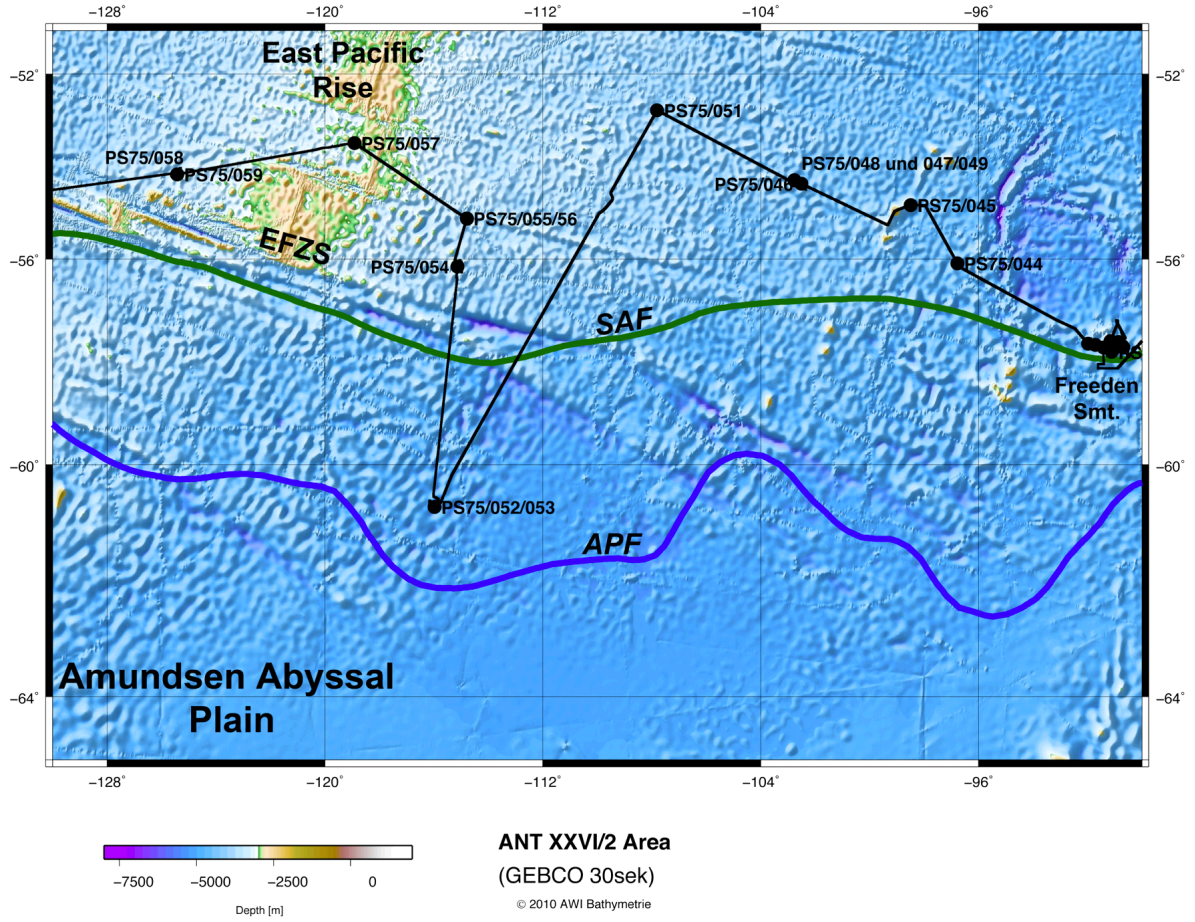


*Abb. 1.2: Fahrtroute und Stationen im Bereich östlich und auf dem Ostpazifischen Rücken. EFZS: Eltanin Fracture Zone System, APF: Antarktische Polarfront, SAF: Subantarktische Front. Lage der Fronten nach Orsi (1995).*

*Fig. 1.2: Track and stations east of and at East Pacific Rise, EFZS: Eltanin Fracture Zone System, APF: Antarctic Polar Front, SAF Subantarctic Front. Location of fronts according to Orsi (1995).*

Gestützt auf vorliegende und neu gewonnene PARASOUND-Information wurden acht Positionen (PS75/035-040, PS75/42-43) ausgewählt, an denen während guter Wetterbedingungen (Abb. 2.3) bei Wassertiefen zwischen 3.000 und 5.000 m bis zu 23,5 m lange Sedimentkerne mit dem Kolbenlot gezogen wurden, um die bei dem Einschlag entstandenen Störungen der Sedimentabfolge und den Meteoriten-„fall-out“ zu dokumentieren. Leider gelang es nur an drei Positionen (PS75/036, 038, 040), Sedimente zu gewinnen, die das Einschlagereignis dokumentieren. Zusätzlich wurde vom 3. - 4.12.09 ein Mehrkanalseismik-Survey mit 2 GI-Kanonen und einem 600 m langen Analog-Streamer durchgeführt. Zusammen mit der Sedimentkernentnahme, den bathymetischen und sedimentechographischen Surveys stellen diese seismischen Untersuchungen eine wesentliche Voruntersuchung („pre-site survey“) zur weiteren Beantragung des Tiefseebohrvorhabens 625 - full („Cenozoic Southern Ocean Pacific“,

CESOP) im Rahmen des Integrated Ocean Drilling Programs (IODP) dar, bei dem durch die beim Eltanin-Einschlag entstandene Sedimentabfolgen gebohrt werden soll. Wegen technischer Probleme bei der Datenaufzeichnung musste der seismische Survey leider vorzeitig abgebrochen werden.

Am 5.12.09 wurde das Untersuchungsprogramm im Bereich des Freeden Seamounts beendet und auf nordwestlichem Kurs der südliche Sektor des Ostpazifischen Rückens angesteuert (Abb. 1.2). Dabei wurde eine 5.000 m tiefe Rinnenstruktur gequert, in der neben Beprobungen der Sedimente mit dem Multicorer und dem Kolbenlot auch die Wassersäule hydrographisch vermessen und beprobt werden konnte (Station PS75/044). Am Abend des 6.12.09 wurde eine sichelförmig gebogene Kette von Seamounts angesteuert, die nach vorliegenden bathymetrischen Daten auf eine Wassertiefe von nur 40 m aufsteigen sollten. Die Kartierung dieser Struktur ergab, dass der östlich gelegene Gipfel ein sich über 4 km erstreckendes Plateau aufweist („Guyot"-Struktur), das eine Wassertiefe von 500 m hat (Abb. 6.2). Hier wurde mit dem Multicorer eine Oberflächensedimentprobe gewonnen (Station PS75/045). Auf dem weiteren Weg zum Ostpazifischen Tiefseerücken konnten am 4.000 - 5.000 tiefen Meeresboden keine Sedimente gefunden werden, bei denen es sich gelohnt hätte, Proben zu ziehen. Am 8.12.09 wurde schließlich ein Seamount mit Sedimentbedeckung entdeckt und bei einer Wassertiefe von 3.000 m ein 17,26 m langer Sedimentkern gezogen (Station PS75/046). Westlich dieses Seamounts wurden mächtigere Sedimentpakete angetroffen und ein weiterer „pre-site-survey" (EPR-4A, Abb. 8.1) für das Bohrvorhaben IODP 625 - full mit einem seismischen Kreuzprofil und Sedimentkernentnahmen durchgeführt (Stationen PS75/047-050, Abb. 8.7, 8.8). Nach einer weiteren Station auf dem Weg zum Ostpazifischen Rücken zum nächsten IODP-„pre-site survey" Gebiet (EPR-3A, Abb. 8.1) zwangen extreme Schlechtwetterbedingungen (Abb. 2.5), für die Wellenhöhen von bis zu 9 m vorausgesagt wurden, zu einem Abbruch der geplanten Route und ein rasches Ausweichen in südwestlicher Richtung. Auf dem über 550 nm langen Transit mit vier Maschinen in ruhigere Gewässer im nördlichen Amundsenbecken, bei dem nahe des Eltanin-Fracture-Zone Systems (EFZS) die Subantarktische Front gequert wurde (Abb. 1.2), zeigten sich mächtige Sedimentpakete am Meeresboden.

Am 11.12.09, 23:09 UTC, wurde der Breitengrad 60°S bei 115°07.7´W gequert und das Antarktisvertragsgebiet erreicht, in dem die geowissenschaftlichen Arbeiten unter besonderen Auflagen des Umweltbundesamtes (UBA) durchzuführen waren. Unmittelbar südlich von 60°S war ein weiterer „pre-site survey" für IODP 625 - full (BEL-1B, Abb. 8.1) geplant. Bei hervorragenden Wetter- und Seegangsbedingungen (Abb. 2.3) wurden nach Beprobung der mächtigen Sedimente (Abb. 7.2.2) mit Multicorer und 30 m-Kolbenlot (Stationen PS75/052-053) alle vom UBA vorgeschriebenen Maßnahmen zur Observierung von Großsäugern getroffen, um seismische Untersuchungen durchführen zu können. Leider fanden diese Untersuchungen nicht statt, da die seismischen Aufzeichnungsgeräte wegen technischer Fehlfunktionen nicht gestartet werden konnten. Diese Arbeiten konnten aber erfolgreich bei der nachfolgenden Expedition ANT-XXVI/3 nachgeholt werden (Gohl, 2010). Darauf hin wurde erneut der Ostpazifische Rücken angesteuert und das Antarktisvertragsgebiet am 13.12.09, 00:31 UTC mit nördlichem Kurs verlassen (Abb. 1.2). Nach Querung des EFZS wurde bei einer Wassertiefe von 4.100 m ein weiterer „pre-site survey" mit 30 m-Kolbenlot, Multicorer und einem seismischen Kreuzprofil (Station PS75/054)

(Abb. 8.9, 8.10) durchgeführt. Darüber hinaus konnte ein S-N-Beprobungsprofil der Wassermassen mit CTD, Wasserschöpfer, Fluorometer und Multinetz, das an Station PS75/052 im Amundsenbecken begonnen worden war, weitergeführt werden. Wenig nördlich dieser Station wurde bei einer Tiefe von 3.600 m eine weitere Sedimentbeprobung mit Schwerelot und Multicorer durchgeführt (Stationen PS75/055-056), um ein Tiefenprofil von der Tiefsee bis zum Zentrum des Ostpazifischen Rückens zu erhalten. Der ursprünglich geplante weitere Weg zu der in IOPD 625 - full vorgeschlagenen Bohrlokation EPR-3A musste am 15.12.09 erneut wegen sich rasch verschlechternden Wetter und Seegangsbedingungen in Folge eines weiter nördlich durchziehenden Tiefdruckgebietes abgebrochen werden. Bei Windstärken von über Bft 8 und Wellenhöhen von 6 m (Abb. 2.3), die weitere Stationsarbeiten unter sicheren Arbeitsbedingungen an Deck unmöglich machten, wurde Kurs Nordwest gesetzt, um dem Tiefdruckgebiet auszuweichen (Abb. 1.2). Unmittelbar nach Querung der Spreizungszone wurde die Gipfelregion des Ostpazifischen Rückens bei einer Wassertiefe von 2.900 m geologisch und hydrographisch beprobt. Die weitere Fahrtroute führte entgegen der ursprünglichen Planung nördlich der Subtropischen Front nach Westen. Auf diesem Weg wurde auf dem südwestlichen Ostpazifischen Rücken ersatzweise ein „pre-site survey“ mit zwei Kolbenloteinsätzen, dem Multicorer, der CTD und einem seismischen Kurzprofil durchgeführt (Stationen PS75/058-060)(Abb. 8.11, 8.12). Der Multicorereinsatz blieb erfolglos und beide Kolbenloteinsätze führten zum Abbiegen des Rohres in einer Tiefe um 12 - 15 m. Die Wiederholung des Kolbenloteinsatzes wurde beschlossen, da wegen anhaltender Schlechtwetterbedingungen das Schiff an Station PS75/058 in eine Zone gedriftet war, in der nach dem PARASOUND-Survey die oberen Sedimentpakete vermutlich gestört sind (s. PARASOUND-Aufzeichnung in A.6). Das Abbiegen der Kolbenlotrohre an beiden Positionen ist auf das Vorkommen einer ca. 2 m mächtigen und dichten Karbonatlage aus Kalkalgen („calcareous nannofossil ooze“) in dieser Sedimenttiefe zurückzuführen (s. Kernbeschreibung in A.7), die das weitere Eindringen des Gerätes verhindert hat. Die Karbonatlage kann stratigraphisch dem Marinen Isotopen Stadium (MIS) 11 zugeordnet werden. Sie bildet sich in PARASOUND-Aufzeichnungen als Reflektor ab, der sich über weite Bereiche des polaren Südpazifiks verfolgen lässt (Abb. 7.2.4).

Am 19.12.09 wurde bei unruhiger See (Abb. 2.3) erneut das EFZS gequert und die Suche nach geeigneten Bohrlokationen für IODP 625 - full aufgenommen (UFZ-2A) (Abb. 8.1). Diese Suche im Rückenbereich zwischen EFZS und Udintsev Fracture Zone (UFZ) blieb erfolglos, da bei dem Survey mit PARASOUND keine geeignete Sedimentbedeckung gefunden werden konnte. Mächtige Sedimentpakete wurden auf dem weiteren Weg Richtung Südwest erst im Bereich der UFZ angetroffen, die hier als topographische Führung der Polarfront wirkt (Abb. 1.3). Nördlich und südlich der UFZ und damit auch der Polarfront wurden über 20 m lange Sedimentkerne mit dem Kolbenlot gezogen, für die Sedimentationsraten von ca. 10 cm/1.000 Jahre abgeschätzt werden (Stationen PS75/062-063). In diesem Bereich wurde ein zweites Beprobungsprofil der Wassersäule mit CTD, Wasserschöpfern, Fluorometer und Multinetzfängen begonnen, das bis in die im Winter von Meereis bedeckte Zone des Amundsen-Beckens reicht (Stationen PS75/061-067). Die marin-geologischen Probennahmen auf diesem Untersuchungsschnitt zeigen in der ganzjährig Meereis freien Zone südlich der Polarfront hohe Sedimentationsraten von biogenem Opal.

Südlich davon brechen die Sedimentationsraten ein und die gewonnenen Sedimente erreichen wie im weiter westlich gelegenen Untersuchungsgebiet Alter von über 3 Millionen Jahre (Stationen PS75/065-069, PS75/086-090)(Abb. 7.6.1).

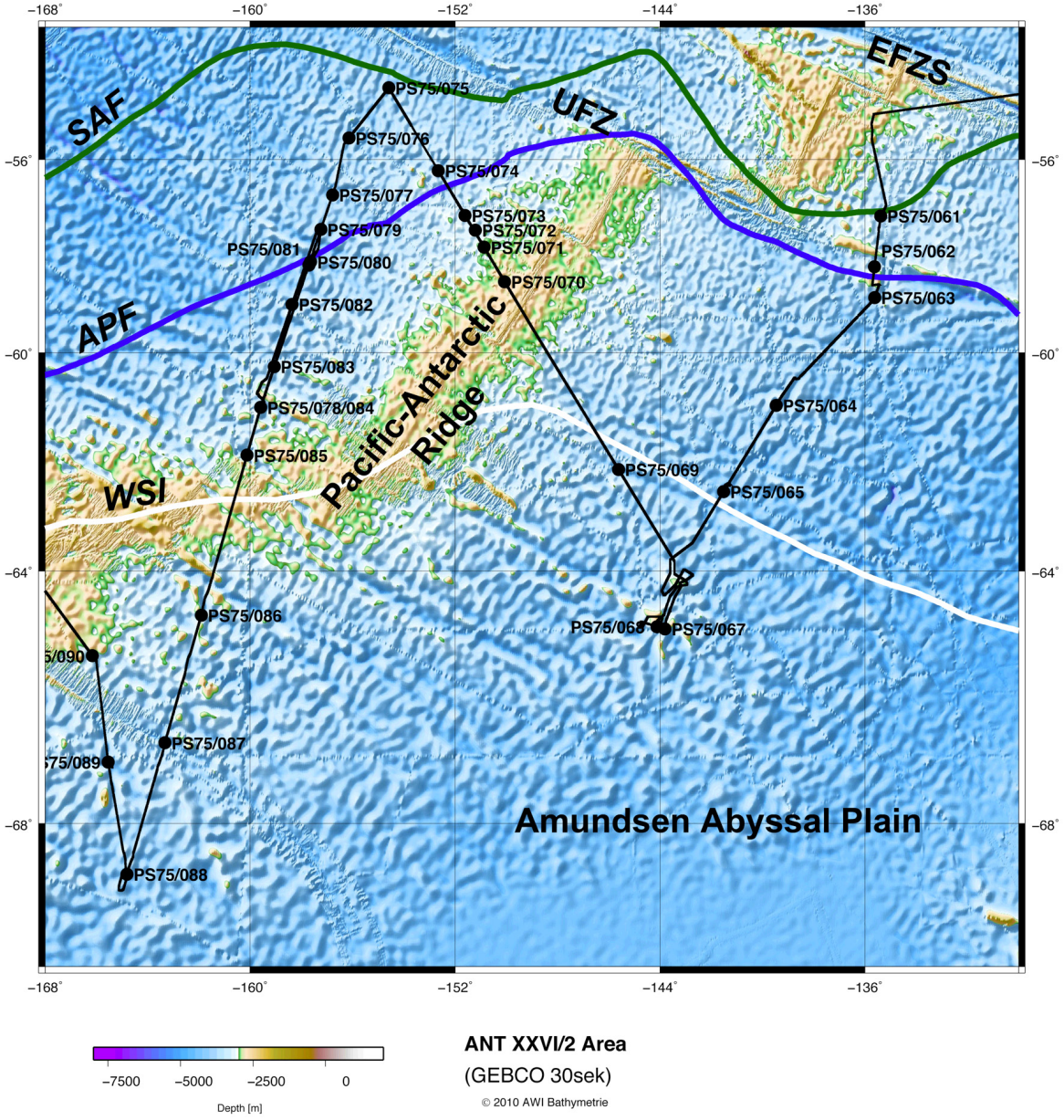


*Abb. 1.3 : Fahrtroute und Stationen südlich des Eltanin Fracture Zone Systems (EFZS) und des östlichen Pazifisch-Antarktischen Rückens. UFZ: Udintsev Fracture Zone. APF: Antarktische Polarfront, SAF: Subantarktische Front nach Orsi (1995). WSI: Wintermeereisgrenze nach Comiso (2003)*

*Fig. 1.3: Track and stations south of Eltanin Fracture Zone System (EFZS). UFZ: Udintsev Fracture Zone. APF: Antarctic Polar Front, SAF Subantarctic Front according to Orsi (1995). WSI: winter sea ice extent according to Comiso (2003).*

Am 22.12.09, 16:03 UTC, wurde auf dem Untersuchungsschnitt in das westliche Amundsenbecken erneut das Antarktisvertragsgebiet und am 25.12.09 bei ca. 64°58´S das südlichste Arbeitsgebiet des Schnittes erreicht (Abb. 1.3). Südlich von 60°S sanken

die Luft- und Wassertemperaturen auf 0 - 1°C ab (Abb. 2.4) und es wurde eine größerer Anzahl von Tafeleisbergen gesichtet. Am 24.12.09 wurden die Arbeiten ab 15:00 Bordzeit für ca. 24 Stunden auf hydroakustische Vermessungen mit PARASOUND und HYDROSWEEP beschränkt. Dabei wurde ein Gebiet vermessen, in dem sich nach bathymetrischen Karten (GEBCO_08) ein ausgebreitetes topographisches Hochgebiet befinden soll. Dies konnte nicht bestätigt werden (Abb. 6.4). Am Abend des 24.12.09 wurden die Weihnachtsfeierlichkeiten bei kaltem, aber ruhigem Wetter mit einem Empfang im „Blauen Salon“ begonnen, dem ein gemütliches Zusammensein in verschiedenen Räumen des Schiffes folgte.

Der folgende Untersuchungsschnitt, mit einer Länge von ca. 700 nm, führte in nordwestlicher Richtung über den Pazifisch-Antarktischen Rücken hinweg zur Subantarktischen Front im Südwestpazifischen Becken (Abb. 1.3). Dabei wurde am 28.12.09, 7:10 UTC, das Antarktisvertragsgebiet erneut verlassen. Auf dem Weg nach Norden konnten bei überwiegend ruhigen Seegangsbedingungen mit Wellenhöhen um 3 m sieben Stationen mit Kolbenlot, Multicorer und CTD durchgeführt werden (PS75/069-075). An der flachsten Station im Gipfelbereich des Tiefseerückens (PS75/070, 2.840 m) an der erneut karbonatische Abfolgen zu erwarten waren, wurde das 15 m lange Gestänge des Kolbenlotes am Meeresboden abgerissen. Lediglich der Gewichtsträger mit Schere und das Voreillot, in dem sich ein 0,9 m langer Sedimentkern befand, konnten geborgen werden. Die Arbeiten an den anderen Stationen waren erfolgreich und ergaben 15 - 21 m lange Sedimentkerne, die die Klimageschichte der letzten 300.000 - 600.000 Jahre dokumentieren. An Station PS75/073 wurde bei einer Wassertiefe von 3.230 m der einzige Einsatz eines Kastenlotes (30 x 30 cm Kastendurchmesser) durchgeführt, um einen großvolumigen Sedimentkern zu gewinnen. Dabei konnte ein 3,68 m langer Kern gewonnen werden. Die nördlichste Position des Profils wurde zum Jahreswechsel 2009/2010 erreicht. Eine ursprünglich geplante kurze Arbeitspause zur Feier des Jahreswechsels wurde kurzfristig um 24 Stunden verschoben, da sich innerhalb kürzester Zeit aus einem unscheinbaren Tiefdruckgebiet ein massiver Tiefdruckwirbel entwickelt hatte und vor Wetterverschlechterung weitere Arbeiten im nördlichen Bereich des folgenden Untersuchungsschnitts durchgeführt werden sollten. Der traditionelle Empfang auf der Brücke während des Jahreswechsels konnte stattfinden. Nach Durchführung der Arbeiten am 31.12.09 und 1.1.10, die schließlich an Station PS75/077 wegen der sich zunehmend schlechten Wetterbedingungen abgebrochen werden mussten, wurde beschlossen, auf schnellstem Wege nach Süden auszuweichen. Da das Schiff durch Wind und See geschoben wurde, konnte auf der 200 nm langen Fahrtstrecke bis in den Kammbereich des Pazifisch-Antarktischen Rückens trotz „ökonomischer“ Fahrweise (2 Maschinen) eine Geschwindigkeit von 12 - 13 kn erreicht werden (Abb. 1.1, 1.3). Am 2.1.10, 18:29 UTC, wurde das Antarktisvertragsgebiet zum dritten Mal erreicht. Für die folgende Nacht wurde das Schiff aufgestoppt und bei Windstärken bis zu Bft 8 und Wellenhöhen bis 7 m für ca. 12 Stunden zum Abwettern in den Wind gelegt. Danach wurde das geowissenschaftliche Stationsprogramm im Kammbereich des Pazifisch-Antarktischen Rückens bei einer Wassertiefe von ca. 3.300 m erneut aufgenommen. Wegen der andauernden unruhigen See konnte an Station PS75/078 kein Kolbenlot eingesetzt werden. Das Schwerelot erbrachte in den karbonatischen Abfolgen des Rückens einen Sedimentkern mit einer Länge von nur 3,83 m. Die Beprobung der Oberflächensedimente mit Multicorer und Großkastengreifer blieb

ohne Erfolg. Auf dem Rückweg Richtung Polarfront wurde der Breitengrad 60°S am 3.1.10, 22:45 UTC gequert (Abb. 1.3). Am 4.1.10 wurde der Bereich der Polarfront erneut erreicht und von dort aus an fünf während der Hin- und Rückfahrt mit Hilfe des hydroakustischen Surveys festgelegten Positionen in Richtung Rossmeer ein Beprobungsprofil abgearbeitet, auf dem Sedimentkerne mit Längen bis zu 19,7 m gewonnen werden konnten (Stationen PS75/080, 081, 082, 083,085). Zwischen den Stationen PS75/082 und /083 wurde am 6.1.10, 02:18 UTC, das Antarktisvertragsgebiet zum vierten Mal erreicht. Auf dem weiteren Weg nach Süden konnten an der Position von PS75/078 Oberflächensedimente gewonnen werden (PS75/084). An den folgenden Stationen PS75/086 und /087, beide südlich der Wintermeereisgrenze, wurden mit dem Schwerelot Sedimenkerne mit pliozänem Basisalter gezogen (Abb. 7.6.1).

Am 9.1.10 wurde bei 68°43´S, 164°48´W die südlichste Position der Expedition erreicht (Abb. 1.1, 1.4). In diesem Gebiet befanden sich zahlreiche Tafeleisberge, die wahrscheinlich aus dem Bereich des Ross-Eisschelfes stammten. Das antarktische Meereis hatte sich aus diesem Bereich erst ca. zwei Wochen vorher nach Süden zurückgezogen. Zeuge dieser Entwicklung war eine ausgeprägte Schichtung des Oberflächenwassers, bedingt durch ein Salzgehaltsminimum (Abb. 3.1.10). Gleichzeitig war deutlich erhöhte Primärproduktion und damit einhergehend eine $CO_2$-Senke zu beobachten (Abb. 3.1.16, 3.2.1). Die südlichste Position war Beginn des längsten latitudinalen Beprobungsprofiles der Expedition ANT-XXVI/2, das über eine Distanz von ca. 1700 nm bis zur Subtropischen Front südlich des Zielhafens Wellington reicht. Auf diesem Profil wurden an 18 Stationen (PS75/088-105) Beprobungen der Wassersäule mit CTD und Wasserschöpfer, Multinetz und Planktonnetz und/oder der Sedimente mit Multicorer sowie Schwerelot oder Kolbenlot durchgeführt (Abb. 1.4). Dabei durchgeführte hydroakustische Surveys (HYDROSWEEP, PARASOUND) und geowissenschaftliche Probennahmen waren gleichzeitig als Teil des „pre-site-surveys“ für den Bohrvorschlag IODP-625 - full geplant, in dem vier Bohrlokationen auf einem Schnitt über den Pazifisch-Atlantischen Rücken hinweg (PAR-1A – PAR-4A) vorgeschlagen worden sind (Abb. 8.1). Die seismischen Arbeiten für den „pre-site-survey“ wurden teilweise während der folgenden ANT-XXVI/3 Expedition durchgeführt (Gohl, 2010).

Während die Arbeiten südlich des Pazifisch-Antarktischen Rückens bei Temperaturen um 0°C (Abb. 2.10) noch unter ruhigen Wetterbedingungen durchgeführt werden konnten, kamen mit Erreichen des Rückenkamms am 12.1.10 erneut Schlechtwetterbedingungen mit Windstärken über Bft 7 und Wellenhöhen von 4 - 5 m auf. Um dem durchziehenden Schlechtwettergebiet auszuweichen, musste nach Abschluss der Arbeiten an Station PS75/091 eine Strecke mit nördlichem Kurs gefahren werden, die bis in den Bereich der Antarktischen Polarfront reichte (Abb. 1.4). Nach einer Station an der Polarfront (PS75/092) hatten sich die Wetterbedingungen wieder so weit beruhigt, dass weitere Arbeiten an zwei südlich gelegenen Positionen durchgeführt werden konnten (PS75/093, /094).

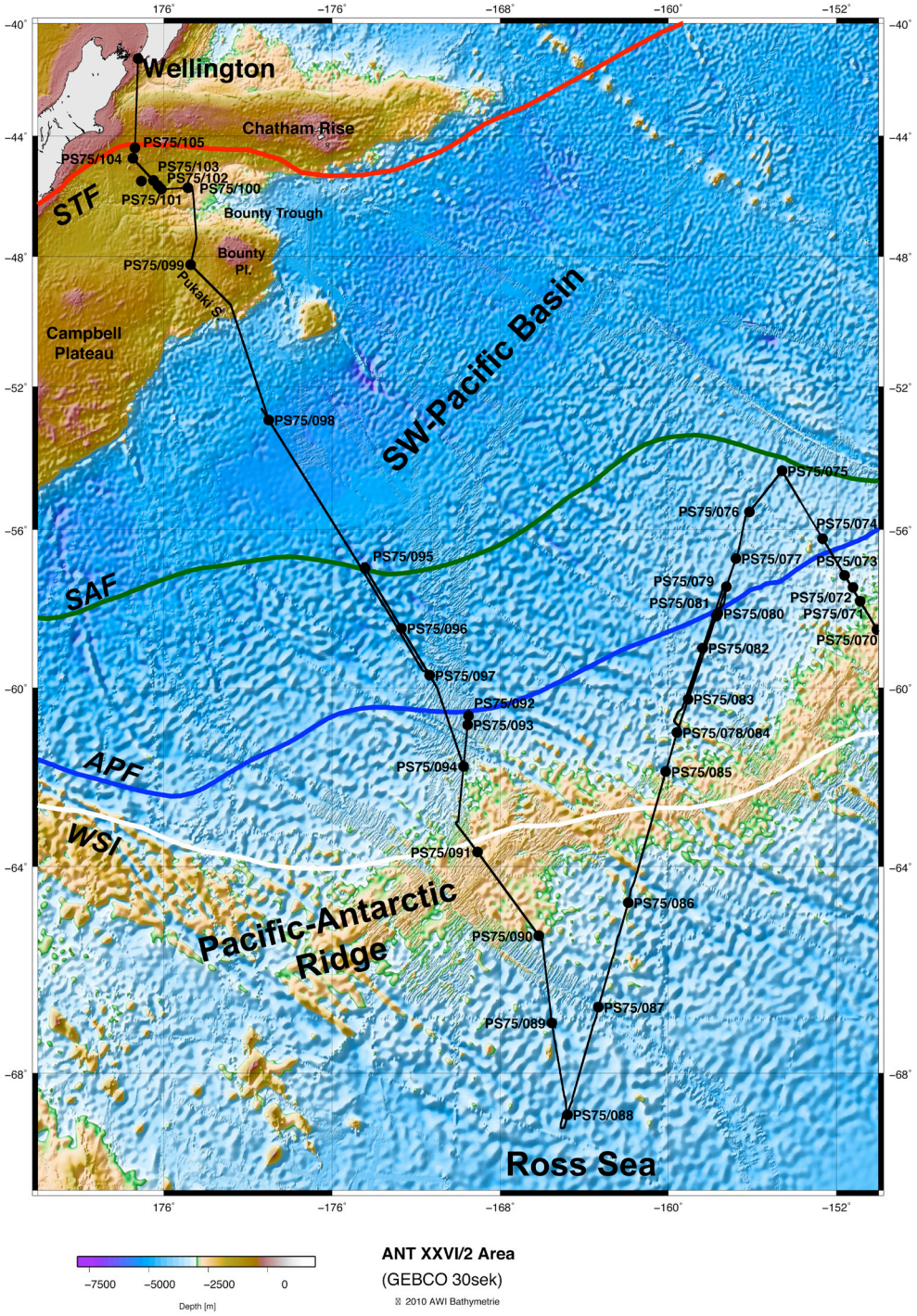


*Abb. 1.4: Fahrtroute und Stationen am Pazifisch-Antarktischen Rücken, im SW-Pazifischen Becken und in neuseeländischen Hoheitsgewässern. APF: Antarktische Polarfront, SAF: Subantarktische Front, STF: Subtropische Front nach Orsi (1995). WSI: Wintermeereisgrenze nach Comiso (2003)*

*Fig. 1.4: Track and stations around the Pacific-Antarctic Ridge, in the SW Pacific Basin and the New Zealand EEZ. APF: Antarctic Polar Front, SAF: Subantarctic Front, STF. Subtopical Front according to Orsi (1995). WSI: winter sea ice extent according to Comiso (2003).*

Ausgehend von der Station PS75/094 wurde am Morgen des 14.1.10 Kurs auf Wellington gesetzt und nach Querung der Polarfront das Antarktisvertragsgebiet um 20:49 UTC des selben Tages verlassen (Abb. 1.4). Die weiteren Arbeiten im Bereich der Polarfrontzone wurden erneut durch Schlechtwetterbedingungen gestört. Auf der 320 nm langen Dampfstrecke bis zur Subantarktischen Front herrschten mit Windstärken bis Bft 8 und Wellenhöhen über 4 m Bedingungen, die keine Stationsarbeiten ermöglichten. Nach Wetterbesserung wurden diese Arbeiten von der Subantarktischen Front aus (PS75/095) auf einer erneuten Rückfahrstrecke an drei Positionen nachgeholt. Von der nördlich der Polarfront liegenden Station PS75/097 aus wurde dann über sieben Breitengrade hinweg ohne weitere Stationsarbeiten bis in den nördlichen Bereich des Südwestpazifischen Beckens gefahren, wo wenig außerhalb der neuseeländischen Hoheitsgewässer bei einer Wassertiefe von 5.190 m die letzte Tiefwasserstation der Expedition ANT-XXVI/2 durchgeführt wurde (PS75/098) (Abb. 1.4).

Am 21.1.10 wurde das neuseeländische Hoheitsgebiet erreicht. Vor Einlaufen in Wellington wurden sieben weitere Stationen durchgeführt: eine im Pukaki-Sattel zwischen Bounty-und Campbell-Plateau bei 1.270 m Wassertiefe und sechs Stationen auf einem Tiefenprofil von 2.500 bis 670 m Wassertiefe, das vom Bounty-Trog bis auf den südwestlichen ChathamRücken reicht (PS75/100-105). Die flachsten Stationen liegen dabei im Bereich der Subtropischen Front (1.4).

In der Nacht zum 26.1.10 kam der Lotse an Bord. Vor Einlaufen in den Hafen von Wellington musste eine kritische Schwelle gequert, bei der nur wenige Dezimeter Wasser unter dem Kiel von *Polarstern* blieben. In den frühen Morgenstunden des 26.1.10 machte das Schiff im Containerhafen von Wellington (Aotea Quay) fest. Die örtlichen Behörden kamen an Bord, Schiffsbesatzung und wissenschaftliche Fahrtteilnehmer wurden einzeln von Zoll, Einwanderungs- und Quarantänebehörden überprüft. Gegen Mittag des 26.1.10 wurden die wissenschaftlichen Fahrtteilnehmer ausgeschifft und die Expedition ANT-XXVI/2 beendet.

## Zusammenfassung

Schwerpunkt der Expedition ANT-XXVI/2, die Polarstern über eine Distanz von 9.757 nm zum ersten Mal über den gesamten polaren Südpazifik nach Neuseeland gebracht hat, sind marin-geowissenschaftliche Probennahmen, die entlang der gesamten Fahrtroute durch bathymetrische (HYDROSWEEP) und sedimentechographische (PARASOUND) Vermessungen über 9.273 nm begleitet worden sind. Die Fahrtroute lässt sich in fünf Untersuchungsschnitte unterteilen:

Transekt 1 (Ost-West): Mornington Abyssal Plain (MAP) – Eltanin Fracture Zone System (EFZS),

Transekt 2 (Nord-Süd): Eltanin Fracture Zone System (EFZS) – Amundsen Abyssal Plain (AAP),

Transekt 3 (Süd-Nord): Amundsen-Abyssal Plain (AAP) – SW-Pacific Basin (SWP)

Transekt 4 (Nord-Süd): SW-Pacific Basin (SWP) – Ross Sea (ROS)

Transekt 5 (Süd-Nord): Ross Sea (ROS) – New Zealand Margin (NZM).

Während Transekt 1 den östlichen und den zentralen polaren Südpazifik im Bereich um die Polarfrontzone abdeckt, reichen die vier latitudinalen Schnitte im westlichen Südpazifik insgesamt von der saisonal meereisbedeckten Zone bis an die Subtropische Front (Abb. 1.2.1).

Insgesamt wurden Arbeiten an 72 Stationen (PS75/034 – PS75/105) durchgeführt. Bei Einsätzen des Kolbenlotes (49), Schwerelotes (7) und Kastenlotes (1) wurden insgesamt 1.030,31 m Sedimentkern gewonnen (Tabelle 1.2.1). Oberflächensedimente konnten bei 50 Einsätzen an 39 Positionen mit dem Multicorer und an einer Position zusätzlich mit dem Großkastengreifer beprobt werden. Gestützt auf das geowissenschaftliche Proben- und Datenmaterial sollen Funktion, Entwicklung und Wirkung klimarelevanter Mechanismen wie biologische Pumpe, Bildung, Zirkulation und Stratifikation von Wassermassen, Meereisausdehnung, Gasaustausch zwischen Atmosphäre und Ozean, Atmosphärenzirkulation und die Dynamik der Antarktischen Eisschilde auf geologischen Zeitskalen erfasst werden. Die Sedimentkerne aus dem Gebiet nördlich der Wintermeereisgrenze werden solche Untersuchungen in zeitlicher Auflösung von $10^2$ – $10^3$ Jahren für den Zeitraum der letzten 900.000 Jahre und für den Bereich des saisonal meereisbedeckten Amundsenbeckens und Rossmeeres in geringerer Auflösung für den Zeitraum der letzten 4,5 Millionen Jahre erlauben. Bislang liegen dazu nur wenige Ergebnisse aus dem polaren Südpazifik vor, der Bildungsgebiet von Wassermassen und darüber hinaus Schlüsselregion für das Verständnis der Geschichte und Dynamik antarktischer Eisschilde ist, da ca. 70 % des westantarktischen Eises in den polaren Südpazifik abfließen. Mit Hilfe der Oberflächensedimentproben und der Proben und Daten aus der Wassersäule soll die Entwicklung von Methoden zur geowissenschaftlichen Rekonstruktion von Umwelt- und Klimabedingungen („Proxy"-Entwicklung) weiter vorangetrieben werden. Neben paläozeanographisch orientierten Probennahmen galten die geowissenschaftlichen Arbeiten auch der weiteren Erkundung und Dokumentation des Eltanin-Asteroideneinschlages vor 2,5 Mio. Jahre im Bereich des Freeden Seamounts. Darüber hinaus konnten durch Kombination von Sedimentprobennahme mit seismischen, bathymetrischen und sedimentechographischen Surveys Voruntersuchungen („pre-site survey") durchgeführt werden, die für die weitere Beantragung des Bohrvorschlages 625 - full („Cenozoic Southern Ocean Pacific", CESOP) (Gersonde et al., 2008) im Rahmen von Integrated Ocean Drilling Program (IODP) benötigt werden.

Ergänzend wurden Probennahme von Staub aus der Atmosphäre sowie hydrographische Untersuchungen in der Wassersäule an 28 Stationen mit CTD und Kranzwasserschöpfer und darüber hinaus Planktonprobennahmen in den oberen 1.500 m der Wassersäule mit einem vertikalen Schließnetz (Multinetz) an 22 Stationen, über die oberen 100 m mit dem Nansen-Netz (23 Netzfänge an 13 Stationen) und aus den wissenschaftlichen Pumpsystemen des Schiffes durchgeführt. Damit kann erstmals der Staubeintrag aus Neuseeland und vom australischen Kontinent in den polaren Südpazifik dokumentiert werden. Die ozeanographischen Messungen und Probennahmen ergeben neue Datensätze zur Hydrographie, Nährstoffverteilung und der Isotopenzusammensetzung in der Wassersäule. Die Auswertung der Messungen kann u.a. Hinweise darauf ergeben, in welcher Wechselwirkung der polare Südpazifik mit einem außerordentlich stark ausgeprägten El-Niño-Ereignis im zentralen Äquatorialpazifik steht, wie es für 2009/10 beobachtet worden ist (Lee und McPhaden, 2010). Die Auswertungen biologischer

Planktonproben werden neue Hinweise zur Verteilung des Mikroplanktons im Südozean liefern, wobei ein besonderer Schwerpunkt bei den Gruppen liegt, die in Sedimenten überlieferbare Schalen und Skelettteile ausbilden (u.a. Foraminiferen, Radiolarien, Diatomeen, kalkiges Nannoplankton, Dinoflagellaten). Die Planktonprobennahmen wurden durch die Erfassung von Parametern zur Bestimmung der biologischen Produktion und Messung des Gasaustausches zwischen Ozean und Atmosphäre begleitet. Im westlichen polaren Südpazifik wurde in der saisonal meereisbedeckten Zone eine ausgeprägte Stratifikation des Oberflächenwassers festgestellt, die mit stark erhöhter Primärproduktion und einer deutlichen $CO_2$-Senke verbunden ist. Solche Bedingungen stellen möglicherweise ein Szenario für glaziale Umweltbedingungen dar.

Die Auswertung des Daten- und Probenmaterials erfolgt in nationaler und internationaler Zusammenarbeit im Rahmen des AWI-Programms PACES, der Programme des DFG-Forschungszentrums „The Ocean in the Earth System“ und der EU-Projektes „Past4Future“, des Integrated Ocean Drilling Program (IODP) und einer Reihe von einzelnen nationalen (DFG) und internationalen Projekten.

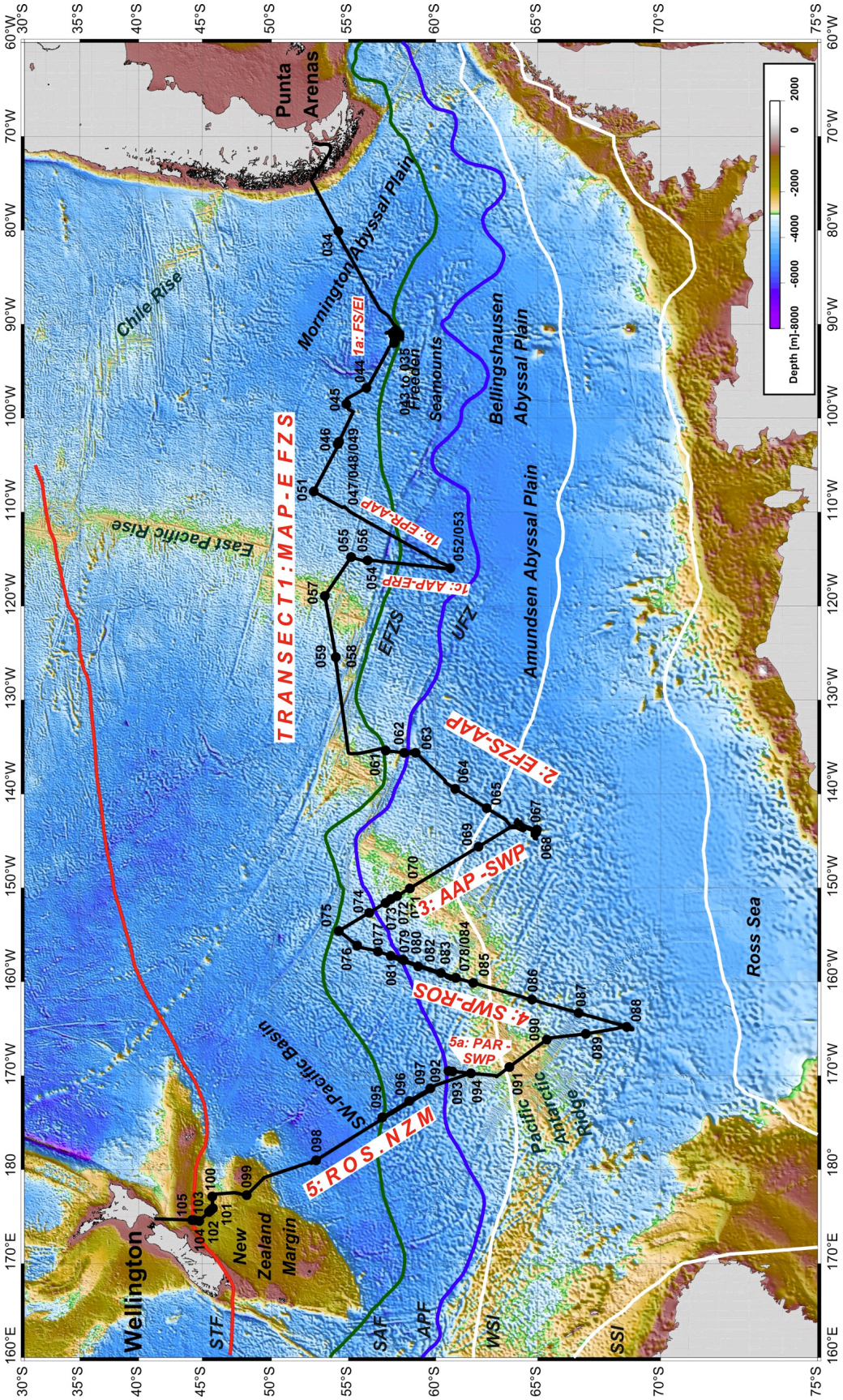


*Abb. 1.2.1: Übersicht der fünf ANT-XXVI/2 Untersuchungsschnitte und 72 Stationen*
*Fig. 1.2.1: Overview map showing the five ANT-XXVI/2 transects and 72 stations*

**Tabelle 1.2.1:** Zusammenstellung und Summierung der ANT-XXVI/2 Stationen mit Wassertiefe, Anzahl der CTD- (und Rosette), Multinetz- (MN), Planktonnetz (PLA)-Einsätze, Anzahl der gewonnen Multicorerrohre (MUC), Kerngewinn (m) des Großkastengreifers (GKG), des Kolbenlotes (KOL), KOL-Voreillotes (KOL TC), Schwerelotes (SL), Kastenlotes (KAL) und Länge der seismischen Surveys (nm). *Station mit ausschließlich PARASOUND und HYDROSWEEP-Vermessung (24.-25.12.2009)

**Table 1.2.1:** Summary of ANT-XXVI/2 station work including water depth, number of CTD (and rosette), multin-net (MN) and Nansen plankon net (PLA) deployments, number of recovered cores with the multi-corer (MUC), recovery of large box corer (GKG), piston corer (KOL), trigger corer of piston corer (KOL TC), gravity corer (SL) and kasten corer (KAL) as awell as the lenghts of seismic surveys in nautical miles (nm). *site decicated solely to survey with PARASOUND and HYDROSWEEP (December 24 - 25, 2009).

| Station | Depth (m) | CTD | MN | PLA | MUC (tubes) | GKG (m) | KOL Core (m) | KOL TC (m) | SL Core (m) | KAL Core (m) | Seismic Survey (nm) |
|---|---|---|---|---|---|---|---|---|---|---|---|
| PS75/034 | 4425 | 1 | | | 12 | | 18.08 | 0.92 | | | |
| PS75/035 | 5224 | | | | | | 22.53 | 0.91 | | | |
| PS75/036 | 5313 | | | | | | 22.74 | 0.52 | | | |
| PS75/037 | 4879 | | | | | | 22.73 | 0.87 | | | |
| PS75/038 | 4208 | | | | | | 21.83 | 1.00 | | | |
| PS75/039 | 5231 | | | | | | 22.15 | 0.53 | | | |
| PS75/040 | 3400 | 1 | 1 | | | | 9.36 | 0.93 | | | |
| PS75/041 | | | | | | | | | | | 20 |
| PS75/042 | 4917 | | | | | | 23.54 | 1.00 | | | |
| PS75/043 | 4619 | | | | | | 23.48 | 0.82 | | | |
| PS75/044 | 5000 | 1 | 1 | | 1 | | 20.93 | 0.33 | | | |
| PS75/045 | 531 | | | | 1 | | | | | | |
| PS75/046 | 2984 | | | | 6 | | 17.26 | 0.17 | | | |
| PS75/047 | 4480 | | | | | | 22.98 | 0.83 | | | |
| PS75/048 | 4516 | | | | | | 19.88 | 0.87 | | | |
| PS75/049 | 4482 | | | | 11 | | | | | | |
| PS75/050 | | | | | | | | | | | 12 |
| PS75/051 | 3949 | | | | 12 | | 18.73 | 1.01 | | | |
| PS75/052 | 5130 | 1 | 1 | | | | 23.17 | 0.41 | | | |
| PS75/053 | 5115 | | | | 11 | | | | | | |
| PS75/054 | 4113 | 1 | 1 | | 0 | | 22.38 | 0.91 | | | 16 |
| PS75/055 | 3602 | | | | 2 | | | | | | |
| PS75/056 | 3581 | | | | | | | | 10.21 | | |
| PS75/057 | 2888 | 1 | 1 | | 0 | | 18.12 | 0.92 | | | |
| PS75/058 | 3629 | 1 | | | | | 12.96 | 0.93 | | | |
| PS75/059 | 3613 | | | | 0 | | 13.98 | 0.90 | | | |
| PS75/060 | | | | | | | | | | | 16 |
| PS75/061 | 3091 | 1 | 1 | | 0 | | | | | | |
| PS75/062 | 4165 | | | | 7 | | 21.09 | 0.65 | | | |
| PS75/063 | 3795 | | | | 6 | | 22.46 | 0.67 | | | |
| PS75/064 | 4600 | 1 | 1 | | 2 | | 15.43 | 0.27 | | | |

| Station | Depth (m) | CTD | MN | PLA | MUC (tubes) | GKG (m) | KOL Core (m) | KOL TC (m) | SL Core (m) | KAL Core (m) | Seismic Survey (nm) |
|---|---|---|---|---|---|---|---|---|---|---|---|
| PS75/065 | 4499 | 1 | 1 | | 9 | | 18.6 | 0.67 | | | |
| PS75/066* | | | | | | | | | | | |
| PS75/067 | 4151 | 1 | 1 | | 6 | | 17.95 | 0.82 | | | |
| PS75/068 | 3728 | | | | 5 | | 14.12 | 0.91 | | | |
| PS75/069 | 4334 | | | | 7 | | 18.46 | 0.65 | | | |
| PS75/070 | 2842 | 1 | | | 10 | | 0 | 0.90 | | | |
| PS75/071 | 2926 | | | | 0 | | 11.36 | 0.95 | | | |
| PS75/072 | 3098 | 1 | | | 11 | | 14.97 | 0.50 | 9.61 | | |
| PS75/073 | 3238 | | | | | | 17.04 | 0.68 | | 3.68 | |
| PS75/074 | 3295 | 1 | | | 6 | | 20.95 | 0.54 | | | |
| PS75/075 | 4096 | 1 | | | 0 | | 18.35 | 0.92 | | | |
| PS75/076 | 3742 | | | | 12 | | 20.59 | 0.65 | | | |
| PS75/077 | 4101 | | | | 0 | | | | | | |
| PS75/078 | 3315 | | | | 0 | 0 | | | 3.83 | | |
| PS75/079 | 3770 | | | | 0 | | 18.51 | 0.67 | | | |
| PS75/080 | 3874 | | | | 11 | | 12.2 | 0.89 | | | |
| PS75/081 | 3857 | | | | | | 13.71 | 0.97 | | | |
| PS75/082 | 4000 | | | | 12 | | 10.88 | 0.89 | | | |
| PS75/083 | 3599 | | | | 0 | | 13.13 | 0.37 | | | |
| PS75/084 | 3734 | | | | 10 | | | | | | |
| PS75/085 | 4065 | | | | 11 | | 19.74 | 0.00 | | | |
| PS75/086 | 4406 | | | | 12 | | | | 12.74 | | |
| PS75/087 | 3857 | | | | 7 | | | | 11.28 | | |
| PS75/088 | 3857 | 1 | 1 | 2 | 12 | | | | 12.4 | | |
| PS75/089 | 4126 | 1 | 1 | 2 | 7 | | | | 11.12 | | |
| PS75/090 | 3478 | 1 | 1 | 2 | 7 | | 17.91 | 0.92 | | | |
| PS75/091 | 2940 | 1 | 1 | 2 | 4 | | 13.44 | 0.26 | | | |
| PS75/092 | 3833 | 1 | 1 | 2 | 7 | | | | | | |
| PS75/093 | 3762 | | | | | | 12.84 | 0.92 | | | |
| PS75/094 | 3270 | 1 | 1 | 2 | 10 | | 9.7 | 0.92 | | | |
| PS75/095 | 4853 | 1 | 1 | 2 | 11 | | 17.85 | 1.01 | | | |
| PS75/096 | 5057 | 1 | 1 | 1 | 0 | | 22.79 | 0.69 | | | |
| PS75/097 | 4672 | 1 | 1 | 1 | 11 | | 17.47 | 0.69 | | | |
| PS75/098 | 5189 | 1 | 1 | 2 | 6 | | 22.83 | 0.82 | | | |
| PS75/099 | 1272 | 1 | 1 | 2 | 6 | 0.29 | 7.71 | 0.00 | | | |
| PS75/100 | 2498 | 1 | 1 | 2 | 7 | | 14.77 | 0.29 | | | |
| PS75/101 | 1770 | | | | 12 | | 11.8 | 0.12 | | | |
| PS75/102 | 1621 | | | | | | 12.96 | 0.48 | | | |
| PS75/103 | 1390 | | | | | | 13.15 | 0.57 | | | |
| PS75/104 | 835 | 1 | 1 | 1 | 9 | | 12.71 | 0.00 | | | |
| PS75/105 | 675 | | | | 12 | | 15.09 | 0.11 | | | |
| **Total 72** | | **28** | **22** | **23** | **321** | **0.29** | **919.39** | **36.15** | **71.19** | **3.68** | **64** |

# ITINERARY AND SUMMARY

## Itinerary

On November 27, 2009, at 22:30h local time, expedition ANT-XXVI/2 started from the bunker pier Cabo Negro near the Chilean town Punta Arenas. It was here that the *Polarstern* had been fueled during the day with 1,400 $m^3$ of Marine Diesel for the long cruise to New Zealand. On board were 45 crewmembers and 43 scientists, technicians and helicopter personnel. The science crew, including 17 women, is a multicultural mix of nationals from Chile, Germany, France, India, Italy, Korea, Malaysia, Austria, Switzerland, Spain and the USA. Due to a delayed departure from Cabo Negro of almost 5 hours, the narrowest section of the Strait of Magellan was passed in the early hours of November 28. Unfortunately poor visibility and rain diminished the view on the snow and ice-covered mountains of Patagonia and Tierra del Fuego.

Immediately after leaving the Strait of Magellan, heading was set towards the southern Freeden Seamount (ca. 57°30´S, 90°30´W) located between Mornington and Bellingshausen Basin (Fig. 1.1). After leaving Chilean waters on November 29, 14:40 UTC, (52°49.3´S, 79°53.1´W) the acoustic instruments for mapping seafloor topography (swatch echosounder HYDROSWEEP) and sediment distribution (PARASOUND-sediment echosounder), as well as the sea gravimeter were set in registration mode and the first sampling station was completed (PS75/034). The multi-corer, a 20 m-piston corer and the CTD and rosette water sampler were deployed successfully. Problems occurred with the fluorometer on the CTD probe and the multi-net, but both could be fixed on the following day. Only 24 hours after this station the area of the Freeden Seamount was reached. A ca. 1 km-sized asteroid named Eltanin hit this area ca. 2.5 million years before present. This event represents the only known larger-sized asteroid impact in the deep ocean. Available geoscientific results suggest that the impact generated a 20 km wide water-crater that reached the seafloor at 5,000 m water depth, and up to 100 $km^3$ of water together with deep-sea sediments and meteorite debris were ejected at hypervelocity into the atmosphere. A 200 - 300 m thick sediment layer, that had accumulated over 40 million years on the Freeden Seamounts, was literally blown away and the seafloor was plowed. At the edge of the water-crater, a wave-ring several kilometers in height developed and traveled across the globe. It was planned to complement these results especially in the southern area of Freeden Seamount and to locate the yet unknown exact impact site (‘ground zero’). Model simulations of the impact event have hinted at this location.

Based on available and new echosounding survey data (PARASOUND) a total of eight sites were selected (PS75/035-040, PS75/42-43) and up to 23.5 m-long sediment cores were recovered at favorable weather conditions (Fig. 2.3). However, sediments that document the impact could only be recovered at three sites (PS75/036, 038, 040) only. Additionally, a multi-channel seismic survey with two GI-guns and a 600 m long

streamer was completed at Freeden Seamount on December 3 and 4. Together with the bathymetric, echosounding and marine geological sampling survey this represents a pre-site survey in the frame of proposal 625 - full („Cenozoic Southern Ocean Pacific“, CESOP) within the Integrated Ocean Drilling Program (IODP) to drill Eltanin impact related sediments. Due to technical problems with the registration of the seismic data the survey could not be completed at full length.

On December 5, the survey at Freeden Seamount was terminated and heading was set in northwesterly direction towards the East Pacific Rise (Fig. 1.2). On this track a >5,000 m-deep trough structure was sampled with the CTD with rosette, the multi-corer and the piston corer (Station PS75/044). In the evening of December 6 *Polarstern* approached a crescent-shaped chain of seamounts. Available bathymetric maps suggested water depths of only 40 m above the seamounts. However, the mapping of the structure resulted that the eastern seamount has ~4 km wide plateau (guyot structure), which is 500 m rather than 40 m deep (Fig. 6.2). It was possible to obtain a surface sediment sample from the summit of the seamount, which contains exclusively foraminifera (Station PS75/045). On the following way to the East Pacific Rise no sediment deposits appropriate to be sampled were found. Finally, on December 8, a seamount was discovered which is covered by thicker sediment and a 17.26 m-long core was recovered from 3,000 m water depth (Station PS75/046). West of the seamount the PARASOUND showed deposition of thick sediment sequences. In this area another pre-site survey for IODP proposal 625 - full (EPR-4A, Fig. 8.1) combining bathymetric, seismic and marine-geological surveys and sampling was accomplished (Stations PS75/047-050, Figs. 8.7, 8.8). After sampling another site located on the track towards an area on the East Pacific Rise planned to be investigated in the frame of an IODP pre-site survey (EPR-3A, Fig. 8.1) heavy weather conditions with predicted wave heights of up to 9 m (Fig. 2.5) forced a change of heading towards the northern Amundsen Abyssal Plain (Fig. 1.2). Throughout the 550 nm long track to the Amundsen Abyssal Plain and calmer sea state, thick sediment sequences were indicated by PARASOUND. On this transect the Subantarctic Front and the Eltanin Fraction Zone System (EPZS) was crossed (Fig. 1.2).

On December 11, 23:09 UTC, *Polarstern* entered the area of the Antarctic Treaty at 60°S, 115°07.7´W. In the Antarctic treaty area the geoscientific survey and sampling must be conducted according to specific requirements imposed by the Federal German Agency of Environmental Protection (UBA). Close to the northern edge of the Antarctic Treaty area another pre-site survey in the frame of proposal IODP625 - full (proposed site BEL1B, Fig. 8.1) was planned. At perfect weather conditions all means were taken to conduct a short seismic survey considering all requirements for environmental protection requested by UBA. Unfortunately, because of a total failure of the seismic recorder, the survey had to be cancelled. However, the survey could be completed during the following cruise ANT-XXVI/3 (Gohl, 2010). The sediments could be successfully sampled with the multi-corer and a 30 m-piston corer (Stations PS75/052-053). On the way back to the East Pacific Rise the area of the Antarctic treaty was left on December 13, 00:31 UTC (Fig. 1.2). After crossing the EFZS, another pre-site survey (EPR-5A, Figs 8.1) including sediment sampling with the multi-corer, a 30 m-piston corer and a cross-shaped seismic survey was accomplished at a water depth of 4,100 m (Station PS75/054) (Figs 8.9, 8.10). Besides, a S-N sample transect

of the water column with CTD, rosette water sampler, fluorometer and multi-net that had started at Station PS75/052 (Amundsen Basin) was continued. Not far north of the station, sediment sampling with multi-corer and gravity corer was continued at a depth of 3,600 m (Stations PS75/055-056) to allow for the establishment of a sediment sampling depth transect between the deep Amundsen Abyssal Plain and the crest of the southern East Pacific Rise. On December 15, the weather conditions again forced to leave the originally planned route and head westward. Strong wind around Bft 8 and wave heights around 6 m (Fig. 2.3) prevented further safe work on deck. Hence, the second attempt to sample the potential IOPD 605 - full drill site EPR-3A (Fig. 8.1) further north had failed. Immediately after crossing the crest of the East Pacific Rise, sediments and water column have been sampled at a water depth of 2,900 m. The following track in westerly direction was located north of the Subantarctic Front (SAF), instead south of it, as originally planned (Fig. 1.2). On this transect another, alternate pre-site survey including a seismic profile and sediment sampling with the multi-corer and the piston corer was completed (Stations PS75/058-60) (Figs. 8.11, 8.12). The surface sampling was not successful and two attempts to recover long piston cores resulted in the bending of the core tube at 12 - 15 m sediment depth. The repetition of the coring was decided because, due to strong winds and currents, the ship had drifted out of the optimal position during the first attempt (PS75/058), as recorded by PARASOUND (see A.6). The bending of the tubes very probably resulted from the presence of a 2 m thick, stiff calcareous nannofossil ooze layer (see sediment core descriptions in A.7). The stratigraphic age of the ooze can be attributed to Marine Isotope Stage (MIS) 11. The ooze is marked as a prominent reflector in the PARASOUND echosounding records and can be followed over large distance in the polar South Pacific (Fig. 7.2.4).

On December 19, the EFZS was crossed in westward direction and the weather conditions remained unfavorable (Fig. 2.3). West of the EFZS, the search for a potential drill site to be proposed in IODP625 - full (UFZ-2A, Fig. 8.1) was started on the ridge segment between the EFZS and the Udintsev Fracture Zone (UFZ). However, no appropriate sediment deposits could be found in this area. Thicker sediment coverage were only found when the area of the UFZ was reached, which bathymetrically constrains the location of the Subantarctic Front and the Polar Front in this area (Fig. 1.3). Geoscientific sampling was continued north and south of the UFZ and the Polar Front, respectively (Fig. 1.3). The recovered piston cores (Stations PS75/062-063) are longer than 20 m and contain sediments deposited at rates estimated to range around 10 cm/1,000 y. In this area the second latitudinal transect for the sampling of the water column (CTD, rosette, fluorometer, multi-net) was started, which extends from the Polar Front into the seasonal sea ice covered zone of the Amundsen Basin. Recorded sedimentation rates (mostly biogenic opal) in the area between the Polar Front and the winter sea ice edge are high and range around 10 cm/1,000 y. However, south of the winter sea ice edge, sedimentations rates drop drastically to low values and recovered sediments reach back > 3 Ma (Stations PS75/065-069, PS75/086-090) (Fig. 7.6.1).

On December 22, 16:03 UTC, *Polarstern* re-entered the Antarctic Treaty area in the western Amundsen Basin and on December 25, the southernmost position on this transect (at around 64°58´S) was reached (Fig. 1.3). South of 60°S air and water temperatures dropped to values around 0 – 1°C (Fig. 2.4) and a large number of icebergs surrounded the ship. On December 24, work was reduced to a bare minimum

for a period of 24 h, starting at 15:00 ship time. Time was used to map a region with HYDROSWEEP and PARASOUND, marked as topographic high on the bathymetric GEBCO_08 map. This pattern could not be confirmed by the survey (Fig. 6.4). In the evening of December 24 Christmas celebrations were started with a reception in the "Blue Salon" on the B-deck followed by parties in different rooms on the ship.

The subsequent transect with a length of 700 nm crosses the Pacific-Antarctic Ridge and heads towards the Subantarctic Front in the SW-Pacific Basin, making yet another saw-tooth in the cruise track towards the west (Fig. 1.3). On December 28, 7:10 UTC, *Polarstern* left the Antarctic Treaty area for the second time. Mostly calm sea conditions (wave heights around 3 m) allowed for the completion of seven stations with piston corer, multi-corer and CTD (Stations PS75/069-075). At the shallowest station on the ridge (PS75/070, 2,840m water depth), where is was expected to recover sediments rich in biogenic carbonate, the 15 m long tube of the piston corer was lost in the sediment. Only the bomb, the trigger arm and the trigger corer, which had sampled a 90 cm-long core, could be recovered. Recovery of sediment was more successful at all other stations, where 15 – 21 m cores could be collected that document the climate history of the past 300,000 - 600,000 years. On this transect, Station PS75/073 represents the only site of the cruise, where a kasten corer (box diameter 30 x 30 cm) was deployed to recover a large sized sediment core. The resulting sediment core has a length of 3.68 m.

Just in time for New Year, the Subantarctic Front was reached. The original plan to interrupt work at station for a shorter period to allow for the celebration of New Year's Eve was modified because of an unexpected deterioration of the weather conditions. Within a short time a harmless low-pressure system developed into a big storm that moved towards the area of operation at a speed of 40 km/h. It was decided to complete the station work in the vicinity of the Subantarctic Front and to celebrate one day later. However the traditional reception on the bridge at midnight did take place. After the survey and station work on December 31, 2009 and January 1, 2010, which were finally abandoned at Station PS75/077 due to increased wind speeds and wave heights, it was decided to escape the storm system and to steam in southwestward direction. Since wind and waves were moving in the same direction as *Polarstern*, the average speed was around 12 - 13 knots on the 200 nm long transit to the Pacific-Antarctic Ridge (Fig. 1.3), even though the ship's engines operated at economic mode. On January 2, 2010, 18:29 UTC, *Polarstern* re-entered the Antarctic Treaty area for the third time. For the following night *Polarstern* was stopped, turned towards the wind to wait ca. 12 h for the decline of the bad weather conditions with winds up to Bft 8 and wave heights up to 7 m. After this stop the geoscientific sampling programme was continued on the crest of the Pacific-Antarctic Ridge at a water depth of 3,300 m. Because of the agitated sea the gravity corer was deployed at Station PS75/078, instead of the piston corer. The deployment resulted in a 3.83 m long core, rich in biogenic carbonate. Attempts to recover surface sediment with the multi-corer and the box corer failed. On the return track to the Polar Front the area of the Antarctic Treaty was left on January 3, 22:45 UTC (Figs. 1.1, 1.3). On January 4, the Polar Front area was reached and the sampling transect between the Subantarctic Front and the seasonal sea ice covered zone in the northern Ross Sea was resumed. Geoscientific sampling was completed at five sites (Stations PS75/080, 081, 082, 083, 085) that had

been selected on the escape way to the South and the return. The recovered sediment cores are up to 19.7 m long. The fourth entry in the area of the Antarctic Treaty was on January 6, 02:18 UTC, between Stations PS75/082 and /083. On the way further south, surface sediment could be recovered successfully (Station PS75/084) when revisiting the location of Station PS75/078. The following two stations, PS75/086 and /087, both located south of the winter sea ice edge, sediment cores with Pliocene bottom ages were recovered with the gravity corer.

On January 9, the southernmost position of expedition ANT-XXVI/2 was reached at 68°43'S, 164°48'W (Figs. 1.1, 1.4). In this area, *Polarstern* was surrounded by huge icebergs, which very probably originate in the Ross Ice Shelf. The sea ice had retreated from this area only two weeks ago. This was witnessed by strong surface water stratification caused by a salinity minimum (Fig. 3.1.10), which was accompanied by strong primary productivity resulting in the development of a $CO_2$ sink (Figs. 3.1.16, 3.2.1). The southernmost site was the start of the longest latitudinal transect surveyed and sampled during ANT-XXVI/2 ranging over a distance of 1,700 nm to the Subtropical Front south of the harbor Wellington. On this transect the water column and the sediment was sampled at 18 sites (PS75/088-105) using the CTD, the rosette water sampler, the multi-net, the plankton net, and the multi-corer, and the piston and the gravity corer, respectively. The acoustic surveys with HYDROSWEEP and PARASOUND as well as the geological sampling represent part of a pre-site survey for proposal IODP-625 full, which includes a latitudinal drill transect with four sites aligned across the Pacific-Antarctic Ridge (PAR-1A – PAR-4A)(Fig. 8.1). Part of the seismic survey was accomplished during the subsequent expedition ANT-XXVI/3 (Gohl, 2010).

Work at stations located south of the Pacific-Antarctic Ridge was accomplished at cold temperatures (around 0°C, Fig. 2.10) and calm weather conditions. However, with the arrival in the central area of the Pacific-Antarctic Ridge on January 12, the weather situation deteriorated and wind speeds around Bft 8 and wave heights between 4 - 5 m established. To avoid further weather deterioration, heading was set to northerly direction after completion of Station PS75/091 (Fig. 1.4). This short transect ended at the Polar Front. After accomplishment of a short station at the front (PS75/092) weather and sea state had improved allowing for the completion of two stations further to the south (PS75/093, /094).

After accomplishment of work at Station PS 75/095 in the morning of January 14, heading was set to Wellington, the Polar Front was crossed and the area of the Antarctic Treaty was left at 20:49 UTC for the last time (Fig. 1.4). The second attempt towards the north was also disturbed by bad weather conditions, which impeded station work. *Polarstern* steamed 320 nm against 8 Beaufort and > 4 m waves until the Subantarctic Front and calmer conditions were reached. Station work was continued at the Subantarctic Front (PS75/095) and two other stations were accomplished on the return track towards the Polar Front. A longer steam track starting north of the Polar Front and extending over 7 degrees of latitude followed. In the western part of the SW-Pacific Basin, close to the New Zealand EEZ, the last deep water station of expedition ANT-XXVI/2 was accomplished at a water depth of 5,190 m (PS75/098)(Fig. 1.4).

On January 21, *Polarstern* entered the New Zealand EEZ. Before arrival at Wellington water column and sediment sampling was accomplished at 7 sites: the first location

was in the Pukaki Saddle between Bounty and Campbell Plateau, at a water depth of 1,270 m, the six other sites are aligned on a depth transect between 2,500 and 670 m water depth, extending from the Bounty Trough to the southwestern Chatham Rise (PS75/100-105). The last site is in the area of the Subtropical Front (Fig. 1.4).

In the night January 25/26 the pilot came onboard and a critical shallow water ridge in front of the harbor of Wellington was crossed. Only a few decimeter of water remained under the keel of *Polarstern*. In the early morning *Polarstern* moored in the container harbor of Wellington (Aotea Quay). Local authorities came onboard for the purpose of clearance. Around noon the scientific cruise members disembarked and the expedition ANT-XXVI/2 was terminated.

**Summary**

The focus of expedition ANT-XXVI/2, which took *Polarstern* over a distance of 9,757 nm for the first time across the entire polar South Pacific, is marine-geoscientific studies. This was complemented by bathymetric (HYDROSWEEP) and echo-sounding (PARASOUND) surveys along the most of the cruise track (9,273 nm). The track can be divided into five transects:

Transect 1 (east-west): Mornington Abyssal Plain (MAP) – Eltanin Fracture Zone System (EFZS),

Transect 2 (north-south): Eltanin Fracture Zone System (EFZS) – Amundsen Abyssal Plain (AAP),

Transect 3 (south-north): Amundsen Abyssal Plain (AAP) – SW-Pacific Basin (SWP)

Transect 4 (north-south): SW-Pacific Basin (SWP) – Ross Sea (ROS)

Transect 5 (south-north): Ross Sea (ROS) – New Zealand Margin (NZM).

Transect 1 covers the eastern and central sector of the polar South Pacific in the realm of the Polar Front Zone. The four latitudinal transects in the western polar South Pacific range between the seasonal sea ice covered zone to the Subtropical Front (Fig. 1.2.1).

ANT-XXVI/2 station work was completed at 72 sites (PS75/34 – PS75-105). A total of 1,030.31 m sediment core was recovered with a piston corer (49 deployments), a gravity corer (7 deployments) and a kasten corer (1 deployment) (Table 1.2.1). Surface sediment was sampled at 39 sites with the multi-corer and additionally at one site with the box corer. The aim of the studies that can be conducted based on the geoscientific data and samples collected during ANT-XXVI/2 is to document the role, evolution, and impact of climatically relevant mechanisms such as the biological pump, circulation and stratification of the ocean, water masses, sea ice extent, atmosphere-ocean exchange, atmospheric circulation and the volume and dynamic of the Antarctic ice sheets on geological time scales. The sediment cores will allow paleoceanographic and paleoclimatic reconstruction at a resolution of $10^2$-$10^3$ years over the past 900,000 years in the area north of the winter sea ice margin and at lower resolution, but back to ca. 4.5 Million years, in the seasonal sea ice covered area. At the moment very little information is available about climate history and related processes in the Pacific sector of the Southern Ocean, which is an important region of water mass formation, and the key region for understanding of the evolution and

dynamics of the Antarctic ice sheets as it collects ca. 70 % of the West Antarctic ice sheet drainage. The surface sediment samples, data and samples from the water column will further improve geoscientific proxies for the reconstruction of past climate conditions. Besides sampling for paleoceanographic studies additional surveys and sampling were conducted in the area of Freeden Seamount for further improvement of the documentation and reconstruction of the Eltanin asteroid impact around 2.5 Ma. Additionally, pre-site survey was completed as part of drill proposal 625 - full („Cenozoic Southern Ocean Pacific“, CESOP) (Gersonde et al., 2008) in the framework of the Integrated Ocean Drilling Program (IODP). This included the combination of seismic, bathymetry and sediment echo-sounding surveys together with sediment sampling at pre-selected sites.

Additionally, atmospheric dust was sampled along the track to document the deposition of dust from New Zealand and Australia and studies in the water column were completed. This included 28 CTD casts across the water column to measure vertical profiles of temperature, salinity and pacif, 22 net hauls with the multinet to sample plankton at five depth intervals in the upper 1,500 m of the ocean and 23 net hauls in the upper 100 m at 13 sites with the Nansen net. Additionally water samples were collected with the rosette water sampler and the ships pumping systems to measure nutrient and gas concentration, investigate the distribution of microplankton and pigments and to measure stable isotopes in the water column. The hydrographic study may provide new insight into the response of the polar South Pacific Ocean to the strong El Niño event observed during 2009/10 in the central Equatorial Pacific (Lee and McPhaden, 2010). In the seasonal sea ice covered zone of the western polar South Pacific strong stratification of the surface water was encountered together with increased primary productivity and resulting in the establishment of distinct $CO_2$ sink. Such conditions may be representative for a glacial type scenario.

The data and samples are studied in national and international cooperation within the frame of the AWI program PACES, the program of the DFG Research Center „The Ocean in the Earth System“, the EU-Program „Past4Future“, the Integrated Ocean Drilling Program (IODP) and other national (DFG) and international projects.

## References

Comiso, J.C., 2003. Large-scale characteristics and variability of the global sea ice cover. In: Thomas, D.N., Diekmann, G.S. (Eds.), Sea Ice: An introduction to its physics, chemistry, biology, and geology, Blackwell, Oxford, pp. 112–142.

Gersonde, R., et al., 2008. Cenozoic Southern Ocean Pacific (CESOP): A proposal for drilling cenozoic history sites in the Pacific sector of the Southern Ocean. Proposal 625-full to the Integrated Ocean Drilling Program (IODP), 128 p.

Gohl, K., 2010. The Expedition of the research vessel “Polarstern” to the Amundsen Sea, Antarctica, in 2010 (ANT-XXVI/3). Reports on Polar and Marine Research 617, 168 p.

Lee, T. and McPhaden, M.J., 2010. Increasing intensity of El Nino in the central Pacific. Geophy. Res. Letters 37, doi:10.1029/2010GL044007

Orsi, A.H., Whithworth, T., Nowlin, W.D., 1995. On the meridonial extend and fronts of the Antarctic Circumpolar Current. Deep-Sea Research I, 42, 641-673.

# 2. WEATHER CONDITIONS

Harald Rentsch Deutscher Wetterdienst

On November 27, 2009 the weather situation around Punta Arenas was characterized by a low entering the Drake Passage from the Pacific Ocean. As result westerly winds in the Strait of Magellan were increasing up to Bft 7 during the night. This same wind force generated waves of nearly 4 m as we exited the straight on November 28. In the following days cyclones with snow and rain showers as well as gusts up to force 9 from the southwest dominate the weather on our course towards the northwest (Fig. 2.1). Sea surface and air temperatures dropped from 7.5°C and 5°C, respectively, to 5°C and 3°C (Fig. 2.2).

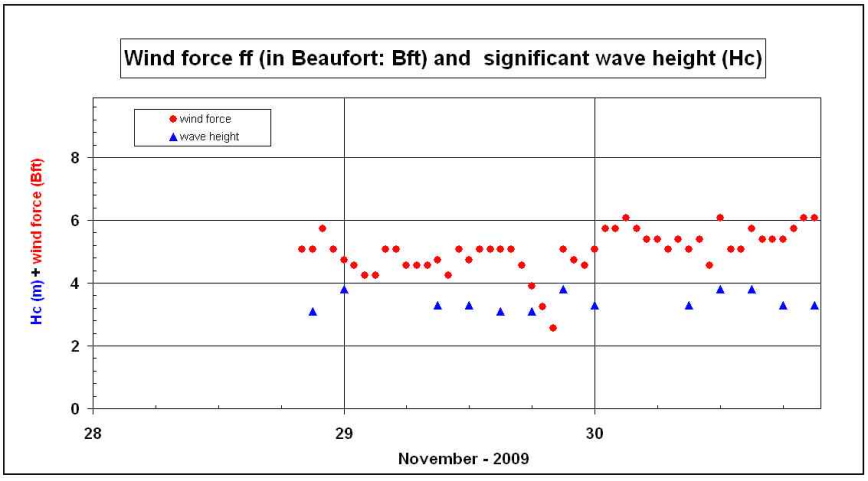


*Fig. 2.1: Time series of wind force and wave height along the track as recorded on November 29 and 30, 2009*

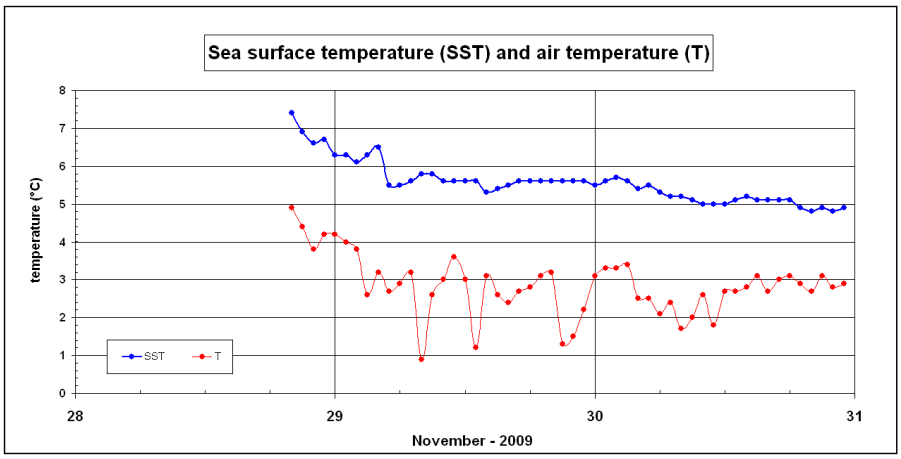


*Fig. 2.2: Time series of sea surface and air temperature along the track as recorded on November 29 and 30, 2009*

In the afternoon of December 1 the ridge of a subtropical high in the South Pacific Ocean (1025 hPa) at 45°S, 120°W began to spread into the working area. Together with this came a calming of winds and the sea state changed to 2.5 m (Fig. 2.3). This opened the possibility of very good working conditions for seismic investigations in the impact area of the Eltanin asteroid. Two days later, as we reached the back side of the cold front, the wind picked up to nearly Bft 7 and sea state reached heights of 3.5 m.

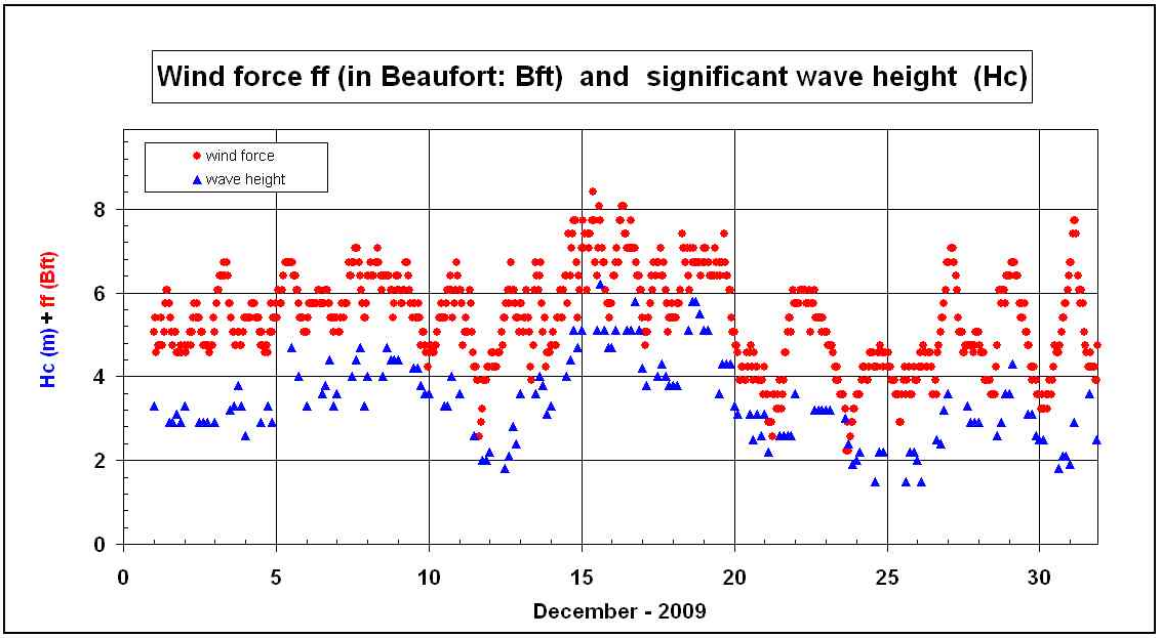


*Fig. 2.3: Time series of wind force and wave height along the track as recorded during December 2009*

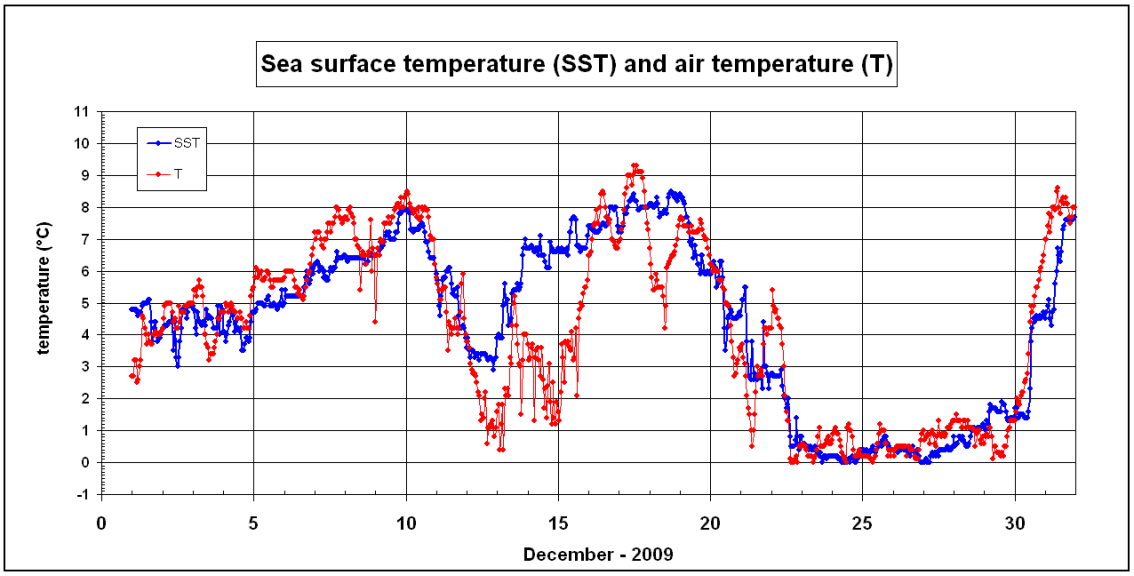


*Fig. 2.4: Time series of sea surface and air temperature along the track as recorded during December 2009*

On December 5, the ships track was close to a cold front, which brought strong cloudiness, and hazy, but dry weather. The winds increased to more than Bft 7 and the swell rose up to 4 m (Fig. 2.3).

On December 7 another cold front passed the cruise track. The strong increase in pressure on the back side of the front caused wave heights of nearly 4.5 m. In addition, due to the instability of the atmosphere there were gusts of up to Bft 9. Sea surface and air temperatures increased as the ship steamed into north-western direction (Figs. 1.1, 2.4)

At this time, the weather models predicted a scenario indicating the development of a strong storm cyclone in the area scheduled to be visited within the following three days (Fig. 2.5). To avoid weather conditions with extreme wind and swell conditions with up to 9 m waves it was decided to change the cruise track and head with full power towards the South, where calmer but colder conditions where established (Figs. 2.3, 2.4).

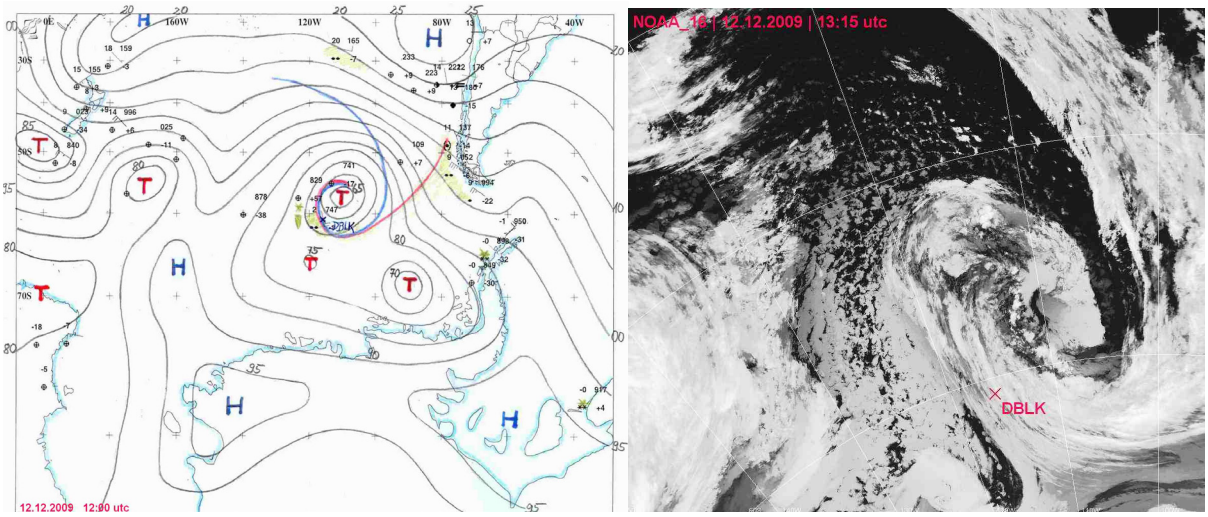


*Fig. 2.5: Surface analysis of the board meteorologist for the date 12/12/2009, 12 UTC (left image) and IR satellite view of the 12/12/2009, 13:15 UTC (right image). The position the Polarstern is marked with a cross and the call sign DBLK.*

With further eastward movement of the cyclone on December 13, a polar unstable stratified cold air mass brought snow-rain showers and wind of up to Bft 8 into the working area. This resulted in a distinct offset between air and sea surface temperatures (Fig. 2.4).

After return into the southernmost area of the East Pacific Rise on December 14 pressure started to increase (approx. 3 hPa per 3 hours) south of 50°S, resulting in a labialization of the lower atmosphere. This caused an increase in wind speeds up to Bft 9 together with an average sea state of 5 m, and peak values up to 6.5 m. Considering that station work was impossible at such conditions the planned expedition track had to be revised once again. Also on the new westward track North of the Subantarctic Front rather windy and unstable weather conditions persisted until December 20. It was only after the change of heading towards the South that calmer conditions with partly sunny weather established. On December 22 the Polar Front was crossed on the way towards the western Amundsen Basin and temperatures dropped to values around 0 to 1°C (Figs. 2.3, 2.4).

Between December 24 and 29 numerous icebergs, some of substantial size, came within sight of our ship along our route. Cold Antarctic air-flow brought strong snowfall and variable weather during the following days. On December 26 and the following days numerous storms developed within the circumpolar west wind drift. The strom systems crossed our track and often produced winds of up to Bft 8, mostly from northerly directions. Sea and swell reached again nearly 5 m.

On the last day of the year 2009 a fine weather window opened up for two days when *Polarstern* reached the area of the Subantarctic Front and the air and sea surface temperature increased to values around 7 to 8°C (Fig. 2.4). This was followed by a complex low pressure system with stormy conditions moved fast into the area of

operation. During the night January 1 to 2, 2010 the forecasted storm started with wave heights of 4.5 m, later up to 6 m, accompanied by Bft 9 (Fig. 2.6). Here the "Furious Fifties" showed their characteristic roughness with steady wind from the west and constant very high swell.

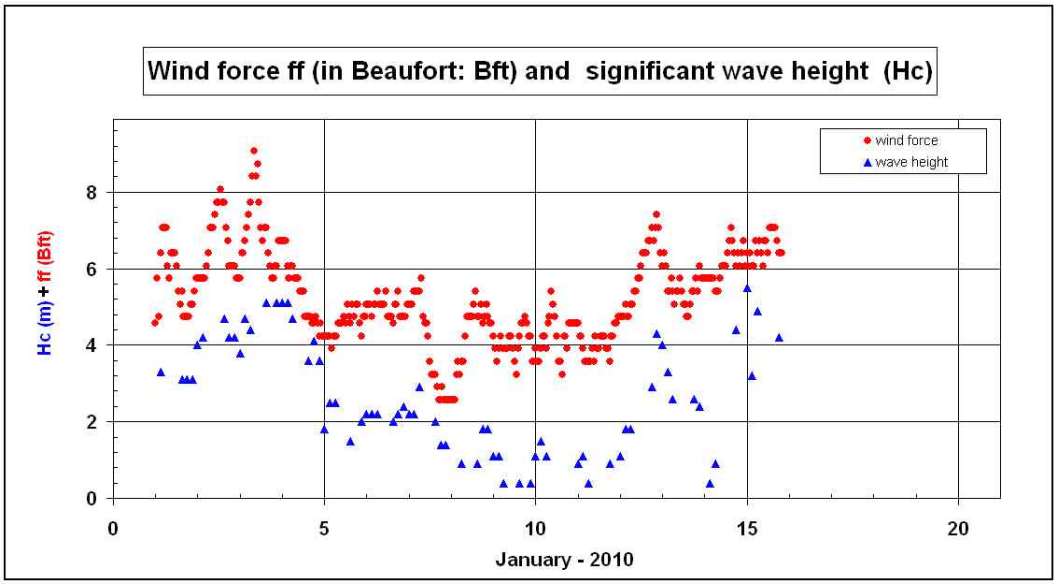


*Fig. 2.6: Time series of wind force and wave height along the track as recorded during the first half of January 2010*

To avoid even worse conditions the ship was moved towards the South. Station work was completed on the transect around the Polar Front until January 6 at more favourable conditions (Fig. 2.6). During the period when the southernmost position of the cruise was reached in the northern Ross Sea weather conditions were marked by low wave heights, calm winds and temperatures around 0°C (Figs. 2.6, 2.7). This cold-water area was characterized by the occurrence of numerous icebergs.

After January 11, the ship came back into a strengthened wind field, with wind forces around Bft 8 and higher waves on the back-side of a weakening, eastward-moving high. Such unfavourable conditions that disturbed the planned station work persisted until the area around 55°S was reached on January 18.

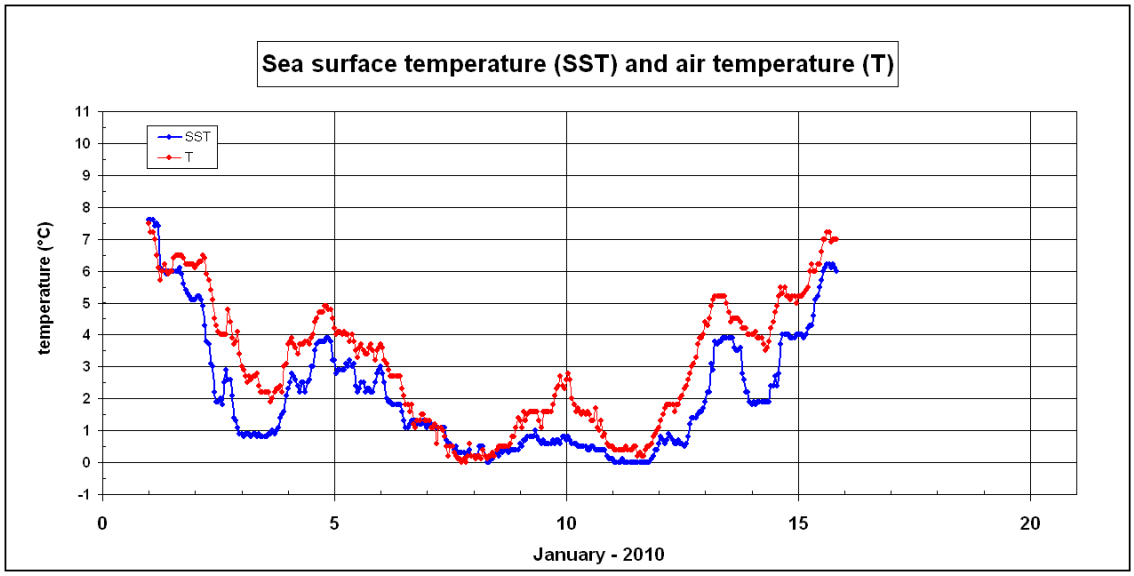


*Fig. 2.7: Time series of sea surface and air temperature along the track as recorded during the first half of January 2010*

The last days of the cruise were marked by a constant north-easterly wind up to Bft 5 and not more than 2.5 m wave heights.

On January 26, 2010 the cruise ended with the entrance into the harbour of Wellington with a light swell from southeast and weak southerly winds.

In summary, the wave heights during ANT-XXVI/2 were centred around 3 m and the wind speeds around Bft 5 - 6 (Figs. 2.8, 2.9). This pattern is due to the fact that the ships track was changed at several occasions to avoid unfavourable weather conditions. The wind direction was mostly West (Fig. 2.10).

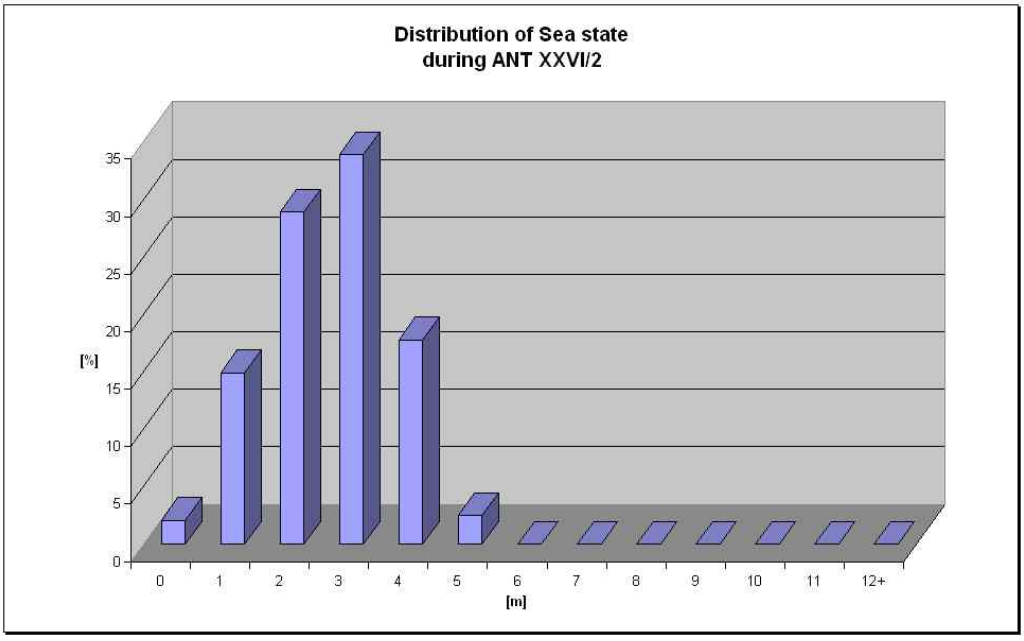


*Fig. 2.8: Distribution of sea state during ANT-XXVI/2*

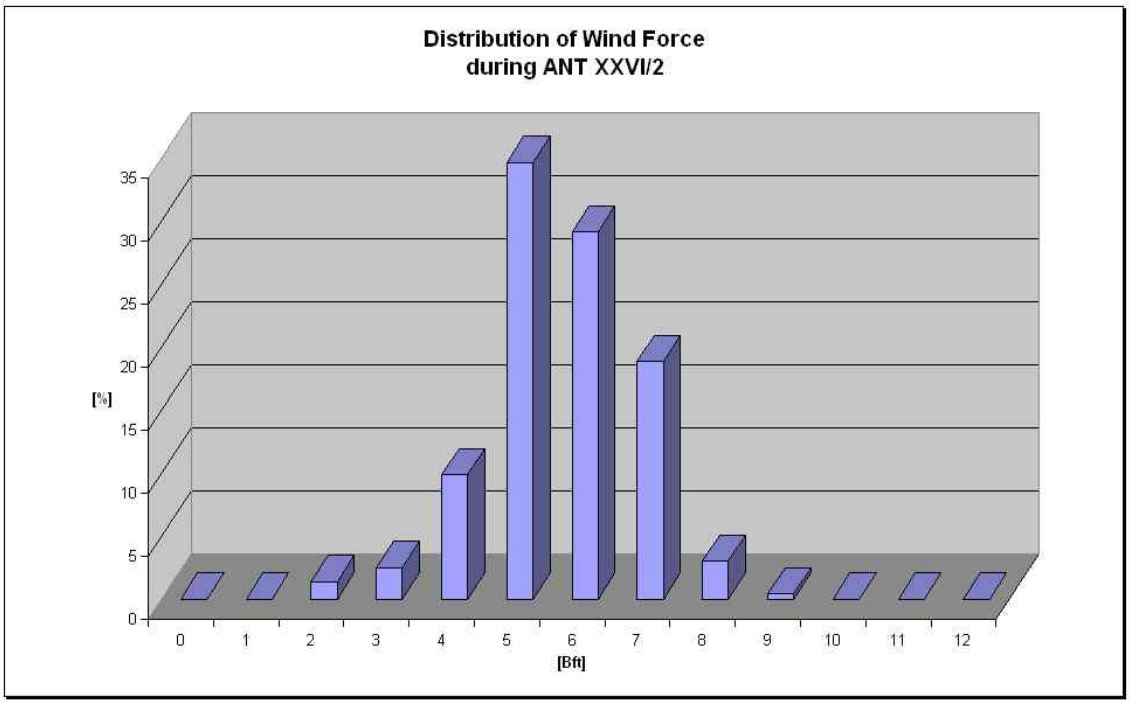


*Fig. 2.9: Distribution of wind force during ANT-XXVI/2*

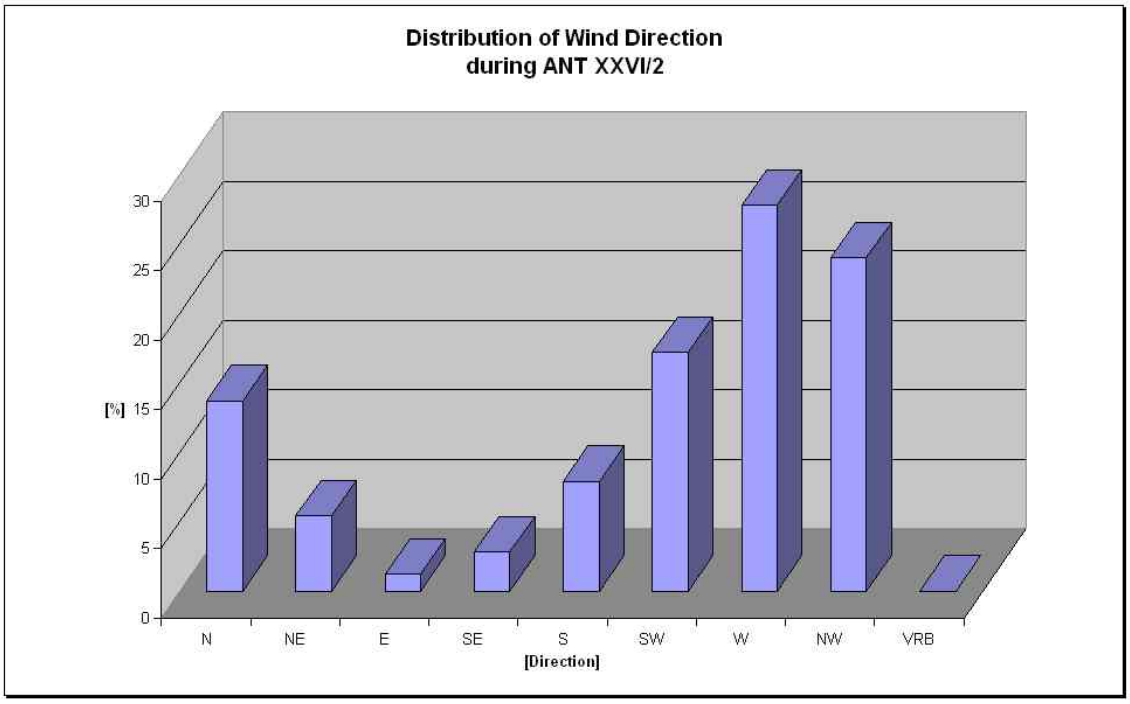


*Fig. 2.10: Distribution of wind direction during ANT-XXVI/2*

# 3. HYDROGRAPHIC AND WATER COLUMN STUDIES

## 3.1 Hydrographic survey

Jana Schnieders[1], Franz Jendersie[1], [1]Alfred-Wegener-Institut
Rainer Gersonde[1], Katharina Pahnke[2] [2]University of Hawaii

### Objectives

The CTD was deployed in order to obtain vertical water column profiles of salinity, temperature, and fluorescence (reflecting chlorophyll a concentrations) along the cruise track in the South Pacific. These data are essential for the identification of surface ocean fronts, water masses and the position of the chlorophyll maximum in the water column, and were directly used to determine the water depths from which to take water samples for the different water column-based projects (chapters 3.2 to 3.5).

### Work at sea

*Instrumentation*

The CTD was attached to a rosette with 24 x 12 l Niskin bottles (OceanTestEquipment Inc.). The bottles were fired by a SBE carousel (SBE32).To survey the water column, a Seabird SBE 9plus sensor (Seabird Electronics Inc.) was used. It measures conductivity (SBE4C), temperature (SBE3plus) at 0.065 s intervals and the pressure at 0.015s intervals. There are two sensors for temperature and conductivity which are supplied by two separate pumps. In addition, a transmissometer (Wetlab Cstar), altimeter (Benthos PSA-916) and fluorometer (Wetlab ECO-AFL/FL) were mounted on the rosette for the measurement of light transmission, water depth, and fluorescence, respectively. As a deck unit, the SBE 11plus from Seabird was used.

The initial accuracy of the measurements is stated to be 0.0003 S/m for conductivity, 0.001°C for temperature, and 0.015 % of the full pressure range (10,000 dbar) (911plusbrochureSep08 by Seabird Electronics Inc.). The initial accuracy given for the A/D inputs is 0.005 V. The pressure sensor was calibrated in 2007, the temperature and conductivity sensors were calibrated in the first half of 2009. For cast observing and data acquisition at the operator PC, the SEASAFE V7 software from SEASOFT was used. Data processing was carried out with the Manage CTD program that transforms the binary data of the downcast into ascii-format.

Surface salinity and temperature were continuously measured (every 5 seconds) and recorded throughout the entire cruise using the Davis ship onboard thermosalinograph (Seabird system, salinity: SBE 38, temperature: SBE 21). Intake is situated at about 11 m depth in the duct keel of the Polarstern. The sensors are regularly calibrated (Davis ship manual, dship_admin.fs-polarstern.de/GESODocu/Index.html).

The chlorophyll a data measured by a FerryBox sensor (scufa) was used for the fluorescence plot in Fig. 3.1.15.

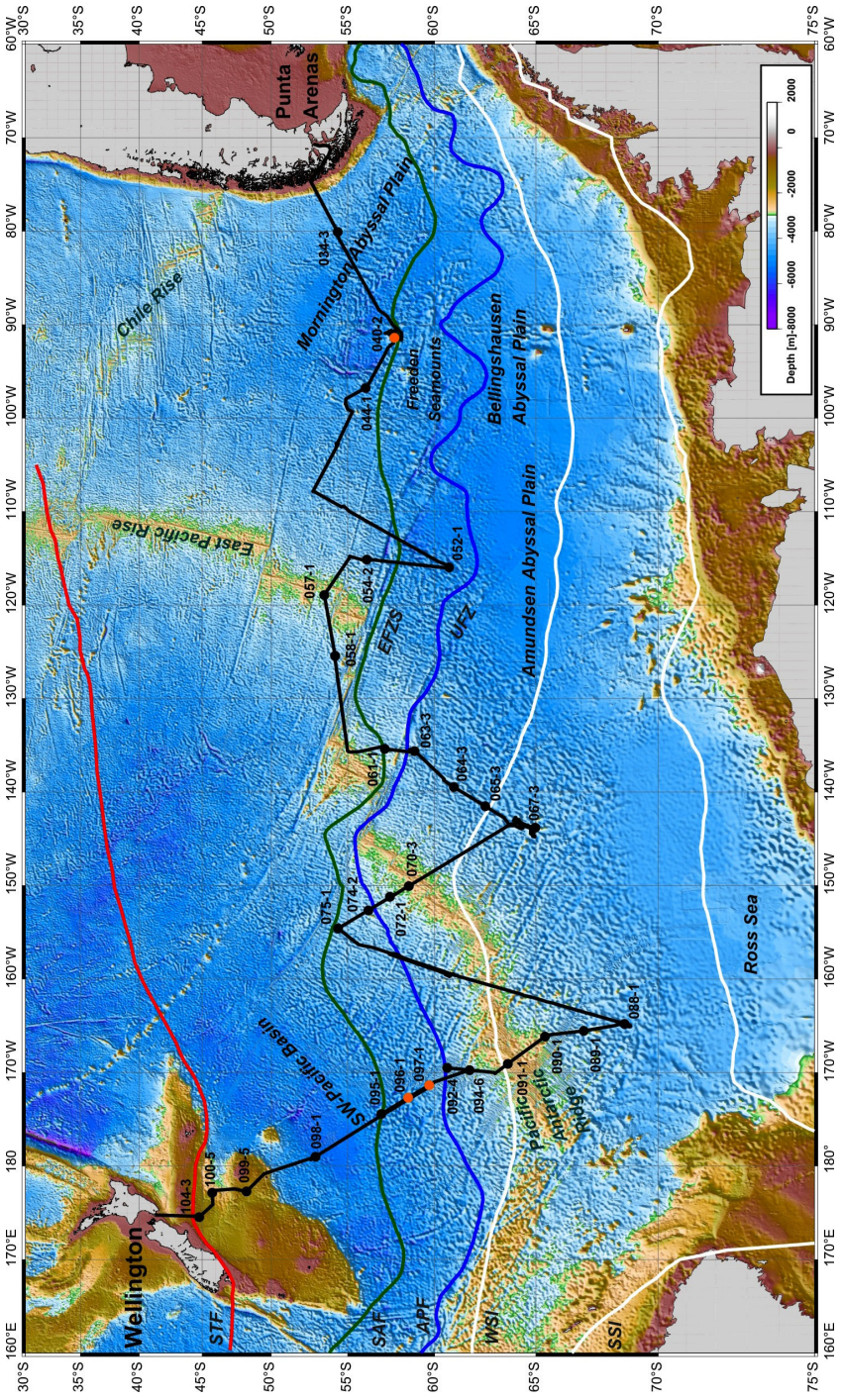


*Fig. 3.1.1: CTD stations during expedition ANT-XXVI/2, including the Subtropical Front (STF), Subantarctic Front (SAF) and Polar Front (APF) according to Orsi et al. (1995), as well as the winter (WSI) and summer (SSI) sea ice boundaries according to Comiso (2003). Orange dots indicate CTD casts to the upper 1,000 m of the water column only.*

*Data collection and water sampling*

The CTD-rosette was deployed at 29 stations along the cruise track (Fig. 3.1.1). Water samples were taken at discrete depths throughout the water column with 24 x 12 L Niskin bottles (chapters 3.2 to 3.5). At the first three stations there were problems with the fluorometer. After changing the sensor, the measured data appeared normal.

**Results**

The CTD was deployed at 29 stations, including 26 stations along four north-south transects and three stations in the Southeast Pacific accomplished during the first days of the cruise. The first CTD station (PS75/034) was a test station. Because of problems with the fluorometer at the first station, the CTD was only deployed to 500 m at the second station to test the fluorometer. The third station (PS75/044) was a deep CTD station that was deployed in the hopes of finding Antarctic Bottom Water (AABW), which was not, however, present at this location.

The 1st N-S transect (T1c + PS75/057) includes three stations (PS75/052-057) and is a meridional section along ~120°00'W from 60°45.871'S to 53°31.782'S. The southernmost station of this transect, PS75/052, is located just north of the Polar Front. There is a clear temperature minimum of slightly below 2°C at around 200 m water depth (determining feature for the location of the APF, Orsi et al., 1995). This temperature minimum is no longer detectable at the two northern stations of the transect (PS75/054, PS75/057), which are located well north of the Polar Front. AABW was penetrated at 4,000 m water depth at this station with a potential temperature of 0.05°C and salinity of 34.68 (potential density 1027 kg/m$^3$). Surface temperature and salinity changed over short distance at around 58°00'S (Fig. 3.1.2), corresponding to the location of the Subantarctic Front (SAF) of Orsi et al. (1995).

The 2nd transect (T2 + PS75/058) (Fig. 3.1.1) is a meridional transect along 139°00'W and starts at 54°12.947'S 125°26.187'W (Stations PS75/058 to PS75/067). As we can clearly see from the salinity and temperature profiles, the starting point of the transect in the north (PS75/058) is still north of the SAF, and crosses the SAF, APF and the Southern Polar Front (SPF) during the transect. Coming from the north, surface temperature and salinity decrease significantly. At 56°00'S there is a drop in surface temperature of ca. 2°C (Fig. 3.1.4), which marks the position of the SAF. The thickness of the surface-mixed layer, as marked by high chlorophyll a concentrations, increases from ca. 50 m at station PS75/058 to ca. 100 m at PS75/067. Additionally, a clear temperature minimum evolves south of the APF and the temperature in the temperature minimum layer above 200 m decreases clearly from ca. 0°C at station PS75/063 to -1.8°C at PS75/067. This is the cold, fresh Antarctic winter water. The higher temperature above the temperature minimum is due to recent spring and summer warming. Station PS75/058 is located north of the SAF. AAIW, as identified by its low salinity of 34.36-34.50 is found at this station as well as stations PS75/061 and PS75/063 but is not found anywhere south of station PS75/063 (59°00'S), as it is formed in the area north of the APF (Gordon and Molinelli, 1986). The salinity maximum rises from ca. 2,500 m at station PS75/058 to 350 m at PS75/067, which is due to the shoaling and eventual outcropping of density surfaces around Antarctica (Reid et al., 1997).

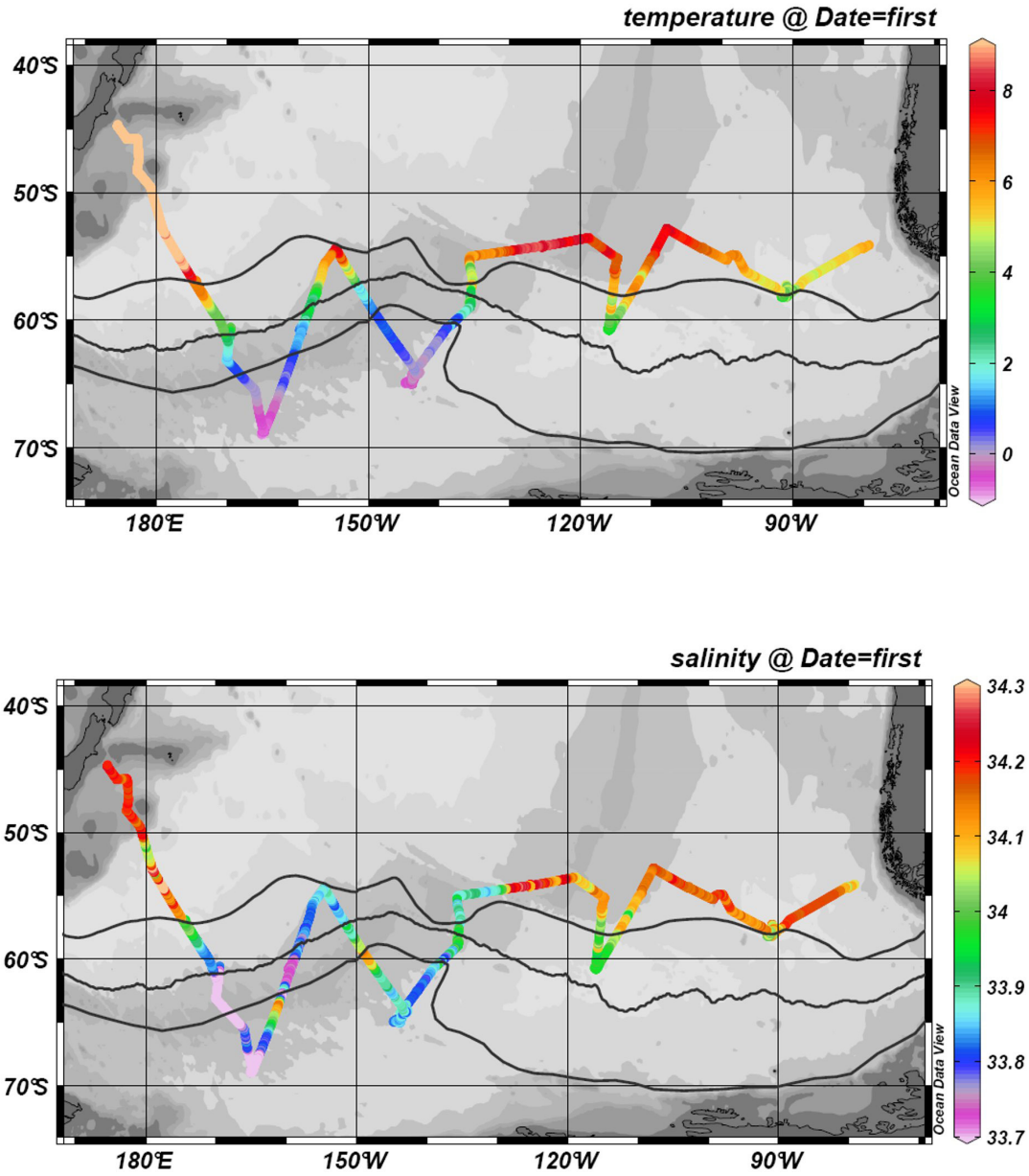


*Fig. 3.1.2: Map of surface water temperature and salinity along the cruise track with continuous data from the dship on-board sensors*

South of the SPF (south of station PS75/63) we reached the area of the Antarctic Zone (AZ), where cold, fresh Antarctic Surface Water (AASW) is found. Cold winter water is located below AASW with temperatures in the temperature minimum below 0°C. The deep water column is dominated by warm and salty Circumpolar Deep Water (CDW) (Orsi et al., 1999; Reid et al., 1997). Bottom water, with a potential temperature of -0.05°C and salinity of 34.68 (potential density: $\sigma_0$= 27.85) was found at the last two stations of this transect. According to the criteria for the surface water characteristics north and south of the fronts given by Orsi et al. (1995) we passed the SAF between stations PS75/058 and PS75/061, the APF between stations PS75/061 and PS75/063, and the SPF between PS75/63 and PS75/064.

We started the 3rd transect (T3) at station PS75/067 at 64°58.23'S while we were still in the Antarctic Zone (Fig. 3.1.1). The water mass distribution here is very similar to that of the previous transect, but the fronts are clearly oriented along the Mid-Pacific Ridge system and therefore further north. The SPF is located between 58°34.886'S and 57°52.381'S on the north side of the Mid-Pacific Ridge. The APF is located between station PS75/072 (57°33.517'S) and station PS75/074 (56°14.67'S). The northernmost station PS75/074 (56°14.67'S) was located slightly south of the SAF. (The temperature at 400 m is still below 4°C and, the salinity above 300 m is still above 34.2.).

The 5th transect (T5) of our cruise starts at station PS75/088 (164°48.046'W, 68°43.780'S) at the southernmost point of this cruise. We found very low surface salinity values (33.64 at PS75/088) in the homogeneous surface mixed layer with a thickness of ca. 40 m and a strong stratification. The lowest surface salinity values (33.36) were found at station PS75/091.

We passed the SPF between stations PS75/090 and PS75/091, the APF between stations PS75/092 and PS75/094 and the SAF between stations PS75/097 and PS75/096 according to the criteria for the surface water characteristics north and south of the fronts given by Orsi et al. (1995).

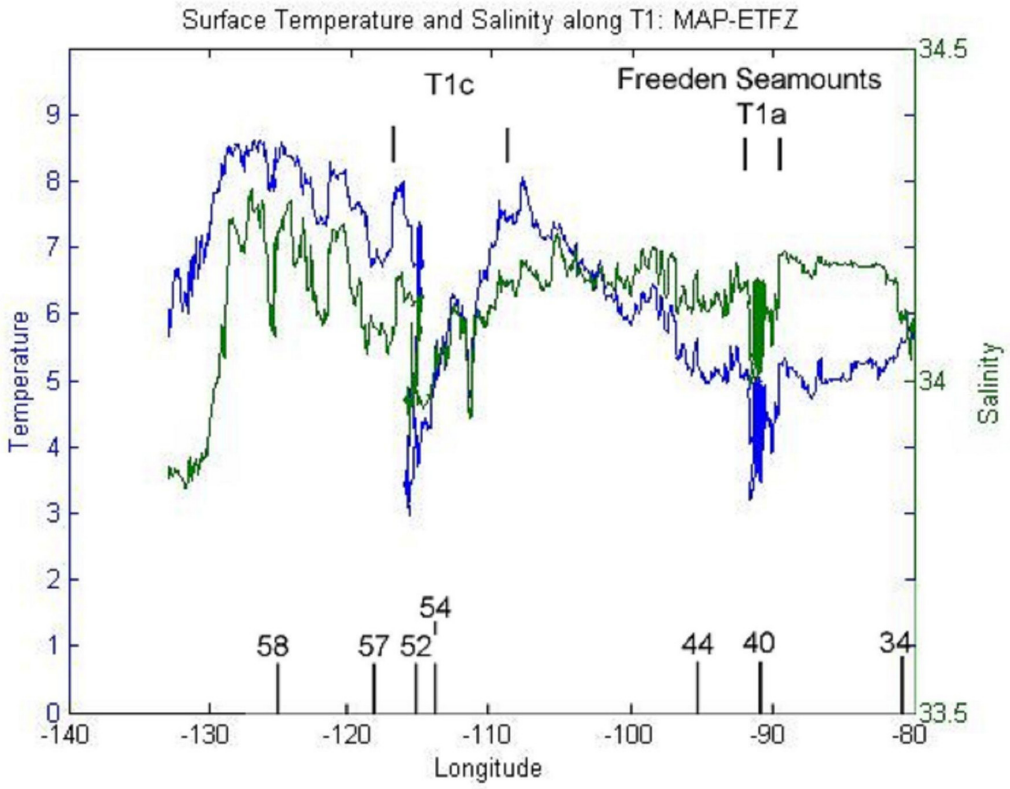


*Fig. 3.1.3: Surface water salinity and temperature along the first transect (T1). The position of stations is given at the bottom.*

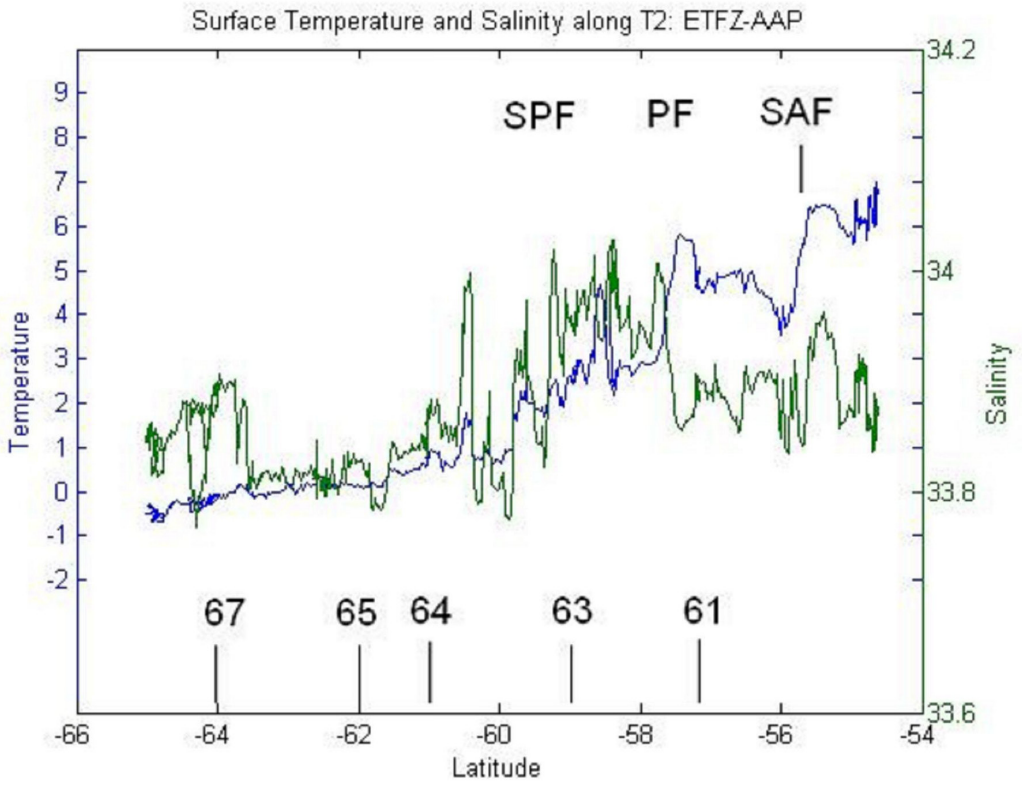


*Fig. 3.1.4: Surface water salinity and temperature along the 2nd transect (140°00'W). The position of stations PS75/061-67 along the transect is noted at the bottom.*

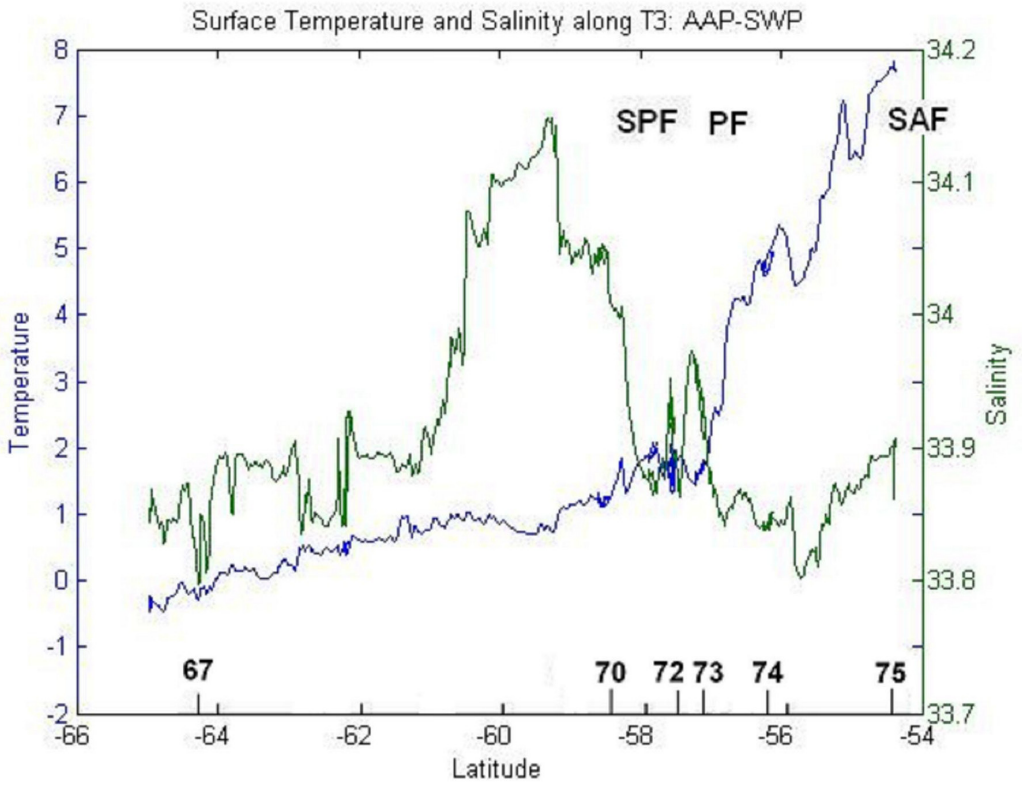


*Fig. 3.1.5: Surface water salinity and temperature along the 3rd transect (150°00'W). The position of stations PS75/067-75 along the transect is noted at the bottom.*

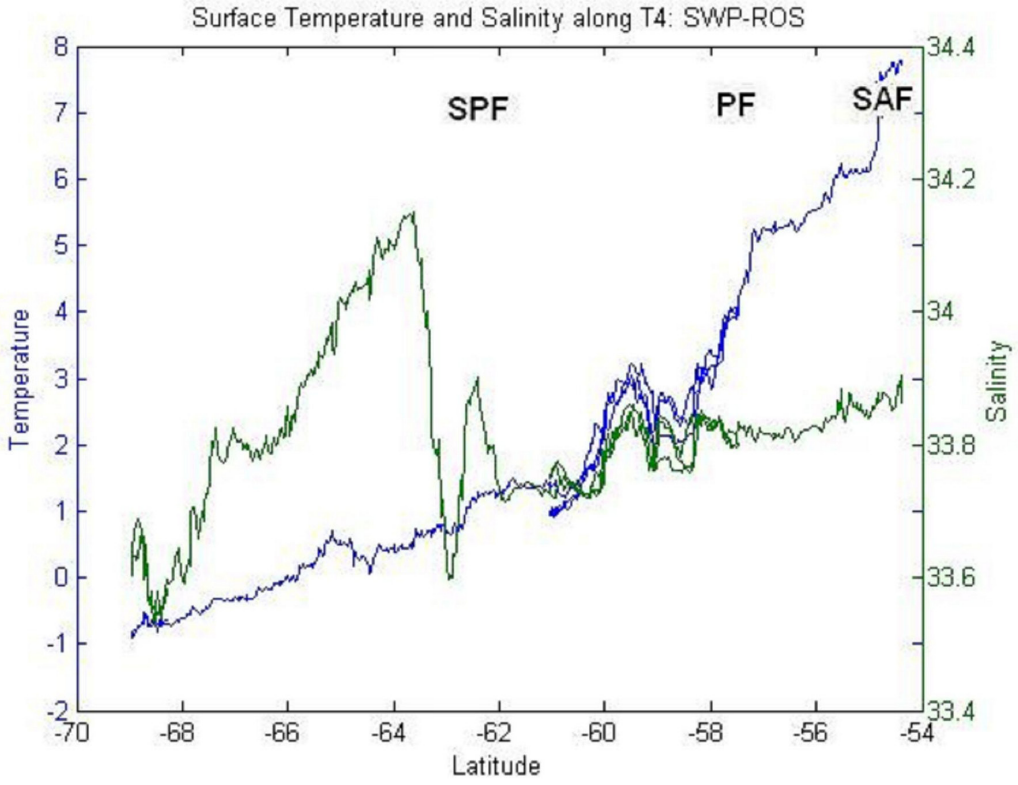


*Fig. 3.1.6: Surface water salinity and temperature along 160°00'W (no CTD transect)*

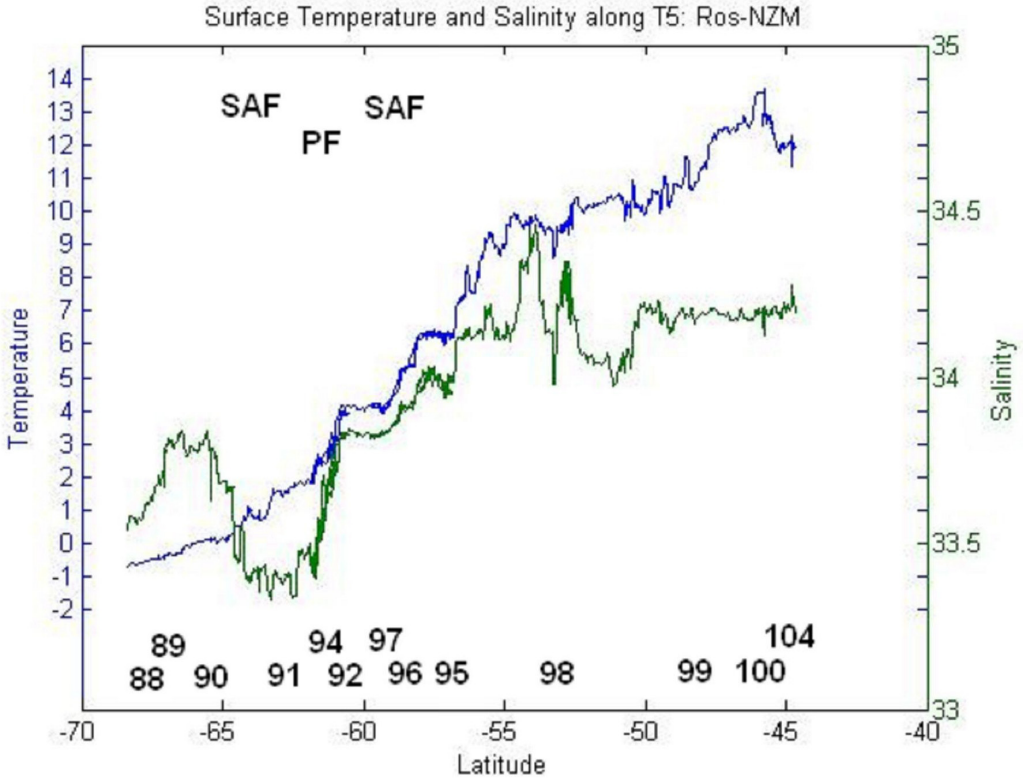


*Fig. 3.1.7: Surface water salinity and temperature along 170°00'W*

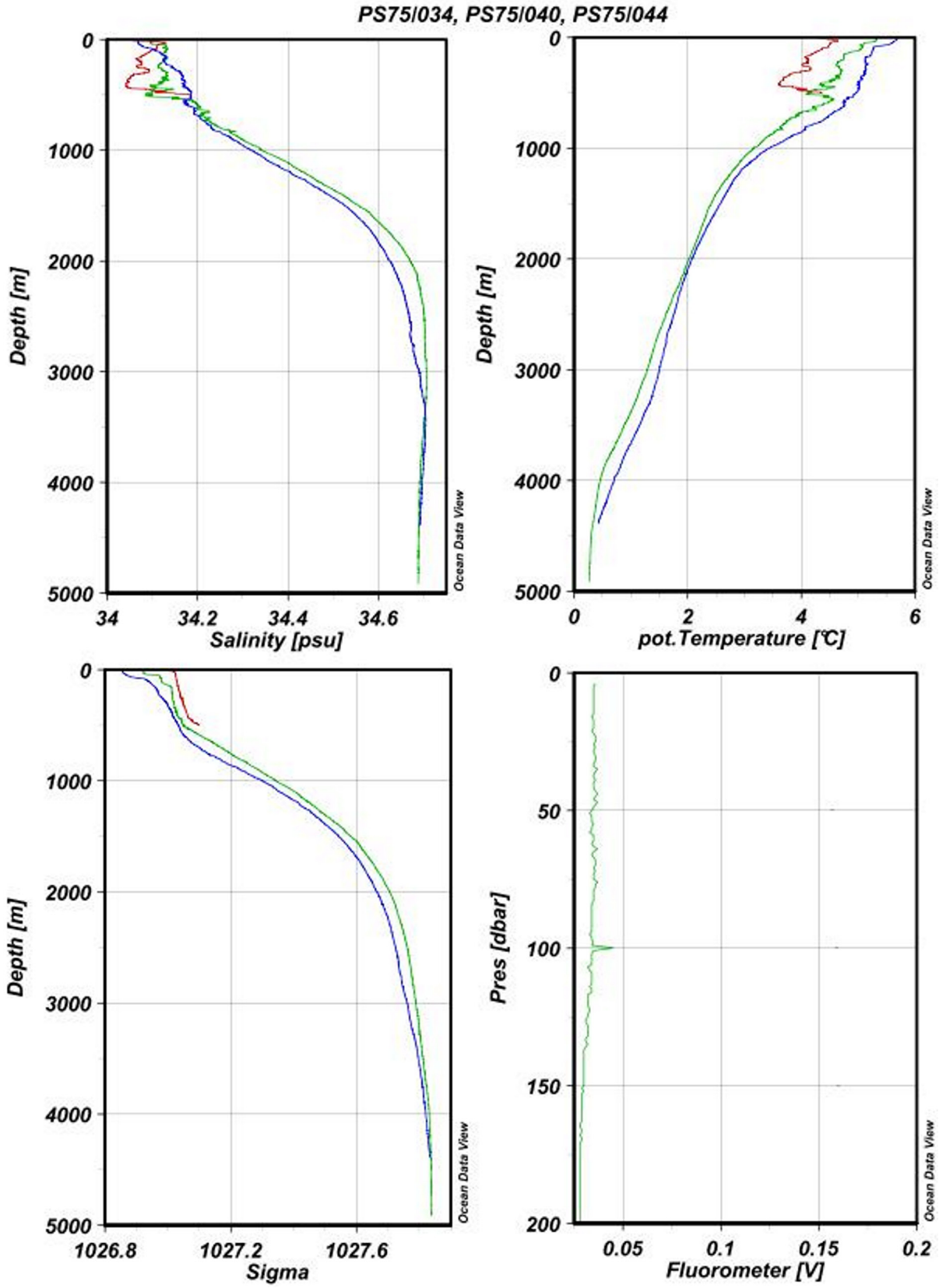


*Fig. 3.1.8: Temperature, salinity, potential density and fluorescence (PS75/034 (blue), PS75/040 (red), PS75/044 (green))*

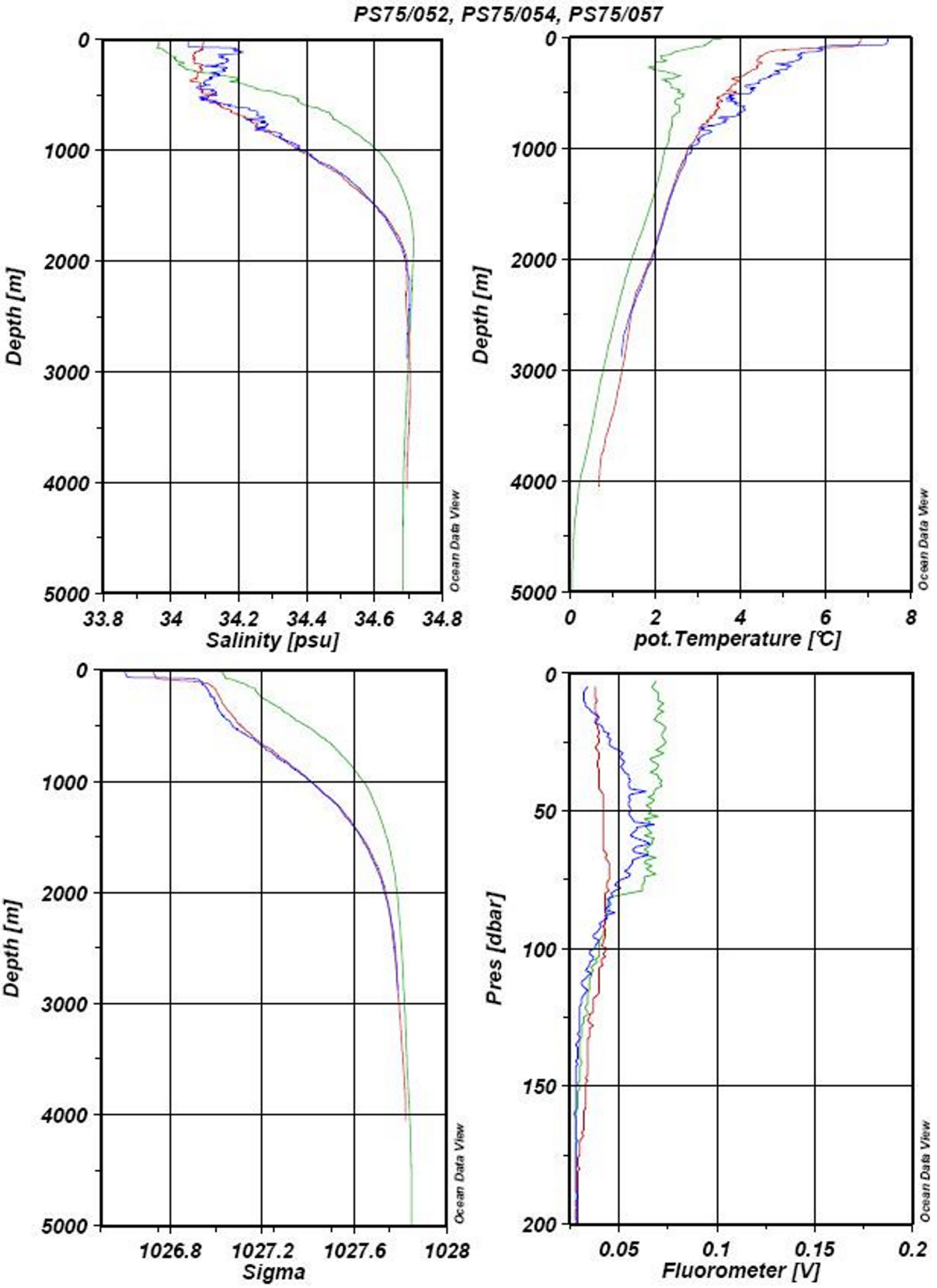


*Fig. 3.1.9: Temperature, salinity, potential density and fluorescence distribution at the first N-S transect (PS75/052 (blue), PS75/054 (red), PS75/057 (green))*

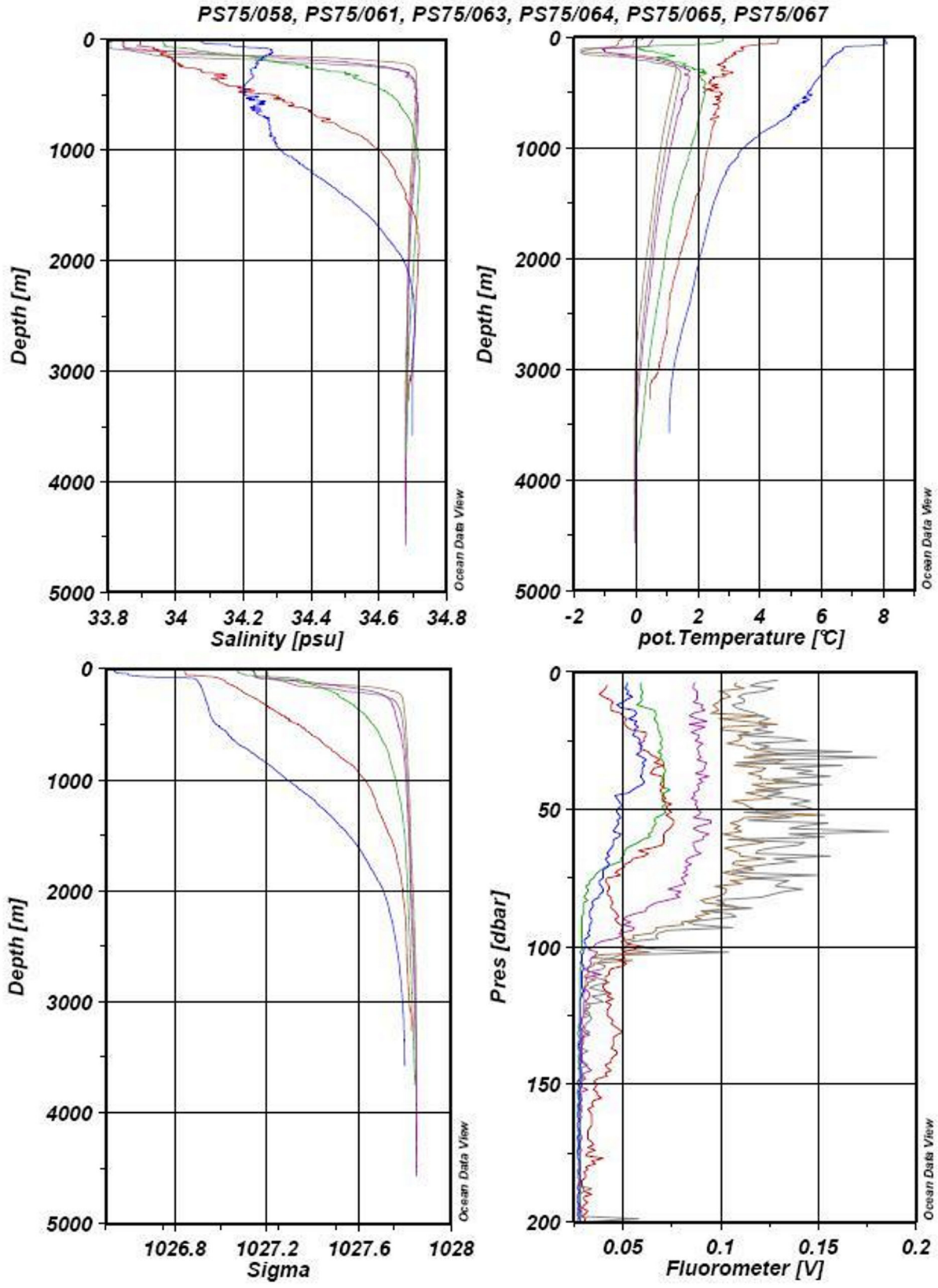


*Fig. 3.1.10: Temperature, salinity, potential density and fluorescence profiles at stations along the 2nd N-S transect (PS75/058 (blue), PS75/061 (red), PS75/063 (green), PS75/064 (magenta), PS75/065 (grey), PS75/067 (brown))*

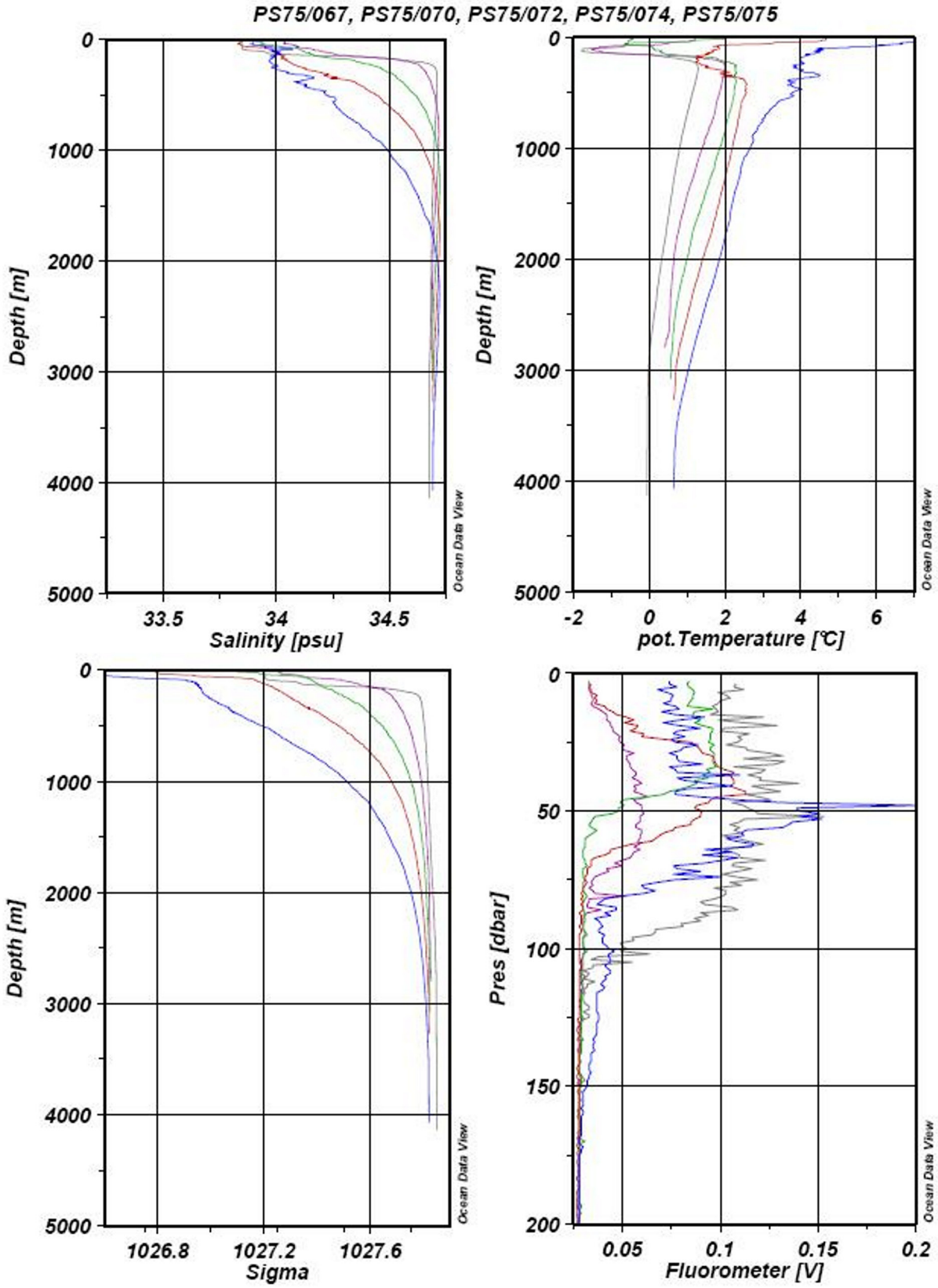


*Fig. 3.1.11: Temperature, salinity, potential density and fluorescence distribution at the 3rd N-S transect (PS75/067 (grey), PS75/070 (purple), PS75/072 (green), PS75/074 (red), PS75/075 (blue)). See above.*

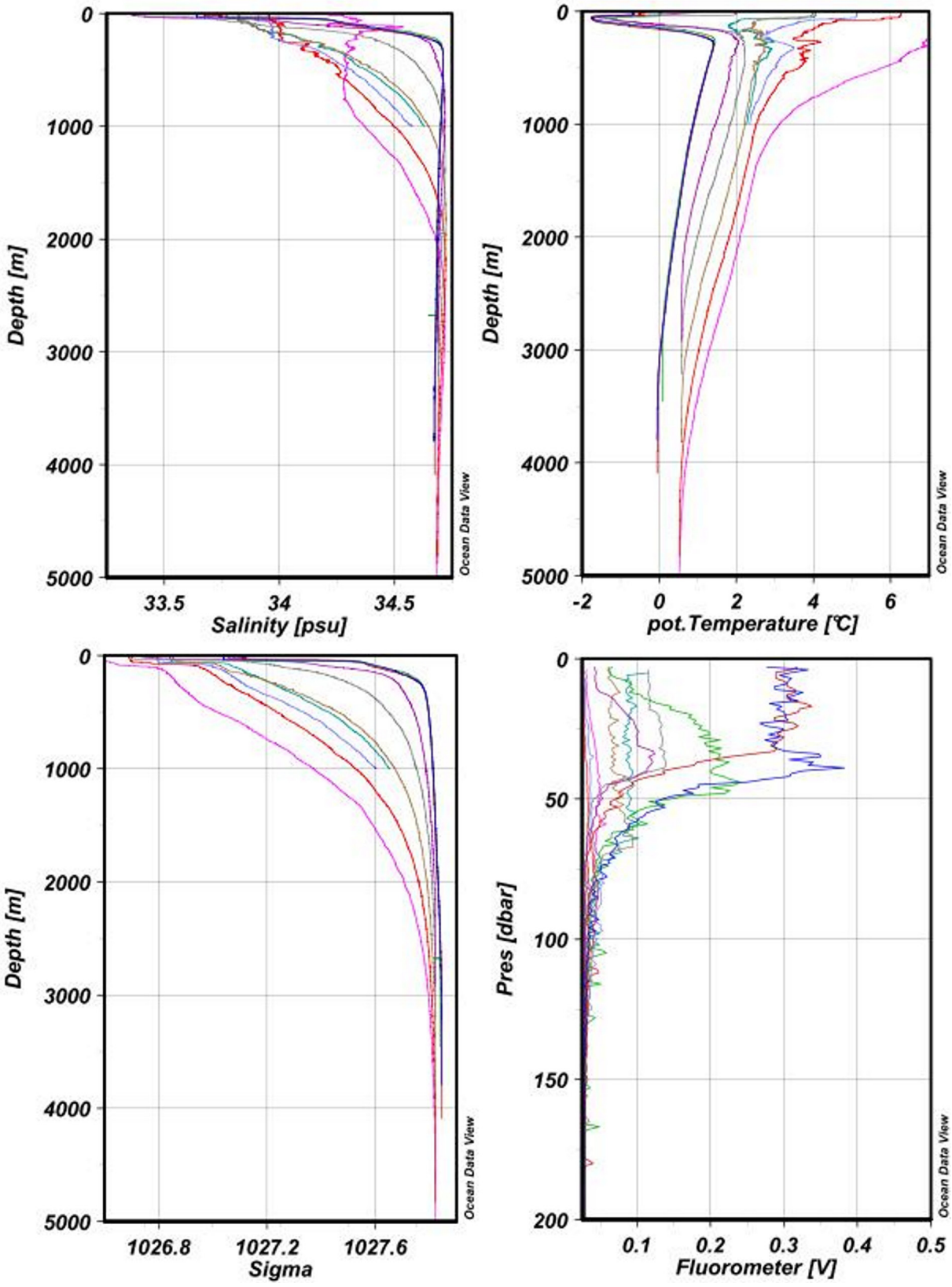


*Fig. 3.1.12: Temperature, salinity, potential density and fluorescence distribution at the first half of the 4th N-S transect (PS75/088 (blue), PS75/089 (red), PS75/090 (green), PS75/091 (purple), PS75/092 (brown), PS75/094 (grey), PS75/095 (light red), PS75/096 (light violet), PS75/097 (turqoise), PS75/098 (pink)).*

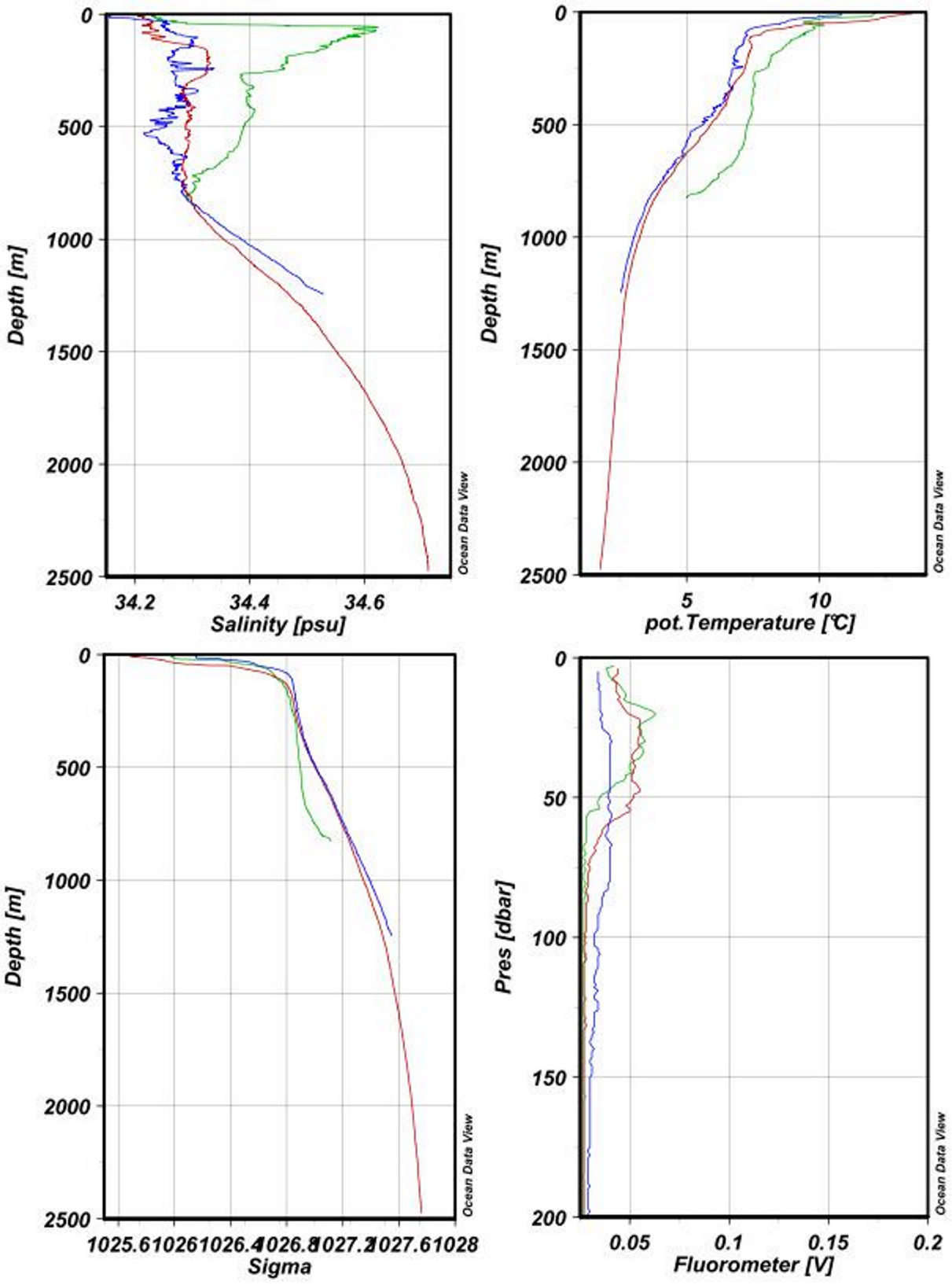


*Fig. 3.1.13: Temperature, salinity, potential density and fluorescence distribution at the second half of the 4th N-S transect (PS75/099 (blue), PS75/0100 (red), PS75/0104 (green)).*

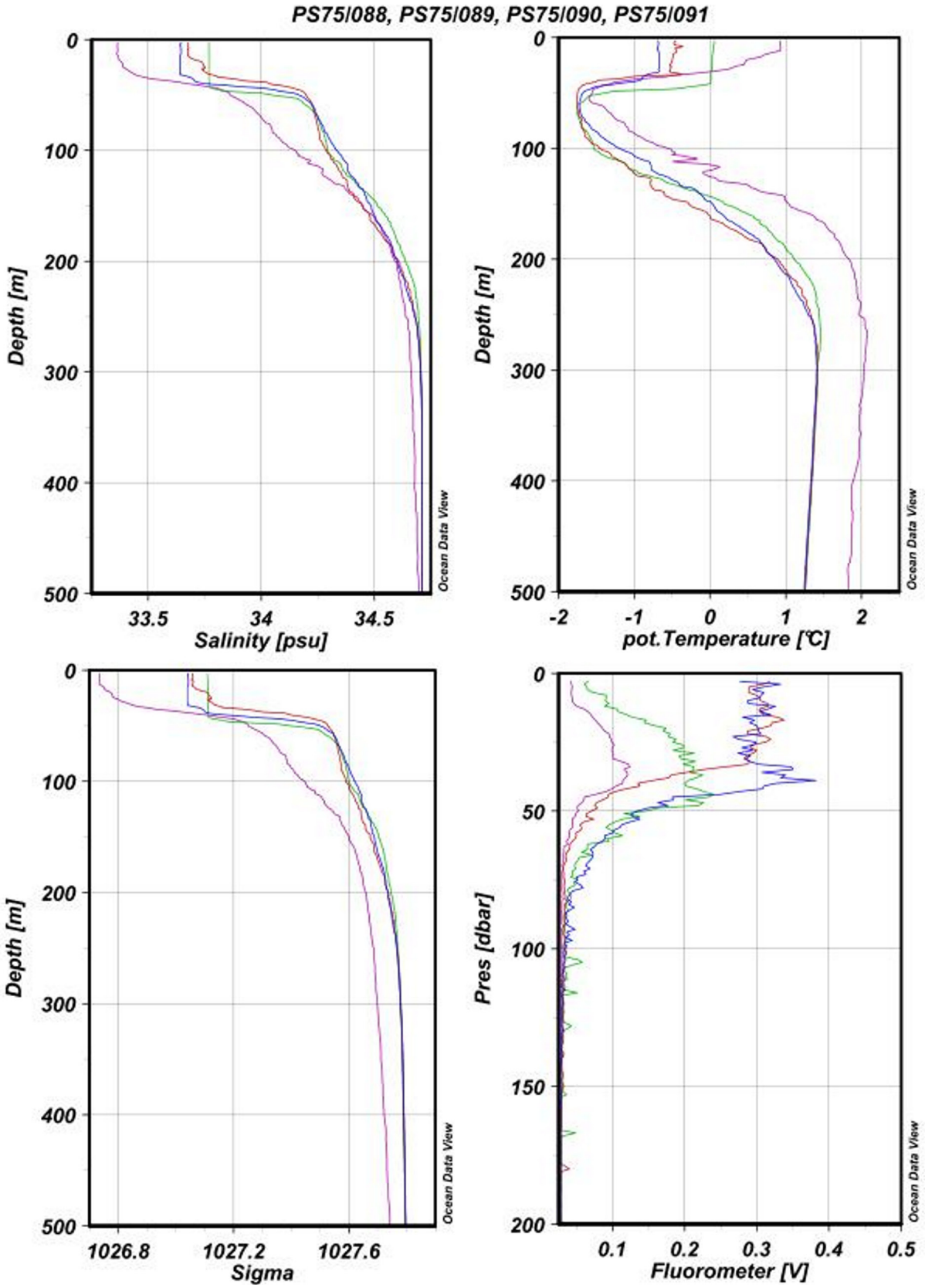


*Fig. 3.1.14: Temperature, salinity, potential density and fluorescence distribution in the first 500 m at four southern stations of the 4th N-S transect (PS75/088 (blue), PS75/089 (red), PS75/090 (green), PS75/091 (magenta)).*

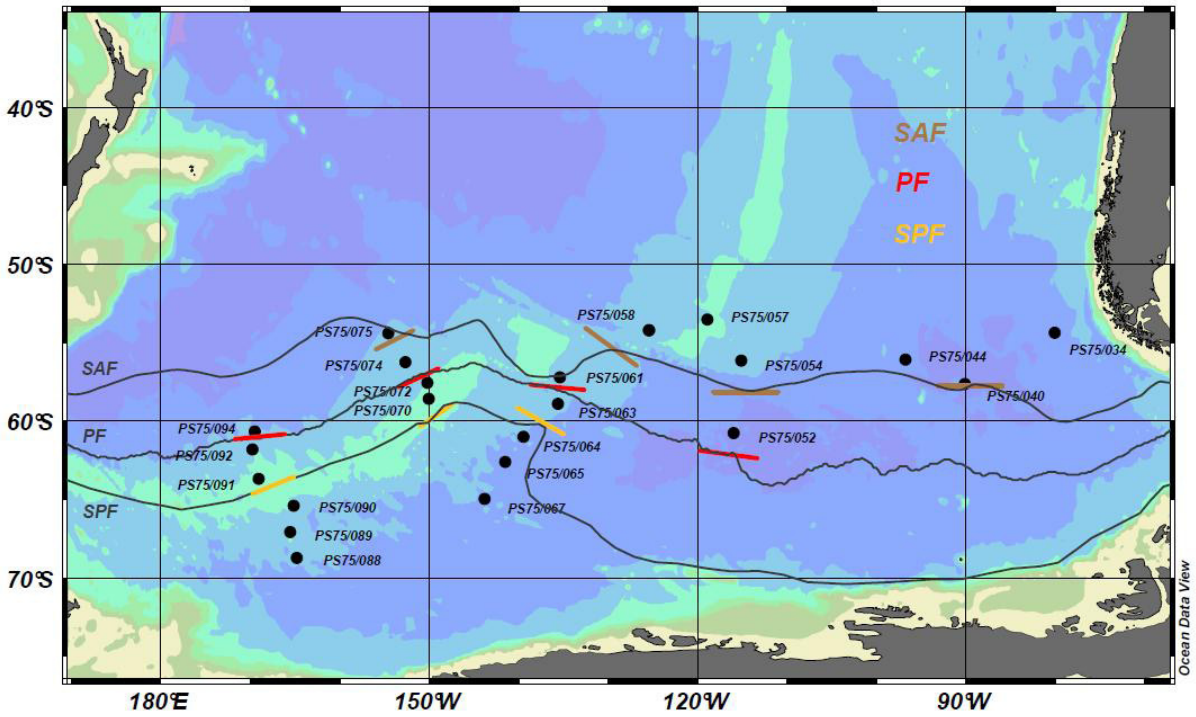


*Fig. 3.1.15: CTD stations during the expedition ANT-XXVI/2, including the Sub Antarctic Front (SAF), Polar Front (PF), Southern Polar Front (SPF) according to Orsi et al. (1995) and the positions of the fronts according to our profile data Orsi et al. (1995)(SAF: brown, PF: red, SPF: yellow).*

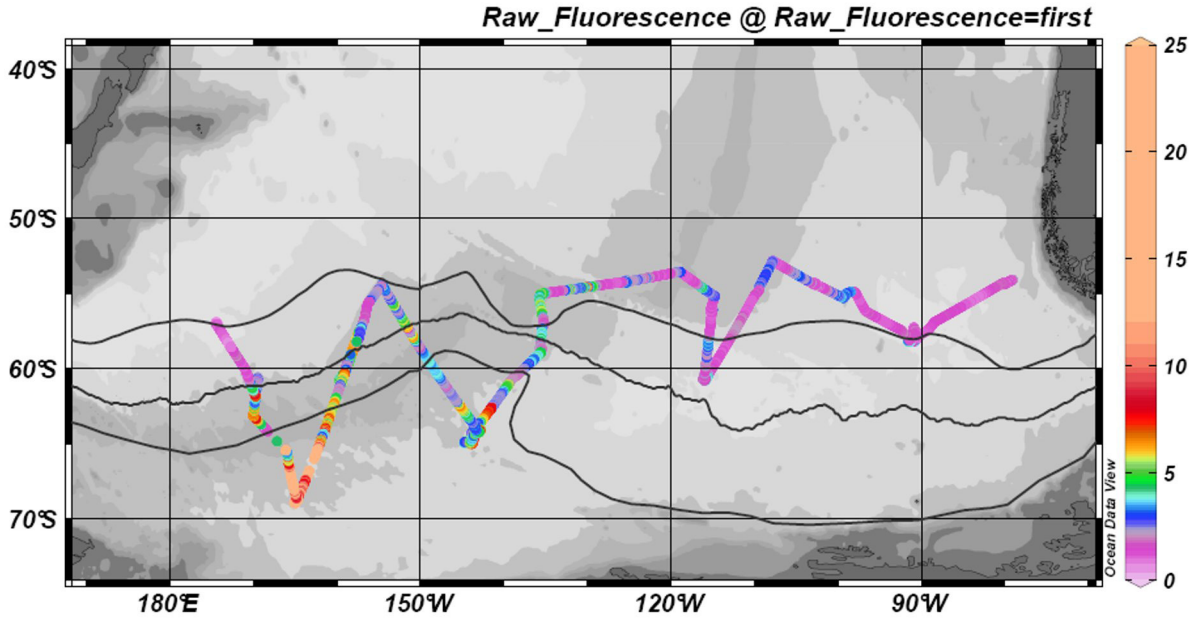


*Fig. 3.1.16: Surface fluorescence along the cruise track with data from the ferrybox*

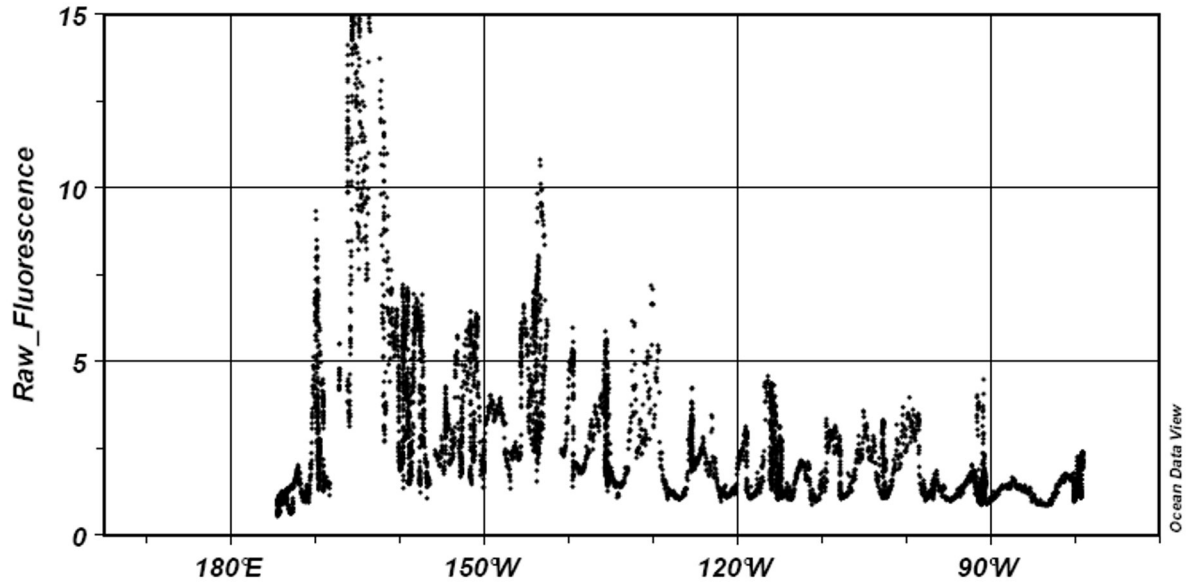


*Fig. 3.1.17: Surface fluorescence plot along the cruise track with data from the ferrybox*

### References

Comiso, J.C., 2003. Large-scale characteristics and variability of the global sea ice cover. In: Thomas, D.N., Diekmann, G.S. (Eds.), Sea Ice: An introduction to its physics, chemistry, biology, and geology, Blackwell, Oxford, pp. 112–142.

Gordon, A.L., Molinelli, E.J., 1986. Southern Ocean Atlas: Rotterdam, Balkema.

Orsi, A.H., Whithworth, T., Nowlin, W.D., 1995. On the meridonial extend and fronts of the Antarctic Circumpolar Current. Deep-Sea Research I, 42, 641-673.

Orsi, A.H., Johnson, G.C., Bullister, J.L., 1999. Circulation, mixing and production of Antarctic Bottom Water. Progress in Oceanography 43, 55–109.

Reid, J.L., 1997. On the total geostrophic circulation of the pacific ocean: flow patterns, tracers and transports. Progress in Oceanography 39, 263-352.

## 3.2 Inorganic carbon system observation

Tae Siek Rhee Korea Polar Research Institute

### Objectives

The Pacific sector of the Southern Ocean plays a crucial role in the global carbon cycle (Daly et al., 2001; Marinov et al., 2006). Atmospheric $CO_2$ is substantially absorbed at the surface and is transported into greater depths with the formation of the Antarctic Intermediate Water (AAIW) off the west coast of the Chile before spreading northwards in the Pacific. In addition, biological activity south of the polar front plays an important role in absorbing atmospheric $CO_2$, which is in turn exported to the deep water. In spite of the significant role of the inorganic carbon cycle of this region, insufficient observations on inorganic carbon distribution and biogeochemical cycles in the interior have been carried out, due largely to remoteness of the area. In this study we will investigate the inorganic carbon system of the water column, its connection to the ecosystem, and the anthropogenic impact in order to fill in the gap of our knowledge

of the carbon cycle in the Southern Ocean and, in particular its the capacity to absorb anthropogenic $CO_2$ emitted to the atmosphere since the industrial revolution.

**Table 3.2.1:** Inorganic carbon and dissolved gas sampling stations and the number of samples collected at the station

| Station ID | Date | Latitude | Longitude | Number of samples | |
|---|---|---|---|---|---|
| | | | | DIC/TA | Dissolved gases |
| PS75/034 | 29/11/2009 | 54°22.111'S | 80°05.187'W | 15 | 15 |
| PS75/040 | 03/12/2009 | 57°38.681'S | 91°08.293W | 11 | 11 |
| PS75/044 | 05/12/2005 | 56°5.188'S | 96°46.559'W | 11 | 6 |
| PS75/052 | 12/12/2009 | 60°45.871'S | 115°57.955'W | 10 | 10 |
| PS75/054 | 13/12/2009 | 56°09.085'S | 115°07.953'W | 11 | 11 |
| PS75/057 | 15/12/2009 | 53°31.782'S | 118°53.782'W | 10 | 10 |
| PS75/058 | 17/12/2009 | 54°12.947'S | 125°26.187'W | 10 | 10 |
| PS75/061 | 20/12/2009 | 57°11.973'S | 135°23.206'W | 11 | 11 |
| PS75/063 | 22/12/2009 | 58°54.223'S | 135°37.242'W | 11 | 11 |
| PS75/064 | 23/12/2009 | 61°01.173'S | 139°27.635'W | 12 | 11 |
| PS75/065 | 24/12/2009 | 62°36.099'S | 141°30.878'W | 12 | 12 |
| PS75/067 | 26/12/2009 | 64°58.252'S | 14348.151'W | 13 | 13 |
| PS75/070 | 27/12/2009 | 58°34.847'S | 150°03.920'W | 10 | 11 |
| PS75/072 | 28/12/2009 | 57°33.517'S | 151°12.922'W | 11 | 11 |
| PS75/074 | 30/12/2009 | 56°14.673'S | 152°39.263'W | 11 | 11 |
| PS75/075 | 31/12/2009 | 54°24.256'S | 154°35.184'W | 12 | 12 |
| PS75/088 | 08/01/2010 | 68°43.780'S | 164°48.046'W | 11 | 11 |
| PS75/089 | 09/01/2010 | 67°04.969'S | 165°32.417'W | 12 | 12 |
| PS75/090 | 10/01/2010 | 65°24.672'S | 166°09.376'W | 12 | 12 |
| PS75/091 | 11/01/2010 | 63°41.650'S | 169°04.485'W | 11 | 11 |
| PS75/092 | 13/01/2010 | 60°40.018'S | 169°30.078'W | 11 | 14 |
| PS75/094 | 14/01/2010 | 61°48.985'S | 169°45.001'W | 12 | 12 |
| PS75/095 | 16/01/2010 | 57°01.148'S | 174°25.785'W | 12 | 12 |
| PS75/096 | 16/01/2010 | 58°32.820'S | 172°41.986'W | 10 | 10 |
| PS75/097 | 17/01/2010 | 59°42.022'S | 171°21.213'W | 10 | 10 |
| PS75/098 | 20/01/2010 | 52°57.688'S | 179°00.834'W | 12 | 12 |
| PS75/099 | 21/01/2010 | 48°15.713'S | 177°16.370'E | 10 | 10 |
| PS75/100 | 22/01/2010 | 45°45.421'S | 177°08.861'E | 10 | 10 |

**Work at sea**

The Inorganic carbon system was investigated by measuring dissolved $CO_2$ ($pCO_2$), dissolved inorganic carbon (DIC), and total alkalinity (TA) in two dimensions: horizontal monitoring along the ship track and vertical profiling at the hydro-casting stations. $pCO_2$ was measured using two different instruments: a non-dispersive infrared (NDIR) detecting system mounted on board by NIOZ (Steven van Heuven) and AWI (Mario Hoppema), and a gas chromatographic system by KOPRI. The former was dedicated to measuring $pCO_2$ underway, whereas the latter was used for both underway measurements and for analyzing discrete samples collected at the hydro-casting stations. Underway measurements of $pCO_2$ were carried out by supplying uncontaminated seawater to a Weiss-type equilibrator, from which headspace air was

delivered to the analytical system. For analyzing $pCO_2$ in the seawater samples collected at the station, a specially designed glass bottle was used to avoid any contamination from the air during sampling and storage. Atmospheric $CO_2$ in the marine boundary layer was analyzed using the same instruments by injecting the ambient air at regular intervals. The systems for analyzing $pCO_2$ were calibrated using a series of standard gases. Dissolved inorganic carbon (DIC) was analyzed by coulometric titration using a system similar to a SOMMA analyzer (Johnson et al., 1993). Total alkalinity (TA) was measured by potentiometric titration with HCl in an open cell. The analytical system for DIC and TA was calibrated twice a day using a certified reference material provided by Andrew Dickson (Scripps Institution of Oceanography). The number of samples collected at the hydro-casting stations is listed in Table 3.2.1.

**Preliminary results**

The NDIR detecting system for $pCO_2$ is equipped with streamlined software that provides the values in situ, while the gas chromatographic technique requires computation to determine $pCO_2$ based on the calibration runs which were carried out between sample runs. In the cruise report we use preliminary data from the NDIR detecting system. In Figure 3.2.1 the difference of $CO_2$ mole fraction ($\Delta xCO_2$) between air and water are shown against time together with seawater temperature and salinity. Positive $\Delta xCO_2$ indicates supersaturation of $CO_2$ with respect to the atmospheric $CO_2$ above the seawater, resulting in the emission of $CO_2$ and negative values for undersaturated surface.

In general, most of the surface seawaters along the cruise track were undersaturated and act as a sink for atmospheric $CO_2$. Supersaturated seawater was encountered four times for short period. Dissolved $CO_2$ concentration seems to be lower to the south of the polar front than to the north. In particular, the lowest value of dissolved $CO_2$ was observed at the southernmost part of the cruise track where biomass in the surface water was high. In fact, biomass content in the eastern part of the cruise track was low (personal communication with Y.N. Kim). Thus, the biological pump seems to be the major factor controlling the strength of atmospheric $CO_2$ sink in this region. This hypothesis should be tested further with results from various parameters relevant to physical and biological processes in the future.

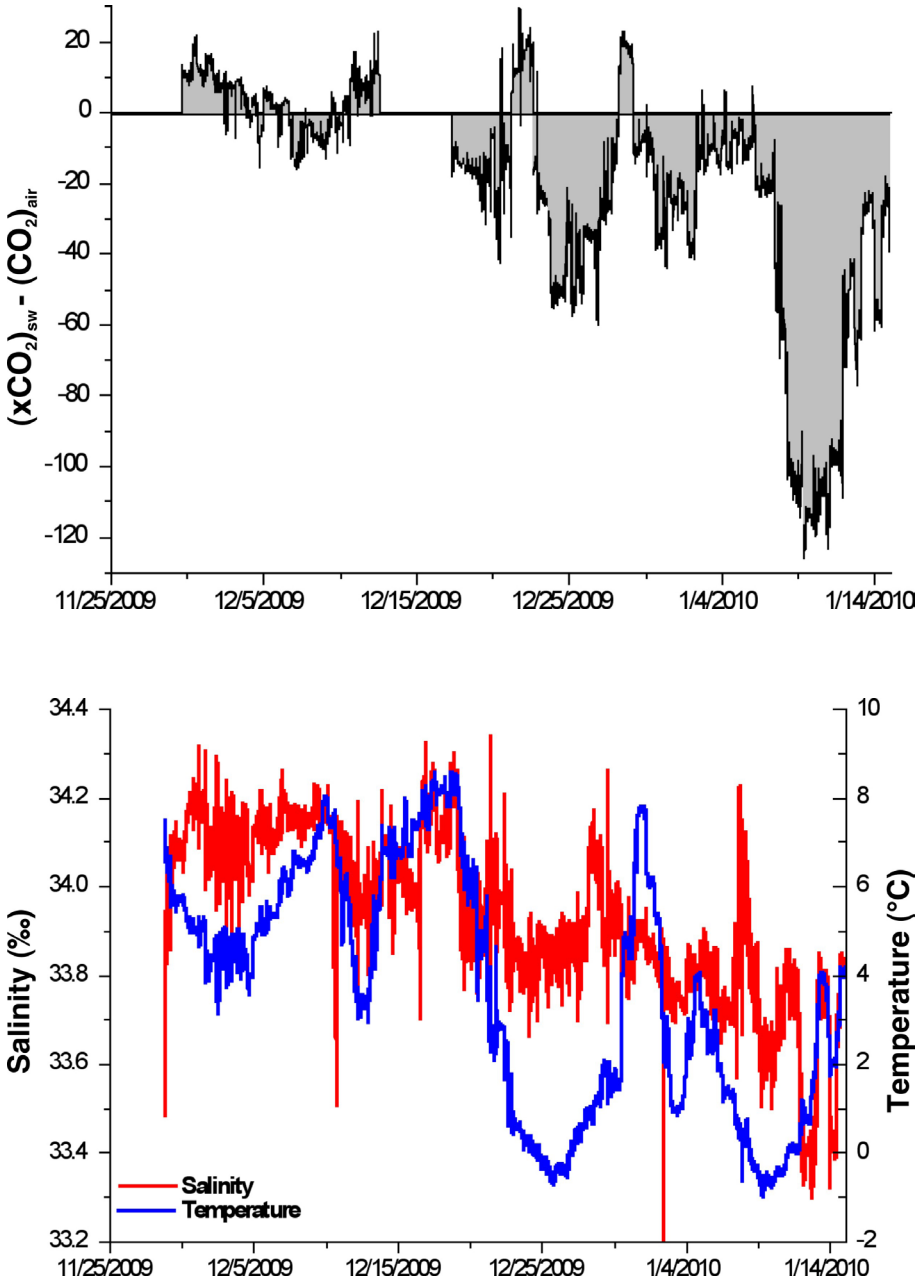


*Figure 3.2.1: $DxCO_2$ (a), seawater temperature and salinity (b) along the cruise track*

## References

Daly, K.L., Smith Jr, W.O., Johnson, G.C., DiTullio, G.R., Jones, D.R., Mordy, C.W., Feely, R.A., Hansell, D.A., Zhang, J.-Z., 2001. Hydrography, nutrients, and carbon pools in the Pacific sector of the Southern Ocean: Implications for carbon flux. Journal of Geophysical Research 106, 7107-7124.

Johnson, K.M., Wills, K.D., Butler, D.B., Johnson, W.K., Wong, C.S., 1993. Coulometric total carbon dioxide analysis for marine studies: Maximizing the performance of an automated gas extraction system and coulometric detector. Marine Chemistry 44, 167-187.

Marinov, I., Gnanadesikan, A., Toggweiler, J.R., Sarmiento, J.L., 2006. The Southern Ocean biogeochemical divide. Nature 441, 964-967.

## 3.3 Non-$CO_2$ greenhouse gases survey

Tae Siek Rhee Korea Polar Research Institute

### Objectives

The present climate change is driven by human activities by which a variety of greenhouse gases in the atmosphere accumulate exponentially. While $CO_2$ is the primary driver, $CH_4$, $N_2O$, $O_3$, and halocarbons altogether are compatible with $CO_2$ in radiative forcing (Forster et al., 2007). CO and $H_2$ are not direct greenhouse gases. However, as reacting with OH radical, which destroys $CH_4$ in the atmosphere and being a precursor of $O_3$ for CO, they contribute to global radiative forcing in an indirect way. The ocean acts as a source of $CH_4$, $N_2O$, $H_2$, and CO (e.g., Bates et al., 1995; Rhee et al., 2009). Microbes produce $CH_4$ and $N_2O$ in the water column while photochemical degradation of organic matters is a major source of CO and likely for $H_2$ in the ocean. However, oceanic source strengths of these gases to the atmospheric budget are not well quantified mainly due to insufficient observations in the ocean. In this expedition, we aim to estimate emission rates of these gases in the Southern Ocean, which shall help to narrow the uncertainty of source strength of the ocean.

### Work at sea

As for inorganic carbon analyses, non-$CO_2$ greenhouse gases ($N_2O$, $CH_4$, $H_2$, and CO) were monitored along the cruise track in the marine boundary layer and in the surface seawater in a regular interval. An air sampling inlet was mounted on the roof of the bridge, ~23 m above the sea surface. The air-sampling inlet was positioned to avoid the flow of contaminated air from ship's exhaust. Air samples were withdrawn through the polyethylene inner-coated aluminum tubing (Dekabon) using a pump. The total length of tubing was ~60 m. The inlet was capped with a funnel to prevent rainwater or sea spray from entering the tubing and a filter pack was mounted at the tip of the inlet to protect the tubing and analyzing system from inhaling solidified sea salts. Uncontaminated surface seawater was supplied at a depth of ~10 m into two Weiss-type equilibrators in which the headspace air equilibrates with dissolved gases in seawater. The headspace air was introduced to gas chromatographic analyzers every hour to determine the dissolved gas concentrations. To keep the analyzing system from being wet, sample and calibration gases were forced to flow through a drying agent ($P_2O_5$). To investigate the distribution of these gases in the water column, aliquots of seawater samples were drawn into glass containers from the Niskin bottles mounted on CTD-rosette. In the laboratory a precisely known volume of "zero air" was injected into the glass containers to make headspace. After equilibration with dissolved gases, the headspace air was taken using a syringe and injected into sample loops equipped in the gas chromatographs. $CH_4$ and $N_2O$ were separated in packed columns, detected by flame ionization detector and electron capture detector, respectively, and quantified by calibrating the gas chromatographic system using a series of calibration gases. CO and $H_2$ were separated in a molecular sieve packed column and detected by Hg vapour which was quantitatively produced by the reaction of CO and $H_2$ with HgO in a hot bed at ~250°C. The gas chromatograph for CO and $H_2$ measurements was calibrated for every sample from the equilibrator or from the marine boundary layer.

### Preliminary results

Over 2,000 samples from the surface seawater and the marine boundary layer along the cruise track and about 250 seawater samples collected at the hydro-casting stations were analyzed for $CH_4$, $N_2O$, $H_2$, and CO on board. The number of samples collected at each station is listed in Table 3.2.1. These raw data will be converted to the values of concentration ashore counting on various parameters observed on board, e.g., temperatures in the air and the surface seawater, salinity, humidity, atmospheric pressure after correcting drifts of the instrumental signal. Underway measurement will provide important information on the estimation of air-sea fluxes of these gases in the Pacific sector of the Southern Ocean. Vertical profiles of the dissolved gases in the water column will give us insight on the biogeochemical cycles occurring in the interior of the ocean. Several observations of these gases showed that the ocean is supersaturated with respect to the atmosphere. Thereby it is expected the same feature during this cruise. However, the magnitude of superasaturation will depend on the net production rates of these gases in the ocean, in particular in the surface mixed layer. According to the preliminary results of fluorescence (Figures 3.1.15 and 3.1.16) and $pCO_2$ (Figure 3.2.1), biological settings would be different along the cruise track, in particular, across the Sub-Antarctic Front, the polar front, and the extension of winter sea-ice. Overall, as this cruise is unique to cover various Polar Regions, the outcome could be beyond what one anticipates based on the previous observations.

### References

Bates, T., Kelly, K.C., Johnson, J.E., Gammon, R.H., 1995. Regional and seasonal variations of in the flux of oceanic carbon monoxide to the atmosphere. Journal of Geophysical Research 100, 23093-23101.

Forster, P., Ramaswamy, V., Artaxo, P., Berntsen, T., Betts, R., Fahey, D.W., Haywood, J., Lean, J., Lowe, D.C., Myhre, G., Nganga, J., Prinn, R., Raga, G., Schulz, M., Van Dorland, R., 2007. Changes in Atmospheric Constituents and in Radiative Forcing. In: Climate Change 2007: The Physical Science Basis. Contribution of Working Group I to the Fourth Assessment Report of the Intergovernmental Panel on Climate Change [Solomon, S., Qin, D., Manning, M., Chen, Z., Marquis, M., Averyt, K.B., Tignor, M., Miller, H.L. (eds.)]. Cambridge University Press, Cambridge, United Kingdom and New York, NY, USA.

Rhee, T.S., Kettle, A.J., Andreae, M.O., 2009. Methane and nitrous oxide emissions from the ocean: A reassessment using basin-wide observations in the Atlantic. Journal of Geophysical Research 114, D12304.

## 3.4. Stable isotope ($\delta^{13}C$, $\delta^{18}O$) signatures of South Pacific water masses

Silke Steph[1,2]
not on board: Ralf Tiedemann[1], Andreas Mackensen[1]

[1]Alfred-Wegener-Institut
[2]Potsdam University

### Objectives

Since different water masses in the global ocean can be distinguished by their carbon and oxygen isotope signatures ($\delta^{13}C$, $\delta^{18}O$), these stable isotope ratios are frequently used as tools for reconstructing past changes in deep and surface ocean circulation. The distribution of $\delta^{13}C$ of dissolved inorganic carbon ($\delta^{13}C_{DIC}$) within the modern ocean is closely linked to nutrient and oxygen contents, and is controlled by the interaction of biological uptake at the sea surface, air/sea gas exchange as well as the

decomposition in deeper water masses with the general circulation of the ocean (e.g. Kroopnick, 1985). $\delta^{18}O$ of modern seawater is mainly a measure of salinity. Although these proxies are generally well established, a broad database for $\delta^{13}C$ and $\delta^{18}O$ of modern water masses is needed to improve our understanding and interpretation of stable isotope records used for paleoceanographic reconstructions. Yet information on the modern $\delta^{13}C$ and $\delta^{18}O$ of seawater in the Pacific sector of the Southern Ocean is still sparse. The objectives of this study are thus 1) to determine the stable isotope signatures of modern deep and intermediate water masses and their variability in different sectors of the Pacific Southern Ocean (specifically Subantarctic Mode Water; Antarctic Intermediate Water, Circumpolar Deep Water, Antarctic Bottom Water), and 2) to document changes in $\delta^{18}O$ and $\delta^{13}C$ of modern surface water samples collected on latitudinal transects across the South Pacific frontal system.

**Work at sea**

Seawater samples for stable isotope measurements were taken from 24 to 11 different water depths (surface to deep) at 27 stations along the cruise track (see chapter 3.1 and Table 3.4.1). Surface samples were generally collected from the ship's pump (11 m water depth), subsurface samples were taken from 12L Niskin bottles of the CTD rosette. Water samples for carbon isotope analysis (d13C of dissolved inorganic carbon (d13CDIC)) were slowly filled into 50 ml glass bottles and 150 µl $HgCl_2$ were added to stop biological activity. Water samples for oxygen isotope analyses ($\delta^{18}O$) were slowly filled into 100 ml glass bottles. Subsequently all sample bottles were sealed with wax in order to avoid fractionation processes, and the glass bottles were stored at a temperature of 4°C and transported to Bremerhaven.

**Preliminary (expected) results**

1) Vertical temperature, salinity and potential density profiles indicate that the CTD casts along the ANT-XXVI/2 cruise track sampled Antarctic Bottom Water, Circumpolar Deep Water, Antarctic Intermediate Water and Subantarctic Mode Water at several hydrographic stations (see Chapter 3.1 for details). Vertical stable isotope profiles combined with CTD data will thus provide valuable information on variations in $\delta^{13}C$ and $\delta^{18}O$ with respect to the water mass distribution in different hydrographic areas of the Pacific Southern Ocean.

2) Water samples collected at CTD stations along North-South transects (see Chapter 3.1 for details) allow for a detailed characterization of changes in surface water $\delta^{13}C$ and $\delta^{18}O$ signatures across the Southern Pacific frontal system during austral summer.

**Tab. 3.4.1:** Seawater samples for stable isotope measurements

| Station No. | Latitude (deg/min) | Longitude (deg/min) | Sampling Depths (m) |
|---|---|---|---|
| PS75/034-3 | 54°22.115'S | 80°5.220'W | Bottom (4390)/4001/3257/2001/1500/1000/800/500/300/200/150/120/91/75/61/40/20/10.5 |
| PS75/044-1 | 56°5.135'S | 96°46.781'W | Bottom (4912)/4000/3000/2000/1000/500/100/40/10 |
| PS75/052-1 | 60°45.871'S | 115°57.955'W | Bottom (5083)/4000/3000/2000/1000/500/100/60/40/22/11 (ships pump) |
| PS75/054-2 | 56°9.085'S | 115°7.953'W | Bottom (4050)/3000/2300/2000/1500/1000/500/100/60/40/20/11 (ships pump) |
| PS75/057-1 | 53°31.782'S | 118°53.782'W | Bottom (2873)/2000/1500/1000/500/100/60/40/20/11 (ships pump) |
| PS75/058-1 | 54°12.947'S | 125°26.187'W | Bottom (3573)/2500/2000/1000/500/100/60/40/20/10 |
| PS75/061-1 | 57°11.973'S | 135°23.206'W | Bottom (3266)/2500/1800/1000/500/100/55/40/20/11 (ships pump) |
| PS75/063-3 | 58°54.223'S | 135°37.242'W | Bottom (3747)/3000/2000/1200/500/150/100/60/40/20/11 (ships pump) |
| PS75/064-3 | 61°1.173'S | 139°27.635'W | Bottom (4571)/4000/3000/2000/800/500/150/100/60/40/20/11 (ships pump) |
| PS75/065-3 | 62°36.099'S | 141°30.878'W | Bottom (4464)/4000/3000/2000/1000/500/150/100/60/40/20/11 (ships pump) |
| PS75/067-3 | 64°58.252'S | 143°48.151'W | Bottom (4133)/3000/2000/1000/500/350/150/100/60/40/20/11 (ships pump) |
| PS75/070-3 | 58°34.847'S | 150°3.920'W | Bottom (2796)/2000/1000/850/500/150/100/55/40/20/11(ships pump) |
| PS75/072-1 | 57°33.517'S | 151°12.922'W | Bottom (3073)/2000/1300/1000/500/150/100/60/35/20/11 (ships pump) |
| PS75/074-2 | 56°14.673'S | 152°39.263'W | Bottom (3265)/2500/1700/1000/500/150/100/60/40/20/11 (ships pump) |
| PS75/075-1 | 54°24.256'S | 154°35.184'W | Bottom (4065)/3500/3000/2200/1000/500/150/100/65/50/20/11 (ships pump) |
| PS75/088-1 | 68°43.780'S | 164°48.046'W | Bottom (3795)/3000/2000/1000/500/150/100/60/40/20/11 (ships pump) |
| PS75/089-1 | 67°4.969'S | 165°32.417'W | Bottom (4090)/3000/2000/1000/500/300/150/100/60/40/20/11 (ships pump) |
| PS75/090-1 | 65°24.672'S | 166°9.376'W | Bottom (3458)/3000/2000/1000/500/60/40/20/11 (ships pump) |
| PS75/091-1 | 63°41.650'S | 169°4.485'W | Bottom (2920)/2000/1000/500/270/150/100/60/35/20/11(ships pump) |
| PS75/092-4 | 60°40.018'S | 169°30.078'W | Bottom (3812)/3000/1800/1000/500/150/100/60/40/20/11 (ships pump) |

| | | | |
|---|---|---|---|
| PS75/094-6 | 61°48.985'S | 169°45.001'W | Bottom (3212)/3000/2000/1500/1000/500/150/100/60/35/20/10 |
| PS75/095-1 | 57°1.148'S | 174°25.785'W | Bottom (4822)/4000/3000/2000/1000/500/150/80/40/20/11 (ships pump) |
| PS75/096-1 | 58°32.820'S | 172°41.986'W | 1000/800/500/150/100/80/60/40/20/10 |
| PS75/098-1 | 52°57.688'S | 179°0.834'W | Bottom (5162)/4000/2800/2000/1000/600/150/100/60/45/20/11 (ships pump) |
| PS75/099-5 | 48°15.713'S | 177°16.370'W | Bottom (1245)/800/500/300/150/100/60/40/20/10 |
| PS75/100-5 | 45°45.421'S | 177°8.861'W | Bottom (2475)/2000/1000/500/150/100/60/40/20/11 |
| PS75/104-3 | 44°46.147'S | 174°31.503'W | Bottom (824)/700/500/400/300/250/150/100/60/40/10 |

## References

Kroopnick, P., 1985. The distribution of carbon-13 in the world oceans. Deep Sea Research 32, 57-84.

## 3.5 Distribution of neodymium isotopes in the Pacific sector of the Southern Ocean

Katharina Pahnke University of Hawaii

### Objectives

The objectives of this study are 1) to determine the neodymium isotopic composition ($^{143}Nd/^{144}Nd$, expressed in $\varepsilon_{Nd}$ notation) of South Pacific water masses, 2) to assess the modern contributions of Antarctica, South America and New Zealand to the seawater Nd isotope signal of the South Pacific, and 3) to trace the export of Antarctic Bottom Water (AABW) formed in the Ross Sea into the South Pacific both at present (using seawater $\varepsilon_{Nd}$) and in the past (using terrigenous Nd and Sr isotope ratios).

Neodymium isotope ratios in the ocean and marine and terrigneous sediments have been recognized as an important tracer for the origin of terrigenous material as well as the flow paths of water masses in the ocean (e.g., GEOTRACES Science Plan, 2006). However, many questions remain regarding the sources, sinks and the internal cycling of dissolved Nd in the ocean. Detailed mapping of the distribution of Nd isotopes in the ocean is therefore required. ANT-XXVI/2 provides a unique opportunity to study dissolved Nd isotope ratios in the South Pacific.

The Nd isotopic signature of the Ross Sea region is distinct from those in other areas of Antarctica and surrounding continents (South America, New Zealand, Australia) (e.g., van de Flierdt et al., 2006; Hemming et al., 2007; Roy et al., 2007). Therefore, the hypothesis is that this isotopic 'fingerprint' should be imprinted on seawater originating in the Ross Sea i.e., Antarctic Bottom Water (AABW) formed in the Ross Sea (RSBW). Moreover, the terrigenous fine fraction transported by RSWB with its distinct Nd and Sr isotopic signature, should be traceable along the RSBW flow path. The analysis of dissolved Nd isotope ratios in bottom waters and the Nd and Sr isotope ratios in surface sediments along the cruise track should allow tracing of RSBW from the Ross

Sea into the southeast Pacific. The terrigenous Nd and Sr isotope ratios in sediment cores from >4,000 m water depths will afford reconstructing past AABW flow in the South Pacific.

Additionally, Nd isotope ratios in the authigenic Fe-Mn oxide fraction of marine sediments can be used to reconstruct past seawater $\varepsilon_{Nd}$, and due to the distinct $\varepsilon_{Nd}$ signature of different water masses is then used to reconstruct past circulation changes. The analysis of authigenic $\varepsilon_{Nd}$ in surface sediments along the cruise track (multi-corer samples) will add important information on the use of this proxy in the South Pacific.

**Tab. 3.5.1:** Stations sampled for Nd isotope analysis in seawater.

| Station No. | Latitude [deg/min] | Longitude [deg/min] | deepest sample [m] | number of samples |
|---|---|---|---|---|
| **PS75/034-3** | 54°22.111'S | 80°05.187'W | 4390 | 8 |
| **PS75/044-1** | 56°5.188'S | 96°46.559'W | 4912 | 7 |
| **PS75/052-1** | 60°45.871'S | 115°57.955'W | 5083 | 7 |
| **PS75/057-1** | 53°31.782'S | 118°53.782'W | 2878 | 7 |
| **PS75/065-3** | 62°36.099'S | 141°30.878'W | 4466 | 7 |
| **PS75/067-3** | 64°58.252'S | 143°48.151'W | 4135 | 1 |
| **PS75/088-1** | 68°43.780'S | 164°48.046'W | 3795 | 6 |
| **PS75/089-1** | 67°04.969'S | 165°32.417'W | 4090 | 7 |
| **PS75/095-1** | 57°01.148'S | 174°25.785'W | 4822 | 8 |
| **PS75/098-1** | 52°57.688´S | 179°00.834´W | 5188 | 7 |
| **PS75/100-5** | 45°45.421´S | 177°08.861´E | 2497 | 5 |

**Work at sea**

Seawater samples were taken at 11 stations along the cruise track from 1 - 8 different water depths (surface to deep) at each station (Chapter 3.1 and Table 3.5.1). All deep samples were taken from 12 L Niskin bottles of the CTD rosette, while additional surface samples were taken from the ship's membrane pump. Samples were filtered directly from the Niskin bottles using AcroPak 500 filter cartridges (0.8/0.45 μm pore size). Each filter cartridge was dedicated to one specific depth and used at each station. From each water depth, 7 - 10 L of seawater were filtered into 10 L LDPE cubitainers for Nd isotope ratios, and 0.5 L were filtered into LDPE bottles for Nd and rare-earth element (REE) concentrations. The samples for Nd and REE concentrations were acidified to pH = 2 and those for Nd isotope analyses to pH = 3.5 using quartz-distilled 6N hydrochloric acid. The latter samples were preconcentrated on board using $C_{18}$ SepPak cartridges loaded with a REE complexant (HDEHP/HMEHP) (Shabani et al., 1992; Lacan and Jeandel, 2001). In order to avoid contamination, all acidifications and preconcentrations were carried out under a temporary 'bubble' that was set up in one of the wet labs on the *Polarstern* using plastic sheets.

**Preliminary (expected) results**

The CTD temperature, salinity and potential density profiles show that AABW was penetrated and sampled at stations PS75/052, PS75/065, PS75/067, PS75/088, PS75/089, PS75/095, and PS75/098 (Chapter 3.1). Antarctic Intermediate Water

(AAIW), with a core potential density of $\sigma_0$ = 27.2 (Piola and Georgi, 1982; Talley, 1996), was sampled at stations PS75/034, PS75/044, PS75/057, PS75/098 and PS75/100 at water depths of 600-800 m (salinity around 34.2-34.3, Chapter 3.1).

Stations PS75/052, PS75/065, PS75/067, PS75/088, and PS75/089 are located south of the Pacific-Antarctic Ridge and east of the East-Pacific Rise and therefore in the flow path of RSBW. Stations PS75/095, and PS75/098 are located north of the ridge and should therefore sample AABW formed along the Adélie Coast and in the Weddell Sea. If AABW carries the $\varepsilon_{Nd}$ signatures of its source regions, the deepest samples from these two sets of stations should show contrasting $\varepsilon_{Nd}$ values and should therefore allow the tracing of these water masses away from their source region.

## References

GEOTRACES Planning Group (2006). GEOTRACES Science Plan, Scientific Committee on Oceanic Research, Baltimore, Maryland.

Hemming, S.R., van de Flierdt, T., Goldstein, S.L., Franzese, A.M., Roy, M., Gastineau, G., Landrot, G., 2007. Strontium isotope tracing of terrigenous sediment dispersal in the Antarctic Circumpolar Current: Implications for constraining frontal positions Geochemistry Geophyscs Geosystems, 8, Q06N13, doi:10.1029/2006GC001441.

Lacan, F., Jeandel, C., 2001. Tracing Papua New Guinea imprint on the central Equatorial Pacific Ocean using neodymium isotopic compositions and Rare Earth Element patterns, Earth and Planetary Science Letters, 186(3-4), 497-512.

Piola, A.R., Georgi, D.T., 1982. Circumpolar properties of Antarctic Intermediate Water and Subantarctic Mode Water, Deep-Sea Research, 29, 687-711.

Roy, M., van de Flierdt, T., Hemming, S.R., Goldstein, S.L., 2007. $^{40}Ar/^{39}Ar$ ages of hornblende grains and bulk Sm/Nd isotopes of circum-Antarctic glacio-marine sediments: Implications for sediment provenance in the southern ocean, Chemical Geology, 244, 507-519.

Shabani, M.B., Akagi, T., Masuda, A., 1992. Preconcentration of trace rare-earth elements in seawater by complexation with bis(2-ethylhexyl) hydrogen phosphate and 2-ethylhexyl dihydrogen phosphate adsorbed on a C18 cartridge and determination by inductively coupled plasma mass-spectrometry, Analytical Chemistry, 64, 737-743.

Talley, L.D., 1996. Antarctic Intermediate Water in the South Atlantic, in: The South Atlantic: Present and Past Circulation, Wefer, G., Berger, W.H., Siedler, G., Webb, D. J. (eds.), pp. 219-238.

van de Flierdt, T., Hemming, S.R., Goldstein, S.J., Abouchami, W., 2006. Radiogenic isotope fingerprint of Wilkes Land-Adélie Coast Bottom Water in the circum-Antarctic Ocean, Geophysical Research Letters, 33.

# 4. CARBON CYCLE, PRODUCTIVITY, MICRO–PLANKTON AND BIOMARKER STUDIES

## 4.1 Nutrients and productivity

Oliver Esper, Ute Bock, Daniela Nowka Alfred-Wegener-Institut

### Objectives

Biological and physical processes in the Southern Ocean play a crucial role in initiating and shaping climatic changes. The Southern Ocean is the largest High-Nutrient-Low Chlorophyll (HNCL) area in the world and thus has the potential to become a major $CO_2$ sink when the efficiency of the biological pump increased as it has been postulated for glacial periods. Furthermore, air-sea interactions in the Southern Ocean have a strong impact on the global ocean circulation loop and are supposed to be important in setting the rate of global overturning. The hard parts of siliceous, calcareous and organic walled microorganisms (diatoms, radiolarians, planktic foraminifers, calcareous nannoplankton, dinoflagellates) are crucial tools to reconstruct past environmental conditions in the Southern Ocean by using paleobiological and geochemical methods. For the interpretation of the paleobiological and geochemical data obtained from the microfossils and the understanding of the complex mechanisms ecological information (latitudinal distribution and depth habitat) of living species in combination with hydrographic data, information on the concentration and distribution of chlorophyll and nutrients (nitrate, phosphate, trace elements like iron) in the water column are needed.

### Work at sea

To gain insight into the hydrographic structure of the water column of the Pacific sector of the Southern Ocean, *in-situ* measurements of hydrographic variables had been carried out with a CTD probe (see Chapter 3.1). These measurements were accompanied by simultaneous water sampling with a water collector (rosette) for the determination of chlorophyll *a* and dissolved nutrient (nitrate, phosphate, silicon) concentrations. In addition to the CTD probe measuring instruments the CTD device consists of a 24-bottle water collector, the so-called rosette. Each of the 24 10-liter bottles of the rosette can be closed separately via the data wire of the winch cable. Before deployment, all the bottles have to be opened; the closing mechanism of each bottle has to be connected with the release-switches of the central controlling device. When triggered via computer command from the board unit a magnetic switch releases strong rubber bands, which close the selected bottle immediately. When all bottles are closed/filled and the device is back on deck, small vents on top and bottom of each bottle allow for an easy access to the collected water. These vents should be closed during the deployment. Release of the bottles took place only during the up-casts after the CTD and rosette had reached its lower most position in the water colum and was heaved up again.

To measure the nutrient concentration at different water depth, 50 ml water samples were taken at 29 stations along specific depth profiles (Table 4.1.1), treated with $HgCl_2$ solution to conserve the samples and were stored at 4°C. In addition, 2 l water samples were taken from selected depths (Tab. 4.1.2) of each CTD + rosette deployment for chlorophyll *a* measurements. The samples were filtered with 25 mm glass microfibre filters (GF/F); the filters were afterwards packed in aluminium foil and stored at –20°C. Once the filters are analyzed for chlorophyll *a* concentration, a calibration for the fluorescence data measured by the CTD can be made. At some stations (see Tables 4.1.1. and 4.1.2.) water from the ships water pump instead of the uppermost CTD depth was taken.

**Tab. 4.1.1:** Nutrient samples (50 ml) from CTD casts at specific water depths (meter)

| **Station** | **1** | **2** | **3** | **4** | **5** | **6** | **7** | **8** | **9** | **10** | **11** | **12** |
|---|---|---|---|---|---|---|---|---|---|---|---|---|
| **034-3** | 4390 | 4001 | 3257 | 2001 | 1500 | 1000 | 800 | 500 | 300 | 200 | 150 | 120 |
| | **13** | **14** | **15** | **16** | **17** | **18** | **19** | **20** | **21** | **22** | **23** | **24** |
| | 91 | 91 | 75 | 75 | 61 | 61 | 40 | 40 | 20 | 20 | 10.5 | 10.5 |
| **Station** | **1** | **2** | **3** | **4** | **5** | **6** | **7** | **8** | **9** | **10** | **11** | **12** |
| **040-2** | 500 | 400 | 300 | 200 | 148 | 100 | 75 | 59 | 40 | 18 | 10 | |
| **044-1** | 4912 | 4000 | 3000 | 2000 | 1000 | 500 | 100 | 60 | 40 | 20 | 10 | |
| **052-2** | 5083 | 4000 | 3000 | 1800 | 1000 | 500 | 100 | 60 | 40 | 22 | 11 | |
| **054-2** | 4050 | 3000 | 2300 | 2000 | 1500 | 1000 | 500 | 100 | 60 | 40 | 20 | 11* |
| **057-1** | 2873 | 2000 | 1500 | 1000 | 500 | 100 | 60 | 40 | 20 | 11 | | |
| **058-1** | 3573 | 2500 | 2000 | 1000 | 500 | 100 | 60 | 40 | 20 | 10 | | |
| **061-1** | 3266 | 2500 | 1800 | 1000 | 500 | 150 | 100 | 55 | 40 | 20 | 11 | |
| **063-3** | 3747 | 3000 | 2000 | 1200 | 500 | 150 | 100 | 60 | 40 | 20 | 11 | |
| **064-3** | 4571 | 4000 | 3000 | 2000 | 800 | 500 | 150 | 100 | 60 | 40 | 20 | 11* |
| **065-3** | 4464 | 4000 | 3000 | 2000 | 1000 | 500 | 150 | 100 | 60 | 40 | 20 | 11* |
| **067-3** | 4133 | 3000 | 2000 | 1000 | 500 | 350 | 150 | 100 | 60 | 40 | 20 | 11* |
| **070-3** | 2796 | 2000 | 1000 | 850 | 500 | 150 | 100 | 55 | 40 | 20 | 11 | |
| **072-1** | 3073 | 2000 | 1300 | 1000 | 500 | 150 | 100 | 60 | 35 | 20 | 11 | |
| **074-2** | 3265 | 2500 | 1700 | 1000 | 500 | 150 | 100 | 60 | 40 | 20 | 11 | |
| **075-1** | 4065 | 3500 | 3000 | 2200 | 1000 | 500 | 150 | 100 | 65 | 50 | 20 | 11* |
| **088-1** | 3795 | 3000 | 2000 | 1000 | 500 | 150 | 100 | 60 | 40 | 20 | 11 | |
| **089-1** | 4090 | 3000 | 2000 | 1000 | 500 | 300 | 150 | 100 | 60 | 40 | 20 | 11* |
| **090-1** | 3458 | 3000 | 2000 | 1000 | 500 | 150 | 100 | 60 | 40 | 20 | 11 | |
| **091-1** | 2920 | 2000 | 1000 | 500 | 270 | 150 | 100 | 60 | 35 | 20 | 11 | |
| **092-4** | 3812 | 3000 | 1800 | 1000 | 500 | 150 | 100 | 60 | 40 | 20 | 11 | |
| **094-6** | 3212 | 3000 | 2000 | 1500 | 1000 | 500 | 150 | 100 | 60 | 35 | 20 | 10 |
| **095-1** | 4822 | 4000 | 3000 | 2000 | 1000 | 500 | 150 | 80 | 60 | 40 | 20 | 11* |
| **096-1** | 1000 | 800 | 500 | 150 | 100 | 80 | 60 | 40 | 20 | 10 | | |
| **097-1** | 1000 | 800 | 500 | 150 | 100 | 80 | 60 | 40 | 20 | 10 | | |
| **098-1** | 5162 | 4000 | 2800 | 2000 | 1000 | 600 | 150 | 100 | 60 | 45 | 20 | 11* |
| **099-5** | 1245 | 800 | 500 | 300 | 150 | 100 | 60 | 40 | 20 | 10 | | |
| **100-5** | 2475 | 2000 | 1000 | 500 | 150 | 100 | 60 | 40 | 20 | 11 | | |
| **104-3** | 824 | 700 | 500 | 400 | 300 | 250 | 150 | 100 | 60 | 40 | 20 | 10 |

*water collected with ships rotary pump

**Tab. 4.1.2:** Filtered 2l-chlorophyll-*a* samples from CTD casts at specific water depth

| Station | 1 | 2 | 3 | 4 | 5 | 6 | 7 | 8 | 9 | 10 | 11 | 12 |
|---|---|---|---|---|---|---|---|---|---|---|---|---|
| **034-3** | 4390 | 4001 | 3257 | 2001 | 1500 | 1000 | 800 | 500 | 300 | 200 | 150 | 120 |
| **040-2** | 500 | 400 | 300 | 200 | 148 | 100 | 75 | 59 | 40 | 18 | 10 | |
| **044-1** | 500 | 100 | 60 | 40 | 20 | 10 | | | | | | |
| **052-2** | 500 | 100 | 60 | 40 | 22 | 11* | | | | | | |
| **054-2** | 500 | 100 | 60 | 40 | 22 | 11* | | | | | | |
| **057-1** | 500 | 100 | 60 | 40 | 22 | 11* | | | | | | |
| **058-1** | 500 | 100 | 60 | 40 | 20 | 10 | | | | | | |
| **061-1** | 500 | 150 | 100 | 55 | 40 | 20 | 11* | | | | | |
| **063-3** | 500 | 150 | 100 | 60 | 40 | 20 | 11* | | | | | |
| **064-3** | 500 | 150 | 100 | 60 | 40 | 20 | 11* | | | | | |
| **065-3** | 500 | 150 | 100 | 60 | 40 | 20 | 11* | | | | | |
| **067-3** | 500 | 150 | 100 | 60 | 40 | 20 | 11* | | | | | |
| **070-3** | 500 | 150 | 100 | 55 | 40 | 20 | 11* | | | | | |
| **072-1** | 500 | 150 | 100 | 60 | 35 | 20 | 11* | | | | | |
| **074-2** | 500 | 150 | 100 | 60 | 40 | 20 | 11* | | | | | |
| **075-1** | 500 | 150 | 100 | 65 | 50 | 20 | 11* | | | | | |
| **088-1** | 500 | 150 | 100 | 60 | 40 | 20 | 11* | | | | | |
| **089-1** | 500 | 150 | 100 | 60 | 40 | 20 | 11* | | | | | |
| **090-1** | 500 | 150 | 100 | 60 | 40 | 20 | 11* | | | | | |
| **091-1** | 500 | 150 | 100 | 60 | 35 | 20 | 11* | | | | | |
| **092-4** | 500 | 150 | 100 | 60 | 40 | 20 | 11* | | | | | |
| **094-6** | 500 | 150 | 100 | 60 | 35 | 20 | 10 | | | | | |
| **095-1** | 500 | 150 | 80 | 60 | 40 | 20 | 11* | | | | | |
| **096-1** | 500 | 150 | 100 | 80 | 60 | 40 | 20 | 10 | | | | |
| **097-1** | 500 | 150 | 100 | 80 | 60 | 40 | 20 | 10 | | | | |
| **098-1** | 600 | 150 | 100 | 60 | 45 | 20 | 11* | | | | | |
| **099-5** | 500 | 300 | 150 | 100 | 60 | 40 | 20 | 10 | | | | |
| **100-5** | 500 | 150 | 100 | 60 | 40 | 20 | 11 | | | | | |
| **104-3** | 500 | 150 | 100 | 60 | 40 | 20 | 10 | | | | | |

*water collected with ships rotary pump

## 4.2 Pelagic ecosystem survey

Giuseppe Cortese[1], Oliver Esper[2], Rainer Gersonde[2], Young Nam Kim[3], Silke Steph[2,4], Mariem Saavedra-Pellitero[5]

[1]GNS Science
[2]Alfred-Wegener-Institut
[3]KOPRI
[4]University of Potsdam
[5]University of Salamanca

### Objectives

In the oceanic ecosystem, $CO_2$ is converted to organic matter by photosynthetic activity of phytoplankton and enters the pelagic food web via a variety of heterotrophic organisms. The downward transport of organic carbon from surface waters to the deep ocean as a result of biological productivity is known as the “biological pump”. In oceanic areas where the biological pump is working actively, sea surface $CO_2$ decreases and

promotes the draw-down of $CO_2$ from the atmosphere. Plankton plays a key role in this oceanic carbon flux and are one of the principal mechanisms for transfer of carbon out of the atmosphere into the surface waters and eventually the deep ocean and sediments (Turner, 2002). Global climate change may have a substantial effect on plankton community structure and dynamics (Hays et al., 2005), and consequently the carbon cycle in the oceans. Plankton community studies by size spectra and pigment analysis have been performed in several environments on a variety of local to regional scales. However, there is a lack of integrated studies covering the Southern Ocean.

The aim of this study is outlined by the following questions:

1) Will key species in the Antarctic be affected by climate change?

Analysis of the present-day biogeography of some of the major groups constituting the phytoplankton community with respect to present-day oceanographic conditions (T, S, water regime, nutrients…) will provide crucial background information on the present-day situation. This biogeographic distribution will most likely be strongly affected by climatic change and especially by global warming, resulting in more temperate species being able to occupy habitats currently occupied by polar species, and also affecting endemic polar species, which risk losing their own typical habitat.

2) How do environmental variables affect plankton distribution and community structure in the Southern Ocean?

The distribution of plankton and community structure in the water column of the Southwest Pacific is not well known. For this reason and in order to improve the interpretation of the surface sediment study of plankton species distribution (see 7.3), a species census in multinet, plankton net and CTD samples will also be carried out. This information will be combined with results from the CTD survey, which will act as a baseline and allow for a comparison of the vertical extent of different water masses along the main transects sampled during the cruise. Additionally, a comparison with surface sediment will be also possible at some locations. Pigment analysis and mycosporine-like aminoacids (MAA) analysis will allow us to understand the adaptation of phytoplankton to enviromental stress, such as UV radiation and iron limitation in this area. Finally, to better understand the roles and strategies of primary producers within the ocean, a quantification of the $CaCO_3$ contribution by some phytoplankton groups (i.e., coccolithophores) will be done using the mass equation of Young and Ziveri (2002).

3) Can we monitor the changes of Phytoplankon Functional Types (PFTs) with satellite data in the Antarctic?

Field studies have the inherent problem of only covering limited space and time of a given ocean region. Although it will be always impossible to distinguish different phytoplankton species from space, a major new advantage would be to identify PFTs, which can be tracked via satellite. This study shall deliver the ground-based data set for the development and ulterior validation of the PhytoDOAS method of Bracher et al. (2009).

**Tab. 4.2.1:** Location of the filtered samples that will be used for future research on coccolithophores sorted by longitude (note that the source of the sea water filtered was indicated, but not the different depths from the CTD).

| Latitude | Longitude | Source |
|---|---|---|
| -49.53 | 178.82 | Ship pump |
| -50.58 | 178.28 | Ship pump |
| -45.76 | 176.85 | CTD |
| -48.26 | 176.73 | CTD |
| -54.37 | -80.09 | Ship pump |
| -54.37 | -80.09 | Ship pump |
| -55.93 | -85.41 | CTD |
| -57.77 | -90.67 | Ship pump |
| -57.77 | -90.68 | Ship pump |
| -57.37 | -90.82 | Ship pump |
| -57.35 | -90.85 | Ship pump |
| -57.85 | -91.03 | Ship pump |
| -57.86 | -91.08 | Ship pump |
| -57.64 | -91.14 | CTD |
| -57.78 | -91.41 | Ship pump |
| -57.70 | -91.98 | Ship pump |
| -56.40 | -95.90 | Ship pump |
| -56.09 | -96.78 | CTD |
| -54.87 | -98.09 | Ship pump |
| -54.41 | -102.50 | Ship pump |
| -54.31 | -102.84 | Ship pump |
| -52.81 | -107.81 | Ship pump |
| -55.33 | -110.22 | Ship pump |
| -58.63 | -113.62 | Ship pump |
| -59.57 | -114.65 | Ship pump |
| -56.15 | -115.13 | CTD |
| -56.19 | -115.14 | Ship pump |
| -55.92 | -115.18 | Ship pump |
| -56.74 | -115.22 | Ship pump |
| -60.53 | -115.62 | Ship pump |
| -59.25 | -115.73 | Ship pump |
| -60.77 | -115.98 | CTD |
| -60.76 | -116.02 | Ship pump |
| -54.12 | -117.45 | Ship pump |
| -53.71 | -118.47 | Ship pump |
| -53.57 | -118.82 | CTD |
| -53.76 | -121.08 | Ship pump |
| -54.21 | -125.44 | Ship pump |
| -54.21 | -125.44 | CTD |
| -54.33 | -127.30 | Ship pump |
| -54.53 | -129.82 | Ship pump |
| -54.76 | -132.66 | Ship pump |
| -57.08 | -135.25 | Ship pump |
| -57.22 | -135.39 | CTD |
| -54.98 | -135.46 | Ship pump |
| -58.68 | -135.47 | Ship pump |
| -58.90 | -135.62 | Ship pump |
| -58.90 | -135.62 | CTD |
| -61.02 | -139.46 | Ship pump |
| -61.01 | -139.46 | CTD |
| -62.36 | -141.19 | Ship pump |
| -62.60 | -141.51 | CTD |
| -64.04 | -143.43 | Ship pump |
| -64.08 | -143.65 | Ship pump |
| -64.97 | -143.80 | CTD |
| -64.97 | -143.80 | Ship pump |
| -62.73 | -144.93 | Ship pump |
| -61.91 | -146.00 | Ship pump |
| -60.30 | -148.03 | Ship pump |
| -58.58 | -150.07 | CTD |
| -58.54 | -150.11 | Ship pump |
| -57.95 | -150.79 | Ship pump |
| -57.55 | -151.20 | CTD |
| -56.24 | -152.65 | CTD |
| -56.24 | -152.65 | Ship pump |
| -54.41 | -154.59 | CTD |
| -56.62 | -156.69 | Ship pump |
| -59.30 | -158.51 | Ship pump |
| -61.05 | -159.59 | Ship pump |
| -68.73 | -164.81 | CTD |
| -67.08 | -165.54 | CTD |
| -65.41 | -166.15 | CTD |
| -63.69 | -169.07 | CTD |
| -63.69 | -169.07 | Ship pump |
| -60.67 | -169.50 | CTD |
| -61.82 | -169.75 | CTD |
| -61.93 | -169.76 | Ship pump |
| -59.70 | -171.36 | CTD |
| -58.92 | -172.28 | Ship pump |
| -58.92 | -172.28 | Ship pump |
| -58.55 | -172.70 | CTD |
| -57.02 | -174.43 | CTD |
| -55.32 | -176.51 | Ship pump |
| -52.97 | -179.01 | CTD |
| -52.65 | -179.34 | Ship pump |

**Work at sea**

The multi-net has been deployed at 22 stations to obtain plankton samples from 5 different water depth profiles between 1,000 m and the sea surface. The profile depths have been chosen in advance according to the hydrographic structure of the upper 1,000 m of the water column, based on the results of the CTD measurements. In order to collect larger plankton fractions such as zooplankton (radiolarians, foraminifera, dinoflagellates), the net beakers have been equipped with 41 $\mu$m mesh size gaze. The samples were stored in 1,000 ml bottles and were fixed with formalin (2 % end concentration). Additionally, a plankton net with a 10 $\mu$m mesh size was towed vertically at 0.3 m $sec^{-1}$ between surface to 100 m depth at 9 stations along the transect for fecal pellet study.

The distribution of siliceous microzooplankton (radiolarians) in the water column of the Southwest Pacific is unknown. For this reason, and in order to improve the interpretation of the surface sediment study of radiolarian species distribution (see Chapter 7.3), a radiolarian species census in multinet and plankton net samples will also be carried out.

For the study of coccolithophore assemblages, 2 - 3 liter water column samples were taken using the membrane pump and CTD casts (4 - 6 samples from the photic zone) and were filtered through cellulose membranes, with 0.45 $\mu$m pore size (Table 4.2.1). In order to study the phytoplankton community, pigment, fatty acids, MAA, size fractionated chl a, and DNA-chip technology (phylochips) samples were collected.

**Expected results**

This study will provide a basin wide comparison and an extensive analysis within the pelagic ecosystem focused mainly on plankton. The results derived from this cruise will allow us to improve the present-day knowledge on the distribution (both latitudinally and within the water column), biodiversity and environmental adaptation of plankton, ranging from primary (e.g. pico-, nanoplankton, diatoms, dinoflagellate) to secondary producers (e.g. radiolaria, foraminifers).

The multi-net and plankton net samples will allow the determination of the vertical distribution in the water column of the various radiolarian species encountered in the samples. This information will be combined with the main results of the CTD survey, which will allow to baseline the vertical extent of different water masses along the main transects sampled during the cruise.

Furthermore, extensive pigment data (more than 300 samples) will be complemented by comparison with other studies, such as biomarkers, coccolithophore abundance, CHEMTAX data set, physiological parameters and carbon flux process study.

**References**

Bracher, A.U., Vountas, M., Dinter, T., Burrows, J.P., Röttgers, R., Peeken, I., 2009. Quantitative observation of cyanobacteria and diatoms from space using PhytoDOAS on SCIAMACHY data. Biogeosciences 6, 751-764.

Hays, G.C., Richardson, A.J., Robinson, C., 2005. Climate change and marine plankton. Trends in Ecology and Evolution 20, 337-344.

Turner, J.T., 2002. Zooplankton fecal pellets, marine snow and sinking phytoplankton blooms. Aquatic Microbial Ecology 27, 57-102.

Young, J., Ziveri, P., 2000. Calculation of coccolith volume and its use in calibration of carbonate flux estimates. Deep-Sea Research II 47, 1679-1700.

## 4.3 Pelagic ecosystem processes

Young Nam Kim Korea Polar Research Institute

### Objectives

Knowledge of the rate of energy or carbon flux within marine ecosystem is important for ecological studies of global change. In the oceanic ecosystem, $CO_2$ is converted to organic matter by the photosynthetic activity of phytoplankton, and enters the pelagic food web via a variety of heterotrophic organisms. The downward transport of organic carbon from surface waters to the deep ocean as a result of biological productivity is known as the “biological pump”. In oceanic areas where the biological pump is working actively, sea surface $CO_2$ decreases and promotes the draw-down of $CO_2$ from the atmosphere. Plankton plays a key role in this oceanic carbon flux and are one of the principal mechanisms for transfer of carbon out of the atmosphere into the surface waters and eventually the deep ocean and sediments (Turner, 2002). Global climate change may have a substantial effect on plankton community structure and dynamics (Hays et al., 2005), and consequently the carbon cycle in the oceans. Plankton community study by size spectra and pigments analysis have been studied in several environments on a variety local or regional scales. However, there is a lack of integrated studies covering in the Southern Ocean.

In general, nutrients and light are the key environment factors for phytoplankton. However, except these two factors, solar ultraviolet radiation (UVR, 280 - 400 nm) and iron concentration are natural stress factors that have the potential to affect negatively phytoplankton organisms by reducing both growth and photosynthetic rates in the Southern Ocean. The penetration of increased amounts of UV light in the Antarctic region has caused great concern over the health of marine phytoplankton (Weiler and Penhale, 1994). The natural protective response of phytoplankton to increased UV is to produce more photoprotective pigments or produce screening substances called mycosporine-like aminoacids (MAA). Fatty acids are also sensitve to oxidation by UV radiations (Skerratt et al., 1998). And iron has wide ranging direct and indirect effects on phytoplankton photophysiology as a consequence of its role in photosynthetic and nutrient acquisition machinery of phytoplankton cells. Iron limitation causes impairment of pigment synthesis and efficient functioning of the electron transport system, reducing the photosynthetic yield per unit of chlorophyll. As a result, iron limited cells with reduced photosynthetic efficiency are more likely to be light-limited due to higher requirement of irradiance. Therefore, studying pigment, fatty acids, and MAA can revealed the stress mechanisms of UV radiation and iron.

This study will be the basin-scale comparative and extensive analysis in the pelagic ecosystem mainly focused on phytoplankton. A further and related goal is how the natural environmental factors, such as UV radiation and iron concentration, affect to the phytoplankton community structure in this area.

**Work at sea**

Vertical seawater samples were taken at 5 depths (surface to 100 m) in all CTD stations (for CTD station, see chapter 3.1). Water samples were decanted into either plastic bottles or directly into sample bottles from Niskin bottles and ship's membrane pump (~7 m depth) using non-toxic silicon tubing. Each of 2 to 6 litres of water were filtered for pigment and fatty acids & MAA analysis, and a total number of samples were around 300 each. Size fractionated chlorophyll *a* and flow cytometry samples were collected 1 to 2 selected depths. Micro zooplankton samples were collected at 4 depths on selected station to compare with plankton net results. All samples were stored in -20°C freezer and -80°C deep freezer for further analysis.

The plankton net with 10 $\mu$m mesh size was towed vertically at 0.3 m $sec^{-1}$ between surface to 100 m depth at 9 stations along the transect. These samples were preserved in borax-buffered 4 % formaldehyde/sea water solution for further fecal pellet study.

A total of 101 sea surface water samples were collected from the ship's own pump for phytoplankton pigment analysis. These samples were taken every 4 to 6 hours when ship was moving. Samples for fatty acids, MAA, size fractionated chlorophyll, microscopy, flow cytometry were also taken on selected positions.

Water samples for on deck incubation experiments were carried out 8 times at selected CTD stations (Table 4.3.1). Stations were chosen considering incubation time and physio-chemical characteristics of water environment. Surface seawater (~11m depth) was collected with ship's pump system. Water was collected into acid-cleaned two of 6 litres quartz bottles and three of 9 litres polycarbonate bottles. These bottles were given different UV light intensity and iron concentration and incubated on deck with circulated surface seawater jacket for 48 hours or 96 hours. After the incubation, pigments, nutrients, DIC, size fractionated chlorophyll *a,* flow cytometry, micro zooplankton, $CO_2$ and greenhouse gases, fatty acids, MAA, microscopy samples, and carbon uptake rate were taken or measured.

**Tab. 4.3.1:** Stations sampled for on deck incubation experiments

| Station No. | Latitude [deg/min] | Longitude [deg/min] | Control factors | Incubation time |
|---|---|---|---|---|
| **PS75/035** | 57°46.166'S | 90°40.019'W | UV, Iron | 96 hr. |
| **PS75/051** | 52°48.73'S | 107°48.33'W | UV, Iron | 96 hr. |
| **PS75/058** | 54°12.947'S | 125°26.187'W | UV, Iron | 96 hr. |
| **PS75/067** | 64°58.252'S | 143°48.213'W | UV, Iron | 96 hr. |
| **PS75/075** | 54°24.256'S | 154°35.184'W | UV, Iron | 96 hr. |
| **PS75/088** | 68°43.811'S | 164°48.074'W | UV, Iron | 96 hr. |
| **PS75/094** | 61°49.364'S | 169°44.444'W | UV, Iron | 96 hr. |
| **PS75/098** | 52°57.032'S | 179°00.732'W | UV, Iron | 48 hr |

### Expected results

During this study, more than 600 samples of pigments, fatty acids, and MAA were collected from the CTD casts, underway and in incubation experiments. Zooplankton fecal pellets, size fractionated chlorophyll, and picoplankton biomass samples were also collected. This extensive plankton data will be extending the understanding of plankton community structure and the effects of environmental factors to plankton, especially UV radiation and iron limitation in this area.

Furthermore, pigment data will be compared with those from other studies, such as biomarkers, coccilothophore counting, CHEMTAX data set, physiological parameters, and carbon flux.

### References

Hays, G.C., Richardson, A.J., and Robinson, C., 2005. Climate change and marine plankton. Trends in Ecology and Evolution 20, 337-344.

Turner, J.T., 2002. Zooplankton fecal pellets, marine snow and sinking phytoplankton blooms. Aquatic Microbial Ecology 27, 57-102.

Weiler, C.S., Penhale, P.A. (Eds), 1994. Ultraviolet Radiation in Antarctica: Measurements and Biological Effects. Antarctic Research Series 62.

Skerratt, J.H., Davidson, A.D., Nichols, P.D., McMeekin, T.A., 1998. Effect of UV-B on lipid content of three Antarctic marine phytoplankton. Phytochemistry 49, 999-1007.

## 4.4 Biomarker studies

Susanne Fietz[1], Alfredo Martinez-Garcia[2], Gemma Rueda [1]
not on board: Antoni Rosell-Melé [1]

[1]Universitat Autonoma de Barcelona
[2]ETH Zürich

### Objectives

The main objective of this study is to obtain modern samples to constrain the calibration of various paleotemperature and productivity biomarkers that are widely applied for paleoceoceanographic reconstructions (alkenones, pigments and GDGTs) given that they are not yet calibrated in polar regions, particulary in the Pacific sector of the Southern Ocean (Conte et al., 2006; Kim et al., 2008). Samples from the water column and surface sediments (Chapter 7.7.1) will be analyzed to measure their biomarkers contents. This will allow us to calibrate and constrain the different paleotemperature indexes ($U^{K'}_{37}$/$U^{K}_{37'}$ and $TEX_{86}$ for SST), and productivity proxies (alkenone and pigment fluxes,) against *in-situ* measured variables, coccoliths counts (Chapter 4.2) and pelagic ecosystem analyses (Chapter 4.3) in the Pacific Southern Ocean.

The newly established SST-index $TEX_{86}$ (Schouten et al., 2002, Kim et al., 2008) and related proxies for paleo-reconstructions (Chapter 7.7) offer a promising new tool for paleoceanographic reconstructions in the polar regions. However, one possible caveat to this method is that the Archaea producing the GDGTs are ubiquitous and, in contrast to the photosynthetic alkenone producers (Brassell et al., 1986; Prahl and Wackeham, 1987), likely live in the whole water column. Surveys of particulate organic matter in the ocean (Wuchter et al., 2005) as well as the recent global core-top calibration of $TEX_{86}$ (Kim et al., 2008) suggest that the temperature of the upper mixed layer (100 - 200 m) is generally integrated into the sedimentary GDGT signal. However, it has

been found that not all regions follow the same pattern. In the Santa Barbara basin, for instance, sea surface temperatures colder than those instrumentally recorded were reconstructed using the $TEX_{86}$ in sediments (Huguet et al., 2007). Therefore, further studies are needed to constrain the depths of GDGT production in the water column and its relationship to the signal recorded in the sediment. Therefore, one of the major aims of this study is to assess the distribution of GDGTs in the water column and surface sediment in order to constrain the ecology of the GDGTs producers in the present ocean, and consequently to interpret the signals preserved in the geologic record.

A related goal of this study is to take advantage of the water samples collected for the biomarker studies to analyze the accumulation of organic pollutants in the Southern High Latitudes and their deposition into the Southern Ocean. The dissolved pollutants will be studied along with the particulates in selected locations. In order to study the hypothesized increase in aeolian input of organic pollutants towards the polar zone as well as their export towards the sea floor, surface water samples were combined with air samples (Chapter 5) during steaming transects and with bottom water samples gathered from the CTD-rosette.

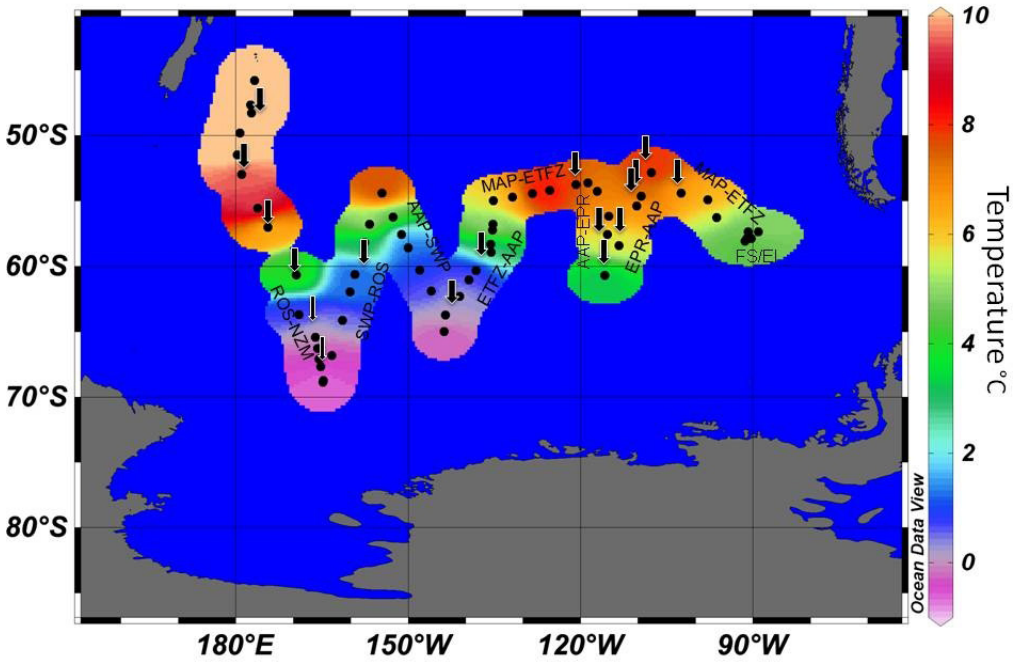


*Fig. 4.4.1: Map tracking surface water samples for biomarker calibration (black circles) and pollutant deposition (black arrows) during ANT-XXVI/2*

**Work at sea**

We collected water samples from the CTD rosette from the chlorophyll maximum, intermediate water masses and bottom waters. The chlorophyll maximum was determined with a fluorescence probe attached to the CTD, which transmitted real-time data (Chapter 3.1 for CTD-rosette and probes description). The CTD stations are shown

in Fig. 3.1.1. We collected 36 L to 48 L for the bottom and intermediate water masses and usually up to 5 L but occasionally up to 24 L for the chlorophyll maximum. Water collected from the CTD rosette was filtered by a fixed filter ramp with two connected vacuum pumps. Environmental data were obtained from the CTD probes (Chapter 3.1). In addition, a total of 59 surface water samples were collected both at the CTD stations and while underway (Fig. 4.4.1) using the underway clean seawater pump (6 m). We connected the water flow directly into four parallel filter systems. Salinity and temperature were monitored during filtering with the thermosalinograph (DSHIP). Moreover at 17 CTD stations, water-sediment interface waters were collected from the Multicorer tubes (Chapter 7.3 for multicorer and Fig. 7.3.1 for station locations). At each station we collected between 3 to 10 L. Hence, at each station we got data from surface, chlorophyll maximum, intermediate and CTD bottom water (approx. 20 m above sea floor) as well as water-sediment interface water. For all samples Whatman GF/F filters were used. All filters were stored frozen at -20ºC.

In addition, fourteen sites (Fig. 4.4.1) were chosen during the transects to study the pollutants dissolved in the surface water, and four sites to study the export towards the bottom water. Whatman GF/F filters were used to collect the particulate fraction and C18 disks for the dissolved pollutants. Up to 10 L were filtered per sample.

## Expected results

The set of surface water samples collected during the ANT-XXVI/2 cruise will allow the measurement the $U^{K'}_{37}$ and $TEX_{86}$ paleothermometers in modern water samples and the comparison of the SST estimates to the *in-situ* measurements obtained on board from the thermosalinograph (DSHIP). This will allow us to obtain a calibration of $TEX_{86}$ and $U^{K'}_{37}$ SST estimates against present-day environmental variables for the first time in the Pacific Southern Ocean.

Additionally, the analysis of samples collected from different water depths, will allow us to better understand depth habitats of the GDGTs producers and hence the origin of the temperature signal recorded in marine sediments. Comparison with the findings on the pelagic ecosystem (Chapters 4.2 and 4.3) will give further hints at the ecology of the GDGT producers in the Southern Pacific Ocean.

After analysis of both particulate and dissolved organic pollutants in the surface and bottom water samples, we expect to be able to outline the distribution of these compounds in this region as such a study has not yet been performed in the Pacific Southern Ocean.

## References

Brassell, S.C., Eglinton, G., Marlowe, I.T., Pflaumann, U., Sarnthein, M., 1986. Molecular Stratigraphy: A New Tool For Climatic Assessment. Nature 320(6058), 129-133.

Conte, M.H., Sicre, M.A., Rühlemann, C., Weber, J.C., Schulte, S., Schulz-Bull, D., Blanz, T., 2006. Global temperature calibration of the alkenone unsaturation index (UK 37') in surface waters and comparison with surface sediments. Geochemisty Geophysics Geosystems 7.

Huguet, C., Schimmelmann, A., Thunell, R., Lourens, L.J., Sinninghe Damsté, J.S., Schouten, S., 2007. A study of the TEX86 paleothermometer in the water column and sediments of the

Santa Barbara Basin, California. Paleoceanography 22(3).

Kim, J.H., Schouten, S., Hopmans, E.C., Donner, B., Sinninghe Damsté, J.S., 2008. Global sediment core-top calibration of the TEX86 paleothermometer in the ocean. Geochimica et Cosmochimica Acta 72, 1154-1173.

Prahl, F.G., Wakeham, S.G., 1987. Calibration of unsaturation patterns in long-chain ketone compositions for paleotemperature assessment. Nature 330(6146), 367-369.

Schouten, S., Hopmans, E.C., Schefuss, E., Sinninghe Damsté, J.S., 2002. Distributional variations in marine crenarchaeotal membrane lipids: A new tool for reconstructing ancient sea water temperatures? Earth and Planetary Science Letters 204(1-2), 265-274.

Wuchter, C., Schouten, S., Wakeham, S.G., Sinninghe Damsté, J.S., 2005. Temporal and spatial variation in tetraether membrane lipids of marine Crenarchaeota in particulate organic matter: Implications for TEX86 paleothermometry. Paleoceanography 20(3), PA3013 10.1029/2004PA001110.

# 5. DUST SAMPLING

Susanne Fietz[1], Alfredo Martinez-Garcia[2], Gemma Rueda [1]
not on board: Antoni Rosell-Melé [1]

[1]Universitat Autonma de Barcelona
[2]ETH-Zürich

## Objectives

Dust plays an important role in global climate by influencing the radiative balance of the atmosphere. Moreover, it can be also an important source for limiting micro nutrients (e.g. iron) to the ocean that are thought to play an important role in driving marine productivity in the high-nutrient low-chlorophyll (HNLC) regions of the world (mainly the Southern Ocean and the North Pacific). However, little is known about the distribution of wind-born terrigenous material in the Pacific sector of the Southern Ocean.

The main objective of this study is to map out the distribution of terrigenous biomarkers (n-alkanes and branched GDGTs) and measure the isotopic composition of n-alkanes ($\delta^{13}C$) in the present-day ocean in order to link it to the source of the terrigenous organic matter and the position of the westerlies. For that purpose we installed a high volume air sampler on the foredeck and collected air particulates to measure long range transport of terrigenous organic matter and link its composition to air mass trajectories during the cruise. The distribution of terrigenous biomarkers in the water column will be also analyzed in the samples taken from the CTD-rosette and the ship's sea water supply (Chapter 4.4.), as well as in the surface sediments recovered with the multicorer (Chapter 7.7.3), with the objective to study the transport of these components from the atmosphere to the sea floor.

A related goal of this study is to take advantage of the modern samples (Chapter 4.4) collected to analyze the organic pollutants, and their accumulation in the southern high latitudes and their deposition into the Southern Ocean.

## Work at sea

An active air sampler (TE-PNY1123, Tisch Environmental Inc.) was installed on the foredeck above the bridge to collect total suspended (airborne) particulates (TSP) whenever the ship was moving. This was especially important when nearing the CTD stations, in order to link air and water samples (Chapter 4.4 for water sampling) and, hence, study the incorporation from the atmosphere into the ocean. A total of 20 TSP samples were collected during the cruise (Fig. 5.1).

## Expected results

The samples collected during the cruise ANT-XXVI/2 will allow us to characterize the present-day distribution of terrigenous biomarkers in the atmosphere, the water column and surface sediments in the Pacific sector of the Southern Ocean. This will add new insights to the main sources and transport mechanisms of these compounds

from the source areas to the deep ocean, providing a new calibration dataset for the interpretation of the data generated in the paleoceanographic studies carried out in this area.

Additionally, the samples collected will provide the first insight on the accumulation and wind transport of organic pollutants to the high southern latitudes and their fate in the water column after the deposition in the Pacific sector of the Southern Ocean.

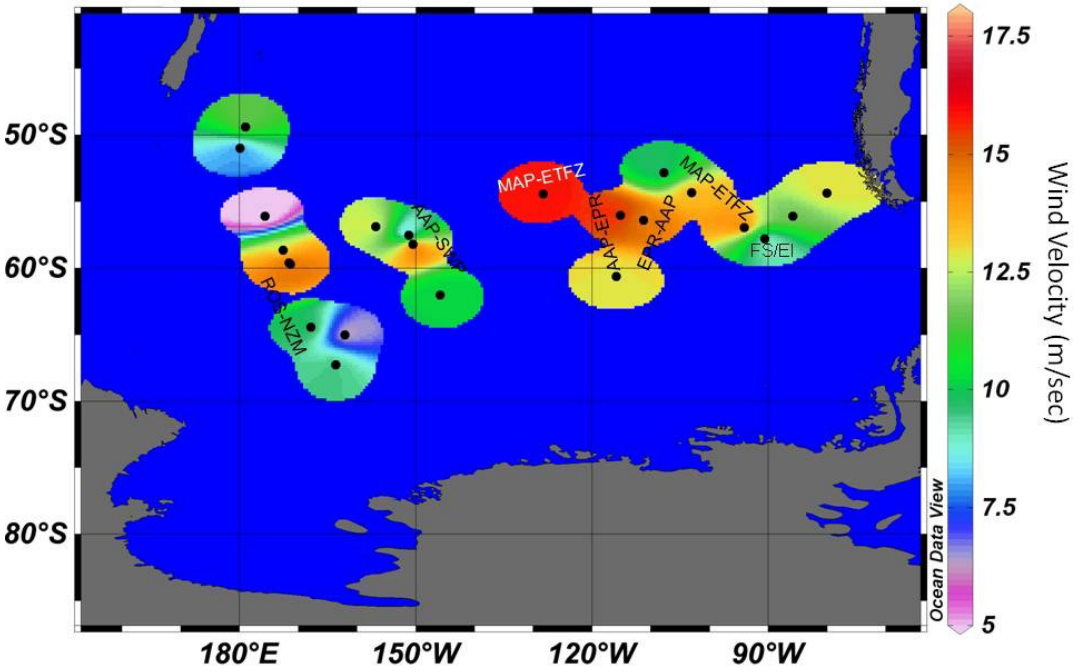


*Fig. 5.1: Map tracking air samples filtered for terrigenous input and pollutant accumulation studies (black circles) during ANT-XXVI/2. Related surface water sample locations for dust and pollutant deposition into the water column are shown in Fig. 4.4.1.*

# 6. BATHYMETRIC SURVEY

Daniel Damaske, Cornelia Heinzl, Hartmut Seidel — Alfred-Wegener-Institut

## Objectives

The seafloor topography in the region visited during the ANT-XXVI/2 expedition is largely unknown. Only predicted bathymetry based on satellite radar altimetry data published by Smith and Sandwell (1997) and sparse bathymetric data measured by research vessels on transits convey a first picture of the bathymetry in the Southern Ocean and the South Pacific. This data is also included in the *General Bathymetric Chart of the Oceans (GEBCO)*. The global *GEBCO_08 Grid, version 20081212 (http:/ www.gebco.net)* was used as primary dataset for track planning during ANT-XXVI/2. However, these data are insufficient for precision deep-sea research.

The bathymetry group organized and monitored the acquisition of swath soundings throughout the expedition using the multi-beam system HYDROSWEEP DS2 from ATLAS Hydrographic aboard *Polarstern*. To avoid possible data loss due to measurement errors, failures or a system crash, the multi-beam system was operated and monitored in a 24 hours watch.

Bathymetric data free of outliers, blunders and systematic errors and a reliable DTM form the geo-data base indispensable for the selection of marine-geological coring sites. Concurrently to the HYDROSWEEP operation and data acquisition, the multi-beam data were processed on board to create detailed bathymetric charts during the cruise to assist geological planning and sampling, and support geophysical interpretation. Furthermore, the bathymetry group provided overview maps for daily briefings.

To extend knowledge of the seafloor topography in this region, the data collected along the tracks will be added to the IHO/DCDB (International Hydrographic Organization/ Data Centre for Digital Bathymetry) archive. The data will also be utilized for the recently established ocean mapping programs Bathymetric Chart of the South East Pacific (IBCSEP) established by the Intergovernmental Oceanographic Commission (IOC), and the International Bathymetric Chart of the Southern Ocean (IBCSO). Finally, detailed information of the seafloor topography in form of multi-beam data is a fundamental requirement for the geophysical/geological pre-site survey in preparation of site-proposals to the Integrated Ocean Drilling Program (IODP).

## Work at sea, technical settings, operation conditions

Data acquisition started on 29 November 2009 at 1500 UTC, at the end of the expedition the multi beam device was switched off on 24 January 2010 at 2300 UTC. The deep-sea multi-beam echo-sounder ATLAS HYDROSWEEP DS2 was in operation to collect

data throughout the cruise. Only during less than 4 h no data was recorded due to system failure.

The HYDROSWEEP system was set to hardbeam mode, using 59 pre-formed beams (PFB) per ping, using a frequency of 15.5 kHz. The multi-beam opening angle is adoptable to the water depth and can be set to 90° or 120°. By setting the fan angle to 90° the multi-beam device can operate down to 11,000 m water depth. Using an angle of 120°, the depth measurement is restricted to 4,700 m. Due to lower resolution in the 120° mode a reduced data quality especially at the outer PFBs was observed. With respect to the water depth of more than 4,700 m in the working area, the opening angle was set to 90°. Using a 90° aperture, the coverage on the seafloor is about two times the water depth. In order to correct the slant sonar beams in terms of the refraction in the water column, a refraction correction must be applied to the individual PFB's. For this purpose a sound velocity profile (SVP) has to be determined. The mean sound speed in the water column is calculated using the integrated *Cross-Fan-Calibration* function of HYDROSWEEP. Alternatively a SVP can be determined from CTD-measurements (Conductivity, Temperature, Depth). CTD-casts were conducted during the cruise mainly at marine geological coring-sites and used to correct the HYDROSWEEP-measurements *(see chapter: Measuring sound velocity in the water column*).

In order to meet the administrative requirements of the *German Federal Environmental Agency (Umweltbundesamt)* based on the Antarctic Treaty, it was ensured that - while on station south of 60°S latitude - HYDROSWEEP could be switched off at any time by the watch keeper in the event of a whale sighting within a radius of 100 m around the ship.

**Data management**

Strong movements of the ship caused by heavy weather conditions can produce large blunders or outliners in depth measurements. These errors must be identified and eliminated during post-processing. The HYDROSWEEP raw data is recorded and post-processed in blocks of eight hours, in following steps:

The raw data are at first converted into the *Hydromap Online SURF-Format.* Position errors are detected and analysed using the *position editor, a component* of *Atlas Hydromap Offline*. As next step the SURF-data is imported into CARIS-HIPS/SIPS for manually editing of outliers, blunders and systematic errors. The cleaned data is then exported from CARIS and converted into the Atlas file output format *dux*.

The individual eight hour blocks are combined into one-day files and simultaneously converted to other formats (e.g. xyz-file) used for subsequent DTM processing and visualization. The *ACSII* format xyz (longitude, latitude, depth) for example can be utilized with the *Generic Mapping Tool (GMT)* software to produce quick-look plots and bathymetric charts. Navigation data from *D-Ship* (data export program aboard *Polarstern*) were downloaded daily to use navigation data from additional sensors for evaluation and comparisons.

**Measuring sound velocity in the water column**

The slant sonar beams must be corrected due to the ray bending caused by differing physical properties in the water column. The refraction correction is determined on

the base of a sound velocity profile (SVP) reflecting the variations of the water sound velocity. The physical parameters of sea water needed for the calculation of the SVP are measured by performing CTD casts. A mean value for the sound velocity is also required to determine the absolute water depth. Due to regional variations of the physical properties of seawater, it is necessary to periodically update the SVP data to avoid systematic refraction errors during the survey and to acquire precise depth data.

The HYDROSWEEP system can be operated in the so-called *Cross-Fan-Calibration* mode, to directly determine a mean sound velocity ($c_m$) of the water column. This operation mode is used during transits and when no CTD measurements are possible. The sound velocity is also measured directly at the ship's keel using a special c-probe. Using the *Cross-Fan-Calibration* large refraction errors can be avoided along transits.

Deep-sea tests have demonstrated that an accuracy of 0.5 % of the water depth (WD) can be achieved for the centre beams and 1% for the outer beams (Schenke und Schreiber, 1989). However, by applying SVP from CTD-data and using the sound velocity at the ship‘s keel the depth measurement accuracy ranges within the entire swath between 0.5 % and 1% of the WD.

During ANT-XXVI/2, data from 19 CTD-casts were used to determine sound velocity profiles. The system was switched to *Cross-Fan-Calibration* mode when physical water conditions were expected to change, for example, when crossing oceanic fronts. During long transits the system was operated mostly in the *Cross-Fan-Calibration* mode.

**Processing of CTD measurements**

CTD data is processed with the *Sea-Bird Electronics Inc. (SBE)* program *SBE Data Processing, Version 7.17a.* The data processing steps are as follows:

- Data conversion [Data Setup; Scans to skip over: 0, Output format: ASCII output, Convert data from: Downcast, Create converted data (.CNV-file) only]
- calculate Bin average [Data Setup; Bin type: Depth, Bin size: 1 meter, Exclude scans marked bad, Scans to skip over: 0, Cast to process: Downcast].

The data of the CTD profile is reduced to 20 significant points and converted to a *Hydromap Online* sound velocity file output using the *Sound Velocity Profile Viewer Version 1.1b.* The final output data is transferred to *Hydromap Online*. Fig. 6.1 shows the workflow of CTD data processing aboard *Polarstern*.

**Results**

*General*

Almost all multi-beam data collected during ANT-XXVI/2 were post-processed by the end of the expedition. Navigation errors were deleted; manual depth editing using *CARIS-HIPS* and all necessary format conversions were performed, as these allow the creation of bathymetric charts with *GMT* or Fledermaus.

The track length of the multi-beam survey during the expedition amounts to 9,273 nm (17,174 km), the multi-beam raw-data volume acquired over 56 days accumulated to a data storage of 13.1 GB. The *CARIS* files are split-up into 173 separate files with a total data volume of 2.9 GB. The files contain 23,359,516 soundings within 395,924 multi-beam pings. The shallowest depth measured was 371 m and the greatest recorded depth was 6,348 m.

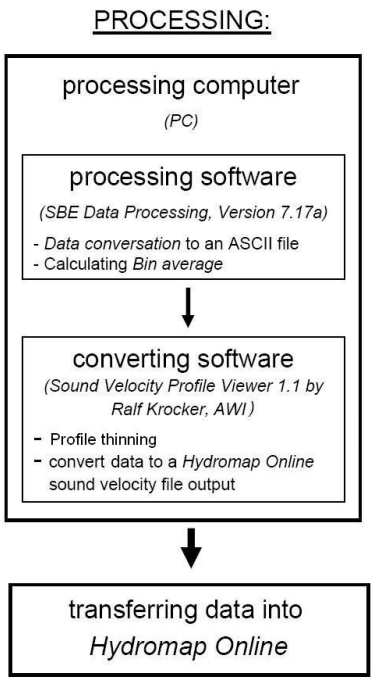


*Fig. 6.1: Workflow of CTD data processing on board Polarstern*

*Freeden Seamount / Eltanin Impact Area*

On 01 Dec. 2009 *Polarstern* reached the Freeden Seamount located in the Eltanin meteorite impact area. New bathymetric data was obtained in the southern part of the region. The new data will be added to the already existing dataset collected during ANT-XII/4 and ANT-XVIII/5 and included in the DTM. While leaving the area on 04 Dec. 2009, the dataset was also extended westward. Fig. 8.5 shows the tracks of all three expeditions

*Seamounts at the west of the Mornington Abyssal Plain*

On 07 Dec. 2009 *Polarstern* passed the top of two unnamed seamounts west of the Mornington Abyssal Plain at 54°52'S/98°30'W and 55°00'S/99°05'W. The shallowest depth values from both seamounts as shown the *GEBCO_08-dataset* are about 50 m. However, the shallowest depth measured over these seamounts was about 500 m. Fig. 6.2 shows the predicted bathymetry (top) and the measured multi-beam track over the seamount.

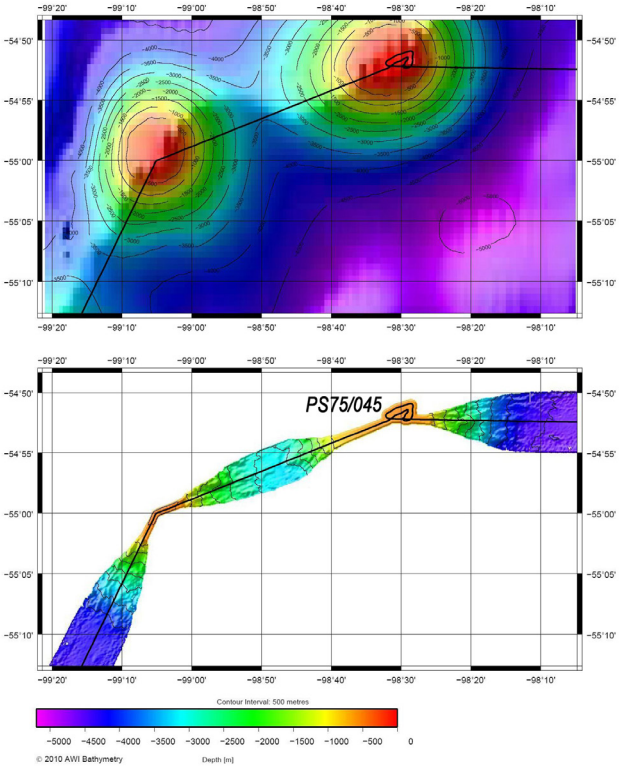


*Fig. 6.2: Seamounts at the west of the Mornington Abyssal Plain (top: GEBCO_08, bottom: swath bathymetry)*

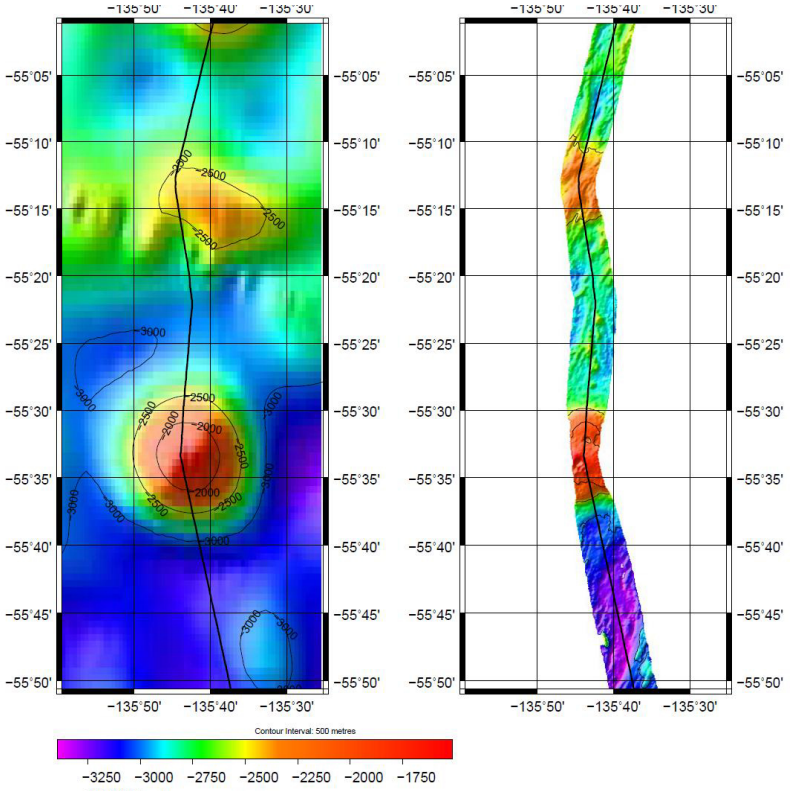


*Fig. 6.3: Seamounts at the north-eastern flank of the Pacific Antarctic Ridge (left: GEBCO_08, right: swath bathymetry)*

*Seamounts at the north-eastern flank of the Pacific Antarctic Ridge*

On 20 Dec. 2009 on the north-eastern flank of the Pacific Antarctic Ridge *Polarstern* again passed two unnamed seamounts at 55°13'S/135°45'W and 55°34'S/135°46'W, which are shown in the *GEBCO_08-bathymerty* (Fig. 6.3). The shallowest depth measured at the northern and southern seamounts are 2,254 m and 1,513 m respectively.

*Survey in the western Amundsen Abyssal Plain*

During the search for a coring station in the western Amundsen Abyssal Plain from 24 to 26 Dec. 2009, a survey was conducted in the area around 64°30'S/143°40'W. The *GEBCO_08-bathymerty* data indicate large seamounts at this position. However, the existence of the suspected seamounts could not be confirmed. Fig. 6.4 shows the predicted and measured bathymetry. The depth difference between both data sets amounts in some areas to more then 1,000 m.

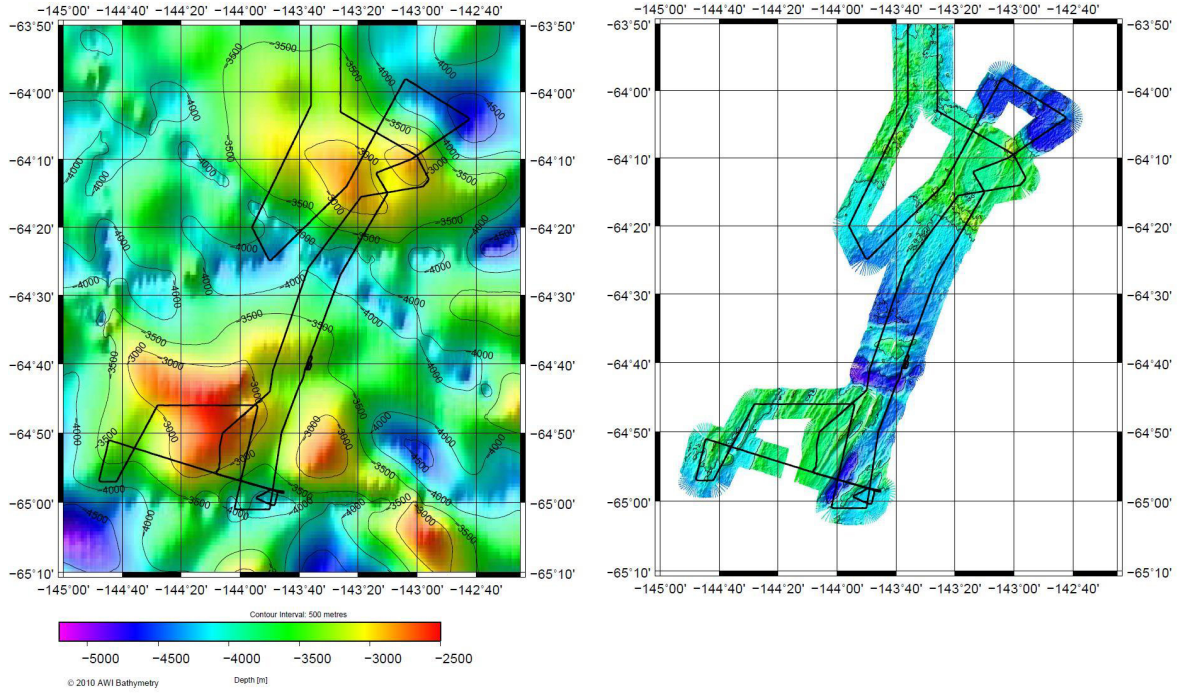


*Fig. 6.4: Suspected seamounts in the western Amundsen Abyssal Plain (left: GEBCO_08, right: swath bathymetry)*

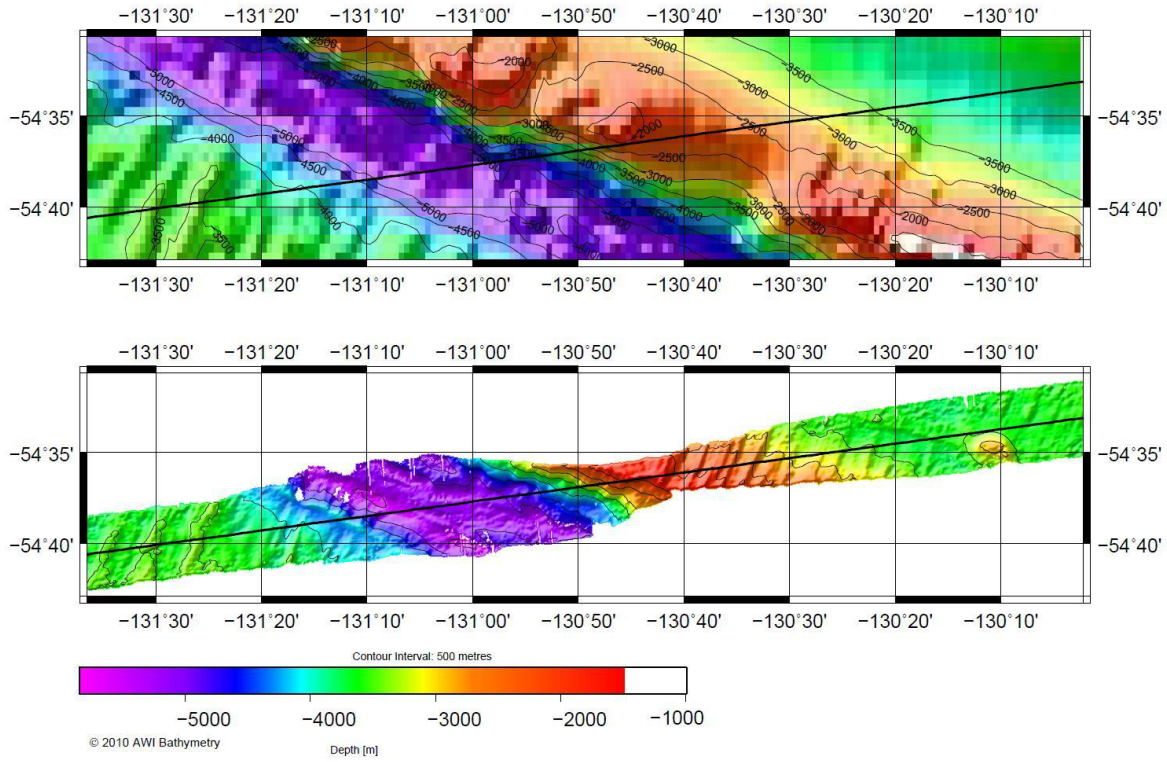


*Fig. 6.5: Tharp Fracture Zone west of the South Pacific Rise (top: GEBCO_08, bottom: swath bathymetry)*

*Eltanin Fracture Zone System*

The Eltanin Fracture Zone System (EFZS), which is subdivided into the Heezen Fracture Zone and the Tharp Fracture Zone, was crossed three times during the cruise. Fig. 6.5 shows the *GEBCO_08* and the multi-beam swathes as part of the Tharp Fracture Zone west of the South Pacific Rise in the area around 54°37'S/ 130°50'W. Due to the good conformity between *GEBCO* and the multi-beam data it is assumed that the *GEBCO_08-dataset* already comprises multi-beam bathymetry in this region. The bathymetry shown on the GEBCO_08 DTM is similar to the *Polarstern* multi-beam data.

Fig. 6.6 shows a section of the Heezen Fracture Zone east of the South Pacific Rise in the area around 57°35'S/112°30'W, based on both predicted and measured bathymetry. In this case the GEBCO_08-bathymetry differs from the *Polarstern* swath bathymetry.

*Ridge and valley structure of the northern Pacific Antarctic Ridge*

Fig. 6.7 shows an example of the bathymetry of the northern Pacific Antarctic Ridge in the area around 57°38'S/151°05'W. Seafloor spreading forms small parallel ridges with difference in elevation up to 400 m.

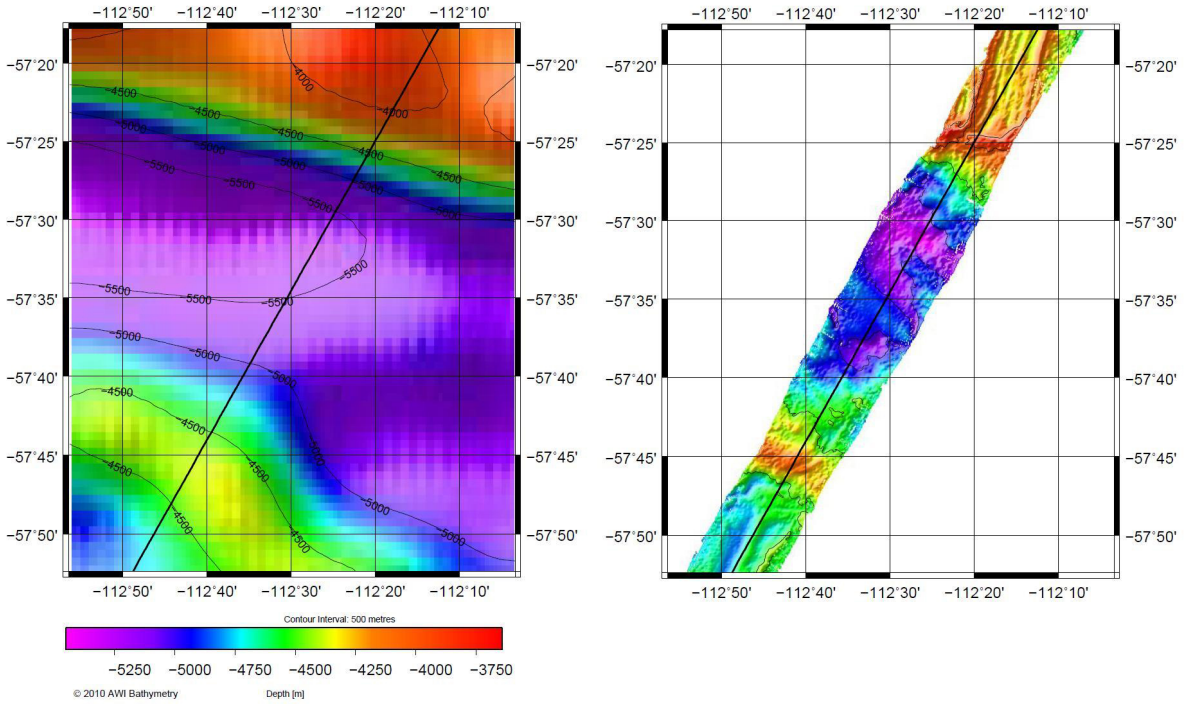


*Fig. 6.6: Heezen Fracture Zone east of the South Pacific Rise (left: GEBCO_08, right: swath bathymetry)*

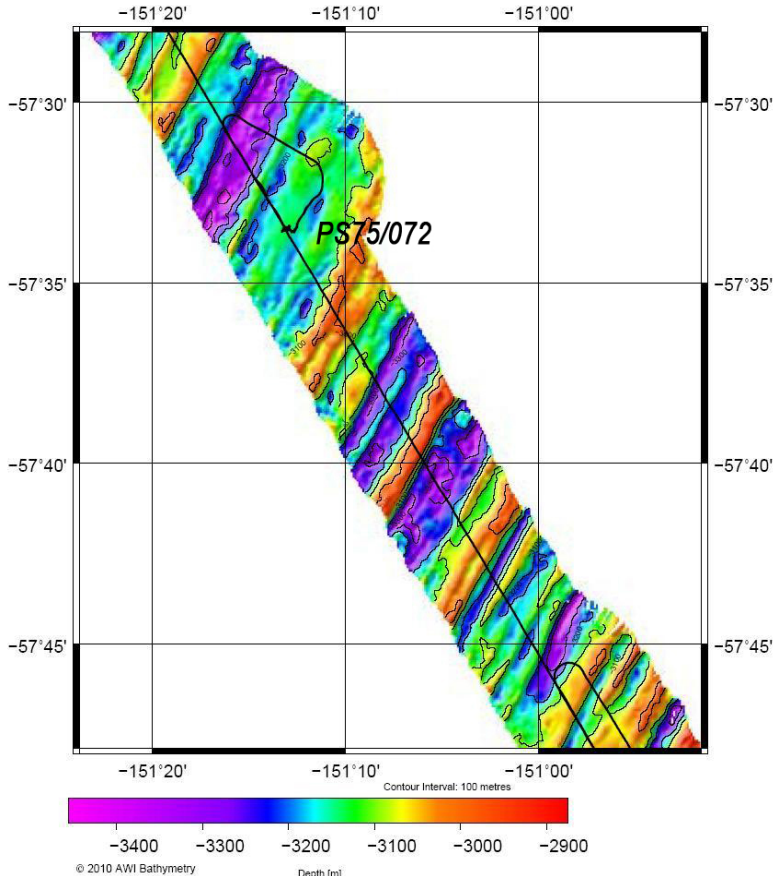


*Fig. 6.7: Ridge and valley structures of the northern Pacific-Antarctic-Ridge (swath bathymetry)*

## References

Sandwell D. T., Smith W. H. F., 1997. Marine gravity anomaly from Geosat and ERS-1 satellite altimetry, Journal of Geophysical Research, 102, No. B5, 10039-10054

Schenke, H.W., Schreiber, R., 1989. Efficient hydrographic surveying of EEZ with new multi-beam echosounder technology for shallow and deep water. Proc. International Ocean Technology Congress, Honolulu, Hawaii, 316-330.

# 7. MARINE GEOLOGICAL STUDIES AND SURVEYS

## 7.1 Background of marine geological studies

Rainer Gersonde, Frank Lamy Alfred-Wegener-Institut

In the Southern Ocean, processes such as the biological pump, the circulation and stratification of water masses, the formation and distribution of sea ice, atmospheric circulation, water vapor transport, and the volume and stability of continental ice on Antarctica play key roles in driving and amplifying Quaternary climate change. The Southern Ocean is also one of the ocean's primary sites of water mass formation, and a "junction box" where mixing occurs among major water masses from all large ocean basins. This makes the modern Southern Ocean to a key area for the transmission of climate change across the globe. So far, our picture of Southern Ocean climate development is primarily based on paleoceanographic studies from the Atlantic and Indian Ocean sectors of the Southern Ocean and very little information is presently available from the Pacific Sector though it is representing the largest portion of the Southern Ocean. The Pacific Sector represents for example a major site of deep and intermediate water formation and it represents the prime candidate to learn more on Antarctic ice sheet stability, as it collects about 70 % of the West Antarctic Ice Sheet drainage.

ANT-XXVI/2 has generated an enormous new set of bathymetric and sediment-echo-sounding data (9,273 nm) together with surface sediment samples and up to 23 m long sediment cores from latitudinal and longitudinal transects on the eastern central and western sectors of the polar South Pacific. The total of 1,030.41 m recovered sediment core from 62 sites will allow for extensive paleoceanographic work in all zones and at depth transects between 669 m and 5,313 m in the polar South Pacific. This will help to close critical gaps in our understanding of the Southern Ocean´s role in the Quaternary climate development. The new data and material allow for addressing paleoceanographic topics such as:

- The timing and response of Pacific Southern Ocean paleoceanography to external forcing mechanisms, past climate tele-connections and inter-hemispheric links (see 7.7.2),
- Pleistocene changes in Pacific Southern Ocean physical environment and ecosystem/export productivity regimes and their relation to atmospheric $pCO_2$ and the global nutrient regime (see 7.7.3),
- Pleistocene changes in South Pacific intermediate and bottom water circulation (see 7.7.4)
- Southern Ocean climate at the Last Glacial Maximum (LGM) and the last glacial/ interglacial transition (see 7.7.5),

- Pleistocene warmer than present environments in the South Pacific and implications for Antarctic ice sheet and global climate history (see 7.7.6),
- Pliocene-Pleistocene climate evolution in the Pacific Southern Ocean and implications for the West Antarctic Ice Sheet (WAIS) history (see 7.7.7).

Other scientific topics that can be addressed concern:

- Further documentation of the Eltanin-asteroid impact in the Bellingshausen Sea (see 7.7.8),
- Refinement of the geomagnetic dating of Holocene-Pleistocene Southern Ocean sediment records (see 7.7.9),
- Refinement of Southern Ocean Plio-Pleistocene biostratigraphic zonations (see 7.7.10),

and

- Establishment of new surface sediment data sets for documentation of modern sedimentation patterns and paleoceanographic proxy calibration (see 7.7.1)

The assignment of the recovered sediment records to the different scientific topics is summarized in Table 7.1.

**Table 7.1:** Scientific projects related to ANT-XXVI/2 sediment cores

| Core | Length [m] | CC Age [Ma]* | Project | | | | | | | | |
|---|---|---|---|---|---|---|---|---|---|---|---|
| | | | 1 | 2 | 3 | 4 | 5 | 6 | 7 | 8 | 9 |
| PS75/034-2 | 18.08 | 0.75 | X | X | X | X | X | | | X | |
| PS75/035-1 | 22.53 | 0.65 | X | X | | X | X | | | | |
| PS75/036-1 | 22.74 | 37.6 | | | | | | | X | X | X |
| PS75/037-1 | 22.73 | 1.8 | X | X | | | | | | | X |
| PS75/038-1 | 21.83 | 48.6 | | | | | | | X | X | X |
| PS75/039-1 | 22.15 | 1.1 | X | X | | | | | | | X |
| PS75/040-1 | 9.36 | 37.2 | | | | | | | X | X | X |
| PS75/042-1 | 23.54 | 1.3 | X | X | | | | | | | X |
| PS75/043-1 | 23.48 | 1.8 | | | | | | | | | X |
| PS75/044-4 | 20.93 | 2.4 | | | | | | | | | |
| PS75/046-2 | 17.26 | 1.02 | X | X | | | | | | | X |
| PS75/047-1 | 22.98 | 0.91 | X | X | | | | | | | X |
| PS75/048-1 | 19.88 | 1.9 | | | | | | | | | X |
| PS75/051-1 | 18.73 | 1.1 | X | X | X | | | | | | X |
| PS75/052-3 | 23.17 | 0.24 | X | X | X | X | X | | | | |
| PS75/054-1 | 22.38 | 0.19 | X | X | X | X | X | | | | |
| PS75/056-1 | 10.21 | 0.29 | X | X | X | X | X | | | | |
| PS75/057-3 | 18.12 | 1.1 | X | X | X | | | | | | X |
| PS75/058-2 | 12.96 | 0.41 | X | X | | X | X | | | | |
| PS75/059-2 | 13.98 | 0.41 | X | X | | | X | | | | |
| PS75/062-2 | 21.09 | 0.15 | X | X | X | X | X | | | | |
| PS75/063-1 | 22.46 | 0.19 | X | X | X | X | X | | | | |
| PS75/064-1 | 15.43 | 0.13 | X | X | X | X | X | | | | |
| PS75/065-1 | 18.6 | 4.5 | | | | | | X | | X | X |
| PS75/067-1 | 17.95 | 2.6 | | | | | | X | | X | X |
| PS75/068-2 | 14.12 | 12.5 | | | | | | X | | | X |
| PS75/069-1 | 18.46 | 1.4 | | | | | | | | | X |

| Core | Length [m] | CC Age [Ma]* | Project | | | | | | | | |
|---|---|---|---|---|---|---|---|---|---|---|---|
| | | | 1 | 2 | 3 | 4 | 5 | 6 | 7 | 8 | 9 |
| PS75/071-2 | 11.36 | 1.1 | X | X | | | | | | | X |
| PS75/072-2 | 14.97 | 0.42 | X | X | X | | X | | | | |
| PS75/072-4 | 9.61 | 0.28 | X | X | X | X | X | | | | |
| PS75/073-1 | 17.04 | 0.19 | X | X | | X | X | | | | |
| PS75/073-2 | 3.68 | 0.19 | X | X | | X | X | | | X | |
| PS75/074-3 | 20.95 | 0.91 | X | X | | | | | | | X |
| PS75/075-3 | 18.35 | 1.1 | X | X | | | | | | | X |
| PS75/076-2 | 20.95 | 1.1 | X | X | | | | | | | X |
| PS75/078-1 | 3.83 | 0.19 | X | X | | X | X | | | | |
| PS75/079-2 | 18.51 | 0.42 | X | X | X | X | X | | | | |
| PS75/080-1 | 12.20 | 0.19 | X | X | | X | X | | | | |
| PS75/081-1 | 13.71 | 0.42 | X | X | | X | X | | | | |
| PS75/082-1 | 10.88 | 0.16 | X | X | | X | X | | | | |
| PS75/083-1 | 13.13 | 0.42 | X | X | | X | X | | | | |
| PS75/085-1 | 19.74 | 0.19 | X | X | | X | X | | | | |
| PS75/086-2 | 12.47 | 2.8 | | | | | | X | | | X |
| PS75/087-1 | 11.28 | 3.5 | | | | | | X | | | X |
| PS75/088-6 | 12.40 | 0.42 | X | X | | X | X | | | | |
| PS75/089-3 | 11.12 | 3.5 | | | | | | X | | X | X |
| PS75/090-3 | 17.91 | 3.8 | | | | | | X | | X | X |
| PS75/091-3 | 13.44 | 1.1 | X | X | | | | | | | X |
| PS75/093-1 | 12.84 | 0.42 | X | X | | X | X | | | | |
| PS75/094-1 | 9.7 | 0.42 | X | X | X | X | X | | | | |
| PS75/095-5 | 17.85 | 0.65 | X | X | | X | X | | | | X |
| PS75/096-4 | 22.79 | 0.42 | X | X | | X | X | | | | |
| PS75/097-4 | 17.46 | 0.65 | X | X | | X | X | | | | X |
| PS75/098-5 | 22.83 | 1.1 | X | X | | | | | | | X |
| PS75/099-4 | 7.71 | 0.44 | X | X | X | X | X | | | | |
| PS75/100-4 | 14.77 | 0.44 | X | X | X | X | X | | | | |
| PS75/101-1 | 11.8 | 0.42 | X | X | X | X | X | | | | |
| PS75/102-1 | 12.96 | 0.42 | X | X | X | X | X | | | | |
| PS75/103-1 | 13.15 | 0.37 | X | X | X | X | X | | | | |
| PS75/104-1 | 12.39 | 0.13 | X | X | X | X | X | | | | |
| PS75/105-2 | 15.09 | 0.13 | | | X | ? | X | | | | |

Project 1:BIPOMAC (Timing and response of Pacific SO paleoceanography to external forcing mechanisms (Chapter 7.7.2)

Project 2:Pleistocene changes in Pacific Southern Ocean physical environment and ecosystem/export productivity regimes (Chapter 7.7.3)

Project 3:Pleistocene changes in South Pacific intermediate and bottom water circulation (Chapter 7.7.4)

Project 4:Last Glacial Maximum and glacial/interglacial transition (Chapter 7.7.5)

Project 5:Pleistocene warmer than present environments (Chapter 7.7.6)

Project 6:Pliocene-Pleistocene climate evolution ( Chapter 7.7.7)

Project 7:Further documentation of the Eltanin-asteroid impact in the Bellingshausen Sea (Chapter 7.7.8)

Project 8:Refinement of geomagnetic dating of Holocene-Pleistocene SO sediment records (Chapter 7.7.9)

Project 9:Refinement of Plio-Pleistocene biostratigraphic zonations (Chapter 7.7.10)

*CC (core catcher) age is a composite age of nannofossil and diatom ages (see Table 7.6.1)

## 7.2 Marine sediment echo-sounding using PARASOUND

Tanja Dufek, Rainer Gersonde, Frank Lamy — Alfred-Wegener-Institut

### Objectives, technical settings and operation condition

The sediment echo-sounder PARASOUND DS III - P70 (Atlas Hydrographic, Bremen, Germany) is permanently installed aboard *Polarstern*. It records sea floor and sub-bottom reflection patterns and thus characterizes the upper sediment layers according to their acoustic behavior.

The objectives of sediment echo-sounding during ANT-XXVI/2 included:

- selection of coring stations based on acoustic patterns and backscatter
- obtaining different patterns of high-resolution acoustic stratigraphy useful for lateral correlation over shorter and longer distances thereby aiding correlation of sediment cores retrieved during the cruise (Fig. 7.2.4).
- providing a high-resolution supplement of the uppermost sediments as part of the IODP seismic pre-site survey
- improvement of information on the sediment distribution in the Southern Ocean.

A transducer array is mounted in the ship's hull. It transmits an acoustic signal, which propagates through the water column down to the sea floor where parts of the signal are reflected. Other parts penetrate the sea floor and are reflected at boundaries between sediment layers. In Fig. 7.2.1, a comparison of the returning echo, the PARASOUND online echogram and the density record of core PS75/047-1 is shown. The correlation between the size of amplitude of the returning echo and the density of the upper sediment layers can be seen clearly. The denser a sediment layer the larger the reflected signal.

PARASOUND uses the parametric effect. It produces additional frequencies through non-linear acoustic interactions of finite amplitude waves. By emitting two primary sound waves of higher frequency (18.8 and 22.8 kHz) a signal of the differential frequency (4 kHz) is generated. Due to its longer wavelength the secondary low frequency (SLF) signal allows a sub-bottom penetration up to 200 m (depending on the thickness of the sediment cover and its density and composition) with a vertical resolution of 30 cm. Due to the parametric effect the pulse is generated within the narrow emission cone (4°) of the primary high frequencies (PHF) and thereby a very high lateral resolution compared to conventional 4 kHz-systems is provided. The secondary high frequency (SHF) is a sum signal of the primary frequency and was not used during ANT-XXVI/2.

The PARASOUND system is controlled by two operator software packages (ATLAS HYDROMAP CONTROL, ATLAS PARASTORE-3) and server software running in the background. These processes are running simultaneously on a PC using a Windows XP operating system. ATLAS HYDROMAP CONTROL is the control software for the echosounder. It is used to set the modes of operation, sounding options and ranges. ATLAS PARASTORE-3 is an acquisition and visualisation software.

Before the system was switched on, a software update for PARASTORE-3 was

installed. During station work south of 60°00' S, whale watching was carried out. In the event that a whale would have been observed closer than 100 m to the vessel, the acoustic systems PARASOUND and HYDROSWEEP DS2 would have been switched off immediately.

Time windows with data of special interest (e.g. geological structures at or near stations) were replayed during the cruise using optimal settings of ATLAS PARASTORE-3. The software SeNT (University of Bremen) was used for visualizing PS3 files of the SLF signal for interesting areas. The echograms of all coring stations are shown in Appendix A.6.

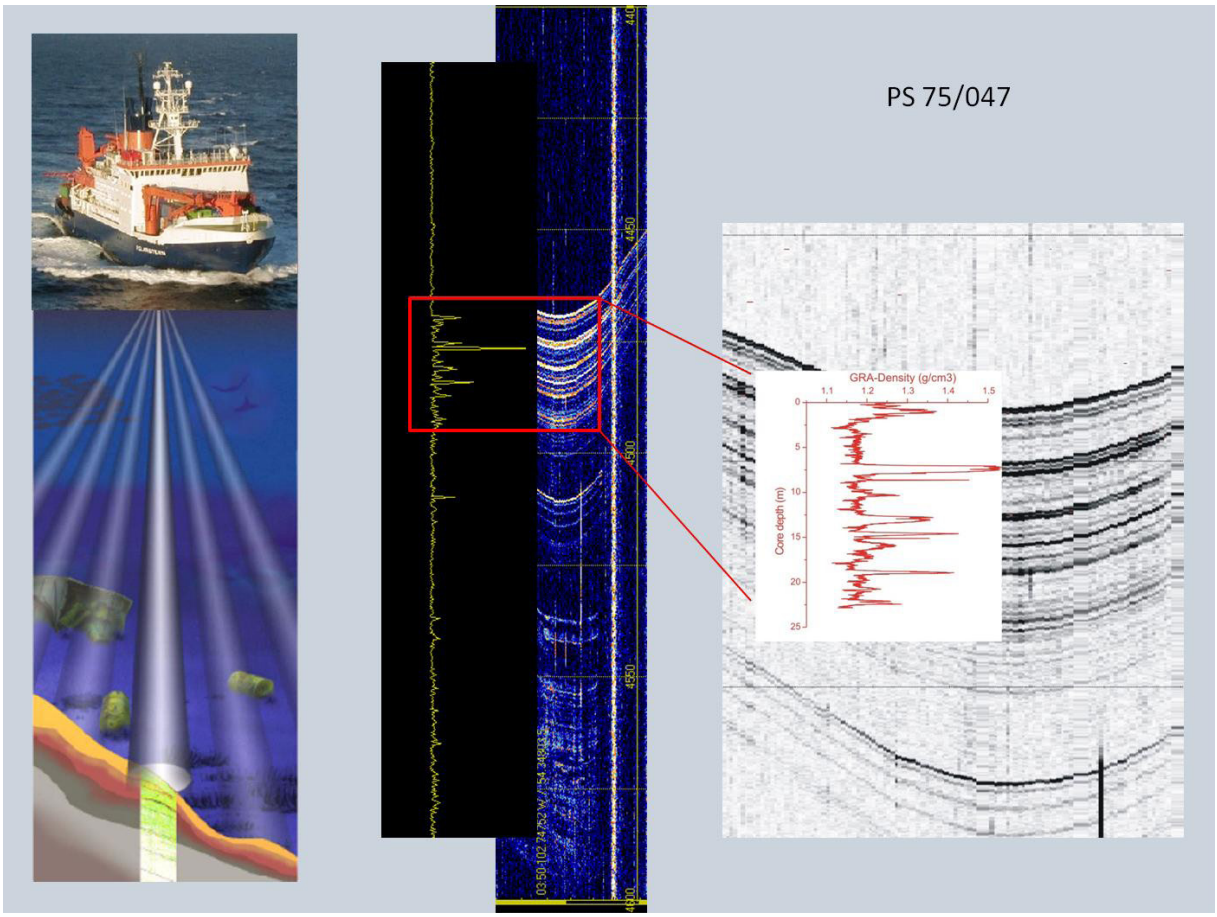


*Fig.7.2.1: Comparison of returning echo, PARASOUND online echogram and GRA-density record of Core PS75/047-1*

**Data management**

During ANT-XXVI/2 data acquisition and storage was switched on after leaving the Chilean EEZ on November 29, 2009 at 15:00 UTC and was switched off on January 24, 2010 at 23:00 UTC. Acquisition included PHF and SLF data. Both frequencies were stored in ASD (Atlas Sounding Data) format. This is a raw file format and stores the complete sounding profiles including reflections from the water column, the seafloor,

and the subsurface echoes down to 200 m bottom penetration. The SLF signal was additionally stored in PS3 and SEG-Y format. These formats only save data that is displayed in the PARASTORE reception window (200 m depth window). Both PHF and SLF traces were visualized as online profiles on the screen. Furthermore, navigation data and general PARASOUND settings as well as ATLAS PARASTORE-3 settings were stored in ASCII format for the duration of data acquisition. SLF profiles (200 m depth window) and online status prints were printed on A4 pages.

While steaming, the quasi-equidistant transmission mode for signal transmission was used. The desired time interval between signal transmissions was set between 1,000 and 2,000 ms. During station work, the transmission mode was set to single pulse in order to reduce data volume. The system was operator-controlled during ANT-XXVI/2 (watch keeping). Book keeping was carried out including basic PARASOUND system settings, some navigation information, and remarks concerning e.g. station work and system failures. Additionally, a low-resolution and hand-drawn bathymetry plot with sketches of SLF online profiles was included to allow points of interest to be located quickly.

At the beginning of the cruise the system depth source was set to the Deep Water Sounder (DWS). Depth measurements were not stable and regular failures occurred. Therefore, the system depth was entered into the system manually during the first days. Thereafter, the system depth source was set to the multi-beam echo-sounder HYDROSWEEP DS2, and no further problems occurred. In total six system crashes were observed. Two of them affected PARASTORE-3 only. These occurred during station work and data storage could be restarted quickly without large loss of data. In four cases, the PARASOUND crashed during transits due to problems with the system software (Windows) and it was necessary to restart the operator PC. During the ~30 minutes required for the restart process, no PARASOUND-data could be recorded.

**Work at sea and results**

After pre-selection of working areas based on oceanographic and marine geological background information, PARASOUND acoustic profiles played an important role in locating coring stations. Site selection was based on acoustic patterns such as the strength of characteristic reflectors, their spacing, and the total sub-bottom penetration. A short outline regarding the general sediment cover and sub-bottom penetration as well as special geological structures recorded with the PARASOUND system within the individual transects of ANT-XXVI/2 is given below (for location of transects see Fig. 7.4.1; Chapter 7.4).

*Transect 1: Mornington Abyssal Plain – Eltanin-Tharp Fracture Zone (MAP-ETFZ)*

The PARASOUND system was switched on after leaving the Chilean EEZ and the first coring station was found shortly afterwards in an area of thick sediment cover. On Subtransect 1a covering the Freeden Seamounts/Eltanin (FS/ET) area, locations of sediment cores were chosen in areas of comparatively low sedimentation-rates (closely spaced reflectors) and reduced sub-bottom penetration in order to obtain cores reaching the Eltanin meteorite debris ejecta layer and the reworked sediment package below. This was successful at three of eight stations (Chapter 7.4) as the impact-related deposits were not clearly indentified in the PARASOUND profiles.

The first part of the E-W transect from the FS/EI area towards the East Pacific Rise (EPR) is generally characterized by good sub-bottom penetration (~50 - 100 m) and selection of coring stations was easy (PS75/047 to PS75/051). The first deep station (PS75/044) was found in an area of moderate sub-bottom penetration. The crossing of seamounts with depths as shallow as ~500 m revealed only thin sediment cover (a multicorer at station PS075/045 recovered foraminifera sand). Approximately 140 nm further west, a deeper seamount shows ~40 m sub-bottom penetration from which a ~18 m sequence of calcareous ooze has been recovered (PS75/046-2; Chapter 7.4). Sub-bottom penetration increased southwards towards the northern Amundsen Abyssal Plain (AAP) (Subtransects 1a and 1b) where core PS75/052-3 was collected in an area of >200 m penetration (Fig. 7.2.2). The PARASOUND data suggest mostly moderate but not continuous sediment cover (~10 - 30 m) across the crest of the EPR which decreases to the west where at station PS75/058-59 calcareous ooze was recovered and core barrels were bent in the process.

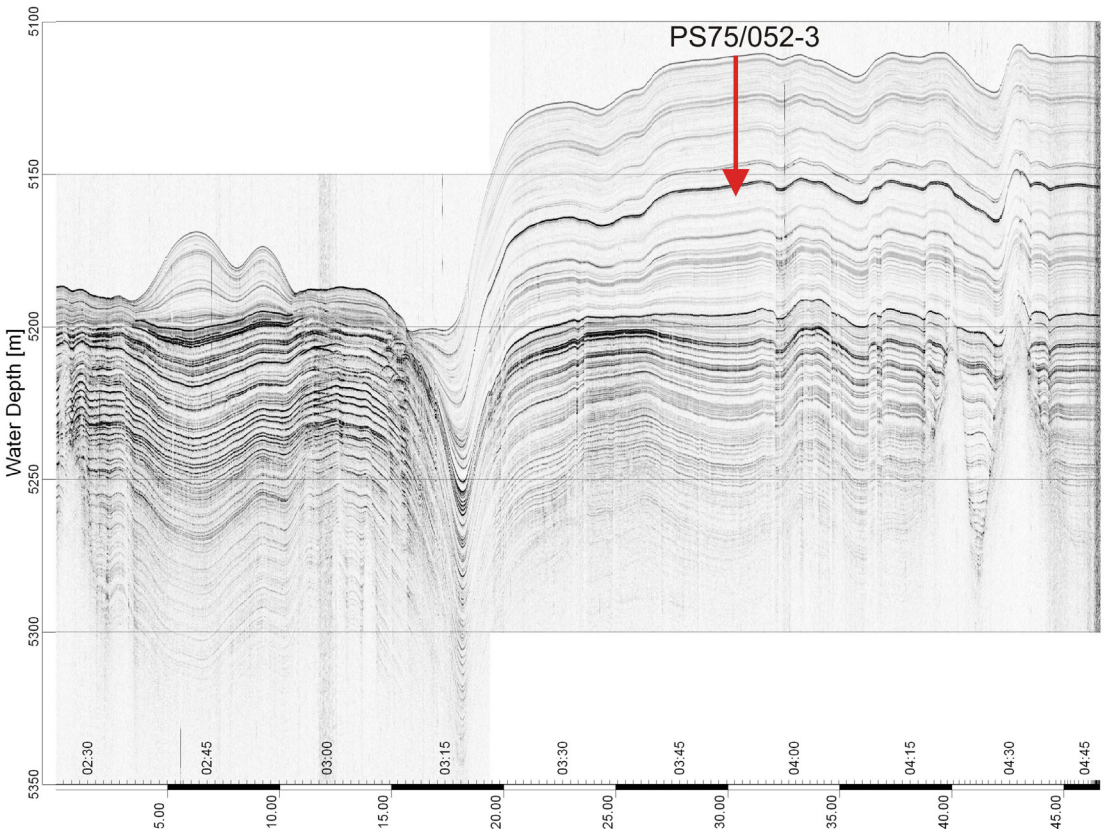


*Fig. 7.2.2: Echogram showing the area of core location PS75/052-3 on a sediment drift(horizontal bars indicate distance of 5 km). The basal age of the core is ~220 kyr.*

*Transect 2: ETFZ-AAP*

Acoustically visible sediment cover was nearly absent south of the ETFZ and on the whole eastern flank of the ridge system south to the Udintsev Fracture Zone (UFZ) (Fig. 7.2.3). A multicorer recovered no sediments at station PS75/061. Directly south of the UFZ ~150 m sub-bottom penetration reveals significant sediment cover. In the vicinity of the Polar Front, two >20 m long sediment cores were recovered (PS75/062-063), which consist of diatom ooze and display high sedimentation rates (Chapter 7.1). Further SE, sub-bottom penetration was moderately high (~20 - 50 m) until station PS75/064 where sediments similar to those at PS75/062-063 were recovered (Chapter 7.4). Acoustically visible sediment cover is significantly reduced south of PS75/064 into the northern AAP. A detailed PARASOUND survey of several seamounts at the southern end of the transect in order to find suitable coring locations in shallower water depths revealed very little sediment cover in this area, which is characterized by rough topography. Two sediment cores extracted from small areas of restricted sub-bottom penetration contain deep-sea sediments with slow accumulation rates and Pliocene basal ages (PS75/067-068; Chapter 7.3 and 7.6).

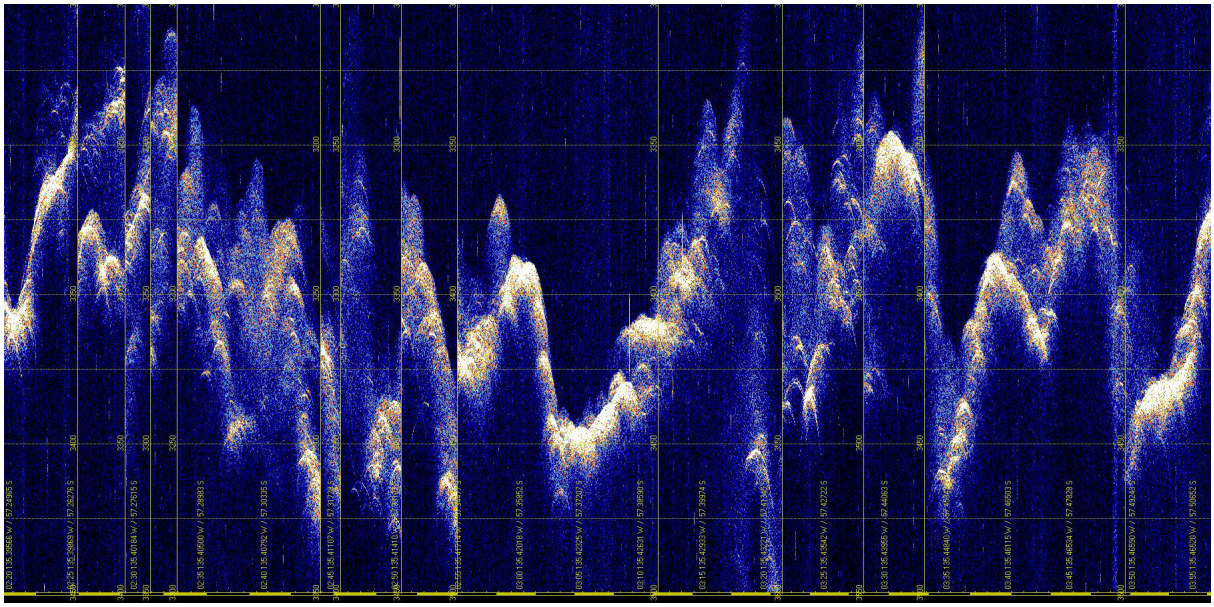

*Fig. 7.2.3: Online echogram of Udintsev Fracture Zone (UFZ) (horizontal bars indicate distance of 1 km)*

*Transect 3: AAP-Southwest-Pacific Basin (SWP)*

Similar conditions prevailed during the first part of this SE-NW transect until the crest of the Pacific Antarctic Ridge (PAR). Directly NW of the crest, a thin sediment cover was present locally, but an attempt to recover a short piston core was unsuccessful, and all tubes were lost. Approximately 50 nm further NW, a thin (~10 - 15 m) sediment cover was visible with the PARASOUND system, and is consistent with the 11.36 m-long core PS75/071-2 that possibly penetrated to the basement (basalt fragments in the

core catcher; Chapter 7.3). The remaining part of the NW PAR flank (i.e., south of the PF and in the Polar Front Zone) generally revealed higher sub-bottom penetration in the range of ~50 - 70 m.

*Transect 4: SWP-northern Ross Sea (ROS)*

The same applies for the corresponding section of the following NNE-SSW transect, where penetration frequently reached up to ~90 m. Correlation of characteristic reflectors in the echograms of stations PS75/080-083 and 085 was possible and is consistent with lithological, biostratigraphic, and physical property data (Fig. 7.2.4). Sediment cover abruptly decreased close to the crest of the PAR and remained low as far as the northern ROS. In this area, stations were selected in isolated areas of moderate sediment penetration of up to ~50 m and recovered comparatively slowly accumulated deep-sea sediments (Chapter 7.4 and 7.5).

*Transect 5: ROS-New Zealand Margin (NZM)*

On the last SSE-NNW transect across the PAR, the situation was similar to the southern part of the previous transect northward up to station PS75/090. On the subsequent NNW flank of the PAR, no sediments could be detected acoustically. Just north of the crest, the PARASOUND penetration started to increase again (station PS75/091) and nearly continuous sediment cover with moderate sub-bottom penetration (~10 - 40 m) extends northward to the PF. On a parallel track across the PF 45 nm to the west, sub-bottom penetration was higher and reached up to ~100 m. Acoustically visible sediment cover was again slightly reduced and patchier in the Polar Front Zone. An exception is the area close to station PS75/095 where a larger-scale elongated basin on a topographic high with sub-bottom penetration of ~70 m was found. The subsequent crossing of the deepest part of the SWP revealed moderate sub-bottom penetration (up to ~50 m) south to ~54°00'S, a short section of reduced penetration between ~54°00'S and ~53 °30'S, and a thick sediment cover NW of ~54°00'S. Sediment core PS75/098-4 was recovered from an area of ~110 m of acoustically visible sediment cover. Approaching the outer NZM, the uppermost sediment cover becomes more and more condensed (Campbell drift) consistent with sediment cores from the area, which recovered a thin Plio-Pleistocene sequence above Cretaceous drift sediments (ODP Site 1121; Carter et al., 2004).

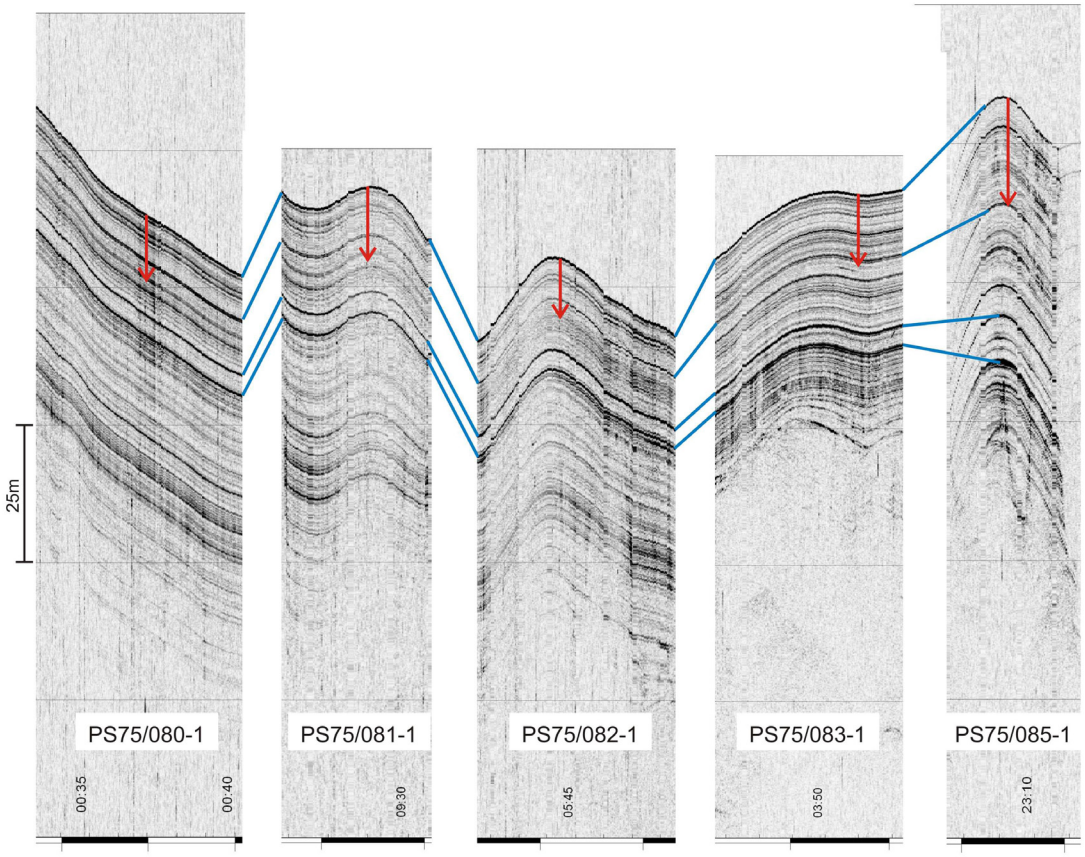


*Fig 7.2.4: Correlation of characteristic reflectors in echograms of stations PS75/080-083 & 085. Red arrow indicates approximate core penetration. The distance between stations PS75/080 and 085 is ~240 nm.*

At the NZM, we crossed the Pukaki Saddle between the Campbell Rise and the Bounty Plateau. On the saddle, a continuous sediment cover with ~100 m sub-bottom penetration and strong reflectors in the uppermost ~8 m is present. Core PS75/099-4 penetrated to the base of this unit. Leaving the Pukaki Saddle, we passed the Bounty Channel and reached the Bounty Trough. Approximately ~30 nm north of the channel, the ship track changed in westerly direction and proceeded upslope with respect to the Bounty Trough. In this area, PARASOUND data suggest strong faulting and significant discordances below a thin Late Quaternary sediment layer (Fig. 7.2.5). Thicker late Quaternary sediments occur in restricted small-scale slope basins (Station PS75/100). Further upslope, sediment cover increases and becomes more continuous (stations PS75/101 to PS75/105).

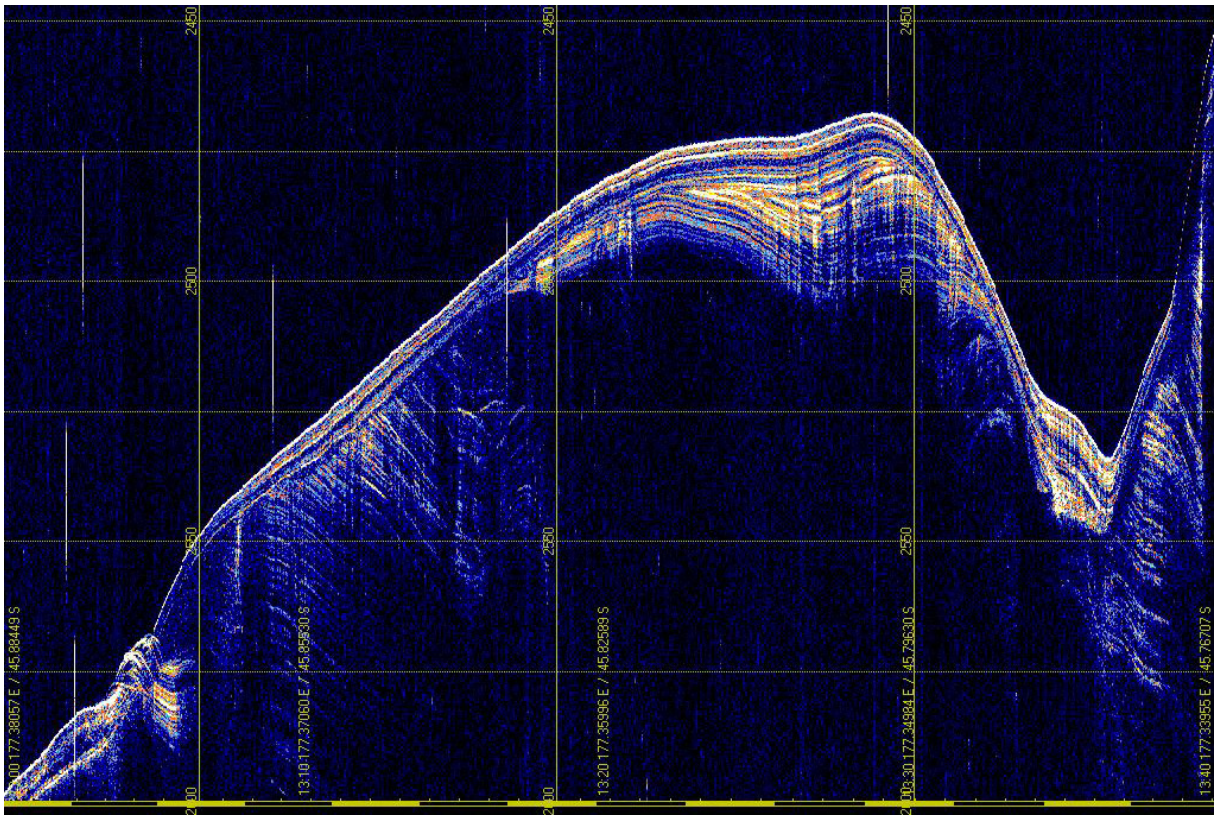

*Fig 7.2.5: Online echogram in the area of the lower Bounty Trough showing significant discordances. (Horizontal bars indicate distance of 1 km)*

## References

Carter, R.M., McCave, I.N., and Carter, L., 2004. Leg 181 synthesis: fronts, flows, drifts, volcanoes, and the evolution of the southwestern gateway to the Pacific Ocean, eastern New Zealand. In Richter, C. (Ed.), Proc. ODP, Sci. Results, 181, 1–111 [Online].

## 7.3 Surface sediment sampling

Oliver Esper, Sze Ling Ho, Franziska Kersten, Silke Steph — Alfred-Wegener-Institut

## Objectives

The acquisition of surface samples is required to document modern sedimentation pattern, understand sedimentation processes and to generate reference data sets for paleoceanographic proxy calibration (for details see 7.7.1).

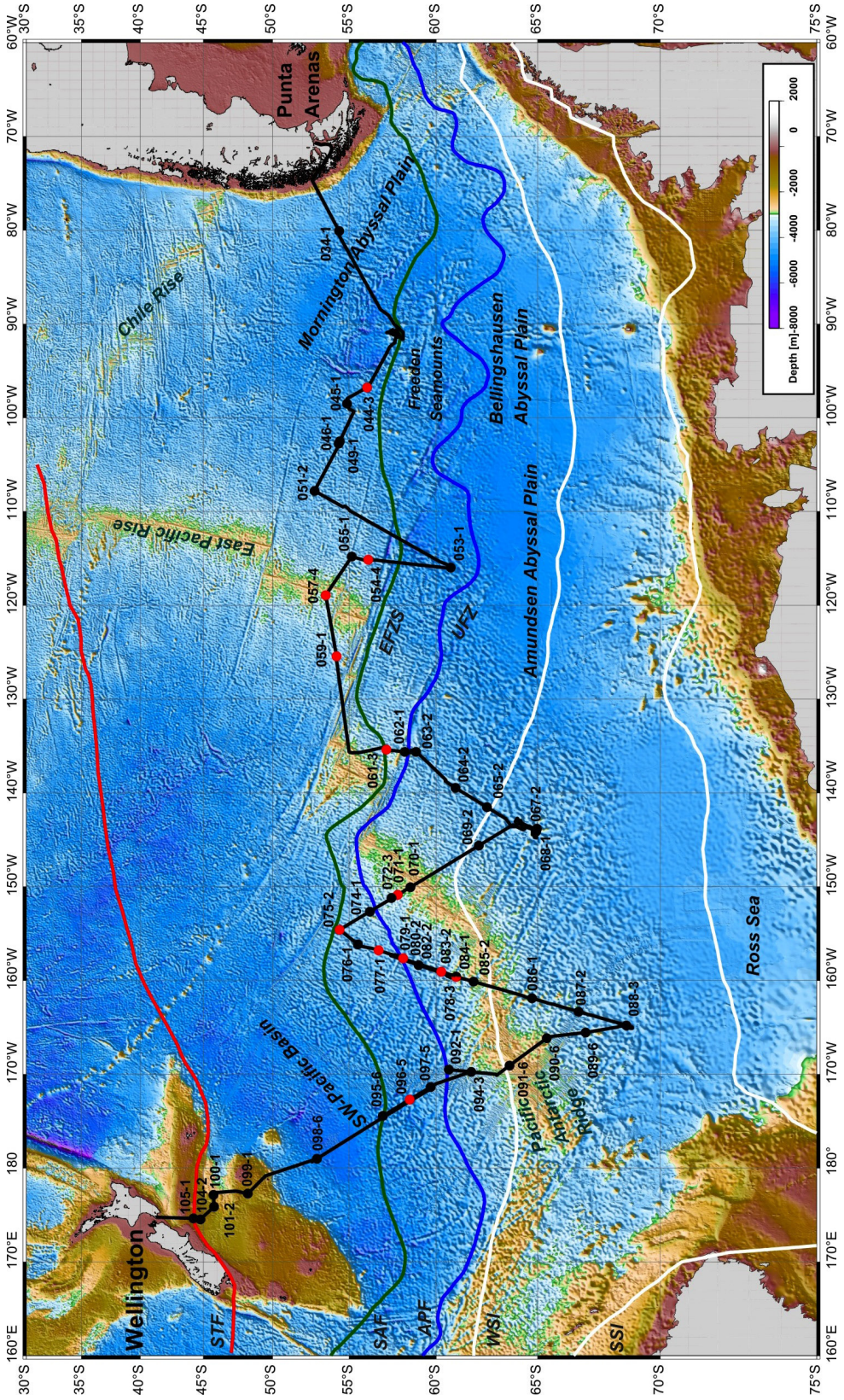


*Fig. 7.3.1: Location of surface sediment sampling sites (multi-corer, box corer). Red dots indicate sites no surface sediment was recovered (see Table 7.3.1)*

**Work at sea**

To recover surface sediment a multi-corer (MUC) consisting of 12 tubes, 60 cm in length and 6 cm in diameter was deployed at 50 sites was deployed at 50 sites. Additionally a large box corer (size of box 50x50x60 cm) was deployed at two sites. The sampling with the MUC was successful at 39 sites and a total of 321 MUC-cores was recovered with lengths between 3 and 47 cm (Figs. 7.3.1, 7.3.2, Table 7.3.1). Reasons for low or no recovery include strong ship's heave due to heavy weather conditions, high carbonate content of surface sediment, and possible mechanical problems. After unsuccessful deployments at stations PS75/057 - /061, a spare MUC was successfully deployed at stations PS75/061 to PS75/070. Unfortunately this MUC got mechanical problems leading to the non-release of one tube row, which could not be solved near-term. Consequently the first MUC was deployed again starting at Site PS75/083 until it broke at PS75/083 due to an incident with the wire. It was then replaced by the spare MUC, which was used until the end of the cruise. The sediment type of the recovered sediment cores varies strongly within the different regions and depositional milieus covered by the cruise including deep-sea clay, diatom and nannofossil oozes, and foraminiferal sands. At several locations manganese nodules were recovered at the recovered sediment surface (Table 7.3.1).

The sediment filled MUC tubes were frozen at -20°C for at least 24 hours. Then the cores were pushed out of the MUC tube and sealed in plastic bags. One third of the recovered cores were wrapped in aluminum foil to allow for later biogeochemical analyses. The frozen cores were stored at –20°C.

The large box corer (GKG) was deployed at two sites (PS75/078, PS75/099), but only at the second site surface sediment was recovered. For surface sediment sampling the upper 1 cm of sediment was removed with a spoon over an area of 14.5 x 27 cm and stored in a nalgene bottle. Additionally two gravity core liner tubes were pushed in the sediment and stored for later analyses.

Besides sediment, at some stations bottom water above the recovered sediment surfaces was samples for biogeochemical analyses to determine possible sources of specific biomarkers and for the determination of GDGT *in-situ* formation (see Chapter 4.4).

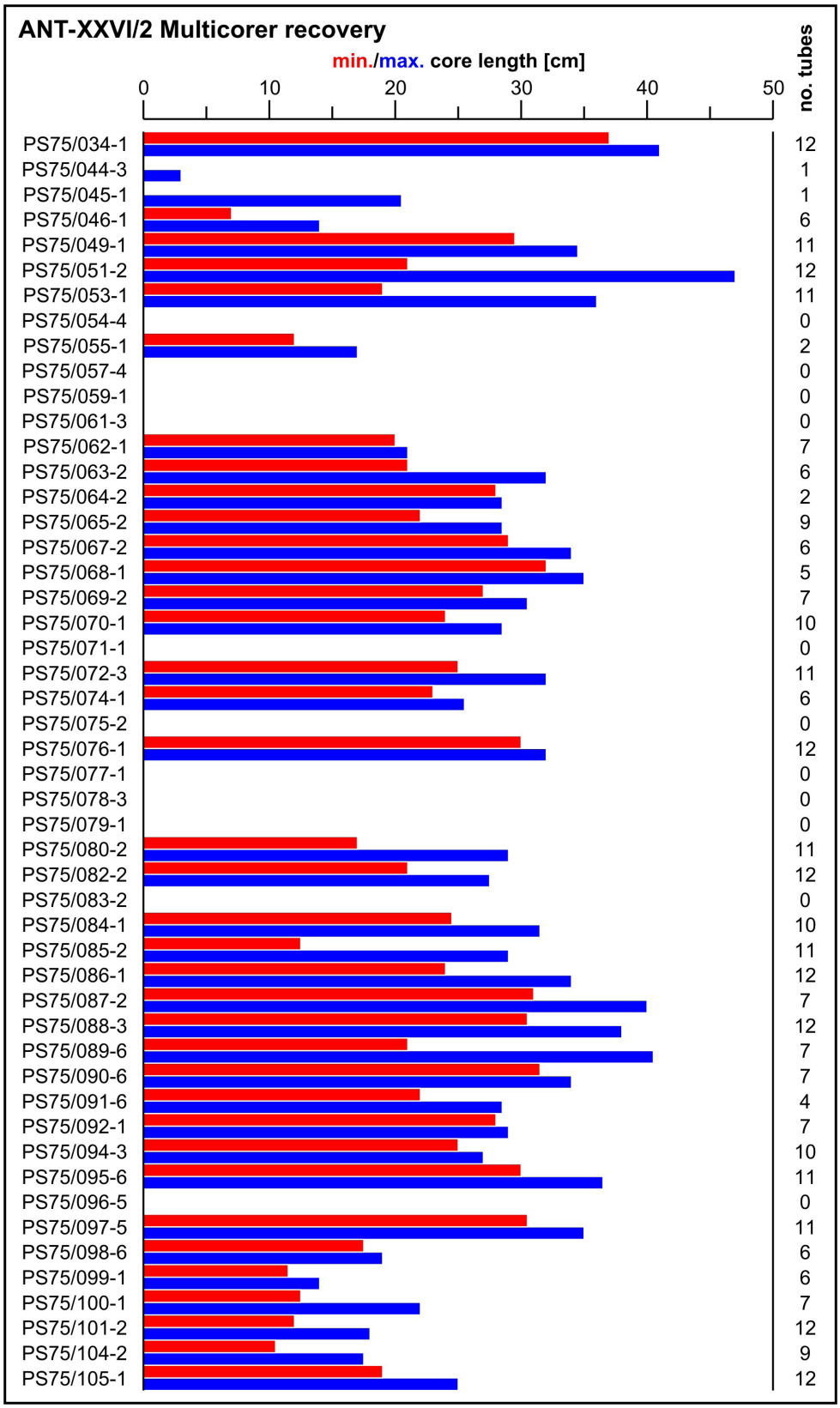


*Fig. 7.3.2: Multi-corer recovery diagram*

**Tab. 7.3.1:** Recovery of surface sediments (red numbers indicate partial outflow)

| Station (PS75/...) | length of multicores [cm] | | | | | | | | | | | | Remarks |
|---|---|---|---|---|---|---|---|---|---|---|---|---|---|
| | 1 | 2 | 3 | 4 | 5 | 6 | 7 | 8 | 9 | 10 | 11 | 12 | |
| 034-1 | 39.0 | 38.0 | 39.0 | 41.0 | 41.0 | 41.0 | 38.0 | 38.0 | 38.0 | 37.0 | 38.0 | 39.0 | |
| 044-3 | 3.0 | - | - | - | - | - | - | - | - | - | - | - | Outflow |
| 045-1 | 20.5 | | | | | | | | | | | | Outflow |
| 046-1 | 14.0 | 7.0 | 13.0 | 9.0 | 8.5 | 10.5 | - | - | - | - | - | - | |
| 049-1 | 34.0 | 34.0 | 34.5 | 34.0 | 34.5 | 31.0 | 29.5 | 32.5 | 29.5 | 28.0 | 30.0 | - | |
| 051-2 | 47.0 | 45.5 | 47.0 | 46.0 | 47.0 | 46.0 | 47.0 | 45.0 | 42.0 | 45.0 | 45.5 | 21.0 | |
| 053-1 | 19.0 | 29.0 | 28.5 | 30.0 | 36.0 | 33.0 | 32.0 | 32.0 | 28.0 | 29.0 | 32.0 | - | |
| 054-4 | - | - | - | - | - | - | - | - | - | - | - | - | Outflow |
| 055-1 | 17.0 | 12.0 | - | - | - | - | - | - | - | - | - | - | Outflow |
| 057-4 | - | - | - | - | - | - | - | - | - | - | - | - | Outflow |
| 059-1 | - | - | - | - | - | - | - | - | - | - | - | - | Outflow |
| 061-3* | - | - | - | - | - | - | - | - | - | - | - | - | Outflow |
| 062-1 | 21.0 | 21.0 | 21.0 | 21.0 | 21.0 | 21.0 | 20.0 | - | - | - | - | - | no release |
| 063-2 | 29.0 | 28.0 | 21.0 | 30.0 | 32.0 | 30.0 | - | - | - | - | - | - | no release |
| 064-2 | 28.0 | 28.5 | - | - | - | - | - | - | - | - | - | - | no release |
| 065-2 | 27.5 | 25.0 | 27.0 | 26.5 | 28.0 | 28.0 | 26.5 | 28.5 | 22.0 | - | - | - | mang.nod. |
| 067-2 | 32.0 | 29.0 | 32.0 | 33.0 | 34.0 | 30.0 | | | | | | | mang.nod |
| 068-1 | 32.0 | 32.0 | 35.0 | 33.0 | 33.0 | - | - | - | - | - | - | - | mang.nod |
| 069-2 | 30.5 | 30.0 | 29.5 | 29.0 | 27.0 | 29.0 | 27.5 | - | - | - | - | - | no release |
| 070-1 | 26.0 | 27.0 | 26.5 | 27.5 | 28.5 | 28.0 | 27.0 | 28.0 | 24.0 | 28.0 | - | - | |
| 071-1 | - | - | - | - | - | - | - | - | - | - | - | - | Outflow |
| 072-3** | 28.0 | 25.0 | 30.0 | 32.0 | 31.0 | 30.0 | 30.0 | 29.5 | 29.0 | 27.0 | 26.0 | - | |
| 074-1 | 24.5 | 25.5 | 25.0 | 24.0 | 23.0 | 23.0 | - | - | - | - | - | - | |
| 075-2 | - | - | - | - | - | - | - | - | - | - | - | - | Outflow |
| 076-1 | 30.5 | 30.0 | 31.0 | 31.0 | 32.0 | 30.0 | 31.0 | 30.5 | 30.0 | 31.0 | 31.0 | 31.0 | |
| 077-1 | - | - | - | - | - | - | - | - | - | - | - | - | Outflow |
| 078-3 | - | - | - | - | - | - | - | - | - | - | - | - | Outflow |
| 079-1 | - | - | - | - | - | - | - | - | - | - | - | - | Outflow |
| 080-2 | 26.0 | 29.0 | 26.0 | 25.0 | 26.0 | 28.0 | 26.0 | 27.0 | 24.0 | 27.0 | 17.0 | - | |
| 082-2 | 27.5 | 25.0 | 27.0 | 27.0 | 27.0 | 21.0 | 27.5 | 27.0 | 23.0 | 26.5 | 25.0 | 21.0 | |
| 083-2*** | - | - | - | - | - | - | - | - | - | - | - | - | M U C broken |
| 084-1 | 29.5 | 31.5 | 30.5 | 29.0 | 28.5 | 30.5 | 24.5 | 30.5 | 28.0 | 28.0 | - | - | |
| 085-2 | 12.5 | 27.5 | 29.0 | 25.0 | 27.0 | 16.5 | 28.0 | 19.5 | 27.0 | 22.0 | 25.0 | - | |
| 086-1 | 33.0 | 32.5 | 33.5 | 34.0 | 33.0 | 32.5 | 30.0 | 32.0 | 24.0 | 33.0 | 31.0 | 32.0 | mang.nod |
| 087-2 | 31.0 | 38.0 | 38.0 | 37.5 | 37.0 | 38.0 | 40.0 | - | - | - | - | - | no release |
| 088-3 | 35.5 | 36.0 | 38.0 | 37.0 | 38.0 | 36.5 | 35.0 | 35.0 | 35.0 | 32.0 | 36.6 | 30.5 | |
| 089-6 | 39.5 | 21.0 | 40.5 | 40.0 | 40.0 | 40.0 | 39.0 | - | - | - | - | - | no release |
| 090-6 | 33.0 | 33.5 | 34.0 | 34.0 | 31.5 | 33.0 | 34.0 | - | - | - | - | - | no release |
| 091-6 | 22.0 | 28.5 | 23.5 | 25.0 | - | - | - | - | - | - | - | - | no release |
| 092-1 | 29.0 | 28.0 | 29.0 | 29.0 | 29.0 | 28.0 | 28.0 | - | - | - | - | - | no release |
| 094-3 | 25.0 | 26.0 | 26.5 | 25.0 | 25.5 | 25.0 | 26.5 | 26.0 | 27.0 | 26.0 | - | - | |
| 095-6 | 36.0 | 36.5 | 36.0 | 35.0 | 34.5 | 36.0 | 36.0 | 35.0 | 30.0 | 35.0 | 34.0 | - | |

| Station (PS75/...) | length of multicores [cm] | | | | | | | | | | | | Remarks |
|---|---|---|---|---|---|---|---|---|---|---|---|---|---|
| | 1 | 2 | 3 | 4 | 5 | 6 | 7 | 8 | 9 | 10 | 11 | 12 | |
| 096-5 | - | - | - | - | - | - | - | - | - | - | - | - | Outflow |
| 097-5 | 34.5 | 35.0 | 34.5 | 33.0 | 33.5 | 34.5 | 30.5 | 33.0 | 32.5 | 30.5 | 33.0 | - | |
| 098-6 | 38.0 | 35.5 | 35.0 | 37.0 | 37.5 | 38.0 | - | - | - | - | - | - | no release |
| 099-1 | 14.0 | 14.0 | 14.0 | 11.5 | 13.0 | 13.5 | - | - | - | - | - | - | no release |
| 099-7**** | 29.0 | 26.0 | 1.0 | 1.0 | 1.0 | 1.0 | 1.0 | 1.0 | - | - | - | - | GKG |
| 100-1 | 22.0 | 15.5 | 16.0 | 15.0 | 15.0 | 12.5 | 14.0 | - | - | - | - | - | no release |
| 101-2 | 18.0 | 12.0 | 13.0 | 14.0 | 15.0 | 12.0 | 15.5 | 15.0 | 16.0 | 16.0 | 18.0 | 17.5 | |
| 104-2 | 15.0 | 16.0 | 15.0 | 16.5 | 15.0 | 17.5 | 14.0 | 11.0 | 10.5 | - | - | - | |
| 105-1 | 23.5 | 23.5 | 21.5 | 22.0 | 22.5 | 23.0 | 19.0 | 23.5 | 23.0 | 24.5 | 25.0 | 24.0 | |

* due to several outflow incidents the first MUC was replaced by the second MUC (second MUC had sometimes problems to release both 5-tube rows; this is indicated as **no release**)

** due to severe releasement problems of the second MUC the first MUC was re-employed

*** the first MUC broke and was substituted again by the second MUC

**** at station PS75/099 a large box corer (GKG) was deployed in addition to the multi-corer

## 7.4 Sediment coring, core documentation, storage, and on-board sampling

Marcelo Arevalo[1], Ute Bock[1], Ulrich Breitsprecher[1], Giuseppe Cortese[2], Oliver Esper[1], Susanne Fietz[3], Rainer Gersonde[1], Thomas Gölles[1], Sze-Ling Ho[1], Lorenz Hutzler[1], Franziska Kersten[1], Matt Konfirst[4], Frank Lamy[1], Norbert Lensch[1], Alfredo Martinez-Garcia[5], Marie Meheust[1], Katharina Pahnke[6], Gemma Rueda[3], Mariem Saavedra-Pellitero[7],Timo Schaper[1], Ina Schulze[1], Silke Steph[1,8], Marietta Straub[5]

[1]Alfred-Wegener-Institut
[2]GNS Science
[3]Universitat Autònoma de Barcelona
[4]Northern Illinois University
[5]ETH-Zürich
[6]University of Hawaii
[7]University of Salamanca
[8]University of Potsdam

### 7.4.1 Methods

During ANT-XXVI/2 54 piston corers with core barrel length between 15 and 30 m (KOL), 7 gravity corers with length between 13 and 20 m (SL), and one 12 m long kasten corer were used to recover long sedimentary sequences. Of those, 61 deployments were successful and resulted in a total core recovery of 1,030.41 m including 36.15 m core length recovered by the pilot corer (TC) triggering the KOL (Tables 1.2.1, 7.4.1; Fig. 7.4.1). At station PS75/070 all barrels of the piston corer were lost, however the trigger corer recovered 0.9 m of sediment. The gear types and the length of the coring devices were chosen based on sediment acoustic profiles with the PARASOUND echo-sounding system considering acoustic patterns such as the strength of characteristic

reflectors, their spacing, and the total sub-bottom penetration (Chapter 7.2).

The sediment cores taken with piston and gravity corers were cut into 1 m long segments on board *Polarstern*. Before closing the core segments with plastic caps, smear slides were taken from each segment top for biostratigraphic analyses and initial carbonate content determinations were performed using 15 %-hydrochloric acid. After the measurement of physical properties with two multi-sensor core loggers (see 7.5), segments, which were not opened on board *Polarstern* were stored in a reefer container at a temperature of 4° C and transported to Bremerhaven.

Based on initial biostratigraphic analyses and physical property data, cores were selected for opening and restricted on-board sampling. At a few stations, the uppermost one or two segments were not split in order to avoid disturbance of water-rich sediments. Additionally, selected segments of three piston cores recovered in the Freeden Seamounts area were opened and sampled to identify deposits related to the Eltanin asteroid impact. These segments were chosen based on preliminary biostratigraphic analyses and on the correlation of ANT-XXVI/2 sediment cores to cores previously recovered in the area (ANT- XII/4, ANT-XVIII/5a) by means of magnetic susceptibility.

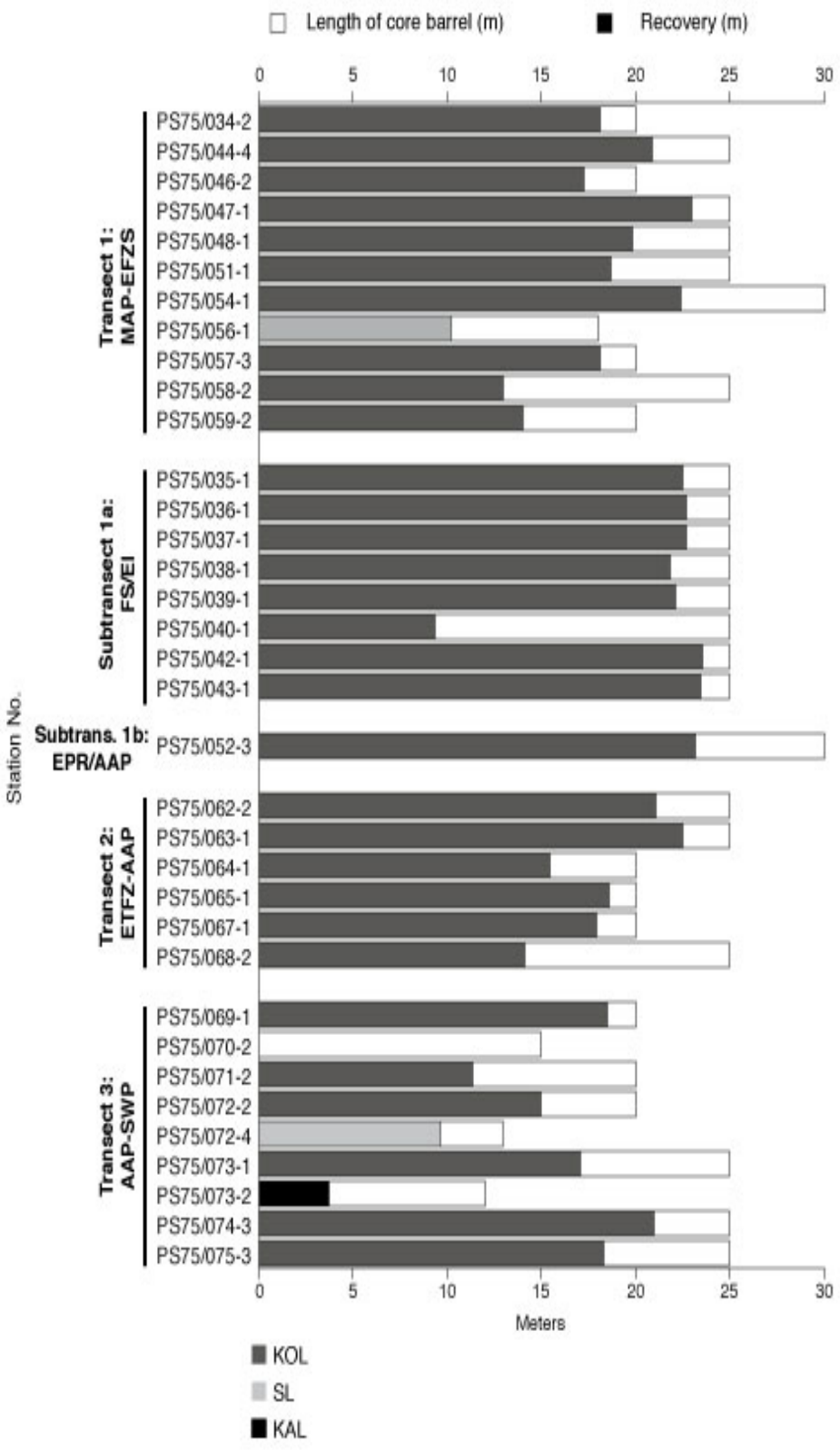


*Fig.7.4.1: Length of core barrel and core recovery (m) of piston corers (KOL), gravity corers (SL) and kasten corers (KAL) deployed during ANT-XXVI/2*

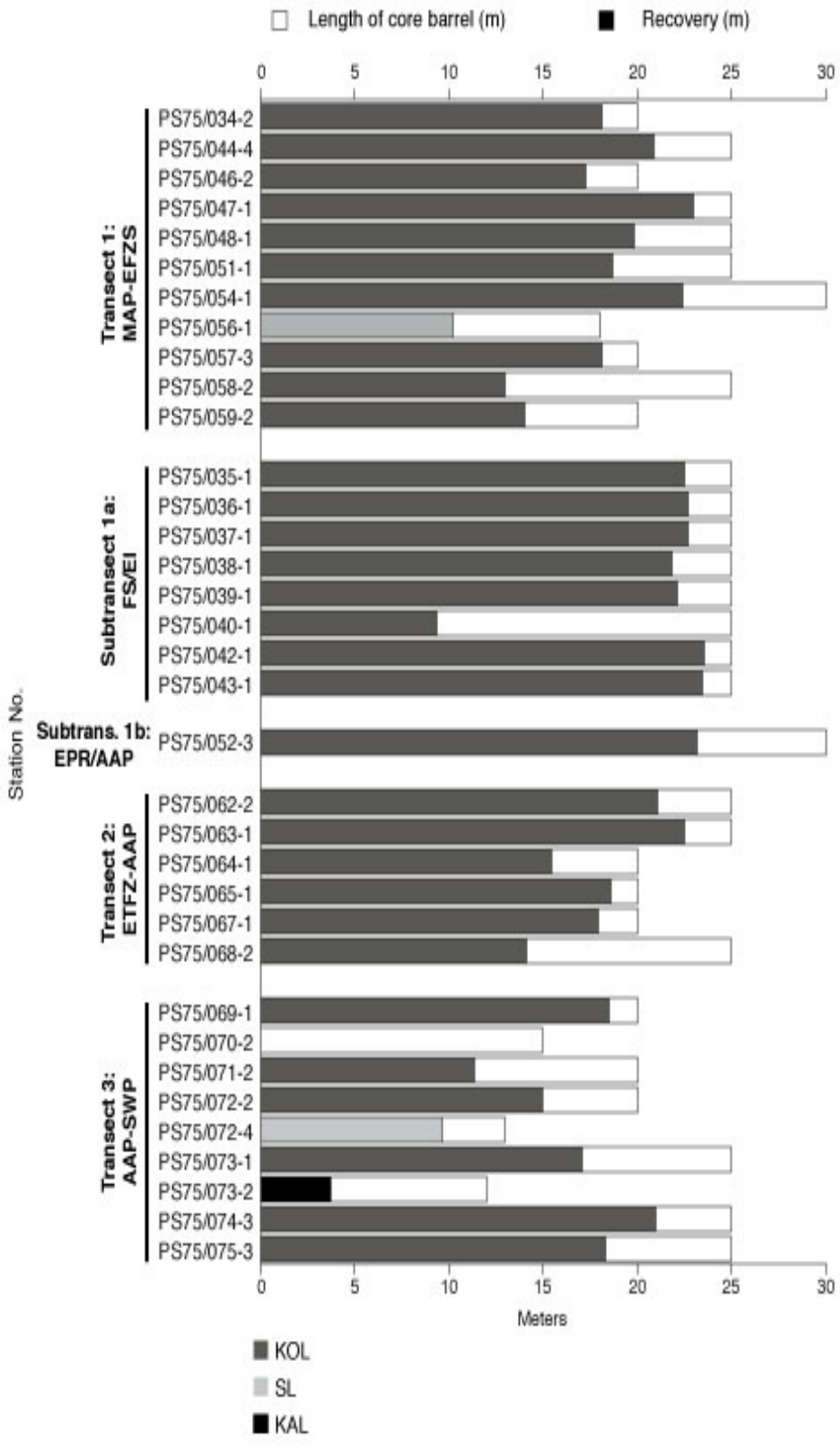


*Fig.7.4.1: (Continued)*

After opening and splitting, the sections were photographed. Sediment core description was performed on the archive half. Sediment colors were determined using a “Munsell Soil Color Chart“. Visual core description was complemented by microscopic analysis

of sediment smear slides from all major lithologies found in the individual cores. The lithological classification followed the scheme suggested by Mazzullo et al. (1988). According to this classification, sediments encountered during ANT-XXVI/2 are granular sediments consisting of pelagic and, subordinately, siliciclastic particles. Pelagic particles are defined as bioclastic grains composed of the skeletal remains of open-marine calcareous and siliceous microfauna and microflora derived from foraminifers, nannofossils, diatoms, and radiolarians as well as minor amounts of sponge spicules and silicoflagellates. The siliciclastic components encountered during ANT-XXVI/2 consist of terrigenous mineral and rock fragments primarily including silt and clay-sized minerals (we defined the sum of both as “mud”). In some cases, sand- and gravel-sized material of glaciogenic origin (ice-rafted debris (IRD)) was found. In the Freeden Seamounts area, we recovered cores documenting the Eltanin asteroid impact (Gersonde et al., 1997) at three sites. Two of the cores contain a sequence of sediment including a layer of meteorite ejecta above sediment excavated by the impact and an undisturbed sequence deposited during the late/middle Eocene.

Sediment names consist of a principal name related to the major biogenic component and the degree of compaction. During ANT-XXVI/2, we only encountered unconsolidated calcareous and/or siliceous biogenic sediments (ooze). For siliciclastic sediments, the principal name describes the texture (gravel, sand, mud (silt+clay)) based on the Udden-Wentworth grain-size scale (Wentworth, 1922). The principal name of biogenic and siliciclastic sediments is preceded by major modifiers and followed by minor modifiers that may refer to mixed biogenic, siliciclastic, and volcaniclastic components:

1. 25 % - 50 %: components in this range modify the principal name.

2.10 % - 24 %: components in this range are added with the suffix “-bearing” (e.g., foraminifer-bearing).

3. 0 % - 9 %: components with these abundances are not named, unless they are of significant importance for the interpretation. In these cases we used (~5 % “with”; ~1 % “with traces of”).

On-board sampling carried out on the work half only included samples for bulk parameters (water content, density, contents of $CaCO_3$, $C_{org}$, and biogenic silica) and paleomagnetic investigations. The bulk parameters samples (~6 -10 $cm^3$ in volume each) were taken with syringes and stored in pre-weighed glasses. For obtaining oriented paleomagnetic samples, plastic cubes (2 x 2 x 1.6 cm) were inserted into the sediment for post-cruise sampling. In total, 360 core meters were opened and sampled. Information regarding the sample types and sample volumes is given in Table 7.4.2 and is also available in the PANGAEA data bank at the AWI (http://www.pangaea.de).

The kasten core PS75/073-2 was sampled completely on board. After opening of the box and exposure of the sediment content, the outer 2 cm of the sediment margins were removed by pushing a steel string through the sediment and manual picking of the produced sediment laps. The sediment was sampled in three layers. The first layer was put into two rows of plastic boxes including one row with 99 cm long plastic boxes (8 x 15 cm in diameter) and a second row with smaller boxes (8 x 8 cm in diameter). The middle layer was sampled with one row of the 8 x 15 cm plastic boxes. In addition, U-Channels for paleomagnetic studies and bulk parameters samples (water content,

density, contents of $CaCO_3$, $C_{org}$, and biogenic silica) were taken at 10-cm intervals. Large samples, comprising 5-cm steps, were collected for the later determination of sand and pebble concentrations. One row of the third layer was sampled again into 8x15 cm plastic boxes. For x-ray radiography, 1-cm thick slices of the remaining part were put onto 25-cm long plastic trays and sealed in plastic foil.

### 7.4.2 Coring transects

Sediment cores were recovered on five transects (Fig. 7.4.2). Transect 1 (Mornington Abyssal Plain (MAP) – Eltanin-Tharp Fracture Zone (ETFZ) is primarily a latitudinal transect located directly north of the Subantarctic Front (SAF) starting outside the Chilean EEZ and ending west of the southern East Pacific Rise at the ETFZ. Within this long transect, we further distinguish Subtransect 1a in the Freeden Seamounts/ Eltanin Impact (FS/EI) area and Subtransects 1b/1c that cover a southward excursion into the northern Amundsen Abyssal Plain where one sediment core (PS75/052-1) was recovered slightly north of the present Polar Front (PF). Transect 2 extends in NE-SW direction from the ETFZ into the northern Amundsen Abyssal Plain (AAP) with sediment cores around the PF and southward across the Permanently Open Ocean Zone (POOZ) into the northern part of the Seasonally Ice-covered Zone (SIZ). Transect 3 crosses the Pacific Antarctic Ridge (PAR) northwestwards into the SW-Pacific Basin (SWP) and primarily covers the POOZ and the Polar Front Zone (PFZ). Transect 4 extends southwestwards across the PAR into the northern Ross Sea (ROS) with sediment cores in the PFZ, POOZ, and south of the winter-sea ice margin (WSI) within the SIZ. The final Transect 5 contains again sediment cores primarily in the POOZ and PFZ but extends into the New Zealand EEZ close to the Subtropical Front (SF) where sediment cores have been recovered from the Campbell Plateau and on a depth transect from the Bounty Trough up the SE New Zealand continental slope (New Zealand Margin (NZM)). Information on core length and recovery is given in Table 7.4.1 and Fig. 7.4.1. The coring locations are shown on Fig. 7.4.2. The graphical core descriptions and photographs can be found in appendix A.7. An overview of the major lithologies in each core is provided in Fig. 7.4.3.

*Transect 1: MAP-ETFZ*

Ten piston cores and one gravity core have been recovered on an ~E-W transect from the MAP across the EPR in the Subantartic Zone directly north of the SAF between ~53°S and 56°S (except Subtransects 1a and 1b). Barrel lengths were mostly 20 or 25 m for the piston cores (except PS75/054-1 with 30 m) and 18 m for the gravity core (PS75/056-1). Core PS75/058-2 was bent during coring using 25 m barrel length. A second core (PS75/059-1) with 20 m barrel length was obtained nearby but was likewise bent. Nevertheless, the cores contained 12.96 m and 13.98 m of undisturbed sediment. The remaining core lengths on this transect range from 17.26 m to 22.98 m and the gravity core is 10.21 m long. Seven cores from this transect were opened on-board *Polarstern*.

Approximately 200 nm offshore Chile, a 18.08 m long piston core (PS75/034-2; barrel length 20 m) was recovered at the MAP (water depth (WD) 4,425 m). Between ca. 10 and 15 m core depth, the liner imploded, probably not disturbing the sediment sequence. The core has not been opened but lithological observations at section

breaks as well as magnetic susceptibility and gamma-ray attenuation (GRA) density data (Chapter 7.5) suggest cyclic changes of more carbonate-rich and more siliceous intervals on m-scale. Comparatively high magnetic susceptibilities point to a significant amount of siliciclastic components in core PS75/034-2. The latitudinal transect continues NW of the FS/EI (see Subtransect 1a) where core PS75/044-4 (WD 5,000 m) is characterized by diatom ooze, that is occasionally mud-bearing with some radiolaria. Several intervals contain diatom mats and two 3 - 4 cm-large dropstones were found at 0.85 m (granite) and 12.09 m core depth (siltstone).

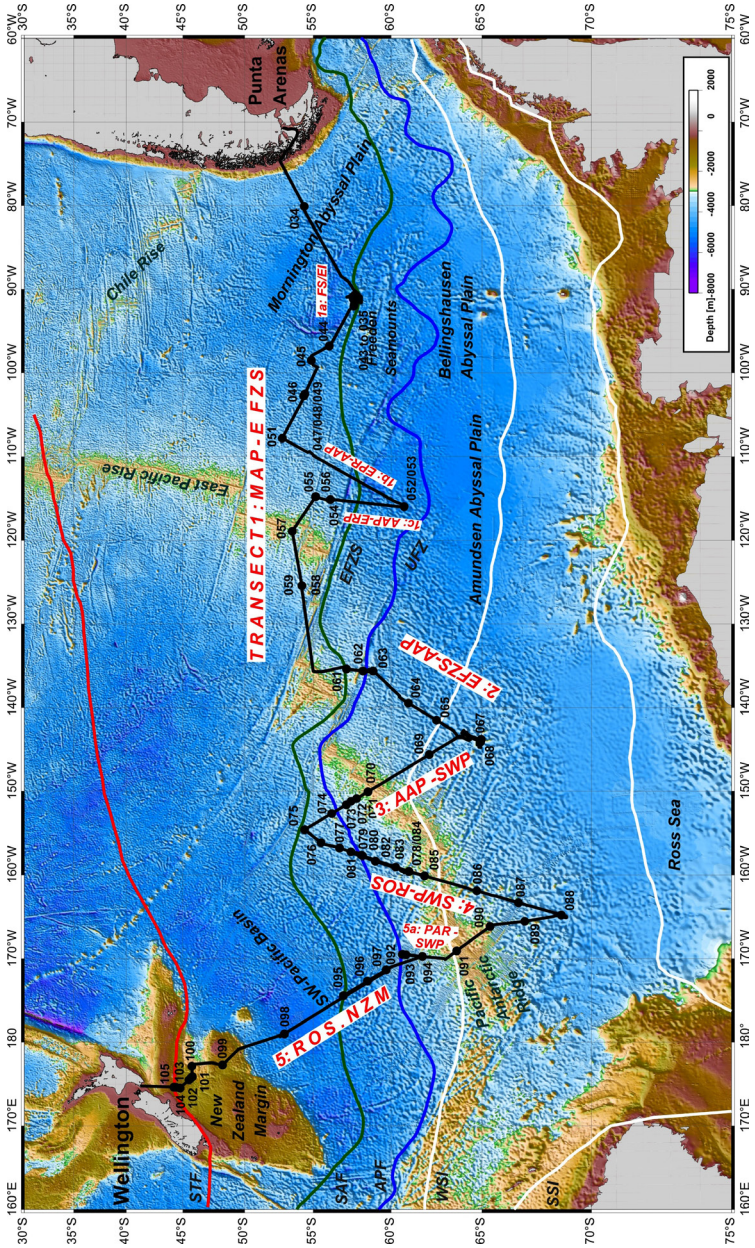


*Fig.7.4.2: Overview map showing the cruise track and all coring stations during ANT-XXVI/2. Locations of the different coring transects are indicated in red: Transect 1: Mornington Abyssal Plain (MAP) to Eltanin-Tharp Fracture Zone (ETFZ). Subtransect 1a: Freeden Seamounts (FS)/Eltanin Impact (EI). Subtransect 1b: Southern EPR/Amundsen Abyssal Plain; Transect 2: ETFZ to Amundsen Abyssal Plain (AAP); Transect 3: AAP to South West Pacific Basin (SWP); Transect 4: SWP to Ross Sea (ROS). Transect 5: ROS to New Zealand Margin (NZM).*

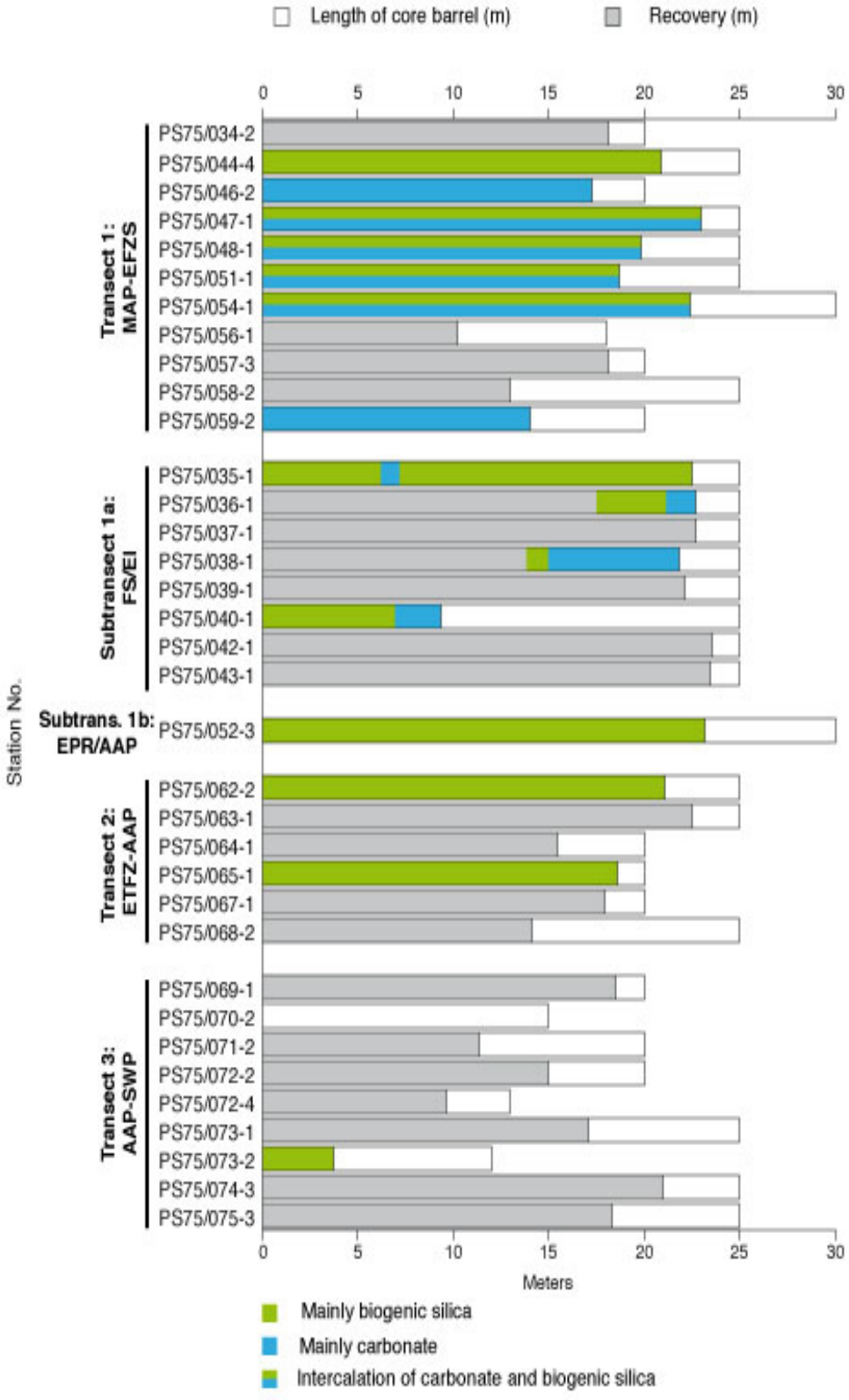


*Fig.7.4.3: Overview of major lithologies of the opened sediment cores recovered during ANT-XXVI/2*

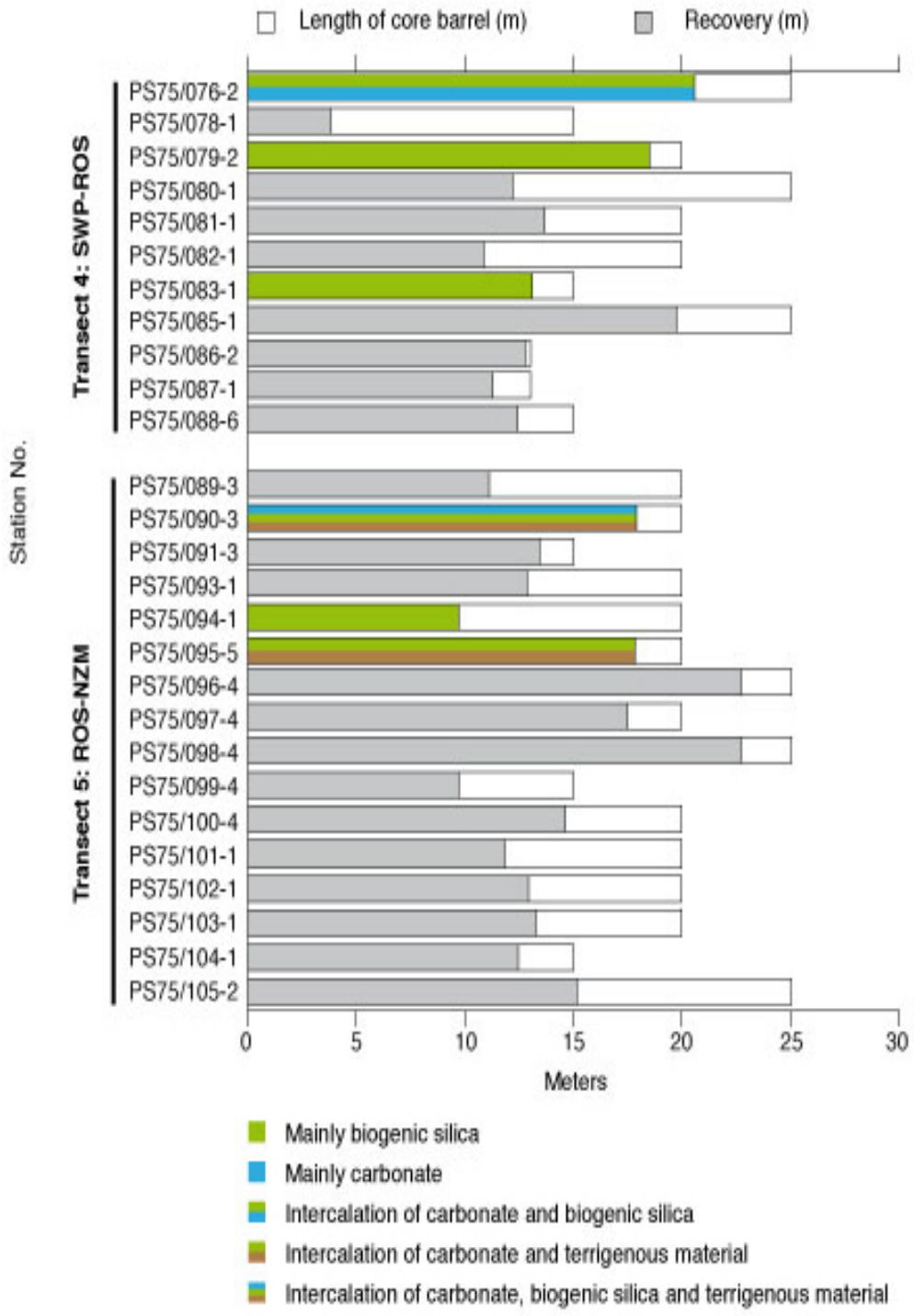


*Fig.7.4.3: (Continued)*

Core PS75/046-2 was recovered on top of an unnamed seamount (WD 2,984 m) and is dominated by calcareous ooze primarily composed of nannofossils and foraminifera. Diatoms are present in minor amounts and a few intervals contain manganese micronodules and some mud. Core PS75/047-1 (WD 4,480 m) contains an intercalation

of more siliceous (primarily diatoms) and more calcareous (primarily foraminifera) intervals on m-scale. A distinct interval of white nannofossil ooze is found at 7.02 m to 8.22 m core depth. A 5 cm-thick graded foraminifera ooze layer (possibly turbidite) and a 2 cm-large dropstone occur at 8.60 m and 8.85 m core depth, respectively. PARASOUND data suggested that nearby core PS75/048-1 (WD 4,516 m) penetrated deeper into the same sedimentary sequence (with lower sedimentation-rates). Indeed, both cores can be correlated using physical property data (Chapter 7.5) and lithological findings. Thus, lithologies within the upper ~12 m of core PS75/048-1 are the same as in the ~23 m-long core PS75/047-1 but more condensed. Below, the content of calcareous microfossils generally decreases and a notable mud content is observed. Core PS75/051-1 (WD 3,949 m) located ~200 nm WNW of PS75/048-1 likewise contains a sequence of mixed siliceous (mainly diatoms, subordinate radiolaria) and calcareous oozes (foraminifera and nannofossils). Compared to the previous cores, carbonate contents are higher. A distinct nannofossil ooze unit is again present (4.90 - 6.30 m core depth). Core PS75/054-1 (WD 4,113 m) contains nannofossil-diatom ooze close to the top, and mud and nannofossil-bearing diatom ooze down to 2 m that is underlain by a ~7 m-sequence of mm- to cm-scale laminated diatom ooze with diatom mats and a notable $H_2S$-smell. The lithology of the lower half of the core is diatom ooze, mostly foraminifera and nannofossil-bearing. Some intervals are foraminifera-bearing nannofossil-diatom ooze. Core PS75/059-2 (WD 3,613 m) retrieved west of the EPR crest is again carbonate rich and primarily composed of foraminifera-bearing nannofossil ooze. Except for a “pure” nannofossil ooze unit close to the base of the core, all lithologies in core PS75/059-2 contain minor amounts of diatoms (mostly diatom-bearing).

*Subtransect 1a: FS/EI*

Within the FS/EI area, eight piston cores (barrel lengths 25 m) were recovered with sediment lengths ranging between 21.83 m to 23.54 m, except for core PS75/040-1 which was bent during coring and recovered only 9.36 m of sediment. Initial biostratigraphic analyses and comparison of magnetic susceptibility records to data from previous cruises in the area suggest that three sediment cores (PS75/036-1, PS75/038-1, and PS75/040-1) penetrated through the Eltanin metorite debris ejecta (EMD) layer. The relevant sections of these cores have been opened (core PS75/040 completely; cores PS75/036-1 and PS75/038-1 only from ca. 3 m above the EMD to the bottom of the core). Core PS75/036-1 records the EMD at a depth of ca. 21 m with a thin layer containing very few, primarily sand-sized vesicular melt rock particles. Below this layer, very homogenous nannofossil ooze is present down to the base of the core. Core PS75/038-1 contains a distinct EMD layer at a core depth of 15.44 m underlain by a cm-scale laminated unit of nannofossil-foraminifera ooze. From 16.30 m to 19.66 m a chaotic mixture of primarily nannofossil ooze with up to dm-large sediment clasts (dark brown clay) containing several cm-large manganese nodules was found. Below an abrupt erosional transition, homogenous nannofossil ooze proceeds down to the base of the core. In this unit, a 5-cm diameter basaltic stone (dropstone?) is present at a depth of 19.99 m. Core PS75/040-1 from shallower WD (4,208 m) mainly contains diatom-foraminifera ooze down to 7.85 m where opaque sand-sized particles were interpreted as traces of EMD layer. Below the EMD layer, homogenous nannofossil ooze is present. We further opened core PS75/035-1 not penetrating down to the EMD

layer. This core from a greater WD (5,224 m) is dominated by diatom ooze (partly mud-bearing) and contains a ~50 cm section of nannofossil-diatom ooze with a 7-cm thick foraminifera ooze at the base that might represent a turbidite. Several thin (<1 cm) coarser layers with foraminifera within the nannofossil ooze and the underlying ~ 2 m of diatom ooze are likely reworked as well. A 8 cm-large dropstone was found at a core depth of ~14.50 m.

*Subtransect 1b: EPR/AAP*

One piston core (PS75/052-3; WD 5,130 m; barrel length 30 m; recovery 23.17 m) was recovered from the AAP within the PFZ. This core complements the AAP core transect obtained during ANT-XVIII-5a. Sediments in core PS75/052-3 are characterized by mostly laminated (mm-scale) diatom ooze with a notable $H_2S$-smell throughout. A 6 cm-large drop-stone (sandstone) occurs at a core depth of 15.63 m.

*Transect 2: ETFZ-AAP*

Six piston cores were taken on a NE-SW transect starting directly north of the PF at the Udintsev-Fracture Zone (UFZ; ~58°S) and ending at ~65°S in the Amundsen Sea (within the SIZ). Barrel lengths were 20 m to 25 m. Core recoveries were high for the northernmost cores (21.09 m and 22.46 m) and reduced further south (14.12 m to 18.6 m). The northernmost core PS75/062-2 (WD 4,165 m) was opened and sampled. The core is entirely composed of diatom oozes, which contain minor amounts of foraminifera, nannofossils, and mud only in the uppermost 0.8 m. Many intervals of the diatom ooze reveal a weak lamination with slightly reddish and, in some cases, bluish laminae. A $H_2S$-smell was often noted during core splitting. Lithological observations at core breaks as well as physical property data (Chapter 7.5) suggest that the unopened cores PS75/063-1 (WD 3,795 m; located directly south of the PF) and PS75/064-1 (WD 4,600 m; located approximately half-way between the PF and the winter sea-ice margin (WSI)) contain similar lithologies as core PS75/062-2. This is consistent with shipboard biostratigraphic data indicating a similar core catcher age of the three cores (Chapter 7.6). The second core from this transect that was opened (core PS75/065-1; WD 4,499 m; located close to the modern WSI) is dominated by mud-bearing diatom ooze, primarily dark brown in color. Three levels with cm-scale manganese nodules occur close to the top, at ~2 m and at ~9.7 m core depth. Two small dropstones of up to 1 cm diameter were found between 8.25 m and 8.8 m core depth. Based on lithological observations at core breaks and physical property data, the southernmost core PS75/067-1 (WD 4,151 m) contains a similar sequence as PS 75/065-1 (dark brown muddy diatom ooze). Core PS75/068-2 (WD 3,728 m) may contain such sediments in the upper ~9 m, while low magnetic susceptibilities combined with low GRA-densities between ~9 and 13 m core depth suggest a lower siliciclastic component (“pure” diatom ooze). The lowermost part of this core reveals high densities and low magnetic susceptibility reflecting calcareous lithologies. Biostratigraphic data suggest a substantial stratigraphic hiatus at ~9 m core depth (upper Pliocene to middle Miocene; Chapter 7.6).

*Transect 3: AAP-SWP*

This transect primarily covers the NW flank of the PAR from the center of the Permanently Open Ocean Zone (POOZ) to the SAF. Due to very sparse sediment cover further

south, only one core was retrieved just south of the present WSI within the SIZ (core PS75/069-1; WD 4,334 m; barrel length 20 m, core recovery 18.46 m). This core has not been opened but is both lithologically and biostratigraphically roughly similar to core PS75/065 from the previous transect.

About 35 nm NW of the PAR crest, the intent to recover a 15 m barrel length piston core was unsuccessful and all tubes were lost except for the TC (PS75/070-2; WD 2,842 m). Five piston cores, one gravity core, and one kasten core were recovered on the NW PAR flank, mostly from comparatively shallow WD ranging from ~2,900 m to ~3,300 m (except PS75/075-3; WD 4,096 m). Barrel lengths of the piston cores were 20 m or 25 m and core recoveries range from 11.36 m (PS75/071-2) to 20.95 m (PS75/074-3). Core PS75/071-2 (WD 2,926 m) was bent during coring and revealed basalt fragments in the core catcher either representing pieces of a large dropstone or basaltic basement as the PARASOUND penetration was only very limited at this site. The core has not been opened but physical property data are consistent with more calcareous lithologies as observed at core breaks. Core PS75/072-2 was opened and primarily contains diatom ooze, which is partly mud-bearing. Only the lowermost 1.5 m are more calcareous and consist of diatom-nannofossil ooze. Gravity core PS75/072-4 from the same location covers the uppermost ~11 m of piston core PS75/072-2 in 9.61 m, indicating moderate compression of sediments in the gravity core. At site PS75/073, a 17.04 m long piston core and 3.68 m long box core were recovered. The kasten core (PS75/073-2) consists of mud- and nannofossil-bearing diatom ooze with some foraminifera down to ~1.8 m core depth, underlain by mud-bearing diatom ooze grading into “pure” diatom ooze towards the base of the core. Several small drop-stones occur at core depths of 1.12 m and around 3.4 m. Cores PS75/074-3 and PS75/075-3 retrieved north of the PF contain an intercalation of biogenic oozes with varying amounts of siliceous and calcareous components. Using physical properties, particularly core PS75/074-3 can be correlated in detail to PS75/076-3 from the following transect (see below).

*Transect 4: SWP-ROS*

On a detailed NNE-SSW transect from the SAF across the PF and the WSI into the northern ROS, seven piston cores and four gravity cores were recovered. Barrel lengths for the piston cores were 20 m and 25 m (except for PS75/083-1 with 15 m). Gravity core barrel lengths were 13 m or 15 m. Core recoveries are variable. At four stations (PS75/080-1, PS75/081-1m, PS75/082-1, and PS75/085-1), implosion of core liners occurred resulting in coring disturbance of the upper 2-4 m. In addition, core PS75/080-1 was bent during coring. However, the undisturbed sections of these cores (below ~4 m) can be correlated in detail to the undisturbed piston core PS75/083-1 using physical property data (Chapter 7.5).

Cores PS75/076-2 (WD 3,742 m), PS75/078-1 (WD 3,315 m), and PS75/079-2 (WD 3,770 m) located north of the PF can be correlated to each other (and to PS75/074-3 from the previous transect) using the magnetic susceptibility and GRA-density records (Chapter 7.5). These correlations are consistent with shipboard biostratigraphic findings (Chapter 7.6). Core PS75/076-2 has been opened and contains a cyclic succession of more calcareous oozes and “purer” diatom oozes. The more calcareous oozes are mostly foraminifera-bearing nannofossil-diatom oozes. Between ~10.5 m

and 11.5 m, a distinct nannofossil ooze unit occurs. Three thinner (~30 cm thick) "pure" nannofossil ooze units are found between ~16 m and 18.5 m core depth. Sediments are mud-bearing in the upper ~3 m of the core. Core PS75/079-2 reveals roughly two-times higher sedimentation-rates than PS75/076-2 and can be used as a link to the higher resolution cores directly to the south within the POOZ. Sediments in this core are substantially more siliceous (primarily diatom ooze) with regular intervals of more foraminifera- and nannofossil-bearing diatom oozes. A foraminifera-bearing diatom-nannofossil ooze unit between 16 m and 16.78 m core depth correlates to the massive nannofossil ooze sections in the northern cores. Compared to these northern cores, sediments in core PS75/079-2 contain higher contents of siliciclastic components (mostly mud-bearing oozes). Three levels with small (<1 cm) dropstones occur at ~ 2 m, ~6 m, and ~16.5 m core depth. Within the POOZ, undisturbed core PS75/083-1 (WD 3,599 m) has been opened on-board. Sediments are primarily diatom oozes and contain only three levels with notable calcareous microfossil contents (0.42 - 0.75 m, 7.07 - 7.41 m, and 12.45 - 12.59 m core depth). The upper ~3 m and three shorter intervals downcore are mud-bearing. These sections also contain radiolaria and partly small dropstones. Additionally, we obtained a short gravity core (PS75/078-1, barrel length 15 m; core length 3.83 m) from shallower water depth (WD 3,315 m) at a ridge within the POOZ. The core has not been opened but biostratigraphic data (Chapter 7.6) and lithological information at core breaks suggest that it contains a more condensed diatom ooze sequence with higher carbonate contents close to the base of the core.

South of the WSI, three gravity cores were recovered that have not been opened. Lithological observations at core breaks, biostratigraphic data (Chapter 7.6), and the magnetic susceptibility records suggest that cores PS75/086-2 (WD 4,065 m) and PS75/087-1 (WD 4,406 m) contain similar lithologies as core PS75/065-1 retrieved from a similar oceanographic setting within the southern part of Transects 2 and 3.

*Transect 5: ROS-NZM*

In total 15 piston cores and one gravity core were obtained on the long ~SSE-NNW transect from the northern ROS across the PAR, the SWP to the NZM. Barrel lengths and core recoveries were variable but generally higher in the SWP and reduced on the northern flank of the PAR (in the POOZ). SSW of the PAR crest (and the WSI), two cores (PS75/089-3 and PS75/090-3) with Pliocene core-catcher ages were recovered (Chapter 7.6). Piston core PS75/090-3 (WD 3,478 m; core length 17.91 m) was opened on-board. The upper ~4 m consist of diatom-bearing mud with several manganese nodules. Further down-core (~4-15 m core depth), more calcareous sediments are predominant (mainly mud- and diatom-bearing foraminifera ooze), except for a short interval of mud-bearing diatom ooze around 8 m core depth. A number of small (<1 cm) dropstones occur between ~6 and 7 m core depth. The lowermost ~3 m of the core are diatom-bearing mud and mud-bearing diatom ooze that is partly laminated on mm-scale. From the three cores within the POOZ, core PS75/094 was opened (WD 3,270 m; core length 9.7 m). Despite its shallow water depth, sediments are nearly barren of carbonate and are primarily composed of diatom-ooze that is partly mud-bearing. Correlations using physical property data suggest that similar lithologies are present in cores PS75/091-3 and PS75/093-1. Three additional cores were recovered within the PFZ and contain more siliciclastic material compared to the PFZ cores recovered on the previous transects. Core PS75/095-5 (WD 4,853 m; core length 17.85 m), which

was opened on-board, primarily consists of muddy diatom ooze frequently laminated on mm-scale. At ~4.6 m core depth, a distinct layer containing up to sand-sized opaque particles (IRD?) was observed. The lowermost ~0.2 m of sediment are composed of diatom-bearing foraminifera-nannofossil ooze. Lithological observations at core breaks and physical property data suggest that core PS75/096-4 (WD 5,057 m; core length 22.74 m) contains a similar sedimentary sequence as core PS75/95-5 with higher sedimentation rates. The same applies to core PS75/097-4 (WD 4,672 m; core length 17.46 m) where sedimentation-rates appear to be similar to those in core PS75/095-5.

**Tab. 7.4.1:** Piston, gravity and kasten corer deployments and recoveries

| station no. | gear | latitude | longitude | water depth (DWS) [m] | rope length [m] | core recov. [m] | TC recov. [m] |
|---|---|---|---|---|---|---|---|
| ***TRANSECT 1: MAP- ETFZ ( Mornington Abyssal Plain (MAP) - southern East Pacific Rise (EPR) - Eltanin-Tharp Fracture Zone (ETFZ))*** | | | | | | | |
| PS75/034-2 | KOL | 54°22.112´S | 80°05.380´W | 4425 | 4433 | 18.08 | 0.92 |
| PS75/044-4 | KOL | 56°05.15´S | 96°46.82´W | 5000 | 4887 | 20.93 | 0.33 |
| PS75/046-2 | KOL | 54°24.92'S | 102°30.22'W | 2984 | 2930 | 17.26 | 0.17 |
| PS75/047-1 | KOL | 54°20.771'S | 102°44.82'W | 4480 | 4429 | 22.98 | 0.83 |
| PS75/048-1 | KOL | 54°20.35'S | 102°45.51'W | 4516 | 4422 | 19.88 | 0.87 |
| PS75/051-1 | KOL | 52°48.73'S | 107°48.33'W | 3949 | 3920 | 18.73 | 1.01 |
| PS75/054-1 | KOL | 56°09.11'S | 115°07.98'W | 4113 | 4083 | 22.38 | 0.91 |
| PS75/056-1 | SL | 55°09.74'S | 114°47.31'W | 3581 | 3587 | 10.21 | - |
| PS75/057-3 | KOL | 53°31.98'S | 118°54.98'W | 2888 | 2856 | 18.12 | 0.92 |
| PS75/058-2 | KOL | 54°12.86'S | 125°26.20'W | 3629 | 3568 | 12.96 | 0.91 |
| PS75/059-2 | KOL | 54°12.90'S | 125°25.53'W | 3613 | 3579 | 13.98 | 0.90 |
| ***Subtransect 1a: FS/EI (Freeden Seamounts (FS)/Eltanin Impact (EI))*** | | | | | | | |
| PS75/035-1 | KOL | 57°46.17´S | 90°41.019´W | 5224 | 5191 | 22.53 | 0.91 |
| PS75/036-1 | KOL | 57°44.44´S | 90°43.560´W | 5313 | 5279 | 22.74 | 0.52 |
| PS75/037-1 | KOL | 57°46.50´S | 91°24.689´W | 4879 | 4816 | 22.73 | 0.87 |
| PS75/038-1 | KOL | 57°51.70´S | 91°06.84´W | 4208 | 4152 | 21.83 | 1.00 |
| PS75/039-1 | KOL | 57°39.98´S | 90°51.76´W | 5231 | 5177 | 22.15 | 0.53 |
| PS75/040-1 | KOL | 57°38.88´S | 91°09.14´W | 3400 | 3336 | 9.36 | 0.93 |
| PS75/042-1 | KOL | 57°43.41´S | 91°42.77´W | 4917 | 4850 | 23.54 | 1.00 |
| PS75/043-1 | KOL | 57°42.01´S | 91°58.61´W | 4619 | 4597 | 23.48 | 0.82 |
| ***Subtransect 1b: EPR/AAP (southern EPR - Amundsen Abyssal Plain)*** | | | | | | | |
| PS75/052-3 | KOL | 60°45.12'S | 115°58.74'W | 5130 | 5063 | 23.17 | 0.41 |
| ***TRANSECT 2: ETFZ-AAP (Eltanin-Tharp Fracture Zone - northern Amundsen Abyssal Plain)*** | | | | | | | |
| PS75/062-2 | KOL | 58°16.60'S | 135°37.61'W | 4165 | 4099 | 21.09 | 0.66 |
| PS75/063-1 | KOL | 58°54.24'S | 135°37.23'W | 3795 | 3736 | 22.46 | 0.67 |
| PS75/064-1 | KOL | 61°00.74'S | 139°27.85'W | 4600 | 4552 | 15.43 | 0.27 |
| PS75/065-1 | KOL | 62°36.21'S | 141°30.90'W | 4499 | 4451 | 18.60 | 0.67 |
| PS75/067-1 | KOL | 64°58.23'S | 143°48.22'W | 4151 | 4116 | 17.95 | 0.82 |
| PS75/068-2 | KOL | 64°56.01'S | 144°06.81'W | 3728 | 3678 | 14.12 | 0.91 |
| ***TRANSECT 3: AAP-SWP (Amundsen Abyssal Plain - northern Pacific-Antarctic Ridge - Southwest-Pacific Basin)*** | | | | | | | |
| PS75/069-1 | KOL | 62°12.24'S | 145°37.11'W | 4334 | 4283 | 18.46 | 0.65 |
| PS75/070-2 | KOL | 58°34.87'S | 150°03.97'W | 2842 | 2816 | 0.00 | 0.90 |
| PS75/071-2 | KOL | 57°52.40'S | 150°52.11'W | 2926 | 2883 | 11.36 | 0.95 |
| PS75/072-2 | KOL | 57°33.51'S | 151°13.11'W | 3098 | 3066 | 14.97 | 0.50 |
| PS75/072-4 | SL | 57°33.51'S | 151°13.17'W | 3099 | 3098 | 9.61 | |
| PS75/073-1 | KOL | 57°12.26'S | 151°36.63'W | 3238 | 3193 | 17.04 | 0.68 |
| PS75/073-2 | KAL | 57°12.26'S | 151°36.65'W | 3234 | 3224 | 3.68 | |

| station no. | gear | latitude | longitude | water depth (DWS) [m] | rope length [m] | core recov. [m] | TC recov. [m] |
|---|---|---|---|---|---|---|---|
| PS75/074-3 | KOL | 56°14.65'S | 152°39.30'W | 3295 | 3255 | 20.95 | 0.54 |
| PS75/075-3 | KOL | 54°24.23'S | 154°35.18'W | 4096 | 4059 | 18.35 | 0.92 |
| ***TRANSECT 4: SWP-ROS (Southwest-Pacific Basin - Pacific-Antarctic Ridge - northern Ross Sea)*** | | | | | | | |
| PS75/076-2 | KOL | 55°31.71'S | 156°08.39'W | 3742 | 3696 | 20.59 | 0.65 |
| PS75/078-1 | SL | 61°03.00'S | 159°35.18'W | 3315 | 3305 | 3.83 | |
| PS75/079-2 | KOL | 57°30.16'S | 157°14.25'W | 3770 | 3814 | 18.51 | 0.67 |
| PS75/080-1 | KOL | 58°10.63'S | 157°38.19'W | 3874 | 3798 | 12.20 | 0.89 |
| PS75/081-1 | KOL | 58°14.49'S | 157°42.44'W | 3857 | 3797 | 13.71 | 0.97 |
| PS75/082-1 | KOL | 59°02.48'S | 158°21.82'W | 4000 | 3934 | 10.88 | 0.89 |
| PS75/083-1 | KOL | 60°16.13'S | 159°03.59'W | 3599 | 3526 | 13.13 | 0.37 |
| PS75/085-1 | KOL | 61°56.38'S | 160°07.10'W | 3734 | 3657 | 19.74 | |
| PS75/086-2 | SL | 64°44.64'S | 161°54.19'W | 4065 | 4044 | 12.74 | |
| PS75/087-1 | SL | 66°47.29'S | 163°19.47'W | 4406 | 4390 | 11.28 | |
| PS75/088-6 | SL | 68°43.82'S | 164°48.95'W | 3857 | 3816 | 12.40 | |
| ***TRANSECT 5: ROS - NZM (northern Ross Sea - Pacific-Antarctic Ridge - Southwest-Pacific Basin - eastern New Zealand margin )*** | | | | | | | |
| PS75/089-3 | SL | 67°05.01'S | 165°32.46'W | 4126 | 4109 | 11.12 | |
| PS75/090-3 | KOL | 65°24.66'S | 166°09.28'W | 3478 | 3443 | 17.91 | 0.92 |
| PS75/091-3 | KOL | 63°41.66'S | 169°04.47'W | 2940 | 2914 | 13.44 | 0.26 |
| PS75/093-1 | KOL | 60°52.33'S | 169°32.89'W | 3762 | 3712 | 12.84 | 0.92 |
| PS75/094-1 | KOL | 61°49.34'S | 169°44.69'W | 3270 | 3227 | 9.70 | 0.92 |
| PS75/095-5 | KOL | 57°01.18'S | 174°25.80'W | 4853 | 4814 | 17.85 | 1.01 |
| PS75/096-4 | KOL | 58°32.86'S | 172°42.06'W | 5057 | 5011 | 22.74 | 0.69 |
| PS75/097-4 | KOL | 59°42.02'S | 171°21.44'W | 4672 | 4623 | 17.46 | 0.69 |
| PS75/098-5 | KOL | 52°57.93'S | 179°00.62'W | 5189 | 5143 | 22.83 | 0.82 |
| PS75/099-4 | KOL | 48°15.72'S | 177°16.35'E | 1272 | 1242 | 7.71 | 0.29 |
| PS75/100-4 | KOL | 45°45.41'S | 177°08.93'E | 2498 | 2463 | 14.77 | 0.29 |
| PS75/101-1 | KOL | 45°48.42'S | 175°52.66'E | 1770 | 1739 | 11.80 | 0.12 |
| PS75/102-1 | KOL | 45°41.20'S | 175°43.29'E | 1621 | 1585 | 12.96 | 0.48 |
| PS75/103-1 | KOL | 45°30.93'S | 175°29.99'E | 1390 | 1356 | 13.15 | 0.57 |
| PS75/104-1 | KOL | 44°46.15'S | 174°31.53'E | 835 | 817 | 12.39 | |
| PS75/105-1 | KOL | 44°24.52'S | 174°37.47'E | 669 | 685 | 15.09 | 0.11 |

**Tab.7.4.2:** Sample types and sample numbers taken from sediment cores

| Gear No. | Bulk (water content, density, $CaCO_3$, Corg, Biogenic Silica) | Paleomagnetics | Grain size, clay mineralogy | Radiograph slice |
|---|---|---|---|---|
| PS75/035-1 TC | - | 10 | | |
| PS75/035-1 KOL | 226 | 217 | | |
| PS75/036-1 KOL | 49 | - | | |
| PS75/038-1 KOL | - | 27 | | 6 |
| PS75/040-1 KOL | - | - | | |
| PS75/044-4 TC | 9 | - | | |
| PS75/044-4 KOL | 208 | 208 | | |
| PS75/046-2 TC | 1 | | | |
| PS75/046-2 KOL | 171 | 10 | | |
| PS75/047-1 TC | 9 | 9 | | |
| PS75/047-1 KOL | 230 | 230 | | |
| PS75/048-1 TC | 9 | 9 | | |

| Gear No. | Bulk (water content, density, $CaCO_3$, Corg, Biogenic Silica) | Paleomagnetics | Grain size, clay mineralogy | Radiograph slice |
|---|---|---|---|---|
| PS75/048-1 KOL | 199 | 199 | | |
| PS75/051-1 TC | 10 | 11 | | |
| PS75/051-1 KOL | 181 | 181 | | |
| PS75/052-3 TC | 5 | 5 | | |
| PS75/052-3 KOL | 226 | 231 | | |
| PS75/054-1 TC | 9 | | | |
| PS75/054-1 KOL | 224 | - | | |
| PS75/059-2 TC | 8 | - | | |
| PS75/059-2 KOL | 139 | - | | |
| PS75/062-2 TC | 7 | - | | |
| PS75/062-2 KOL | 210 | - | | |
| PS75/065-1 TC | 7 | 7 | | |
| PS75/065-1 KOL | 186 | 186 | | |
| PS75/072-2 TC | 5 | | | |
| PS75/072-2 KOL | 95 | - | | |
| PS75/073-2 KAL | 37 | - | 75 | 25 |
| PS75/076-2 TC | 6 | 6 | | |
| PS75/076-2 KOL | 206 | 203 | | |
| PS75/079-2 KOL | 179 | 179 | | |
| PS75/083-1 KOL | 126 | 126 | | |
| PS75/090-3 KOL | 176 | 351 | | |

We further recovered one sediment core (PS75/098-4; WD 5,189 m; core length 22.83 m) from the SWP ~250 nm SE of the Campbell Plateau. The core was not opened but lithological observations at core breaks suggest a sequence of mud-bearing diatom ooze similar to the lithologies found in the previous PFZ cores. Seven cores from the NZM margin were recovered during the last three days of the cruise and were not opened. Core PS75/099-4 (WD 1,272; core length 7.71 m) was recovered from the Pukaki Saddle between the Campbell Rise and the Bounty Plateau. Cores PS75/100-4, PS75/101-1; PS75/102-1, PS75/103-1; PS75/104-1, and PS75/105-1 (core lengths 11.8 to 15.9 m) constitute a depth transect from the northern margin of the Bounty Trough upslope in northwesterly direction. These cores cover a depth range from ~2,500 m to ~700 m. Lithological core-break information suggests that all NZM sediment cores are dominated by mud-bearing to muddy nannofossil and foraminifera-nannofossil oozes.

## References

Gersonde, R, Kyte, F.T., Bleil, U., Diekmann, B., Flores, J. A., Gohl, K., Grahl, G., Hagen, R., Kuhn, G., Sierro, F. J., Völker, D., Abelmann, A., and Bostwick J. A., 1997. Geological record and reconstruction of the late Pliocene impact of the Eltanin asteroid in the Southern Ocean, Nature 390, 357-363.

Mazzullo, J.M., Meyer, A., and Kidd, R.B., 1988. New sediment classification scheme for the Ocean Drilling Program. In: Mazzullo, J., and Graham, A.G. (Eds.), Handbook for Shipboard Sedimentologists. ODP Tech. Note, 8:45–67.

Wentworth, C.K., 1922. A scale of grade and class terms of clastic sediments. J. Geol., 30, 377–392.

## 7.5 Core logging and physical properties

Sze Ling Ho[1], Frank Lamy[1],
Abhinav Gogoi[2], Bastian Kühl[2],
Lucia Reichelt[2]

[1]Alfred-Wegener-Institut
[2]University of Bremen

### Objectives

Physical properties were measured on board *Polarstern* on all sediment cores including piston cores (KOL), the pilot cores (TC) triggering the KOL, gravity cores (SL), and on the box core (KAL). Because of the relatively restricted diversity of the major lithologies recovered during ANT-XXVI/2 (Chapter 7.4) with contrasting physical properties, the data were often easy to interpret in terms of lithology. Furthermore, by combining particular magnetic susceptibility and Gamma-Ray-Attenuation (GRA)-density data with shipboard biostratigraphic findings, the development of preliminary age-models for many of the recovered cores during ANT-XXVI/2 was possible (Chapter 7.6). The physical property data will be stored in the database PANGAEA (www.pangaea.de) after verification.

### Instruments

After the cores were cut into ~1-m-segments and labelled, they were brought to the Dry Laboratory (Trockenlabor) 1 - 3 on *Polarstern*. The cores were laid on the floor for at least 12 hours (KOL) and 24 hours (SL), in order to allow the sediment cores to reach room temperature. A constant temperature is required for the some of the physical property parameters.

Two devices were used for the on-board measurements:

(1) One of the devices was a GEOTEK Multi-Sensor Core Logger (MSCL) provided by the AWI. This device was used for whole-core measurements of p-wave-velocity, GRA-density, and magnetic susceptibility. Furthermore, temperature and core diameter were measured for the calculation of the parameter values. This device was initially used only for the measurements of the piston cores. In some parts deformed or taped segments did not fit through the susceptibility coil of the device. These segments were not measured on this device. Due to the amount of cores and time constraints, it was not possible to alter the susceptibility coil on the device for each core individually. Gravity cores were measured at the end of the cruise after installing a larger-diameter susceptibility coil.

The length of each segment had to be adjusted manually and was not detected with a laser. The segments were placed one after the other. At the beginning of each core a 20 cm liner filled with demineralised water was measured. At the end of the core a 18 cm plastic (POM) piece (with a diameter of 90 mm) was measured to push the whole core through all the sensors. After this short water liner, a 94.8 cm long water-filled liner was used as a core pusher. The first 20 cm-liner and the POM provide a guide for the beginning and end of the core.

The measurement resolution was 1 cm and the time required for each measurement was 10 seconds. It took about 25 - 30 minutes to measure each ~1-m-core segment.

We used the Geotek MSCL 6.2 software and the Geotek Utilities 6.1 software for measurements and data-processing. All physical property data have been corrected for section breaks and faulty values at core section boundaries due to disturbances, and gaps between the caps have been deleted.

(2) A second core-logging device on board was the GEOTEK Multi-Sensor Core Logger (MSCL) from the University of Bremen (GeoB). This device provided the opportunity to measure magnetic susceptibility, electrical resistivity and in addition the temperature. All cores were measured on this device (KOL, including the deformed segments, TC, SL, and the small 8 x 8 x 100 cm-KAL-boxes) as the susceptibility coil was much bigger than that of the AWI device. The parameters were measured utilizing a stepper motor to convey core segments along a track and through a series of sensors. Positions and lengths are automatically detected with a laser. The separate logging measurements were controlled and rapidly collated by the systems computer terminal. In order to make an accurate end-correction at the base of each segment and to assess the drift of the susceptibility meter, a spacer cylinder of 29.5 cm length was placed between each segment during the measurement procedure.

The general spacing of the measurements was 2 cm and the time for each measurement was 10 seconds. It took about 20 minutes to measure one core segment of about 1 m length, including the spacer. Data were measured and processed using the Geotek MSCL 7.5 software and the Geotek Utilities 7.5 software. For further processing, we used an Excel-Macro developed at GeoB. An example of the processed data is given in Fig. 7.5.1.

Additionally, the GeoB-device was used for obtaining high-resolution line scan images of the split cores and spectral light reflectance with a resolution of 0.01 cm. For this purpose, the sediment surface of the split cores (archive-halves) was carefully scraped to create an even surface before scanning. We used the Imaging program 2.3 and Image Tools 2.3 for data processing. An example is shown in Fig. 7.5.1.

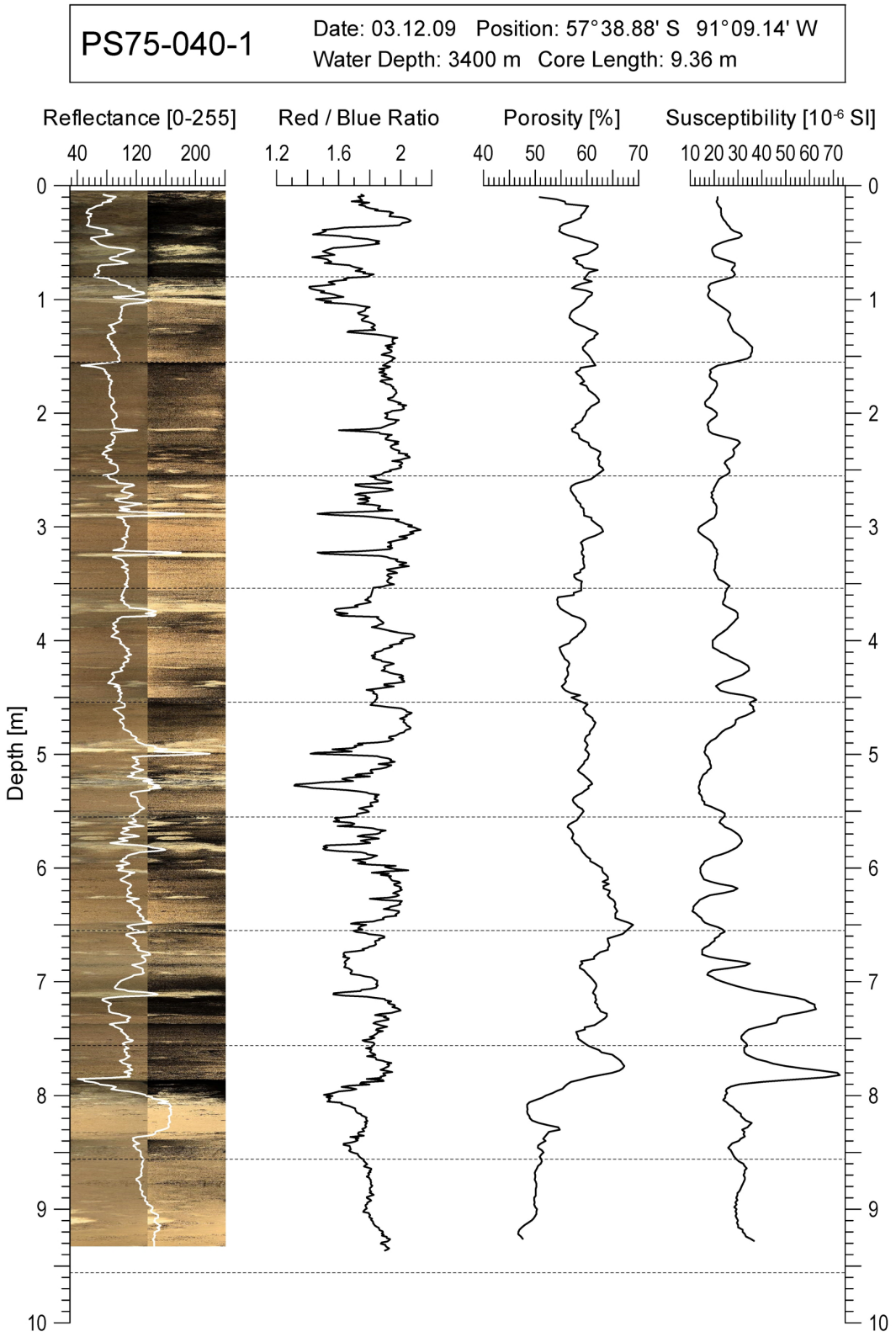


*Fig. 7.5.1: Example of the processed physical property data measured with the GeoB MSCL device (core PS75/040-1). Data include magnetic susceptibility, porosity, red-blue ratio, and the digital core image (left part: genuine colors; right part: contrast-enhanced colors).*

**Parameters**

*Magnetic Susceptibility (AWI-device and GeoB-device)*
The magnetic volume susceptibility $\kappa$ is defined by the equations

$$B = \mu_0 \cdot \mu_r \cdot H = \mu_0 \cdot (1 + \kappa) \cdot H = \mu_0 \cdot H + \mu_0 \kappa \cdot H = B_0 + M$$

with magnetic induction B, absolute and relative permeabilities $\mu_0$ and $\mu_r$, magnetizing field H, magnetic volume susceptibility $\kappa$ and volume magnetization M. As can be seen from the third term, $\kappa$ is a dimensionless physical quantity. It records the amount to which a material is magnetized by an external magnetic field.

For marine sedients the magnetic susceptibility may vary from an absolute minimum value of $-15 \cdot 10^{-6}$ (diamagnetic minerals such as pure carbonate or silicate) to a maximum of some $10.000 \times 10^{-6}$ for basaltic debris rich in (titano-) magnetite. In most cases $\kappa$ is primarily determined by the concentration of ferrimagnetic minerals, while paramagnetic matrix components such as clays are of minor importance. Enhanced susceptibilities generally indicate higher concentrations of lithogenic or authigenic components.

The GeoB core logger is mounted with a commercial Bartington M.S.2 susceptibility meter with a 140 mm loop sensor. Due to the sensor's size, its sensitivity extends over a core interval of about 8 cm. Consequently, sharp susceptibility changes in the sediment column will appear smoothed in the $\kappa$ core log and thin layers cannot be appropriately resolved in most cases. During the processing of the data created with the GeoB-core logger, all data related to void sections were removed to provide a continuous composite core log. The measurements taken at the centre of the spacer were used to assess and compensate the instrumental drift. In case of piston and kasten cores, a calibration factor of 14.03 was applied to convert the digital readings of the M.S.2 into volume magnetic susceptibility values in $10^{-6}$ SI units. The factor is in accordance with the equation given in the GEOTEK MSCL manual:

$$k_{rel} = 4.8566\ (d/D)^2 - 3.0163\ (d/D) + 0.6448 = 0.713 \rightarrow 1/k_{rel}\ 10 = 14.03$$

with d = core diameter = 90 mm, D = loop diameter = 140 mm

In case of gravity cores with a diameter d = 120 mm, a factor of $1/k_{rel}\ 10 = 6.14$ was applied.

For the AWI MSCL, we likewise used a commercial Bartington M.S.2 susceptibility meter. Piston cores were measured with a 100 mm loop sensor (#203) and the gravity cores with a 140 mm loop sensor (#208). Due to the smaller diameter of the piston core loop sensor, the magnetic susceptibility data obtained with the AWI device are less smoothed compared to the GeoB logger.

*Gamma-Ray-Attenuation (GRA)-density (AWI-device)*
Beside the magnetic susceptibility, the GRA-density records were a very useful tool for core-correlation and to obtain information about the lithology of the un-opened cores (Chapter 7.5.3). For the measurements of the GRA-density, a Caesium-137

source (activity: 356 MBq, energy: 0.662 MeV) was used. The aperture diameter of 5.0 mm was used for both piston cores and gravity cores. The gamma ray detector was a Gammasearch2, Model SD302D, Serial Number 3047, John Caunt Scientific Ltd. The count time for each value was 10 seconds. For later processing, before the measurement of each core a density-pyramid was measured.

*P-Wave Velocity, core diameter and core thickness measurement*
The P-wave velocity was measured with P-Wave plate-Transducers (PWTs) with a diameter of 4 cm. Transmitter pulse frequency was 500 kHz. Pulse repetition rate: 1 kHz. Recorded pulse resolution: 50 ns. Gate: 2800. Delay: 10 s. P-wave velocity data were calibrated with water core of known temperature and theoretical sound velocity. The core thickness was calibrated with distance pieces of known length.

*Electric Resistivity and Porosity (GeoB-device)*
The electric sediment resistivity Rs was determined using an inductive non-contact sensor. The system applies high-frequency magnetic fields by a transmitter coil inducing electrical eddy currents in the sediment, which are proportional to conductivity. Their secondary field is recorded and yields raw and calibrated values for conductivity and resistivity. Porosity was calculated according to the empirical Archie's equation

$$R_s/R_w = k \cdot \phi^{-m}$$

where the ratio of sediment resistivity $R_s$ and pore water resistivity $R_w$ can be approximated by a power function of porosity $\phi$. Following a recommendation by Boyce (1968), suitable for sea water saturated clay-rich sediments, values of 1.30 and 1.45 were used for the constants k and m, respectively. The calculated porosity $\phi$ is subsequently converted to wet bulk density $\rho_{wet}$ using the equation (Boyce, 1976)

$$\rho_{wet} = \phi \cdot \rho_f + (1 - \phi) \cdot \rho_m$$

with a pore water density $\rho_f$ of 1,030 kg/m$^3$ and a matrix density $\rho_m$ of 2.670 kg/m$^3$. For a uniform treatment of all cores, these empirical coefficients were not adapted to individual sediment lithologies. Yet, relative porosity and density changes should be well documented.

The resistivity sensor averages over approximately 12 cm core length. A platinum thermometer inserted into a segment continuously measures sediment temperature for temperature compensation. Absolute sensor calibrations using a series of saline standards are performed daily. For subsequent drift and segment end correction, 29.5 cm long insulating spacers were placed between segments during logging. Thus, the characteristic decay of the eddy currents nearby the end-caps was separately recorded for each segment and corrected on basis of a model curve. This method provides a continuous composite record, however the first 2 - 3 data points from each intersection were discarded due to some overshooting.

During the measurements of the resistivity some jumps occurred. This problem seemed to be fixed after changing first a plug and later a plug-in, but it showed up later again, so that there might be problems with the reliability of some of the electrical resistivity-data.

*Temperature*
The temperature measurement with the GeoB-core logger (as explained above) is used for calculating the temperature compensation. The AWI-core logger uses a bimetal sensor, which was calibrated both with a Hg-thermometer and a digital thermometer.

*Digital Imaging – Color Scanning (GeoB-device)*
Spectral light reflectance is a measure of the relative amount of light reflected by a material under incident white light. It is expressed within an absolute range from 0 (minimum) to 255 (maximum) and specified as average value for the red (600 - 700 nm), green (500 - 600 nm) and blue (400 - 500 nm) color band (RGB system). The reflectance properties of sediments relate to their chemistry and structure and are dominated by pigmented trace constituents, typically Fe and Mn bearing minerals (clays, oxides, sulfides) and organic enrichments. Reflectance logs provide high-resolution records of terrigenous content (total reflectance) and redox state (red/blue ratio). Scanned at high spatial resolution, reflectance images provide sharp, undistorted, true-color core photographs scarcely affected by undesirable artefacts known from classical core photography (shadows, reflections etc.).

The digital imaging module of the GEOTEK MSCL consists of a camera containing three separate 3*1024 pixel CCD detectors mounted in the focal planes of split light beams ~40 cm above the surface of the sediment and equipped with red, green and blue dichroic filters. This camera captures consecutive, strictly orthogonal line images of the bypassing split core surface. The sediment is illuminated from above by two white fluorescent tubes. Freshly cut archive halves were carefully leveled to prevent shadows from residual surface roughness. All cores were scanned at an axial resolution setting of 100, corresponding to 1 row of pixels for every 100 $\mu$m in core depth. The resolution achieved across the core is nearly equivalent. The brightest part of each core was selected to determine the lens aperture value, which allows the entire core to be measured on the same setting without saturating any of the color channels. Each reflectance value is calibrated against the range defined by a white tile (white calibration) and a closed lens cap (black calibration). Color test cards were measured before and after each core to determine and linearly correct drift effects of the CCD sensors.

A specific post-processing software was used on-board to perform all necessary image corrections and calculations. The processing starts out by cropping end-cap and cavity sections and by removing spurious color stripes caused by a non-uniform response of individual color channels. This task is efficiently solved by normalizing the means within each down-core column of data to the same mean-core value. The individual segment images are then merged into a full core image and numerically compressed in various ways. The median value of each data row was chosen as representative reflectance value in the depth series of red, green and blue reflectance, total reflectance (mean value of R, G and B) and for the red/blue ratio.

Contrast-enhanced color images were produced to improve the identification of layers, gradients, and textures (Fig. 7.5.1). For this purpose, the RGB images were transformed to the equivalent hue, saturation and value (HSV) color system. By linearly expanding the data range of the value (intensity) parameter, the available contrast is broadened without shifting hue (dominant wavelength) and saturation (degree of purity) of each

colour, hence, the specific aspects of mineral color. In the standard processing, the 10 % and 90 % percentiles of V were determined for each core and linearly rescaled to a value range reaching from 25 % to 75 % total reflectance.

### Interpretation

Of the physical property data, particularly magnetic susceptibility and GRA-density data were very useful to distinguish the major lithologies found in the sediment cores. Sediments recovered during ANT-XXVI/2 were primarily composed of siliceous and calcareous microfossils and generally minor amounts of siliciclastic material. Within this three-component system, siliceous ooze is characterized by low magnetic susceptibility and low GRA-density, calcareous ooze by low magnetic susceptibility and high GRA-density, and more siliciclastic (lithogenic) sediments (mostly mud-bearing biogenic ooze) by comparatively high magnetic susceptibility combined with high GRA-density (Fig. 7.5.2).

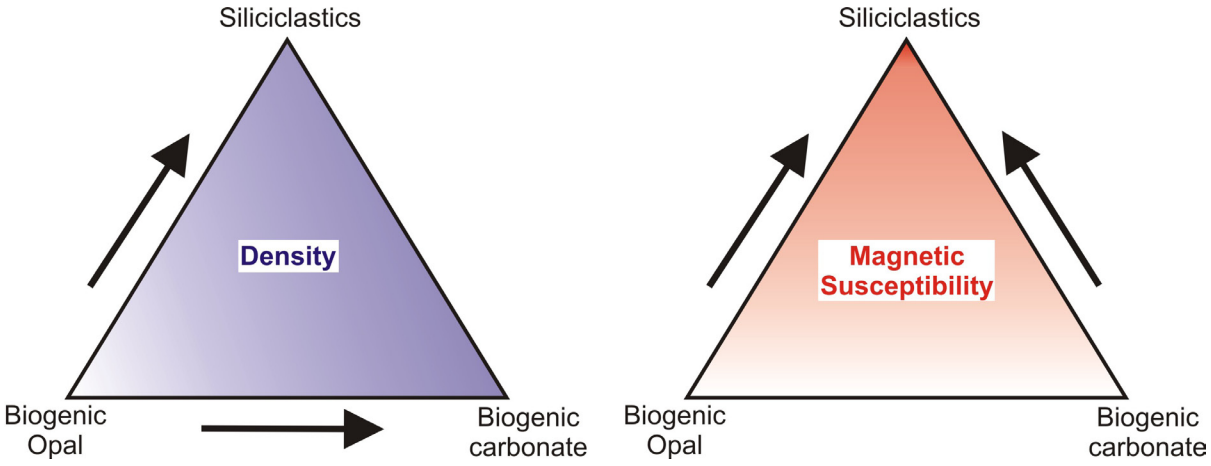


*Fig. 7.5.2: Simplified view of the three-component system describing the major lithological components of sediments recovered during ANT-XXVI/2 in terms of physical properties*

By comparing the GRA-density and magnetic susceptibility records of the individual cores, the major lithologies can mostly be distinguished and lithological information from opened sediment cores can be transferred to those not opened on-board. Fig. 7.5.3 shows an example of a core (PS75/035-1) in which magnetic susceptibility and GRA-density reveal largely parallel fluctuations suggesting an intercalation of diatom-ooze (low magnetic susceptibility, low density) with mud-bearing diatom ooze (high magnetic susceptibility, high density) except for a nannofossil-ooze layer between ~6 m and 7 m core depth (Chapter 7.4; Appendix A7), which is characterized by low magnetic susceptibility and high GRA-density.

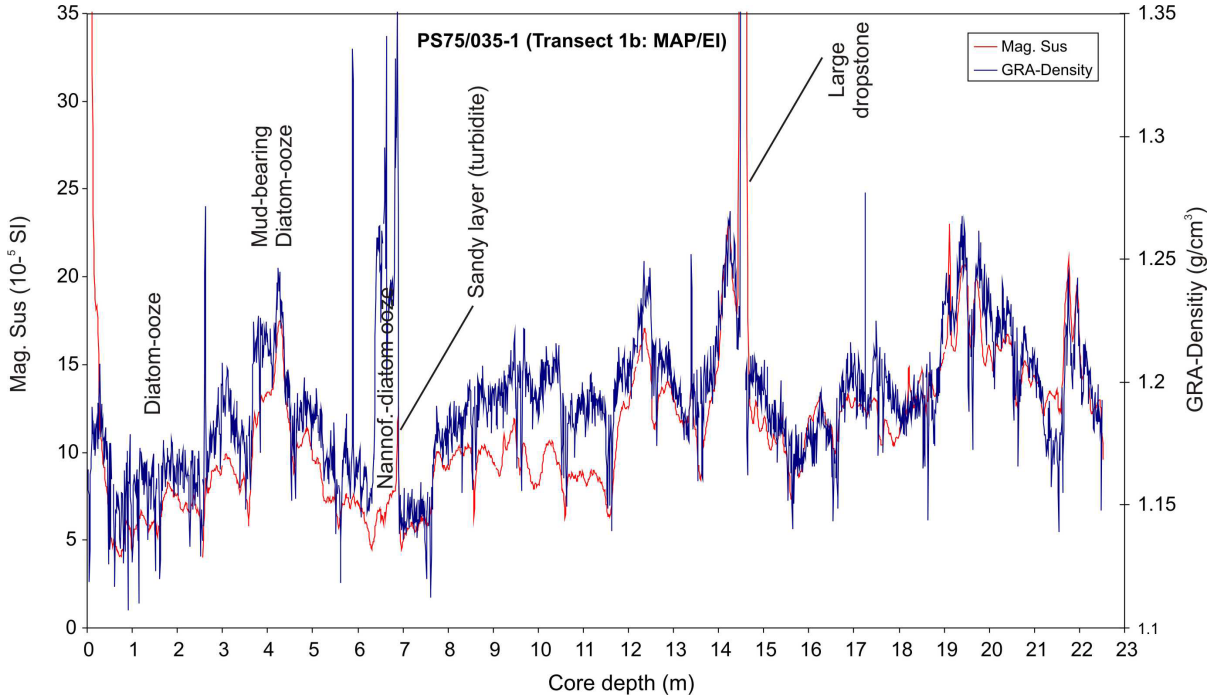


*Fig. 7.5.3: Magnetic susceptibility and GRA-density record of core PS75/035-1 with assignment of major lithologies found in the core*

A second example is shown in Fig. 7.5.4. In this core, magnetic susceptibility and GRA-density changes are largely anti-phased, consistent with the intercalation of calcareous *versus* more diatom/siliciclastic-rich lithologies found in the core (Chapter 7.4; Appendix A7).

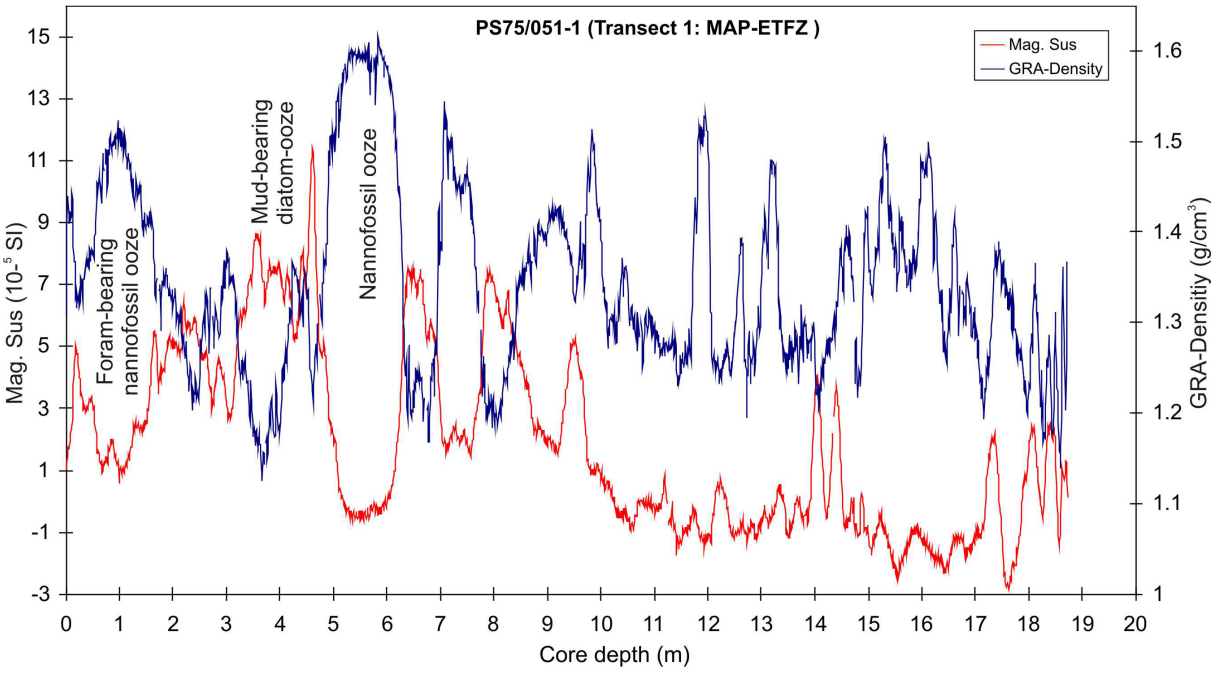


*Fig. 7.5.4: Magnetic susceptibility and GRA-density record of core PS75/051-1 with assignment of major lithologies found in the core*

**References**

Boyce, R.E., 1968. Electrical resistivity of modern marine sediments from the Bering Sea. Journal of Geophysical Research 73, 4759-4766.

## 7.6 Ship-board stratigraphy

Giuseppe Cortese[1], Oliver Esper[2], Rainer Gersonde[2], Matt Konfirst[3], Frank Lamy[2], Mariem Saavedra-Pellitero[4]

[1]GNS Science
[2]Alfred-Wegener-Institut
[3]Northern Illinois University
[4]University of Salamanca

### Objectives

The development of preliminary age-models on-board is a major prerequisite for assessing the suitability of the recovered sediment cores for envisaged post-cruise marine geological studies (Chapter 7.1 and 7.7) and for correlating sediment cores along the different transects. A combination of diatom, calcareous nannofossil, and radiolarian ages are used to obtain bottom (core-catcher) ages of all cores in order to estimate average sedimentation-rates (Table 7.6.1). For the majority of the cores, more detailed preliminary age-models could be provided shipboard. These age-models are based on a combination of the biostratigraphic findings with lithological and physical property data (Chapter 7.4-7.5). Physical property data (particularly magnetic susceptibility and GRA-density records (Chapter 7.5)) provided a very useful tool in order to link lithological changes to Pleistocene glacial/interglacial cycles. Identification of Southern Ocean microfossil biozones was used to assign Marine Isotope Stages to cycles observed in the physical property data.

### Work at Sea

Sediment samples were taken from the tops of each of the ~1-meter core segments and the core catcher from each of the cores collected during the expedition ANT-XXVI/2. Smear slides were prepared using meltmount in toluene for the diatom samples and Canada balsam for the calcareous nannofossil samples and examined under the light microscope. Radiolarians were present in low quantities, and for this reason it was preferred to disaggregate and sieve the core catcher samples to concentrate the specimens before preparing them for taxonomic analysis. This was done for 12 cores and provided more accurate radiolarian age determinations. Maximum ages were determined from core catcher samples at the base of each core. More detailed diatom and calcareous nannofossil biostratigraphic characterization was performed on selected cores to aid in correlation of sediment layers present at different sites. Ship-board diatom identification and dating follows the published work of Harwood and Maruyama (1992), Censarek and Gersonde (2002), Zielinski and Gersonde (2002) and Zielinski et al. (2002). Calcareous nannofossil identification and dating follows Perch-Nielsen (1985), Bown and Young (1998), Hine and Weaver (1998), Young (1998) and Lourens et al. (2004). The dating of samples by radiolarian biostratigraphy follows the biozonation for the Southern Ocean proposed by Lazarus (1992). Details on physical property measurements including their interpretation in terms of lithological changes are given in Chapter 7.5.

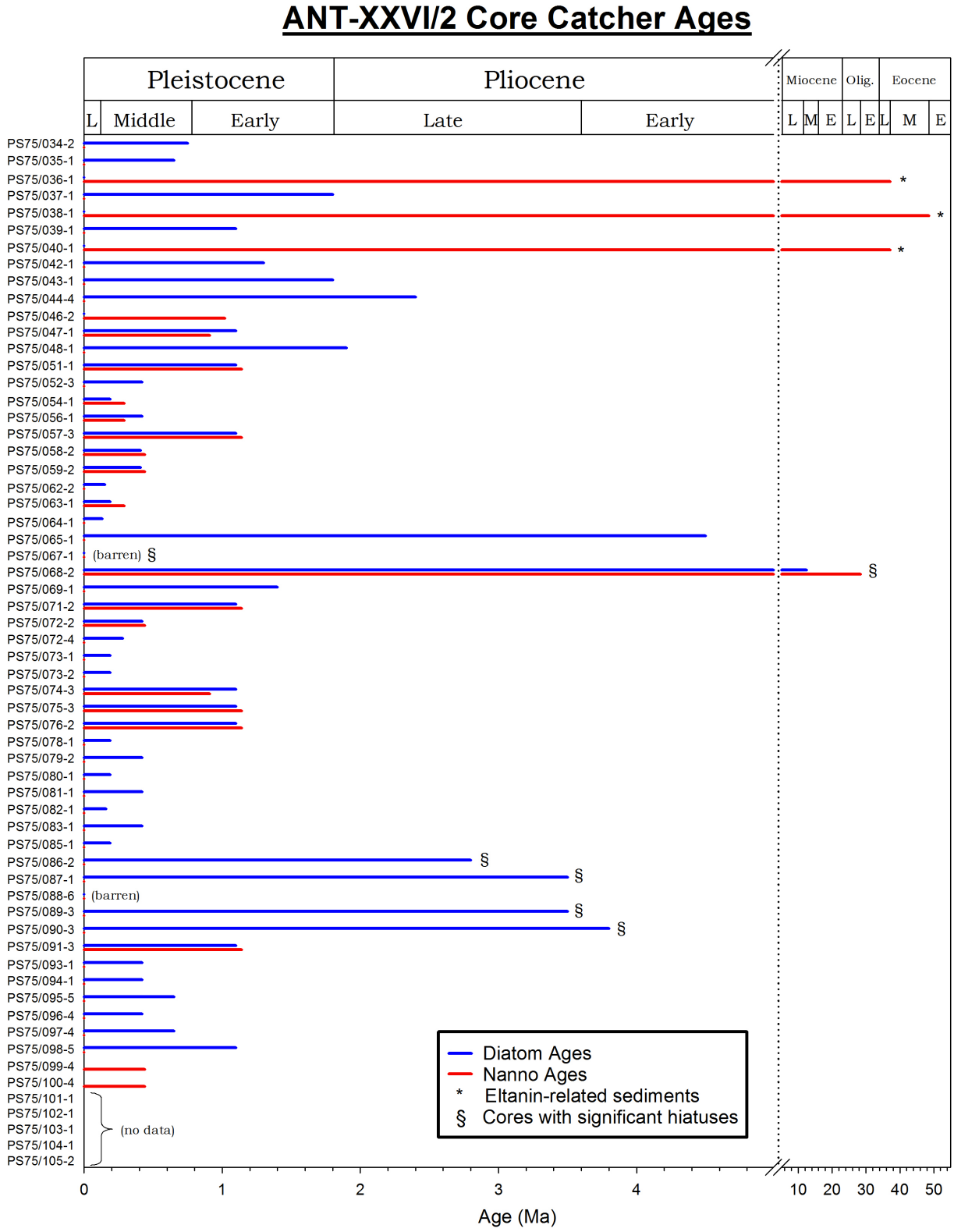


*Fig. 7.6.1: Diatom and calcareous nannofossils were used to determine the maximum age of each of the sediment cores taken during the expedition ANT-XXVI/2.*

**Tab. 7.6.1:** Absolute ages of cores collected from ANT-XXVI/2 as determined by diatom and calcareous nannofossil assemblages

**Biostratigraphic Ages and Average Sedimentation Rates of ANT-XXVI/2 Sediment Cores**

| Station No. | Latitude | Longitude | Water depth (DWS) | Core length (m) | Diatom CC-age (Ma) | Nanno CC-age (Ma) | Composite CC-age (Ma) | Sed-rates (cm/kyr) |
|---|---|---|---|---|---|---|---|---|
| ***TRANSECT 1: MAP- ETFZ ( Mornington Abyssal Plain (MAP) - southern East Pacific Rise (EPR) - Eltanin-Tharp Fracture Zone (ETFZ))*** | | | | | | | | |
| PS75/034-2 | 54°22.112´S | 80°05.380´W | 4425 | 18.08 | 0.75 | (barren) | 0.75 | 2.4 |
| PS75/044-4 | 56°05.15´S | 96°46.82´W | 5000 | 20.93 | ≤ 2.4 | (barren) | 2.4 | 0.9 |
| PS75/046-2 | 54°24.92'S | 102°30.22'W | 2984 | 17.26 | (barren) | ≤ 1.02 | 1.02 | 1.7 |
| PS75/047-1 | 54°20.771'S | 102°44.82'W | 4480 | 22.98 | < 1.1 | ≤ 0.91 | 0.91 | 2.5 |
| PS75/048-1 | 54°20.35'S | 102°45.51'W | 4516 | 19.88 | ≤ 1.9 | (barren) | 1.9 | 1.0 |
| PS75/051-1 | 52°48.73'S | 107°48.33'W | 3949 | 18.73 | ≤ 1.1 | < 1.14 | 1.1 | 1.7 |
| PS75/054-1 | 56°09.105'S | 115° 07.982'W | 4113 | 22.38 | ≤ 0.19 | < 0.29 | 0.19 | 11.8 |
| PS75/056-1 | 55°09.74'S | 114°47.31'W | 3581 | 10.21 | < 0.42 | ≤ 0.29 | 0.29 | 3.5 |
| PS75/057-3 | 53°31.98'S | 118°54.98'W | 2888 | 18.12 | ≤ 1.1 | < 1.14 | 1.1 | 1.6 |
| PS75/058-2 | 54°12.86'S | 125°26.20'W | 3629 | 12.96 | ≤ 0.41 | < 0.44 | 0.41 | 3.2 |
| PS75/059-2 | 54°12.90'S | 125°25.53'W | 3613 | 13.98 | ≤ 0.41 | < 0.44 | 0.41 | 3.4 |
| ***Subtransect 1a: FS/El (Freeden Seamounts (FS)/Eltanin Impact (El))*** | | | | | | | | |
| PS75/035-1 | 57°46.17´S | 90°41.02´W | 5224 | 22.53 | ≤ 0.65 | (barren) | 0.65 | 3.5 |
| *PS75/036-1 | 57°44.44´S | 90°43.56´W | 5313 | 22.74 | (barren) | ≤ 37.2 | 37.2 | 0.1 |
| PS75/037-1 | 57°46.50´S | 91°24.69´W | 4879 | 22.73 | ≤ 1.8 | (barren) | 1.8 | 1.3 |
| *PS75/038-1 | 57°51.70´S | 91°06.84´W | 4208 | 21.83 | (barren) | ≤ 48.6 | 48.6 | 0.0 |
| PS75/039-1 | 57°39.98´S | 90°51.76´W | 5231 | 22.15 | ≤ 1.1 | (barren) | 1.1 | 2.0 |
| *PS75/040-1 | 57°38.88´S | 91°09.14´W | 3400 | 9.36 | (barren) | ≤ 37.2 | 37.2 | 0.0 |
| PS75/042-1 | 57°43.41´S | 91°42.77´W | 4917 | 23.54 | 1.3 | (barren) | 1.3 | 1.8 |
| PS75/043-1 | 57°42.01´S | 91°58.61´W | 4619 | 23.48 | 1.8 | (barren) | 1.8 | 1.3 |
| ***Subtransect 1b: EPR-AAP (southern EPR - Amundsen Abyssal Plain)*** | | | | | | | | |
| PS75/052-3 | 60°45.12'S | 115°58.74'W | 5130 | 23.17 | ≤ 0.42 | (barren) | 0.42 | 5.5 |
| ***TRANSECT 2: ETFZ-AAP (Eltanin-Tharp Fracture Zone - northern Amundsen Abyssal Plain)*** | | | | | | | | |
| PS75/062-2 | 58°16.60'S | 135°37.61'W | 4165 | 21.09 | ≤ 0.15 | (barren) | 0.15 | 14.1 |
| PS75/063-1 | 58°54.24'S | 135°37.23'W | 3795 | 22.46 | ≤ 0.19 | < 0.29 | 0.19 | 11.8 |
| PS75/064-1 | 61°00.74'S | 139°27.85'W | 4600 | 15.43 | ≤ 0.13 | (barren) | 0.13 | 11.9 |
| PS75/065-1 | 62°36.21'S | 141°30.90'W | 4499 | 18.6 | ≤ 4.5 | (barren) | 4.5 | 0.4 |
| §PS75/067-1 | 64°58.23'S | 143°48.22'W | 4151 | 17.95 | (barren) | (barren) | --- | --- |
| §PS75/068-2 | 64°56.01'S | 144°06.81'W | 3728 | 14.12 | ≤ 12.5 | < 28.4 | 12.5 | 0.1 |
| ***TRANSECT 3: AAP-SWP (northern Amundsen Abyssal Plain - northern Pacific-Antarctic Ridge - Southwest-Pacific Basin)*** | | | | | | | | |
| PS75/069-1 | 62°12.24'S | 145°37.11'W | 4334 | 18.46 | ≤ 1.4 | (barren) | 1.4 | 1.3 |
| PS75/070-2 | 58°34.87'S | 150°03.97'W | 2842 | 0 | --- | --- | --- | --- |
| PS75/071-2 | 57°52.40'S | 150°52.11'W | 2926 | 11.36 | ≤ 1.1 | < 1.14 | 1.1 | 1.0 |
| PS75/072-2 | 57°33.51'S | 151°13.11'W | 3098 | 14.97 | ≤ 0.42 | < 0.44 | 0.42 | 3.6 |
| PS75/072-4 | 57°33.51'S | 151°13.17'W | 3099 | 9.61 | ≤ 0.28 | (barren) | 0.28 | 3.4 |
| PS75/073-1 | 57°12.26'S | 151°36.63'W | 3238 | 17.04 | ≤ 0.19 | (barren) | 0.19 | 9.0 |
| PS75/073-2 | 57°12.26'S | 151°36.65'W | 3234 | 3.68 | ≤ 0.19 | (barren) | 0.19 | --- |
| PS75/074-3 | 56°14.65'S | 152°39.30'W | 3295 | 20.95 | < 1.1 | ≤ 0.91 | 0.91 | 2.3 |
| PS75/075-3 | 54°24.23'S | 154°35.18'W | 4096 | 18.35 | ≤ 1.1 | < 1.14 | 1.1 | 1.7 |
| ***TRANSECT 4: SWP-ROS (Southwest-Pacific Basin - Pacific-Antarctic Ridge - northern Ross Sea)*** | | | | | | | | |
| PS75/076-2 | 55°31.71'S | 156°08.39'W | 3742 | 20.59 | ≤ 1.1 | < 1.14 | 1.1 | 1.9 |
| PS75/078-1 | 61°03.00'S | 159°35.18'W | 3315 | 3.83 | ≤ 0.19 | (barren) | 0.19 | 2.0 |
| PS75/079-2 | 57°30.16'S | 157°14.25'W | 3770 | 18.51 | ≤ 0.42 | (barren) | 0.42 | 4.4 |
| PS75/080-1 | 58°10.63'S | 157°38.19'W | 3874 | 12.2 | ≤ 0.19 | (barren) | 0.19 | 6.4 |
| PS75/081-1 | 58°14.486'S | 157°42.44'W | 3857 | 13.71 | ≤ 0.42 | (barren) | 0.42 | 3.3 |
| PS75/082-1 | 59°02.48'S | 158°21.82'W | 4000 | 10.88 | ≤ 0.16 | (barren) | 0.16 | 6.8 |
| PS75/083-1 | 60°16.13'S | 159°03.59'W | 3599 | 13.13 | ≤ 0.42 | (barren) | 0.42 | 3.1 |
| PS75/085-1 | 61°56.38'S | 160°07.10'W | 3734 | 19.74 | < 0.19 | (barren) | 0.19 | 10.4 |
| §PS75/086-2 | 64°44.64'S | 161°54.19'W | 4065 | 12.74 | ≥ 2.8 | (barren) | 2.8 | 0.5 |
| §PS75/087-1 | 66°47.29'S | 163°19.47'W | 4406 | 11.28 | ≤ 3.5 | (barren) | 3.5 | 0.3 |
| PS75/088-6 | 68°43.82'S | 164°48.95'W | 3857 | 12.4 | (barren) | (barren) | --- | --- |
| ***TRANSECT 5: ROS - NZM (northern Ross Sea - Pacific-Antarctic Ridge - Southwest-Pacific Basin - eastern New Zealand margin )*** | | | | | | | | |
| §PS75/089-3 | 67°05.01'S | 165°32.46'W | 4126 | 11.12 | ~3.5 | (barren) | 3.5 | 0.3 |
| §PS75/090-3 | 65°24.66'S | 166°09.28'W | 3478 | 17.91 | ≤ 3.8 | (barren) | 3.8 | 0.5 |
| PS75/091-3 | 63°41.66'S | 169°04.47'W | 2940 | 13.44 | ≤ 1.1 | < 1.14 | 1.1 | 1.2 |
| PS75/093-1 | 60°52.33'S | 169°32.89'W | 3762 | 12.84 | ≤ 0.42 | (barren) | 0.42 | 3.1 |
| PS75/094-1 | 61°49.34'S | 169°44.69'W | 3270 | 9.7 | ≤ 0.42 | (barren) | 0.42 | 2.3 |
| PS75/095-5 | 57°01.18'S | 174°25.80'W | 4853 | 17.85 | ≤ 0.65 | (barren) | 0.65 | 2.7 |
| PS75/096-4 | 58°32.86'S | 172°42.06'W | 5057 | 22.79 | ≤ 0.42 | (barren) | 0.42 | 5.4 |
| PS75/097-4 | 59°42.02'S | 171°21.44'W | 4672 | 17.46 | ≤ 0.65 | (barren) | 0.65 | 2.7 |
| PS75/098-5 | 52°57.93'S | 179°00.62'W | 5189 | 22.83 | ≤ 1.1 | (barren) | 1.1 | 2.1 |
| PS75/099-4 | 48°15.72'S | 177°16.35'E | 1272 | 7.71 | (no data) | ≤ 0.44 | 0.44 | 1.8 |
| PS75/100-5 | 45°45.41'S | 177°08.93'E | 2497 | 14.77 | (no data) | ≤ 0.44 | 0.44 | 3.4 |
| PS75/101-1 | 45°48.42'S | 175°52.66'E | 1770 | 11.8 | (no data) | (no data) | --- | --- |
| PS75/102-1 | 45°41.20'S | 175°43.29'E | 1621 | 12.96 | (no data) | (no data) | --- | --- |
| PS75/103-1 | 45°30.93'S | 175°29.99'E | 1390 | 13.15 | (no data) | (no data) | --- | --- |
| PS75/104-1 | 45°46.15'S | 174°31.53'E | 835 | 12.39 | (no data) | (no data) | --- | --- |
| PS75/105-2 | 44°24.51'S | 174°37.51'E | 668 | 15.09 | (no data) | (no data) | --- | --- |

* Eltanin-related sediments

§ Cores with significant hiatuses

## Preliminary Results

Maximum core ages are plotted in figure 7.6.1 and absolute ages of core catcher samples are given in table 7.6.1. Estimates of basal ages based on diatoms and calcareous nannofossils are generally in good agreement with one another within the resolution of the respective fossil groups. However, coccolithophores are absent in many of the cores, particularly those collected from more south of the Polar Front (PF).

Thirty-six out of the fifty cores displayed in Table 7.6.1 had a Pleistocene basal age. Particularly high sedimentation rates (>10 cm/kyr) were recorded close to the PF (cores PS75/052-3, PS75/062-2, and PS75/063-1), in the Permanent Open Ocean Zone (POOZ) (cores PS75/064-1 and PS75/085-1), and in one occasion slightly to the north of the Subantarctic Front (SAF) (core PS75/054-1). Several cores contained a low-resolution record covering the last 3 - 3.5 Ma (approximately the whole Pliocene-Pleistocene interval): PS75/069-1 (basal age: lower Pliocene); PS75/086-2, PS75/087-1, and PS75/089-3 (Pliocene); and PS75/090-3 (late Pliocene). A few cores collected along transect 2 (ETFZ-AAP) displayed signs of reworking/mixing of sediment (e.g., cores PS75/065-1 and PS75/067-1), or presence of widespread hiatuses (e.g., core PS75/068-2, where most of the Pliocene is missing).

Three cores of Subtransect 1a (FS/EI) contain sediments with Eocene basal ages, which were barren of diatoms. Therefore, basal ages are based on coccolithophores alone. These cores document the Eltanin asteroid impact (Gersonde et al., 1997). For more details see Subchapter 7.7.8.

## References

Bown, P. R, Young, J.R., 1998. Introduction. In: Bown, P. R. (Ed.) Calcareous nannofossil biostratigraphy, Chapman & Hall, London, pp. 1-15.

Censarek, B., Gersonde, R., 2002. Miocene diatom biostratigraphy at ODP Sites 689, 690, 1088, 1092 (Atlantic sector of the Southern Ocean). Marine Micropaleontology, 45, 309-356.

Gersonde, R, Kyte, F.T., Bleil, U., Diekmann, B., Flores, J. A., Gohl, K., Grahl, G., Hagen, R., Kuhn, G., Sierro, F. J., Völker, D., Abelmann, A., and Bostwick J. A., 1997. Geological record and reconstruction of the late Pliocene impact of the Eltanin asteroid in the Southern Ocean. Nature 390, 357-363.

Harwood, D. M., Maruyama, T., 1992. Middle Eocene to Pleistocene diatom biostratigraphy of Southern Ocean sediments from the Kerguelen Plateau, Leg 120. Proceedings of the Ocean Drilling Program, Scientific Results, Vol. 120, 683-733.

Hine, N., Weaver, P. P. E., 1998. Quaternary. In: Bown, P. R. (Ed.) Calcareous nannofossil biostratigraphy, Chapman & Hall, London, pp. 265-278.

Lazarus, D., 1992. Antarctic Neogene radiolarians from the Kerguelen Plateau, Legs 119 and 120. In: Wise, S.W. Jr. and Schlich, R., et al. (Eds.), Proceedings of the Ocean Drilling Program, Scientific Results, Volume 120, 785-809.

Lourens, L. J., Hilgen, F. J., Shackleton, N. J., Laskar, J., Wilson, D., 2004. The Neogene Period. In: Gradstein, F. M., Ogg J. G., Smith, A. G. (Eds.), A Geological Time Scale, Cambridge University Press, Cambridge, pp. 409-440.

Perch-Nielsen, K., 1985. Cenozoic calcareous nannofossils. In: Bolli, H. M., Saunders, J. B., Perch-Nielsen, Y.K. (Eds.), Plankton Stratigraphy, Cambridge University Press, Cambridge, pp. 427-555.

Young, J., 1998. Neogene. In: Bown, P. R. (Ed.) Calcareous nannofossil biostratigraphy,

Chapman & Hall, London, pp. 225-265.

Zielinski, U., Gersonde, R., 2002. Plio-Pleistocene biostratigraphy from ODP Leg 177, Atlantic Sector of the Southern Ocean. Marine Micropaleontology 45, 225-268.

Zielinski, U., Bianchi, C., Gersonde, R., Kunz-Pirrung, M., 2002. Last occurrence datums of the diatoms Rouxia leventerae and Rouxia constricta: indicators for marine isotope stages 6 and 8 in Southern Ocean sediments. Marine Micropaleontology 45, 127-137.

## 7.7 Marine geological projects

### 7.7.1 Surface sediment data sets for documentation of modern sedimentation patterns and paleoceanographic proxy calibration

Rainer Gersonde[1], Giuseppe Cortese[2], Oliver Esper[1], Susanne Fietz[3], Sze Ling Ho[1], Alfredo Martinez-Garcia[4], Marie Meheust[1], Katharina Pahnke[5], Gemma Rueda[3], Mariem Saavedra-Pellitero[6], Silke Steph[1,7]

[1]Alfred-Wegener-Institut
[2]GNS Science
[3]Universitat Autònoma de Barcelona
[4]ETH-Zürich
[5]University of Hawaii
[6]University of Salamanca
[7]University of Potsdam

**Objectives**

The study of surface samples is required a) to document the modern sedimentation pattern and related flux rates of biogenic, terrestrial and eolian components, b) to understand the processes that lead the deposition of a sedimentary signal and based on this c) to generate reference data sets for paleoceanographic proxy calibration, which represent a critical prerequisite for paleoceanographic reconstructions. The latter concerns established proxies such as census-based siliceous, calcareous and organic-walled microfossil assemblages (diatoms, radiolarians, coccoliths, planktic foraminifers and dinoflagellate cysts), stable isotope signatures of benthic and planktic foraminifers, foraminiferal-based Mg/Ca temperatures and alkenone-derived SSTs, but also new organic biomarker SST proxies such as $TEX_{86}$ that has a great potential for temperature reconstructions in high latitudes. In this respect the study of surface sediment samples will allow to fill the temperature range missing in the present calibration ca. 0 - 10ºC (Kim et al., 2008) and hopefully make $TEX_{86}$ an applicable proxy in the polar regions. Further proxies that will be studied in the polar South Pacific are alkenone isotopes as a salinity proxy, the flux of alkenones and pigments as productivity proxies, the isotopic composition of microfossil-bound Nitrogen, Neodymium isotopes as water mass tracer, and the distribution of terrigenous biomarkers and their isotopic values to link it with the source of the terrigenous organic matter.

**Expected results**

The surface sediment samples recovered from the different environmental regimes and water depth in the Polar South Pacific can be used for different sedimentological, geochemical and micropaleontological analyses. This includes analyses of a) the isotopic composition of diatoms, foraminifers and radiolarians for paleoenvironmental reconstructions (e.g. productivity and sea surface salinity), b) ice-rafted debris for iceberg drift reconstructions, c) diatom and radiolarian assemblages for paleoceanographic

reconstructions, d) dinoflagellate cysts for the reconstruction of past sea-surface conditions (e.g. sea surface temperature, sea surface salinity, sea-ice cover and primary productivity), e) phytoplankton pigments and sterols for the reconstruction of paleoproductivity, f) sediment geochemical and grain size analyses, g) surface sediment age determination with radiometeric methods ($^{210}$Pb, $^{14}$C bulk, $^{14}$C foraminifera), g) trace metal mapping, h) radionuclide flux (e.g. $_{ex}^{230}$Th, $^{231}$Pa, $^{4}$He), i) Mg/Ca ratios in foraminiferal calcite tests, j) $U^{k'}_{37}$ measurements on alkenones, k) TEX86 determination based on archaeal lipids (SST reconstructions), and l) determination of the dust flux into the sediments (for details see Chapter 5).

### References

Kim J. H., Schouten S., Hopmans E. C., Donner B., Sinninghe Damsté J. S., 2008. Global sediment core-top calibration of the $TEX_{86}$ paleothermometer in the ocean. Geochimica et Cosmochimica Acta 72, 1154-1173.

## 7.7.2 Timing and response of Pacific Southern Ocean paleoceanography to external forcing mechanisms, past climate tele-connections and interhemispheric links

Rainer Gersonde[1], Frank Lamy[1], Giuseppe Cortese[2], Oliver Esper[1], Susanne Fietz[3], Sze Ling Ho[1], Alfredo Martinez-Garcia[4], Katharina Pahnke[5], Silke Steph[1,6]

[1]Alfred-Wegener-Institut
[2]GNS Science
[3]Universitat Autònoma de Barcelona
[4]ETH-Zürich
[5]University of Hawaii
[6]University of Potsdam

### Objectives

The response of the southern high latitudes on millennial/centennial and orbital times-scales to both external climate drivers (insolation, solar variability), and internal amplifiers (e.g. thermohaline circulation, changes in the carbon cycle, sea ice albedo) is still not sufficiently established. Multiple studies have pointed out the role of North Atlantic Deep Water (NADW) formation in amplifying millennial climate variability during glacial periods. Although NADW variability may be linked to meltwater surges into the North Atlantic (e.g. Ganopolski and Rahmstorf 2001), other studies have emphasized the importance of the SO sea-ice for NADW formation and suggested that the glacial “on” and “off” mode of global circulation was linked to a very different mode of deep-water formation in the SO (Keeling and Stephens, 2001). While a number of high resolution records document the Pleistocene climate development of the Atlantic and Indian sector, the behavior and role of the Pacific southern-high latitude sector, which links the low and high latitude Pacific with the Atlantic is still relatively unexplored. Consequently, a number of leading hypotheses postulating that changes in this sector could play an active role in triggering and propagating abrupt ocean-climate changes remain untested. For example, numerical model studies suggest that the discharge of melt-water from the WAIS and related reductions in surface water salinity could trigger a seesaw mechanism that has global scale consequences for ocean circulation and climate (Mikolajewicz, 1998, Weaver et al., 2003). Some available records from the mid-latitude South Pacific continental margins (i.e., off Chile and New Zealand) suggest that changes in Southern Ocean climate, southern westerly winds, and southern hemisphere water mass ventilation are all part and parcel of global millennial-

scale climate events (e.g., Lamy et al., 2004; Pahnke et al., 2003).

Even on orbital time-scales regional differences between the Southern Ocean sectors are evident. Although showing a similar pattern e.g. with Atlantic Southern Ocean records, the few available SST records from the Pacific Southern Ocean display lower glacial/interglacial amplitudes compared with the Atlantic sector. Reasons for this difference, which is also obvious from a Mg/Ca derived Subantarctic Pacific SST record (Mashiotta et al., 1999, core *E11-2* recovered near PS75/054) and a circum-Antarctic mapping of LGM SST and sea ice (Gersonde et al., 2005) still need to be resolved.

**Preliminary results**

Sediment cores with high average sedimentation rates of >10 cm/kyr suitable for millennial-scale studies have been recovered at six sites during ANT-XXVI/2. These cores are located close to the Polar Front (PF) (cores PS75/052-3, PS75/062-2, and PS75/063-1), in the Permanent Open Ocean Zone (POOZ) (cores PS75/064-1 and PS75/085-1), and, in one occasion, slightly to the north of the Subpolar Front (SF) (core PS75/054-1) (Chapter 7.6). The PF cores and the POOZ cores are primarily composed of siliceous ooze and are thus particularly suitable for diatom-based paleoceanographic studies. Moreover, low carbonate contents and occasional calcareous nannofossils observed in smear slides (e.g. cores PS75/062-1 and PS75/63-1), suggest that alkenone-based SST estimates will be possible at most of the sites. Furthermore, we plan to apply $TEX_{86}$ paleothermometry at selected sites and compare these biomarker-based SST estimates to those derived from diatom assemblages. Carbonate contents are substantially higher at site PS75/054 located north of the SF. This core will likely allow to derive an oxygen isotope record at least on planktic foraminifera and potentially even Mg/Ca paleotemperatures. This site will thus be a key location for a detailed multi-proxy study involving a large variety of biomarker, carbonate, and opal-based paleoceanographic proxies.

Moderate average sedimentation-rates (~3 to 9 cm/kyr) characterize most other cores from the POOZ section of Transects 3, 4 and 5. Further north, cores from the PFZ at Transects 3 and 4 show sedimentation-rates in the order of ~2 cm/kyr and contain substantially higher amounts of calcareous microfossils These cores may thus be particularly suitable for carbonate-based proxy studies on orbital and possibly even sub-orbital time-scales.

A major prerequisite for studying interhemsipheric links and past-climate teleconnections are reliable and highly resolved age models. We plan to generate oxygen isotope stratigraphies on the sediment cores with moderate sedimentation-rates from the PFZ in Transects 4 and 5, that may be transferred to lower-carbonate POOZ cores from these transects by physical properties correlation (7.6). At the diatom-dominated sites, we will primarily rely on biostratigraphy and correlation of e.g. SST and/or dust records to Antarctic ice-cores. Paleomagnetic dating may be helpful at the western South Pacific sites (Transects 4 and 5) where the content of siliciclastic components is higher. Younger sediments will be also radiocarbon dated depending on the availability of datable material (preferably foraminifera).

Finally, we recovered a number of sediment cores on a depth transect from ~2,500 m to ~700 m water depth at the New Zealand continental margin (Bounty trough) shortly

before arriving at Wellington. These cores have not been opened and biostratigraphic data is not yet available. However, carbonate content estimates and lithological observations at core breaks during the cutting of segments, suggest that at least the shallower cores (PS75/103-1 to PS75/105-1) contain hemipelagic sediments with moderate to high sedimentation-rates. These cores will be easily datable (radiocarbon dating and oxygen isotope records) and used for reconstructing changes in Antarctic Intermediate Water over the past two glacial-interglacial cycles (Chapter 7.7.4).

### References

Ganopolski, A., Rahmstorf, S., 2001. Rapid changes of glacial climate simulated in a coupled climate model. Nature 409, 153-158.

Gersonde, R., Crosta, X., Abelmann, A., Armand, L., 2005. Sea-surface temperature and sea ice distribution of the Southern ocean at the EPILOG Last Glacial Maximum – a circum-Antarctic view based on siliceous microfossils. Quaternary Science Reviews 24, 869-896.

Keeling, R. F., Stephens, B.B., 2001. Antarctic sea ice and the control of pleistocene climate instability. Palaeogeography 16, 112-131.

Lamy, F., Kaiser, J., Ninnemann, U., Hebbeln, D., Arz, H. W., Stoner, J., 2004 . Antarctic Timing of Surface Water Changes off Chile and Patagonian Ice Sheet Response. Science 304, 1959-1962.

Mashiotta, T. A., Lea, D. W., Spero, H., 1999. Glacial-interglacial changes in Subantarctic sea surface temperature and d18O-water using foraminiferal Mg. Earth and Planetary Science Letters 170, 417-432.

Mikolajewicz, U., 1998. Effect of meltwater input from the Antarctic ice sheet on the thermohaline circulation. Annals of Glaciology 27, 311-320.

Pahnke, K., Zahn, R., Elderfield, H, Schulz, M., 2003. 340,000-year centennial-scale marine record of Southern hemisphere climate oscillation. Science 301, 948-952.

Weaver, A. J., Saenko, O. A. et al., 2003. Meltwater pulse 1A from Antarctica as a trigger of the Boelling-Alleroed Warm Interval. Science 299, 1709-1713.

## 7.7.3 Pleistocene changes in Pacific Southern Ocean physical environment and ecosystem/export productivity regimes and their relation to atmospheric $pCO_2$ variability and the global nutrient regime

Rainer Gersonde[1], Frank Lamy[1], Oliver Esper[1], Alfredo Martinez-Garcia[2], Marietta Straub[2]

[1]Alfred-Wegener-Institut
[2]ETH-Zürich

### Obectives

Southern Ocean physical and biological processes exert a strong impact on global ocean biogeochemical cycles and influence atmospheric $CO_2$ concentration. Crucial processes include ocean ventilation/stratification, sea ice extent/seasonality, and biological productivity/export. These processes may have acted as feedbacks that significantly contributed to the Cenozoic climate development. Especially sea ice, which represents a fast changing variable with strong albedo feedback that profoundly affects the physical, chemical, and biological properties of Southern Ocean surface

water, ocean ventilation and atmospheric circulation. High-resolution records of past sea-ice variability based on the diatom record in the Atlantic and Indian sectors of the SW reveal a close correlation between sea-ice variability and atmospheric $CO_2$ at Pleistocene terminations. Such pattern supports models calling for a role of sea ice in glacial-to-interglacial variations in atmospheric $CO_2$, but the magnitude of the sea-ice impact is yet under discussion as the models are still limited in accurate sea-ice reconstruction and only constricted circum-Antarctic sea-ice reconstructions based on the sediment record are yet available. Indeed, reconstruction of the LGM winter sea ice field and surface water temperatures point to a different behavior of these physical parameters in the Pacific sector during the LGM compared with the other sectors of the Southern Ocean. However, this observation relies on a small number of available samples from the Pacific sector calling for the urgent need to increase the set of sediment cores from this sector.

Biogeochemical models simulating modern global ocean nutrient (N, Si) distribution indicate that biological productivity at mid- and low-latitudes is controlled by physical and biological processes occurring at high latitudes, the Southern Ocean playing a primary role. Based on opal isotope measurements ($\delta^{30}Si$, $\delta^{15}N$), some studies postulate increased northward export of silicon during glacials and suggest that the Pacific may be an area of major silicon export, having strong implications on the productivity regimes in coastal upwelling areas and atmospheric $CO_2$ concentration. Such scenario needs to be tested on latitudinal sediment core transects from the Pacific sector.

**Expected results**

Representing a High-Nutrient-Low-Chlorophyll (HNLC) area during warm climate modes the Southern Ocean has strong potential to represent a major $CO_2$ sink during glacial conditions, when increased input of the micronutrient iron enhances the biological pump. The sediment cores from the Pacific sector retrieved during the cruise ANT-XXVI/2 will provide a unique set of samples to assess to what extent glacial dust/iron import from the Australian continent and New Zealand has impacted Pacific Southern Ocean productivity, carbon export, and burial of biogenic particles. In these records a multi-proxy approach based on a combination of organic biomarkers (e.g. alkenones, chlorines, TOC), inorganic redox sensitive tracers (authigenic U, Re, Mo, V, ect), micropaleonthological assemblages, and vertical flux normalizing methods (e.g. $^{230}Th_{ex}$), will be applied. These records will be tied to Antarctic ice core records for a general understanding how changes in greenhouse gas concentration such as $CO_2$ are linked to the deposition of dust, dust-born iron, as well as to Southern Ocean temperature, stratification, biological productivity regimes and related carbon sequestration.

Nitrogen is a main component of the marine biomass and a required nutrient by all marine phytoplankton, therefore, nitrogen isotopes provide information about the patterns of biochemical cycling in the ocean and changes in the nitrate inventory that can be linked to the oceanic gas exchange within the atmosphere and the surface waters. Therefore, the reconstruction of past changes in nutrient utilization will provide important additional information to complement the information obtained from the export production reconstructions, contributing to assess the role of this region in the global biological pump.

Variations in nutrient utilization in the SO during the last glacial period have been intensively studied for more than a decade by measuring the isotopic composition of bulk sedimentary nitrogen. The use of this proxy relies on the observation that the $^{15}N/^{14}N$ of sinking organic mater reflects the utilization of nitrate by marine organisms in regions where nitrate is not completely consumed. Possible caveats of this method include the acknowledged potential for diagenetic artefacts due to the alteration of the isotopic signal during sinking and sedimentation (Altabet and François, 1994), and the possible contribution of foreign (e.g. terrestrial) nitrogen to the bulk sedimentary signal (Ren et al., 2009). However, in recent years a new methodology based on the analysis the isotopic composition of nitrogen bound within microfossil shells (e.g. diatom silica frustules, and carbonate foraminiferal tests), has been developed to overcome these potential biases (Ren et al., 2009; Robinson et al., 2004; Sigman et al., 1999). The idea behind this novel methodology is that the organic material incorporated during the construction of microfossil structures is protected from diagenetic alteration and allochtonous interferences, providing a nitrogen archive directly related to the primary photosynthetic signal that is free of sedimentary artifacts. The novel method employs the denitrifying bacteria *Pseudomonas chlororaphis* and *Pseudomonas aureofaciens* to produce nitrous oxide ($N_2O$) of the nitrate extracted from the organic matter, which is sheltered within the microfossil shells, increasing the sensitivity of the analytical method and allowing the measurement of the isotopic composition of the nitrogen bound within microfossil shells in geologic samples (Sigman et al., 1994)

Hence, the use of microfossil-bound N proxies offers a promising tool to yield a consistent picture of nutrient utilization in the different regions of the SO during last glacial stage and beyond. However, the available microfossil bound dataset from the Pacific sector of the Southern Ocean (Robinson et al., 2008) is far too sparse to asses the nutrient status of the SO during ice ages and its role in controlling atmospheric carbon dioxide concentrations through time. The samples collected during the cruise ANT-XXVI/2, especially those located south of the present day Polar Front and with good carbonate preservation (e.g. PS75/072-4), will provide a unique dataset to assess the contribution of this mechanism to the glacial-interglacial atmospheric $CO_2$ variability observed in the Antarctic ice cores.

## References

Altabet, M.A., Francois, R., 1994. Sedimentary Nitrogen Isotopic Ratio as a Recorder for Surface Ocean Nitrate Utilization. Global Biogeochemical Cycles, 8.

Ren, H., Sigman, D.M., Meckler, A.N., Plessen, B., Robinson, R.S., Rosenthal, Y.,Haug, G.H., 2009. Foraminiferal Isotope Evidence of Reduced Nitrogen Fixation in the Ice Age Atlantic Ocean. Science, 323(5911), 244-248.

Robinson RS, Brunelle BS, and Sigman DM (2004). Revisiting nutrient utilization in the glacial Antarctic: Evidence from a new method for diatom-bound N isotopic analysis, Paleoceanography, 19, PA3001.

Robinson, R.S., Sigman, D.M., 2008. Nitrogen isotopic evidence for a poleward decrease in surface nitrate within the ice age Antarctic. Quaternary Science Reviews, 27(9-10), 1076-1090.

Sigman, D.M., Altabet, M.A., Francois, R., McCorkle, D.C., Gaillard, J.F., 1999. The Isotopic Composition of Diatom-Bound Nitrogen in Southern Ocean Sediments. Paleoceanography, 14(2), 118-134.

### 7.7.4 Pleistocene changes in South Pacific intermediate and bottom water circulation

Silke Steph[1,2], Katharina Pahnke[3]

[1]Alfred-Wegener-Institut
[2]University of Potsdam
[3]University of Hawaii

#### Objectives

*Antarctic Bottom Water*

The Late Pleistocene history of Antarctic Bottom Water (AABW) circulation is still largely unknown. Available nutrient proxy data (benthic $\delta^{13}C$, Cd/Ca) indicate that AABW filled an extended depth range of the Atlantic Ocean during the last glacial period (e.g., Curry and Oppo, 2005; Marchitto and Broecker, 2006), but whether this is due to an actual increase in its formation or simply the result of reduced North Atlantic Deep Water (NADW) production, is not clear.

Radiogenic isotopes of the terrigenous fine fraction of marine sediments that is transported by bottom currents can be used as a tracer to study the past flow-path of water masses. In particular, the distinct isotopic 'fingerprint' of the Ross Sea region, with $^{87}Sr/^{86}Sr$ ratios >0.71 and $^{143}Nd/^{144}Nd$ ratios (expressed in $\varepsilon_{Nd}$ units) of $\varepsilon_{Nd}$ <-5 (Lang Farmer et al., 2006; Roy et al., 2007) affords tracing of Ross Sea Bottom Water (RSBW) into the southeast Pacific. Using these isotopic fingerprints in the fine fraction of terrigenous material in fossil sediments from the southeast Pacific, we are planning to study past changes in AABW export from the Ross Sea on glacial-interglacial to millennial time scales. Initially, surface sediments recovered using the multi-corer (MUC) will be analyzed for their isotopic signatures and compared to the bottom water Nd isotopic composition at stations where seawater samples were collected (see Chapter 3.5 and Tab. 3.5.1) as well as the modern flow-path of RSBW as known from physical oceanographic studies (e.g., Orsi et al., 1999) (see Tab. 7.7.4.1). Finally, we will apply the above to down-core records along the modern flow-path of RSBW in the South Pacific, with an initial focus on the last glacial-interglacial transition including the LGM, ACR, and the Holocene.

*Mid-depth stratification of the Southern Ocean during glacials*

Carbon isotope records support a mechanism proposed by Toggweiler (1999) that describes the boundary between mid-depth and deep waters as a chemical divide between low $CO_2$ water above and high $CO_2$ water below (Hodell and Venz-Curtis 2006). This approach is consistent with Last Glacial Maximum (LGM) isotope data indicating a strong bathyal front between mid-depth and deep waters (Kallel et al., 1988) and deep-water temperature near the freezing point (Duplessy et al., 2002). Such changes in ventilation that should be related to several interrelated processes in the SO (e.g. sea surface temperature, sea ice, surface stratification, decreased Ekman-induced upwelling) may have acted as a positive feedback to Late Plio-Pleistocene climate cooling through the carbon cycle, especially enhancing Northern Hemisphere Glaciation. The cooling co-occurs with a major switch of the tropics/subtropics into the modern mode of circulation with relatively strong Walker circulation and cool subtropical temperatures (Ravelo et al., 2004) and marks the period when reductions

in the ventilation of South Atlantic deep water further intensified in glacial periods, making this basin the most poorly ventilated in the ocean (Hodell and Venz-Curtis, 2006). The magnitude of the gradient in ventilation between the polar South Pacific, and South Atlantic can only be elucidated if benthic $\delta^{13}C$ records become available from the polar South Pacific. Such knowledge, which is crucial for understanding the potential of SO ventilation to reduce atmospheric $CO_2$ as proposed by Toggweiler (1999), should be obtained from ANT-XXVI/2 sediment records gathered above the CCD on depth transects across the East Pacific Rise and the Pacific Antarctic Ridge.

**Table 7.7.4.1:** Potential piston and multi-cores for the study of past AABW flow in the South Pacific

**Piston cores**

| Station No. | Latitude [deg/min] | Longitude [deg/min] | water depth [m] | recovery [m] | bottom age [ka] | sed.rate [cm/ka] |
|---|---|---|---|---|---|---|
| **PS75/034-2** | 54°22.12'S | 80°05.40'W | 4436 | 18.08 | 1100 | 1.6 |
| **PS75/052-3** | 60°45.12'S | 115°58.74'W | 5130 | 23.17 | 220 | 10.5 |
| **PS75/054-1** | 56°09.11'S | 115°07.98'W | 4113 | 22.38 | 190 | 11.8 |
| **PS75/062-2** | 58°16.60'S | 135°37.61'W | 4165 | 21.09 | 150 | 14.1 |
| **PS75/063-1** | 58°54.24'S | 135°37.23'W | 3795 | 22.46 | 190 | 11.8 |
| **PS75/064-1** | 61°00.74'S | 139°27.85'W | 4600 | 15.43 | 130 | 11.9 |

**Multi-cores**

| Station No. | Latitude [deg/min] | Longitude [deg/min] | water depth [m] | recovery [tubes] |
|---|---|---|---|---|
| **PS75/034-1** | 54°22.11'S | 80°05.38'W | 4450 | 12 |
| **PS75/044-3** | 56°5.14'S | 96°46.82'W | 5011 | 1 |
| **PS75/049-1** | 54°20.79'S | 102°44.82'W | 4482 | 11 |
| **PS75/053-1** | 60°46.15'S | 115°58.79'W | 5132 | 11 |
| **PS75/062-1** | 58°16.62'S | 135°37.55'W | 4147 | 7 |
| **PS75/063-2** | 58°54.25'S | 135°37.25'W | 3790 | 6 |
| **PS75/064-2** | 61°00.75'S | 139°27.79'W | 4595 | 2 |
| **PS75/065-2** | 62°36.23'S | 141°30.91'W | 4488 | 9 |
| **PS75/067-2** | 64°58.25'S | 143°48.21'W | 4153 | 6 |
| **PS75/069-2** | 62°12.33'S | 145°37.16'W | 4328 | 7 |
| **PS75/087-2** | 66°47.27'S | 163°19.50'W | 4411 | 7 |
| **PS75/088-3** | 68°43.82'S | 164°48.08'W | 3849 | 12 |
| **PS75/089-6** | 67°04.98'S | 165°32.50'W | 4121 | 7 |
| **PS75/095-3** | 61°49.34'S | 169°44.44'W | 3274 | 10 |

*Antarctic Intermediate Water/Subantarctic Mode Water*

Today, intermediate water masses originating from the Southern Ocean (Antarctic Intermediate Water; AAIW; Subantarctic Mode Water; SAMW) play an important role for the redistribution of heat and freshwater within the upper ocean, and are potentially one of the main sources for nutrient supply to the tropical thermocline (e.g., Toggweiler et al., 1991; Spero and Lea, 2002; Sarmiento et al., 2004). Furthermore, air-sea gas exchange in their formation regions north of the polar front acts as an important sink

for anthropogenic $CO_2$ (Sabine et al., 2004). This identifies AAIW/SAMW as globally significant water mass with a strong potential to contribute to changes in the global climate system. Yet our knowledge about variations in Southern Hemisphere mid-depth circulation under different climate conditions is still limited. The resulting climate linkages and underlying mechanisms remain ambiguous due to the small number of available sediment archives from intermediate water depths.

The objective of this study is a detailed documentation of past changes in AAIW and SAMW circulation in the Southwest Pacific sector of the Southern Ocean on glacial-interglacial to millennial time scales. We plan to investigate 7 sediment cores along an intermediate water depth transect (669 - 2,498 m water depth) on Chatham Rise off the east coast of New Zealand. Stable isotope measurements on epibenthic foraminifera ($\delta^{13}C$, $\delta^{18}O$) as well as benthic foraminiferal Mg/Ca temperatures will be used to determine changes in the vertical expansion of AAIW, which is relatively fresh and nutrient-poor compared to underlying Upper Circumpolar Deep Water (UCDW). The new proxy records will be compared to existing benthic stable isotope records from intermediate water depths near the study area (MD97-2120, 1,210 m east of New Zealand; Pahnke and Zahn (2005); and MD06-2986, 1,470 m and MD06-2990, 950 m, west of New Zealand, Steph et al., manuscript in prep.). The paleoceanographic investigations will be complemented by comparisons of the physical properties and stable isotopic composition of modern SAMW, AAIW and UCDW sampled during ANT-XXVI/2 CTD casts with stable isotope signatures in benthic foraminifera from core top samples collected with the multi-corer at the same stations.

### Expected results

Suitable multi-cores for the direct comparison of bottom water with surface sediment Nd isotope ratios and piston cores for the study of past bottom water flow in the South Pacific are listed in Table 7.7.4.1. Multi- and piston cores for AABW studies were chosen based on their location along the flow-path of RSBW, their depth below 4,000m water depth, and their age range (Late Pleistocene). Multi- and piston cores for studies of changes in SAMW, AAIW, and CDW circulation will be chosen based on their water depth, carbonate content and age range. Water samples for $\varepsilon_{Nd}$ and stable isotope calibration studies have been taken from the CTD/Rosette on-board *Polarstern* during ANT-XXVI/2 (see chapters 3.4 and 3.5).

### References

Curry, W. B., Oppo, D.W., 2005. Glacial water mass geometry and the distribution of $d^{13}C$ of $SCO_2$ in the western Atlantic Ocean. Paleoceanography 20, PA1017, doi:10.1029/2004PA001021.

Duplessy, J. C., Labeyrie, L. D., Waelbroeck, C., 2002. Constraints on the ocean oxygen isotopic enrichment between the Last Glacial Maximum and the Holocene: Paleoceanographic implications. Quat. Sci. Rev. 21, 315-330.

Hodell, D. A., Venz-Curtis, K. A., 2006. Late Neogene history of deepwater ventilation in the Southern Ocean. Geochem. Geophys. Geosys. 7, doi:10.1029/ 2005GC001211.

Kallel, N., Labeyrie, L. D., Juillet-Leclerc, A., Duplessy, J.-C., 1988. A deep hydrological front between intermediate and deep-water masses in the glacial Indian Ocean, Nature 333 651-655.

Lang Farmer, G., et al., 2006. Isotopic constraints on the provenance of fine-grained sediment in LGM tills from the Ross Embayment, Antarctica. Earth and Planetary Science Letters 249, 90-107.

Marchitto, T. M., Broecker, W. S., 2006. Deep water mass geometry in the glacial Atlantic Ocean: a review of contraints from the paleonutrient proxy Cd/Ca. Geochemistry Geophysics Geosystems 7, doi:10.1029/2006GC001323.

Orsi, A. H., et al., 1999. Circulation, mixing, and production of Antarctic Bottom Water. Progress in Oceanography 43(1), 55-109.

Pahnke, K., Zahn, R., 2005. Southern Hemisphere Water Mass Conversion linked with North Atlantic Climate Variability. Science 307, 1741-1746.

Ravelo, A. C., Andreasen, D. H., Lyle, M., Lyle, A. O., Wara, M. W., 2004. Regional climate shifts caused by gradual global cooling in the Pliocene epoch. Nature 429, 263-267.

Roy, M., et al., 2007. $^{40}Ar/^{39}Ar$ ages of hornblende grains and bulk Sm/Nd isotopes of circum-Antarctic glacio-marine sediments: Implications for sediment provenance in the southern ocean. Chemical Geology 244, 507-519.

Sabine, C. L., Feely, R. A., Gruber, N., Key, R. M., Lee, K., Bullister, J. L., Wanninkhof, R., Wong, C. S., Wallace, D. W. R., Tilbrook, B., Millero, F. J., Peng, T.-H., Kozyr, A., Ono, T., Rios A. F., 2004. The Ocean sink for anthropogenic $CO_2$. Science 305, 367-371.

Sarmiento, J. L., Gruber, N., Brzezinski, M. A., Dunne J. P., 2004. High-latitude controls of thermocline nutrients and low latitude biological productivity. Nature 427, 56-60.

Spero, H. J., and Lea, D. W., 2002. The cause of carbon isotope minimum events on glacial terminations. Science 296, 522-525.

Toggweiler, J. R., Dixon, K., Broecker W. S., 1991. The Peru upwelling and the ventilation of the south Pacific thermocline. J. Geophys. Res. 96, 20467-20497.

Toggweiler, J. R.,1999. Variation of atmospheric $CO_2$ by ventilation of the ocean's deepest water. Paleoceanography 14, 571-588.

### 7.7.5 Southern Ocean climate at the Last Glacial Maximum (LGM) and the last glacial/interglacial transition

Rainer Gersonde, Oliver Esper Alfred-Wegener-Institut

#### Objectives

The recently published synthesis of sea surface temperatures during the LGM from the Multiproxy Approach for the Reconstruction of the Glacial Ocean Surface (MARGO) project clearly reveals the lack of data in the South Pacific and in particular in the Pacific sector of the Southern Ocean (Gersonde et al., 2005, Waelbroeck et al., 2009). The few data available indicate reduced cooling in the Pacific sector and suggest a non-uniform cooling of the glacial Southern Ocean. Similar results have been obtained from sea-ice reconstructions. The scarce data from the Pacific sector point to smaller expansions of the LGM winter sea-ice in this sector. To substantiate the Pacific sector sea ice distribution, more data points are urgently needed. The apparent reduced LGM cooling of the Pacific Southern Ocean is in contrast to strong LGM cooling in the mid-latitude Pacific recorded in continental margin sediments off Chile and New Zealand. The reconstruction of the subsequent glacial/interglacial transition (Termination I) will generate data indicating how last glacial conditions in the Pacific Southern Ocean may have influenced the climate development into the present interglacial.

### Preliminary Results

Based on preliminary dating and core-core correlation based on physical property parameters a total of 31 piston, gravity and kasten cores from the eastern, central and western polar South Pacific and from latitudinal transects ranging from the seasonal sea ice covered zone to the Subtropical Front (Fig. 7.4.2, Table 7.1.1) includes last glacial and Terminaton I sediments, allowing for the reconstruction of past sea surface temperature, sea ice, water mass properties and productivity.

Cores had been recovered during ANT-XXVI/2 to generate a sediment core collection allowing for the documentation of the LGM environmental conditions. This core collection includes LGM sediments from latitudinal transects ranging from the seasonal sea ice covered zone to the Subtropical Front (Fig. 7.4.2).

### References

Gersonde, R., Crosta, X., Abelmann, A., Armand, L., 2005. Sea-surface temperature and sea ice distribution of the Southern Ocean at the EPILOG Last Glacial Maximum a circum-Antarctic view based on siliceous microfossil records, Quaternary Science Reviews, 24, 869-896.

Waelbroeck, C., Paul, A., Kucera, M., Rosell-Mele, A., Weinelt, M., Schneider, R., Mix, A. C., Abelmann, A., Armand, L., Barker, S., Barrows, T. T., Benway, H., Cacho, I., Chen, M. -T., Cortijo, E., Crosta, X., de Vernal, A., Dokken, T., Duprat, J., Elderfield, H., Eynaud, F., Gersonde, R., Hayes, A., Henry, M., Hillaire-Marcel, C., Huang, C. -C., Jansen, E., Juggins, S., Kallel, N., Kiefer, T., Kienast, M., Labeyrie, L., Leclaire, H., Londeix, L., Mangin, S., Matthiessen, J., Marret, F., Meland, M., Morey, A. E., Mulitza, S., Pflaumann, U., Pisias, N. G., Radi, T., Rochon, A., Rohling, E. J., Sbaffi, L., Schäfer-Neth, C., Solignac, S., Spero, H., Tachikawa, K., Turon, J. -L., 2009. Constraints on the magnitude and pattern of ocean cooling at the Last Glacial Maximum. Nature Geoscience, doi 10.1038/NGEO411.

## 7.7.6 Pleistocene warmer than present environments in the South Pacific and implications for Antarctic ice sheet and global climate history

Rainer Gersonde, Frank Lamy, Oliver Esper
Alfred-Wegener-Institut

### Objectives

The present global warming evident from instrumental observation and the predicted temperature increase during the near future (Solomon et al., 2007) call for a better understanding of warmer than present climate conditions as documented in sedimentary and ice core records. Pleistocene warming events at the onset of e.g. Marine Isotope Stages 11, 9, 7, 5 and 1 may be characterized by climate conditions exceeding present climate conditions by up to 2°C warmer than present and thus range in the near-future temperature regime predicted by numerical simulations. The warmings are periods of high sea level stand, exceeding the present sea level by 3 – 7.5 m, according to numerical models (Pollard and DeConto, 2009). This points to contributions by the Antarctic Ice Sheet, besides by the ice on Greenland. The study of marine records from the Pacific Southern Ocean can provide insight into the climate conditions close to the West Antarctic Ice Sheet (WAIS) and its stability history, information that is not available from the near-coast ANDRILL-record (Naish et al., 2009). The early stages of MIS 5,

9, and 11 are characterized by "overshootings" of the atmospheric $CO_2$ concentration, exceeding the average late Pleistocene interglacial values of 280 ppmv, by ca. 10 ppmv (Tzedakis et al., 2009). Biogeochmical and physical processes that are linked with these natural "overshoots" are yet not well known.

### Expected results

The recovery of a large series of sediment cores that document Pleistocene paleoceanographic conditions provides records documenting Pleistocene warmer than present events from all open ocean sectors off the WAIS (Table 7.1.1). These records can be dated with high accuracy and linked with the ice core climate records. The occurrence of a prominent sediment section consisting of biogenic carbonate assigned to early interglacial warmings (e.g. MIS 11) indicates major biogeochemical and physical changes occurring in the Southern Ocean at periods of high natural $CO_2$ levels. Such levels can be mapped over large distance based on the PARASOUND record (Fig. 7.2.4). The multi-proxy based paleoceanographic reconstruction of the warmer than present intervals and the climate development leading to the warmings will provide new insight into the Southern Ocean role governing the warmings and WAIS stability history.

### References

Naish, T, et al. 2009. Obliquity-paced Pliocene West Antarctic ice sheet oscillations. Nature 458, 322-328.

Pollard, D., DeConto, R. M., 2009. Modelling West Antarctic ice sheet growth and collapse through the past five million years. Nature 458, 329-332.

Solomon, S. et al. 2007. Contribution of Working Group I to the Fourth Assessment Report of the Intergovernmental Panel on Climate Change, 2007 Cambridge University Press, Cambridge, United Kingdom and New York, NY, USA.

Tsedakis, P. C., Raynaud, D, McManus, J.F., Berger, A., Brovkin, V., Kiefer, T., 2009. Interglacial diversity. Nature Geoscience 2,751-755

## 7.7.7 Pliocene-Pleistocene climate evolution in the Pacific Sector of the Southern Ocean and implications for the West Antarctic Ice Sheet history

Rainer Gersonde[1] [1]Alfred-Wegener-Institut
Matt Konfirst[2] [2]Northern Illinois University
Alfredo Martinez-Garcia[3] [3]ETH-Zürich

### Objectives

Although not a perfect analog for future warmth, the early to mid Pliocene does represent the most recent period in Earth's history when; (1) long-term climate was on average warmer (by ca. 2 - 3°C above pre-industrial temperature, e.g. Jiang et al., 2005); (2) sea level was higher by 15 - 25 m (Shackleton et al., 1995); (3) thermohaline circulation was enhanced (Kim and Crowley, 2000); and (4) atmospheric $CO_2$ concentrations were likely close to those to be expected in the next decades (Raymo et al., 1996). During this period the geographic configuration of continents and ocean basins that influence the pathways of ocean circulation was close to the present, except for the Central American Seaway that experienced significant shoaling

throughout the Pliocene (e.g., Haug and Tiedemann, 1998; Haug et al., 2001). This makes the early Pliocene a prominent candidate to "help improve predictions of the likely response to increased $CO_2$ in the future, including the ultimate role of the ocean circulation in a globally warmer world" (IPCC 2007; Jansen et al., 2007).

While the establishment of EAIS is relatively well constrained, it is only very recently that drilling results obtained during the *ANDRILL* projects allow for a more detailed picture of the Neogene-Quaternary WAIS history. Although the WAIS volume is equivalent to a sea level change of only 5 - 7 meters, its environmental impact is significant. The large ice shelves (Ross, Filchner-Ronne) associated with the WAIS are critical for the production of cold surface and bottom waters and sea ice. The marine-based WAIS is the world's most unstable large ice sheet (Anderson et al., 2002) and is thus the primary potential melt-water source in southern high-latitudes. The impending global-scale anthropogenic warming and related changes predicted in the climate system during the 21st century are "very likely" to be larger than those observed during the 20th century (IPCC, 2007; Meehl et al., 2007). Thus, it is important to assess the stability of this ice sheet and to resolve any critical thresholds that could be reached in climate periods warmer than present. Indeed paleoclimatic analogs are urgently needed for this assessment because available numerical models do yet not include all relevant processes (Alley et al., 2005) leading to a large uncertainty about what dynamical changes could occur in the WAIS and under which climate conditions. Oppenheimer and Alley (2005) highlight that the WAIS may provide a plausible example of "dangerous anthropogenic interference with the climate system" under Article 2 of the UN Framework Convention on Climate Change. They suggest that the limited evidence presently available indicates that perpetuate global warming of 2°C above present-day represents a threshold beyond which there will be a commitment to a large sea level contribution from the WAIS.

During the 2006/7 field season, the *ANDRILL MIS* (ANtarctic geological DRILLing McMurdo Ice Shelf) project recovered a nearly continuous (~98 % recovery) 1,285 m long sediment core (AND-1B) from beneath the Ross Ice Shelf near Ross Island, Antarctica, with the goal of documenting the history of the Antarctic ice sheets during the late Neogene. The upper 600 m contained 13 discrete diatomite units composing approximately half of the core material and ranging in thickness from 1 to nearly 100 m (Scherer et al., 2007). Age constraints based on diatom biostratigraphy indicate that the upper 600 m of the AND-1B core range from the earliest Pliocene to Pleistocene and provide a unique insight into Antarctic climate evolution from the warm Pliocene and PRISM intervals to modern high amplitude glacial/ interglacial variability. Also demonstrated is an apparent link between the ANDRILL record and obliquity-paced climate forcing (Naish *et al.*, 2009); however, the fragmentary nature of the sedimentary sequence limits the resolution of these interpretations.

The Pacific sector of the Southern Ocean is a drainage basin for the Ross Ice Shelf, which itself is a major outlet for both the East and West Antarctic Ice Sheets and therefore provides a direct link between the climate record contained within the ANDRILL AND-1B core and the cores collected on the ANT-XXVI/2 expedition. Recovery of a number of cores spanning Plio-Pleistocene time in the Pacific sector of the Southern Ocean provides the opportunity to study past links between the Antarctic Shelf and open ocean settings. Additionally, ANT-XXVI/2 core material can provide a more continuous

sedimentary succession as well as generate independent age models, which can be used to further refine our understanding of the interaction of Antarctic continental and marine responses to variability between glacial/ interglacial time periods external insolation forcing in a warmer climatic scenario.

### Preliminary results

Of the 61 cores recovered during the ANT-XXVI/2 expedition, 7 have basal ages in the Pliocene or earlier (Figs 7.6.1; Table 7.6.1). Of these, only two (PS75/065-1 and PS75-090-3) appear to have adequate microfossil preservation for a more detailed study of long-term oceanographic changes in the Pacific Sector of the Southern Ocean. These cores also provide the opportunity for comparison to other Southern Ocean Pliocene records including those in the Atlantic (Gersonde, 1990; Gersonde and Burckle, 1990; Fenner, 1991; Zielinski and Gersonde, 2002; Zielinski *et al.*, 2002) and Indian Ocean Sectors (Baldauf and Barron, 1991; Harwood and Maruyama, 1992) as well as the ANDRILL MIS record (Scherer *et al.*, 2007; Naish *et al.*, 2009).

### References

Alley R.B., Clark P.U., Huybrechts P., Joughin I., 2005. Ice-sheet and sea-level changes. Science, 310 456-460.

Anderson JB, Shipp SS, Lowe AL, Wellner JS, Mosola A., 2002. The Antarctic ice sheet during the last glacial maximum and its subsequent retreat history: a review. Quaternary Science Reviews 21, 49–70.

Baldauf J. G, Barron, J. A., 1991. Diatom biostratigraphy: Kerguelen Plateau and Prydz Bay regions of the Southern Ocean. Proceedings of the Ocean Drilling Program, Scientific Results, Vol. 119, 547-598.

IPCC (2007), Climate Change 2007: The Physical Science Basis. Contribution of Working Group I to the Fourth Assessment Report of the Intergovernmental Panel on Climate Change. Cambridge University Press. Cambridge, United Kingdom and New York, USA.

Fenner, J. M., 1991. Late Pliocene-Quarternary quantitative diatom stratigraphy in the Atlantic Sector of the Southern Ocean. Proceedings of the Ocean Drilling Program, Scientific Results, Vol. 114, 97-121.

Gersonde, R., 1990. Taxonomy and morphostructure of Neogene diatoms from the Southern Ocean, ODP Leg 113. Proceedings of the Ocean Drilling Program, Scientific Results, Vol. 113, 791-802.

Gersonde, R., Burckle, L. H., 1990. Neogene diatom biostratigraphy of ODP Leg 113, Weddell Sea (Antarctic Ocean). Proceedings of the Ocean Drilling Program, Scientific Results, Vol. 113, 761-789.

Harwood, D. M., Maruyama, T., 1992. Middle Eocene to Pleistocene diatom biostratigraphy of Southern Ocean sediments from the Kerguelen Plateau, Leg 120. Proceedings of the Ocean Drilling Program, Scientific Results, Vol. 120, 683-733.Haug, G. H., and R. Tiedemann (1998), Effect of the formation of the Isthmus of Panama on Atlantic Ocean thermohaline circulation. Nature, 393(6686), 673.

Haug, G.H., Tiedemann, R., 1998. Effect of the formation of the Isthmus of Panama on Atlantic Ocean thermohaline circulation. Nature, 393, 673-676.

Haug G.H., Tiedemann R., Zahn, R., Ravelo, A.C., 2001. Role of Panama uplift on oceanic freshwater balance. Geology, 29, 207– 210.

Jansen E, Overpeck J, Briffa KR, Duplessy J-C, Joos F, Masson-Delmotte V, Olago D, Otto-Bliesner B, Peltier WR, Rahmstorf S, Ramesh R, Raynaud D, Rind D, Solomina O, Villalba

R, and Zhang D, 2007. Paleoclimate. In: S. Solomon, et al. (Eds.), Climate Change 2007: The Physical Science Basis. Contribution of Working Group I to the Fourth Assessment Report of the Intergovernmental Panel on Climate Change, Cambridge University Press, Cambridge, UK & New York, USA.

Jiang, D., Wang, H., Ding, Z., Lang, X., Drange, H., 2005. Modeling the middle Pliocene climate with a global atmospheric general circulation model. Journal of Geophysical Research, 110, D14107.

Kim, S.-J., Crowley, T.J., 2000. Increased Pliocene North Atlantic Deep Water: cause or consequence of Pliocene warming? Paleoceanography, 15(4): 451-455.

Meehl, G.A. et al., 2007. Global Climate Projections. In: S. Solomon, et al. (Eds.), Climate Change 2007: The Physical Science Basis. Contribution of Working Group I to the Fourth Assessment Report of the Intergovernmental Panel on Climate Change, Cambridge University Press, Cambridge, UK & New York, USA.

Naish T, Powell R, Levy R, Wilson G, Scherer R, Talarico F, Krissek L, Niessen F, Pompilio M, Wilson T, Carter L, DeConto R, Huybers P, McKay R, Pollard D, Ross J, Winter D, Barrett P, Browne G, Cody R, Cowan E, Crampton J, Dunbar G, Dunbar N, Florindo F, Gebhardt C, Graham I, Hannah M, Hansaraj D, Harwood D, Helling D, Henrys S, Hinnov L, Kuhn G, Kyle P, Läufer A, Maffioli P, Magens D, Mandernack K, McIntosh W, Millan C, Morin R, Ohneiser C, Paulsen T, Persico D, Raine I, Reed J, Riesselman C, Sagnotti L, Schmitt D, Sjunneskog C, Strong P, Taviani M, Vogel S, Wilch T, Williams T, 2009. Obliquity-paced Pliocene West Antarctic ice sheet oscillations. Nature, 458, 322-328.

Oppenheimer M, Alley R.B., 2005. Ice sheets, global warming, and article 2 of the UNFCCC. Climatic Change, 68, 257-267.

Raymo, M.E., Grant, B., Horowitz, M., Rau, G.H., 1996. Mid-Pliocene warmth: stronger greenhouse and stronger conveyor. Marine Micropaleontology, 27: 313-326.

Scherer R, Hannah M, Maffioli P, Persico D, Sjunneskog CP, Strong CP, Taviani M, Winter D, the ANDRILL-MIS Science Team, 2007. Palaeontologic characterisation and analysis of the AND-1B core, ANDRILL McMurdo Ice Shelf Project, Antarctica. Terra Antarctica, 14(3), 223-254.

Shackleton, N.J., Hall, M.A., Pate, D., 1995. Pliocene stable isotope stratigraphy of Site 846. Proceedings of the Ocean Drilling Program, Scientific Results, 138: 337-355.

Zielinski, U., Gersonde, R., 2002. Plio-Pleistocene biostratigraphy from ODP Leg 177, Atlantic Sector of the Southern Ocean. Marine Micropaleontology 45, 225-268.

Zielinski, U., Bianchi, C., Gersonde, R., Kunz-Pirrung, M., 2002. Last occurrence datums of the diatoms *Rouxia leventerae* and *Rouxia constricta*: indicators for marine isotope stages 6 and 8 in Southern Ocean sediments. Marine Micropaleontology 45, 127-137.

### 7.7.8 Further documentation of the Eltanin-asteroid impact in the Bellingshausen Sea

Rainer Gersonde Alfred-Wegener-Institut

**Objectives**

Earlier geological explorations have documented the presence of impact related sediment disturbances and deposition near the Freeden Seamount (57.3°S, 90.5°W) in the northern Bellingshausen Sea (Gersonde et al., 1997). Deposits of the late Pliocene (2.5 Ma) Eltanin impact are unique in the known geological record. The only known example of a km-sized asteroid to impact a deep-ocean (5 km) basin, is the most meterorite-rich locality known. Available sediment core studies showed that sediments

as old as Eocene were eroded by the impact disturbance and re-deposited in three distinct units. The lowermost is a chaotic assemblage of sediment fragments up to 50 cm in size. Above this is a laminated sand-rich unit that deposited as a turbulent flow, and this is overlain by a more fine-grained deposit of silts and clays that settled from a cloud of sediment suspended in the water column. Meteoritic ejecta particles were concentrated near the base of the uppermost unit, where coarse ejecta caught up with the disturbed sediment. More recent numerical modeling has allowed for the prediction of potential ground-zero areas of the impact. These sites are yet unstudied and were visited during ANT-XXVI/2 to validate the impact models, which indicate massive meteorite deposition in area of ground-zero.

**Work at sea**

Based on available and new bathymetric and sediment echo-sounding survey obtained during ANT-XXVI/2 in the southern sector of the Freeden Seamount a total of eight sites were selected (PS75/035-040, PS75/42-43) to recover impact-related sediment sequences in potential ground-zero areas predicted by numerical modeling. At these sites a 25 m long piston corer was deployed. Additionally, a multi-channel seismic survey was completed at Freeden Seamount. Together with the bathymetric, echo-sounding and marine geological sampling survey this represents a pre-site survey in the frame of proposal 625-full („Cenozoic Southern Ocean Pacific“, CESOP) within the Integrated Ocean Drilling Program (IODP) to drill Eltanin impact related sediments (Chapter 8).

**Preliminary results**

Although seven of the recovered cores are longer than 20 m impact related sequences could be encountered only at three locations (PS75/036, 038, 040). While one core (PS75/036) presumably sampled at its base the fine-grained deposits above the ejecta layer, the other cores document the ejecta layer, underlying disturbed sequences and undisturbed Eocene calcareous nannofossil ooze.

**References**

Gersonde, R, Kyte, F.T., Bleil, U., Diekmann, B., Flores, J. A., Gohl, K., Grahl, G., Hagen, R., Kuhn, G., Sierro, F. J., Völker, D., Abelmann, A., and Bostwick J. A., 1997. Geological record and reconstruction of the late Pliocene impact of the Eltanin asteroid in the Southern Ocean. Nature 390, 357-363.

### 7.7.9 Refinement of geomagnetic dating of Holocene-Pleistocene Southern Ocean sediment records

Rainer Gersonde[1] [1]Alfred-Wegener-Institut
Lucia Reichelt[2] [2]University of Bremen

**Objectives**

The sediments of the deep Southern Ocean are mostly barren of biogenic carbonate, which limits the dating of Holocene-Pleistocene records by means of the oxygen isotope stratigraphy based on planktic and benthic foraminifers. New dating approaches include the generation of paleointensity records, which can be correlated over larger areas allowing for dating in combination with radiometric methods, oxygen isotope

stratigraphy and biostratigraphy. However, geomagnetic data from the Southern Ocean is only available from few sites, are mainly located in the Atlantic region (e.g. ODP Leg 177, Channell and Stoner, 2002). The generation of new paleointensity records from sediment recovered during ANT-XXVI/2 from carbonate bearing ridges and deep ocean basins will lead to further enhancement of the dating accuracy of Southern Ocean records.

**Methods – Sampling and measurements**

Initial sampling for paleomagnetic investigations was accomplished aboard *Polarstern* at selected cores. Plastic sampling cubes (2 x 2 x 1.6 $cm^3$) for geomagnetic measurements were oriented and inserted into the working halves of the selected piston cores for post-cruise sampling. All cubes have serial numbers and the arrow on the box is always maintained to point up-core (top). The sampling interval was usually 10 cm and samples come from the depth sampling for bulk geochemistry and water-content has been accomplished. In Core PS75/90-3 the sampling interval was 5 cm. For the sampling of the kasten core (PS75/073-2), U-Channels were used for the continuous sampling of the core. All rock and paleomagnetic analyses of the samples will be carried out at the University of Bremen.

**Expected results**

In combination with radiometric dating, isotope stratigraphy and biostratigraphy, geomagnetic records will be the base for the establishment of accurate age-models. Geomagnetic dating will be based on geomagnetic polarity changes and the variation in the paleointensity. Investigation of the mineralogy of the remanence carriers will provide information on paleocurrent changes.

**References**

Channell, J. E. T., Stoner, J. S., 2002. Plio-Pleistocene magnetic polarity stratigraphies and diagenetic magnetite dissolution at ODP Leg 177 Sites (1089, 1091, 1093 and 1094). Marine Micropaleontology 45, 269-290.

### 7.7.10 Refinement of Southern Ocean Plio-Pleistocene biostratigraphic zonations

Matt Konfirst[1], Mariem Saavedra-Pellitero[2], Oliver Esper[3], Rainer Gersonde[3]

[1]Northern Illinois University
[2]University of Salamanca
[3]Alfred-Wegener-Institut

**Objectives**

The sediments of the deep Southern Ocean are mostly barren of biogenic carbonate, which limits the dating of Plio-Pleistocene records by means of the oxygen isotope stratigraphy based on planktic and benthic foraminifers. New dating approaches include the generation of paleointensity records, which can be correlated over larger areas, allowing for dating in combination with radiometric methods or oxygen isotope stratigraphy. The availability of such records from Southern Ocean sediments is still rather limited. The recovery of sediment records from carbonate bearing ridges and deep ocean basins during ANT-XXVI/2 will lead to further enhancement of this geomagnetic dating method. This in turn can be used to compare the diatom biostratigraphy of the Pacific sector of the Southern Ocean to previous work done in the Atlantic (Censarek

and Gersonde, 2002, Gersonde, 1990; Gersonde and Burckle, 1990; Fenner, 1991; Zielinski and Gersonde, 2002; Zielinski *et al.*, 2002) and Indian sectors (Baldauf and Barron, 1991; Harwood and Maruyama, 1992). Calcareous nannofossil biostratigraphic work will build on that of Perch-Nielsen (1985), Bown and Young (1998), Hine and Weaver (1998), Young (1998) and Lourens *et al.* (2004).

### Preliminary results

Initial dating of core material by biostratigraphic means has identified a number of high resolution Pleistocene records as well as 7 cores containing Pliocene material, one of which extends back to the Late-Middle Miocene (see 7.6). The material collected during this cruise also offers the opportunity to study the evolution of past calcareous nannofossil assemblages from various regions across the Pacific sector of the Southern Ocean. These data together with the siliceous biostratigraphic record will allow us to correlate important paleoceanographic events in the Southern Ocean, such as the calcareous nannofossil ooze that was deposited during MIS 11 and prior to the last occurrence of *Pseudoemiliania lacunosa.*

### References

Baldauf J. G, Barron, J. A., 1991. Diatom biostratigraphy: Kerguelen Plateau and Prydz Bay regions of the Southern Ocean. Proceedings of the Ocean Drilling Program, Scientific Results, Vol. 119, 547-598.

Bown, P. R, Young, J.R., 1998. Introduction. In: Bown, P. R. (Ed.) Calcareous nannofossil biostratigraphy, Chapman & Hall, London, pp. 1-15.

Censarek, B., Gersonde, R., 2002. Miocene diatom biostratigraphy at ODP Sites 689, 690, 1088, 1092 (Atlantic sector of the Southern Ocean). Marine Micropaleontology, 45, 309-356.

Fenner, J. M., 1991. Late Pliocene-Quarternary quantitative diatom stratigraphy in the Atlantic Sector of the Southern Ocean. Proceedings of the Ocean Drilling Program, Scientific Results, Vol. 114, 97-121.

Gersonde, R., 1990. Taxonomy and Morphostructure of Neogene diatoms from the Southern Ocean, ODP Leg 113. Proceedings of the Ocean Drilling Program, Scientific Results, Vol. 113, 791-802.

Gersonde, R., Burckle, L. H., 1990. Neogene diatom biostratigraphy of ODP Leg 113, Weddell Sea (Antarctic Ocean). Proceedings of the Ocean Drilling Program, Scientific Results, Vol. 113, 761-789.

Harwood, D. M., Maruyama, T., 1992. Middle Eocene to Pleistocene diatom biostratigraphy of Southern Ocean sediments from the Kerguelen Plateau, Leg 120. Proceedings of the Ocean Drilling Program, Scientific Results, Vol. 120, 683-733.

Hine, N., Weaver, P. P. E., 1998. Quaternary. In: Bown, P. R. (Ed.) Calcareous nannofossil biostratigraphy, Chapman & Hall, London, pp. 265-278.

Lourens, L. J., Hilgen, F. J., Shackleton, N. J., Laskar, J., Wilson, D., 2004. The Neogene Period. In: Gradstein, F. M., Ogg J. G., Smith, A. G. (Eds.), A Geological Time Scale, Cambridge University Press, Cambridge, pp. 409-440.

Young, J., 1998. Neogene. In: Bown, P. R. (Ed.) Calcareous nannofossil biostratigraphy, Chapman & Hall, London, pp. 225-265.

Zielinski, U., Gersonde, R., 2002. Plio-Pleistocene biostratigraphy from ODP Leg 177, Atlantic Sector of the Southern Ocean. Marine Micropaleontology 45, 225-268.

Zielinski, U., Bianchi, C., Gersonde, R., Kunz-Pirrung, M., 2002. Last occurrence datums of the diatoms Rouxia leventerae and Rouxia constricta: indicators for marine isotope stages 6 and 8 in Southern Ocean sediments. Marine Micropaleontology 45, 127-137.

# 8. MARINE GEOLOGICAL, SEISMIC AND BATHYMETRIC PRE-SITE SURVEY FOR IODP DRILL PROPOSAL 625-FULL (CESOP)

Rainer Gersonde, Jürgen Gossler, Daniel Damaske, Tanja Dufek, Oliver Esper, Frank Lamy

Alfred-Wegener-Institut

**Objectives**

The South Pacific is one of the few areas of the global ocean lacking information on Cenozoic paleoclimatic development from deep-sea drilling records. The Integrated Ocean Drilling Program (IODP) proposal 625-Full *Cenozoic Southern Ocean Pacific (CESOP) - a proposal for drilling Cenozoic history sites in the Pacific sector of the Southern Ocean* (Gersonde et al., 2008) proposes to secure these missing Southern Ocean constraints in order to assemble a sophisticated picture of the power of southern high latitude ocean and ice to drive climate and ocean evolution. The Pacific Southern Ocean is a key area to resolve a number of partly controversially discussed questions that have ultimate implications on past global climate, ocean, cryosphere, and biota evolution:

- What drove Antarctic glaciation at the Eocene/Oligocene transition (EOT)?
- Could the Southern Ocean have acted as an atmospheric $CO_2$ sink prior to the EOT?
- What is the timing of the opening of the Southern Ocean gateways to allow for the establishment of a fully developed ACC?
- What is the relationship between the Southern Ocean, cryosphere development in Antarctica, and the evolution of high latitude biota?
- What is the stability of the Westantactic Ice Sheet (WAIS) and connected Ross Ice Shelf (e.g. in the Pliocene) and what can we learn about future WAIS development in a World with persistent global warming?
- In case of a full early Pliocene WAIS draw down, what would be the effect of a gateway linking the Ross and Weddell Sea on ocean and climate?
- What is the role of Southern Ocean within the chain of responses that led to northern hemisphere glaciation in the Pliocene?
- What is the impact of orbital cycles on the Pacific Southern Ocean and Antarctic ice-sheet development?
- What is the role of the Pacific Southern Ocean in triggering and propagating abrupt ocean-climate changes?
- What is the role of the Pacific Southern Ocean in global deep-water ventilation and $CO_2$ sequestration at glacial/interglacial timescales?

- Is Pleistocene glacial/interglacial amplitude of physical Pacific Southern Ocean surface parameters less developed compared with other Southern Ocean sectors, and if yes what are the reasons for this decoupling?
- What is the nature of ocean-atmosphere dynamic variability and how is this connected to ocean nutrient, carbon cycling, water mass ventilation and sea ice?
- How have ENSO-like conditions impacted the Pacific Southern Ocean climate with potential impact on the WAIS development and propagation of climate signals into the Atlantic?
- How do large-sized asteroid impacts (like Eltanin) affect sediments and basement in the deep ocean?

These questions are all concerning major topics of the IODP science plan and in part requested by ICPP 2009 to be resolved for enhanced projection of future warmer climate conditions. To generate the appropriate sedimentary archives Gersonde et al. (2008) proposed in 625-ful-CESOP the recovery of Paleogene and Neogene sediments and high-resolution Plio-Pleistocene at 14 locations in the frame of IODP (Fig. 8.1).

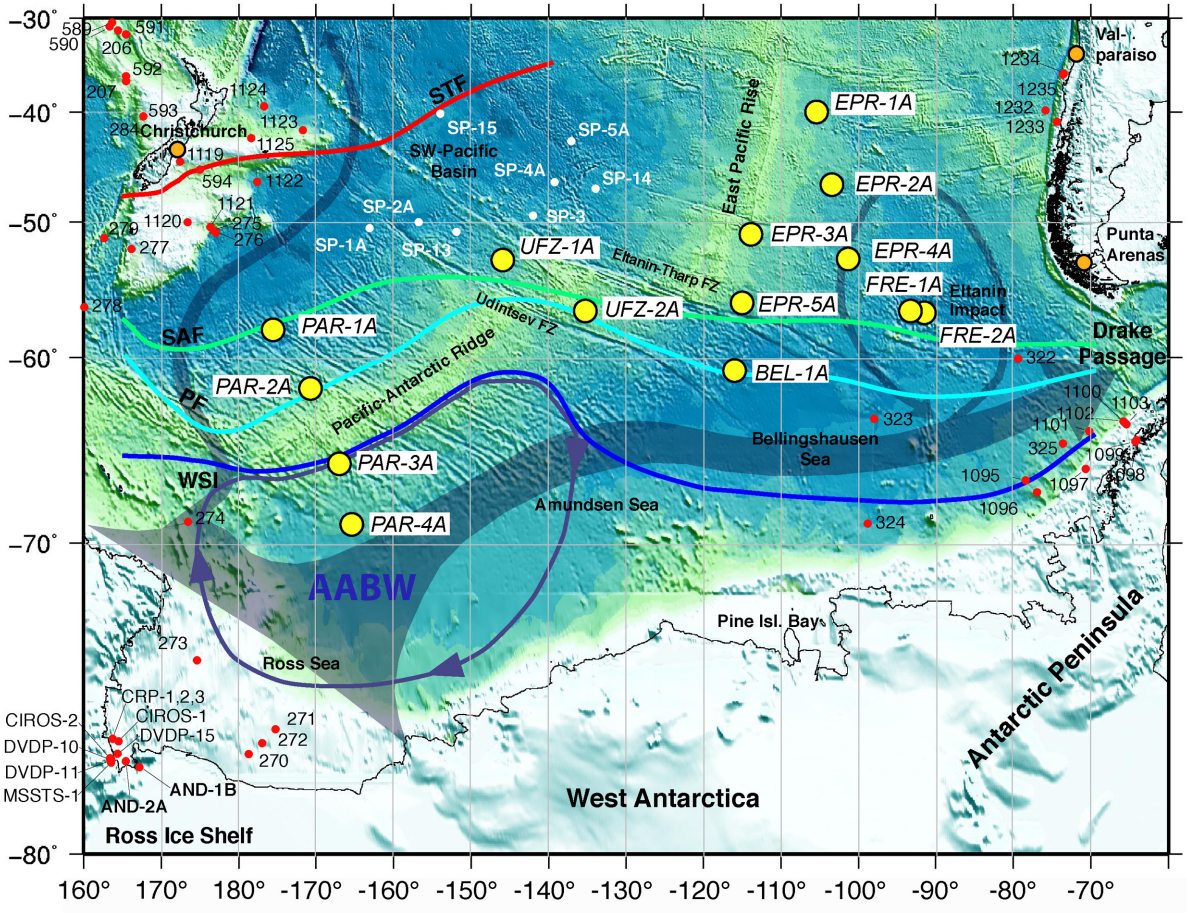


*Fig. 8.1: IODP drill sites proposed for 625-full CESOP (yellow dots) together with previous DSDP/OPD and other drilling (red dots) and proposed sites of IODP-proposal 567-full "Paleogene South Pacific APC transect" (white dots). Also indicated are oceanic fronts (STF, Subtropical Front, SAF, Subantarctic Front, PF, Polar Front) according to Belkin and Gordon (1996), winter sea ice distribution (WSI) (Comiso, 2003), as well as schematic representations of the Antarctic Bottom Water (AABW) pathways (Schlitzer, 2007) and the location of the Ross Gyre according to data from Assmann et al. (2005) (from Gersonde et al., 2008).*

Proposal 625-Full has been positively reviewed by the IODP-SSEP (Science Steering and Evaluation Panel), and the generation of a comprehensive pre-site survey at the proposed sites has been recommended. It was planned to conduct during ANT-XXVI/2 part of the pre-site survey including seismic, echosounding and bathymetric survey as well at sediment sampling at the proposed sites FRE-1A and Fre-1B, both located in the impact area of the Eltanin asteroid (see 7.7.8), at three sites at the southern East-Pacific Ridge (EPR-3A, -4A, -5A), at one site in the northern Bellingshausen Sea (BEL-1B), at one site North of the Udintsev Fracture Zone (UFZ-2A) and, except seismic survey at four sites located on a transect across the Pacific-Antarctic Ridge (PAR-1A, -2A, 3-A, -4A). Seismic survey at the latter four sites is planned to be conducted during the subsequent expedition ANT-XXVI/3 and the full survey programme at the sites EPR-2A and -1A, located north of 50°S on the East-Pacific Ridge should be accomplished during the SOPATRA cruise with RV *Sonne,* scheduled for austral summer 2010/11.

**Work at sea**

For further details on the instrumentation used for bathymetric and sediment echosounding survey at the proposed sites see Chapters 6 and 7.2. Surface sediment sampling and sediment coring techniques applied are described in Chapters 7.3 and 7.4.

*Multi-channel reflection seismics (MCS) - Seismic source, triggering and timing*

High resolution seismic reflection lines were shot using a high-frequency 2 GI-Gun™ cluster to better resolve the expected sedimentary layers (FIG. 8.2). A single GI-Gun is made of two independent airguns within the same body. The first airgun (“Generator”) produces the primary pulse, while the second airgun (“Injector”) is used to control the oscillation of the bubble produced by the “Generator”. We used the “Generator” with a volume of 0.74 liters (45 in³) and fired the “Injector” with a volume of 1.72 liters (105 in³) with a delay of 33 ms, leading to an almost bubble-free signal. The GI-Guns were towed 10 m behind the vessel in 3 m depth and were fired every 10 seconds at 200 bar, leading to an average shot interval of 25 m.

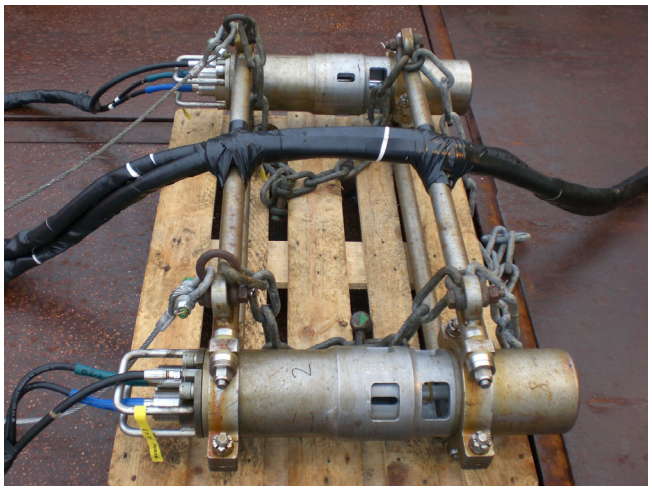

*Fig. 8.2: High-frequency 2 GI-Airgun cluster used for the seismic surveys*

Seismic data acquisition requires a very precise timing system, because seismic sources and recording systems must be synchronised. A combined electric trigger-clock system was in operation in order to provide the firing signal for the electric airgun valves and the time-control of the seismic data recording.

*Fig. 8.3: The 600 m long analogue streamer (Type PRAKLA)*

*Multi-channel reflection recording system*

As part of the multi-channel reflection data acquisition system, a 600 m long (active sections), 96 channel (hydrophones groups) analogue streamer (Type Prakla) was used (Fig. 8.3). To ensure that the streamer was placed deep enough below the water surface we made a control flight by helicopter (Fig. 8.4). This was necessary because

the slipping area of the vessel has been modified in a way that the lead-in point of the streamer cable was several meters more above sea level. We were very content that the streamer could not be seen further than 20 m behind the vessel. The seismic data were recorded at 1 ms sampling interval in SEG-D format on 3,480 cartridge magnetic tapes via a Geometrics EG&G 2420 recording system. Due to a severe hardware problem of the tape control circuit board of the Geometrics EG 2420 main unit, the originally planned seismic survey at Sites FRE-1A and FRE-2A is not continuous and had to be aborted before its completion and the survey around Site BEL-1 had to be cancelled. After identifying the reason of the problem, it could be fixed by replacing the damaged circuit board by another one from a second recording unit we had fortunately with us.

*Processing of multi-channel reflection seismic data*

Only single channel plots of every seismic section had been produced on board. All further seismic data processing will be performed during cruise leg ANT-XXVI/3.

**Preliminary results**

**1. Survey at FRE-1A and FRE-2A (Eltanin impact area)**

The area of the Freeden Seamount located between the Mornington Abyssal Plain and the Bellingshausen Abyssal Plain (Fig. 8.1) is the impact area of the Eltanin asteroid, the yet only known impact site of a large-sized (1 km in diameter) asteroid into the deep ocean. The impact took place in the Late Pliocene (ca. 2.5 Ma) and has disturbed the sediment column in the impact area back to Eocene deposits. Previous studies show that the Eltanin impact has generated a field of meteorite deposition, which represents the most meteorite-rich region known on the surface of the Earth. Marine-geological sampling of the potential ground-zero sites of the impact and a seismic survey provide the baseline for drilling the impact deposits as proposed within IODP proposal 625-Full.

*Fig. 8.4: Polarstern with the towed airgun cluster and 600 m streamer taken during a helicopter control flight to check the correct depth position of the streamer.*

*Bathymetric and echo-sounding survey*

Bathymetric and echo-sounding survey was accomplished to add further information on the bathymetry and sediment deposition pattern with a focus on the southern part of the Freeden Seamount (Fig. 8.5).

*Sediment coring*

Based on available and new bathymetric and sediment echo-sounding survey obtained during ANT-XXVI/2 a total of eight sites were selected (PS75/035-040, PS75/42-43) to recover impact-related sediment sequences in potential ground-zero areas predicted by numerical modeling (Fig. 8.5). Although seven of the recovered cores are longer than 20 m impact related sequences could be encountered only at three locations (PS75/036, 038, 040). While one core (PS75/036) presumably sampled at its base the fine-grained deposits above the ejecta layer, the other cores document the ejecta layer, underlying disturbed sequences and undisturbed Eocene calcareous nannofossil ooze (for PARASOUND profiles from coring sites, sediment core description and fotographic documentation see Appendix A.6, A.7, A.8).

*Seismic survey*

The layout of MCS profiles AWI-20100001-06 covers various bathymetric features like seamounts and the proposed impact location (Fig. 8.5). We connected profile 20100001 to the MCS profile AWI-95224 from 1995 by crossing it perpendicular. Due to the above mentioned hardware problem we could not record the seismic lines 20100001 and 20100004 completely. The further planned profiles 20100005-06 had to be cancelled. The single channel profile plot shows high-resolution signals from the sedimentary layers and underlying basement (Fig. 8.6).

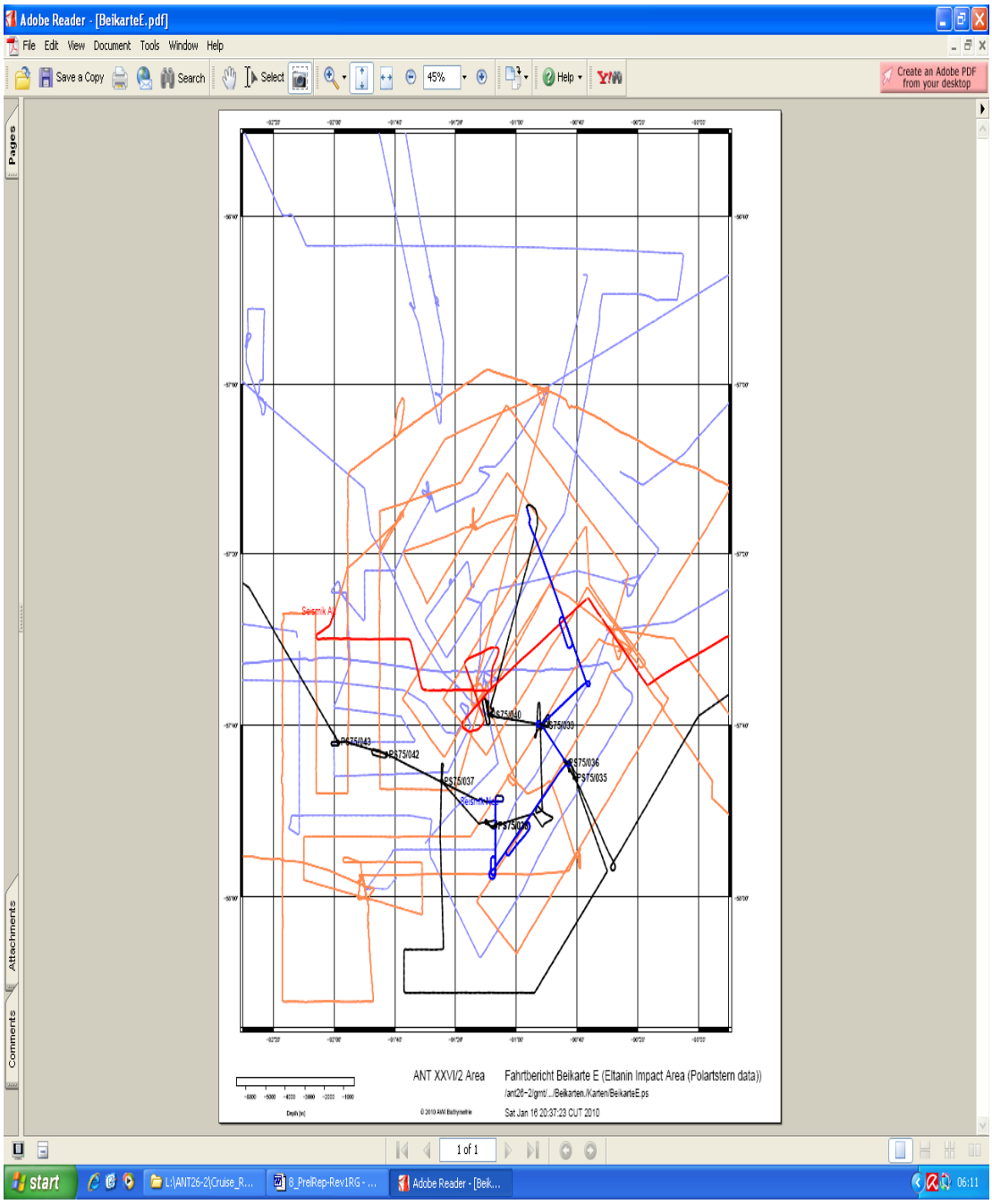


*Fig. 8.5: Map showing bathymetric and sediment-echounding tracks (black line) combined bathymetric, echo-sounding and MCS track (thick blue line) together with acoustic surveys accomplished during previous cruises in the area of Freeden Seamount. Also indicated are sediment sampling sites.*

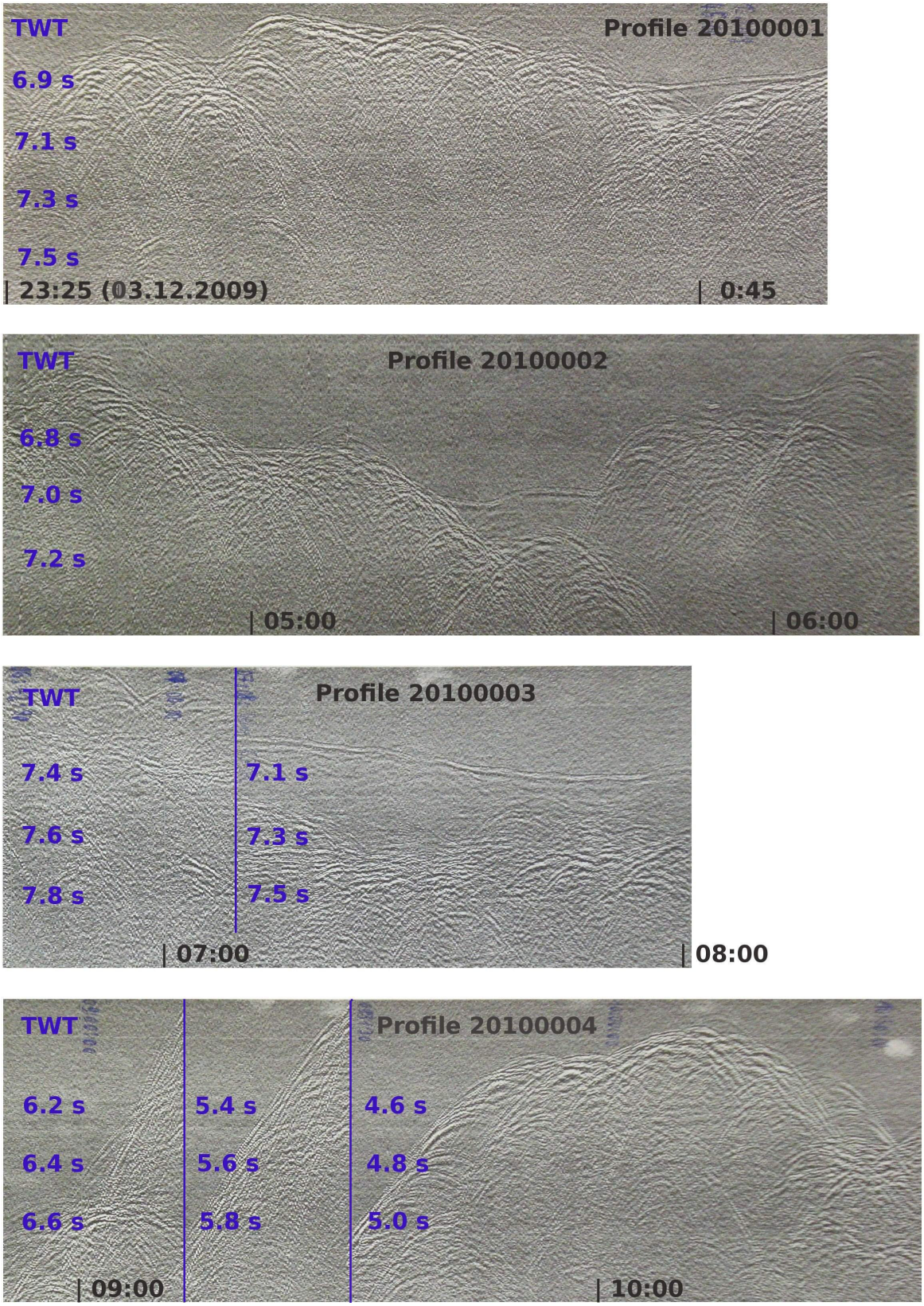


*Fig. 8.6: Single channel plot of seismic reflection signals of profiles AWI-20100001-04. The pre-filtered traces are shown in a two-way traveltime (TWT) plot.*

## 2. Survey at EPR-4A (East Pacific Rise)

*Bathymetric and echo-sounding survey*

Bathymetric and sediment-echosounding surveys were accomplished around the potential drill site (Station PS75/047), located west of a seamount structure (Fig. 8.7).

*Sediment coring*

At the potential drill site, Station PS75/047 was accomplished and a 22.89 m long piston core was recovered at a water depth of 4,480 m (for PARASOUND profiles from coring site, sediment core description and fotographic documentation see Appendix A.6, A.7, A.8) (Fig. 8.7). Preliminary dating of the core indicates a basal age around 0.9 Ma, which results in an average sedimentation rate of 1 cm/1,000 y (Tab. 7.6.1).

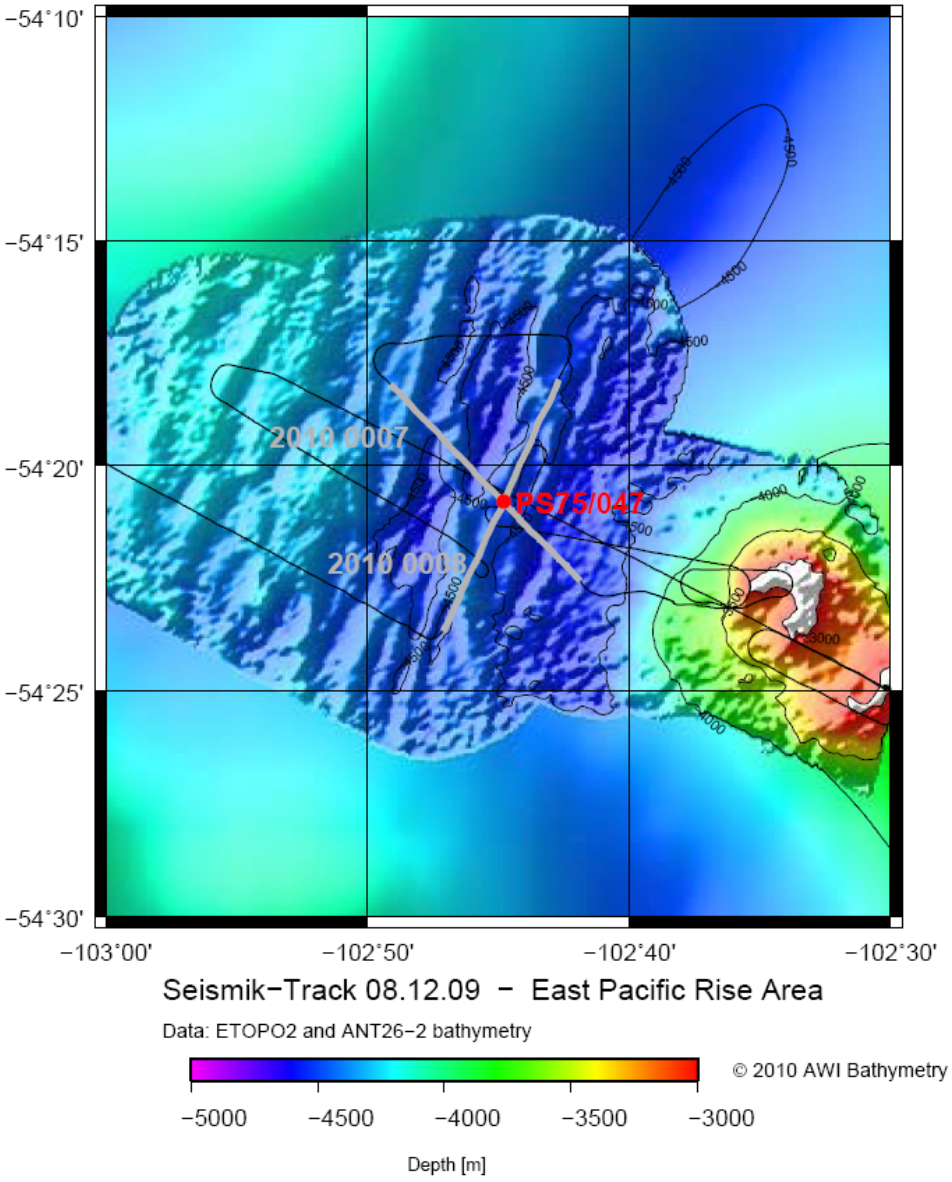


*Fig. 8.7: Bathymetric map of IODP site EPR-4A. The ships track including the MCS lines, profile names and the proposed drill site (Station PS75/047) are indicated.*

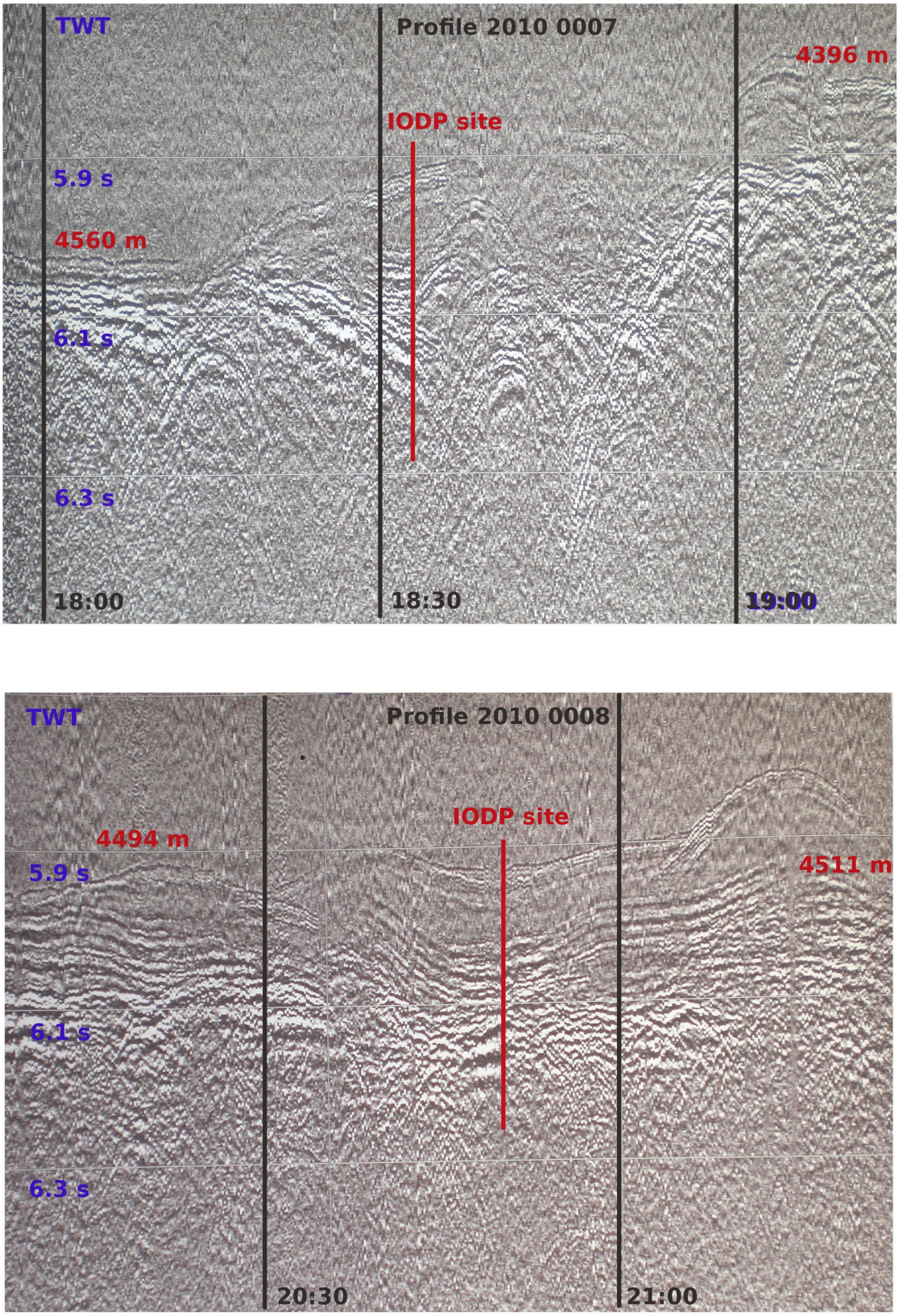


*Fig. 8.8: Pre-filtered single channel reflection seismic traces of profiles AWI-20100007/08. Two-way traveltime (TWT), water depth, IODP location and UTC time are indicated.*

*Seismic survey*

IODP site EPR-4A was surveyed by MCS profiles 20100007-08. The profiles were designed crosswise with an individual length of 6 nautical miles (nm) each. This is less than the initially planned 20 nm to minimize the drop out probability caused by the hardware problem of the recording unit. Profile locations are shown in Fig. 8.7. While profile 20100007 crosses the bathymetric structures showing many diffracted signals, profile 20100008 stretches parallel to the structure indicating a ~500 m thick sedimentary layer above the basement (Fig. 8.8).

**3. Survey at BEL-1B (Northern Amundsen Sea)**

*Bathymetric and echo-sounding survey*

Bathymetric and sediment-echosounding surveys were accomplished around the potential drill site (Station PS75/052), located on top of a sedimentary structure possibly representing a sediment drift deposit.

*Sediment coring*

At the potential drill site, Station PS75/052 was accomplished. A 23.17 m long piston core was recovered at a water depth of 5,130 m (for PARASOUND profiles from coring site, sediment core description and fotographic documentation see Appendix A.6, A.7, A.8). Preliminary dating of the core indicates a basal age around 0.4 Ma, which results in an average sedimentation rate of 5.5 cm/1000 y (Tab. 7.6.1). The coring was complemeted by a CTD cast and a multi-net haul. After cancellation of the planned seismic survey surface sediments were recovered with a multi-corer in the vicinity of the potential drill site (PS75/053).

*Seismic survey*

The seismic survey at this location (profiles 20100009-10) had to be cancelled due to the hardware failure of the recording system. The survey could be completed successfully during the following cruise ANT-XXVI/3 (Gohl, 2010).

**4. Survey at EPR-5A (southernmost East Pacific Rise)**

*Bathymetric and echo-sounding survey*

Bathymetric and sediment-echosounding surveys were accomplished around the potential drill site (Station PS75/054) (Fig. 8.9).

*Sediment coring*

At the potential drill site, Station PS75/054 was accomplished. A 22.38 m long piston core was recovered at a water depth of 4,113 m (for PARASOUND profiles from coring site, sediment core description and fotographic documentation see Appendix A.6, A.7, A.8) (Fig. 8.9). Preliminary dating of the core indicates a basal age around 0.2 Ma, which results in an average sedimentation rate of 11.8 cm/1,000 y (Tab. 7.6.1). The coring was complemeted by a CTD cast and a multi-net haul. The sampling of surface sediment was unsuccessful at the station.

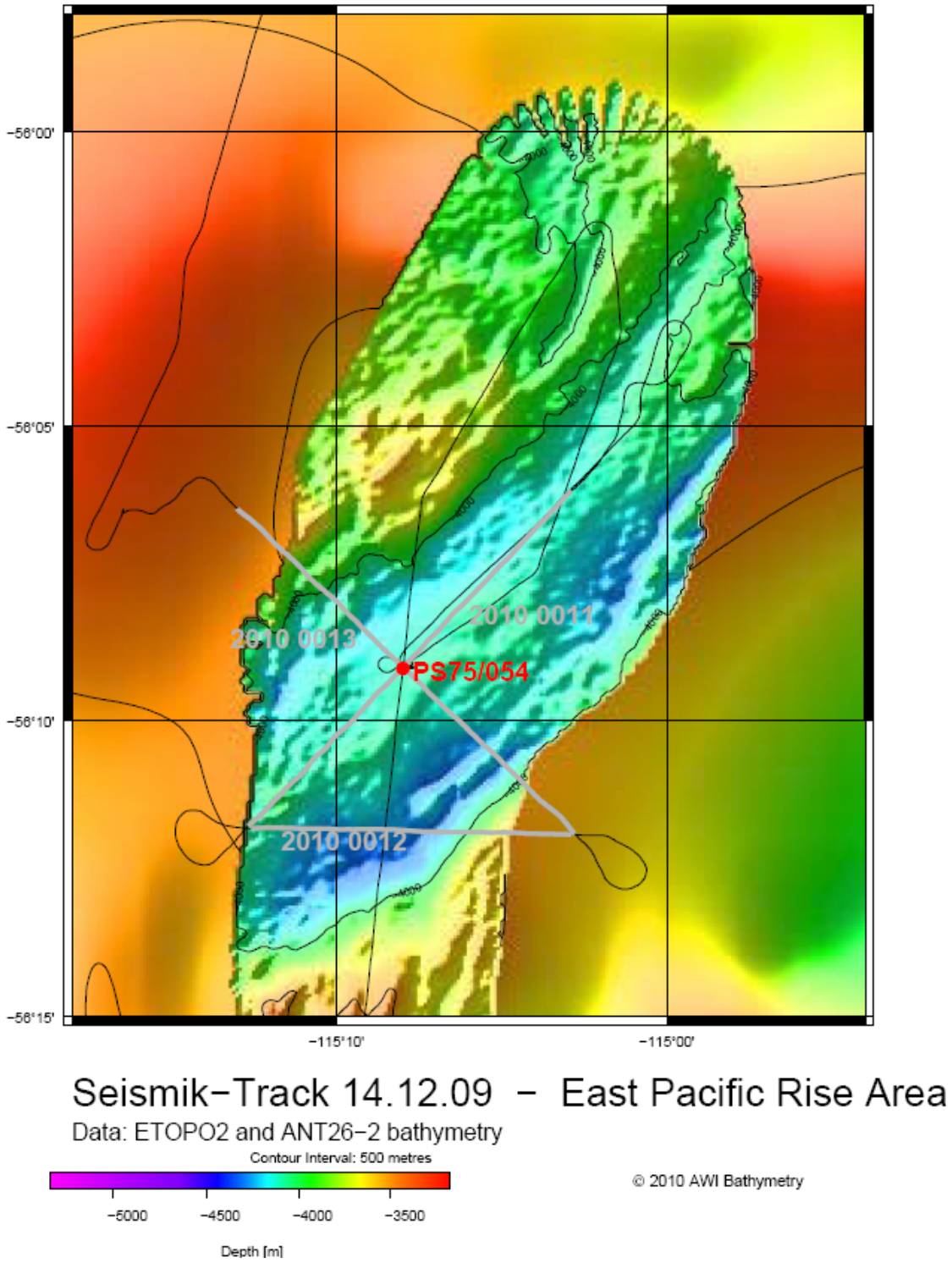


*Fig. 8.9: Bathymetric map of IODP site EPR-5A. The ships track including the MCS lines, profile names and the proposed drill site (Site PS75/054) are indicated.*

*Seismic survey*

MCS lines 20100011-13 were shot north of the Eltanin Fracture Zone ~400 km eastward the East Pacific Rise (EPR*)* (Figs. 8.1, 8.9, 8.10). The additional profile (20100012) was obtained by connecting the end point of profile 20100011 with the starting location of profile 20100013 by a straight line. The cross profiles extend to a length of 8 nm each. MCS profile 20100011 parallels a small hill structure indicating ~1,300-1,500 m thick sediments, while line 20100013 crosses the bathymetric structures perpendicularly (Fig. 8.9). The sedimentary layers of EPR-5A drill site have been resolved clearly and very detailed (Fig. 8.10). The profiles could be shot without any problems after the successful repair of the recording unit.

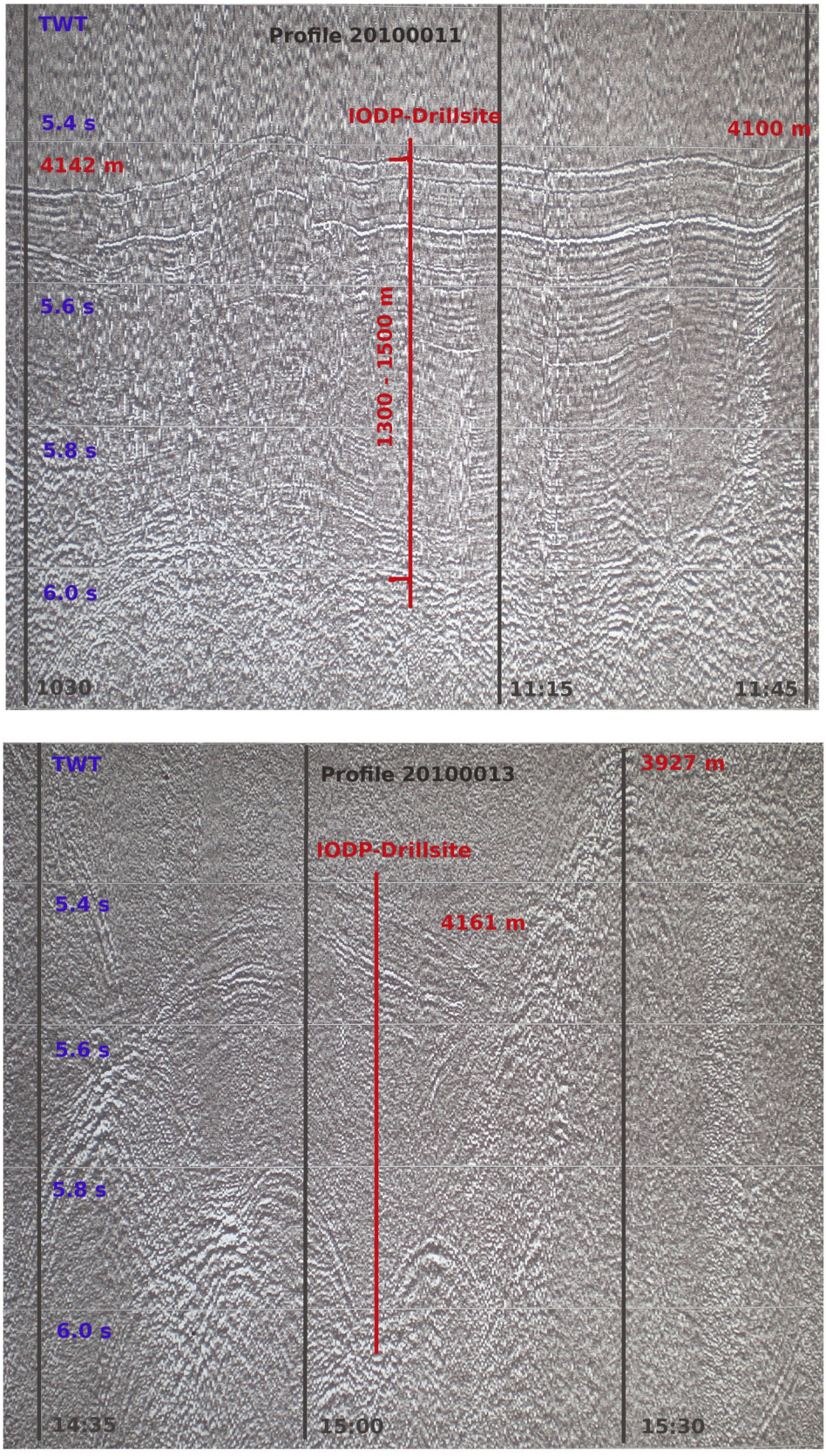


*Fig. 8.10: Pre-filtered single channel reflection seismic traces of profiles AWI-20100011/13 at Site EPR-5A. Two-way traveltime (TWT), water depth, IODP location and UTC time are indicated.*

## 5. Survey at EPR-3A (Southern East Pacific Rise)

The originally planned survey of proposed Site EPR-3A was cancelled because two attempts to reach this position on the southern East Pacific Rise were unsuccessful due to heavy weather conditions. As a consequence it was decided to select an alternate site on the western flank of the East Pacific Rise labelled EPR-6A.

## 6. Alternate survey at western flank of southern East Pacific Rise (EPR-6A)

*Bathymetric and echo-sounding survey*

Bathymetric and sediment-echosounding surveys were accomplished around the alternate potential drill site (Station PS75/059) (Fig. 8.11).

*Sediment coring*

At the potential drill site, Station PS75/059 was accomplished. A 13.98 m long piston core was recovered at a water depth of 3,613 m (for PARASOUND profiles from coring site, sediment core description and fotographic documentation see Appendix A.6, A.7, A.8) (Fig. 8.11). Preliminary dating of the core indicates a basal age around 0.4 Ma, which results in an average sedimentation rate of 3 cm/1,000 y (Tab. 7.6.1). The sampling of surface sediment was unsuccessful at the station.

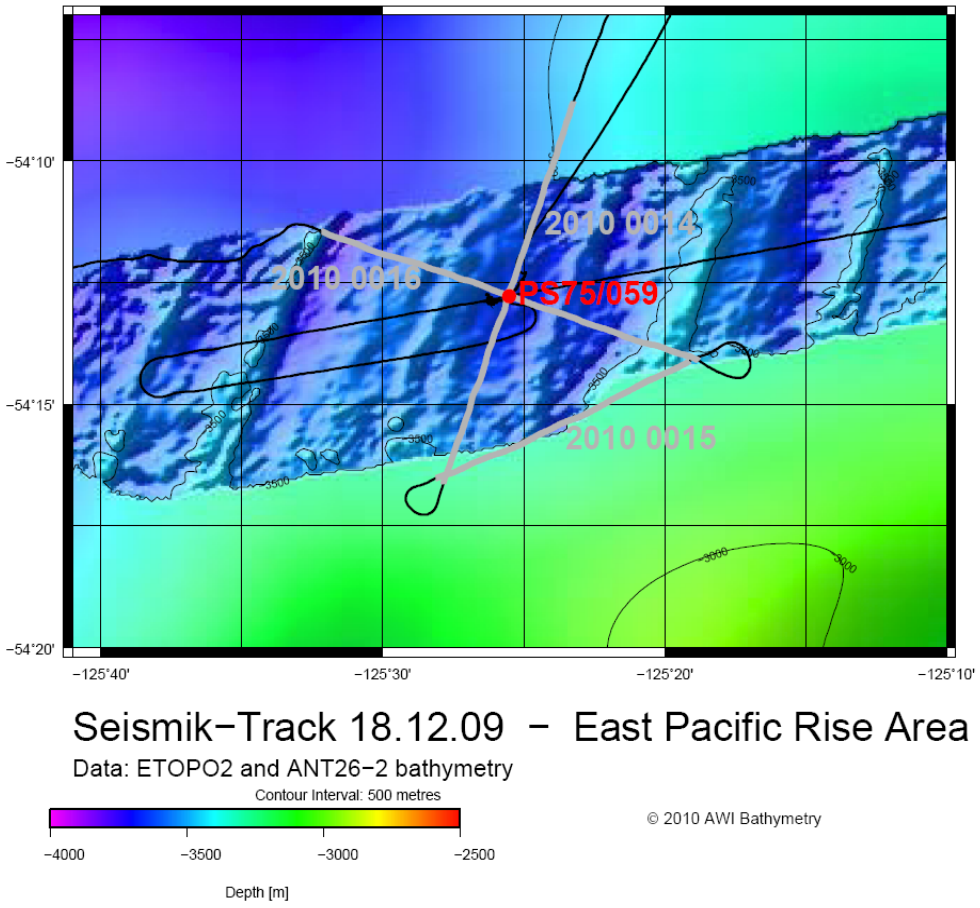


*Fig. 8.11: Bathymetric map of alternate IODP site EPR-6A (Station PS75/059). The ships track including the MCS lines, profile names and the proposed drill site are indicated.*

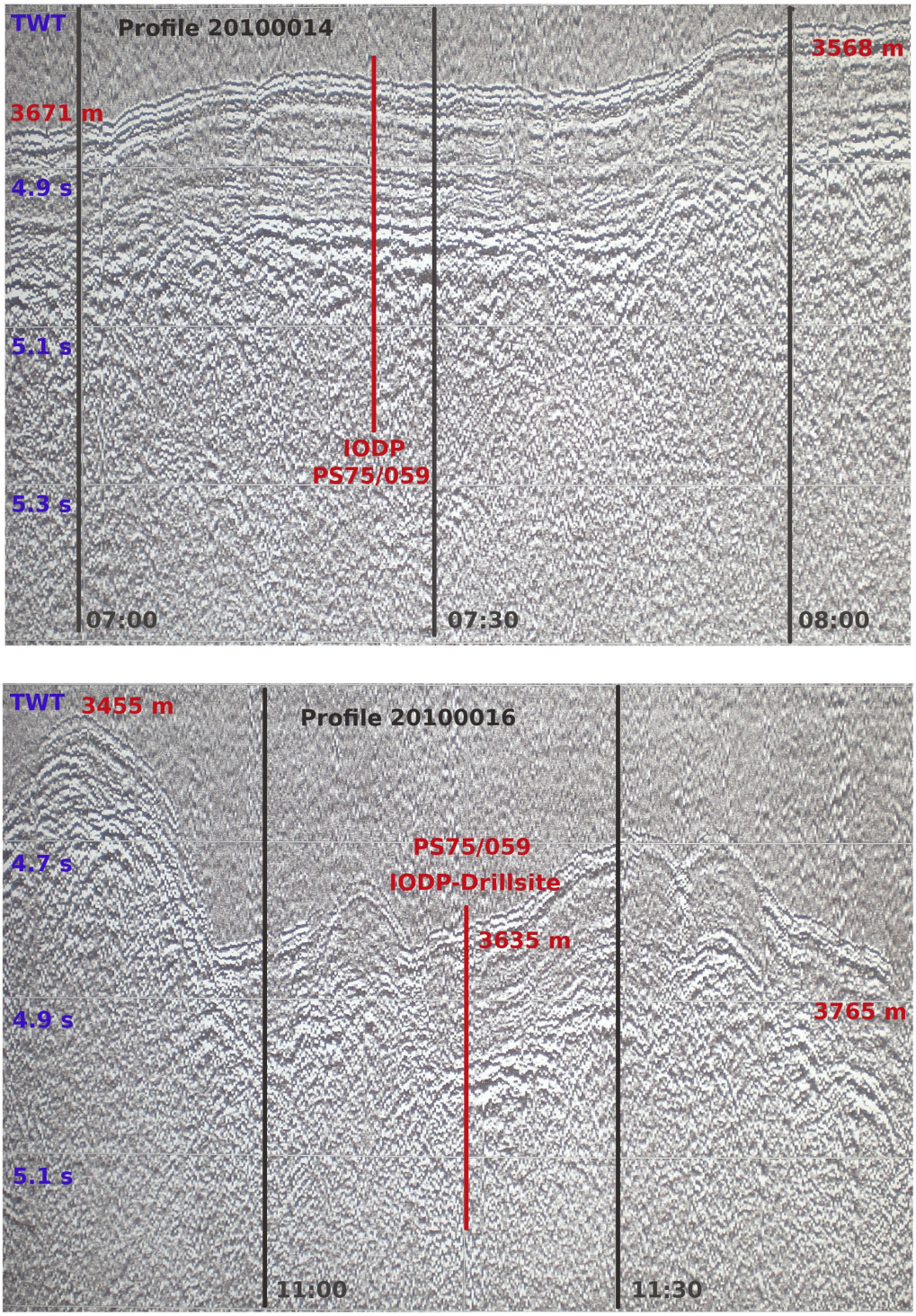


*Fig. 8.12: Pre-filtered single channel reflection seismic traces of profiles AWI-20100014/16. Two-way traveltime (TWT), water depth, IODP location and UTC time are indicated.*

*Seismic survey*

The last seismic survey accomplished during ANT-XXVI/2 took place at EPR-6A, located north of the Eltanin Fracture Zone System and ~300 km west of the crest of the EPR (Fig. 8.11). A similar MCS profile configuration as at the previous site EPR-5 was used. Profile 20100014 was shot along the linear bathymetric structure while profile 20100016 was perpendicular to it. The connecting profile 20100015 was also recorded. Again, well resolved flat ~300-400 m thick sediments covering the basement have been observed on line 20100014, while line 20100016 shows a wiggle structure due to the bathymetric variations (Fig. 8.12).

**6. Survey at UFZ-2A (North of Udintsev Francture Zone)**

Survey at initially proposed locations and UFZ-2A in the vincinity of the Udintsev Fracture Zone (Fig. 8.1) was cancelled due to the lack of sediments in that region.

**7. Survey at PAR-4A (Southern flank of Pacific-Antarctic Ridge, Ross Sea)**

*Bathymetric and echo-sounding survey*

Bathymetric and sediment-echosounding surveys were accomplished around the potential drill site (Station PS75/088), located on top of a sedimentary structure possibly representing a sediment drift deposit.

*Sediment coring*

At the potential drill site, Station PS75/088 was accomplished. A 12.4 m long gravity core was recovered at a water depth of 3,857 m (for PARASOUND profiles from coring site see Appendix A.6). The coring was complemeted by surface sediment sampling, a CTD cast, a multi-net and two plankton net hauls.

*Seismic survey*

The seismic survey at this location was completed successfully during the following cruise ANT-XXVI/3 (Gohl, 2010).

**8. Survey at PAR-3A (Southern flank of Pacific-Antarctic Ridge)**

*Bathymetric and echo-sounding survey*

Bathymetric and sediment-echosounding surveys were accomplished around the potential drill site (Station PS75/090), located in an area of restricted sediment deposition.

*Sediment coring*

At the potential drill site, Station PS75/090 was accomplished. A 17.91 m long piston core was recovered at a water depth of 3,478 m (for PARASOUND profiles from coring site, sediment core description and fotographic documentation see Appendix A.6, A.7, A.8). ). Preliminary dating of the core indicates a basal age in the Pliocene, around 3.8 Ma, which results in an average sedimentation rate of 0.5 cm/1,000 y (Tab. 7.6.1). The coring was complemeted by surface sediment sampling, a CTD cast, a multi-net and

two plankton net hauls. The coring was complemeted by surface sediment sampling, a CTD cast, a multi-net and two plankton net hauls.

*Seismic survey*

No seismic survey was completed during the following cruise ANT-XXVI/3 (Gohl, 2010) at this site.

## 9. Survey at PAR-2A (Northern flank of Pacific-Antarctic Ridge)

*Bathymetric and echo-sounding survey*

Bathymetric and sediment-echosounding surveys were accomplished around the potential drill site (Station PS75/093), located in the vicinity of the Antarctic Polar Front (Fig. 8.1).

*Sediment coring*

At the potential drill site, Station PS75/093 was accomplished. A 12.84 m long piston core was recovered at a water depth of 3,762 m (for PARASOUND profiles from coring site, see Appendix A.6). ). Preliminary dating of the core indicates a basal age around 0.4 Ma, which results in an average sedimentation rate of 3 cm/1,000 y (Tab. 7.6.1).

*Seismic survey*

The seismic survey at this location was completed successfully during the following cruise ANT-XXVI/3 (Gohl, 2010).

## 10. Survey at PAR-1A (Northern flank of Pacific-Antarctic Ridge, Southwest Pacific Basin)

*Bathymetric and echo-sounding survey*

Bathymetric and sediment-echosounding surveys were accomplished around the potential drill site (Station PS75/095), located in the vicinity of the Subantarctic Front (Fig. 8.1).

*Sediment coring*

At the potential drill site, Station PS75/095 was accomplished. A 17.85 m long piston core was recovered at a water depth of 4,853 m (for PARASOUND profiles from coring site, sediment core description and fotographic documentation see Appendix A.6, A.7, A.8). ). Preliminary dating of the core indicates a basal age around 0.65 Ma, which results in an average sedimentation rate of 2.7 cm/1,000 y (Tab. 7.6.1).

*Seismic survey*

Due to technical problems no seismic survey was completed during the following cruise ANT-XXVI/3 (Gohl, 2010) at this site.

Further potential sites for future drilling in the frame of IODP have been discovered on the transect between sites PS75/075 (eastern SW-Pacific Basin) and PS75/088 (northern Ross Sea). These sites very possibly bear sediment sequences that document

the Pliocene-Pleistocene paleoceanographic development in the western sector of the polar South Pacific more favourable than those found at the sites PAR-3A to PAR-1A. Bathymetric and sediment-echosounding information is available from these sites, but the required seismic survey could not be accomplished during the following cruise ANT-XXVI/3 and thus is still lacking.

## References

Assmann, K. M., Hellmer, H. H., Jacobs, S. S., 2005. Amundsen Sea ice production and transport. Journ. Geophys. Res. 110, C12013, doi:10.1029/2004JC002797.

Belkin, I.M., A.L. Gordon, 1996. Southern Ocean fronts from the Greenwich meridian to Tasmania. Journal of Geophysical Research, 101, C12, 28317-28324.

Comiso, J.C., 2003. Large scale characteristics and variability of the global sea ice cover. In: Thomas, D.N., Diekmann, G. S. (Eds.) Sea ice an Introduction to its Physics, Chemistry, Biology and geology, Blackwell, Oxford, 112-142.

Gohl, K., 2010 The Expedition of the research vessel “Polarstern” to the Amundsen Sea, Antarctica, in 2010 (ANT-XXVI/3). Reports on Polar and Marine Research 617, 168 p.

Gersonde, R., et al., 2008: Cenozoic Southern Ocean Pacific (CESOP): A proposal for drilling Cenozoic history sites in the Pacific sector of the Southern Ocean. Proposal 625-full to the Integrated Ocean Drilling Program (IODP), 128 p.

Schlitzer, R., 2007. Assimilation of radiocarbon and chlorofluorocarbon data to constrain deep and bottom water transports in the World Ocean. J. Phys. Oceanogr. 37, 259-27.

# 9. GRAVIMETRIC AND GEOMAGNETIC UNDERWAY MEASUREMENTS

Jürgen Gossler[1] not on board: Andreas Winter[2]

[1]Alfred-Wegener-Institut
[2]FIELAX Gesellschaft für wissenschaftliche Datenverarbeitung mbH

## Objectives

Accurate models of the geodynamic-tectonic evolution contain some of the most important parameters for understanding and reconstruction of the palaeo-environment. Magnetic and gravimetric surveys allow plate-tectonic and oceanic crustal reconstructions.

## Work at sea

### Shipborne gravity

Gravity data were continuously acquired during the expedition using the ship's permanently-mounted KSS31 gravity meter. The data were directly archived in the D-SHIP system at one-second intervals. The gravity data acquisition worked without any problems during the entire cruise leg, except for about 4 hours on January 5 when the cardanic platform failed, so that the system had to be restarted. The gravimeter's heating was never switched of during the whole cruise.

*Onshore gravity measurements*

We conducted two onshore measurements with a LaCoste and Romberg gravity meter in Punta Arenas (Chile) in order to tie the underway data to the International Gravity Station Network (IGSN). It was not possible to measure directly at the nearest located IGSN station at the Port Authority building in Punta Arenas, due to limited time before the ship's departure. Instead, the last available gravity measurement from that station will be used to correct the relative KSS31-measurements. This will be performed on the subsequent cruise leg ANT-XXVI/3.

Measurement at Madones peer, Punta Arenas on November 26th, 2009 (Fig. 9.1):

Coordinates: 53°07.607' S; 70°51.600' W, altitude: 4 m, conditions: strong wind

Instrument temperature: 51°C, feedback on: 1 V ~ 1 scu

| UTC | reading (scu) | Voltage (V) | calc. reading (scu) |
|---|---|---|---|
| 14:02 | 4853,0 | +0,832 | 4853,832 |
| 14:08 | 4854,0 | –0.192 | 4853,808 |
| 14:13 | 4853,5 | +0,328 | 4853,828 |
| 14:17 | 4854,5 | –0,726 | 4853,774 |

Average calc. reading: 4853.811 scu = 4967.718 mgal relative gravity*

* from gravimeter's calibration table


*Fig. 9.1 Land gravity measurement at Madones peer in Punta Arenas, Chile*

*Fig. 9.2 Second gravity measurement at Cabo Negro fuel depot near Punta Arenas.*

Measurement at Cabo Negro fuel depot on November 27, 2009 (Fig. 9.2):

Coordinates: 52°55.954' S; 70°48.277' W, altitude: 4.5 m, conditions: strong wind

Instrument temperature: 51°C, feedback on: 1 V ~ 1 scu

| UTC | reading (scu) | Voltage (V) | calc. reading (scu) |
|---|---|---|---|
| 16:40 | 4835,0 | +1,239 | 4836,239 |
| 16:45 | 4835,5 | +0,731 | 4836,231 |
| 16:47 | 4836,0 | +0,191 | 4836,191 |
| 16:50 | 4837,0 | –0,844 | 4836,156 |

Average calc. reading: 4836.204 scu = 4949.677 mgal relative gravity*

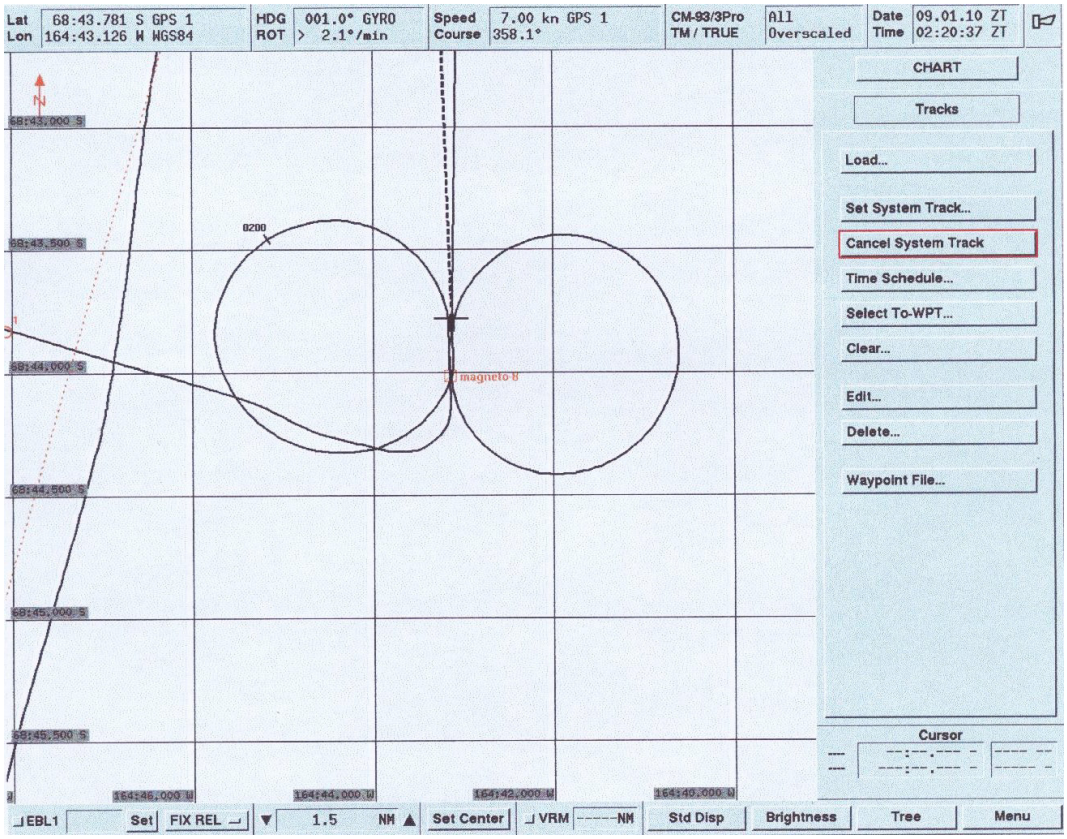


*Fig. 9.3 Ship track of the compensation turn circles to calibrate the magnetic measurements.*

*Shipborne magnetics*

Shipborne magnetic measurements were made by two fluxgate vector magnetometers, which were permanently mounted at the crow's nest. The data were directly saved in the ship's archiving system, D-SHIP, at one-second intervals since January 8. To take account of the influence of the metallic bulk of the ship, the ship undertook two

compensation loops on January 9 (Fig. 9.3). In the small area of a compensation loop the variations of the magnetic field due to crustal magnetisation are assumed to be negligible. The loops thus provide coefficients that relate the ship's heading, roll, and pitch movements to the variations in magnetometer measurements that they cause. Using these coefficients, it is possible to correct the shipborne magnetic measurements in the wider area around the compensation loop.

**Preliminary results**

In the future, after further data reduction and modelling of source body distributions, the ship's gravity and magnetic data will be useful adjuncts to the interpretation of the seismic profiles and other data.

# 10. PUBLIC OUTREACH (SCHOOL & UNIVERSITY)

Ulrich Breitsprecher[1] [1]KGS Stuhr-Brinkum
Abhinav Gogoi[2] [2]University of Bremen

## 10.1 WebBlog Polarstern-AG and Comments by Addy

Ulrich Breitsprecher KGS Stuhr-Brinkum

**Objectives**

The intention is the transfer of knowledge from scientific work to schools. The close link between research and education increases the interest of pupils and students in scientific subjects. Our own experience during the expedition will lead to a more convincing and successful routine in education.


*Fig. 10.1: View of the Addy Website*

### Work at sea

The webblog during the cruise was done in conjunction with the project “Coole Klassen”. The intention is to give pupils the chance to experience research methods and to understand the content of the expedition and how it is currently implemented on *Polarstern*. There are 2 target groups: 1. a younger audience who receives their explanation from Addy and 2. more general audience, who can read about my experiences in the blog. The webadress is: http://www.polarstern-ag.de. The English version was issued on the IPY Website.

The blog was updated every four days, as were the stories of Addy, the Adelie penguin. In total 24 articles were issued in the blog and also on the Addy site. The following aspects of the expedition were discussed: research work, experiences of nature, technical details of the ship, sciencific methods and teamwork.


*Fig. 10.2: View of the Blog*

### Preliminary results

The feedback of the readers is very good. The number of visits to the website is not accessible from the ship but will be evaluated at home.

The future objective is to integrate the experience of scientific work with educational methodes in the classroom, which will be accomplished through the national project “Coole Klassen“. The various science courses should be taught in an interdisciplinary fashion to mirror the way things function aboard.

## 10.2 *Polarstern* Diary Blogspot

Abhinav Gogoi University of Bremen

### Objectives

This project was a Media Project for the Research Project Module for the University of Bremen Masters program (M.Sc. Marine Geosciences). The aim of this project is to present to the public the adventures of living and working on a research vessel in general terms. A lot of people, for example friends and family of participants of such an expedition, school and university students, other faculties and the general public are interested in learning the course of scientific and logistical activities in such an environment, especially within the field of climate research (an important political, scientific and communal topic at present) on board of *Polarstern*. By using documents, pictures and videos, the public's interest for the importance of polar science, its implementation and general overview gained by personal experience and input from others on board the vessel should be enhanced.

### Work at sea

The work on board has been about writing reports on life-on-board in English for the IPY website as mentioned above by Ulrich Breitsprecher. The blog, at the moment, includes these IPY reports. The blog can be found under the link:

www.polarstern-diary.blogspot.com

and is titled: *Polarstern* Cruise XXVI-2 Diary

However, as the title suggests the main objective is a diary about the life-on-board. Hence, a written account has been kept which includes day-to-day stories of work, events and activities on board. It includes information on the different equipment and instruments on board and their applications – how they work and what they are used for? There is also information about life on board such as the working hours and how people go about it, the strategies planned such as escaping bad weather and still continuing with the planned program of stations and sampling, the science involved behind the expedition, the various scientific work done on board, about the facilities on the ship, the social events such as Christmas and New Year's, the intricacies of interdisciplinary work by various scientific groups and everyday adventures seen through the eyes of a scientist. The personal work on board, besides the routine of working in the Physical Properties Lab and keeping the diary, also includes documenting various work and conditions with pictures and videos. The pictures are selected and the videos are edited on board, however, further editing is required when back in Bremen.

### Preliminary results

The result so far has been the set-up of the blog with the reports for the IPY. Tthe response has been positive. The finished product of the diary, the pictures and the videos put-up altogether on the blog will be done by the end of February to be first presented to the Chief Scientist of the cruise Dr. Rainer Gersonde and supervisor of this project Dr. Tilo von Dobeneck and once approved will then be presented in the Research Project Seminar in University Bremen in March 2010. The blog will then be accessible to everyone.

# A.1 TEILNEHMENDE INSTITUTE / PARTICIPATING INSTITUTIONS

| | **Adresse**<br>**Address** |
|---|---|
| AWI | Stiftung Alfred-Wegener-Institut für Polar- und Meeresforschung in der Helmholtz-Gemeinschaft<br>Postfach 120161<br>27515 Bremerhaven/ Germany |
| DWD | Deutscher Wetterdienst<br>Geschäftsbereich Wettervorhersage<br>Seeschifffahrtsberatung<br>Bernhard Nocht Str. 76<br>20359 Hamburg/Germany |
| ETH | Eidgenössische Technische Hochschule Zürich<br>Geologisches Institut<br>Sonneggstrasse 5<br>8092 Zürich/Switzerland |
| GeoB | Marine Geophysik<br>Fachbereich Geowissenschaften<br>Universität Bremen<br>Postfach 330440<br>28344 Bremen/Germany |
| GNS | GNS Science<br>1 Fairway Drive, Avalon<br>PO Box 30368<br>Lower Hutt 5040/New Zealand |
| Heli Service | Heli Service International GmbH<br>Am Luneort 15<br>27572 Bremerhaven/Germany |
| KGS | KGS Stuhr-Brinkum<br>Brunnenweg 2<br>28816 Stuhr/Germany |
| KOPRI | Korea Polar Research Institute, KOPRI<br>Songdo Techno Park, 7-50, Songdo-Dong, Yeonsu-Gu,<br>Incheon, P.O. Box 32, 406-840/Korea |

| | **Adresse**<br>**Address** |
|---|---|
| NIU | Northern Illinois University<br>Department of Geology & Environmental Geosciences<br>Davis Hall<br>Dekalb, IL 60115/USA |
| UAB | Institute of Environmental Sciences and Technologies<br>Universitat Autònoma de Barcelona<br>08193 Cerdanyola del Vallès, Catalonia/Spain |
| UHAM | Department of Geology and Geophysics<br>University of Hawaii at Manoa<br>1680 East-West Road,<br>Honolulu, HI 96822/USA |
| USAL | Department of Geology<br>Faculty of Sciences<br>University of Salamanca<br>Salamanca 37008/Spain |

# A.2 FAHRTTEILNEHMER / CRUISE PARTICIPANTS

Fahrtleiter/Chief Scientist: Rainer Gersonde

Punta Arenas-Wellington

| Name/ Last name | Vorname/ First name | Institut/ Institute | Beruf/ Profession |
|---|---|---|---|
| Arevalo | Marcelo | AWI | Technician, Geology |
| Bock | Ute | AWI | Technician, Geology |
| Brauer | Jens | HeliTransair | Helicopter technician |
| Breitsprecher | Ulrich | KGS | Teacher |
| Büchner | Jürgen | HeliTransair | Helicopter pilot |
| Buldt | Klaus | DWD | Technician, Meteorology |
| Choi | Yu Jeong | KOPRI | Technician, Biology |
| Cortese | Giuseppe | GNS | Scientist, Paleoceanogr. |
| Damaske | Daniel | AWI | Student, Bathymetry |
| Dufek | Tanja | AWI | Student, Parasound |
| Esper | Oliver | AWI | Scientist, Paleoceanogr. |
| Fietz | Susanne | UAB | Scientist, Paleoceanogr. |
| Gall | Fabian | HeliTransair | Helicopter technician |
| Gersonde | Rainer | AWI | Scientist, Paleoceanogr. |
| Gogoi | Abhinav | GeoB | Student, Geomag/Phys.prop |
| Gölles | Thomas | AWI | Student, Geology |
| Gossler | Jürgen | AWI | Scientist, Seismics |
| Heinzl | Cornelia | AWI | Student, Bathymetry |
| Ho | Sze Ling | AWI | Scientist, Paleoceanogr. |
| Hutzler | Lorenz | AWI | Student, Paleoceanogr. |
| Jendersie | Franz | AWI | Student, Oceanography |
| Kersten | Franziska | AWI | Scientist, Paleoceanogr. |
| Kim | Young Nam | KOPRI | Scientist, Biology |
| Konfirst | Matt | NIU | Scientist, Paleoceanogr. |
| Kühl | Bastian | AWI | Student, Geomag/Phys.prop |
| Lamy | Frank | AWI | Scientist, Sedimentology |
| Lensch | Norbert | AWI | Technician, Geology |
| Martinez Garcia | Alfredo | UAB | Scientist, Paleoceanogr. |
| Meheust | Marie | AWI | Scientist, Paleoceanogr. |
| Nowka | Daniela | AWI | Student, Paleoceanogr. |
| Pahnke | Katharina | UH | Scientist, Paleoceanogr. |
| Reichelt | Lucia | GeoB | Scientist, Geomag/Phys.prop. |
| Rentsch | Harald | DWD | Scientist, Meteorology |
| Rhee | Tae Siek | KOPRI | Scientist, Chemistry |
| Rueda | Gemma | UAB | Scientist, Paleoceanogr. |
| Saavedra-Pellitero | Mariem | USAL | Scientist, Paleoceanogr. |
| Schaper | Timo | AWI | Student, Seismics/Geology |
| Schnieders | Jana | AWI | Student, Oceanography |
| Schulze | Ina | AWI | Student, Seismics/Geology |
| Seidel | Hartmut | AWI | Student, Bathymetry |
| Steph | Silke | AWI | Scientist, Paleoceanogr. |
| Straub | Marietta | ETH | Scientist, Paleoceanogr. |
| Zepick | Burkhard | HeliTransair | Helicopter pilot |

## A.3 SCHIFFSBESATZUNG / SHIP‘S CREW

| Name | Rank |
|---|---|
| Schwarze, Stefan | Master |
| Ettlin, Margrith | 1. Offc. |
| Krohn, Günther | Ch. Eng. |
| Fallei, Holger | 2. Offc. |
| Ritter, Michael | 2. Offc. |
| Dugge, Heike | 3. Offc. |
| Türke, Helmut | Doctor |
| Hecht, Andreas | R. Offc. |
| Minzlaff, Hans-Ulrich | 2. Eng. |
| Sümnicht, Stefan | 2. Eng. |
| Schaefer, Marc | 2. Eng. |
| Scholz, Manfred | Elec. Eng. |
| Fröb, Martin | ELO |
| Himmel, Frank | ELO |
| Schulz, Harry | ELO |
| Winter, Andreas | ELO |
| Loidl, Reiner | Boatsw. |
| Lutz, Reise | Carpenter |
| Bäcker, Andreas | A.B. |
| Brickmann, Peter | A.B. |
| Guse, Hartmut | A.B. |
| Hagemann, Manfred | A.B. |
| Pousada Martinez, S. | A.B. |
| Scheel, Sebastian | A.B. |
| Schmidt, Uwe | A.B. |
| Wende, Uwe | A.B. |
| Winkler, Michael | A.B. |
| Preußner, Jörg | Storek. |
| Elsner, Klaus | Mot-man |
| Pinske, Lutz | Mot-man |
| Schütt, Norbert | Mot-man |
| Teichert, Uwe | Mot-man |
| Voy, Bernd | Mot-man |
| Müller-Homburg, R.-D. | Cook |
| Martens, Michael | Cooksmate |
| Silinski, Frank | Cooksmate |
| Jürgens, Monika | 1. Stwdess |
| Wöckener, Martina | Stwdess/N. |
| Czyborra, Bärbel | 2. Stwdess |
| Gaude, Hans-Jürgen | 2. Steward |
| Silinksi, Carmen | 2. Stwdess |
| Huang, Wu-Mei | 2. Steward |
| Möller, Wolfgang | 2. Steward |
| Yu, Kwok Yuen | Laundrym. |
| Apel, Rodney | Trainee |

## A. 4 STATION LIST PS 75

| Station No. | Gear No. | Date (UTC) | Start (UTC) | at seafl. at depth (UTC) | End (UTC) | Latitude (deg/min) | Longitude (deg/min) | Area | HS-water depth (m) | Rope length (m) | Gear | Depth inter-vall (m) | Core re-covery (m) | Remarks |
|---|---|---|---|---|---|---|---|---|---|---|---|---|---|---|
| **PS75/034** | -1 | 29.11.09 | 16:07 | 17:12 | 18:04 | 54°22.112'S | 80°05.380'W | Mornington Abyssal Plain | 4450 | 4433 | MUC | | 12x (0.37-0.41) | |
| | -2 | 29.11.09 | 18:57 | 20:23 | 21:50 | 54°22.120'S | 80°05.400'W | | 4436 | 4386 | KOL (20m) | | **18.08** | **TC 0.92m,** liner imploded between 10-15m |
| | -3 | 29.-30. 11.09 | 22:10 | 23:44 | 01:06 | 54°22.111'S | 80°05.187'W | | 4436 | 4473 | CTD+ROS +FLU | to bottom | | fluorometer failed |
| **PS75/035** | -1 | 01.12.09 | 20:08 | 21:43 | 23:34 | 57°46.166'S | 90°40.019'W | Freeden Smt./Eltanin impact | 5105 | 5191 | KOL (25m) | | **22.53** | **TC 0.91m** |
| **PS75/036** | -1 | 02.12.09 | 01:14 | 03:03 | 04:42 | 57°44.445'S | 90°43.56'W | Freeden Smt./Eltanin impact | 5202 | 5279 | KOL (25m) | | **22.74** | **TC 0.52m** |
| **PS75/037** | -1 | 02.12.09 | 16:21 | 17:45 | 19:26 | 57°46.540'S | 91°24.689'W | Freeden Smt./Eltanin impact | 4879 | 4816 | KOL (25m) | | **22.73** | **TC 0.87m** |
| **PS75/038** | -1 | 02-03. 12.09 | 21:58 | 23:15 | 00:42 | 57°51.70'S | 91°06.84'W | Freeden Smt./Eltanin impact | 4228 | 4152 | KOL (25m) | | **21.83** | **TC 1.0 m** |
| **PS75/039** | -1 | 03.12.09 | 05:55 | 07:39 | 09:12 | 57°39.98'S | 90°51.76'W | Freeden Smt./Eltanin impact | 5231 | 5177 | KOL (25m) | | **22.15** | **TC 0.53m** |
| **PS75/040** | -1 | 03.12.09 | 13:00 | 14:00 | 15:57 | 57°38.88'S | 91°09.14'W | Freeden Smt./Eltanin impact | 3400 | 3336 | KOL (25m) | | **9.36** | **TC 0.93m**, upper 5 cm of core lost, 18 cm of water between sections 836-736 and 736-655, core barrel bent at 9-14 and 14-19 m |
| | -2 | | 17:13 | 17:28 | 17:42 | 57°38.681'S | 91°08.293W | | | | CTD+ROS +FLU | 0- 500 m | | |
| | -3 | | 18:04 | | | 57°28.427'S | 91°07.803'W | | | | MN | | | MN aborted at 18:10, display not working |
| **PS75/041** | -1 | 03.-04. 12.09 | 22:00 | | | 57°14.74'S | 90°56.39'W | Freeden Smt./Eltanin impact | 5305 | | SEIS REFL | | | Begin deployment of 600 m-streamer |

| Station No. | Gear No. | Date (UTC) | Start (UTC) | at seafl. at depth (UTC) | End (UTC) | Latitude (deg/min) | Longitude (deg/min) | Area | HS-water depth (m) | Rope length (m) | Gear | Depth inter-vall (m) | Core re-covery (m) | Remarks |
|---|---|---|---|---|---|---|---|---|---|---|---|---|---|---|
| PS75/041 | -1 | | | | 22:36 | 57°16.62'S | 90°55.63'W | Freeden Smt./Eltanin impact | 5334 | | SEIS REFL | | | End of deployment of streamer and GI-airgun cluster |
| | | | 22:53 | | | 57°17.30'S | 90°54.50'W | | 5334 | | SEIS REFL | | | Begin of profile 2010 0001, course altered by 1° at 0:00 |
| | | | | | 01:00 | 57°28.10'S | 90°43.80'W | | 5140 | | SEIS REFL | | | Data acquisition stopped due to tape drive misfunction |
| | | | 01:00 | | 02:40 | | | | | | SEIS REFL | | | Repair tape drive and return to last profile position |
| | | | 02:40 | | | 57°28.02'S | 90°43.92'W | | 5148 | | SEIS REFL | | | Cont. profile 2010 0001, further tape drive problems, only 3 minutes of data |
| | | | 03:56 | | | 57°34.00'S | 90°38.00'W | | 5020 | | SEIS REFL | | | Cont. profile 2010 0001 |
| | | | | | 04:10 | 57°35.19'S | 90°36.91'W | | 5010 | | SEIS REFL | | | End of profile 2010 0001 |
| | | | 04:29 | | | 57°35.00'S | 90°36.77'W | | 5013 | | SEIS REFL | | | Begin of profile 2010 0002 |
| | | | | | 06:15 | 57°39.98'S | 90°51.66'W | | 5215 | | SEIS REFL | | | End of profile 2010 0002 |
| | | | 06:40 | | | 57°39.98'S | 90°51.84'W | | 5220 | | SEIS REFL | | | Begin of profile 2010 0003 |
| | | | | | 07:54 | 57°44.47'S | 90°43.61'W | | 5337 | | SEIS REFL | | | End of profile 2010 0003 |
| | | | 08:22 | | | 57°44.65'S | 90°43.68'W | | 5337 | | SEIS REFL | | | Begin of profile 2010 0004 |
| | | | | | 10:35 | 57°51.40'S | 90°57.50'W | | 3529 | | SEIS REFL | | | Data acquisition stopped due to tape drive misfunction |
| | | | | | 10:57 | 57°52.50'S | 90°59.00'W | | 3684 | | SEIS REFL | | | Further tape drive problems, only 8 minutes of data |

| Station No. | Gear No. | Date (UTC) | Start (UTC) | at seafl. at depth (UTC) | End (UTC) | Latitude (deg/min) | Longitude (deg/min) | Area | HS-water depth (m) | Rope length (m) | Gear | Depth inter-vall (m) | Core re-covery (m) | Remarks |
|---|---|---|---|---|---|---|---|---|---|---|---|---|---|---|
| **PS75/ 041** | -1 | | 10:57 | | 12:56 | | | Freeden Smt./Eltanin impact | | | SEIS REFL | | | Repair tape drive and return to profile position from 10:35 |
| | | | 12:56 | | | 57°51.75'S | 90°57.75'W | | 3562 | | SEIS REFL | | | Cont. profile 2010 0004, further tape drive problems, no data |
| | | | 13:21 | | | 57°53.05'S | 91°0.20'W | | 3661 | | SEIS REFL | | | Cont. profile 2010 0004 |
| | | | | | 13:57 | 57°54.90'S | 91°3.75'W | | 3884 | | SEIS REFL | | | Data acquisition stopped due to tape drive misfunction |
| | | | | | 14:26 | 57°56.51'S | 91°6.93'W | | 4306 | | SEIS REFL | | | End of profile 2010 0004, no further data acquired |
| | | | 15:15 | | | 57°56.52'S | 91°6.93'W | | 4336 | | SEIS REFL | | | Begin of profile 2010 0005 |
| | | | | | 15:24 | 57°55.73'S | 91°6.84'W | | 4259 | | SEIS REFL | | | Stop profile 2010 0005 due to tape drive failure, no data |
| | | | 15:24 | | 16:16 | | | | | | SEIS REFL | | | Return to begin of profile |
| | | | 16:16 | | | 57°56.62'S | 91°6.95'W | | 4342 | | SEIS REFL | | | Begin of profile 2010 0005 again |
| | | | | | 17:55 | 57°48.99'S | 91°6.85'W | | 4360 | | SEIS REFL | | | End of profile 2010 0005, no data acquired due to tape drive misfunction |
| | | | 18:36 | | | 57°48.95'S | 91°6.90'W | | 4363 | | SEIS REFL | | | Begin of profile 2010 0006 |
| | | | | | 19:00 | 57°48.95'S | 91°10.14'W | | 4563 | | SEIS REFL | | | Stop profile 2010 0006 due to tape drive failure, no data |
| | | | | | 19:11 | 57°48.75'S | 91°11.20'W | | 4281 | | SEIS REFL | | | Airgun on deck |
| | | | | | 19:36 | 57°48.75'S | 91°12.28'W | | 4416 | | SEIS REFL | | | Streamer recovered |

| Station No. | Gear No. | Date (UTC) | Start (UTC) | at seafl. at depth (UTC) | End (UTC) | Latitude (deg/min) | Longitude (deg/min) | Area | HS-water depth (m) | Rope length (m) | Gear | Depth inter-vall (m) | Core re-covery (m) | Remarks |
|---|---|---|---|---|---|---|---|---|---|---|---|---|---|---|
| **PS75/042** | -1 | 04.-05.12.09 | 22:55 | 00:27 | 01:59 | 57°43.41'S | 91°42.77'W | Freeden Smt./Eltanin impact | 4917 | 4850 | KOL (25 m) | | **23.54** | **TC 1.0m** |
| **PS75/043** | -1 | 05.12.09 | 04:15 | 05:45 | 07:18 | 57°42.01'S | 91°58.75'W | Freeden Smt./Eltanin impact | 4619 | 4567 | KOL (25 m) | | **23.48** | **TC 0.82m** |
| **PS75/044** | -1 | 06.12.09 | 03:37 | 05:11 | 06:48 | 56°5.188'S | 96°46.559'W | Mornington Abyssal Plain | 5013 | 5001 | CTD+ROS +FLU | to bottom | | |
| | -2 | | 06:59 | 07:17 | 07:55 | 56°5.177'S | 96°46.756'W | | 4989 | 500 | MN | 0-500m | | |
| | -3 | | 08:05 | 09:21 | 10:27 | 56°5.142'S | 96°46.821'W | | 5011 | 5043 | MUC | | 1x (0.03) | |
| | -4 | | 11:13 | 12:46 | 14:20 | 56°05.15'S | 96°46.82'W | | 5000 | 4887 | KOL (25m) | | **20.93** | **TC 0.33m** |
| **PS75/045** | -1 | 07.12.09 | 01:17 | 01:30 | 01:41 | 54°52.203'S | 98°29.776'W | Mornington Abyssal Plain | 531 | 541 | MUC | | 1x (0.2) | |
| **PS75/046** | -1 | 07.-08.12.09 | 19:59 | 20:39 | 21:21 | 54°24.919'S | 102°30.209'W | southeastern East Pacific Rise | 2984 | 2965 | MUC | | 6x (0.07-0.14) | winch malfunction |
| | -2 | | 22:02 | 23:12 | 00:18 | 54°24.92'S | 102°30.22'W | | 2984 | 2930 | KOL (20m) | | **17.26** | **TC 0.17m** |
| **PS75/047** | -1 | 08.12.09 | 04:27 | 06:03 | 07:14 | 54°20.771'S | 102°44.82'W | southeastern East Pacific Rise | 4480 | 4429 | KOL (25m) | | **22.98** | **TC 0.83m** |
| **PS75/048** | -1 | 08.12.09 | 08:30 | 10:11 | 11:43 | 54°20.35'S | 102°45.51'W | southeastern East Pacific Rise | 4516 | 4422 | KOL (25m) | | **19.88** | **TC 0.87m** |
| **PS75/049** | -1 | 08.12.09 | 12:56 | 13:56 | 14:53 | 54°20.79'S | 102°44.82'W | southeastern East Pacific Rise | 4482 | 4477 | MUC | | 11x (29.5-39.5) | |
| **PS75/050** | -1 | 08.12.09 | 17:01 | | | 54°23.17'S | 102°35.97'W | southeastern East Pacific Rise | 3295 | | SEIS REFL | | | Begin deployment of 600 m-Streamer |
| | | | | | 17:34 | 54°22.93'S | 102°38.76'W | | 3989 | | SEIS REFL | | | End of deployment of Streamer and GI-Airgun Cluster |
| | | | 18:00 | | | 54°22.57'S | 102°41.87'W | | 4560 | | SEIS REFL | | | Begin of profile 2010 0007 |

| Station No. | Gear No. | Date (UTC) | Start (UTC) | at seafl. at depth (UTC) | End (UTC) | Latitude (deg/min) | Longitude (deg/min) | Area | HS-water depth (m) | Rope length (m) | Gear | Depth inter-vall (m) | Core re-covery (m) | Remarks |
|---|---|---|---|---|---|---|---|---|---|---|---|---|---|---|
| **PS75/ 050** | -1 | | | | 19:09 | 54°18.20'S | 102°49.11'W | southeastern East Pacific Rise | 4396 | | SEIS REFL | | | End of profile 2010 0007 |
| | | | 20:14 | | | 54°18.09'S | 102°42.70'W | | 4494 | | SEIS REFL | | | Begin of profile 2010 0008 |
| | | | | | 21:23 | 54°23.67'S | 102°47.12'W | | 4511 | | SEIS REFL | | | End of profile 2010 0008 |
| | | | | | 21:35 | 54°23.71'S | 102°48.16'W | | 4527 | | SEIS REFL | | | Airgun on deck |
| | | | | | 22:00 | 54°23.04'S | 102°50.20'W | | 4463 | | SEIS REFL | | | Streamer recovered |
| **PS75/ 051** | -1 | 09.-10. 12.09 | 20:50 | 22:02 | 23:25 | 52°48.73'S | 107°48.33'W | southeastern East Pacific Rise | 3949 | 3920 | KOL (25m) | | **18.73** | **TC 1.01m** |
| | -2 | | 23:53 | 00:45 | 01:36 | 52°48.738'S | 107°48.307'W | | 3977 | 3962 | MUC | | 12x (21-47) | |
| **PS75/ 052** | -1 | 12.12.09 | 05:02 | 06:36 | 08:12 | 60°45.871'S | 115°57.955'W | northern Amundsen Abyssal Plain | 5121 | 5186 | CTD+ROS +FLU | to bottom | | |
| | -2 | | 08:22 | 09:03 | 10:02 | 60°45.810'S | 115°57.503'W | | 5121 | 1000 | MN | 0-1000m | | |
| | -3 | | 10:33 | 12:16 | 14:04 | 60°45.12'S | 115°58.74'W | | 5130 | 5063 | KOL (30m) | | **23.17** | **TC 0.41m** |
| **PS75/ 053** | -1 | 12.12.09 | 17:40 | 18:45 | 19:47 | 60°46.152'S | 115°58.792'W | northern Amundsen Abyssal Plain | 5132 | 5115 | MUC | | 11x (19-36) | |
| **PS75/ 054** | -1 | 13.-14. 12.09 | 22:52 | 00:14 | 01:35 | 56°09.105'S | 115°07.982'W | southeastern East Pacific Rise | 4113 | 4083 | KOL (30m) | | **22.38** | **TC 0.91m** |
| | -2 | | 02:15 | 03:36 | 04:48 | 56°09.085'S | 115°07.953'W | | 4119 | 4120 | CTD+ROS +FLU | to bottom | | Data used for Hydrosweep calibration at 06:00 |
| | -3 | | 04:55 | 05:33 | 06:29 | 56°09.106'S | 115°07.863'W | | 4117 | 1000 | MN | 0-1000m | | |
| | -4 | | 06:40 | 07:29 | 08:24 | 56°09.139'S | 115°08.025'W | | 4085 | 4081 | MUC | | 0 | all tubes empty due to outflow |

| Station No. | Gear No. | Date (UTC) | Start (UTC) | at seafl. at depth (UTC) | End (UTC) | Latitude (deg/min) | Longitude (deg/min) | Area | HS-water depth (m) | Rope length (m) | Gear | Depth inter-vall (m) | Core re-covery (m) | Remarks |
|---|---|---|---|---|---|---|---|---|---|---|---|---|---|---|
| **PS75/ 054** | -5 | | | | 09:30 | 56° 3.60' S | 114° 59.31' W | southeastern East Pacific Rise | 3992 | | SEIS REFL | | | Streamer and GI-airgun cluster deployed |
| | | | 10:20 | | | 56° 6.11' S | 115° 2.88' W | | 4128 | | SEIS REFL | | | Begin of profile 2010 0011 |
| | | | | | 11:56 | 56° 11.78' S | 115° 12.66' W | | 4089 | | SEIS REFL | | | End of profile 2010 0011 |
| | | | 12:32 | | | 56° 11.83' S | 115° 12.57' W | | 4094 | | SEIS REFL | | | Begin of profile 2010 0012 |
| | | | | | 13:36 | 56° 11.93' S | 115° 2.87' W | | 3812 | | SEIS REFL | | | End of profile 2010 0012 |
| | | | 14:19 | | | 56° 11.91' S | 115° 2.78' W | | 3867 | | SEIS REFL | | | Begin of profile 2010 0013 |
| | | | | | 15:48 | 56° 6.41' S | 115° 13.00' W | | 3571 | | SEIS REFL | | | End of profile 2010 0013 |
| | | | | | 16:02 | 56° 5.96' S | 115° 14.37' W | | 3512 | | SEIS REFL | | | Airgun on deck |
| | | | | | 16:16 | 56° 6.31' S | 115° 15.03' W | | 3571 | | SEIS REFL | | | Streamer recovered |
| **PS75/ 055** | -1 | 14.-15. 12.09 | 23:36 | 00:22 | 01:12 | 55°09.363'S | 114°47.916'W | southeastern East Pacific Rise | 3599 | 3602 | MUC | | 2x(12-17) | MUC not fully functional |
| **PS75/ 056** | -1 | 15.12.09 | 02:30 | 03:15 | 04:04 | 55°09.74'S | 114°47.31'W | southeastern East Pacific Rise | 3581 | 3587 | SL | | **10.21** | |
| **PS75/ 057** | -1 | 15.-16. 12.09 | 23:48 | 24:51:00 | 01:42 | 53°31.782'S | 118°53.782'W | southern East Pacific Rise | 2908 | 2938 | CTD+ROS +FLU | to bottom | | |
| | -2 | | 01:51 | 02:28 | 03:26 | 53°31.629'S | 118°54.523'W | | 2927 | 1000 | MN | 0-1000m | | |
| | -3 | | 04:18 | 05:13 | 06:20 | 53°31.983'S | 118°54.984'W | | 2888 | 2856 | KOL (20m) | | **18.12** | **TC 0.92m** |
| | -4 | | 06:54 | 07:30 | 08:13 | 53°31.967'S | 118°55.03'W | | 2897 | 2898 | MUC | | 0 | |

| Station No. | Gear No. | Date (UTC) | Start (UTC) | at seafl. at depth (UTC) | End (UTC) | Latitude (deg/min) | Longitude (deg/min) | Area | HS-water depth (m) | Rope length (m) | Gear | Depth inter-vall (m) | Core re-covery (m) | Remarks |
|---|---|---|---|---|---|---|---|---|---|---|---|---|---|---|
| **PS75/ 058** | -1 | 17.-18. 12.09 | 16:18 | 17:36 | 18:45 | 54°12.947'S | 125°26.187'W | southwestern East Pacific Rise | 3637 | 3639 | CTD+ROS +FLU | to bottom | | |
| | -2 | | 19:18 | 20:25 | 21:49 | 54°12.86'S | 125°26.20'W | | 3629 | 3568 | KOL (25m) | | **12.96** | **TC 0.93m** (surface missing), core bent between 12-16m |
| **PS75/ 059** | -1 | 17.-18. 12.09 | 23:18 | 23:59 | 00:49 | 54°12.773'S | 125°25.520'W | southwestern East Pacific Rise | 3638 | 3618 | MUC | | 0 | |
| | -2 | | 01:14 | 02:30 | 03:52 | 54°12.90'S | 125°25.53'W | | 3613 | 3579 | KOL (20m) | | **13.98** | **TC 0.90m**, core bent between 12-15m |
| **PS75/ 060** | -1 | 18.12.09 | 05:36 | | | 54° 4.71' S | 125° 18.80' W | southwestern East Pacific Rise | 3689 | | SEIS REFL | | | Begin deployment of 600 m-streamer |
| | | | | 05:50 | | 54° 5.53' S | 125° 19.88' W | | 3680 | | SEIS REFL | | | Streamer and GI-airgun cluster deployed |
| | | | 06:37 | | | 54° 8.78' S | 125° 23.23' W | | 3746 | | SEIS REFL | | | Begin of profile 2010 0014 |
| | | | | 08:13 | | 54° 16.64' S | 125° 27.85' W | | 3572 | | SEIS REFL | | | End of profile 2010 0014 |
| | | | 08:38 | | | 54° 16.53' S | 125° 28.12' W | | 3556 | | SEIS REFL | | | Begin of profile 2010 0015 |
| | | | | 09:53 | | 54° 14.12' S | 125° 19.12' W | | 3541 | | SEIS REFL | | | End of profile 2010 0015 |
| | | | 10:33 | | | 54° 14.11' S | 125° 18.79' W | | 3552 | | SEIS REFL | | | Begin of profile 2010 0016 |
| | | | | 11:59 | | 54° 11.45' S | 125° 32.17' W | | 3578 | | SEIS REFL | | | End of profile 2010 0016 |
| | | | | 12:07 | | 54° 11.37' S | 125° 33.35' W | | 3638 | | SEIS REFL | | | Airgun on deck |
| | | | | 12:26 | | 54° 12.00' S | 125° 35.00' W | | 3676 | | SEIS REFL | | | Streamer recovered |
| **PS75/ 061** | -1 | 20.-21. 12.09 | 19:07 | 20:29 | 21:35 | 57°11.973'S | 135°23.206'W | North of Udintsev Fracture Zone | 3296 | 3340 | CTD+ROS +FLU | to bottom | | |

| Station No. | Gear No. | Date (UTC) | Start (UTC) | at seafl. at depth (UTC) | End (UTC) | Latitude (deg/min) | Longitude (deg/min) | Area | HS-water depth (m) | Rope length (m) | Gear | Depth inter-vall (m) | Core re-covery (m) | Remarks |
|---|---|---|---|---|---|---|---|---|---|---|---|---|---|---|
| **PS75/ 061** | -2 | | 21:44 | 22:20 | 23:26 | 57°10.598'S | 135°22.897'W | North of Udintsev Fracture Zone | 3480 | 1000 | MN | 0-1000m | | |
| | -3 | | 00:11 | 00:57 | 01:51 | 57°12.95'S | 135°23.30'W | | 3091 | 3177 | MUC | | 0 | 2 kn ship speed over ground results in failure of sediment recovery |
| **PS75/ 062** | -1 | 21.12.09 | 10:05 | 11:00 | 11:52 | 58°16.62'S | 135°37.55'W | South of Udintsev Fracture Zone | 4147 | 4174 | MUC | | 7x (20-21) | |
| | -2 | | 12:43 | 14:06 | 15:34 | 58°16.60'S | 135°37.61'W | | 4165 | 4099 | KOL (25m) | | **21.09** | **TC 0.66m** |
| **PS75/ 063** | -1 | 21.-22. 12.09 | 22:44 | 23:59 | 01:16 | 58°54.24'S | 135°37.23'W | South of Udintsev Fracture Zone | 3795 | 3736 | KOL (25m) | | **22.46** | **TC 0.67m** |
| | -2 | | 01:49 | 02:37 | 03:26 | 58°54.251'S | 135°37.246'W | | 3790 | 3775 | MUC | | 6x (21-32) | |
| | -3 | | 03:38 | 04:53 | 06:03 | 58°54.223'S | 135°37.242'W | | 3793 | 3816 | CTD+ROS +FLU | to bottom | | |
| | -4 | | 06:12 | 06:47 | 07:50 | 58°54.207'S | 135°36.824'W | | 3784 | 1000 | MN | 0-1000m | | |
| **PS75/ 064** | -1 | 23.12.09 | 01:20 | 02:55 | 04:16 | 61°00.74'S | 139°27.85'W | western Amundsen Abyssal Plain | 4600 | 4552 | KOL (20m) | | **15.43** | **TC 0.27m**, liner pushed into lower 40 cm of segment 4.86-5.60 m |
| | -2 | | 04:42 | 05:42 | 06:38 | 61°00.749'S | 139°27.788'W | | 4595 | 4588 | MUC | | 2x (28-28.5) | |
| | -3 | | 06:45 | 08:17 | 09:39 | 61°01.173'S | 139°27.635'W | | 4642 | 4682 | CTD+ROS +FLU | to bottom | | |
| | -4 | | 09:45 | 10:21 | 11:16 | 61°01.393'S | 139°26.782'W | | 4596 | 1000 | MN | 0-1000m | | |
| **PS75/ 065** | -1 | 24.12.09 | 01:14 | 02:43 | 04:07 | 62°36.21'S | 141°30.90'W | western Amundsen Abyssal Plain | 4499 | 4451 | KOL (20m) | | **18.6** | **TC 0.67m** |
| | -2 | | 04:28 | 05:27 | 06:24 | 62°36.232'S | 141°30.914'W | | 4488 | 4498 | MUC | | 9x(22-28.5) | |
| | -3 | | 06:24 | 07:59 | 09:18 | 62°36.099'S | 141°30.878'W | | 4492 | 4548 | CTD+ROS +FLU | to bottom | | |
| **PS75/ 065** | -4 | | 09:24 | 10:00 | 11:01 | 62°36.161'S | 141°31.065'W | western Amundsen Abyssal Plain | 4484 | 1000 | MN | 0-1000m | | |
| **PS75/ 066** | -1 | 24.-25. 12.09 | 19:54 | | 19:26 | | | western Amundsen Abyssal Plain | | | HS/ PS | | | Bathymetric/echo-sounding survey |

| Station No. | Gear No. | Date (UTC) | Start (UTC) | at seafl. at depth (UTC) | End (UTC) | Latitude (deg/min) | Longitude (deg/min) | Area | HS-water depth (m) | Rope length (m) | Gear | Depth inter-vall (m) | Core re-covery (m) | Remarks |
|---|---|---|---|---|---|---|---|---|---|---|---|---|---|---|
| **PS75/ 067** | -1 | 25.-26. 12.09 | 23:52 | 01:08 | 02:30 | 64°58.23'S | 143°48.22'W | western Amundsen Abyssal Plain | 4151 | 4116 | KOL (20m) | | **17.95** | **TC 0.82m** |
| | -2 | | 02:45 | 03:40 | 04:34 | 64°58.253'S | 143°48.213'W | | 4153 | 4155 | MUC | | 6x (29-34) | |
| | -3 | | 04:39 | 06:02 | 07:15 | 64°58.252'S | 14348.151'W | | 4155 | 4208 | CTD+ROS +FLU | to bottom | | |
| | -4 | | 07:20 | 07:56 | 08:59 | 64°58.218'S | 143°48.265'W | | 4160 | 1000 | MN | 0-1000m | | |
| **PS75/ 068** | -1 | 26.12.09 | 10:04 | 10:47 | 11:38 | 64°56.007'S | 144°06.890'W | western Amundsen Abyssal Plain | 3727 | 3722 | MUC | | 5x (32-35) | |
| | -2 | | 12:10 | 13:26 | 14:43 | 64°56.01'S | 144°06.81'W | | 3728 | 3678 | KOL (25m) | | **14.12** | **TC 0.91m** |
| **PS75/ 069** | -1 | 27.12.09 | 12:22 | 13:48 | 15:14 | 62°12.24'S | 145°37.11'W | northeastern Pacific-Antarctic Ridge | 4334 | 4283 | KOL (20m) | | **18.46** | **TC 0.65m** |
| | -2 | | 15:26 | 16:24 | 17:17 | 62°12.329'S | 145°37.157'W | | 4328 | 4321 | MUC | | 7x (25-30.5) | |
| **PS75/ 070** | -1 | 28.12.09 | 18:08 | 18:45 | 19:21 | 58°34.886'S | 150°03.946'W | Pacific-Antarctic Ridge | 2839 | 2846 | MUC | | 10x (26-29) | |
| | -2 | | 19:46 | 20:46 | 21:36 | 58°34.87'S | 150°03.97'W | | 2842 | 2816 | KOL (15m) | | 0 | **TC 0.90m**, core tubes lost at seafloor |
| | -3 | | 21:59 | 22:56 | 23:53 | 58°34.847'S | 150°03.920'W | | 2846 | 2847 | CTD+ROS +FLU | | to bottom | |
| **PS75/ 071** | -1 | 29.12.09 | 06:17 | 06:56 | 07:34 | 57°52.381'S | 150°52.095'W | northwestern Pacific-Antarctic Ridge | 2925 | 2929 | MUC | | 0 | |
| | -2 | | 08:09 | 09:12 | 10:21 | 57°52.40'S | 150°52.11'W | | 2926 | 2883 | KOL (20m) | | **11.36** | **TC 0.95m**, core bent around 9 m |
| **PS75/ 072** | -1 | 29.12.09 | 13:58 | 15:06 | 16:08 | 57°33.517'S | 151°12.922'W | northwestern Pacific-Antarctic Ridge | 3111 | 3136 | CTD+ROS +FLU | to bottom | | |
| | -2 | | 16:21 | 17:28 | 18:38 | 57°33.51'S | 151°13.11'W | | 3098 | 3066 | KOL (20m) | | **14.97** | **TC 0.50m** |
| | -3 | | 18:55 | 19:30 | 20:15 | 57°33.593'S | 151°13.159'W | | 3096 | 3105 | MUC | | 11x (25-32) | |
| | -4 | | 21:12 | 21:50 | 22:36 | 57°33.51'S | 151°13.17'W | | 3099 | 3098 | SL (13m) | | **9.61** | |

| Station No. | Gear No. | Date (UTC) | Start (UTC) | at seafl. at depth (UTC) | End (UTC) | Latitude (deg/min) | Longitude (deg/min) | Area | HS-water depth (m) | Rope length (m) | Gear | Depth inter-vall (m) | Core re-covery (m) | Remarks |
|---|---|---|---|---|---|---|---|---|---|---|---|---|---|---|
| **PS75/073** | -1 | 30.12.09 | 03:18 | 04:24 | 05:30 | 57°12.26'S | 151°36.63'W | northwestern Pacific-Antarctic Ridge | 3238 | 3193 | KOL (25m) | | **17.04** | **TC 0.68m** |
| | -2 | | 07:44 | 08:24 | 09:15 | 57°12.26'S | 151°36.65'W | | 3234 | 3224 | KAL (12m) | | **3.68** | Serie 1A 3.68m, Serie 1B 3.71m, Serie 2A 3.68m, Serie 3 3.68m |
| **PS75/074** | -1 | 30.-31. 12.09 | 17:46 | 18:30 | 19:12 | 56°14.67'S | 152°39.29'W | northwestern Pacific-Antarctic Ridge | 3318 | 3298 | MUC | | 6x (23-25.5) | |
| | -2 | | 19:35 | 20:43 | 21:42 | 56°14.673'S | 152°39.263'W | | 3318 | 3327 | CTD+ROS +FLU | to bottom | | |
| | -3 | | 21:51 | 23:00 | 00:16 | 56°14.65'S | 152°39.30'W | | 3295 | 3255 | KOL (25 m) | | **20.95** | **TC 0.54m** |
| **PS75/075** | -1 | 31.12.09-01.01.10 | 16:50 | 18:18 | 19:27 | 54°24.256'S | 154°35.184'W | northwestern Pacific-Antarctic Ridge | 4127 | 4140 | CTD+ROS +FLU | to bottom | | |
| | -2 | | 19:34 | 20:21 | 21:20 | 54°24.206'S | 154°35.215'W | | 4106 | 4099 | MUC | | 0 | |
| | -3 | | 21:47 | 23:07 | 00:27 | 54°24.23'S | 154°35.18'W | | 4096 | 4059 | KOL (25m) | | **18.35** | **TC 0.92m** (top missing), upper 2.27 m of core imploded and disturbed |
| **PS75/076** | -1 | 01.01.10 | 10:21 | 11:11 | 11:57 | 55°31.708'S | 156°08.469'W | northwestern Pacific-Antarctic Ridge | 3745 | 3737 | MUC | | 12x (30-32) | |
| | -2 | | 12:46 | 13:59 | 15:13 | 55°31.71'S | 156°08.39'W | | 3742 | 3696 | KOL (25m) | | **20.59** | **TC 0.65m** |
| **PS75/077** | -1 | 01.-02. 01.10 | 23:38 | 00:30 | 01:23 | 56°46.088'S | 156°46.837'W | northwestern Pacific-Antarctic Ridge | 4101 | 4082 | MUC | | 0 | |
| **PS75/078** | -1 | 03.01.10 | 00:56 | 01:32 | 02:15 | 61°03.00'S | 159°35.175'W | northwestern Pacific-Antarctic Ridge | 3315 | 3305 | SL (15m) | | **3.83** | |
| | -2 | | 02:47 | 03:38 | 04:24 | 61°03.00'S | 159°35.15'W | | 3335 | 3306 | GKG | | 0 | |
| | -3 | | 04:54 | 05:36 | 06:18 | 61°03.012'S | 159°35.195'W | | 3336 | 3323 | MUC | | 0 | |

| Station No. | Gear No. | Date (UTC) | Start (UTC) | at seafl. at depth (UTC) | End (UTC) | Latitude (deg/min) | Longitude (deg/min) | Area | HS-water depth (m) | Rope length (m) | Gear | Depth inter-vall (m) | Core re-covery (m) | Remarks |
|---|---|---|---|---|---|---|---|---|---|---|---|---|---|---|
| **PS75/079** | -1 | 04.01.10 | 15:43 | 16:26 | 17:23 | 57°30.145'S | 157°14.256'W | northwestern Pacific-Antarctic Ridge | 3776 | 3776 | MUC | | 0 | |
| | -2 | | 17:44 | 18:59 | 20:28 | 57°30.16'S | 157°14.25'W | | 3770 | 3814 | KOL (20m) | | **18.51** | **TC 0.67m** |
| **PS75/080** | -1 | 05.01.10 | 01:38 | 02:44 | 05:35 | 58°10.63'S | 157°38.19'W | northwestern Pacific-Antarctic Ridge | 3874 | 3798 | KOL (25m) | | **12.20** | **TC 0.89m**, core bent between 10-15m |
| | -2 | | 04:32 | 05:22 | 06:14 | 58°10.645'S | 157°38.190'W | | 3870 | 3845 | MUC | | 11x (17-28) | |
| **PS75/081** | -1 | 05.01.10 | 07:22 | 08:45 | 10:00 | 58°14.486'S | 157°42.44'W | northwestern Pacific-Antarctic Ridge | 3857 | 3797 | KOL (20m) | | **13.71** | **TC 0.97m** (TC surface disturbed), liner imploded around 4.7 m, no significant core disturbance |
| **PS75/082** | -1 | 05.01.10 | 15:18 | 16:38 | 17:58 | 59°02.48'S | 158°21.82'W | northwestern Pacific-Antarctic Ridge | 4000 | 3934 | KOL (20m) | | **10.88** | **TC 0.89m** |
| | -2 | | 18:11 | 19:04 | 19:55 | 59°02.501'S | 158°21.839'W | | 4004 | 3981 | MUC | | 12x (21-27.5) | |
| **PS75/083** | -1 | 06.01.10 | 04:39 | 05:55 | 07:06 | 60°16.13'S | 159°03.59'W | northwestern Pacific-Antarctic Ridge | 3599 | 3526 | KOL (15m) | | **13.13** | **TC 0.37m** |
| | -2 | | 07:23 | 08:11 | 08:58 | 60°16.138'S | 159°03.589'W | | 3600 | 3559 | MUC | | 0 | 1 MUC arm broken, winch malfunction |
| **PS75/084** | -1 | 06.01.10 | 15:33 | 16:18 | 17:00 | 61°02.986'S | 159°35.193'W | northwestern Pacific-Antarctic Ridge | 3313 | 3310 | MUC | | 10x (24.5-31.5) | |
| **PS75/085** | -1 | 07.01.10 | 00:18 | 01:33 | 02:45 | 61°56.38'S | 160°07.10'W | northern Pacific-Antarctic Ridge | 3734 | 3657 | KOL (25m) | | **19.74** | TC empty |
| | -2 | | 03:18 | 04:09 | 04:57 | 61°56.362'S | 160°07.151'W | | 3724 | 3700 | MUC | | 11x (12.5-29) | |

| Station No. | Gear No. | Date (UTC) | Start (UTC) | at seafl. at depth (UTC) | End (UTC) | Latitude (deg/min) | Longitude (deg/min) | Area | HS-water depth (m) | Rope length (m) | Gear | Depth inter-vall (m) | Core re-covery (m) | Remarks |
|---|---|---|---|---|---|---|---|---|---|---|---|---|---|---|
| **PS75/ 086** | -1 | 07.-08. 01.10 | 22:06 | 22:57 | 23:48 | 64°44.643'S | 161°54.245'W | southern Pacific-Antarctic Ridge | 4064 | 4049 | MUC | | 12x (24-34) | |
| | -2 | | 00:09 | 00:55 | 01:46 | 64°44.64'S | 161°54.19'W | | 4065 | 4044 | SL (13m) | | **12.47** | |
| **PS75/ 087** | -1 | 08.01.10 | 14:39 | 15:27 | 16:19 | 66°47.29'S | 163°19.47'W | southern Pacific-Antarctic Ridge | 4406 | 4390 | SL (13m) | | **11.28** | |
| | -2 | | 16:33 | 17:30 | 18:24 | 66°47.273'S | 163°19.495'W | | 4411 | 4399 | MUC | | 7x (31-40) | |
| **PS75/ 088** | -1 | 09.01.10 | 11:46 | 13:17 | 14:30 | 68°43.780'S | 164°48.046'W | northern Ross Sea | 3852 | 3866 | CTD+ROS +FLU | to bottom | | |
| | -2 | | 14:38 | 15:19 | 16:10 | 68°43.812'S | 164°47.736'W | | 3860 | 1000 | MN | 0-1000m | | |
| | -3 | | 16:45 | 17:35 | 18:20 | 68°43.818'S | 164°48.076'W | | 3849 | 3826 | MUC | | 12x (32-38) | |
| | -4 | | 18:28 | 18:34 | 18:40 | 68°43.811'S | 164°48.074'W | | 3855 | 100 | PLA | 0-100m | | |
| | -5 | | 18:43 | 18:49 | 18:57 | 68°43.833'S | 164°48.061'W | | 3864 | 100 | PLA | 0-100m | | |
| | -6 | | 19:16 | 19:56 | 20:43 | 68°43.82'S | 164°48.95'W | | 3857 | 3816 | SL (15m) | | **12.40** | |
| **PS75/ 089** | -1 | 10.01.10 | 07:52 | 09:18 | 10:33 | 67°04.969'S | 165°32.417'W | southern Pacific-Antarctic Ridge | 4133 | 4165 | CTD+ROS +FLU | to bottom | | |
| | -2 | | 10:46 | 11:22 | 12:27 | 67°05.015'S | 165°32.492'W | | 4141 | 1000 | MN | 0-1000m | | |
| | -3 | | 12:40 | 13:24 | 14:16 | 67°05.01'S | 165°32.46'W | | 4126 | 4109 | SL (20m) | | **11.12** | |
| | -4 | | 14:29 | 14:36 | 14:43 | 67°05.010'S | 165°32.829'W | | 4125 | 100 | PLA | 0-100m | | |
| | -5 | | 14:46 | 14:53 | 14:59 | 67°05.039'S | 165°32.706'W | | 4125 | 100 | PLA | 0-100m | | |
| | -6 | | 15:07 | 16:00 | 16:52 | 67°04.980'S | 165°32.496'W | | 4121 | 4117 | MUC | | 7x (21-40.5) | |

| Station No. | Gear No. | Date (UTC) | Start (UTC) | at seafl. at depth (UTC) | End (UTC) | Latitude (deg/min) | Longitude (deg/min) | Area | HS-water depth (m) | Rope length (m) | Gear | Depth inter-vall (m) | Core re-covery (m) | Remarks |
|---|---|---|---|---|---|---|---|---|---|---|---|---|---|---|
| **PS75/090** | -1 | 11.01.10 | 03:45 | 04:57 | 05:55 | 65°24.672'S | 166°09.376'W | southern Pacific-Antarctic Ridge | 3505 | 3521 | CTD+ROS +FLU | to bottom | | |
| | -2 | | 06:02 | 06:34 | 07:32 | 65°24.677'S | 166°09.261'W | | 3501 | 1000 | MN | 0-1000m | | |
| | -3 | | 07:48 | 09:02 | 10:10 | 65°24.66'S | 166°09.28'W | | 3478 | 3443 | KOL (20m) | | **17.91** | **TC 0.92m** (top missing) |
| | -4 | | 10:22 | 10:28 | 10:34 | 65°24.653'S | 166°09.324'W | | 3481 | 100 | PLA | 0-100m | | |
| | -5 | | 10:36 | 10:43 | 10:49 | 65°24.657'S | 166°09.328'W | | 3481 | 100 | PLA | 0-100m | | |
| | -6 | | 10:55 | 11:40 | 14:02 | 65°24.659'S | 166°09.325'W | | 3480 | 3485 | MUC | | 7x (31.5-34) | winch stopped at 11:55 (2315m) due to alarm |
| **PS75/091** | -1 | 12.01.10 | 04:21 | 05:25 | 06:18 | 63°41.650'S | 169°04.485'W | Pacific-Antarctic Ridge | 2953 | 2974 | CTD+ROS +FLU | to bottom | | |
| | -2 | | 06:24 | 06:57 | 07:57 | 63°41.658'S | 169°04.462'W | | 2955 | 1000 | MN | 0-1000m | | |
| | -3 | | 08:06 | 09:08 | 10:05 | 63°41.66'S | 169°04.47'W | | 2940 | 2914 | KOL (15m) | | **13.44** | **TC 0.26m** |
| | -4 | | 10:16 | 10:22 | 10:28 | 63°41.693'S | 169°04.389'W | | 2951 | 100 | PLA | 0-100m | | |
| **PS75/091** | -5 | | 10:30 | 10:36 | 10:42 | 63°41.655'S | 169°04.374'W | Pacific-Antarctic Ridge | 2942 | 100 | PLA | 0-100m | | |
| | -6 | | 10:49 | 11:27 | 12:05 | 63°41.63'S | 169°04.48'W | | 2944 | 2948 | MUC | | 4x (22-28.5) | |
| **PS75/092** | -1 | 13.01.10 | 07:12 | 08:00 | 08:52 | 60°40.036'S | 169°30.100'W | northern Pacific-Antarctic Ridge | 3833 | 3845 | MUC | | 7x (28-29) | |
| | -2 | | 08:56 | 09:02 | 09:08 | 60°40.011'S | 169°30.112'W | | 3846 | 100 | PLA | 0-100m | | |
| | -3 | | 09:10 | 09:15 | 09:22 | 60°40.059'S | 169°30.178'W | | 3835 | 100 | PLA | 0-100m | | |
| | -4 | | 09:32 | 10:53 | 11:59 | 60°40.018'S | 169°30.078'W | | 3833 | 3883 | CTD+ROS +FLU | to bottom | | |
| | -5 | | 12:08 | 12:46 | 13:43 | 60°40.047'S | 169°30.139'W | | 3849 | 1000 | MN | 0-1000m | | |
| **PS75/093** | -1 | 13.01.10 | 15:39 | 16:49 | 17:59 | 60°52.33'S | 169°32.89'W | northern Pacific-Antarctic Ridge | 3762 | 3712 | KOL (20m) | | **12.84** | **TC 0.92m** (top missing), core imploded between 3 – 5 m, but no significant core disturbance |

| Station No. | Gear No. | Date (UTC) | Start (UTC) | at seafl. at depth (UTC) | End (UTC) | Latitude (deg/min) | Longitude (deg/min) | Area | HS-water depth (m) | Rope length (m) | Gear | Depth inter-vall (m) | Core re-covery (m) | Remarks |
|---|---|---|---|---|---|---|---|---|---|---|---|---|---|---|
| **PS75/ 094** | -1 | 13.-14. 01.10 | 23:33 | 00:38 | 01:44 | 61°49.34'S | 169°44.69'W | northern Pacific-Antarctic Ridge | 3270 | 3227 | KOL (20m) | | **9.70** | TC **0.92**m, core bent between 10 and 12m |
| | -2 | | 01:57 | 02:33 | 03:34 | 61°49.364'S | 169°44.444'W | | 3271 | 1000 | MN | 0-1000m | | |
| | -3 | | 03:44 | 04:28 | 05:09 | 61°49.341'S | 169°44.441'W | | 3274 | 3264 | MUC | | 10x (25-27) | |
| | -4 | | 05:19 | 05:25 | 05:31 | 61°49.006'S | 169°44.842'W | | 3286 | 100 | PLA | 0-100m | | |
| | -5 | | 05:33 | 05:39 | 05:46 | 61°49.020'S | 169°44.876'W | | 3258 | 100 | PLA | 0-100m | | |
| | -6 | | 05:54 | 07:03 | 08:00 | 61°48.985'S | 169°45.001'W | | 3256 | 3271 | CTD+ROS +FLU | to bottom | | |
| **PS75/ 095** | -1 | 16.01.10 | 01:09 | 02:42 | 04:07 | 57°01.148'S | 174°25.785'W | SW-Pacific Basin | 4836 | 4916 | CTD+ROS +FLU | to bottom | | |
| **PS75/ 095** | -2 | | 04:17 | 04:50 | 05:44 | 57°01.186'S | 174°25.786'W | SW-Pacific Basin | 4847 | 1000 | MN | 0-1000m | | |
| | -3 | | 05:52 | 05:58 | 06:03 | 57°00.906's | 174°25.663'W | | 4852 | 100 | PLA | 0-100m | | |
| | -4 | | 06:05 | 06:12 | 06:17 | 57°00.896'S | 174°25.810'W | | 4853 | 100 | PLA | 0-100m | | |
| | -5 | | 06:40 | 08:21 | 09:40 | 57°01.18'S | 174°25.80'W | | 4853 | 4814 | KOL (20m) | | **17.85** | **TC 1.01m** |
| | -6 | | 10:05 | 11:06 | 12:05 | 57°01.176'S | 174°25.866'W | | 4857 | 4857 | MUC | | 11x (30-36.5) | |
| **PS75/ 096** | -1 | 16.-17. 01.10 | 22:41 | 23:04 | 23:28 | 58°32.820'S | 172°41.986'W | SW-Pacific Basin | 5051 | 1014 | CTD+ROS +FLU | 0-1000m | | |
| | -2 | | 23:35 | 00:10 | 01:05 | 58°32.863'S | 172°42.067'W | | 5054 | 1000 | MN | 0-1000m | | |
| | -3 | | 01:13 | 01:16 | 01:26 | 58°32.848'S | 172°42.008'W | | 5060 | 60 | PLA | 0-60m | | |
| | -4 | | 01:33 | 03:19 | 04:48 | 58°32.86'S | 172°42.06'W | | 5057 | 5011 | KOL (25m) | | **22.79** | **TC 0.69m** |
| | -5 | | 05:10 | 06:15 | 07:15 | 58°32.857'S | 172°42.031'W | | 5057 | 5059 | MUC | | 0 | all tubes flown out due to ships movement |

| Station No. | Gear No. | Date (UTC) | Start (UTC) | at seafl. at depth (UTC) | End (UTC) | Latitude (deg/min) | Longitude (deg/min) | Area | HS-water depth (m) | Rope length (m) | Gear | Depth inter-vall (m) | Core re-covery (m) | Remarks |
|---|---|---|---|---|---|---|---|---|---|---|---|---|---|---|
| **PS75/ 097** | -1 | 17.01.10 | 15:27 | 15:53 | 16:21 | 59°42.022'S | 171°21.213'W | northern Pacific-Antarctic Ridge | 4677 | 1014 | CTD+ROS +FLU | 0-1000m | | |
| | -2 | | 16:29 | 17:02 | 18:02 | 59°42.071'S | 171°21.378'W | | 4675 | 1000 | MN | 0-1000m | | |
| | -3 | | 18:09 | 18:14 | 18:22 | 59°42.023'S | 171°21.259'W | | 4678 | 100 | PLA | 0-100m | | |
| | -4 | | 18:29 | 20:00 | 21:25 | 59°42.02'S | 171°21.44'W | | 4672 | 4623 | KOL (20m) | | **17.46** | **TC 0.69m** |
| | -5 | | 21:41 | 22:40 | 23:39 | 59°42.026'S | 171°21.450'W | | 4675 | 4666 | MUC | | 11x (30.5-35) | |
| **PS75/ 098** | -1 | 20.01.10 | 00:34 | 02:18 | 03:46 | 52°57.688'S | 179°00.834'W | SW-Pacific Basin | 5188 | 5272 | CTD+ROS +FLU | to bottom | | |
| **PS75/ 098** | -2 | | 03:58 | 04:31 | 05:31 | 52°57.544'S | 179°00.813'W | SW-Pacific Basin | 5189 | 1000 | MN | 0-1000m | | |
| | -3 | | 05:40 | 05:46 | 05:53 | 52°57.162'W | 179°00.705'W | | 5184 | 100 | PLA | 0-100m | | |
| | -4 | | 05:55 | 06:01 | 06:07 | 52°57.032'W | 179°00.732'W | | 5185 | 100 | PLA | 0-100m | | |
| | -5 | | 06:25 | 08:08 | 09:46 | 52°57.93'S | 179°00.62'W | | 5189 | 5143 | KOL (25 m) | | **22.83** | **TC 0.82m**, minor imposion in section 6.81-7.80 m |
| | -6 | | 10:15 | 11:20 | 12:22 | 52°57.976'S | 179°00.576'W | | 5187 | 5191 | MUC | | 6x (35-38) | |
| **PS75/ 099** | -1 | 21.01.10 | 17:42 | 18:00 | 18:14 | 48°15.707'S | 177°16.393'E | Pukaki Saddle | 1270 | 1272 | MUC | | 6x (11.5-14) | |
| | -2 | | 18:26 | 18:31 | 18:37 | 48°15.709'S | 177°16.398'E | | 1270 | 100 | PLA | 0-100m | | |
| | -3 | | 18:39 | 18:45 | 18:51 | 48°15.721'S | 177°16.381'E | | 1272 | 100 | PLA | 0-100m | | |
| | -4 | | 19:10 | 19:35 | 20:11 | 48°15.718'S | 177°16.353'E | | 1272 | 1242 | KOL (15m) | | **7.71** | TC empty |
| | -5 | | 20:18 | 20:50 | 21:19 | 48°15.713'S | 177°16.370'E | | 1270 | 1269 | CTD+ROS +FLU | to bottom | | |
| | -6 | | 21:26 | 21:58 | 22:57 | 48°15.752'S | 177°16.294'E | | 1272 | 1000 | MN | 0-1000m | | |
| | -7 | | 23:05 | 23:22 | 23:42 | 48°15.676'S | 177°16.417'E | | 1263 | 1268 | GKG | | 0.29 | 2 subcores 0-0.29, 5 surface samples (0-0.01) |

| Station No. | Gear No. | Date (UTC) | Start (UTC) | at seafl. at depth (UTC) | End (UTC) | Latitude (deg/min) | Longitude (deg/min) | Area | HS-water depth (m) | Rope length (m) | Gear | Depth inter-vall (m) | Core re-covery (m) | Remarks |
|---|---|---|---|---|---|---|---|---|---|---|---|---|---|---|
| **PS75/ 100** | -1 | 22.01.10 | 15:10 | 15:43 | 16:15 | 45°45.454'S | 177°08.932'E | Bounty Trough | 2502 | 2505 | MUC | | 7x(14-22) | |
| | -2 | | 16:18 | 16:25 | 16:31 | 45°45.423'S | 177°08.931'E | | 2504 | 100 | PLA | 0-100m | | |
| | -3 | | 16:33 | 16:39 | 16:45 | 45°45.415'S | 177°08.907'E | | 2502 | 100 | PLA | 0-100m | | |
| | -4 | | 16:55 | 17:46 | 18:39 | 45°45.41'S | 177°08.93'E | | 2498 | 2463 | KOL (20m) | | **14.77** | **TC 0.29m** |
| **PS75/ 100** | -5 | | 18:50 | 19:41 | 20:27 | 45°45.421'S | 177°08.861'E | Bounty Trough | 2497 | 2521 | CTD+ROS +FLU | to bottom | | |
| | -6 | | 20:35 | 21:06 | | 45°45.416'S | 177°08.884'E | | 2498 | 1000 | MN | 0-1000m | | |
| **PS75/ 101** | -1 | 23.01.10 | 03:59 | 04:38 | 05:19 | 45°48.42'S | 175°52.66'E | Bounty Trough | 1770 | 1739 | KOL (20m) | | **11.8** | **TC 0.12m** |
| | -2 | | 05:31 | 05:56 | 06:19 | 45°48.371'S | 175°52.540'E | | 1773 | 1778 | MUC | | 12x (12-18) | |
| **PS75/ 102** | -1 | 23.01.10 | 08:44 | 09:21 | 10:00 | 45°41.197'S | 175°43.29'E | Bounty Trough | 1621 | 1585 | KOL (20m) | | **12.96** | **TC 0.48m** |
| **PS75/ 103** | -1 | 23.01.10 | 11:48 | 12:14 | 12:50 | 45°30.93'S | 175°29.99'E | Chatham Rise | 1390 | 1356 | KOL (20m) | | **13.15** | **TC 0.57m** |
| **PS75/ 104** | -1 | 23.01.10 | 19:14 | 19:34 | 19:59 | 44°46.15'S | 174°31.53'E | Chatham Rise | 835 | 817 | KOL (15m) | | **12.39** | TC empty |
| | -2 | | 20:12 | 20:27 | 20:41 | 44°46.158'S | 174°31.546'E | | 835 | 848 | MUC | | 9x (11-16) | |
| | -3 | | 20:53 | 21:13 | 21:32 | 44°46.147'S | 174°31.503'E | | 836 | 841 | CTD+ROS +FLU | to bottom | | |
| | -4 | | 21:41 | 22:02 | 22:35 | 44°46.091'S | 174°31.625'E | | 835 | 600 | MN | | | |
| | -5 | | 22:46 | 22:51 | 22:57 | 44°46.095'S | 174°31.724'E | | 833 | 100 | PLA | 0-100m | | |
| **PS75/ 105** | -1 | 24.01.10 | 01:22 | 01:33 | 01:45 | 44°24.519'S | 174°37.470'E | Chatham Rise | 669 | 685 | MUC | | 12x (19-25) | |
| | -2 | | 02:14 | 02:35 | 03:22 | 44°24.51'S | 174°37.51'E | | 668 | 640 | KOL (25m) | | **12.09** | **TC 0.11m**, core bent above 15m |

# A.5 CTD CASTS

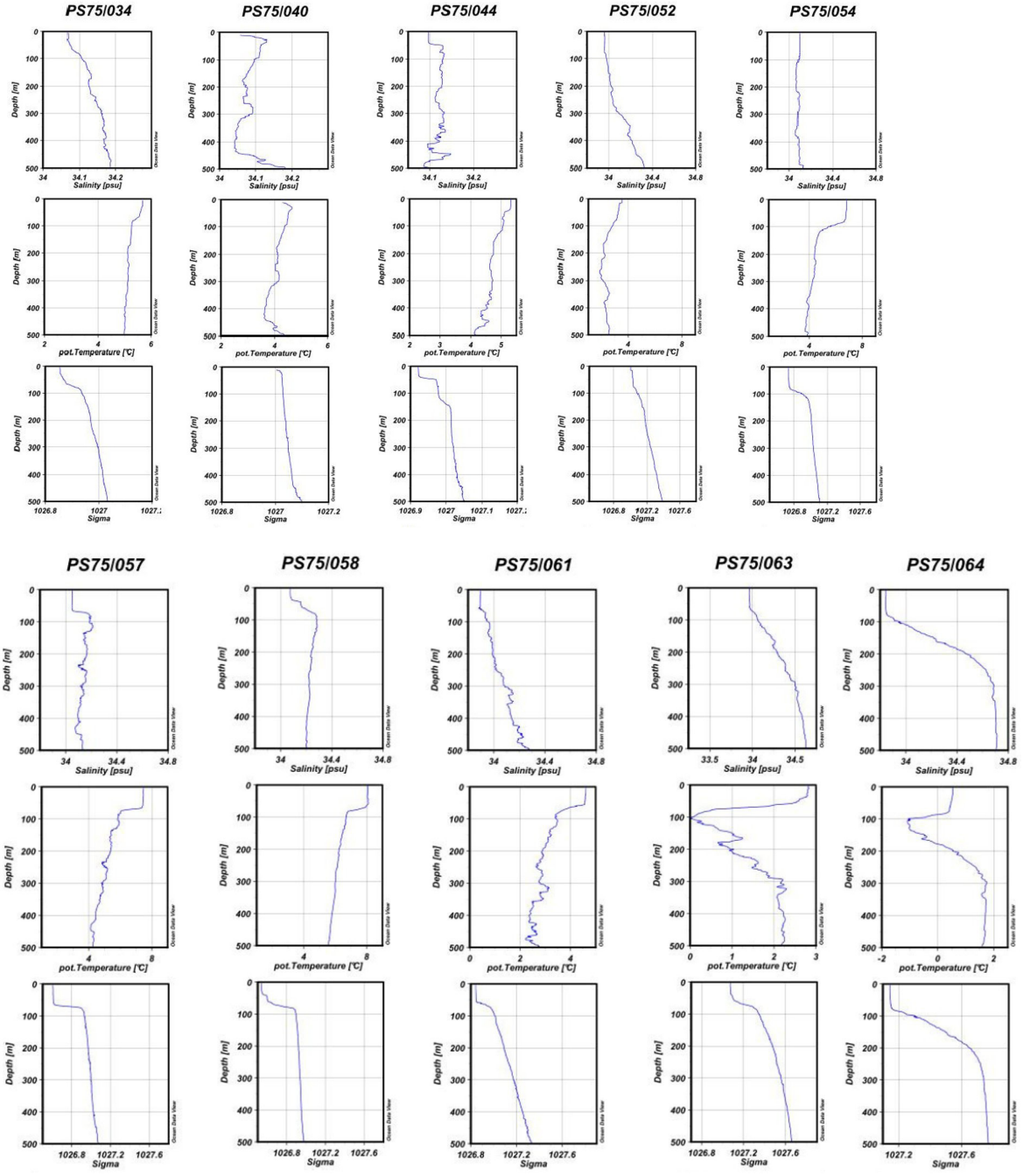
PS75/034
PS75/040
PS75/044
PS75/052
PS75/054
PS75/057
PS75/058
PS75/061
PS75/063
PS75/064
Depth [m]
Salinity [psu]
pot.Temperature [°C]
Sigma
Ocean Data View

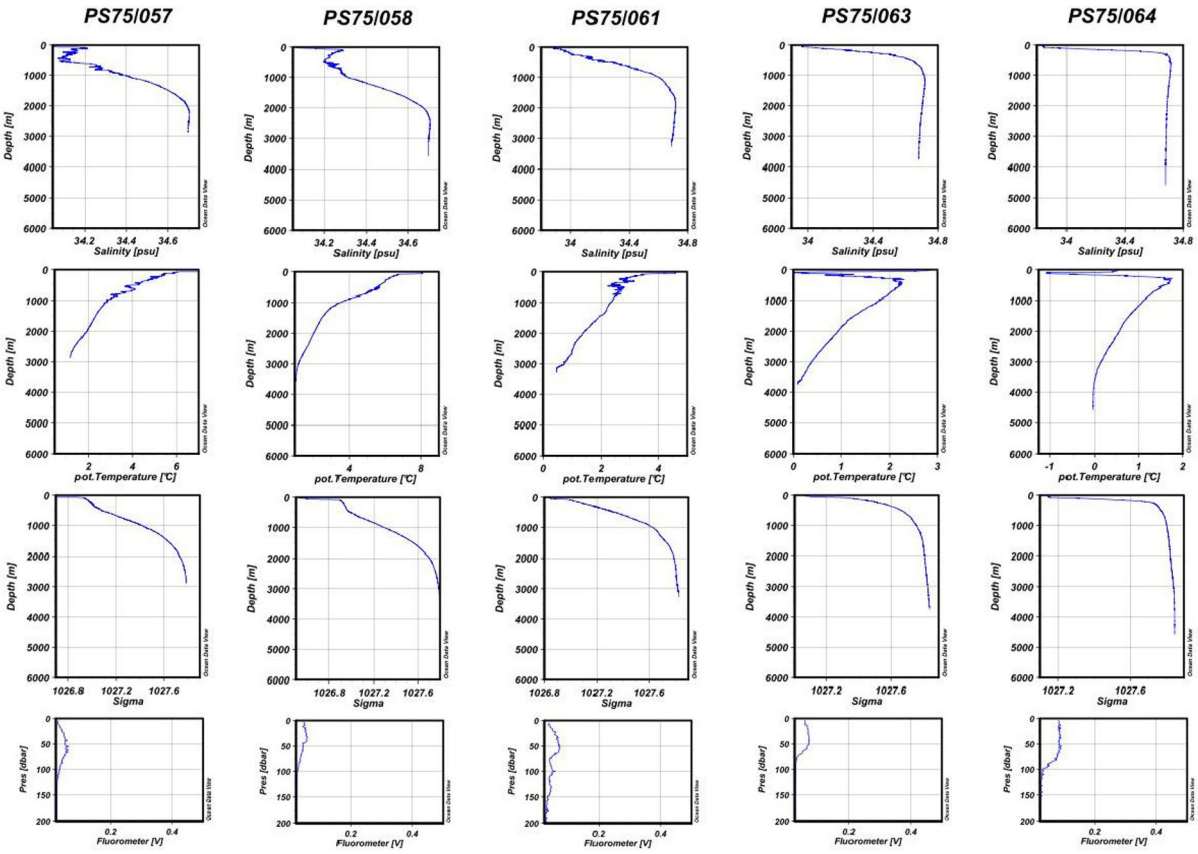
PS75/057
PS75/058
PS75/061
PS75/063
PS75/064
Depth [m]
Salinity [psu]
pot.Temperature [°C]
Sigma
Pres [dbar]
Fluorometer [V]

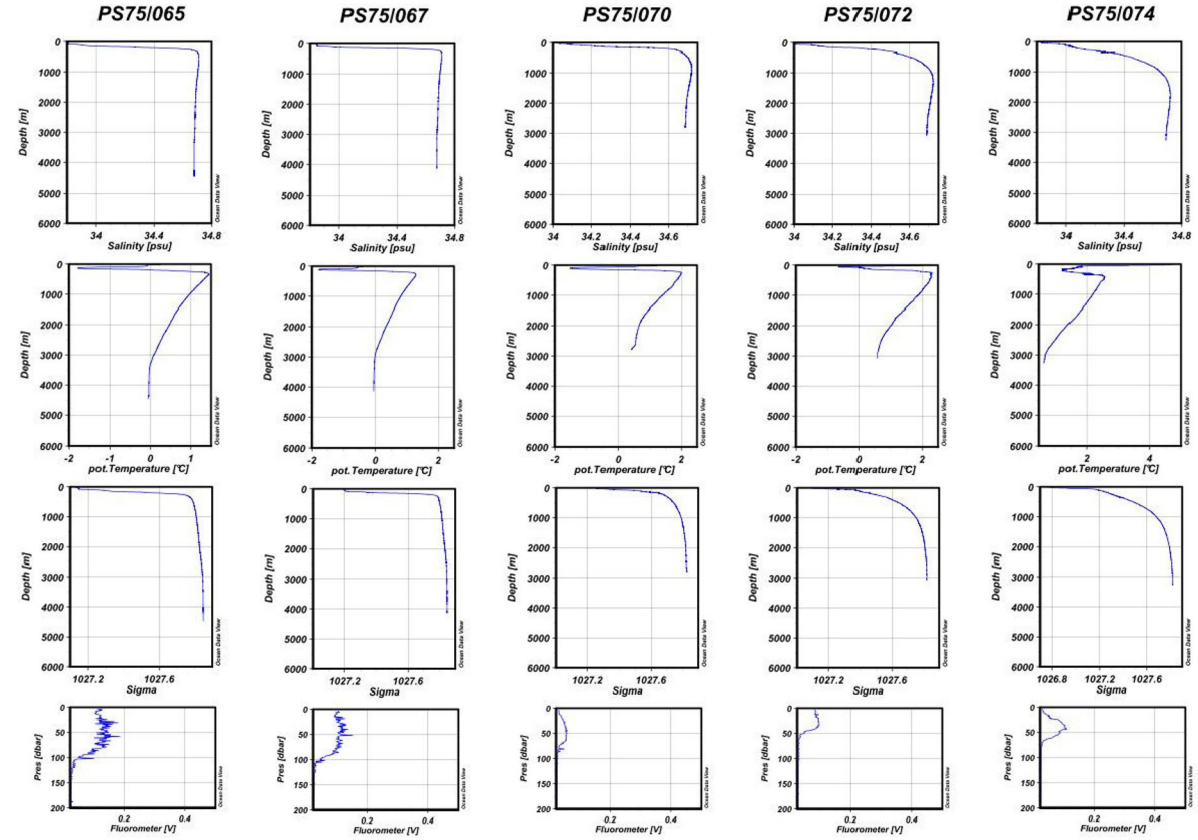
PS75/065
PS75/067
PS75/070
PS75/072
PS75/074
Depth [m]
Salinity [psu]
pot.Temperature [°C]
Sigma
Pres [dbar]
Fluorometer [V]

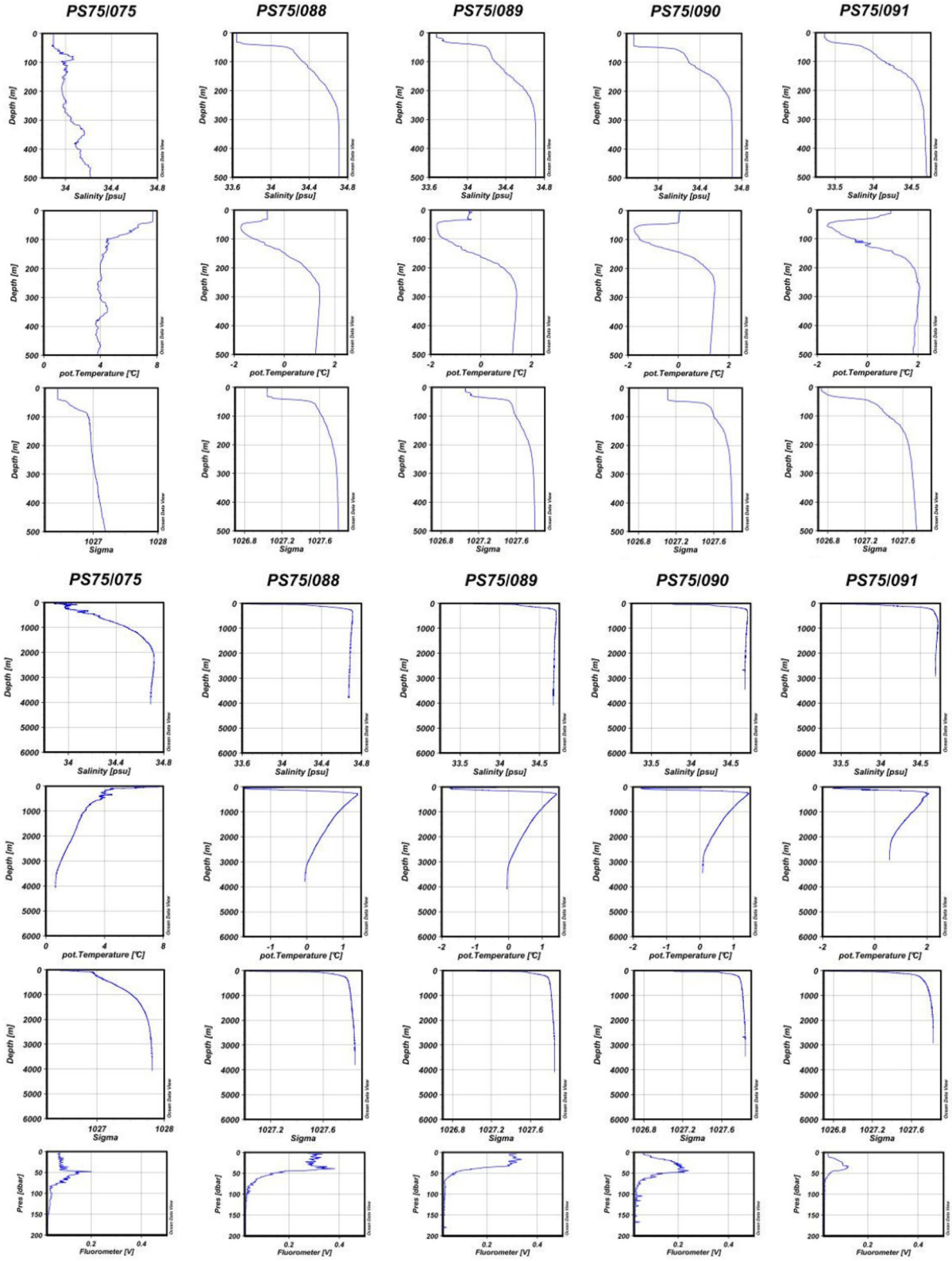
PS75/075
PS75/088
PS75/089
PS75/090
PS75/091
Depth [m]
Salinity [psu]
pot.Temperature [°C]
Sigma
PS75/075
PS75/088
PS75/089
PS75/090
PS75/091
Depth [m]
Salinity [psu]
pot.Temperature [°C]
Sigma
Pres [dbar]
Fluorometer [V]

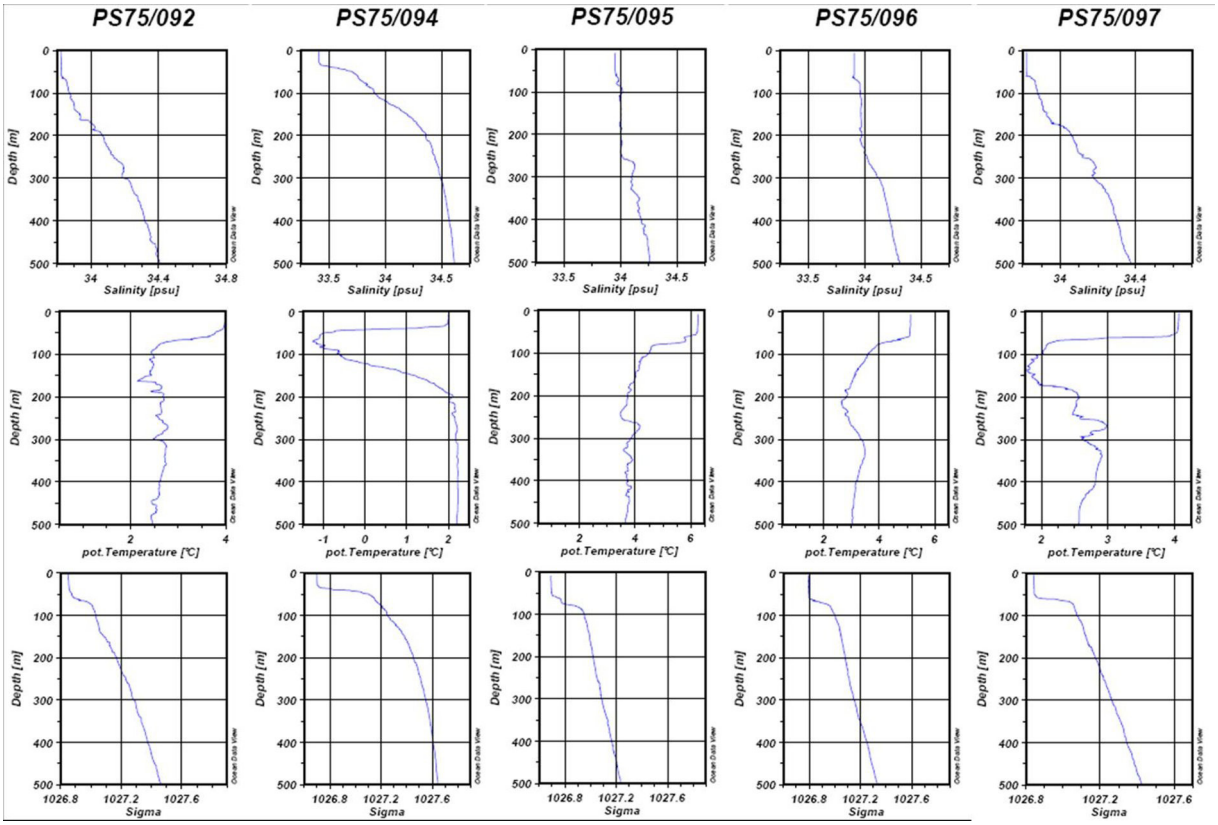
PS75/092
PS75/094
PS75/095
PS75/096
PS75/097
Depth [m]
Salinity [psu]
pot.Temperature [°C]
Sigma

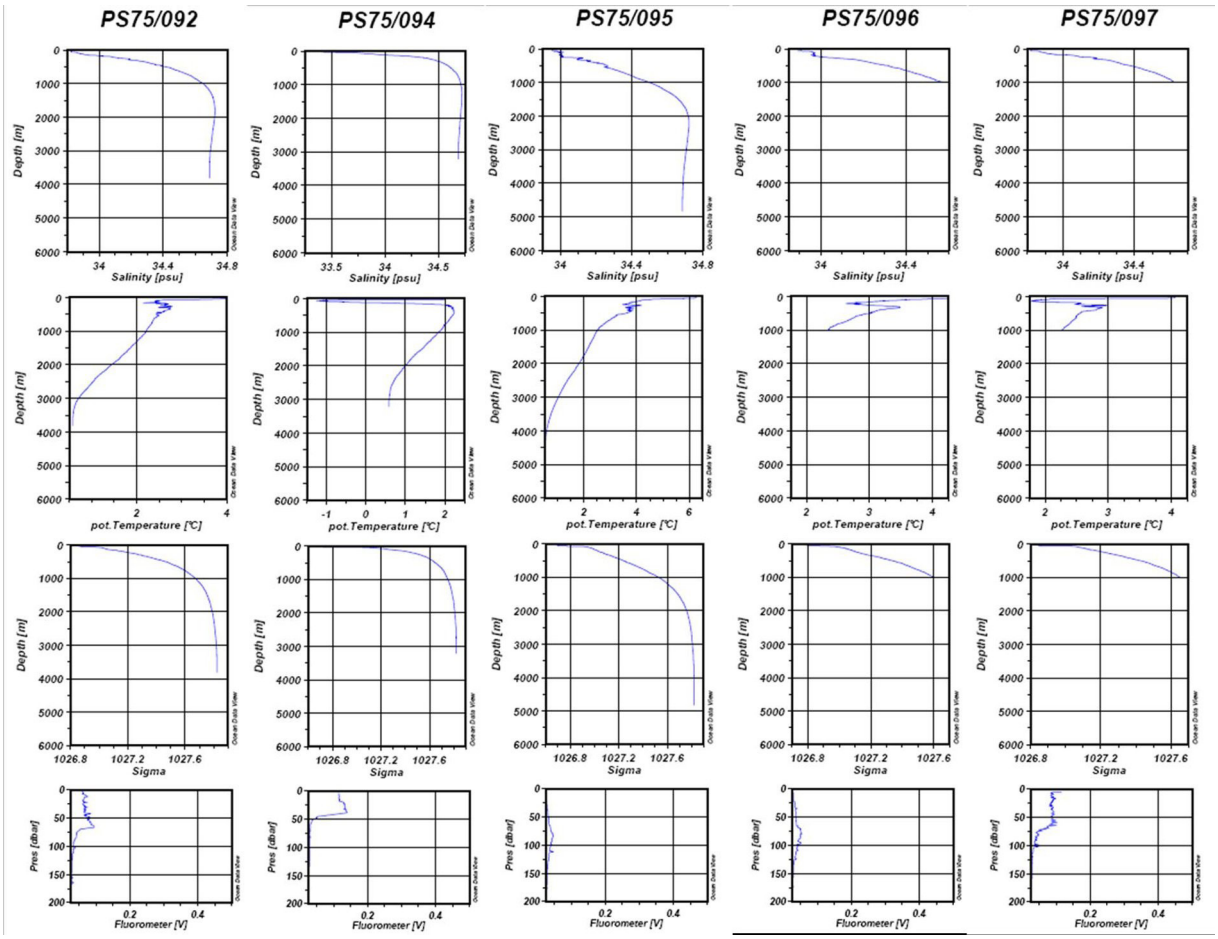
PS75/092
PS75/094
PS75/095
PS75/096
PS75/097
Depth [m]
Salinity [psu]
pot.Temperature [°C]
Sigma
Press [dbar]
Fluorometer [V]

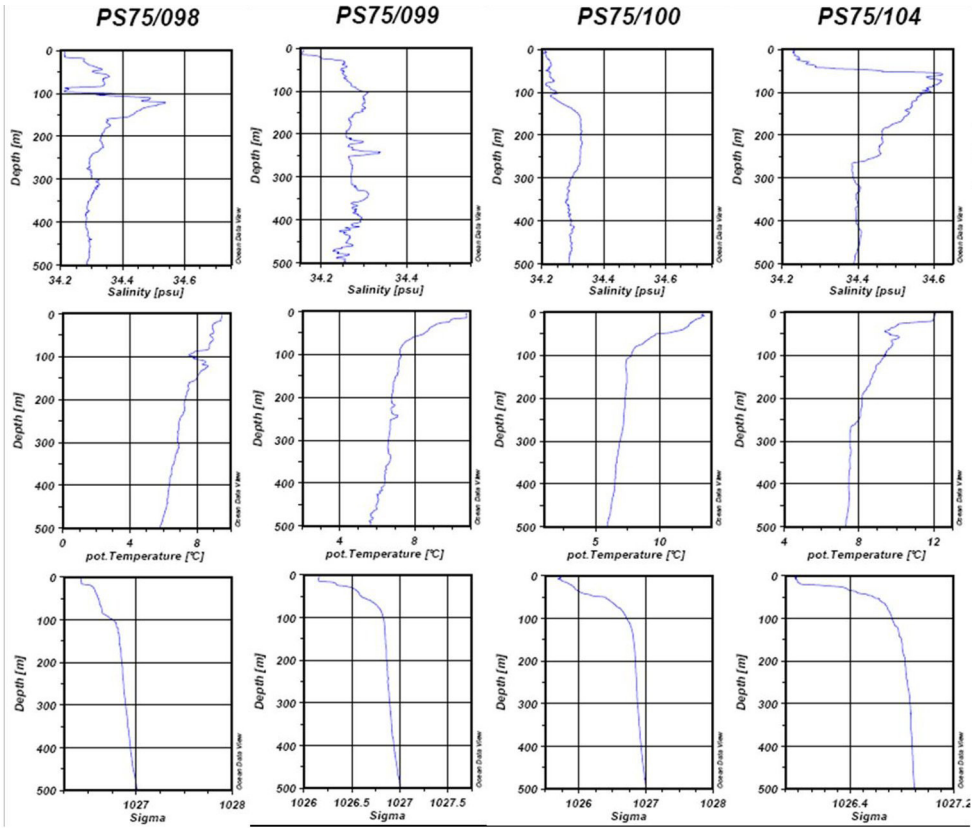
PS75/098
PS75/099
PS75/100
PS75/104
Depth [m]
Salinity [psu]
pot.Temperature [°C]
Sigma

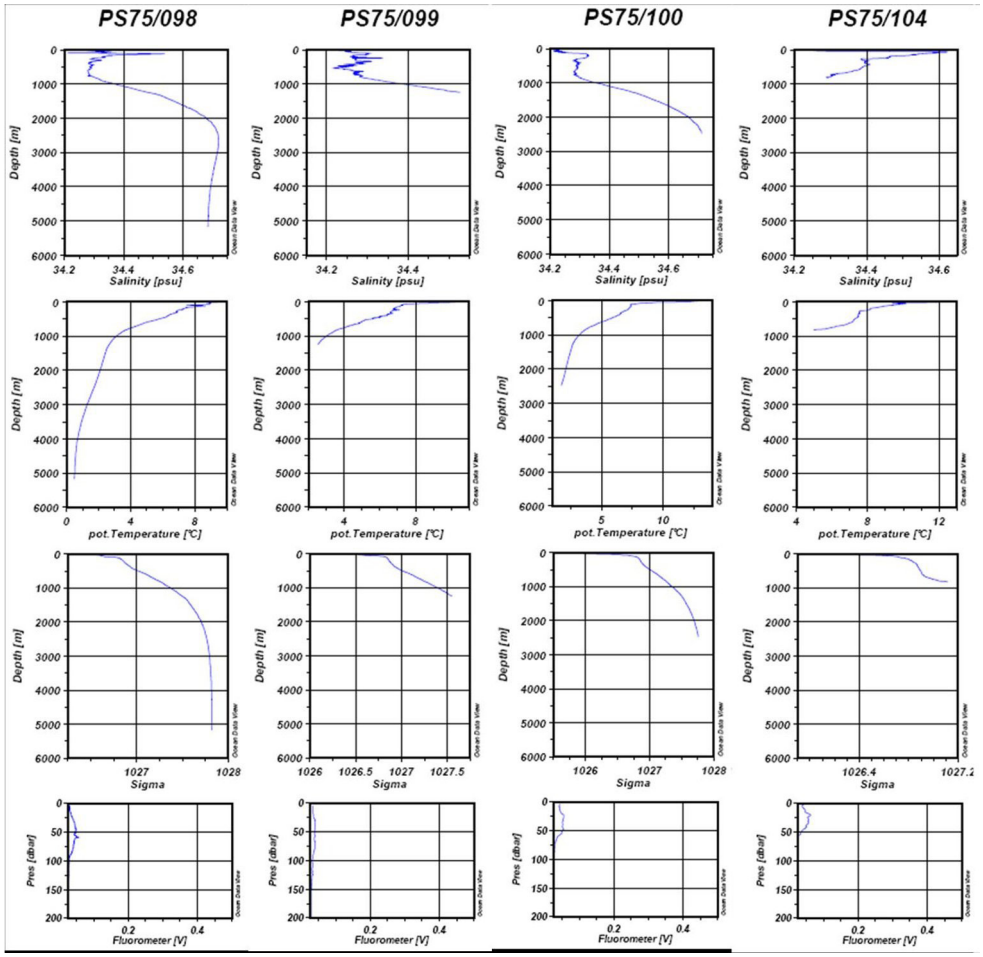
PS75/098
PS75/099
PS75/100
PS75/104
Depth [m]
Salinity [psu]
pot.Temperature [°C]
Sigma
Pres [dBar]
Fluorometer [V]

# A.6 PARASOUND PROFILES AT CORING SITES

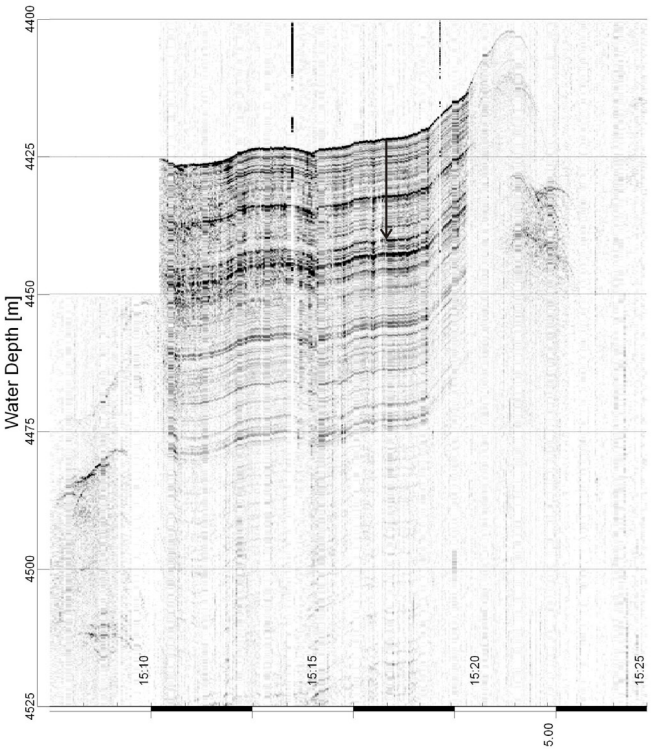


PS75/034-2
KOL 20
18.08 m
0.65-0.75 Ma

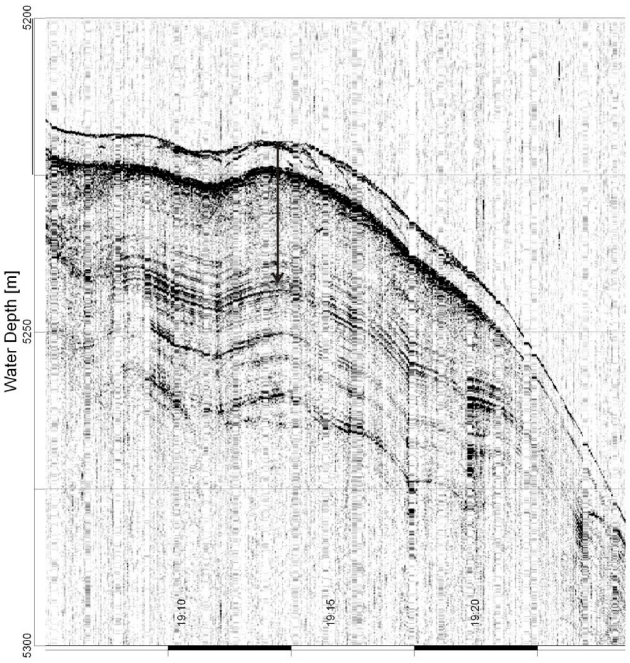


PS75/035-1
KOL 25
22.53 m
0.65-1.04 Ma

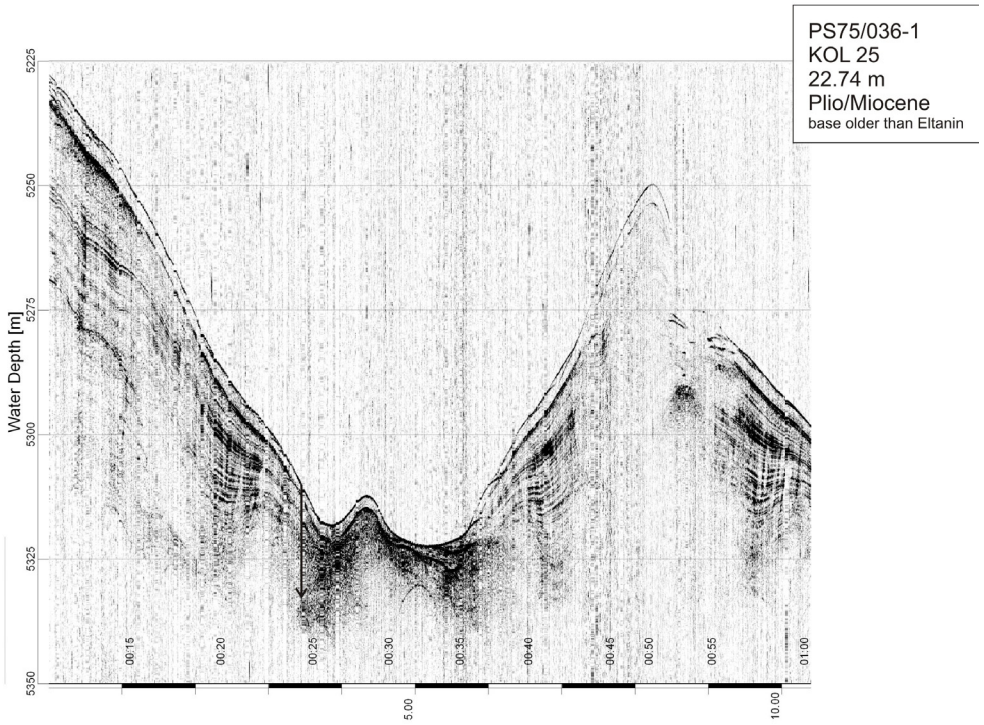
PS75/036-1
KOL 25
22.74 m
Plio/Miocene
base older than Eltanin
Water Depth [m]
5225
5250
5275
5300
5325
5350
00:15
00:20
00:25
00:30
00:35
00:40
00:45
00:50
00:55
01:00
5.00
10.00

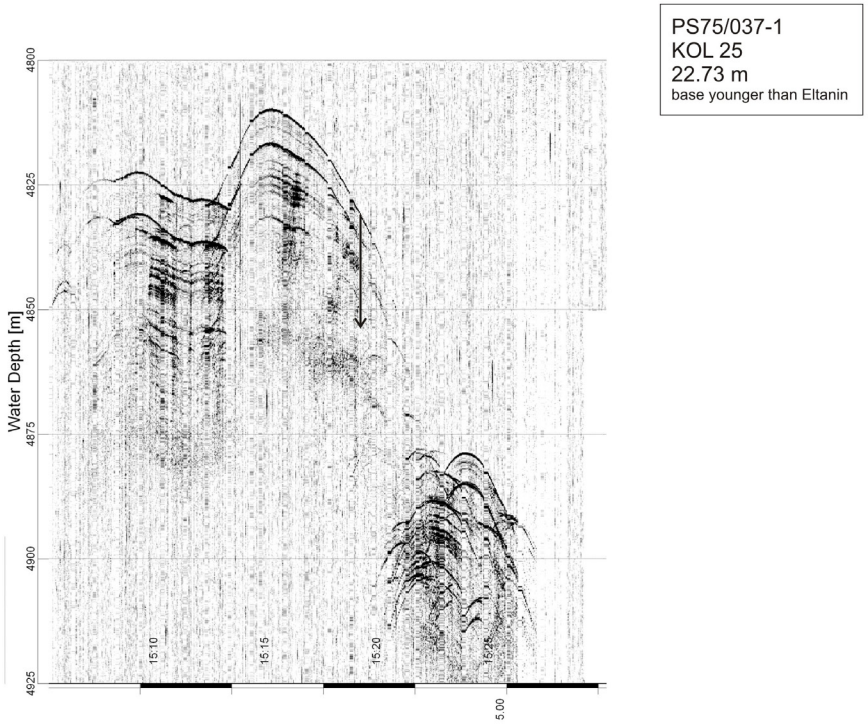
PS75/037-1
KOL 25
22.73 m
base younger than Eltanin
Water Depth [m]
4800
4825
4850
4875
4900
4925
15:10
15:15
15:20
15:25
5.00

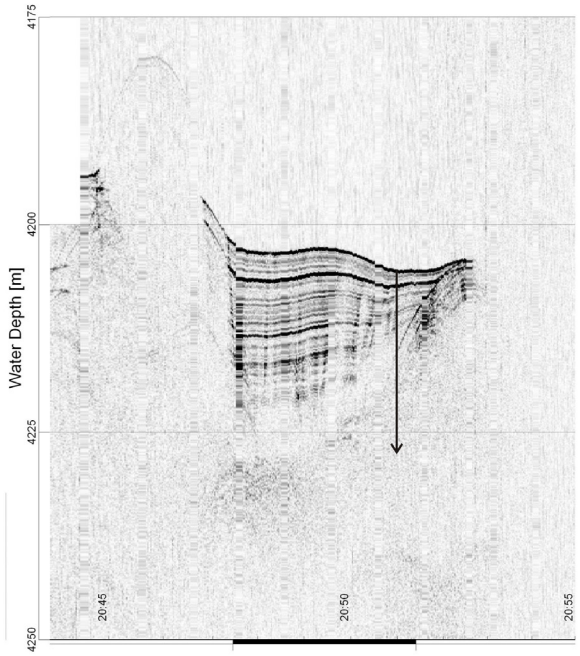


PS75/038-1
KOL 25
21.83 m
base older than Eltanin

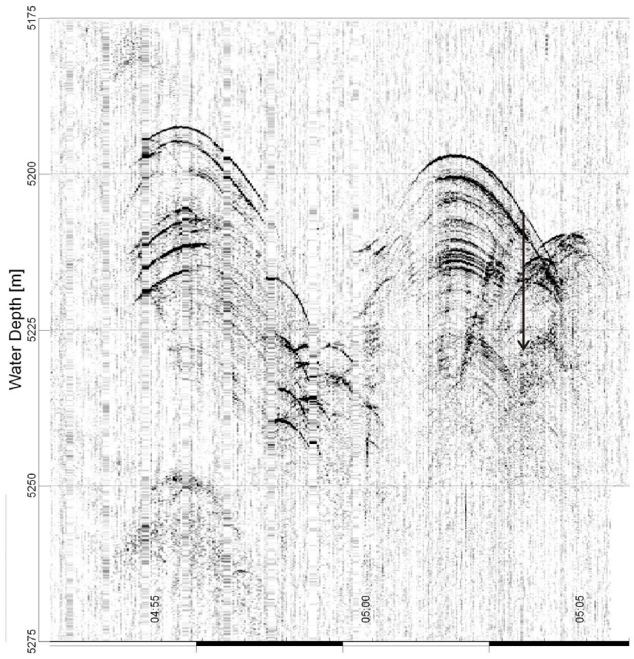


PS75/039-1
KOL 25
22.15 m
base younger than Eltanin

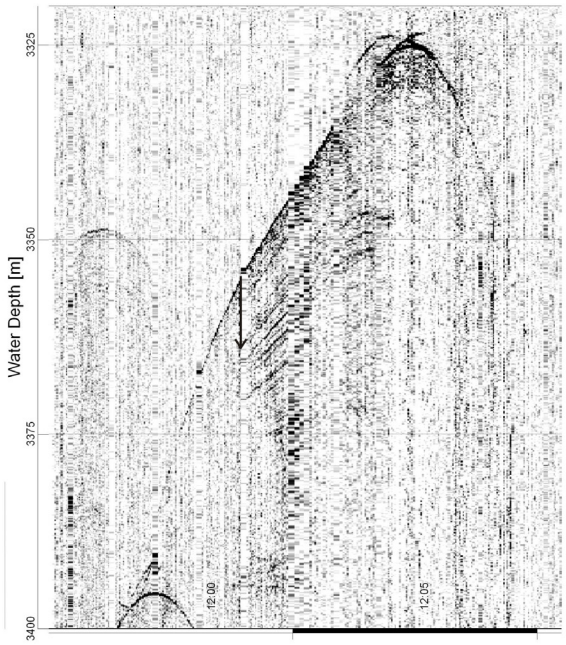


PS75/040-1
KOL 25
9.36 m
base older than Eltanin

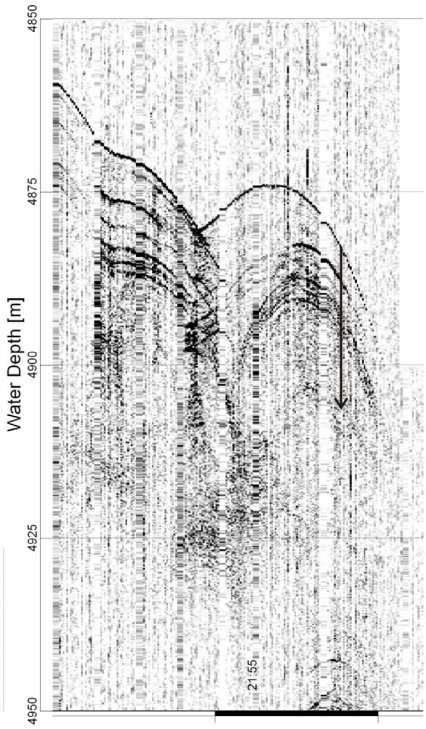


PS75/042-1
KOL 25
23.54 m
base younger than Eltanin

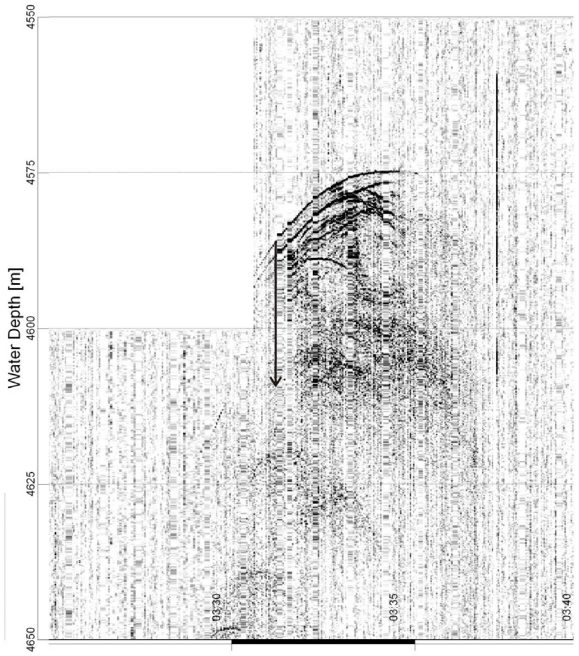


PS75/043-1
KOL 25
23.48 m
base younger than Eltanin

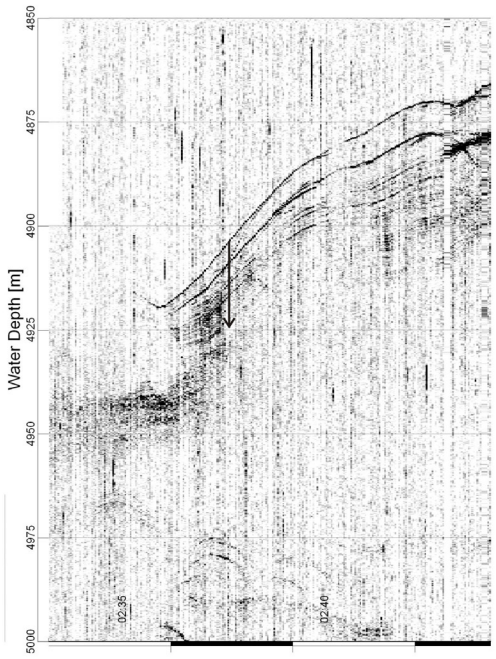


PS75/044-4
KOL 25
20.93 m
~2.3-2.4 Ma

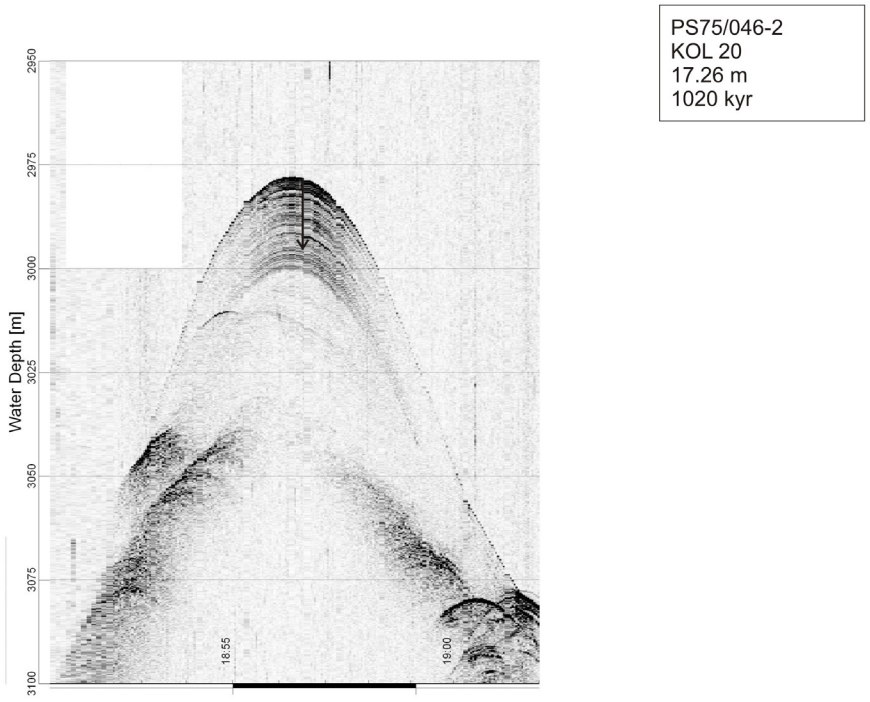
PS75/046-2
KOL 20
17.26 m
1020 kyr
Water Depth [m]
2950
2975
3000
3025
3050
3075
3100
18:55
19:00

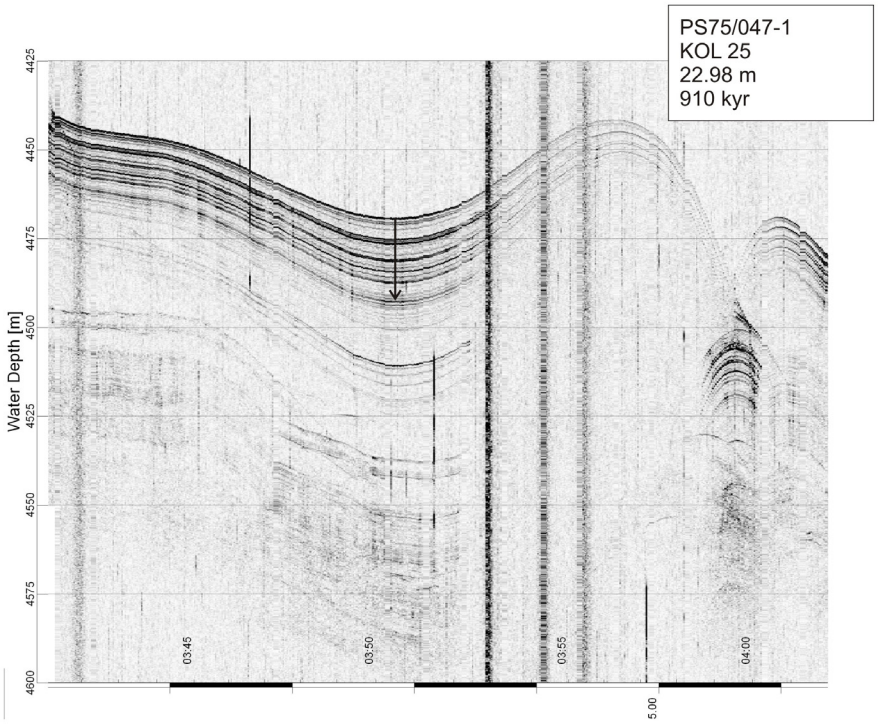
PS75/047-1
KOL 25
22.98 m
910 kyr
Water Depth [m]
4425
4450
4475
4500
4525
4550
4575
4600
03:45
03:50
03:55
04:00
5.00

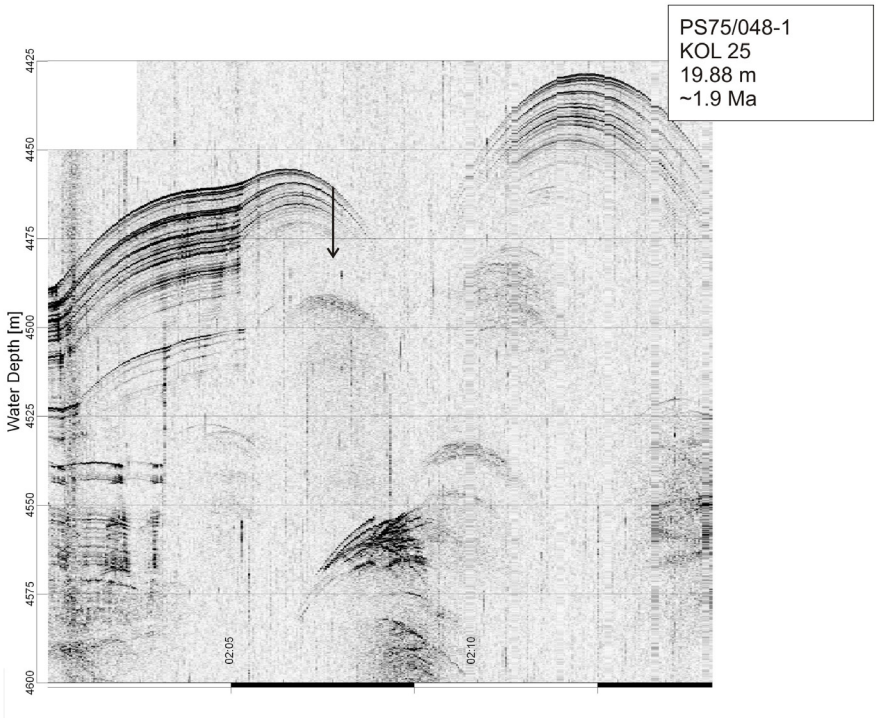
PS75/048-1
KOL 25
19.88 m
~1.9 Ma
Water Depth [m]
4425
4450
4475
4500
4525
4550
4575
4600
02:05
02:10

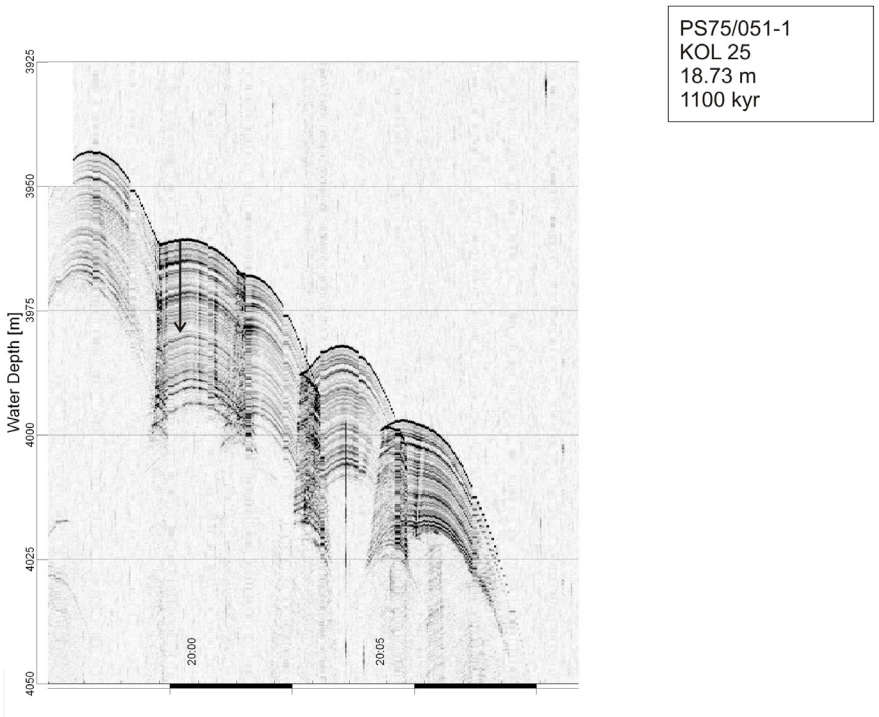
PS75/051-1
KOL 25
18.73 m
1100 kyr
Water Depth [m]
3925
3950
3975
4000
4025
4050
20:00
20:05

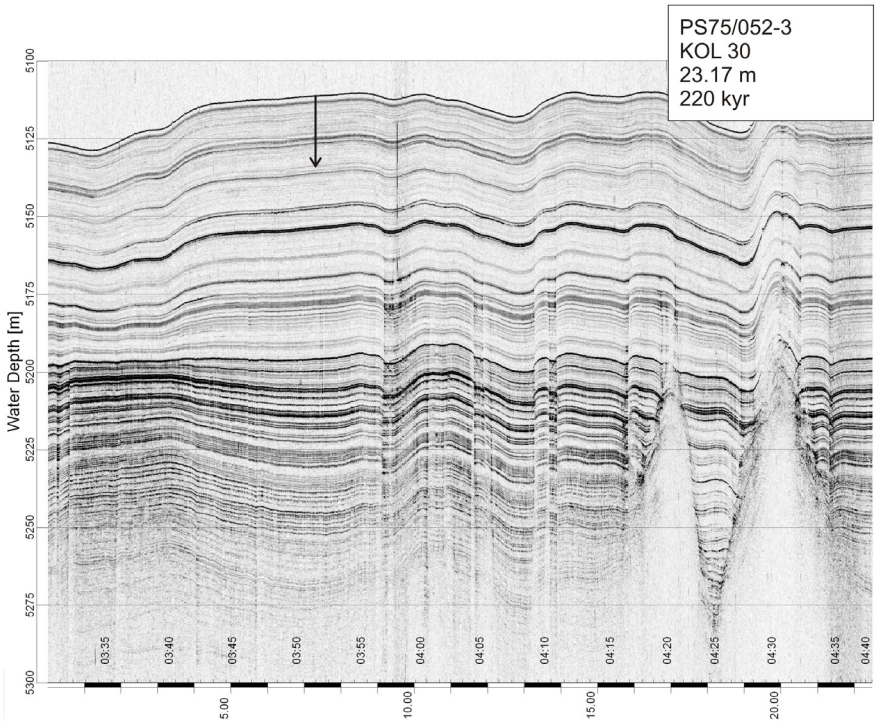
PS75/052-3
KOL 30
23.17 m
220 kyr
Water Depth [m]
5100
5125
5150
5175
5200
5225
5250
5275
5300
03:35
03:40
03:45
03:50
03:55
04:00
04:05
04:10
04:15
04:20
04:25
04:30
04:35
04:40
5.00
10.00
15.00
20.00

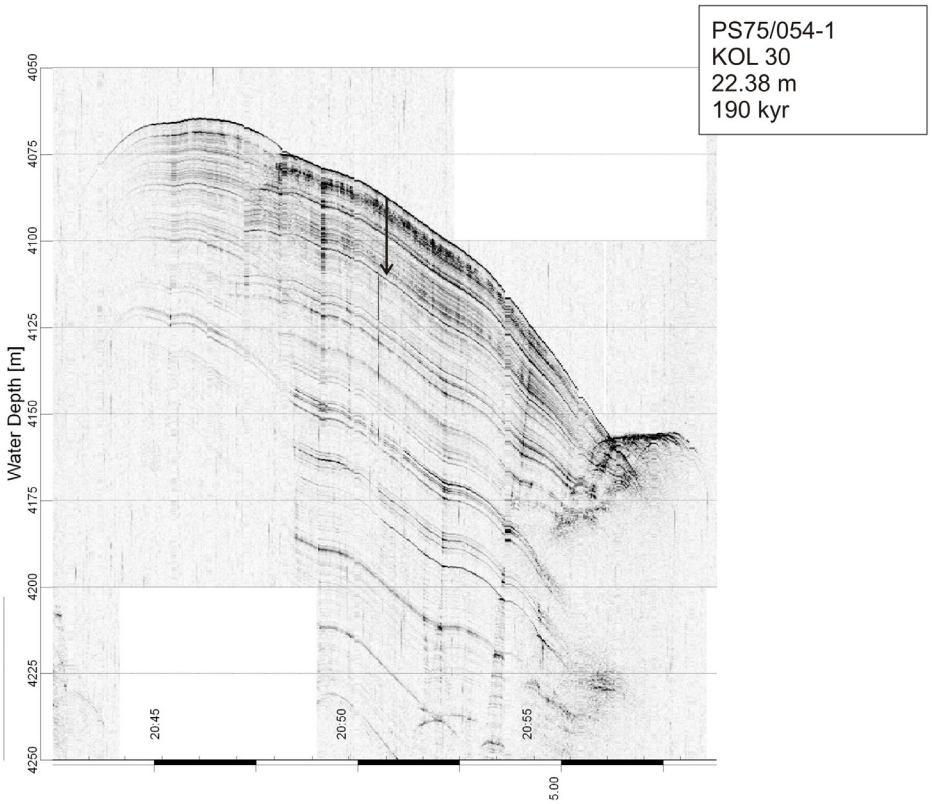
PS75/054-1
KOL 30
22.38 m
190 kyr
Water Depth [m]
4050
4075
4100
4125
4150
4175
4200
4225
4250
20:45
20:50
20:55
5.00

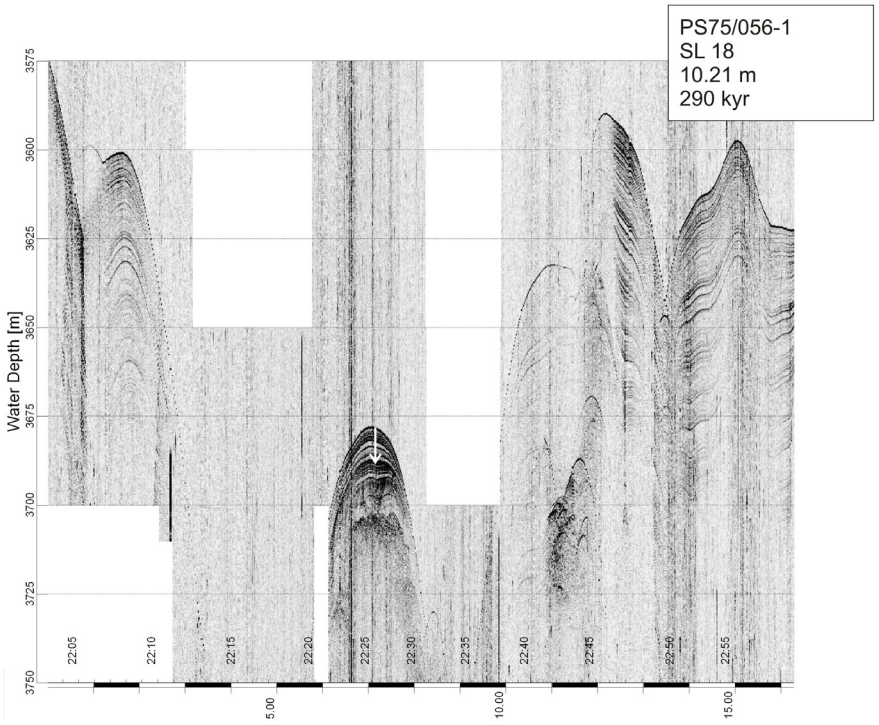
PS75/056-1
SL 18
10.21 m
290 kyr
Water Depth [m]
3575
3600
3625
3650
3675
3700
3725
3750
22:05
22:10
22:15
22:20
22:25
22:30
22:35
22:40
22:45
22:50
22:55
5.00
10.00
15.00

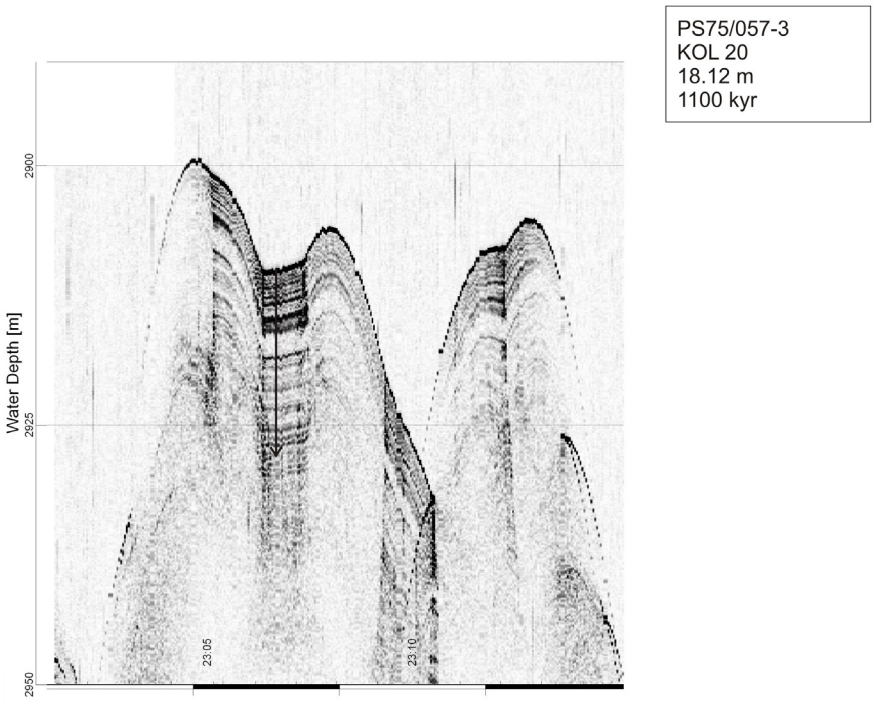
PS75/057-3
KOL 20
18.12 m
1100 kyr
Water Depth [m]
2900
2925
2950
23:05
23:10

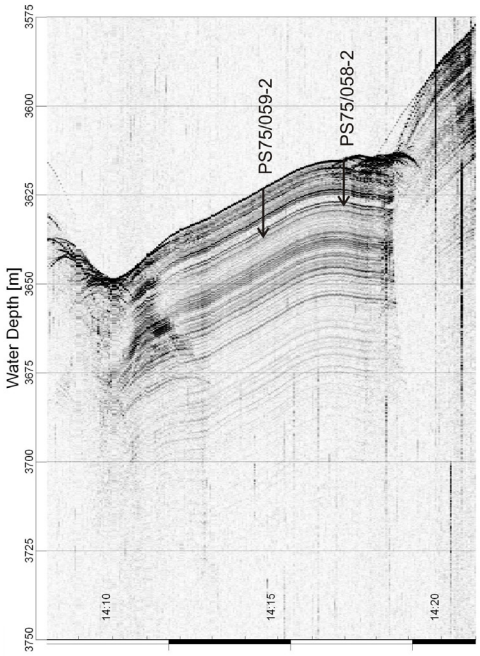


PS75/058-2
KOL 25
12.96 m
410 kyr

PS75/059-2
KOL 20
13.98 m
410 kyr

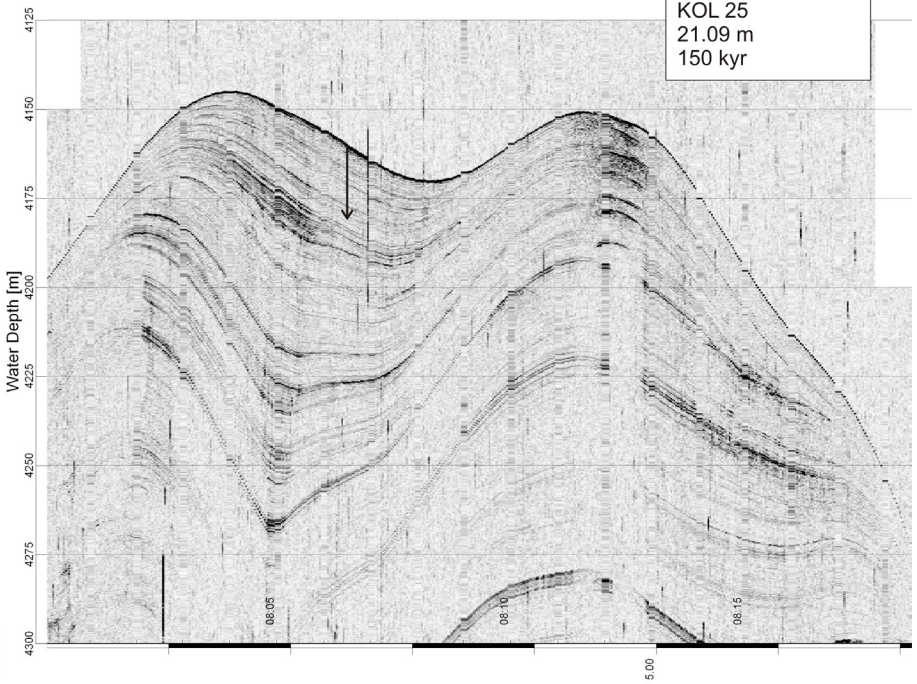


PS75/062-2
KOL 25
21.09 m
150 kyr

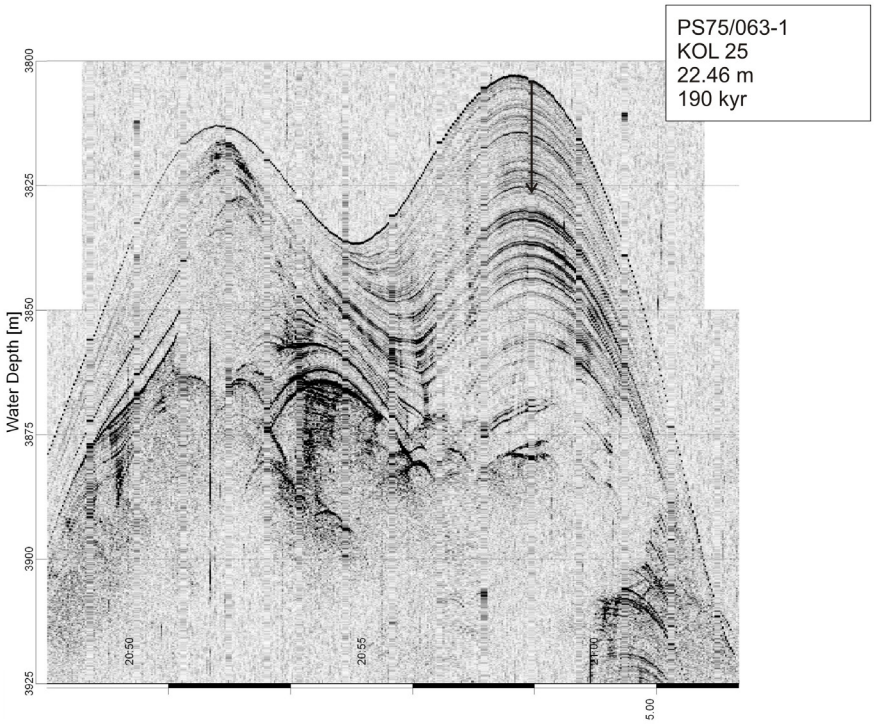
PS75/063-1
KOL 25
22.46 m
190 kyr
Water Depth [m]
3800
3825
3850
3875
3900
3925
20:50
20:55
21:00
5.00

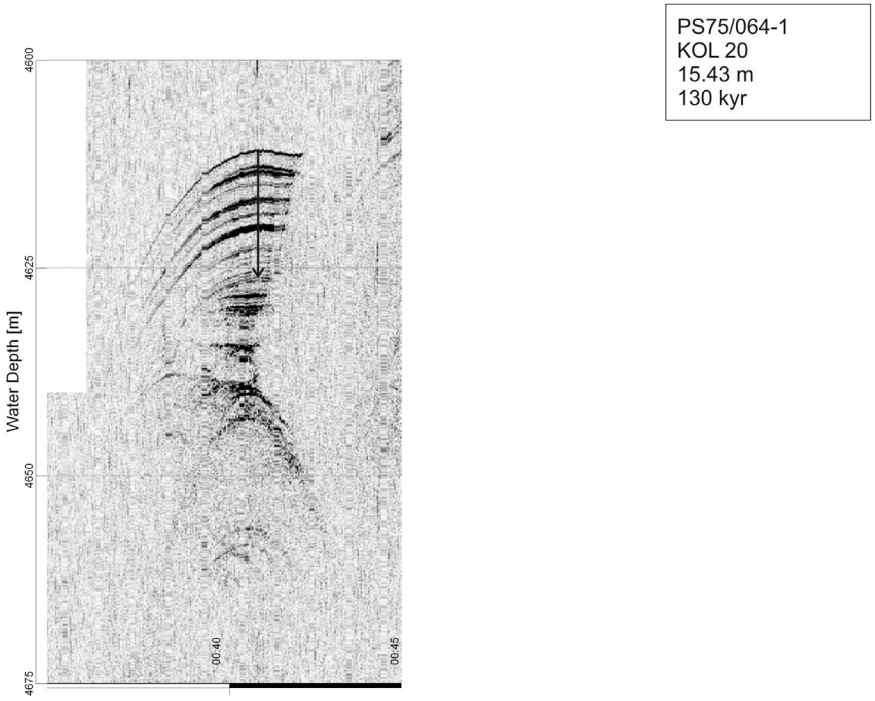
PS75/064-1
KOL 20
15.43 m
130 kyr
Water Depth [m]
4600
4625
4650
4675
00:40
00:45

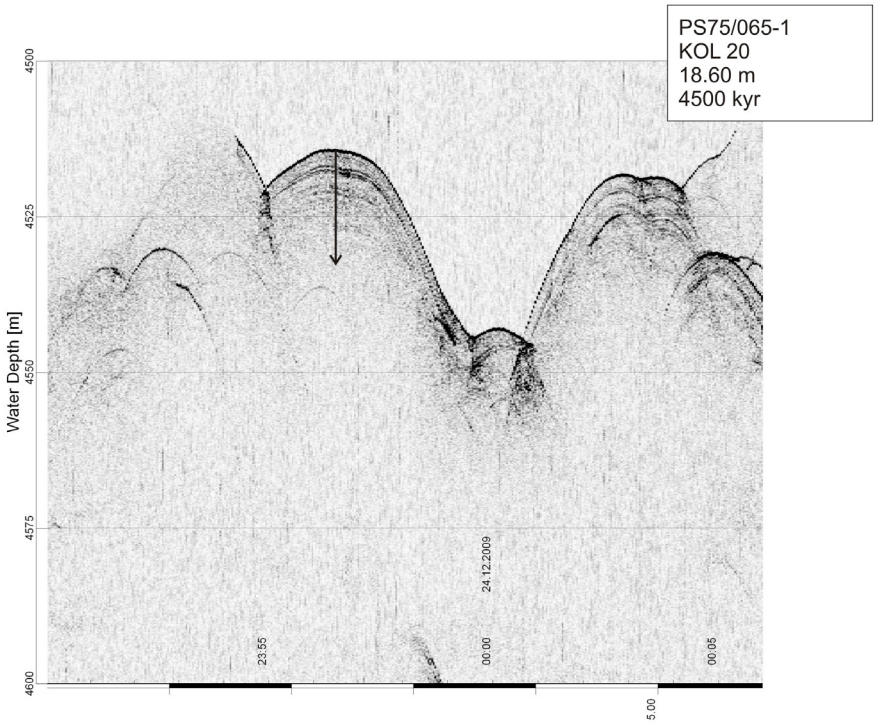
PS75/065-1
KOL 20
18.60 m
4500 kyr
Water Depth [m]
4500
4525
4550
4575
4600
24.12.2009
23:55
00:00
00:05
5.00

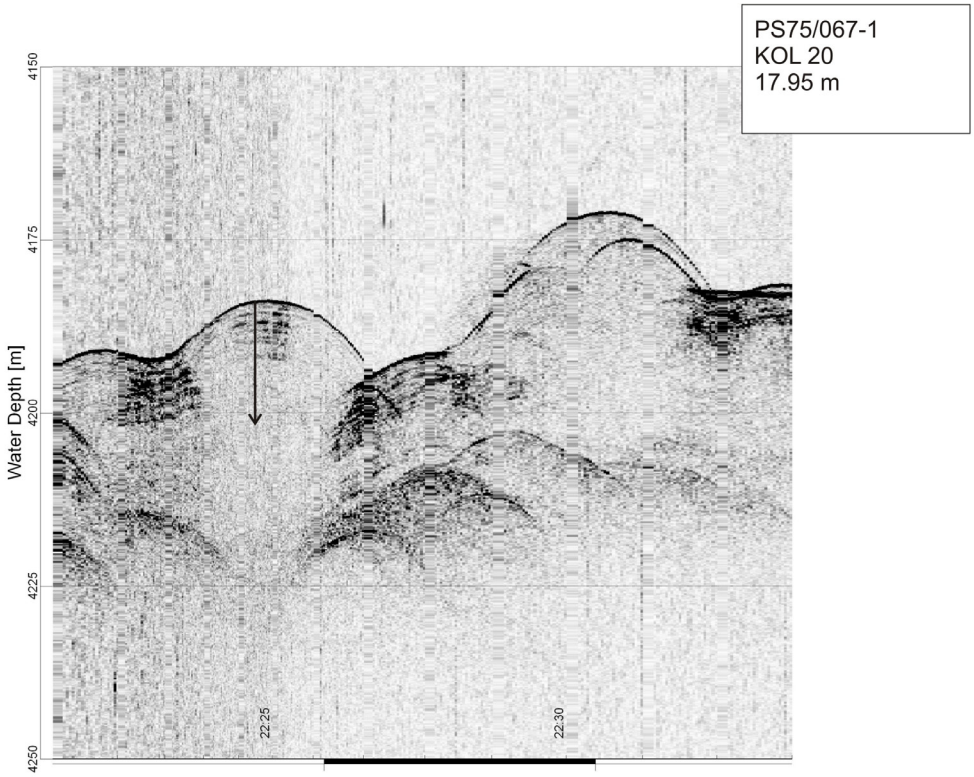
PS75/067-1
KOL 20
17.95 m
Water Depth [m]
4150
4175
4200
4225
4250
22:25
22:30

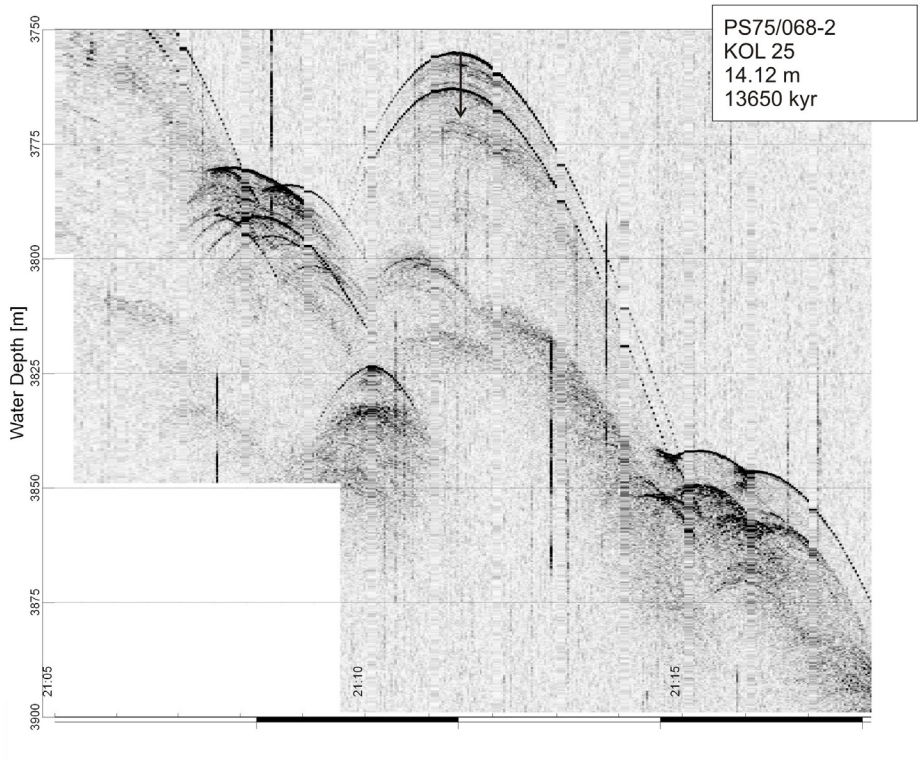
PS75/068-2
KOL 25
14.12 m
13650 kyr
Water Depth [m]
3750
3775
3800
3825
3850
3875
3900
21:05
21:10
21:15

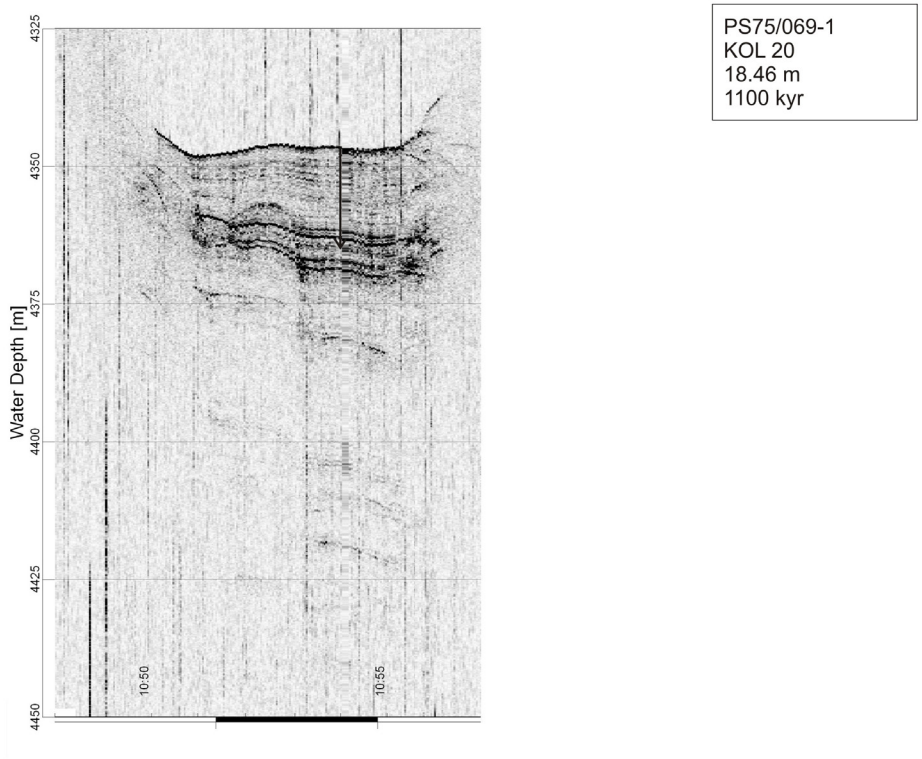
PS75/069-1
KOL 20
18.46 m
1100 kyr
Water Depth [m]
4325
4350
4375
4400
4425
4450
10:50
10:55

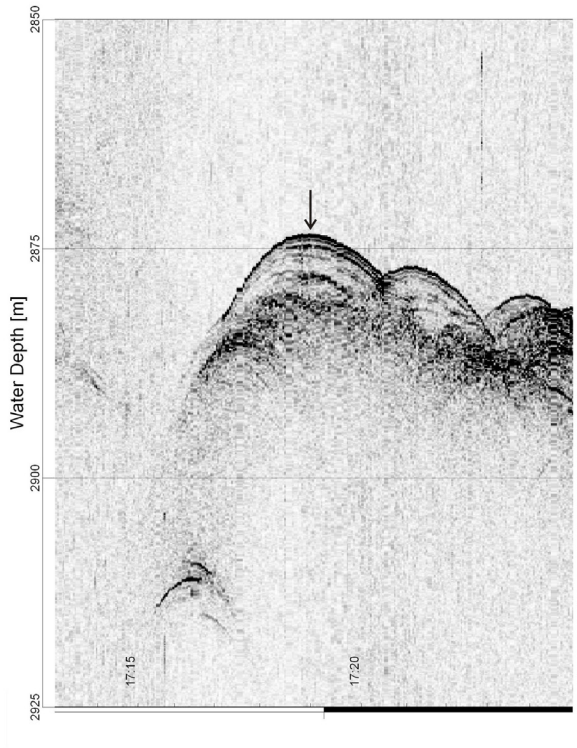
PS75/070-2
KOL 15
0 m (tube lost)
Water Depth [m]
2850
2875
2900
2925
17:15
17:20

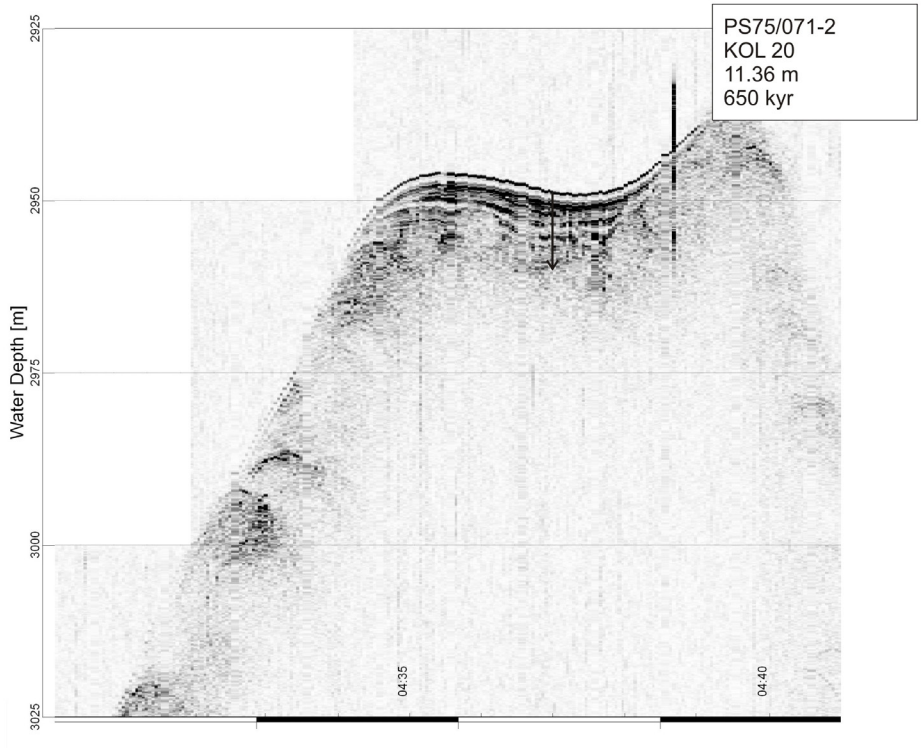
PS75/071-2
KOL 20
11.36 m
650 kyr
Water Depth [m]
2925
2950
2975
3000
3025
04:35
04:40

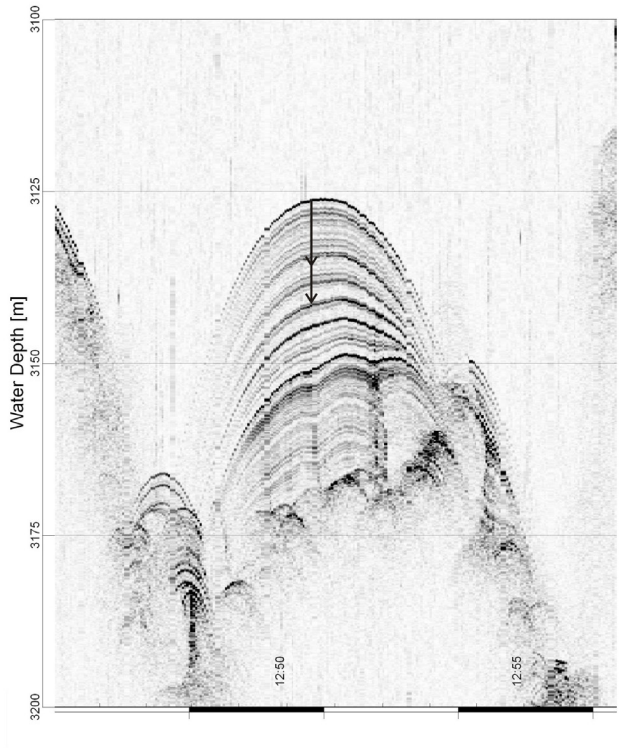


PS75/072-2
KOL 20
14.97 m
420 kyr

PS75/072-4
SL 13
9,61 m
280 kyr

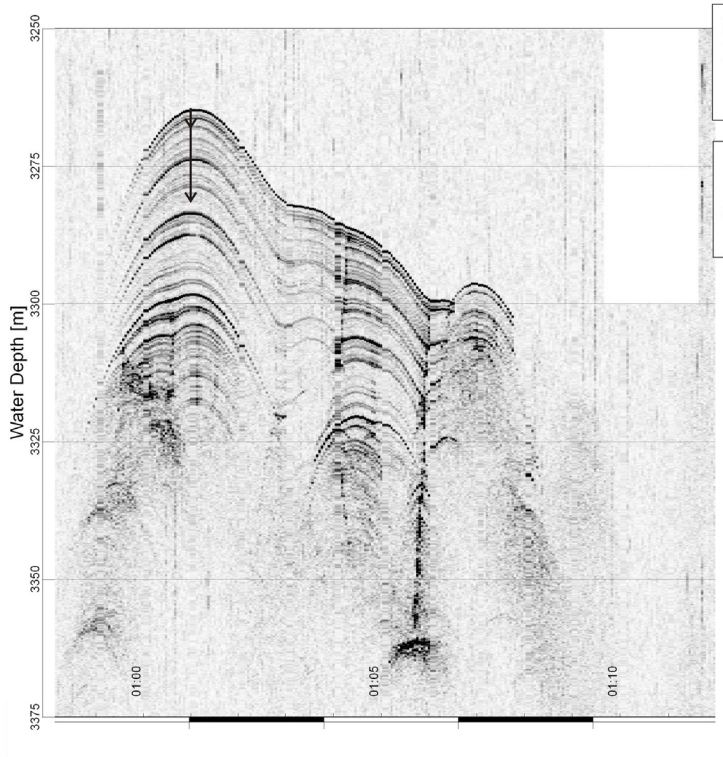


PS75/073-1
KOL 25
17.04 m
190 kyr

PS75/073-2
KAL 12
3.68 m
190 kyr

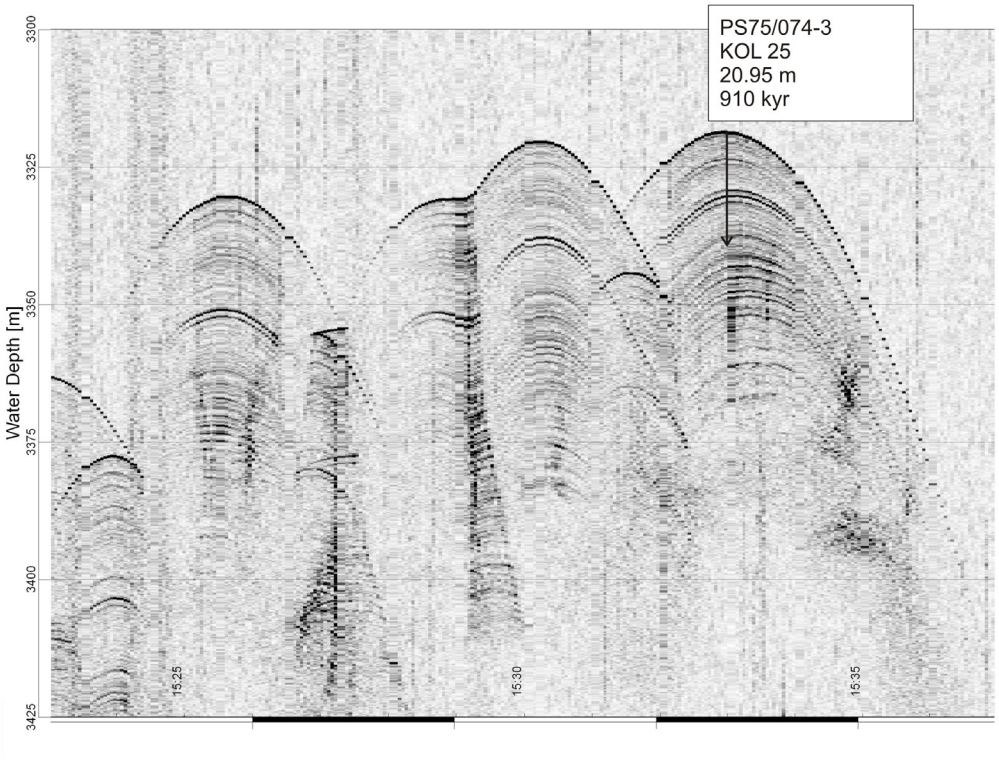
PS75/074-3
KOL 25
20.95 m
910 kyr
Water Depth [m]
3300
3325
3350
3375
3400
3425
15:25
15:30
15:35

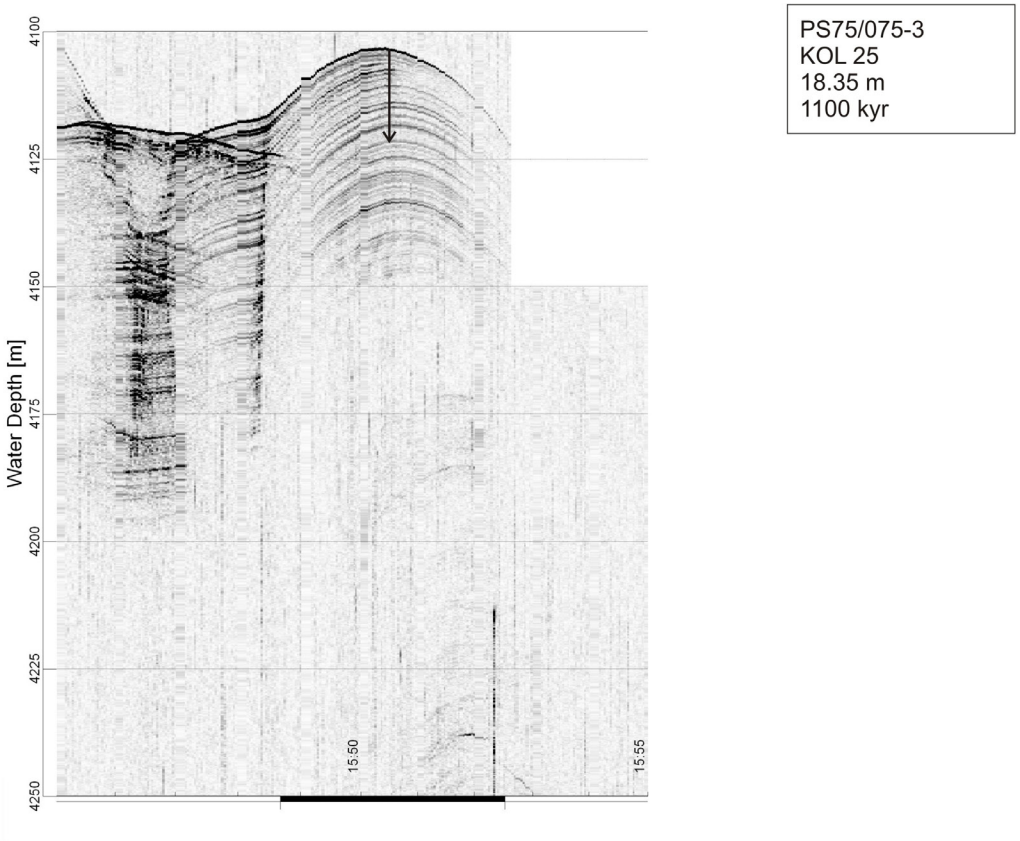
PS75/075-3
KOL 25
18.35 m
1100 kyr
Water Depth [m]
4100
4125
4150
4175
4200
4225
4250
15:50
15:55

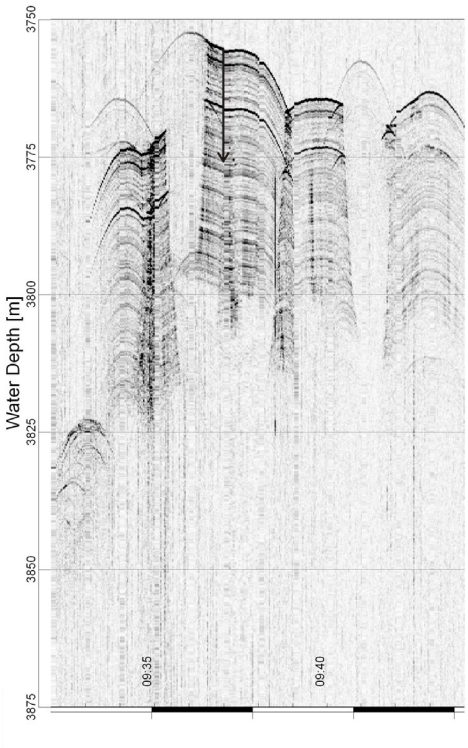


PS75/076-2
KOL 25
20.59 m
1100 kyr

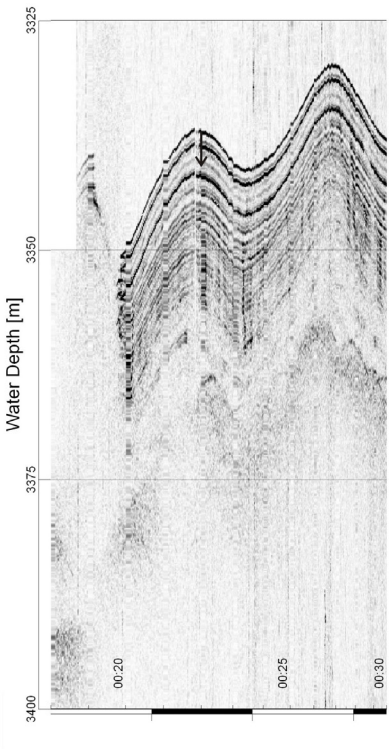


PS75/078-1
SL 15
3.83 m
190 kyr

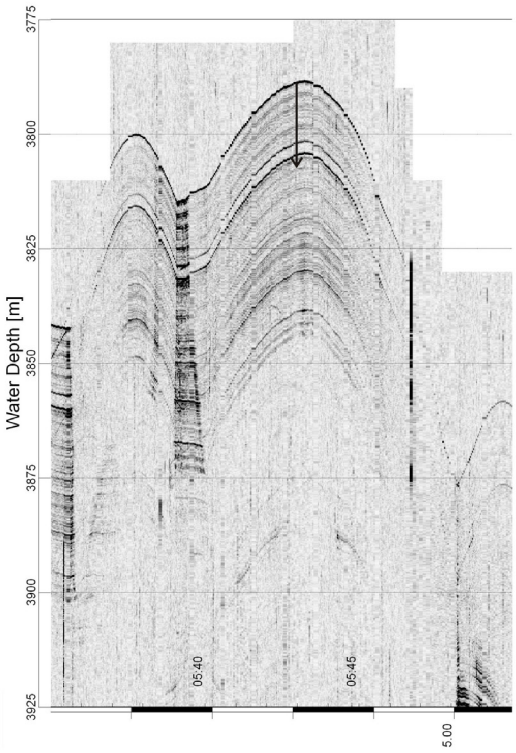


PS75/079-2
KOL 20
18.51 m
420 kyr

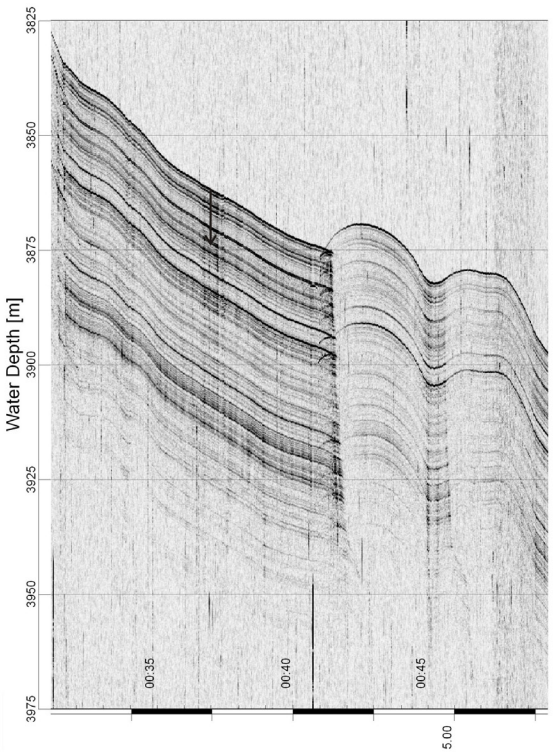


PS75/080-1
KOL 25
12.20 m
190 kyr

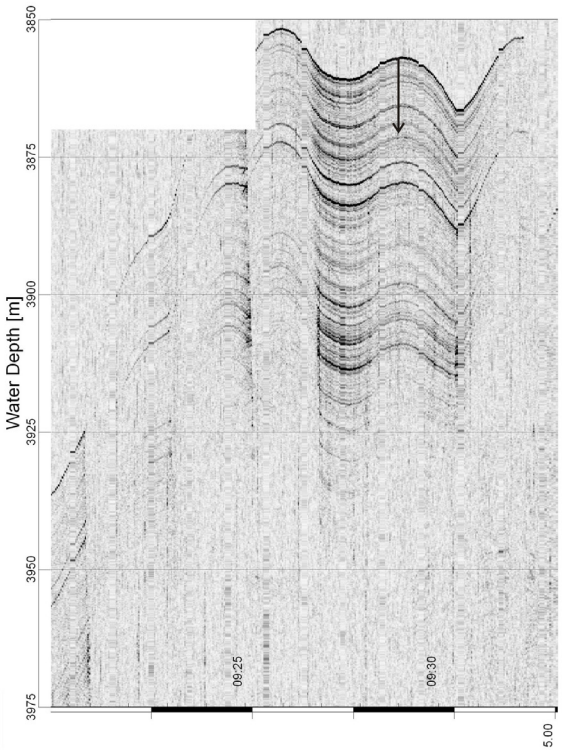


PS75/081-1
KOL 20
13.71 m
160 kyr

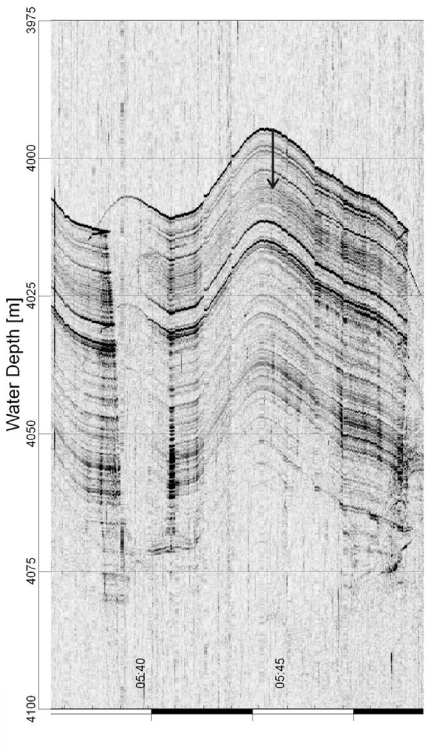


PS75/082-1
KOL 20
10.88 m
160 kyr

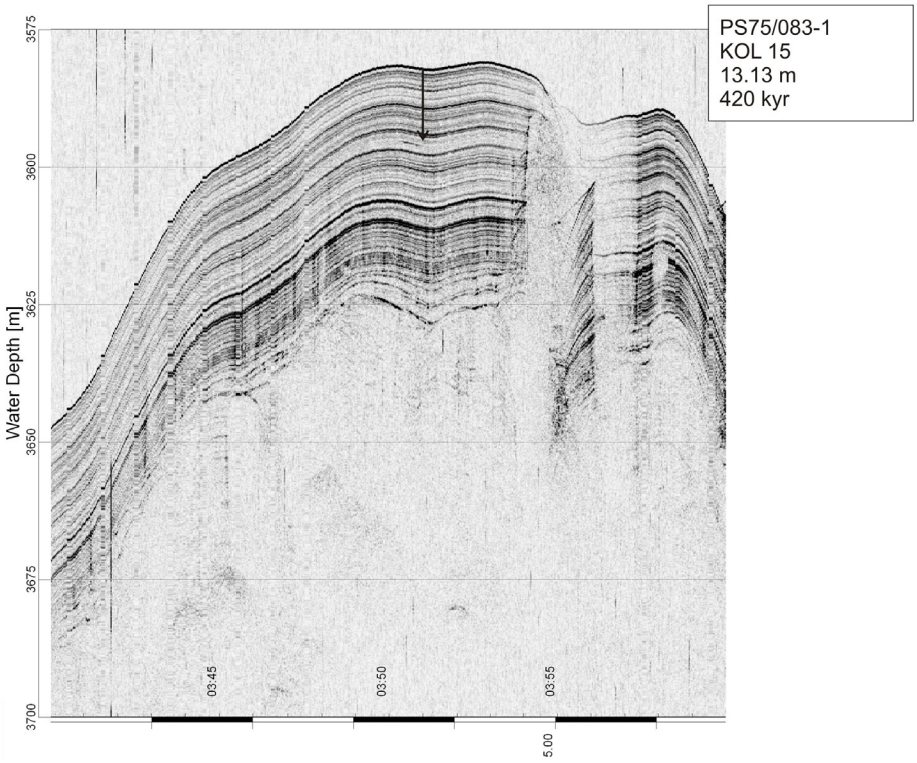
PS75/083-1
KOL 15
13.13 m
420 kyr
Water Depth [m]
3575
3600
3625
3650
3675
3700
03:45
03:50
03:55
5.00

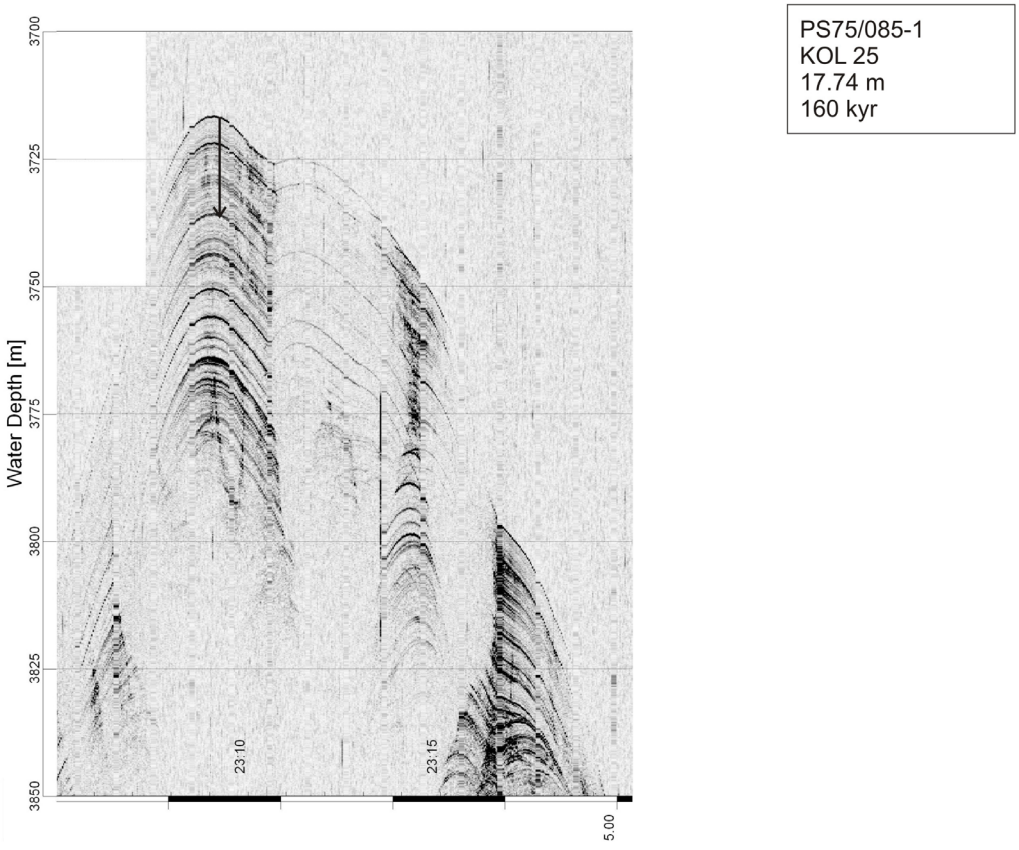
PS75/085-1
KOL 25
17.74 m
160 kyr
Water Depth [m]
3700
3725
3750
3775
3800
3825
3850
23:10
23:15
5.00

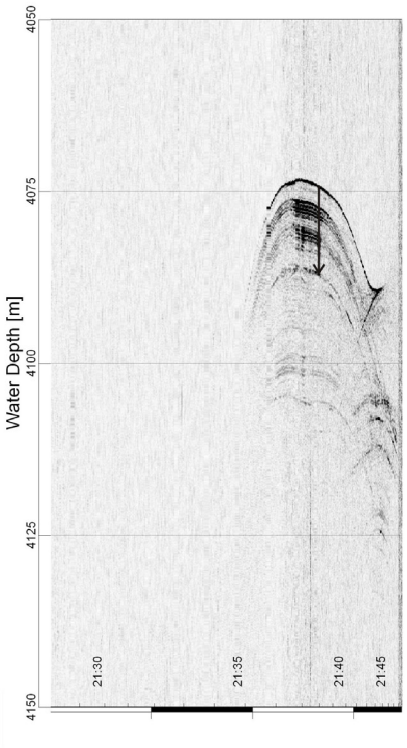


PS75/086-2
SL 13
12.74 m
2800 kyr

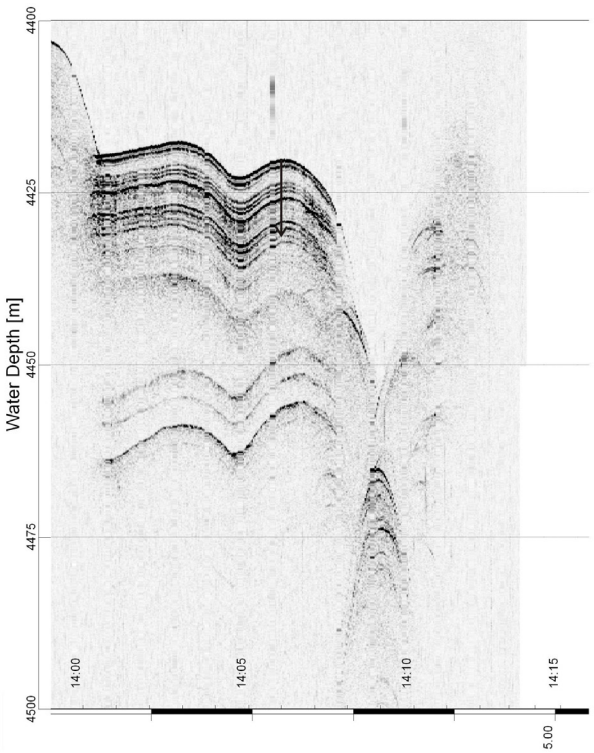


PS75/087-1
SL 13
11.28 m
3500 kyr

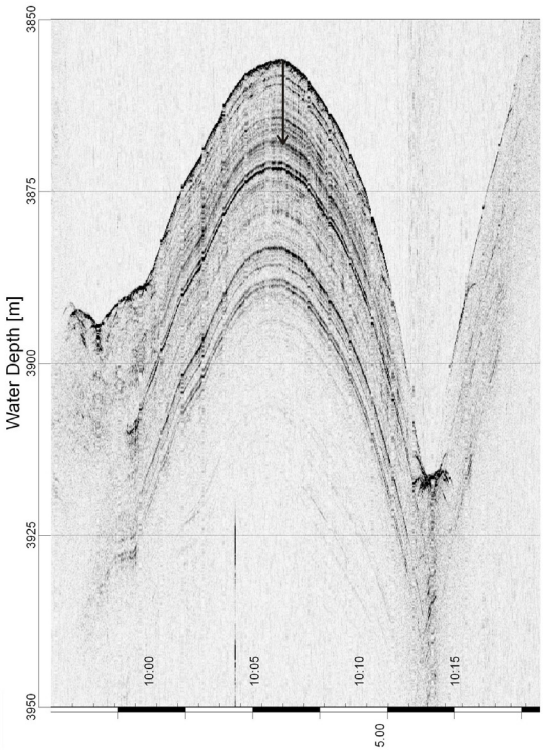


PS75/088-6
SL 15
12.40 m

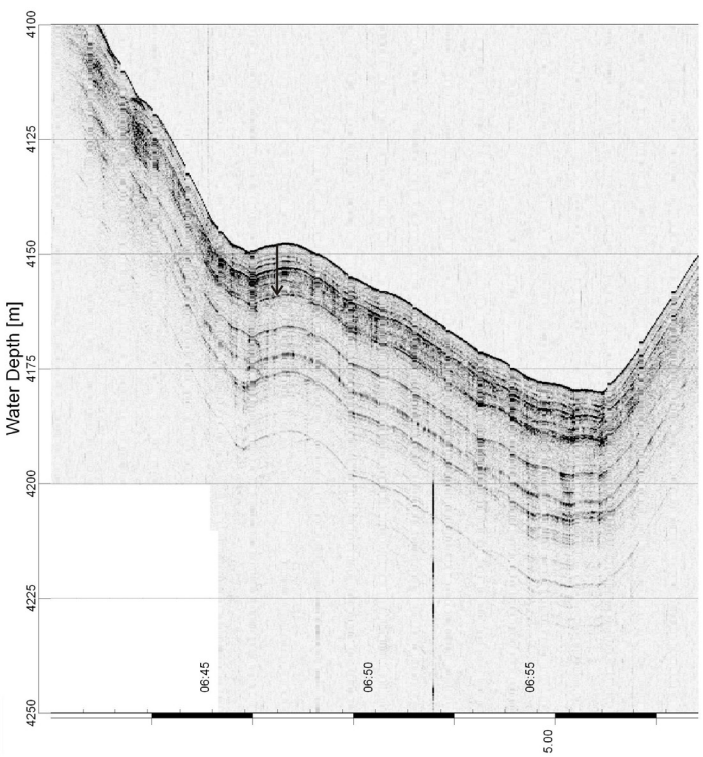


PS75/089-3
SL 20
11.12 m
3500 kyr

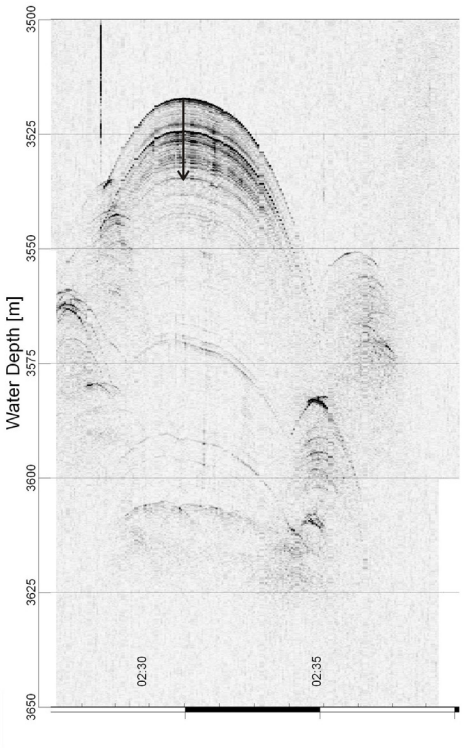


PS75/090-3
KOL 20
17.91 m
3000 kyr

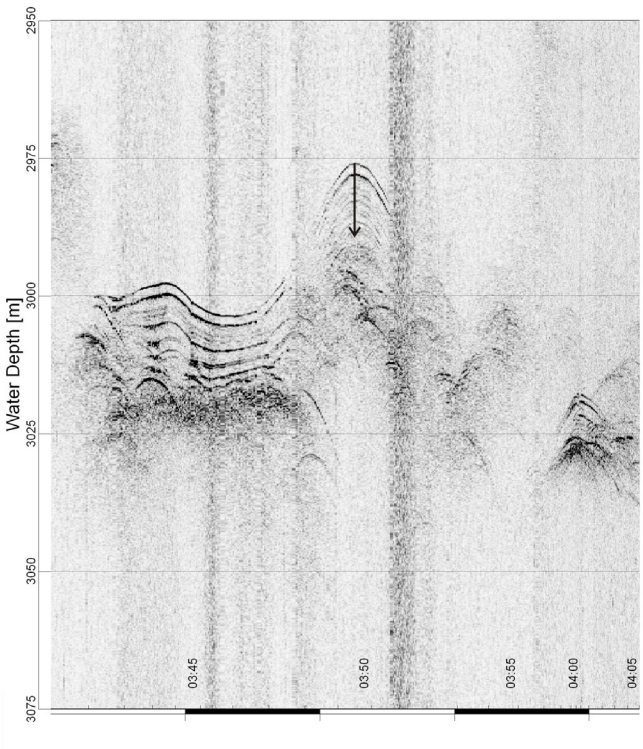


PS75/091-3
KOL 15
13.44 m
1100 kyr

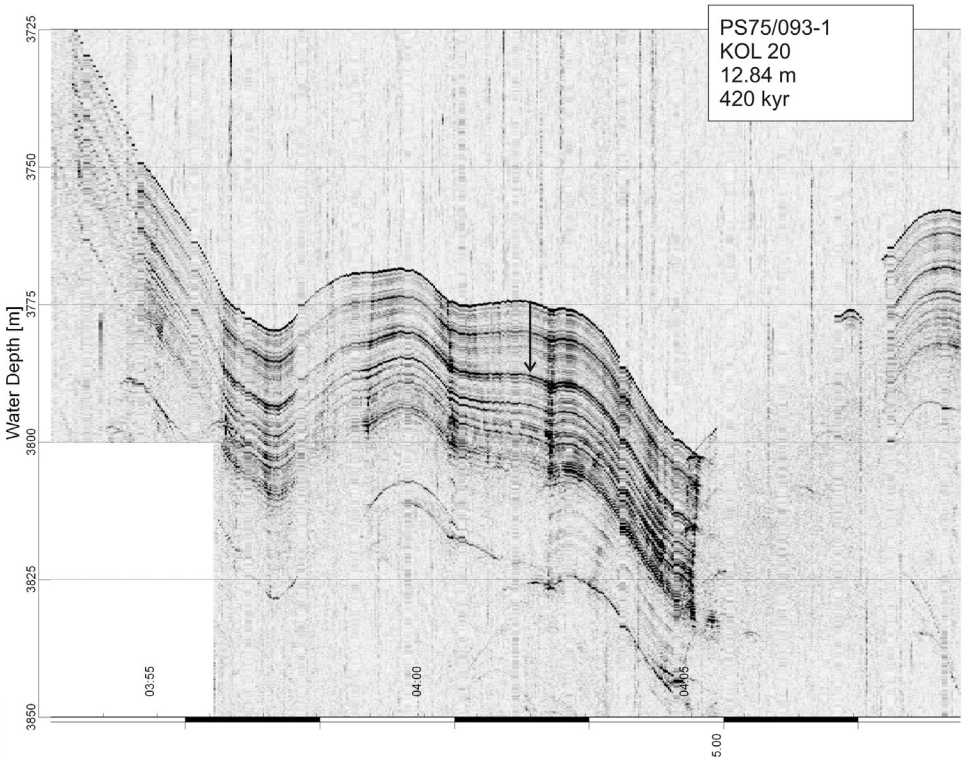
PS75/093-1
KOL 20
12.84 m
420 kyr
Water Depth [m]
3725
3750
3775
3800
3825
3850
03:55
04:00
04:05
5.00

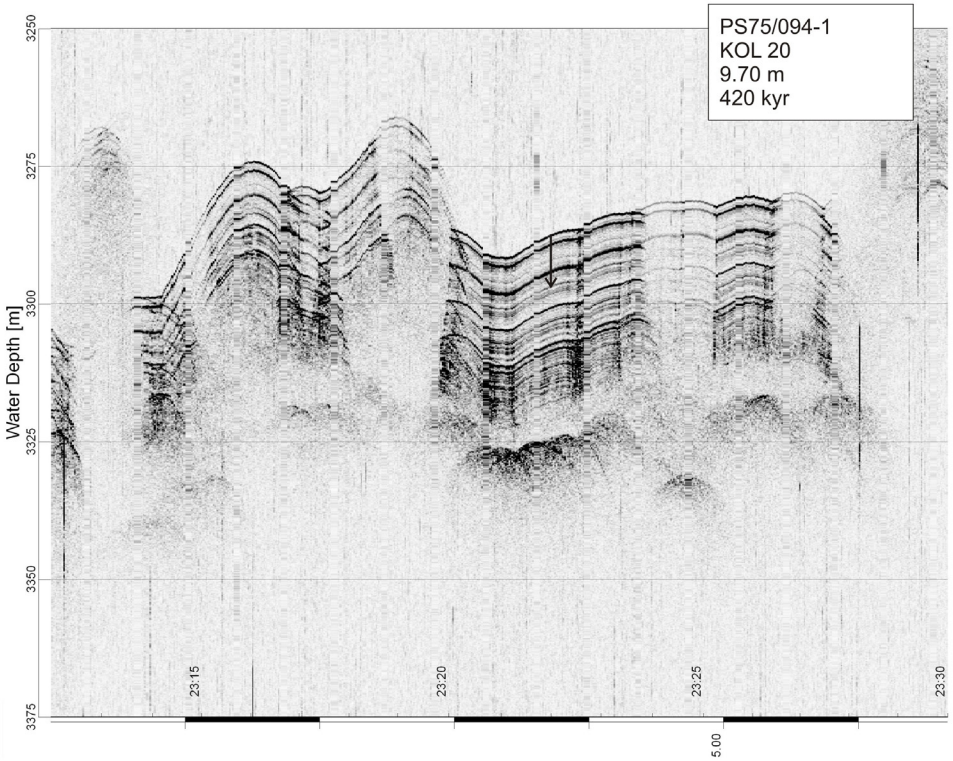
PS75/094-1
KOL 20
9.70 m
420 kyr
Water Depth [m]
3250
3275
3300
3325
3350
3375
23:15
23:20
23:25
23:30
5.00

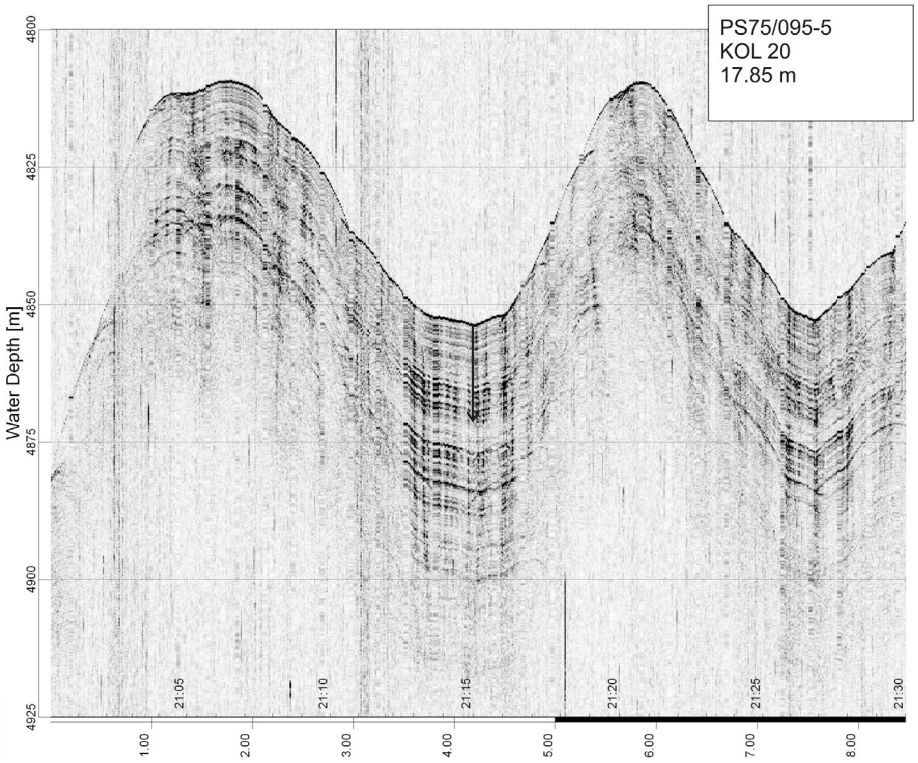
PS75/095-5
KOL 20
17.85 m
Water Depth [m]
4800
4825
4850
4875
4900
4925
21:05
21:10
21:15
21:20
21:25
21:30
1.00
2.00
3.00
4.00
5.00
6.00
7.00
8.00

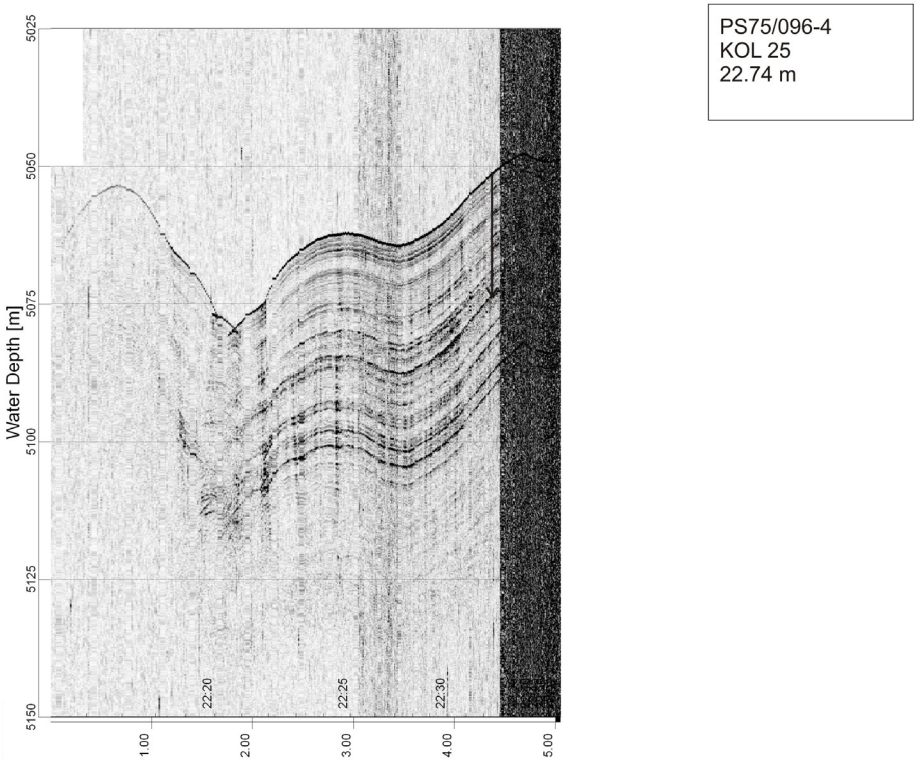
PS75/096-4
KOL 25
22.74 m
Water Depth [m]
5025
5050
5075
5100
5125
5150
22:20
22:25
22:30
1.00
2.00
3.00
4.00
5.00

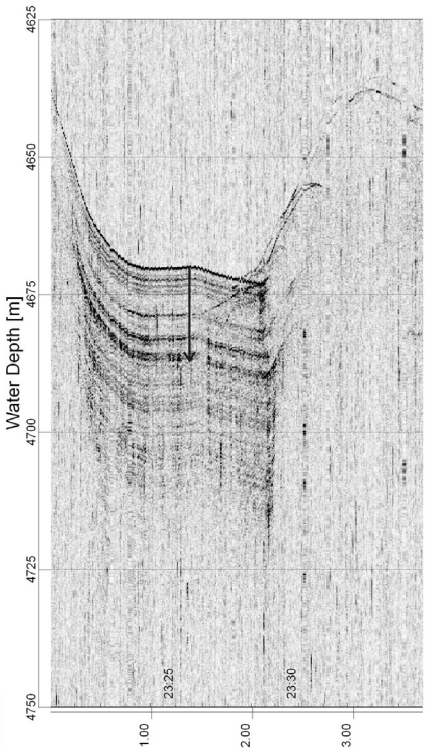


PS75/097-4
KOL 20
17.46 m

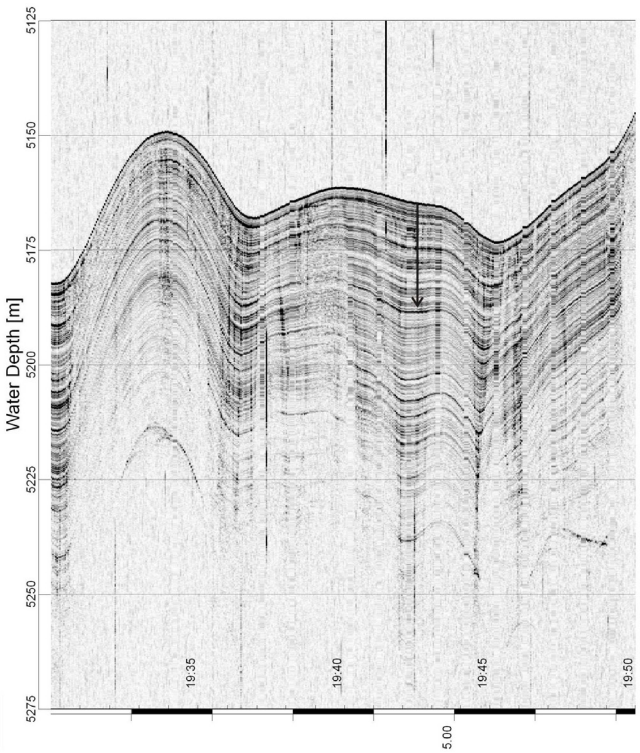


PS75/098-4
KOL 25
22.83 m
600 kyr

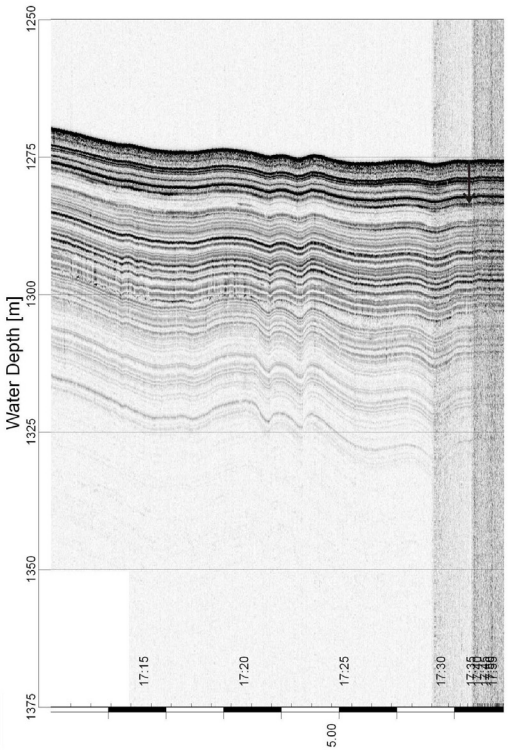


PS75/099-4
KOL 15
7.71 m
~400 kyr

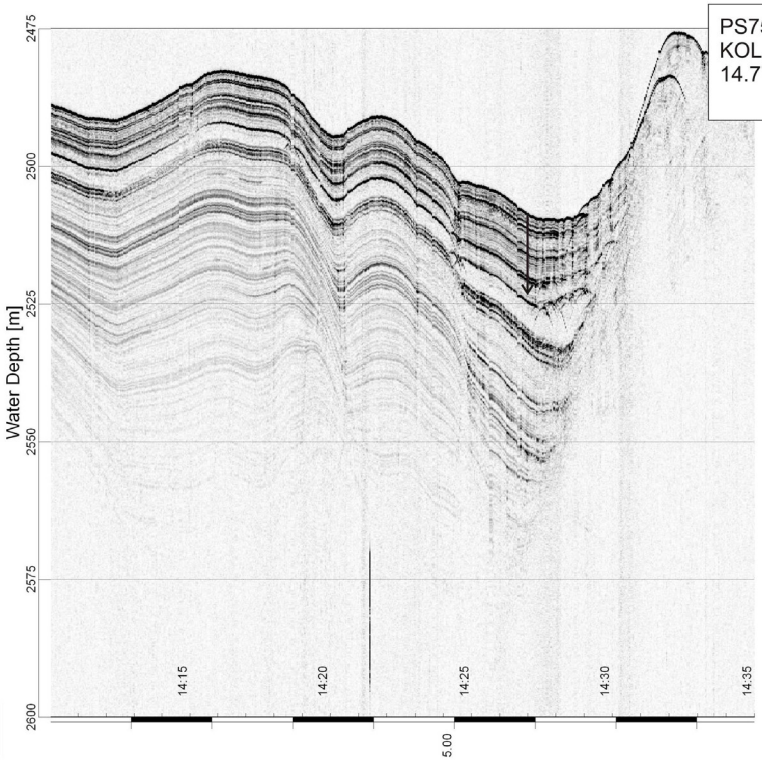


PS75/100-4
KOL 20
14.77 m

# A.7 VISUAL CORE DESCRIPTIONS

## Legend:

### Lithology (biogenic-diatoms):


diatom ooze


radiolarian-bearing diatom ooze

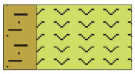
mud-bearing diatom ooze


foraminifera-bearing diatom ooze


nannofossil-bearing diatom ooze


foraminifera- and nannofossil-bearing diatom ooze


nannofossil- and foraminifera-bearing diatom ooze


radiolaria- and foraminifera-bearing diatom ooze


mud- and radiolaria-bearing diatom ooze


foraminifera- and radiolaria-bearing diatom ooze


mud- and nannofossil-bearing diatom ooze


mud- and foraminifera-bearing diatom ooze


nannofossil- and mud-bearing diatom ooze


foraminifera- and mud-bearing diatom ooze


radiolaria-, nannofossil- and foraminifera-bearing diatom ooze

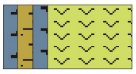
nannofossil-, mud- and foraminifera-bearing diatom ooze

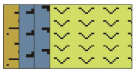
mud-, nannofossil- and foraminifera-bearing diatom ooze

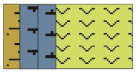
mud-, foraminifera- and nannofossil-bearing diatom ooze


mud-, foraminifera-, radiolaria-, and nannofossil-bearing diatom ooze

### Lithology (biogenic-foraminifera):

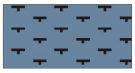
foraminiferal ooze

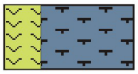
diatom-bearing foraminiferal ooze

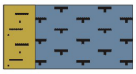
mud-bearing foraminiferal ooze

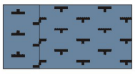
nannofossil-bearing foraminiferal ooze

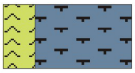
radiolaria-bearing foraminiferal ooze

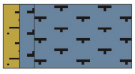
mud- and nannofossil-bearing foraminiferal ooze

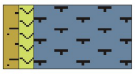
mud- and diatom-bearing foraminiferal ooze

### Lithology (siliciclastic):

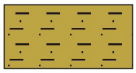
mud

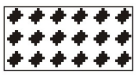
dropstones

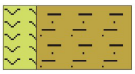
diatom-bearing mud

## Lithology (biogenic-nannofossils):


nannofossil ooze

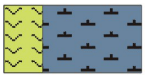
diatom-bearing nannofossil ooze

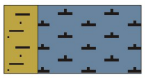
mud-bearing nannofossil ooze

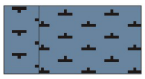
foraminifera-bearing nannofossil ooze

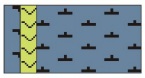
foraminifera- and diatom-bearing nannofossil ooze

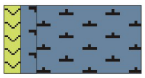
diatom- and foraminifera-bearing nannofossil ooze

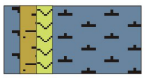
foraminifera-, mud- and diatom-bearing nannofossil ooze

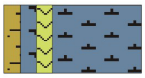
mud-, foraminifera- and diatom-bearing nannofossil ooze

## Lithology (biogenic-two components):


nannofossil and diatom ooze


muddy diatom ooze

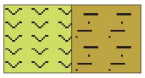
diatomaceous mud


foraminiferal and diatom ooze

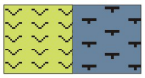
diatom and foraminiferal ooze


diatom and nannofossil ooze

## Lithology (biogenic-two components, continued):


nannofossil and foraminiferal ooze

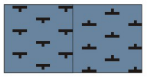
foraminiferal and nannofossil ooze

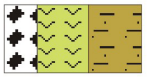
IRD-bearing diatomaceous mud

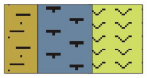
mud-bearing foraminiferal and diatom ooze

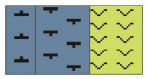
nannofossil-bearing foraminiferal and diatom ooze

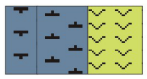
foraminifera-bearing nannofossil and diatom ooze

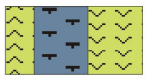
radiolaria-bearing foraminiferal and diatom ooze

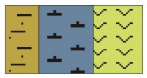
mud-bearing nannofossil and diatom ooze

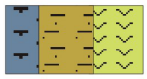
foraminifera-bearing muddy diatom ooze


radiolaria-bearing muddy diatom ooze


foraminifera-bearing diaton and nannofossil ooze


nannofossil-bearing diatom and foraminiferal ooze

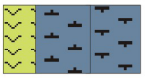
diatom-bearing nannofossil and foraminiferal ooze

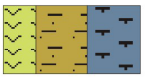
diatom-bearing muddy foraminiferal ooze

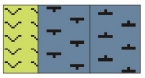
diatom-bearing foraminifer and nannofossil ooze

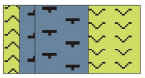
radiolaria- and nannofossil-b foraminiferal and diatom oo

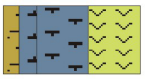
mud- and nannofossil-beari foraminiferal and diatom oo

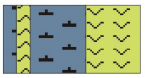
foraminifera- and radiolaria nannofossil and diatom ooz

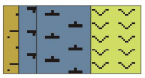
mud- and foraminifera-bea nannofossil and diatom ooz

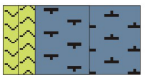
diatom- and radiolaria-bea foraminiferal and nannofoss

## Lithology (biogenic-three components):


nannofossil, foraminiferal and diatom ooze

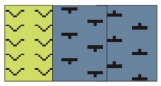
diatom, foraminiferal, and nannofossil ooze

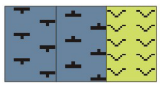
foraminiferal, nannofossil and diatom ooze

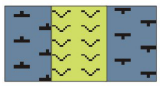
nannofossil, diatom and diatom ooze

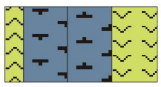
radiolaria-bearing foraminiferal, nannofossil and diatom ooze

## Structure:


sharp boundary


gradational boundary


transition zone


erosive contact

weakly bedded/laminated


bedded/laminated

mm
cm
dm
dimension of bedding


fining upward sequence


coarsening upward sequence

*S* bioturbated (<30% of sediment)
*SS* bioturbated (<30-60% of sediment)
*SSS* bioturbated (>60% of sediment)


manganese nodules


sediment clasts


single dropstone

## Colour

*Munsell value*

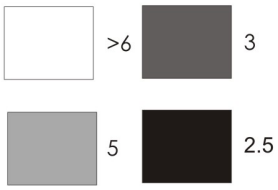

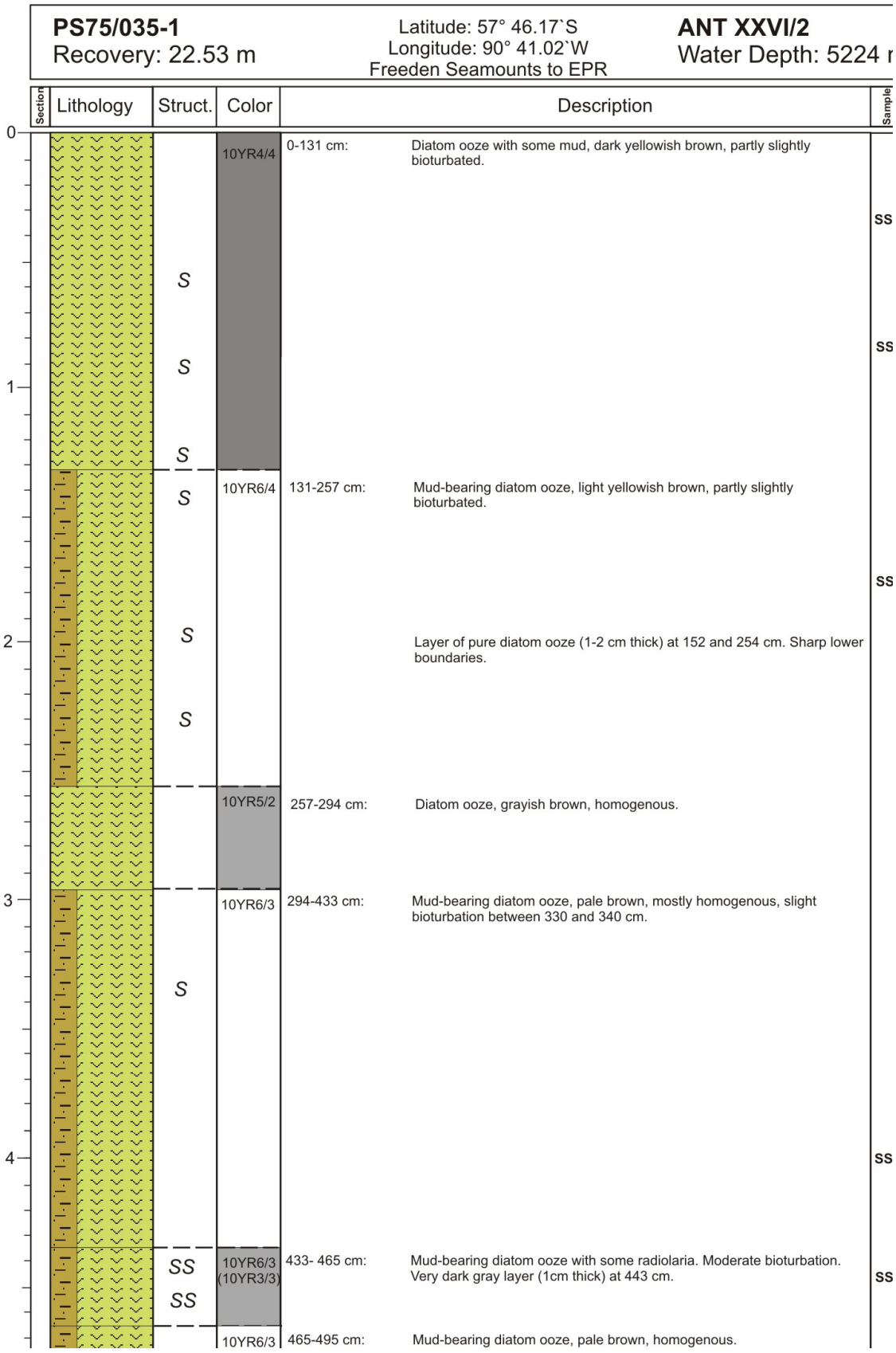
PS75/035-1
Recovery: 22.53 m
Latitude: 57° 46.17`S
Longitude: 90° 41.02`W
Freeden Seamounts to EPR
ANT XXVI/2
Water Depth: 5224 r
Section
Lithology
Struct.
Color
Description
Sample
0
1
2
3
4
10YR4/4
0-131 cm:
Diatom ooze with some mud, dark yellowish brown, partly slightly bioturbated.
S
S
S
SS
SS
10YR6/4
131-257 cm:
Mud-bearing diatom ooze, light yellowish brown, partly slightly bioturbated.
S
S
S
SS
Layer of pure diatom ooze (1-2 cm thick) at 152 and 254 cm. Sharp lower boundaries.
10YR5/2
257-294 cm:
Diatom ooze, grayish brown, homogenous.
10YR6/3
294-433 cm:
Mud-bearing diatom ooze, pale brown, mostly homogenous, slight bioturbation between 330 and 340 cm.
S
SS
10YR6/3
(10YR3/3)
433- 465 cm:
Mud-bearing diatom ooze with some radiolaria. Moderate bioturbation.
Very dark gray layer (1cm thick) at 443 cm.
SS
SS
10YR6/3
465-495 cm:
Mud-bearing diatom ooze, pale brown, homogenous.

**PS75/035-1**
Recovery: 22.53 m

Latitude: 57° 46.17`S
Longitude: 90° 41.02`W
Freeden Seamounts to EPR

**ANT XXVI/2**
Water Depth: 5224 r

| Section | Lithology | Struct. | Color | | Description | Sample |
|---|---|---|---|---|---|---|
| 5 | | S<br>S | 10YR5/2 | 495-539 cm: | Diatom ooze with some mud, dark grayish brown, slightly bioturbated. | |
| | | | 10YR6/3 | 539-566 cm: | Mud bearing diatom ooze, pale brown, homogenous. | |
| | | | 10YR3/1 | 566-580 cm: | Diatom ooze, very dark gray, homogenous. | |
| 6 | | △<br>S | 10YR7/2 | 580-638 cm: | Mud-bearing diatom ooze, light gray, partly slight bioturbation.<br>588-590 cm: Graded sand (mud, radiolarian, and diatom-bearing foraminifera ooze). Likely turbidite. | SS |
| | | ?△ | 10YR8/1 | 638-682 cm: | Nannofossil-diatom ooze with some foraminifera, white. Several thin (0.5-1 cm) coarser layers that may represent distal turbidites. | SS<br>SS |
| | | △ | 10YR8/1 | 682-689 cm: | Sandy layer (diatom and nannofossil-bearing foraminifera ooze) with visible opaque and brown particles. | SS |
| 7 | | ?△ | | 689-762 cm: | Diatom ooze with some mud, very pale brown slightly greenish in the top 10 cm.<br>Thin coarser layer at 718 cm. | SS |
| | | ?△<br>?△<br>?△<br>?△<br>?△ | 10YR6/3 | 762-877 cm: | Diatom ooze with some mud, very pale brown, homogenous. Unit contains numerous thin (0.3-1 cm) coarser layer (light gray foraminifera ooze), most likely representing distal turbidites. | SS |
| 8 | | S<br>?△ | 10YR6/2 | 877-912 cm: | Mud-bearing diatom ooze, light brownish gray, slightly bioturbated. Two thin coarser layers (ca. 0.2 cm). | SS<br>SS |
| 9 | | ?△ | 10YR7/3 and 10YR6/2 and 10YR7/2 | 912-957 cm: | Diatom ooze with some mud. Colour changes on dm-scale between very pale brown, light gray, and light brownish gray.<br>912 and 914 cm: thin coarser layers. | |
| | | | 10YR6/3 (10YR3/1) | 957-1030 cm: | Mud-bearing diatom ooze, primarily very pale brown, a few thin layers of darker sediment (10YR3/1). | |

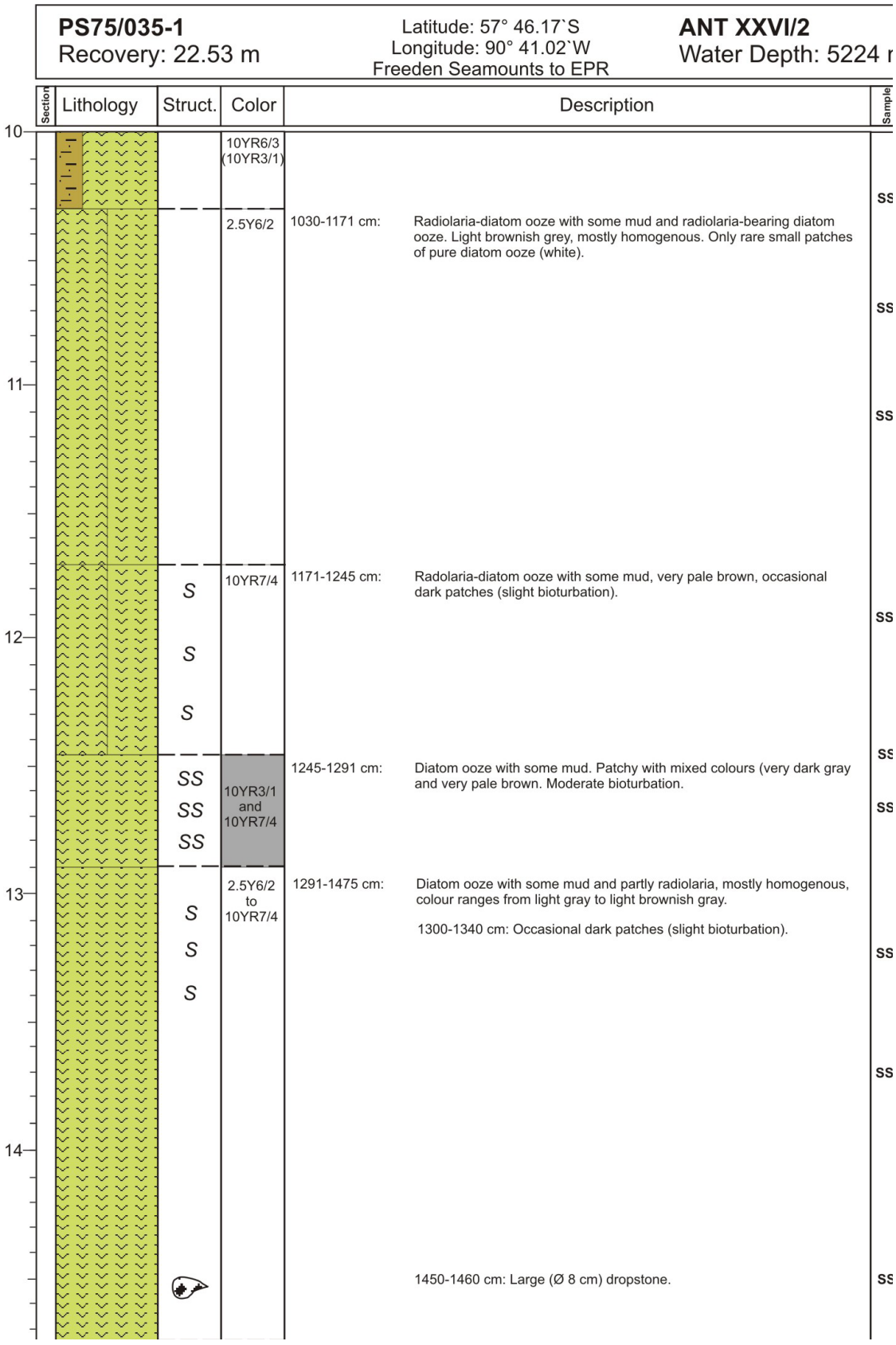
PS75/035-1
Recovery: 22.53 m
Latitude: 57° 46.17`S
Longitude: 90° 41.02`W
Freeden Seamounts to EPR
ANT XXVI/2
Water Depth: 5224 r
Section
Lithology
Struct.
Color
Description
Sample
10
11
12
13
14
10YR6/3
(10YR3/1)
SS
2.5Y6/2
1030-1171 cm:
Radiolaria-diatom ooze with some mud and radiolaria-bearing diatom ooze. Light brownish grey, mostly homogenous. Only rare small patches of pure diatom ooze (white).
SS
SS
S
S
S
10YR7/4
1171-1245 cm:
Radolaria-diatom ooze with some mud, very pale brown, occasional dark patches (slight bioturbation).
SS
SS
SS
SS
10YR3/1
and
10YR7/4
1245-1291 cm:
Diatom ooze with some mud. Patchy with mixed colours (very dark gray and very pale brown. Moderate bioturbation.
SS
S
S
S
2.5Y6/2
to
10YR7/4
1291-1475 cm:
Diatom ooze with some mud and partly radiolaria, mostly homogenous, colour ranges from light gray to light brownish gray.
1300-1340 cm: Occasional dark patches (slight bioturbation).
SS
SS
1450-1460 cm: Large (Ø 8 cm) dropstone.
SS

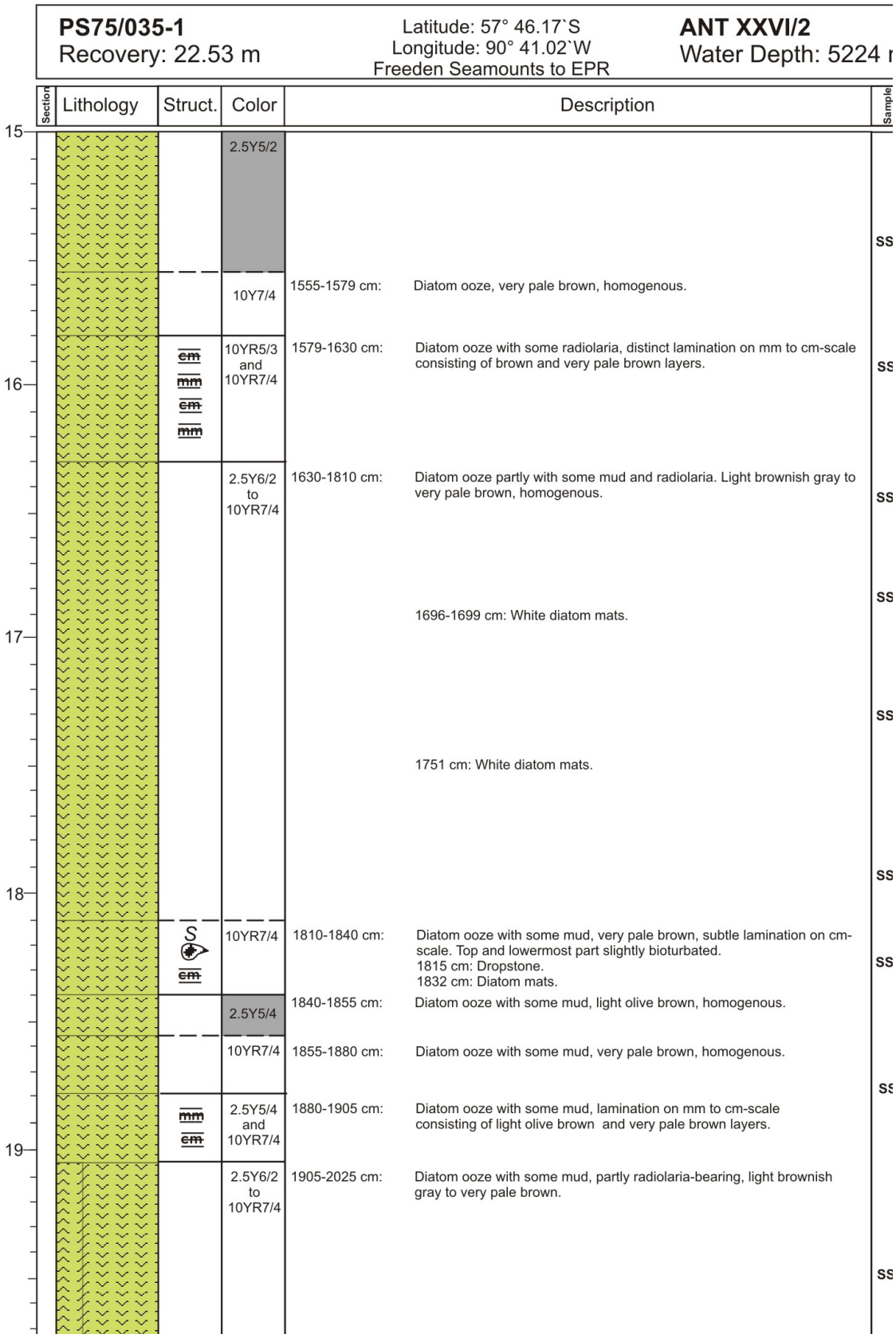
PS75/035-1
Recovery: 22.53 m
Latitude: 57° 46.17`S
Longitude: 90° 41.02`W
Freeden Seamounts to EPR
ANT XXVI/2
Water Depth: 5224 r
Section
Lithology
Struct.
Color
Description
Sample
15
16
17
18
19
2.5Y5/2
10Y7/4
1555-1579 cm: Diatom ooze, very pale brown, homogenous.
10YR5/3 and 10YR7/4
1579-1630 cm: Diatom ooze with some radiolaria, distinct lamination on mm to cm-scale consisting of brown and very pale brown layers.
2.5Y6/2 to 10YR7/4
1630-1810 cm: Diatom ooze partly with some mud and radiolaria. Light brownish gray to very pale brown, homogenous.
1696-1699 cm: White diatom mats.
1751 cm: White diatom mats.
10YR7/4
1810-1840 cm: Diatom ooze with some mud, very pale brown, subtle lamination on cm-scale. Top and lowermost part slightly bioturbated.
1815 cm: Dropstone.
1832 cm: Diatom mats.
2.5Y5/4
1840-1855 cm: Diatom ooze with some mud, light olive brown, homogenous.
10YR7/4
1855-1880 cm: Diatom ooze with some mud, very pale brown, homogenous.
2.5Y5/4 and 10YR7/4
1880-1905 cm: Diatom ooze with some mud, lamination on mm to cm-scale consisting of light olive brown and very pale brown layers.
2.5Y6/2 to 10YR7/4
1905-2025 cm: Diatom ooze with some mud, partly radiolaria-bearing, light brownish gray to very pale brown.
SS

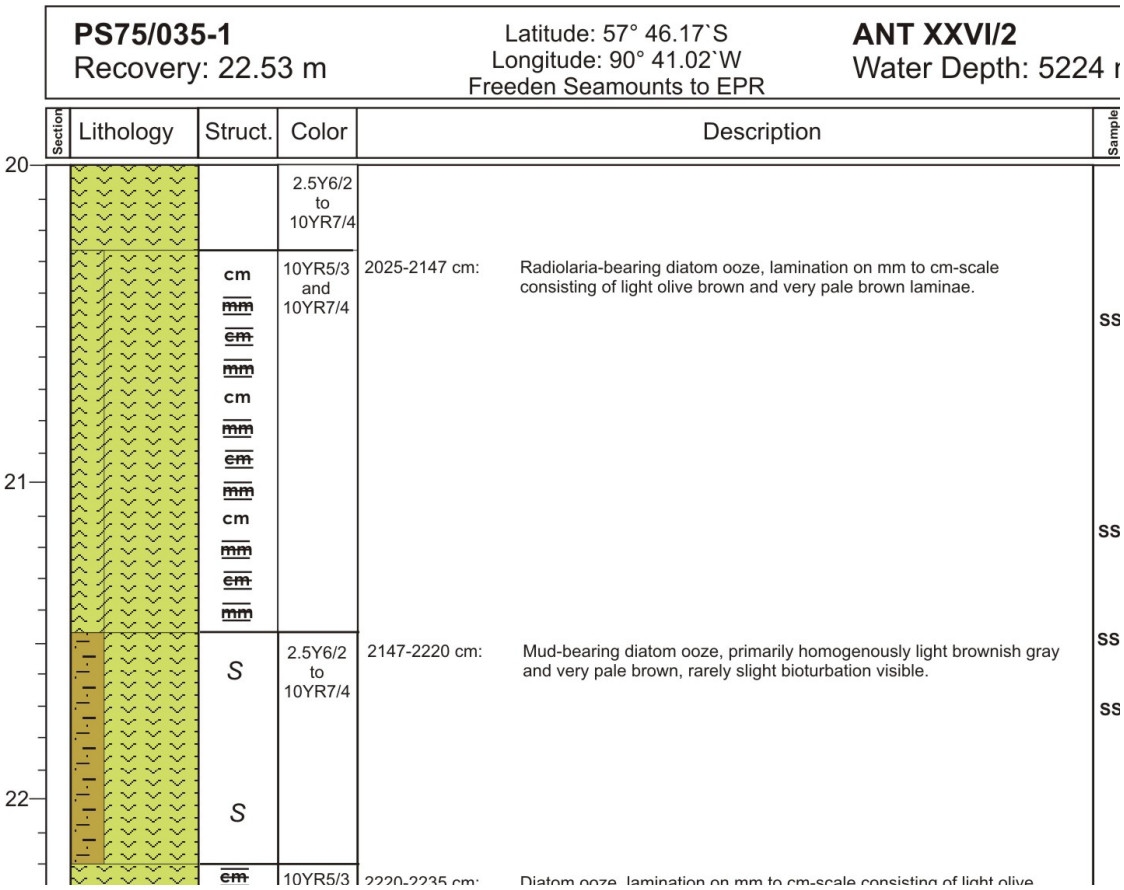
PS75/035-1
Recovery: 22.53 m
Latitude: 57° 46.17`S
Longitude: 90° 41.02`W
Freeden Seamounts to EPR
ANT XXVI/2
Water Depth: 5224 r
Section
Lithology
Struct.
Color
Description
Sample
20
21
22
2.5Y6/2 to 10YR7/4
10YR5/3 and 10YR7/4
2025-2147 cm:
Radiolaria-bearing diatom ooze, lamination on mm to cm-scale consisting of light olive brown and very pale brown laminae.
cm
mm
cm
mm
cm
mm
cm
mm
cm
mm
cm
mm
SS
SS
SS
SS
S
S
2.5Y6/2 to 10YR7/4
2147-2220 cm:
Mud-bearing diatom ooze, primarily homogenously light brownish gray and very pale brown, rarely slight bioturbation visible.
cm
10YR5/3
2220-2235 cm:
Diatom ooze, lamination on mm to cm-scale consisting of light olive

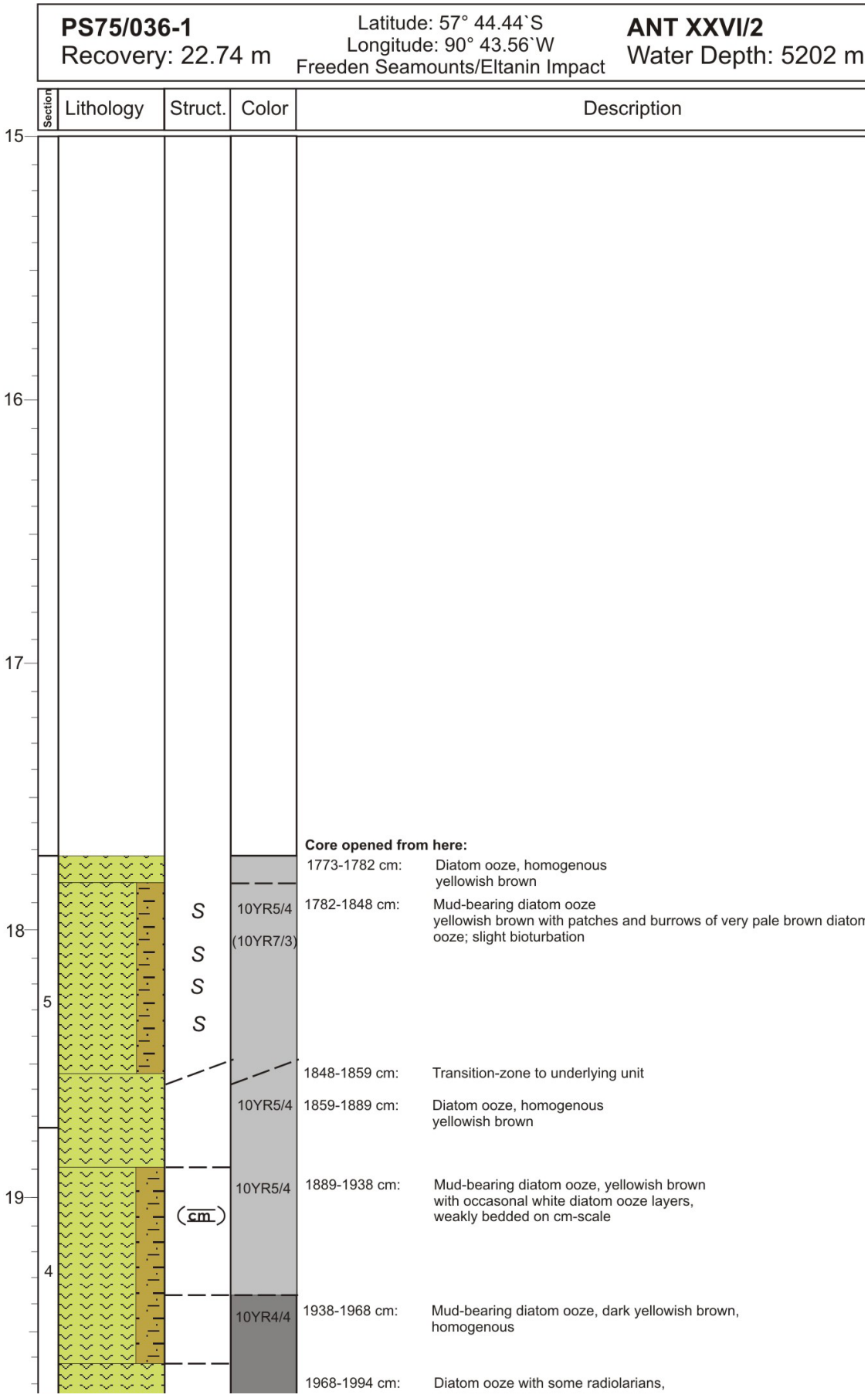
PS75/036-1
Recovery: 22.74 m
Latitude: 57° 44.44`S
Longitude: 90° 43.56`W
Freeden Seamounts/Eltanin Impact
ANT XXVI/2
Water Depth: 5202 m
Section
Lithology
Struct.
Color
Description
15
16
17
18
19
5
4
S
S
S
S
(cm)
10YR5/4
(10YR7/3)
10YR5/4
10YR5/4
10YR4/4
Core opened from here:
1773-1782 cm: Diatom ooze, homogenous yellowish brown
1782-1848 cm: Mud-bearing diatom ooze yellowish brown with patches and burrows of very pale brown diatom ooze; slight bioturbation
1848-1859 cm: Transition-zone to underlying unit
1859-1889 cm: Diatom ooze, homogenous yellowish brown
1889-1938 cm: Mud-bearing diatom ooze, yellowish brown with occasonal white diatom ooze layers, weakly bedded on cm-scale
1938-1968 cm: Mud-bearing diatom ooze, dark yellowish brown, homogenous
1968-1994 cm: Diatom ooze with some radiolarians,

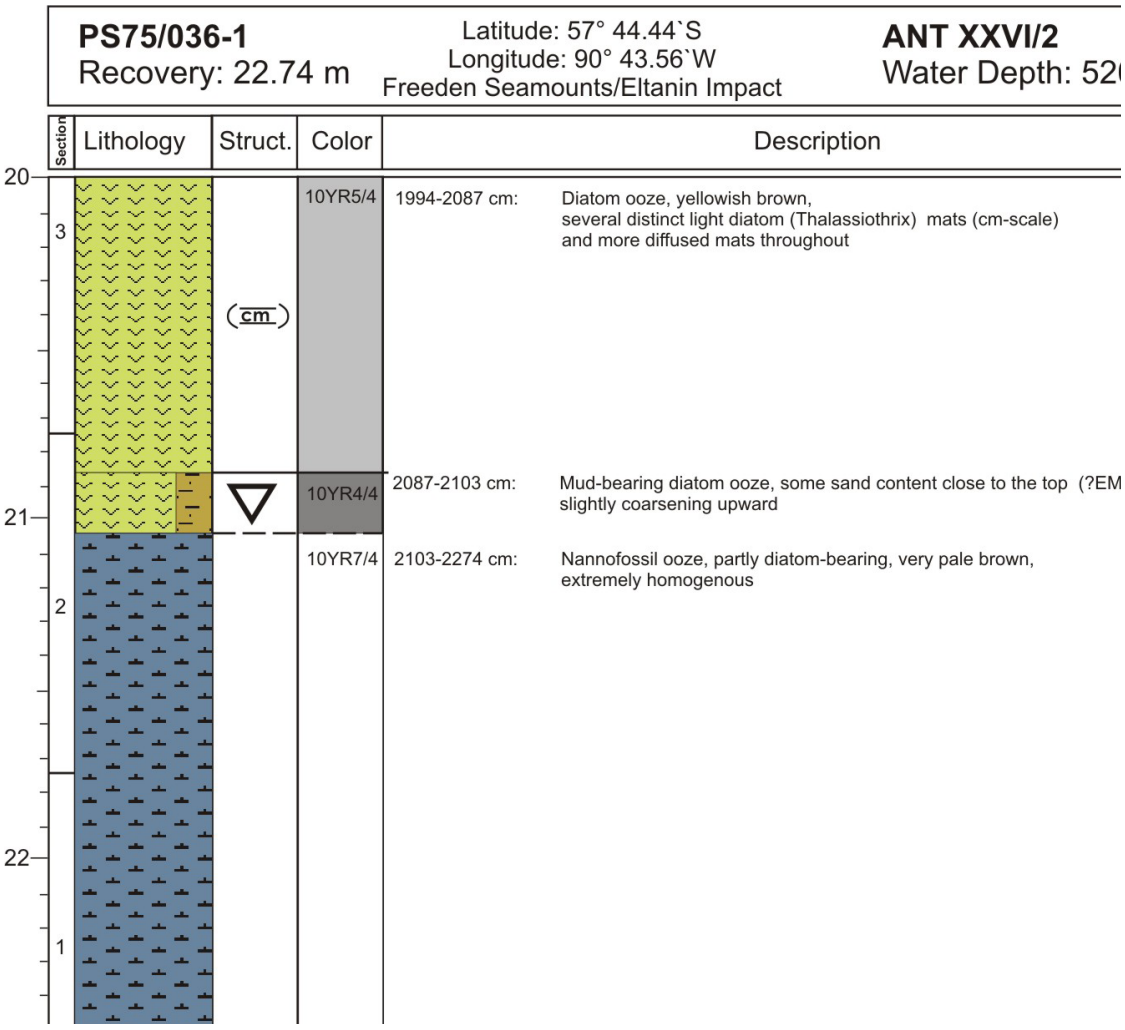
PS75/036-1
Recovery: 22.74 m
Latitude: 57° 44.44`S
Longitude: 90° 43.56`W
Freeden Seamounts/Eltanin Impact
ANT XXVI/2
Water Depth: 52
Section
Lithology
Struct.
Color
Description
20
21
22
3
2
1
cm
10YR5/4
1994-2087 cm:
Diatom ooze, yellowish brown,
several distinct light diatom (Thalassiothrix) mats (cm-scale)
and more diffused mats throughout
10YR4/4
2087-2103 cm:
Mud-bearing diatom ooze, some sand content close to the top (?EM
slightly coarsening upward
10YR7/4
2103-2274 cm:
Nannofossil ooze, partly diatom-bearing, very pale brown,
extremely homogenous

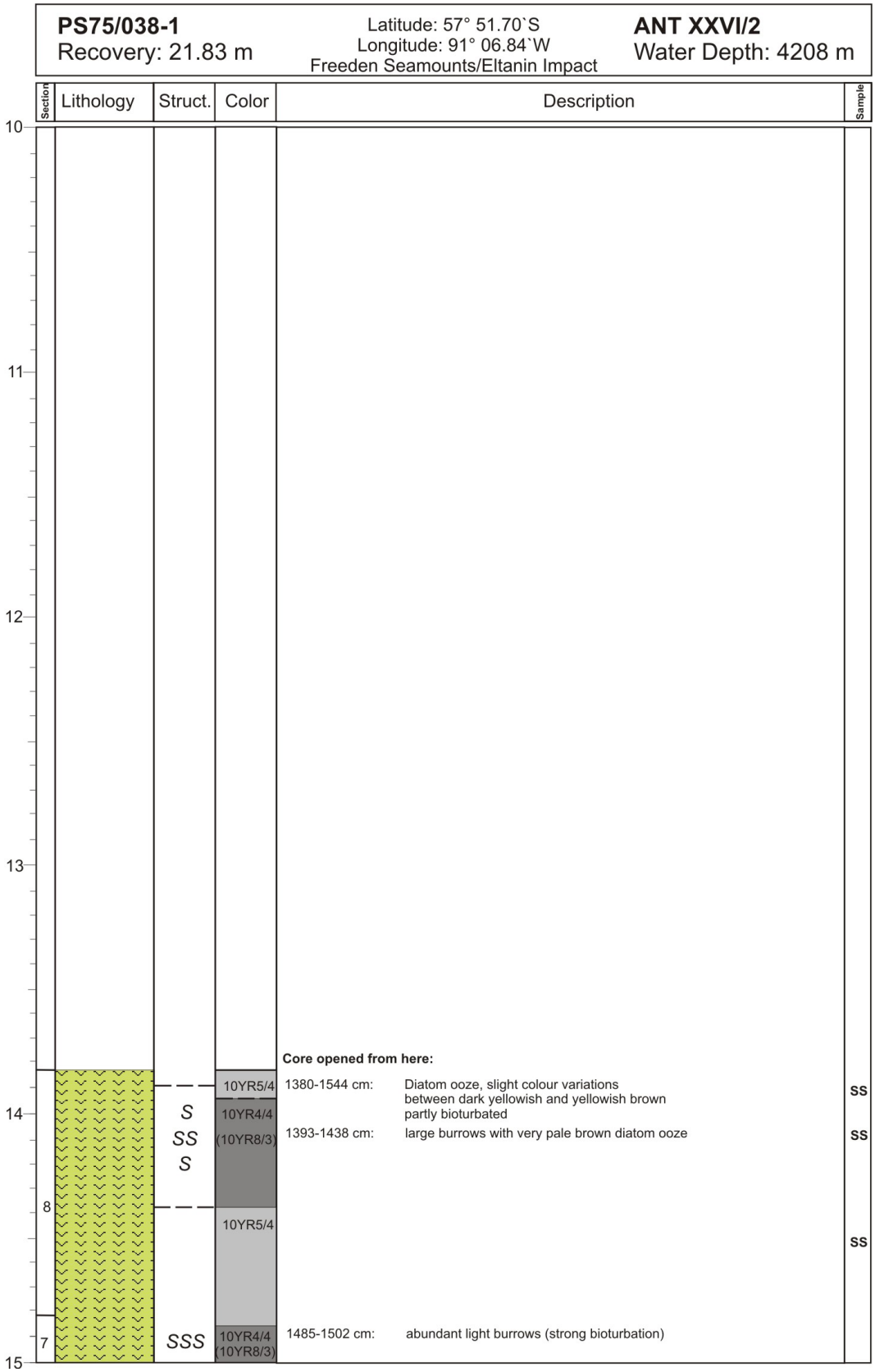
PS75/038-1
Recovery: 21.83 m
Latitude: 57° 51.70`S
Longitude: 91° 06.84`W
Freeden Seamounts/Eltanin Impact
ANT XXVI/2
Water Depth: 4208 m
Section
Lithology
Struct.
Color
Description
Sample
10
11
12
13
14
15
8
7
S
SS
S
SSS
10YR5/4
10YR4/4
(10YR8/3)
10YR5/4
10YR4/4
(10YR8/3)
Core opened from here:
1380-1544 cm:
Diatom ooze, slight colour variations between dark yellowish and yellowish brown partly bioturbated
1393-1438 cm:
large burrows with very pale brown diatom ooze
1485-1502 cm:
abundant light burrows (strong bioturbation)
SS
SS
SS

**PS75/038-1**
Recovery: 21.83 m

Latitude: 57° 51.70`S
Longitude: 91° 06.84`W
Freeden Seamounts/Eltanin Impact

**ANT XXVI/2**
Water Depth: 420

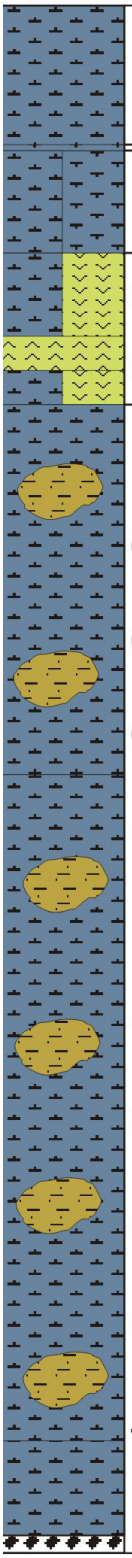

| Struct. | Color | Description |
|---|---|---|
| S<br>S | 10YR4/4 (10YR8/3) | see above |
| cm<br>cm | 10YR4/4 to 10YR6/4 | 1544-1545 cm: Distinct sandy layer (nannofossil-foraminifera ooze) with larger opaque particles partly gravel-size (EMD)<br>1545-1580 cm: Nannofossil-foraminifera ooze, laminated (cm-scale), reworked, light yellowish to dark yellowish brown |
| | 10YR4/4 and 10YR3/3 | 1580-1630 cm: Nannofossil-diatom ooze (dark yellowish brown) with dark brown sediment clasts containing diatom and nannofossil bearing radiolarian ooze, reworked |
| | mixed colours 10YR6/4 and 10YR4/4 and 10YR3/2 | 1630-1750 cm: Chaotic mixture of primarily nannofossil ooze (light yellowish brown) wi dark yellowish brown and dark brown sediment clasts (mostly several c but up to dm-scale). Dark brown sediment clasts contain mud (deep-se clay?).<br>Whole unit reworked |
| | mixed colours 10YR6/4 and 10YR3/3 and 10YR3/2 | 1750-1966 cm: Chaotic mixture of predominantly light yellowish brown nannofossil oo with dark brown and very dark grayish brown muddy sediment clasts.<br>Whole unit reworked.<br>1805 cm: Large (Ø 7 cm) manganese nodule<br>1918 cm: Large (Ø 3-4 cm) manganese nodule<br>1948 cm: Large (Ø 5 cm) manganese nodule |
| | 10YR6/4 | 1966-1976 cm: Inclined abrupt lithology change (erosional)<br>1976-2000 cm: Nannofossil ooze, light yellowish brown, very homogenous.<br>1999 cm: Large black (basalt?) stone (possibly dropstone) |

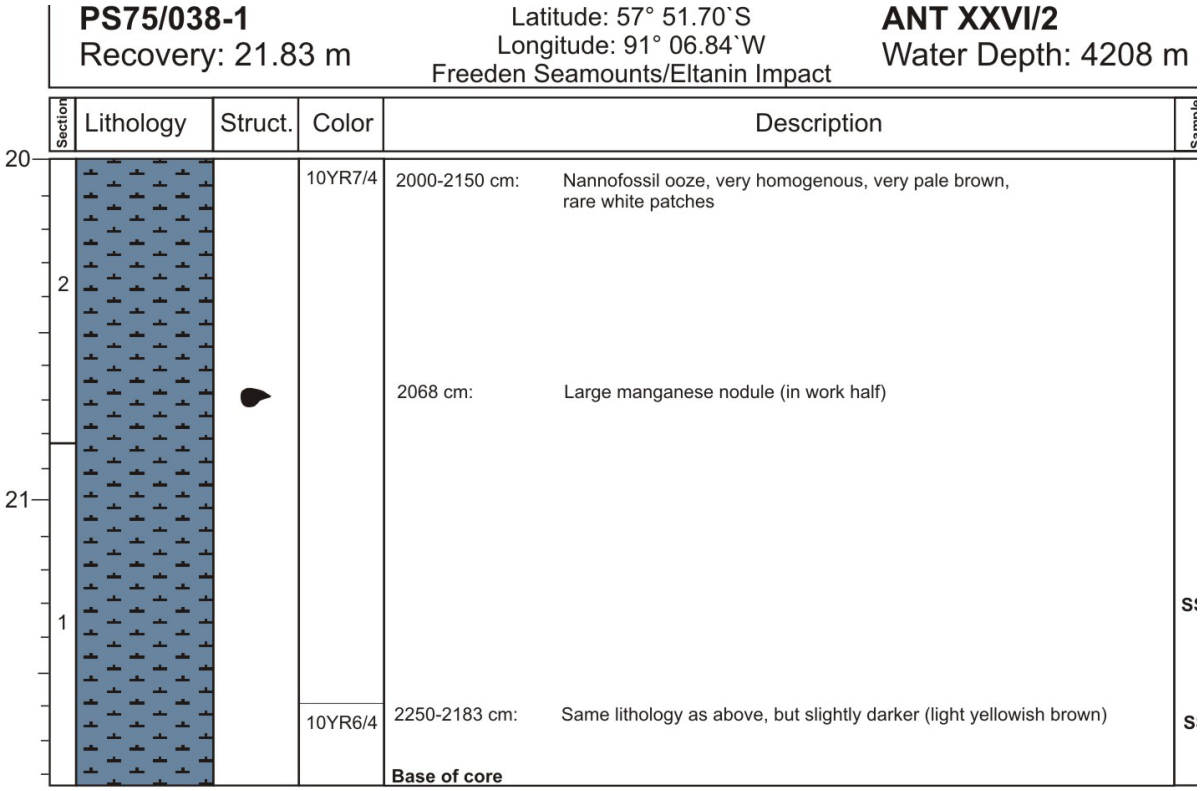
PS75/038-1
Recovery: 21.83 m
Latitude: 57° 51.70`S
Longitude: 91° 06.84`W
Freeden Seamounts/Eltanin Impact
ANT XXVI/2
Water Depth: 4208 m
Section
Lithology
Struct.
Color
Description
20
21
2
1
10YR7/4
2000-2150 cm:
Nannofossil ooze, very homogenous, very pale brown, rare white patches
2068 cm:
Large manganese nodule (in work half)
10YR6/4
2250-2183 cm:
Same lithology as above, but slightly darker (light yellowish brown)
Base of core

**PS75/040-1**
Recovery: 9.36 m

Latitude: 57° 38.88`S
Longitude: 91° 09.14`W
Freeden Seamounts/Eltanin Impact

**ANT XXVI/2**
Water Depth: 4208 m

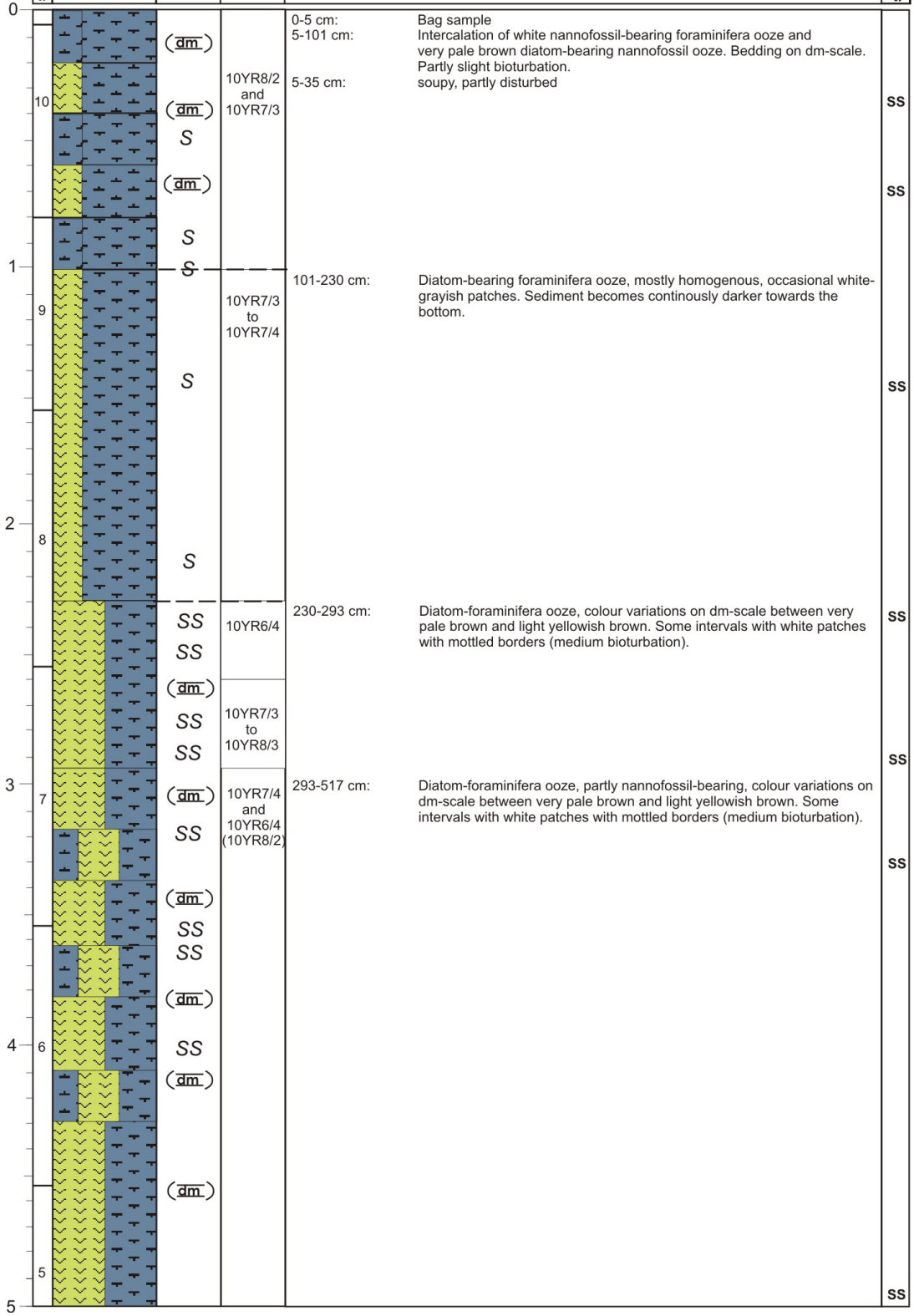

**PS75/040-1**
Recovery: 9.36 m

Latitude: 57° 38.88`S
Longitude: 91° 09.14`W
Freeden Seamounts/Eltanin Impact

**ANT XXVI/2**
Water Depth: 4208 m

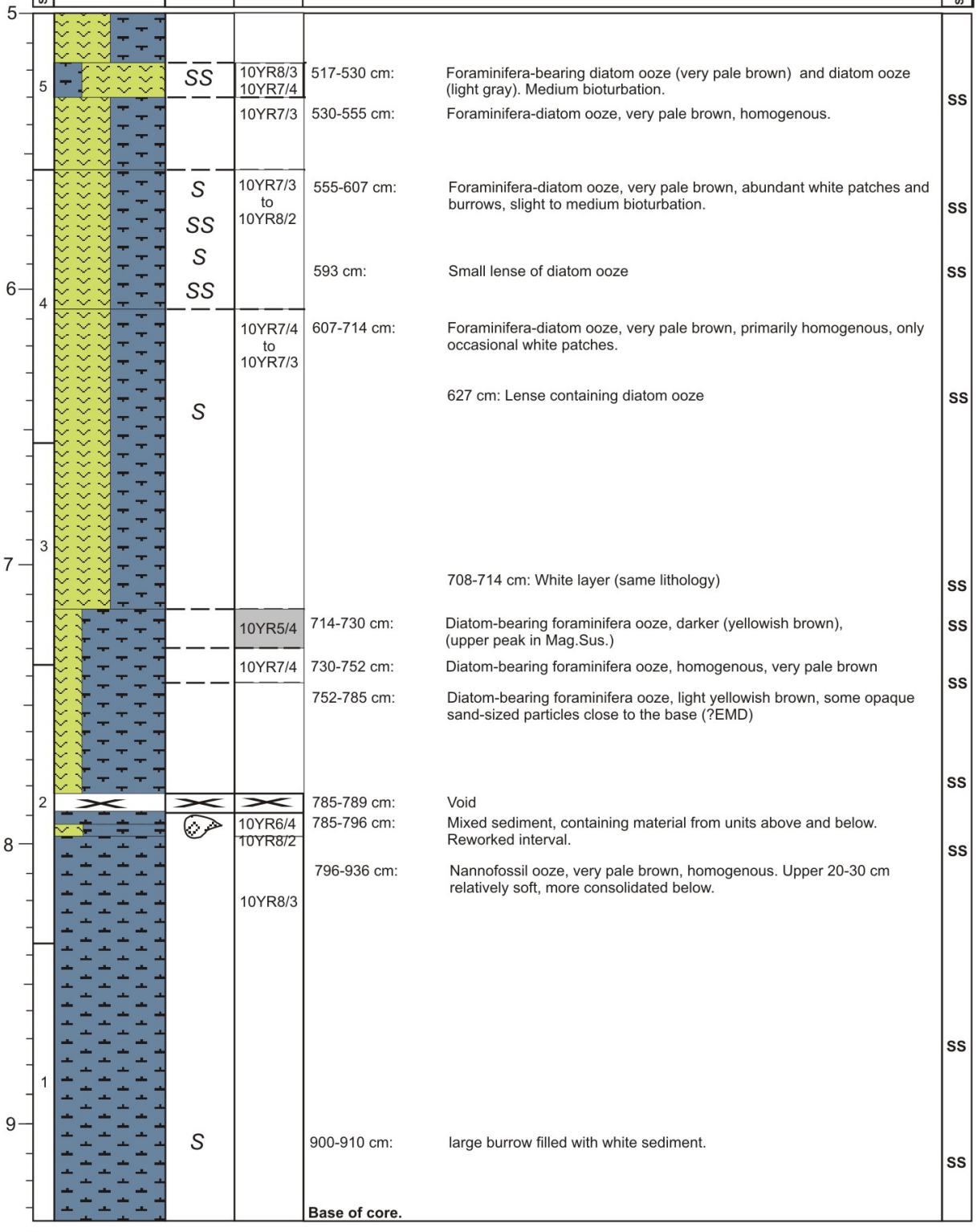

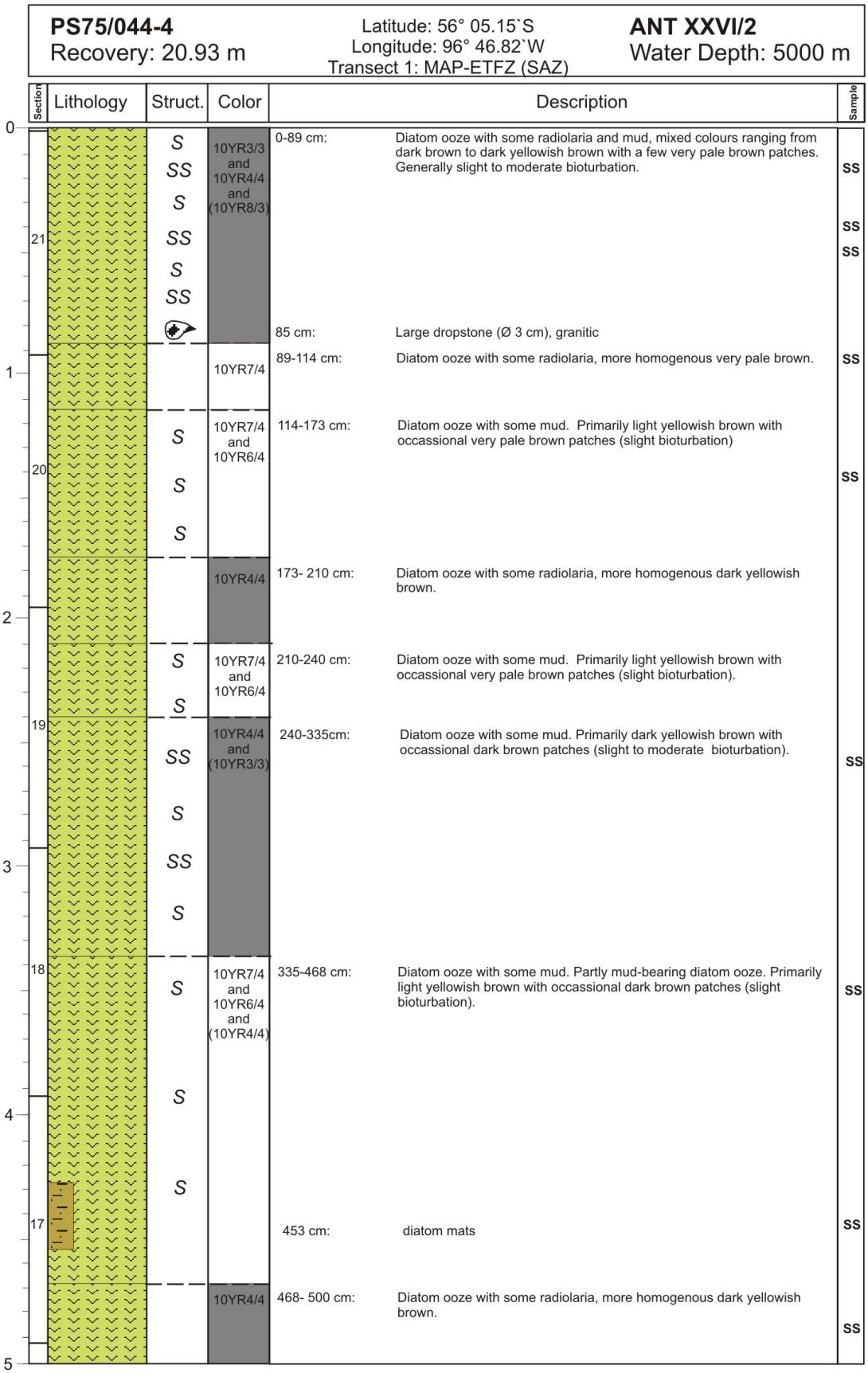
PS75/044-4
Recovery: 20.93 m
Latitude: 56° 05.15`S
Longitude: 96° 46.82`W
Transect 1: MAP-ETFZ (SAZ)
ANT XXVI/2
Water Depth: 5000 m
Section
Lithology
Struct.
Color
Description
Sample
0
1
2
3
4
5
21
20
19
18
17
S
SS
10YR3/3 and 10YR4/4 and (10YR8/3)
0-89 cm:
Diatom ooze with some radiolaria and mud, mixed colours ranging from dark brown to dark yellowish brown with a few very pale brown patches. Generally slight to moderate bioturbation.
85 cm:
Large dropstone (Ø 3 cm), granitic
10YR7/4
89-114 cm:
Diatom ooze with some radiolaria, more homogenous very pale brown.
10YR7/4 and 10YR6/4
114-173 cm:
Diatom ooze with some mud. Primarily light yellowish brown with occassional very pale brown patches (slight bioturbation)
10YR4/4
173- 210 cm:
Diatom ooze with some radiolaria, more homogenous dark yellowish brown.
210-240 cm:
Diatom ooze with some mud. Primarily light yellowish brown with occassional very pale brown patches (slight bioturbation).
10YR4/4 and (10YR3/3)
240-335cm:
Diatom ooze with some mud. Primarily dark yellowish brown with occassional dark brown patches (slight to moderate bioturbation).
10YR7/4 and 10YR6/4 and (10YR4/4)
335-468 cm:
Diatom ooze with some mud. Partly mud-bearing diatom ooze. Primarily light yellowish brown with occassional dark brown patches (slight bioturbation).
453 cm:
diatom mats
10YR4/4
468- 500 cm:
Diatom ooze with some radiolaria, more homogenous dark yellowish brown.
SS

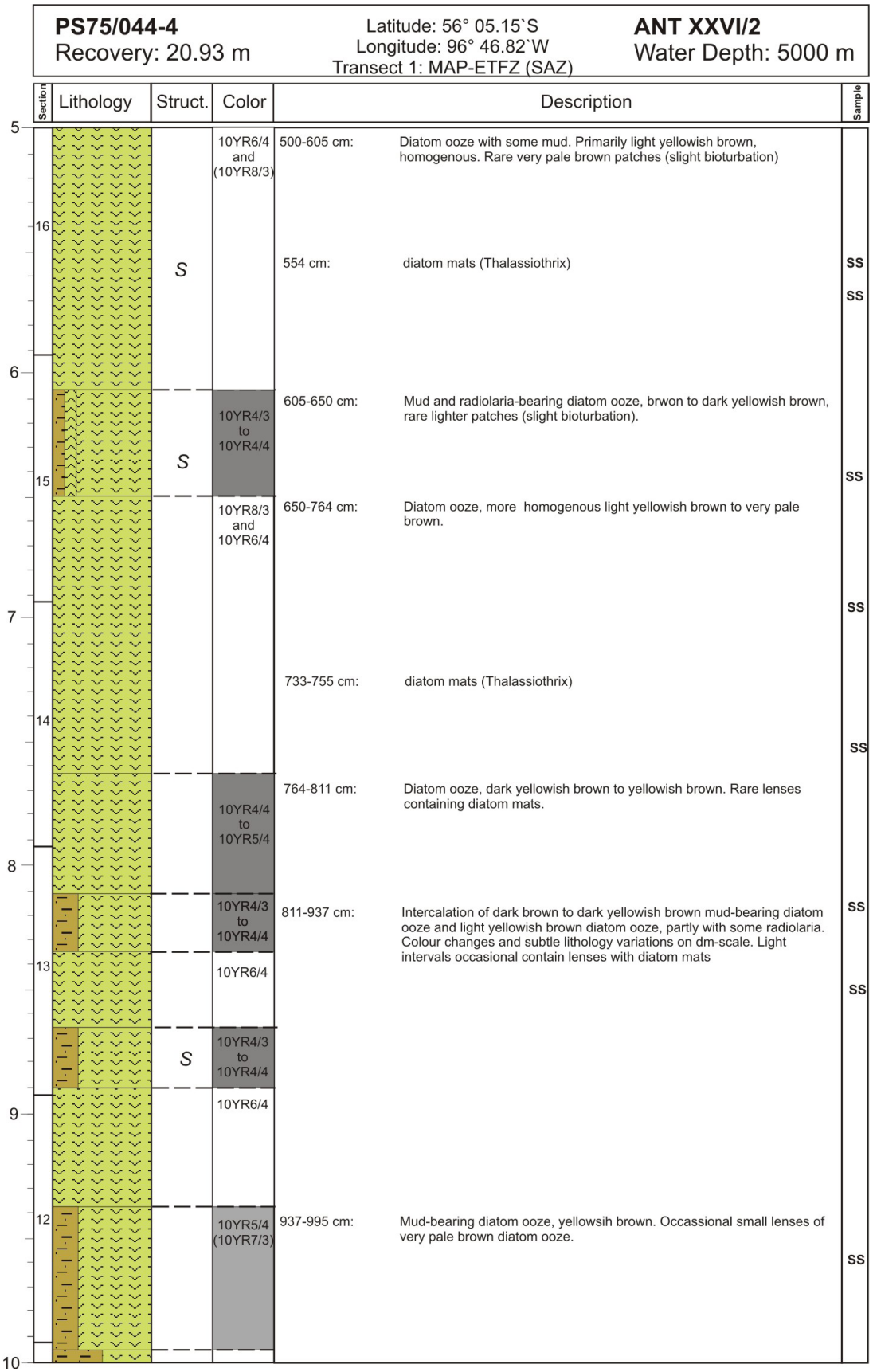
PS75/044-4
Recovery: 20.93 m
Latitude: 56° 05.15`S
Longitude: 96° 46.82`W
Transect 1: MAP-ETFZ (SAZ)
ANT XXVI/2
Water Depth: 5000 m
Section
Lithology
Struct.
Color
Description
Sample
5
16
6
15
7
14
8
13
9
12
10
S
S
S
10YR6/4 and (10YR8/3)
10YR4/3 to 10YR4/4
10YR8/3 and 10YR6/4
10YR4/4 to 10YR5/4
10YR4/3 to 10YR4/4
10YR6/4
10YR4/3 to 10YR4/4
10YR6/4
10YR5/4 (10YR7/3)
500-605 cm:
Diatom ooze with some mud. Primarily light yellowish brown, homogenous. Rare very pale brown patches (slight bioturbation)
554 cm:
diatom mats (Thalassiothrix)
605-650 cm:
Mud and radiolaria-bearing diatom ooze, brwon to dark yellowish brown, rare lighter patches (slight bioturbation).
650-764 cm:
Diatom ooze, more homogenous light yellowish brown to very pale brown.
733-755 cm:
diatom mats (Thalassiothrix)
764-811 cm:
Diatom ooze, dark yellowish brown to yellowish brown. Rare lenses containing diatom mats.
811-937 cm:
Intercalation of dark brown to dark yellowish brown mud-bearing diatom ooze and light yellowish brown diatom ooze, partly with some radiolaria. Colour changes and subtle lithology variations on dm-scale. Light intervals occasional contain lenses with diatom mats
937-995 cm:
Mud-bearing diatom ooze, yellowsih brown. Occassional small lenses of very pale brown diatom ooze.
SS
SS
SS
SS
SS
SS
SS
SS

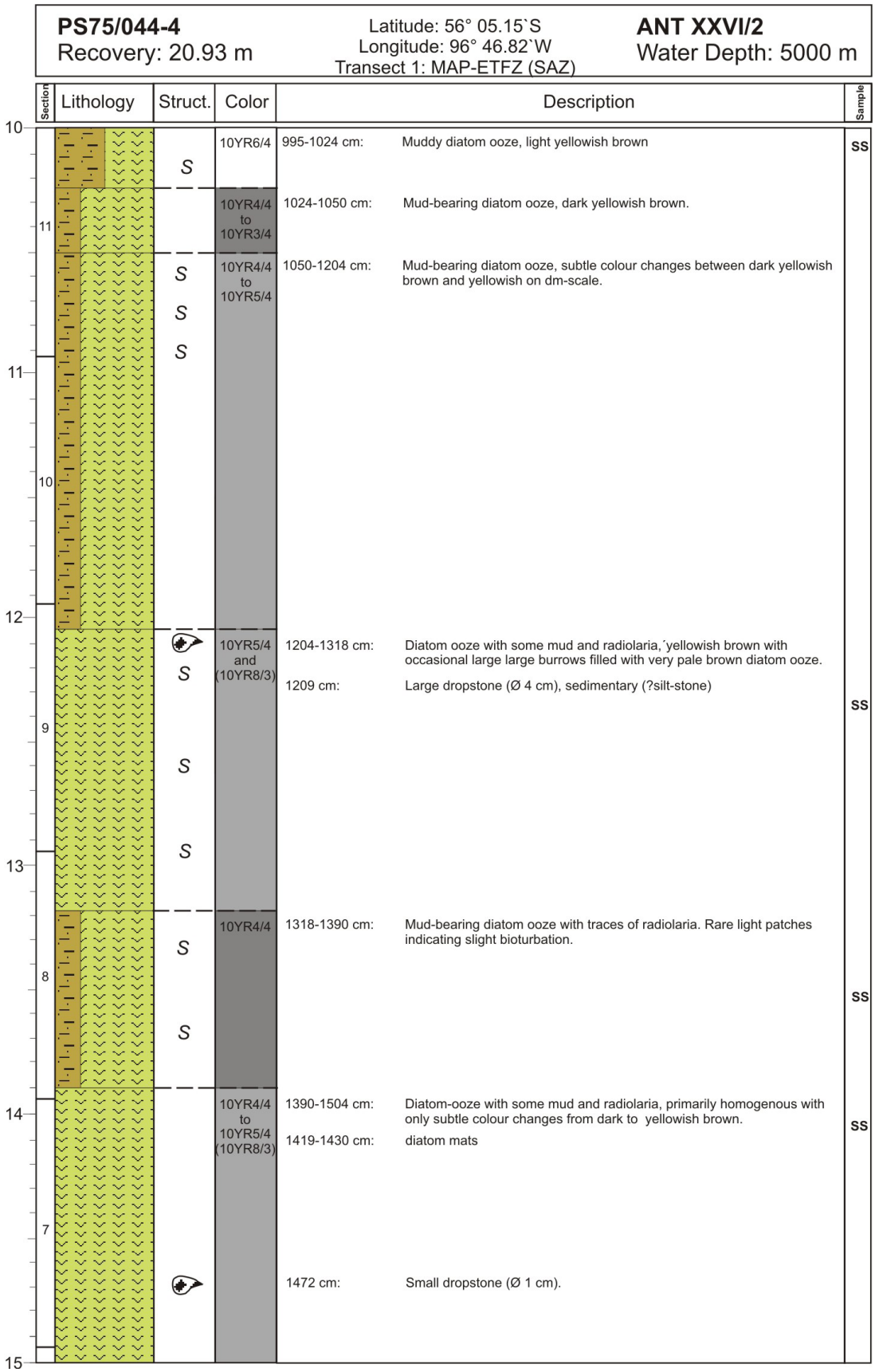
PS75/044-4
Recovery: 20.93 m
Latitude: 56° 05.15`S
Longitude: 96° 46.82`W
Transect 1: MAP-ETFZ (SAZ)
ANT XXVI/2
Water Depth: 5000 m
Section
Lithology
Struct.
Color
Description
Sample
10
11
12
13
14
15
7
8
9
10
11
S
10YR6/4
995-1024 cm:
Muddy diatom ooze, light yellowish brown
SS
10YR4/4 to 10YR3/4
1024-1050 cm:
Mud-bearing diatom ooze, dark yellowish brown.
10YR4/4 to 10YR5/4
1050-1204 cm:
Mud-bearing diatom ooze, subtle colour changes between dark yellowish brown and yellowish on dm-scale.
10YR5/4 and (10YR8/3)
1204-1318 cm:
Diatom ooze with some mud and radiolaria,´yellowish brown with occasional large large burrows filled with very pale brown diatom ooze.
1209 cm:
Large dropstone (Ø 4 cm), sedimentary (?silt-stone)
SS
10YR4/4
1318-1390 cm:
Mud-bearing diatom ooze with traces of radiolaria. Rare light patches indicating slight bioturbation.
SS
10YR4/4 to 10YR5/4 (10YR8/3)
1390-1504 cm:
Diatom-ooze with some mud and radiolaria, primarily homogenous with only subtle colour changes from dark to yellowish brown.
1419-1430 cm:
diatom mats
SS
1472 cm:
Small dropstone (Ø 1 cm).

**PS75/044-4**
Recovery: 20.93 m

Latitude: 56° 05.15`S
Longitude: 96° 46.82`W
Transect 1: MAP-ETFZ (SAZ)

**ANT XXVI/2**
Water Depth: 5000 m

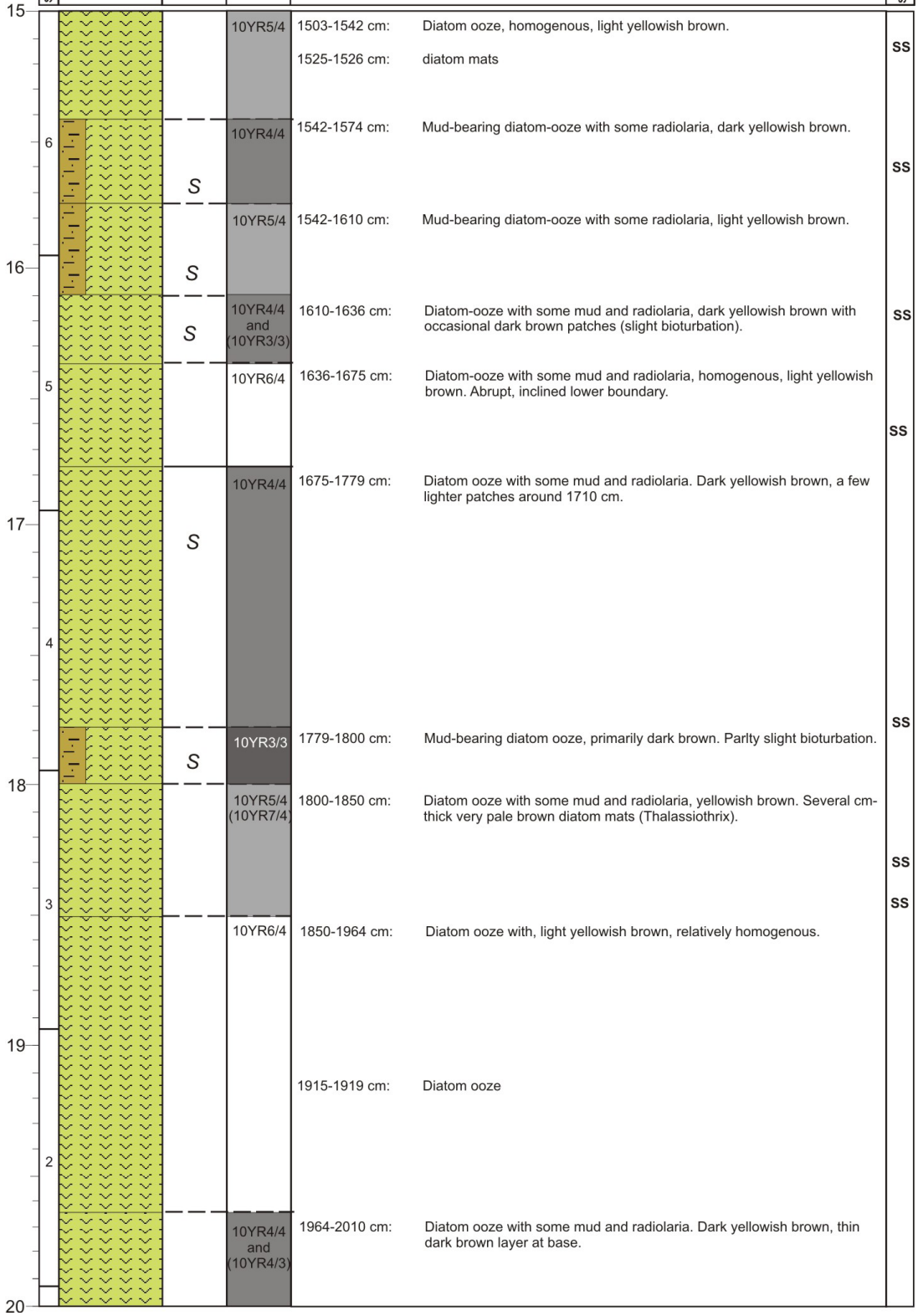

**PS75/044-4**
Recovery: 20.93 m

Latitude: 56° 05.15`S
Longitude: 96° 46.82`W
Transect 1: MAP-ETFZ (SAZ)

**ANT XXVI/2**
Water Depth: 5000 m

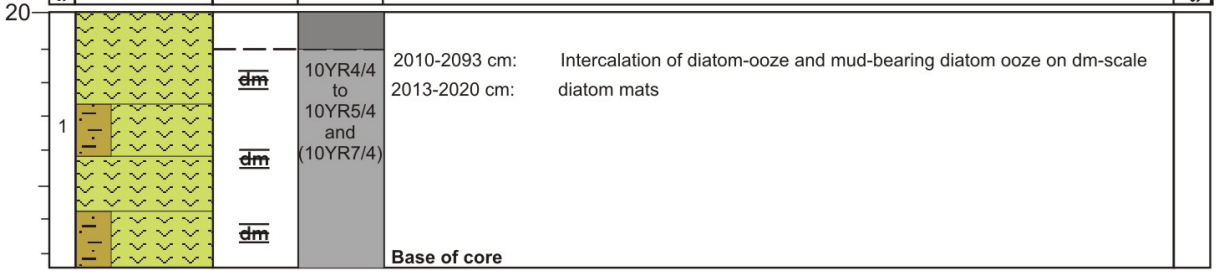

**PS75/046-2**
Recovery: 17.26 m

Latitude: 54° 24.92`S
Longitude: 103° 30.22`W
Transect 1: MAP-ETFZ (SAZ)

**ANT XXVI/2**
Water Depth: 2984 m

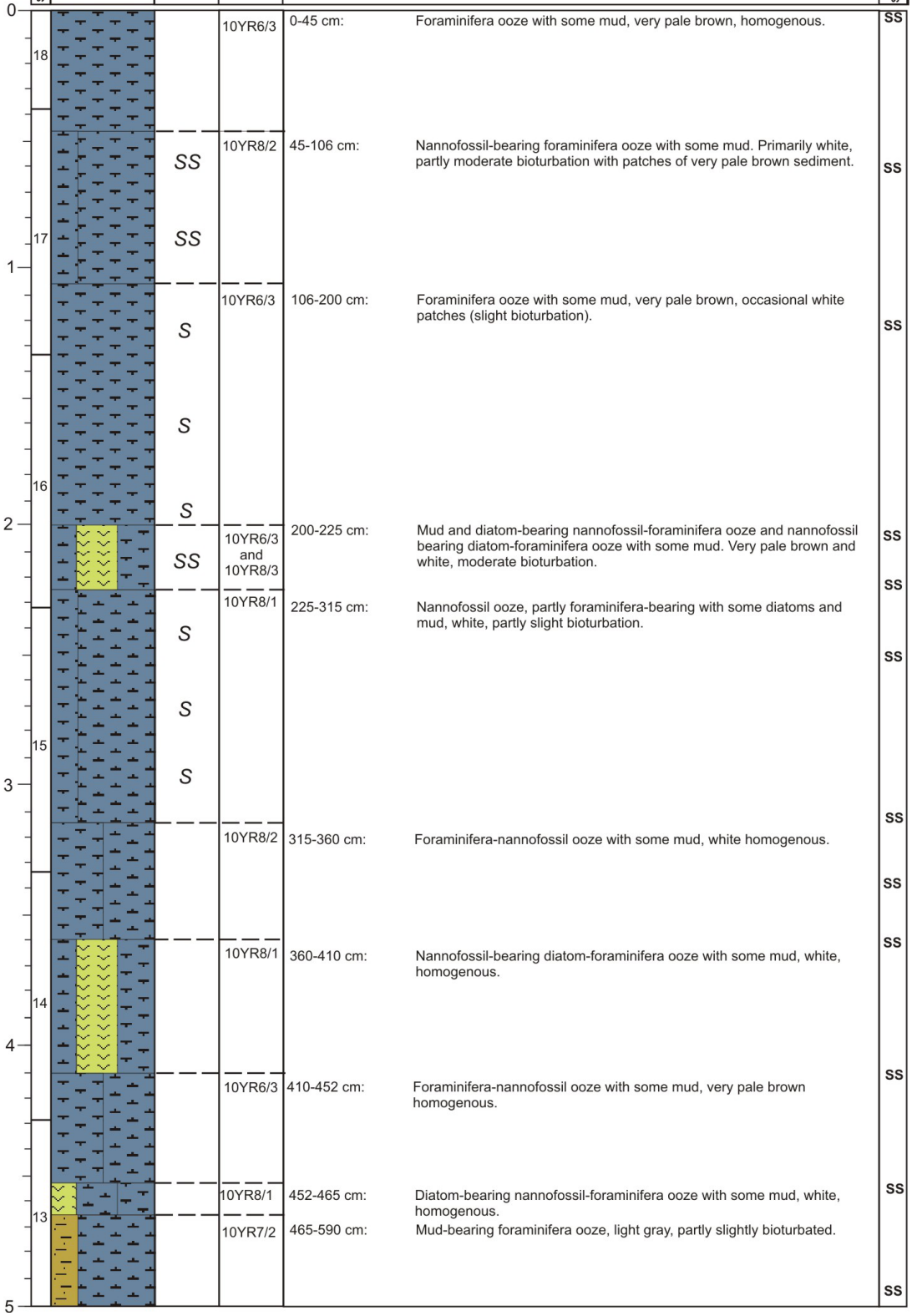

**PS75/046-2**
Recovery: 17.26 m

Latitude: 54° 24.92`S
Longitude: 103° 30.22`W
Transect 1: MAP-ETFZ (SAZ)

**ANT XXVI/2**
Water Depth: 2984 m

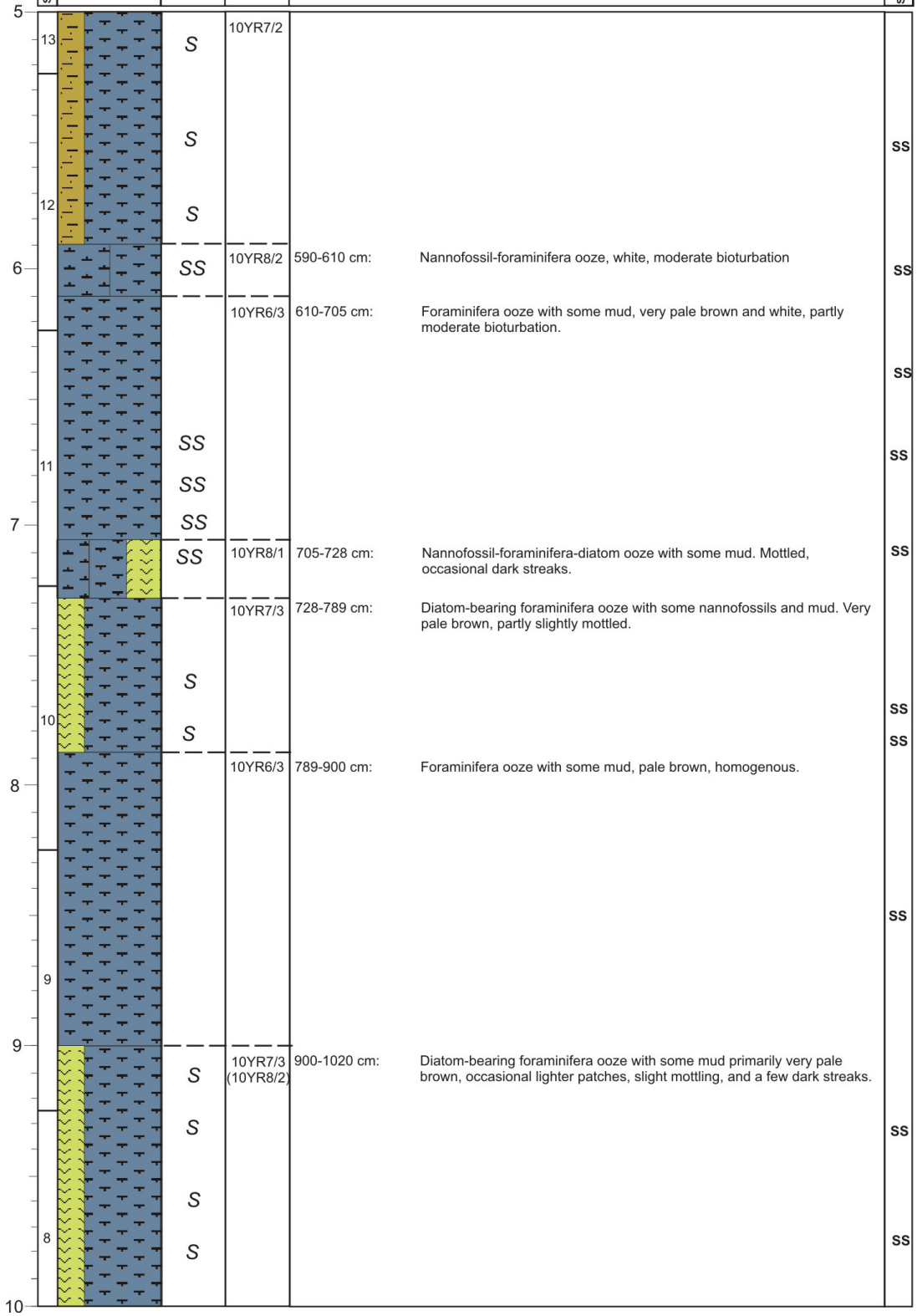

**PS75/046-2**
Recovery: 17.26 m

Latitude: 54° 24.92`S
Longitude: 103° 30.22`W
Transect 1: MAP-ETFZ (SAZ)

**ANT XXVI/2**
Water Depth: 2984 m

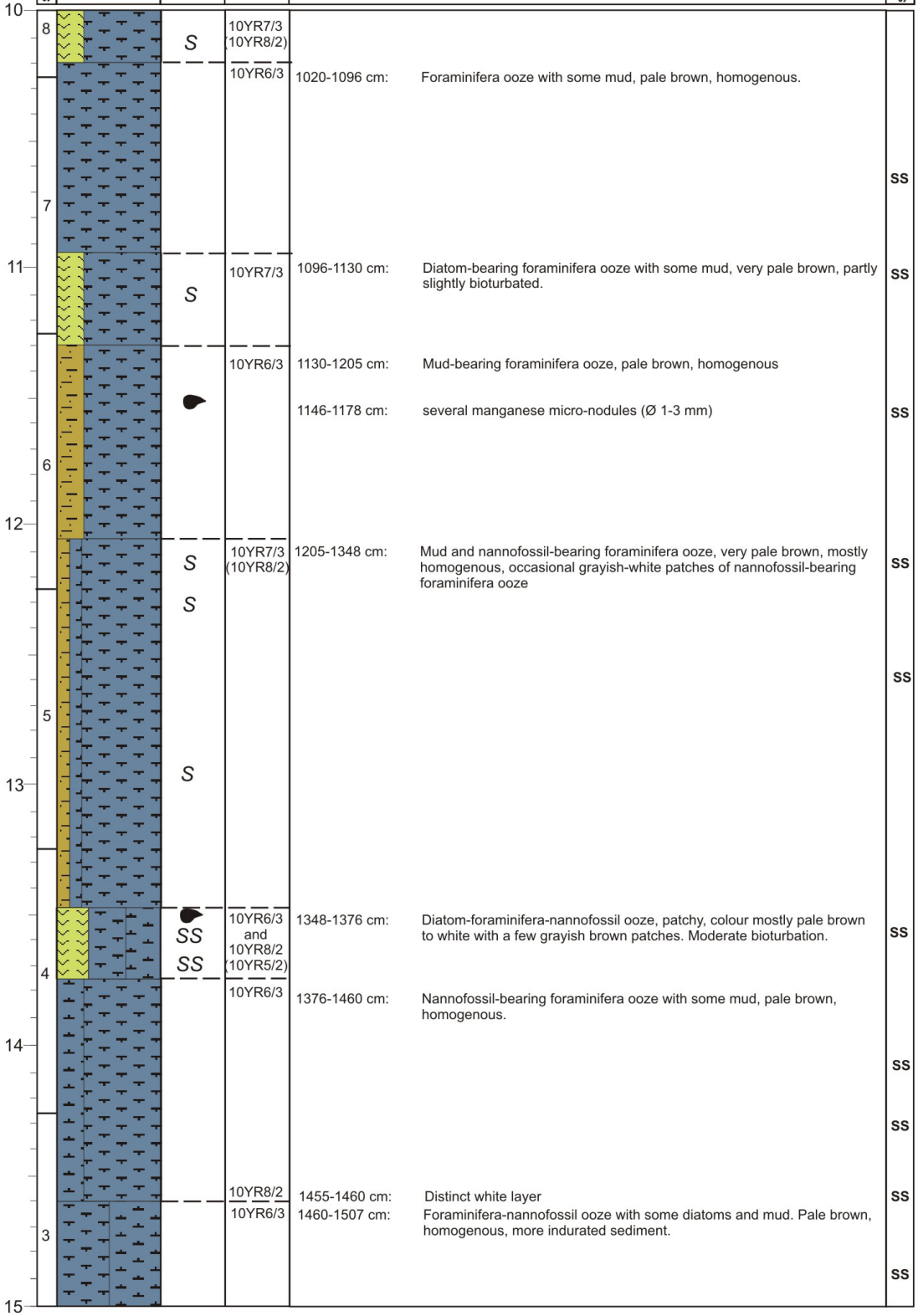

**PS75/046-2**
Recovery: 17.26 m

Latitude: 54° 24.92`S
Longitude: 103° 30.22`W
Transect 1: MAP-ETFZ (SAZ)

**ANT XXVI/2**
Water Depth: 2984 m

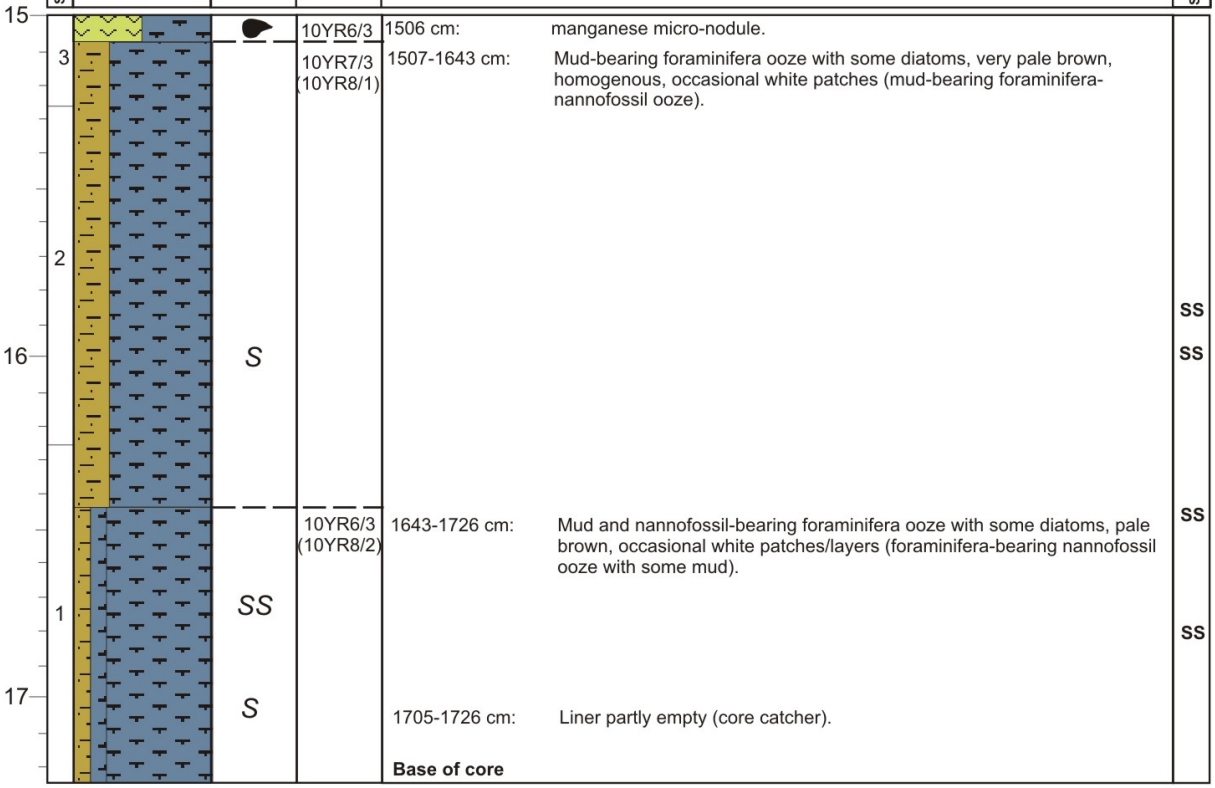

**PS75/047-1**
Recovery: 22.89 m

Latitude: 54° 20.77`S
Longitude: 102° 44.82`W
Transect 1: MAP-ETFZ (SAZ)

**ANT XXVI/2**
Water Depth: 4480 m

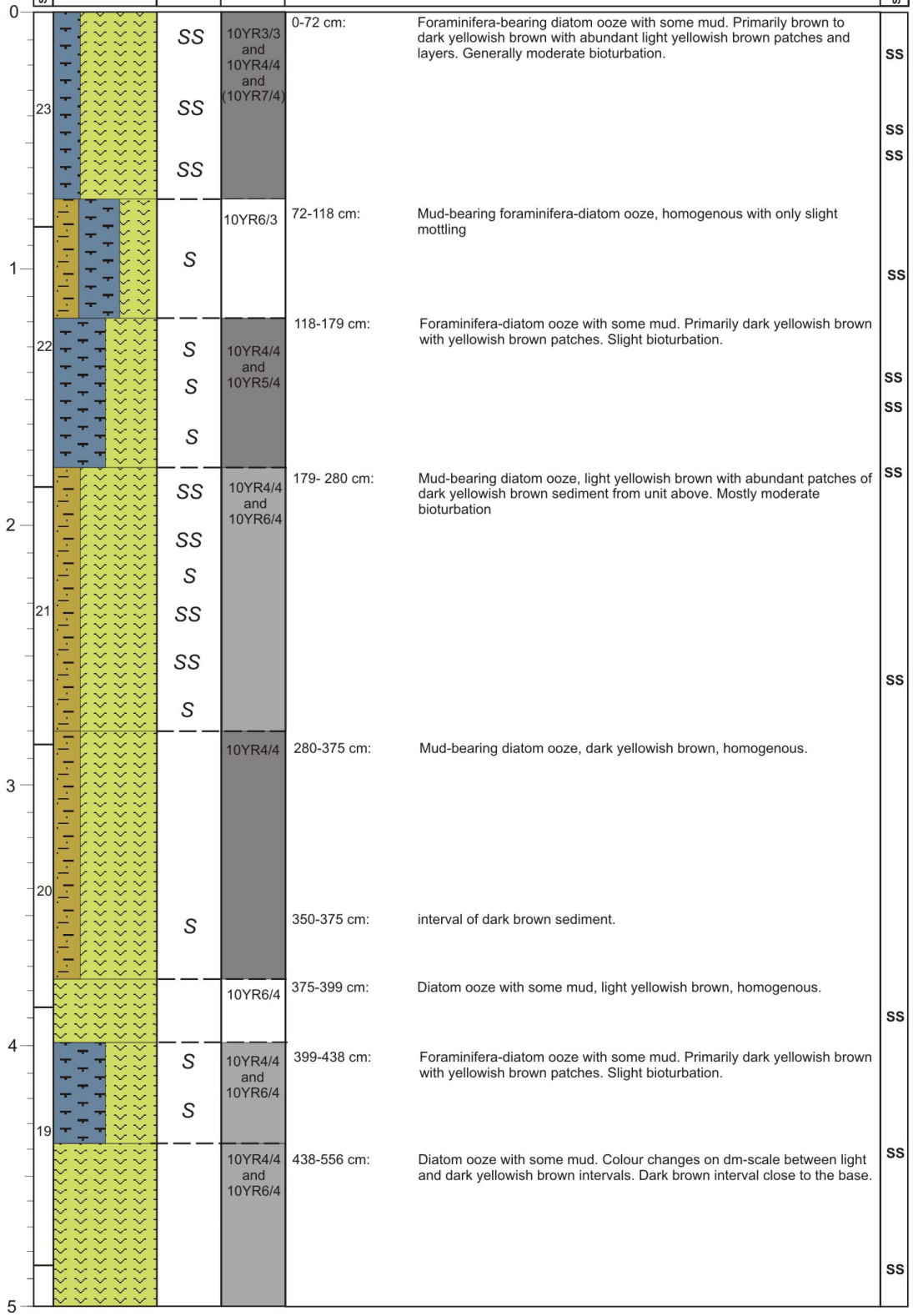

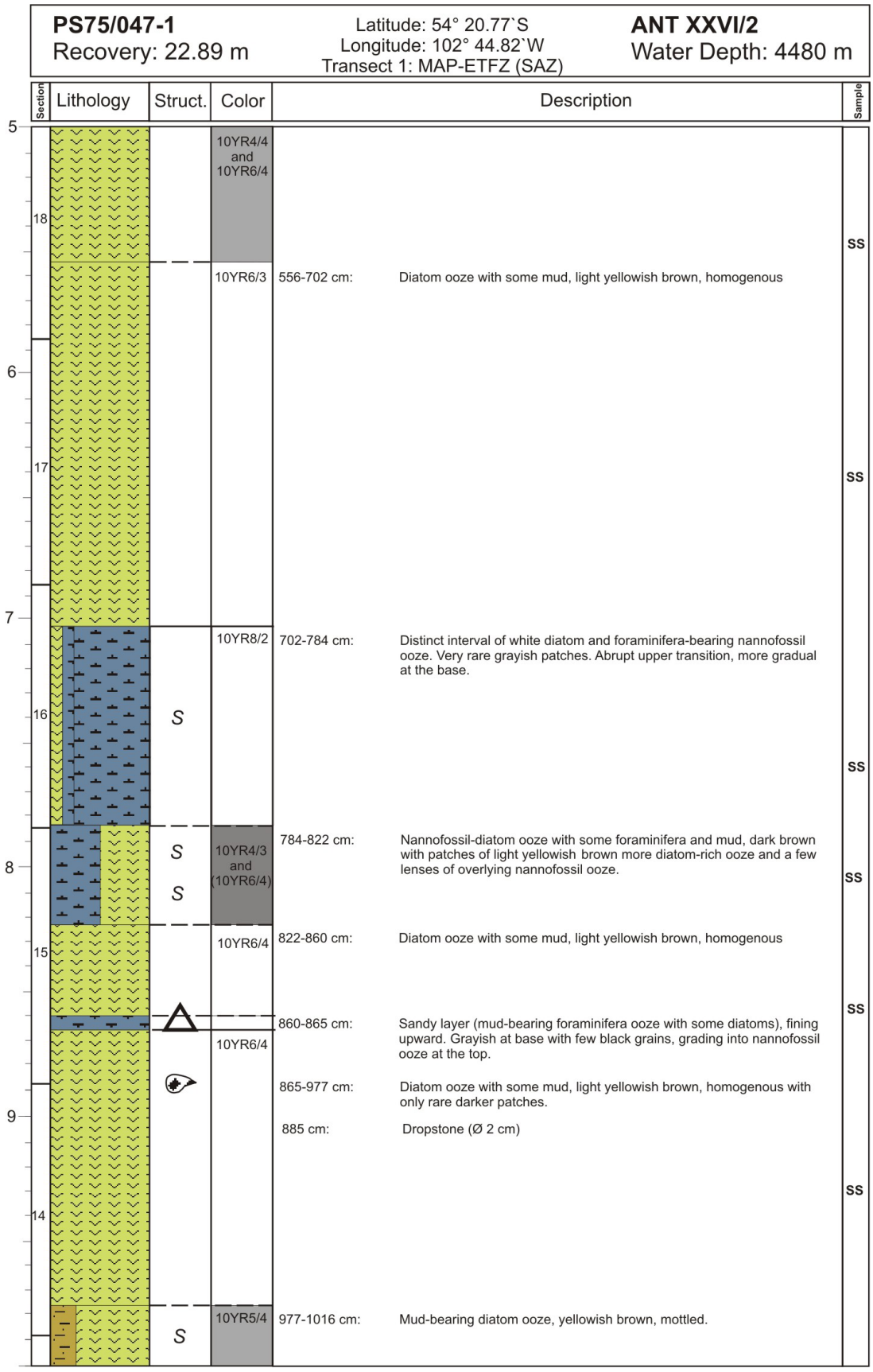
PS75/047-1
Recovery: 22.89 m
Latitude: 54° 20.77`S
Longitude: 102° 44.82`W
Transect 1: MAP-ETFZ (SAZ)
ANT XXVI/2
Water Depth: 4480 m
Section
Lithology
Struct.
Color
Description
Sample
5
6
7
8
9
18
17
16
15
14
10YR4/4 and 10YR6/4
10YR6/3
556-702 cm:
Diatom ooze with some mud, light yellowish brown, homogenous
10YR8/2
702-784 cm:
Distinct interval of white diatom and foraminifera-bearing nannofossil ooze. Very rare grayish patches. Abrupt upper transition, more gradual at the base.
S
10YR4/3 and (10YR6/4)
784-822 cm:
Nannofossil-diatom ooze with some foraminifera and mud, dark brown with patches of light yellowish brown more diatom-rich ooze and a few lenses of overlying nannofossil ooze.
10YR6/4
822-860 cm:
Diatom ooze with some mud, light yellowish brown, homogenous
860-865 cm:
Sandy layer (mud-bearing foraminifera ooze with some diatoms), fining upward. Grayish at base with few black grains, grading into nannofossil ooze at the top.
865-977 cm:
Diatom ooze with some mud, light yellowish brown, homogenous with only rare darker patches.
885 cm:
Dropstone (Ø 2 cm)
10YR5/4
977-1016 cm:
Mud-bearing diatom ooze, yellowish brown, mottled.
SS

**PS75/047-1**
Recovery: 22.89 m

Latitude: 54° 20.77`S
Longitude: 102° 44.82`W
Transect 1: MAP-ETFZ (SAZ)

**ANT XXVI/2**
Water Depth: 4480 m

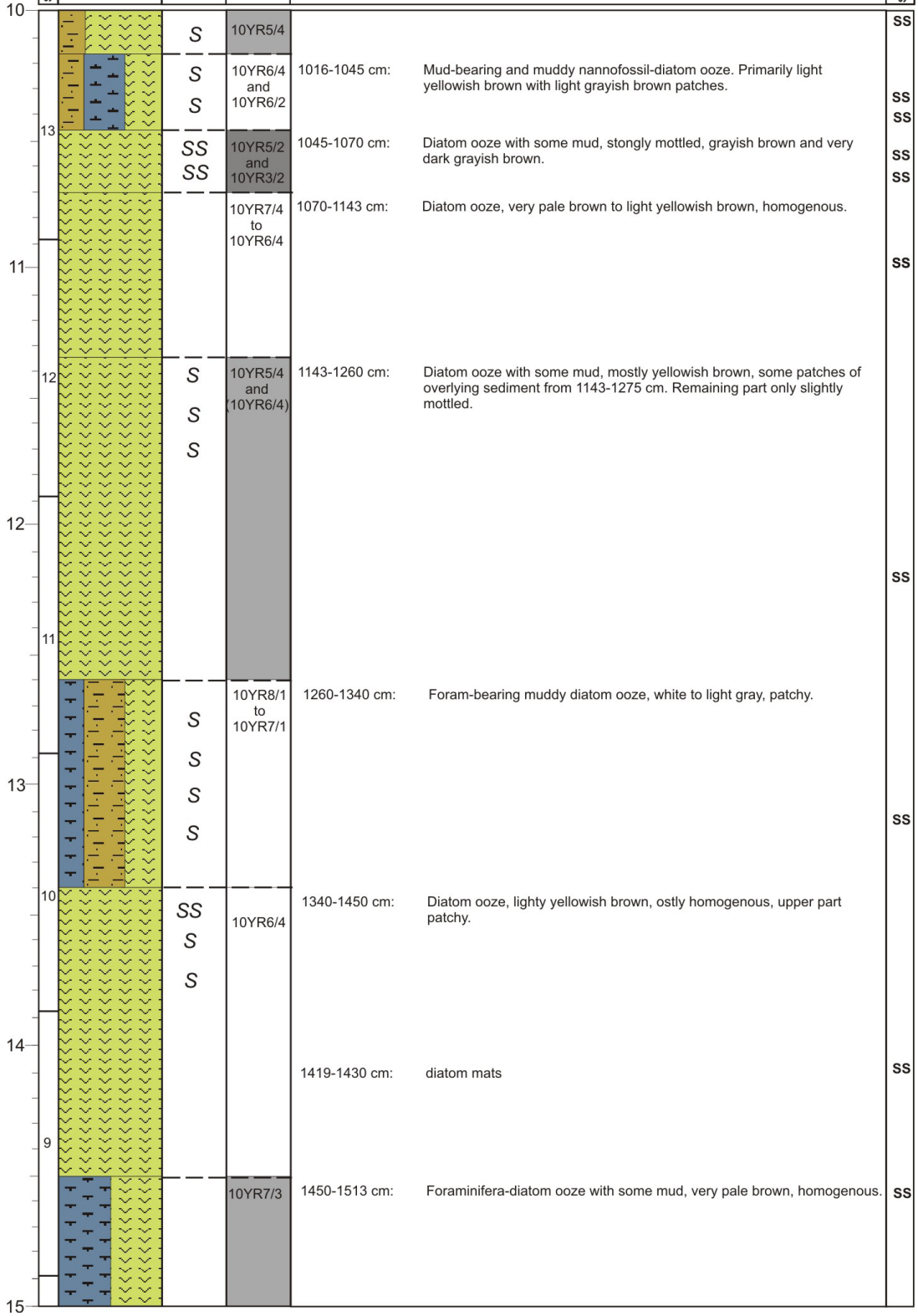

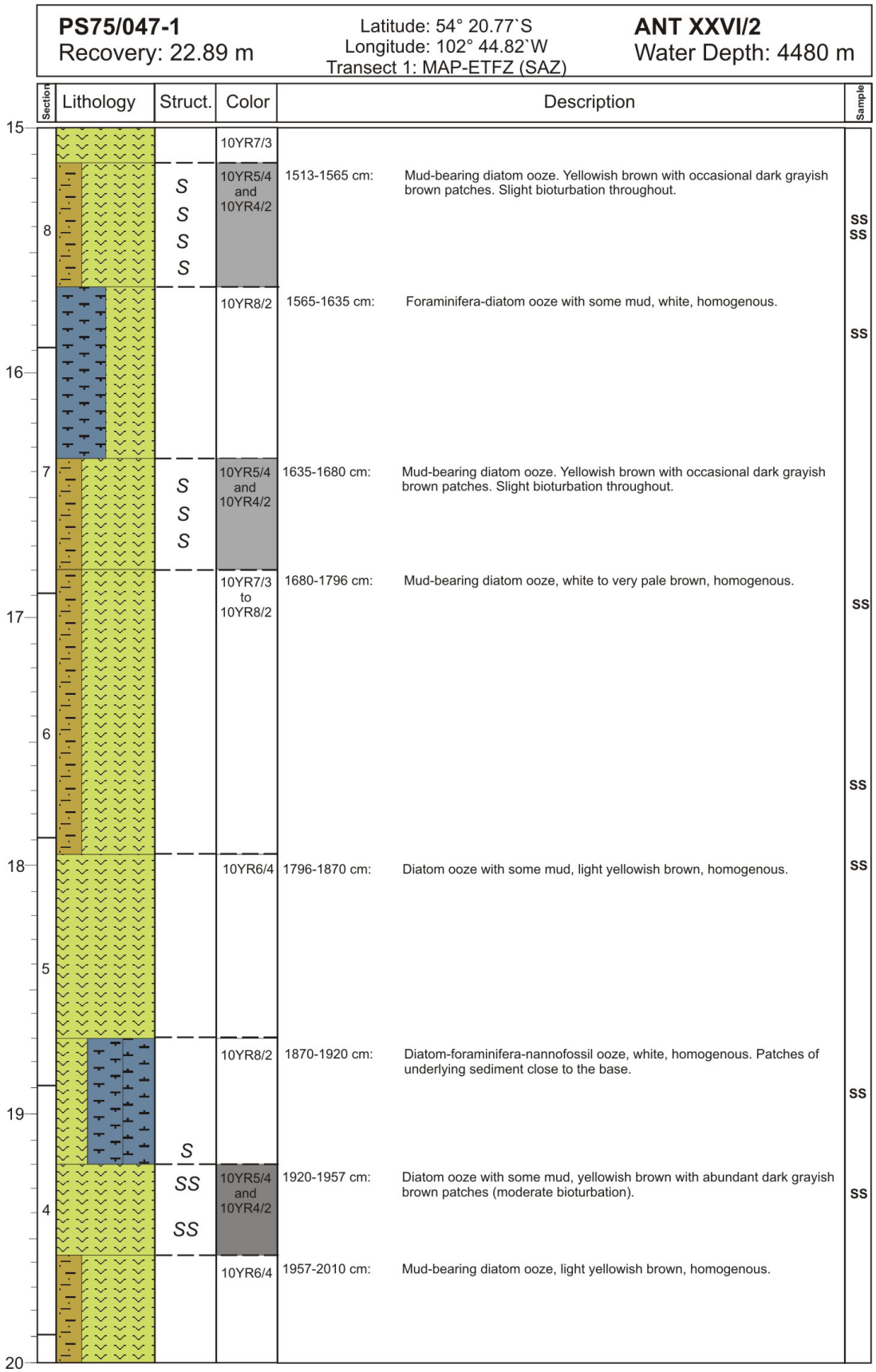
PS75/047-1
Recovery: 22.89 m
Latitude: 54° 20.77`S
Longitude: 102° 44.82`W
Transect 1: MAP-ETFZ (SAZ)
ANT XXVI/2
Water Depth: 4480 m
Section
Lithology
Struct.
Color
Description
Sample
15
16
17
18
19
20
8
7
6
5
4
S
S
S
S
S
S
S
S
SS
SS
10YR7/3
10YR5/4 and 10YR4/2
10YR8/2
10YR5/4 and 10YR4/2
10YR7/3 to 10YR8/2
10YR6/4
10YR8/2
10YR5/4 and 10YR4/2
10YR6/4
1513-1565 cm: Mud-bearing diatom ooze. Yellowish brown with occasional dark grayish brown patches. Slight bioturbation throughout.
1565-1635 cm: Foraminifera-diatom ooze with some mud, white, homogenous.
1635-1680 cm: Mud-bearing diatom ooze. Yellowish brown with occasional dark grayish brown patches. Slight bioturbation throughout.
1680-1796 cm: Mud-bearing diatom ooze, white to very pale brown, homogenous.
1796-1870 cm: Diatom ooze with some mud, light yellowish brown, homogenous.
1870-1920 cm: Diatom-foraminifera-nannofossil ooze, white, homogenous. Patches of underlying sediment close to the base.
1920-1957 cm: Diatom ooze with some mud, yellowish brown with abundant dark grayish brown patches (moderate bioturbation).
1957-2010 cm: Mud-bearing diatom ooze, light yellowish brown, homogenous.
SS
SS
SS
SS
SS
SS
SS

**PS75/047-1**
Recovery: 22.89 m

Latitude: 54° 20.77`S
Longitude: 102° 44.82`W
Transect 1: MAP-ETFZ (SAZ)

**ANT XXVI/2**
Water Depth: 4480 m

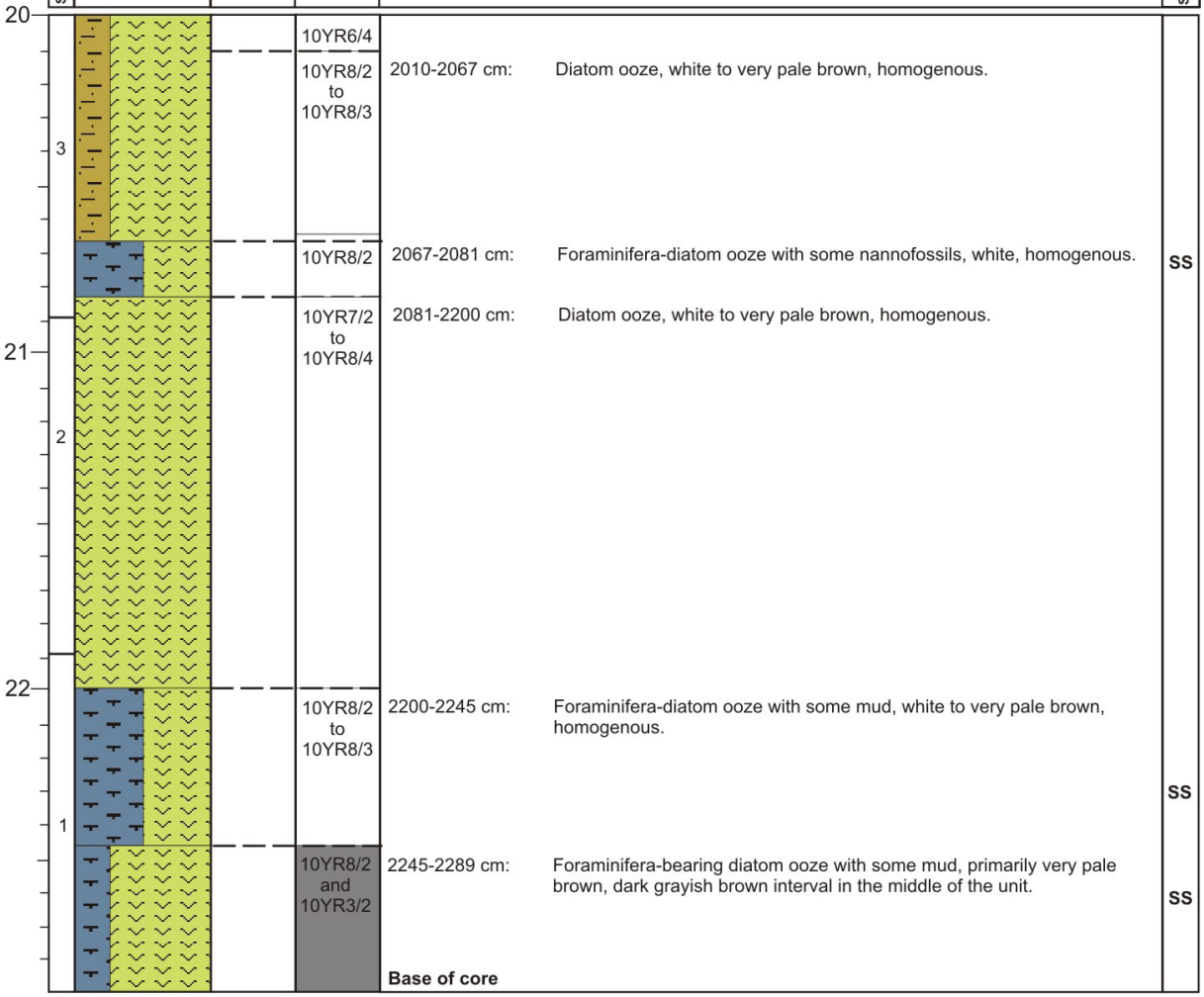

**PS75/048-1**
Recovery: 19.88 m

Latitude: 54° 20.35`S
Longitude: 102° 45.51`W
Transect 1: MAP-ETFZ (SAZ)

**ANT XXVI/2**
Water Depth: 4512 m

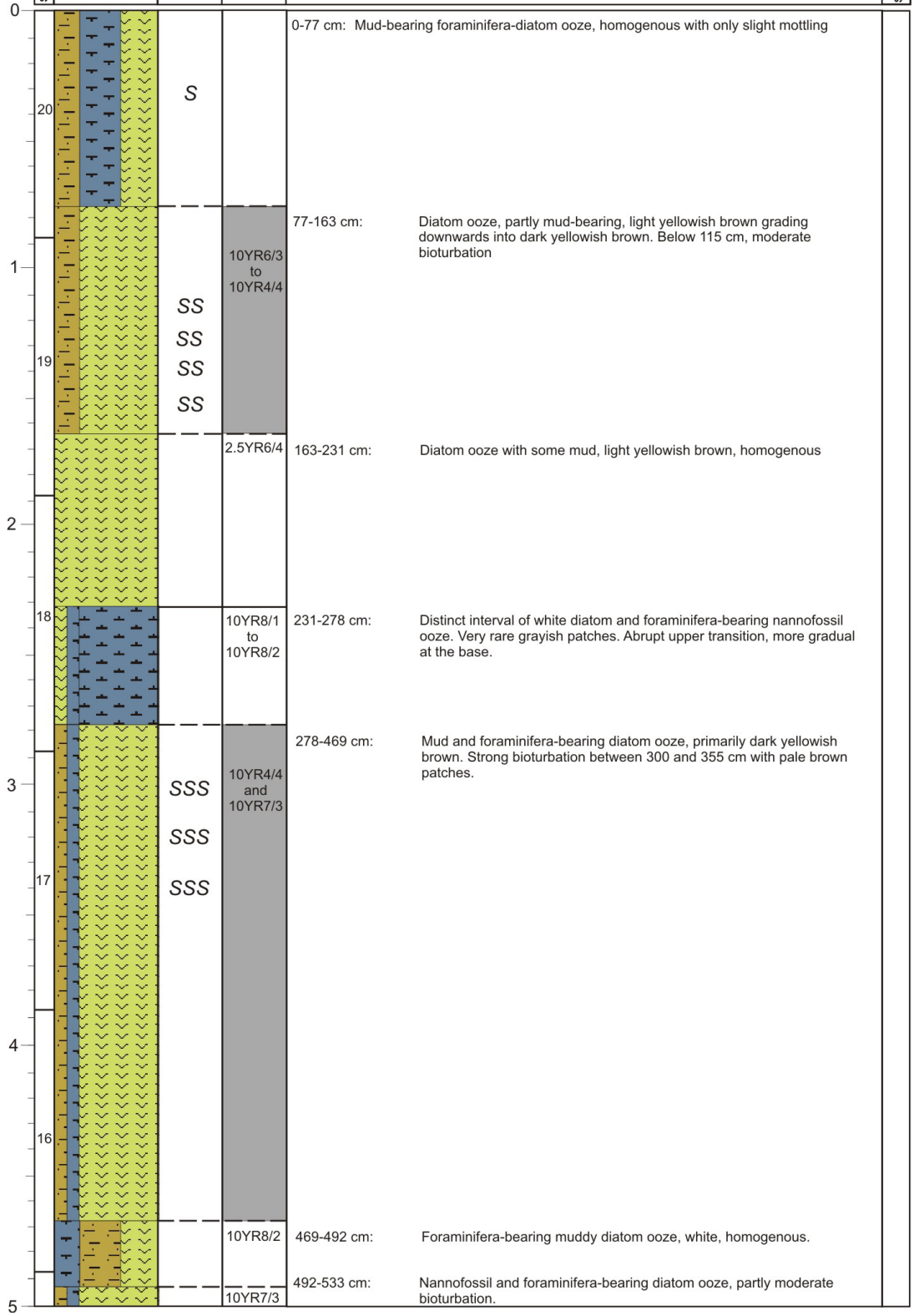

**PS75/048-1**
Recovery: 19.88 m

Latitude: 54° 20.35`S
Longitude: 102° 45.51`W
Transect 1: MAP-ETFZ (SAZ)

**ANT XXVI/2**
Water Depth: 4512 m

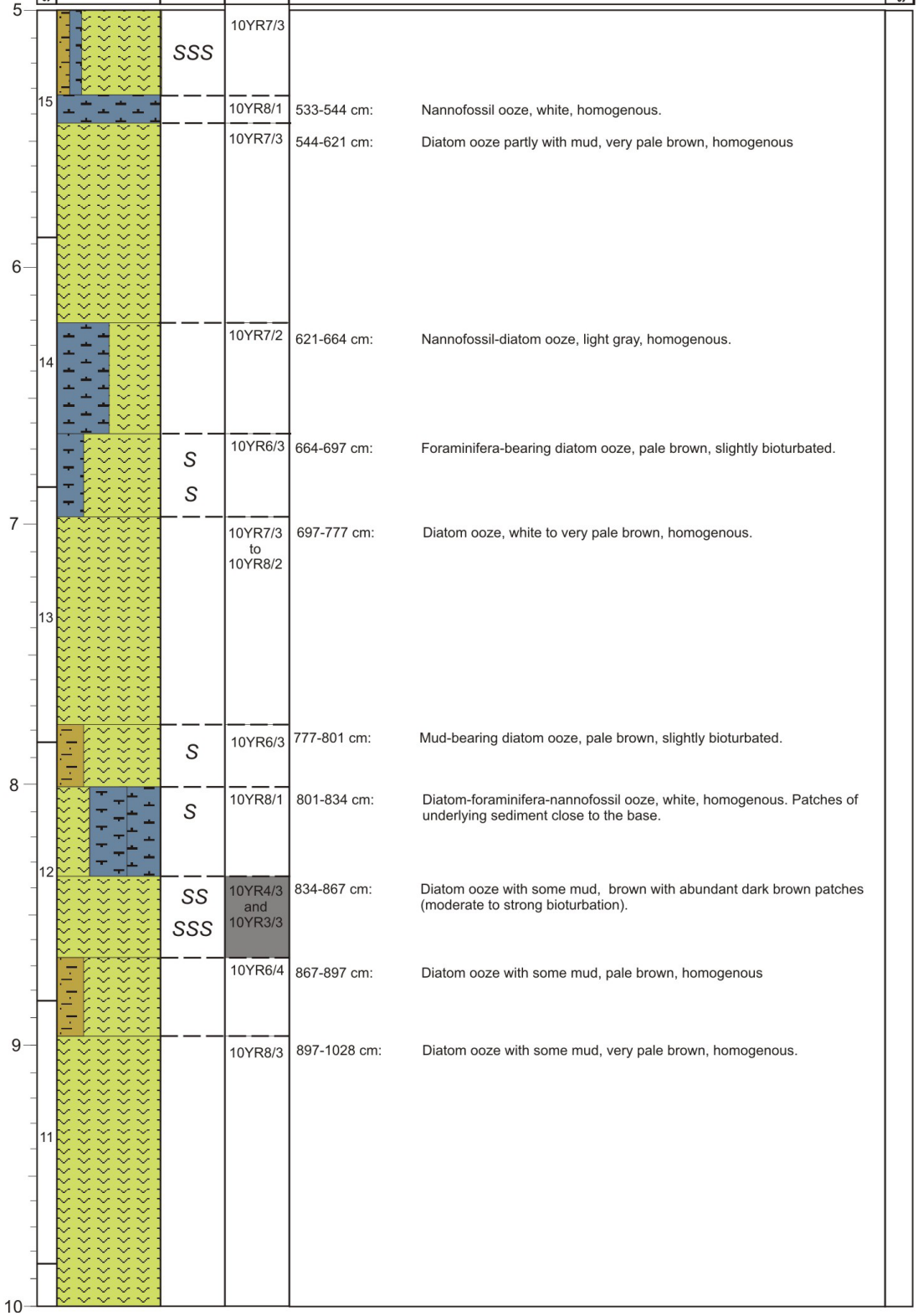

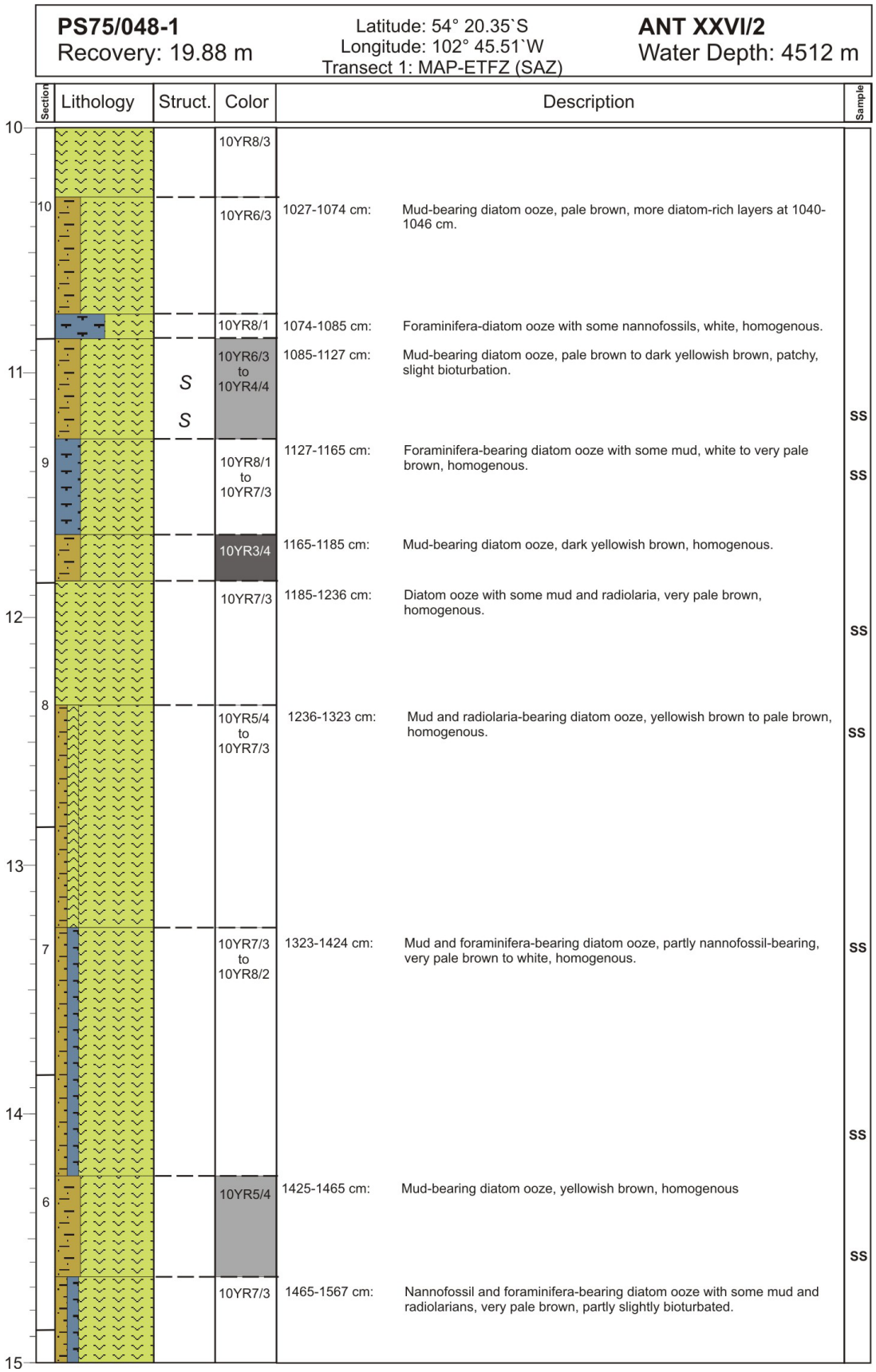
PS75/048-1
Recovery: 19.88 m
Latitude: 54° 20.35`S
Longitude: 102° 45.51`W
Transect 1: MAP-ETFZ (SAZ)
ANT XXVI/2
Water Depth: 4512 m
Section
Lithology
Struct.
Color
Description
Sample
10
11
12
13
14
15
10
9
8
7
6
10YR8/3
10YR6/3
1027-1074 cm: Mud-bearing diatom ooze, pale brown, more diatom-rich layers at 1040-1046 cm.
10YR8/1
1074-1085 cm: Foraminifera-diatom ooze with some nannofossils, white, homogenous.
10YR6/3 to 10YR4/4
1085-1127 cm: Mud-bearing diatom ooze, pale brown to dark yellowish brown, patchy, slight bioturbation.
S
S
SS
10YR8/1 to 10YR7/3
1127-1165 cm: Foraminifera-bearing diatom ooze with some mud, white to very pale brown, homogenous.
SS
10YR3/4
1165-1185 cm: Mud-bearing diatom ooze, dark yellowish brown, homogenous.
10YR7/3
1185-1236 cm: Diatom ooze with some mud and radiolaria, very pale brown, homogenous.
SS
10YR5/4 to 10YR7/3
1236-1323 cm: Mud and radiolaria-bearing diatom ooze, yellowish brown to pale brown, homogenous.
SS
10YR7/3 to 10YR8/2
1323-1424 cm: Mud and foraminifera-bearing diatom ooze, partly nannofossil-bearing, very pale brown to white, homogenous.
SS
SS
10YR5/4
1425-1465 cm: Mud-bearing diatom ooze, yellowish brown, homogenous
SS
10YR7/3
1465-1567 cm: Nannofossil and foraminifera-bearing diatom ooze with some mud and radiolarians, very pale brown, partly slightly bioturbated.

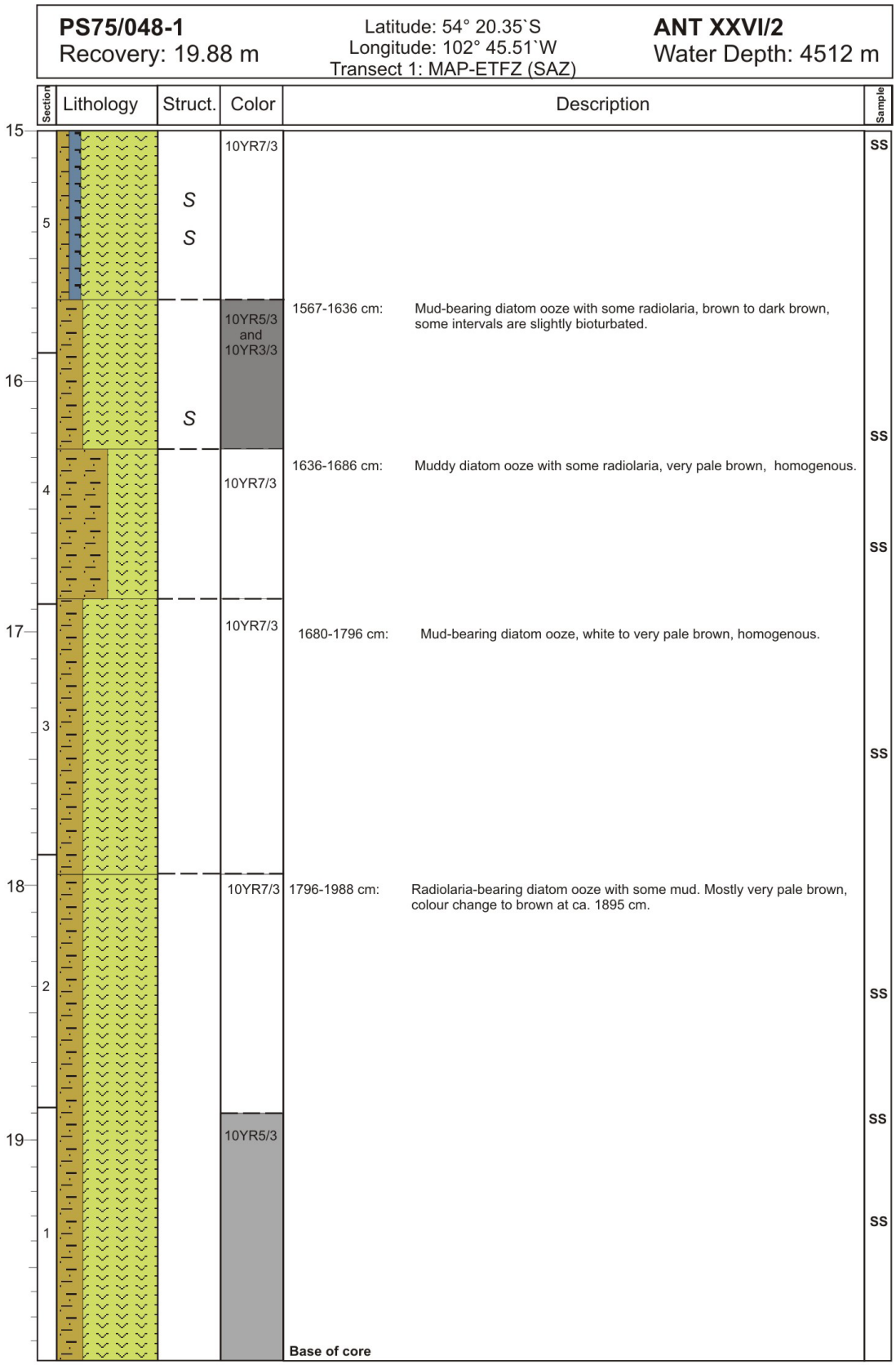
PS75/048-1
Recovery: 19.88 m
Latitude: 54° 20.35`S
Longitude: 102° 45.51`W
Transect 1: MAP-ETFZ (SAZ)
ANT XXVI/2
Water Depth: 4512 m
Section
Lithology
Struct.
Color
Description
Sample
15
16
17
18
19
5
4
3
2
1
S
S
S
10YR7/3
10YR5/3 and 10YR3/3
10YR7/3
10YR7/3
10YR7/3
10YR5/3
1567-1636 cm:
Mud-bearing diatom ooze with some radiolaria, brown to dark brown, some intervals are slightly bioturbated.
1636-1686 cm:
Muddy diatom ooze with some radiolaria, very pale brown, homogenous.
1680-1796 cm:
Mud-bearing diatom ooze, white to very pale brown, homogenous.
1796-1988 cm:
Radiolaria-bearing diatom ooze with some mud. Mostly very pale brown, colour change to brown at ca. 1895 cm.
Base of core
SS
SS
SS
SS
SS
SS
SS

**PS75/051-1**
Recovery: 18.73 m

Latitude: 52° 48.73`S
Longitude: 107° 48.33`W
Transect 1: MAP-ETFZ (SAZ)

**ANT XXVI/2**
Water Depth: 3949 m

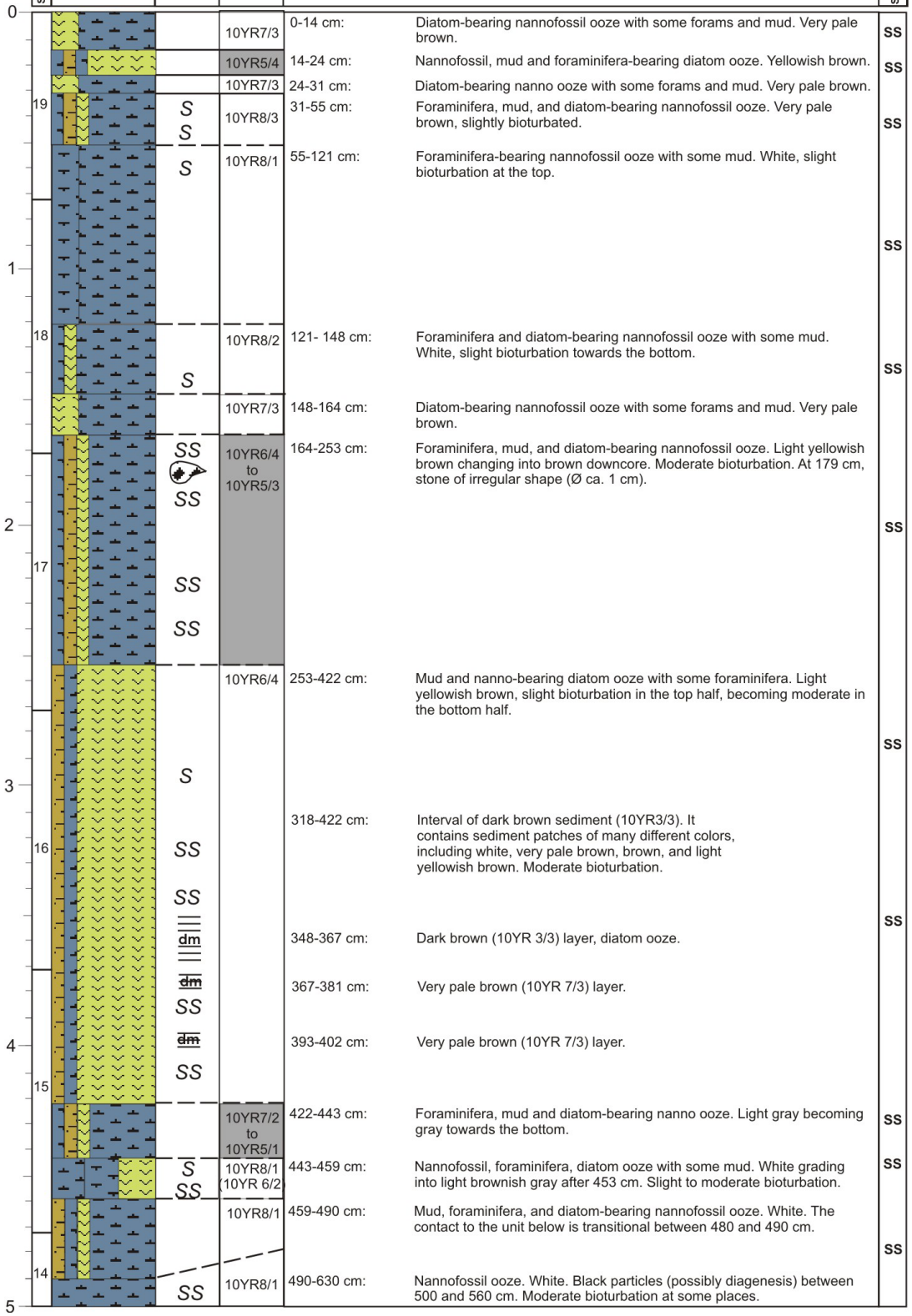

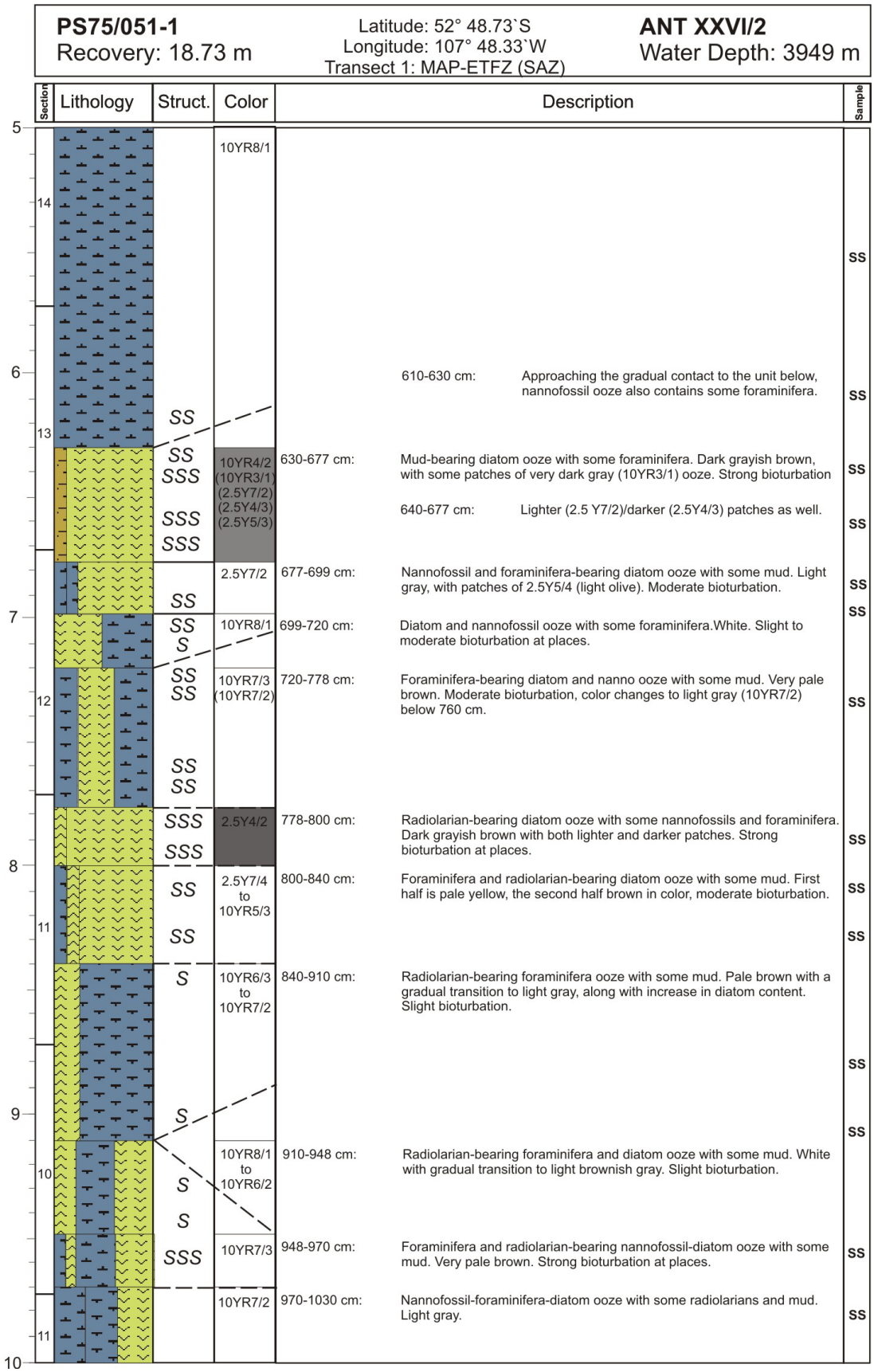
PS75/051-1
Recovery: 18.73 m
Latitude: 52° 48.73`S
Longitude: 107° 48.33`W
Transect 1: MAP-ETFZ (SAZ)
ANT XXVI/2
Water Depth: 3949 m
Section
Lithology
Struct.
Color
Description
Sample
610-630 cm: Approaching the gradual contact to the unit below, nannofossil ooze also contains some foraminifera.
630-677 cm: Mud-bearing diatom ooze with some foraminifera. Dark grayish brown, with some patches of very dark gray (10YR3/1) ooze. Strong bioturbation
640-677 cm: Lighter (2.5 Y7/2)/darker (2.5Y4/3) patches as well.
677-699 cm: Nannofossil and foraminifera-bearing diatom ooze with some mud. Light gray, with patches of 2.5Y5/4 (light olive). Moderate bioturbation.
699-720 cm: Diatom and nannofossil ooze with some foraminifera.White. Slight to moderate bioturbation at places.
720-778 cm: Foraminifera-bearing diatom and nanno ooze with some mud. Very pale brown. Moderate bioturbation, color changes to light gray (10YR7/2) below 760 cm.
778-800 cm: Radiolarian-bearing diatom ooze with some nannofossils and foraminifera. Dark grayish brown with both lighter and darker patches. Strong bioturbation at places.
800-840 cm: Foraminifera and radiolarian-bearing diatom ooze with some mud. First half is pale yellow, the second half brown in color, moderate bioturbation.
840-910 cm: Radiolarian-bearing foraminifera ooze with some mud. Pale brown with a gradual transition to light gray, along with increase in diatom content. Slight bioturbation.
910-948 cm: Radiolarian-bearing foraminifera and diatom ooze with some mud. White with gradual transition to light brownish gray. Slight bioturbation.
948-970 cm: Foraminifera and radiolarian-bearing nannofossil-diatom ooze with some mud. Very pale brown. Strong bioturbation at places.
970-1030 cm: Nannofossil-foraminifera-diatom ooze with some radiolarians and mud. Light gray.

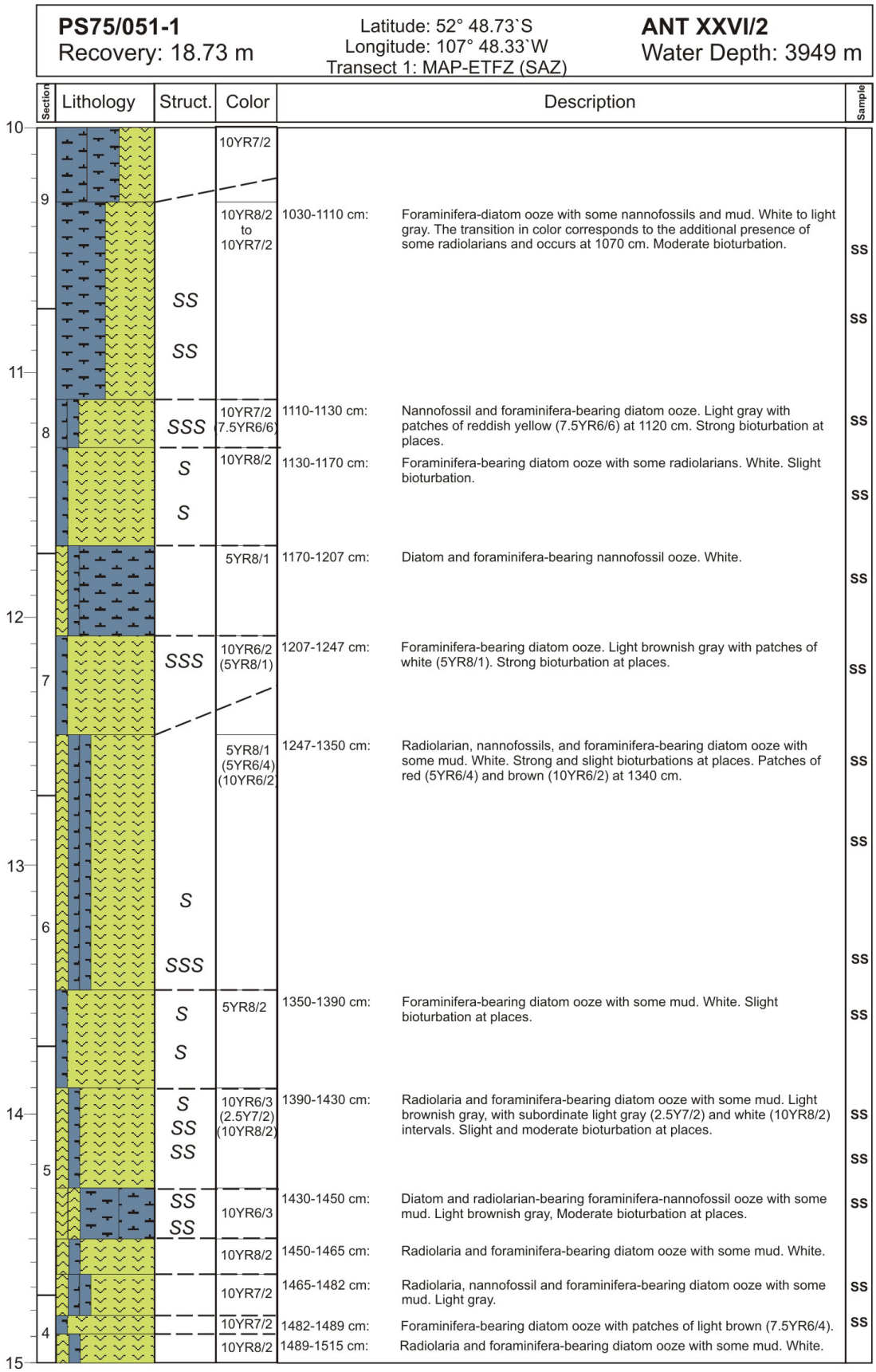
PS75/051-1
Recovery: 18.73 m
Latitude: 52° 48.73`S
Longitude: 107° 48.33`W
Transect 1: MAP-ETFZ (SAZ)
ANT XXVI/2
Water Depth: 3949 m
Section
Lithology
Struct.
Color
Description
Sample
10
11
12
13
14
15
9
8
7
6
5
4
SS
SS
SSS
S
S
SSS
S
S
S
SS
SS
SS
SS
10YR7/2
10YR8/2 to 10YR7/2
1030-1110 cm: Foraminifera-diatom ooze with some nannofossils and mud. White to light gray. The transition in color corresponds to the additional presence of some radiolarians and occurs at 1070 cm. Moderate bioturbation.
10YR7/2 (7.5YR6/6)
1110-1130 cm: Nannofossil and foraminifera-bearing diatom ooze. Light gray with patches of reddish yellow (7.5YR6/6) at 1120 cm. Strong bioturbation at places.
10YR8/2
1130-1170 cm: Foraminifera-bearing diatom ooze with some radiolarians. White. Slight bioturbation.
5YR8/1
1170-1207 cm: Diatom and foraminifera-bearing nannofossil ooze. White.
10YR6/2 (5YR8/1)
1207-1247 cm: Foraminifera-bearing diatom ooze. Light brownish gray with patches of white (5YR8/1). Strong bioturbation at places.
5YR8/1 (5YR6/4) (10YR6/2
1247-1350 cm: Radiolarian, nannofossils, and foraminifera-bearing diatom ooze with some mud. White. Strong and slight bioturbations at places. Patches of red (5YR6/4) and brown (10YR6/2) at 1340 cm.
5YR8/2
1350-1390 cm: Foraminifera-bearing diatom ooze with some mud. White. Slight bioturbation at places.
10YR6/3 (2.5Y7/2) (10YR8/2)
1390-1430 cm: Radiolaria and foraminifera-bearing diatom ooze with some mud. Light brownish gray, with subordinate light gray (2.5Y7/2) and white (10YR8/2) intervals. Slight and moderate bioturbation at places.
10YR6/3
1430-1450 cm: Diatom and radiolarian-bearing foraminifera-nannofossil ooze with some mud. Light brownish gray, Moderate bioturbation at places.
10YR8/2
1450-1465 cm: Radiolaria and foraminifera-bearing diatom ooze with some mud. White.
10YR7/2
1465-1482 cm: Radiolaria, nannofossil and foraminifera-bearing diatom ooze with some mud. Light gray.
10YR7/2
1482-1489 cm: Foraminifera-bearing diatom ooze with patches of light brown (7.5YR6/4).
10YR8/2
1489-1515 cm: Radiolaria and foraminifera-bearing diatom ooze with some mud. White.
SS

**PS75/051-1**
Recovery: 18.73 m

Latitude: 52° 48.73`S
Longitude: 107° 48.33`W
Transect 1: MAP-ETFZ (SAZ)

**ANT XXVI/2**
Water Depth: 3949 m

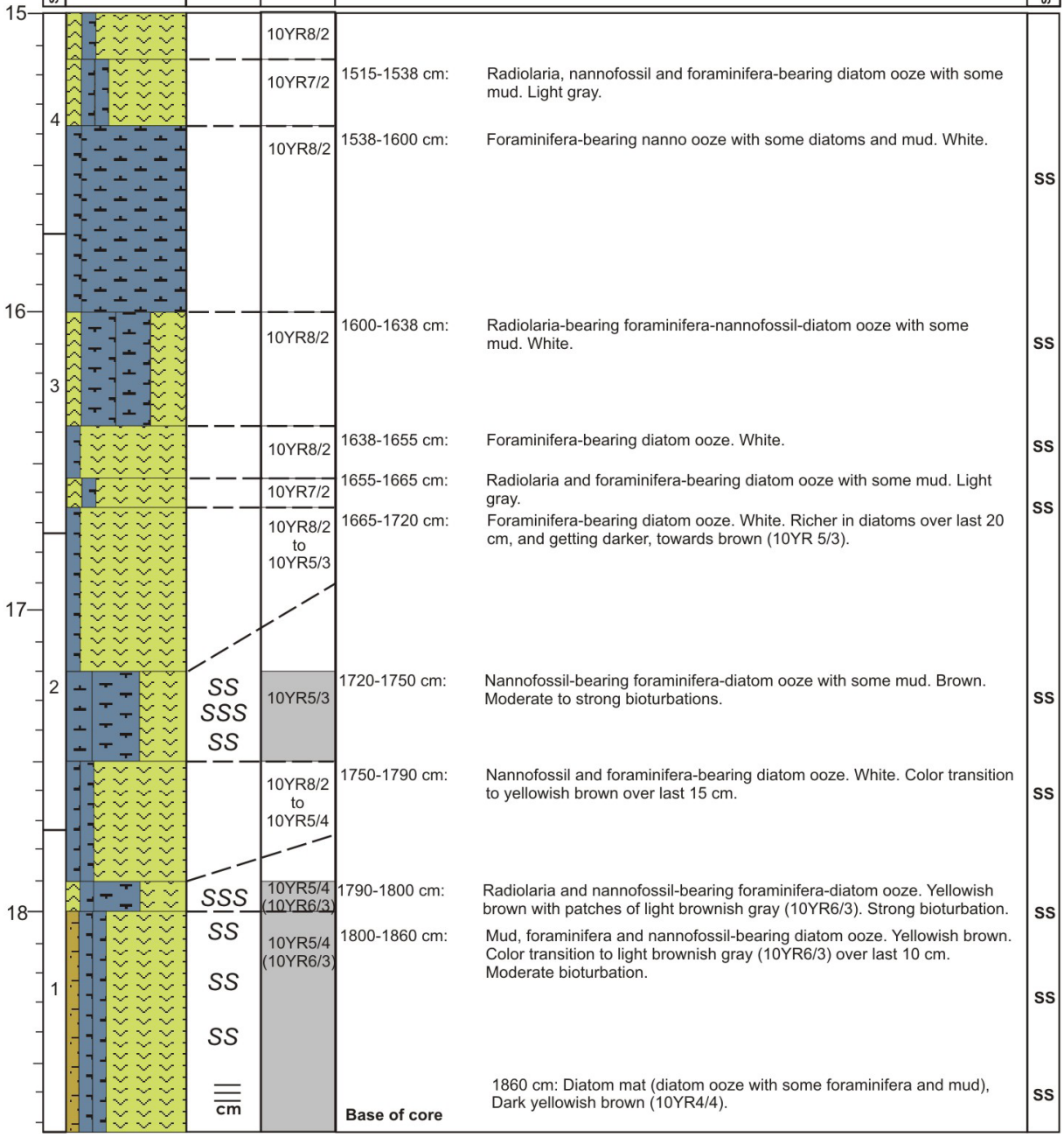

**PS75/052-3**
Recovery: 23.17 m

Latitude: 60° 45.12`S
Longitude: 115° 58.74`W
Amundsen Abyssal Plain (PFZ)

**ANT XXVI/2**
Water Depth: 5130m

| Section | Lithology | Struct. | Color | Description | Sample |
|---|---|---|---|---|---|
| 24 | | S | 10YR4/4 | 0-28 cm: Diatom ooze with some mud. Dark yellowish brown, slight bioturbation. | SS |
| | | | 10YR6/6 | 28-77 cm: Diatom ooze with some mud. Brownish yellow. | SS |
| 23 | | mm<br>cm<br>mm | 10YR6/6 | 77-128 cm: Diatom ooze with some mud. Brownish yellow, ca. 11 gray laminae (0.3 to 2cm thick), the most prominent one at 95cm.<br>95 cm: Diatom ooze with some silicoflagellates and black opaque particles (3%). Many *Thalassiotrix*. Lamina. | SS |
| | | | 5Y6/2 | 128-177 cm: Diatom ooze with some mud. Light olive gray, decreasing siliceous content downcore. | |
| 22 | | | 2.5Y6/4 | 177-270 cm: Diatom ooze. Light yellowish brown, slightly more gray at 211-225cm. | SS |
| 21 | | mm<br>mm<br>mm<br>mm<br>mm<br>mm | 2.5Y6/4 | 270-342 cm: Diatom ooze. Light yellowish brown, ca. 10 gray laminae (0.3 to 1cm thick) | |
| 20 | | mm | 10YR6/4 | 342-382 cm: Diatom ooze. Light yellowish brown, ca. 2-3 gray laminae (less than 0.5cm thick). Higher siliceous content compared to the unit above. | |
| 19 | | mm<br>mm<br>mm<br>mm<br>mm | 2.5Y6/4 | 382-471 cm: Diatom ooze. Light yellowish brown, ca. 18 gray laminae (less than 1cm thick). Siliceous content increases towards the bottom. | |
| | | mm<br>mm | 10YR7/4 | 471-510 cm: Diatom ooze. Very pale brown, ca. 14 gray and brown laminae (0.3 to 0.8cm thick). | |

**PS75/052-3**
Recovery: 23.17 m

Latitude: 60° 45.12`S
Longitude: 115° 58.74`W
Amundsen Abyssal Plain (PFZ)

**ANT XXVI/2**
Water Depth: 5130m

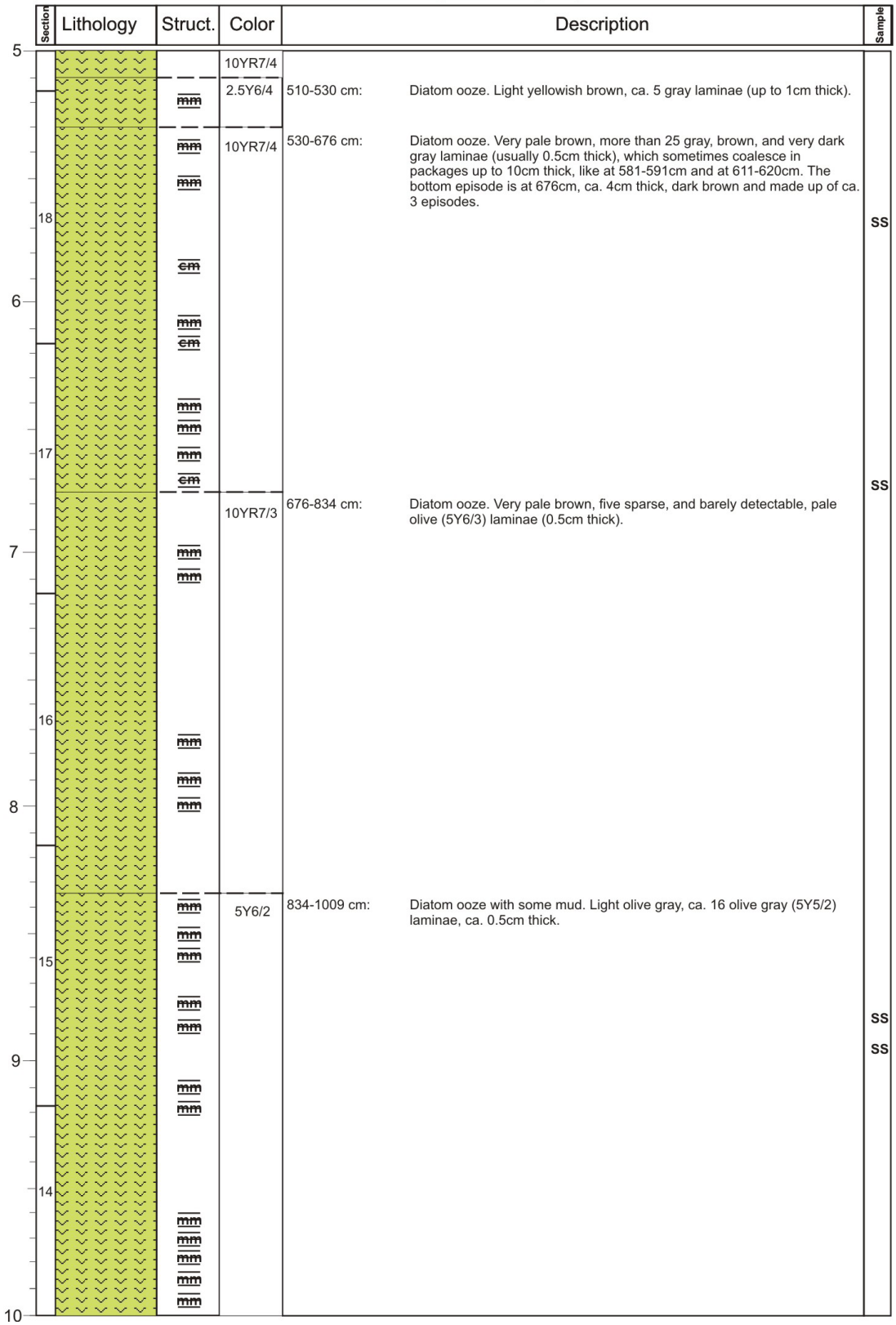

**PS75/052-3**
Recovery: 23.17 m

Latitude: 60° 45.12`S
Longitude: 115° 58.74`W
Amundsen Abyssal Plain (PFZ)

**ANT XXVI/2**
Water Depth: 5130m

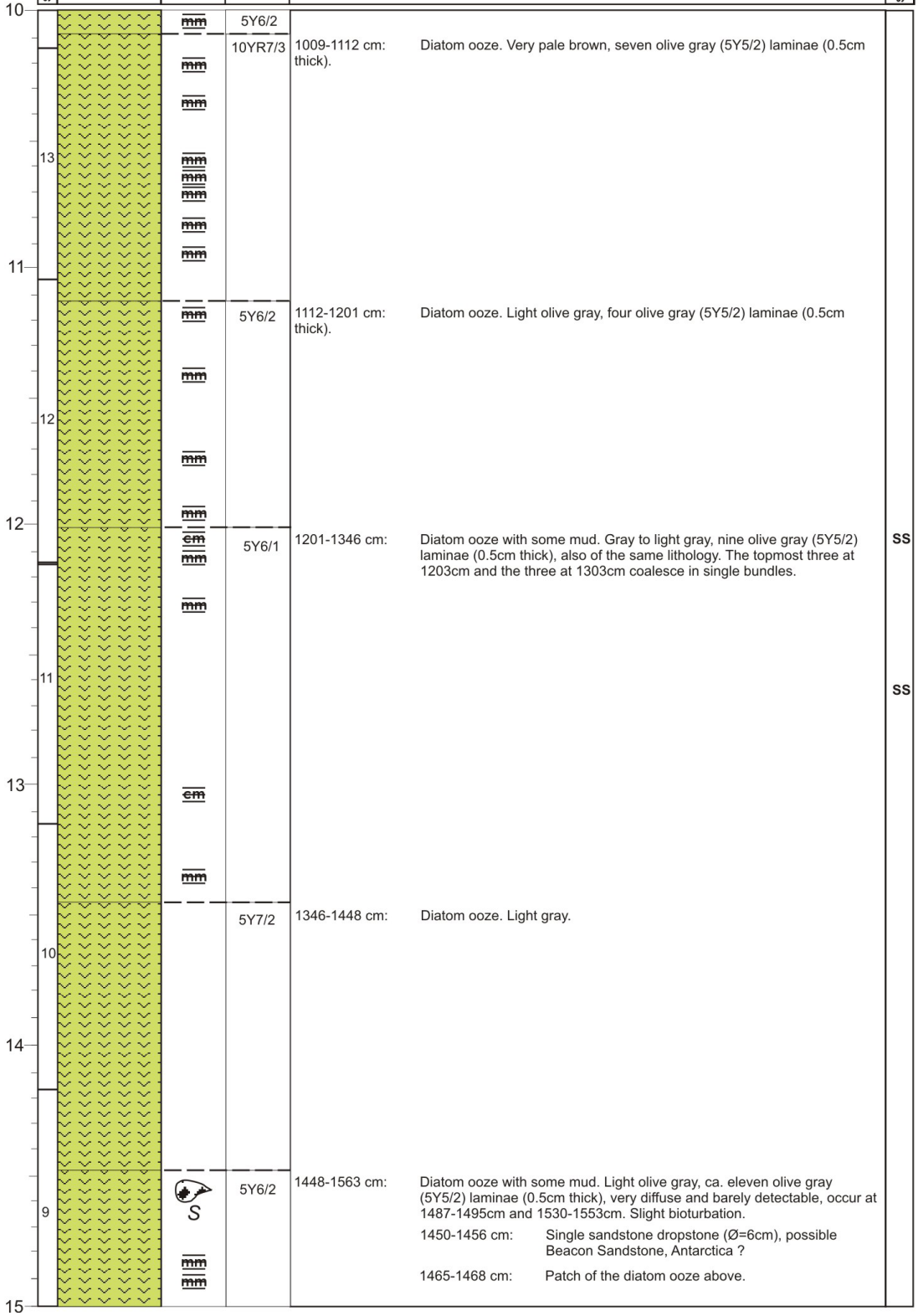

**PS75/052-3**
Recovery: 23.17 m

Latitude: 60° 45.12`S
Longitude: 115° 58.74`W
Amundsen Abyssal Plain (PFZ)

**ANT XXVI/2**
Water Depth: 5130m

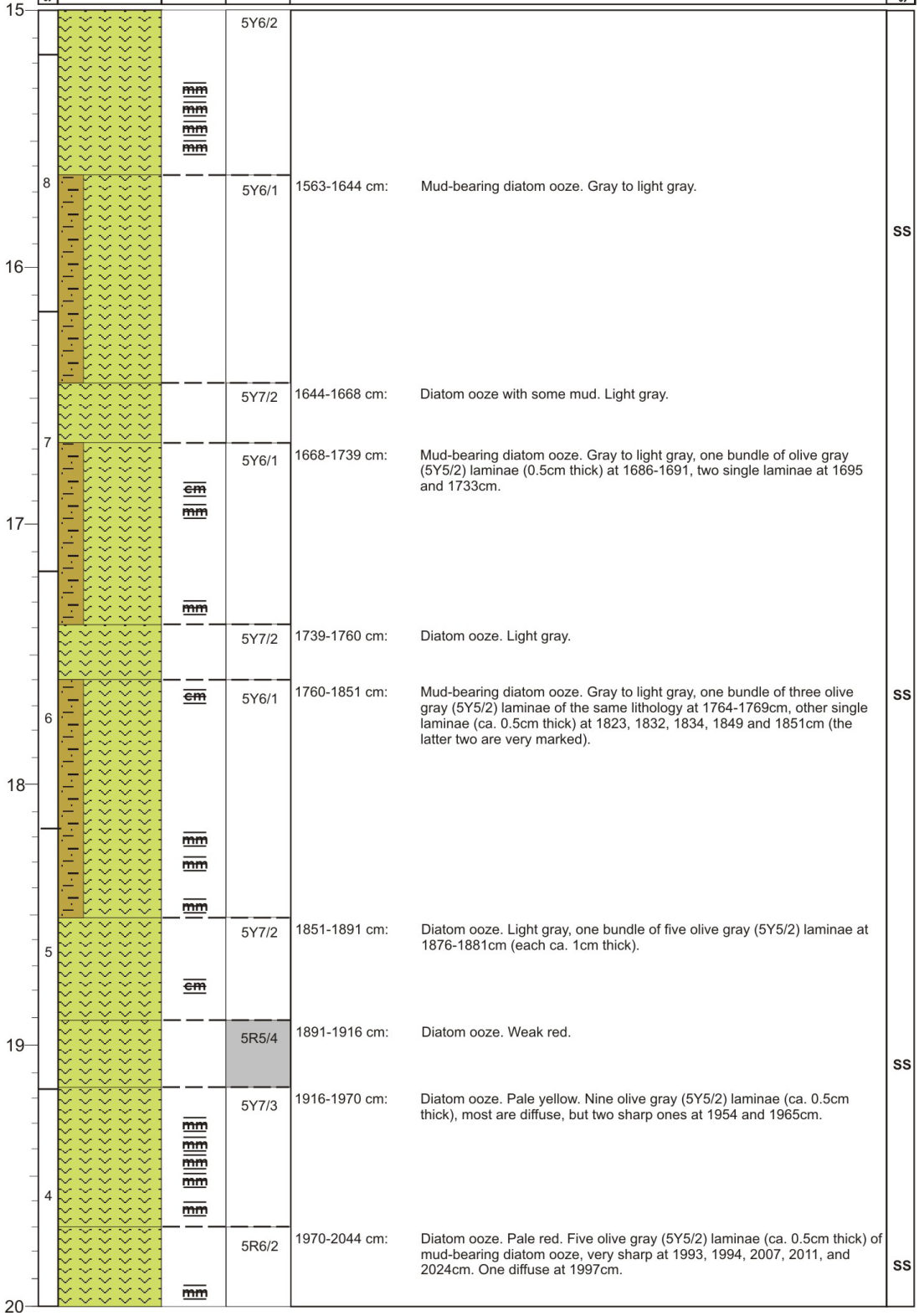

| Section | Color | | Description | Sample |
|---|---|---|---|---|
| | 5Y6/2 | | | |
| 8 | 5Y6/1 | 1563-1644 cm: | Mud-bearing diatom ooze. Gray to light gray. | SS |
| | 5Y7/2 | 1644-1668 cm: | Diatom ooze with some mud. Light gray. | |
| 7 | 5Y6/1 | 1668-1739 cm: | Mud-bearing diatom ooze. Gray to light gray, one bundle of olive gray (5Y5/2) laminae (0.5cm thick) at 1686-1691, two single laminae at 1695 and 1733cm. | |
| | 5Y7/2 | 1739-1760 cm: | Diatom ooze. Light gray. | |
| 6 | 5Y6/1 | 1760-1851 cm: | Mud-bearing diatom ooze. Gray to light gray, one bundle of three olive gray (5Y5/2) laminae of the same lithology at 1764-1769cm, other single laminae (ca. 0.5cm thick) at 1823, 1832, 1834, 1849 and 1851cm (the latter two are very marked). | SS |
| | 5Y7/2 | 1851-1891 cm: | Diatom ooze. Light gray, one bundle of five olive gray (5Y5/2) laminae at 1876-1881cm (each ca. 1cm thick). | |
| 5 | 5R5/4 | 1891-1916 cm: | Diatom ooze. Weak red. | SS |
| | 5Y7/3 | 1916-1970 cm: | Diatom ooze. Pale yellow. Nine olive gray (5Y5/2) laminae (ca. 0.5cm thick), most are diffuse, but two sharp ones at 1954 and 1965cm. | |
| 4 | 5R6/2 | 1970-2044 cm: | Diatom ooze. Pale red. Five olive gray (5Y5/2) laminae (ca. 0.5cm thick) of mud-bearing diatom ooze, very sharp at 1993, 1994, 2007, 2011, and 2024cm. One diffuse at 1997cm. | SS |

**PS75/052-3**
Recovery: 23.17 m

Latitude: 60° 45.12`S
Longitude: 115° 58.74`W
Amundsen Abyssal Plain (PFZ)

**ANT XXVI/2**
Water Depth: 5130m

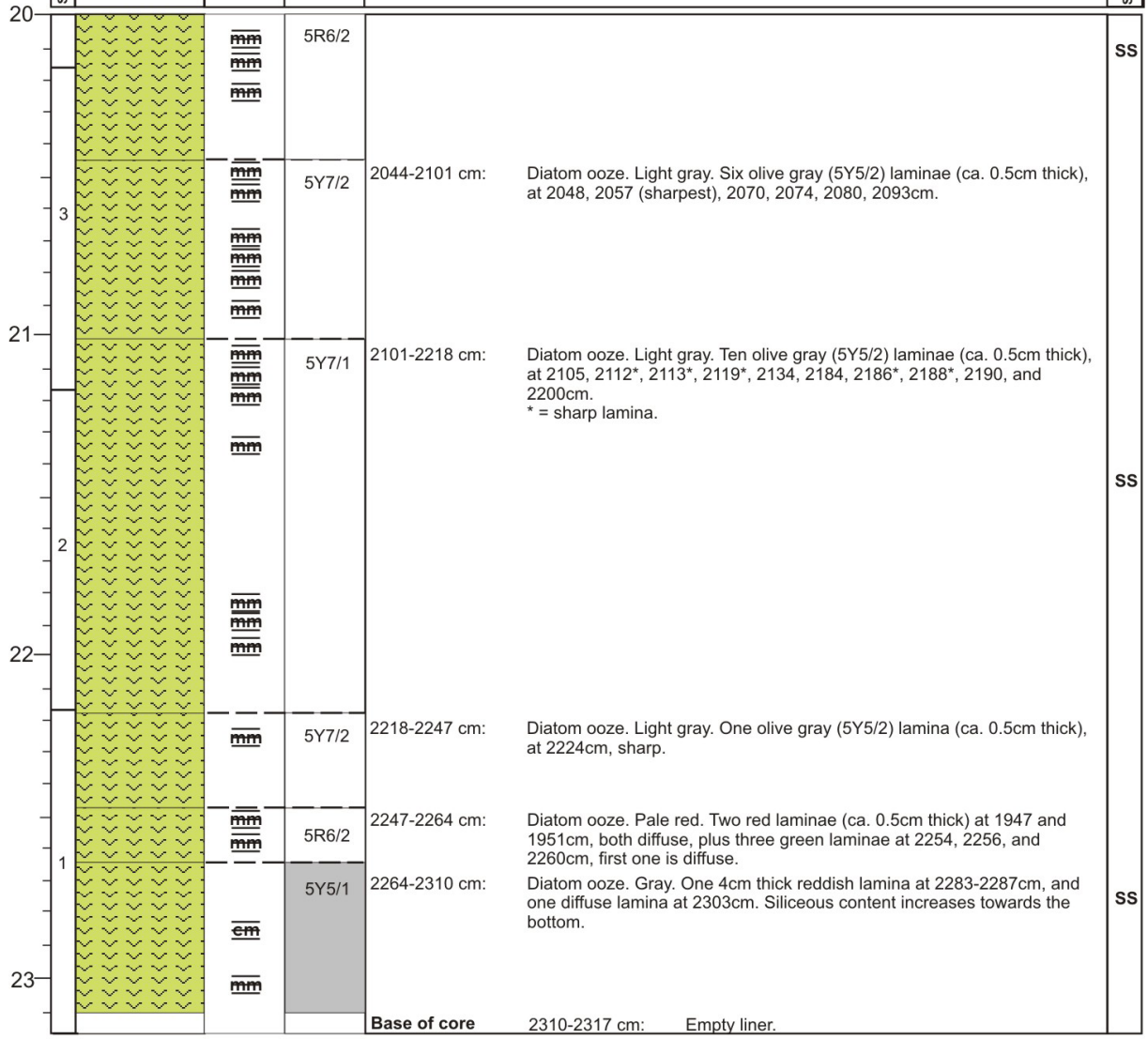


| | | |
|---|---|---|
| 2044-2101 cm: | Diatom ooze. Light gray. Six olive gray (5Y5/2) laminae (ca. 0.5cm thick), at 2048, 2057 (sharpest), 2070, 2074, 2080, 2093cm. | |
| 2101-2218 cm: | Diatom ooze. Light gray. Ten olive gray (5Y5/2) laminae (ca. 0.5cm thick), at 2105, 2112*, 2113*, 2119*, 2134, 2184, 2186*, 2188*, 2190, and 2200cm.<br>* = sharp lamina. | |
| 2218-2247 cm: | Diatom ooze. Light gray. One olive gray (5Y5/2) lamina (ca. 0.5cm thick), at 2224cm, sharp. | |
| 2247-2264 cm: | Diatom ooze. Pale red. Two red laminae (ca. 0.5cm thick) at 1947 and 1951cm, both diffuse, plus three green laminae at 2254, 2256, and 2260cm, first one is diffuse. | |
| 2264-2310 cm: | Diatom ooze. Gray. One 4cm thick reddish lamina at 2283-2287cm, and one diffuse lamina at 2303cm. Siliceous content increases towards the bottom. | |
| **Base of core** | 2310-2317 cm: Empty liner. | |

**PS75/054-1**
Recovery: 22.38 m

Latitude: 56° 09.11`S
Longitude: 115° 07.98`W
Transect 1: MAP-ETFZ (SAZ)

**ANT XXVI/2**
Water Depth: 4113m

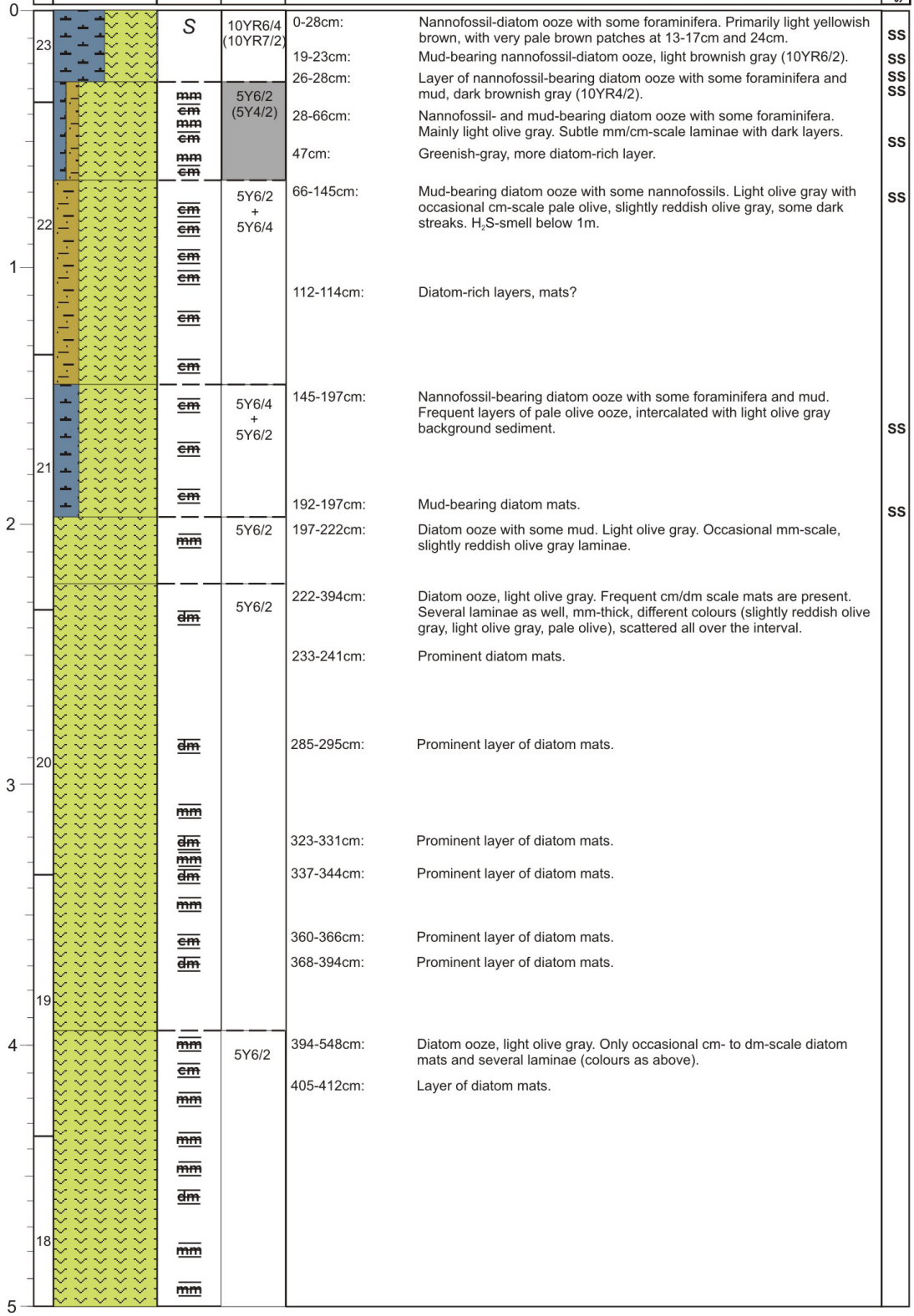

**PS75/054-1**
Recovery: 22.38 m

Latitude: 56° 09.11`S
Longitude: 115° 07.98`W
Transect 1: MAP-ETFZ (SAZ)

**ANT XXVI/2**
Water Depth: 4113m

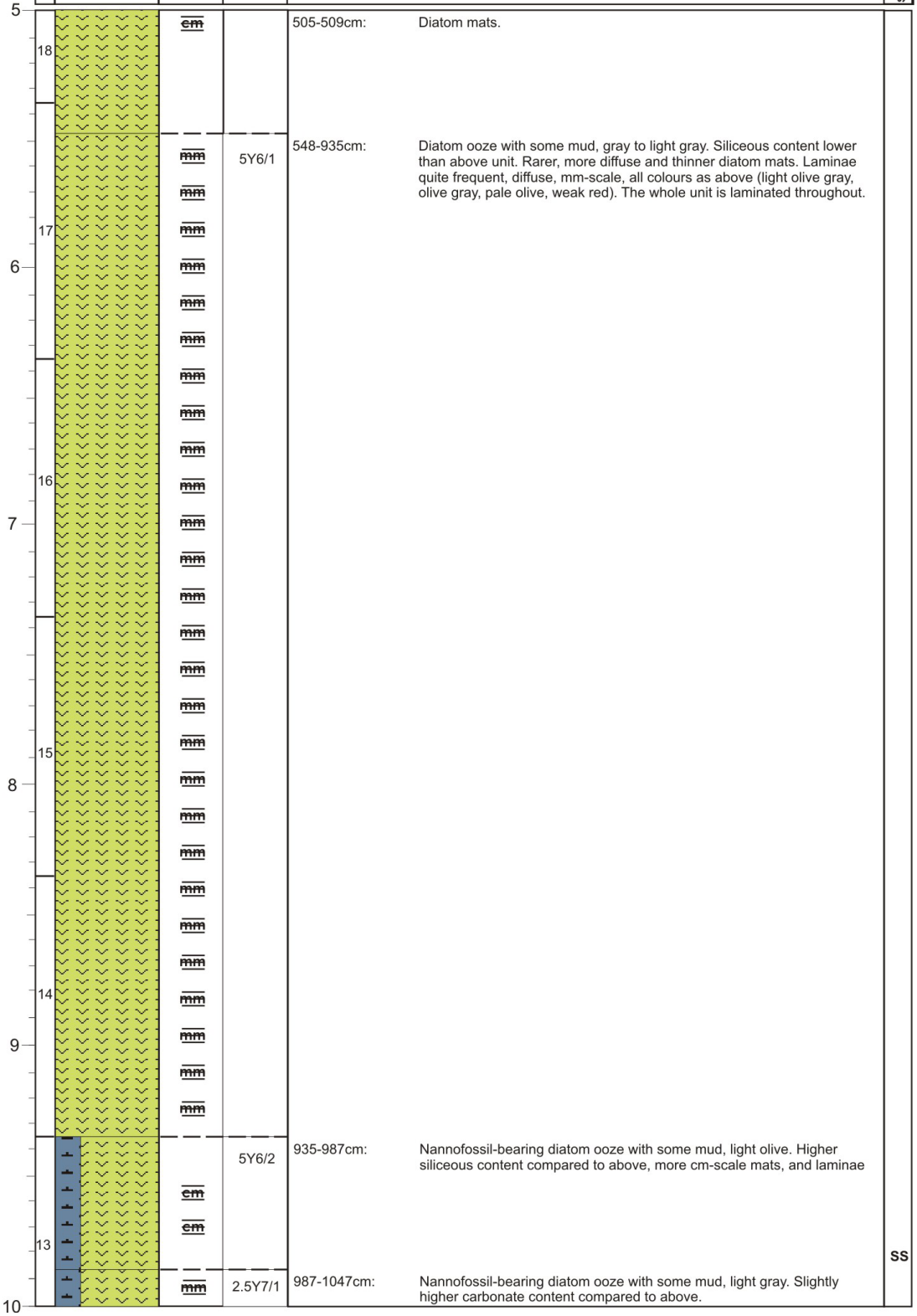

**PS75/054-1**
Recovery: 22.38 m

Latitude: 56° 09.11`S
Longitude: 115° 07.98`W
Transect 1: MAP-ETFZ (SAZ)

**ANT XXVI/2**
Water Depth: 4113m

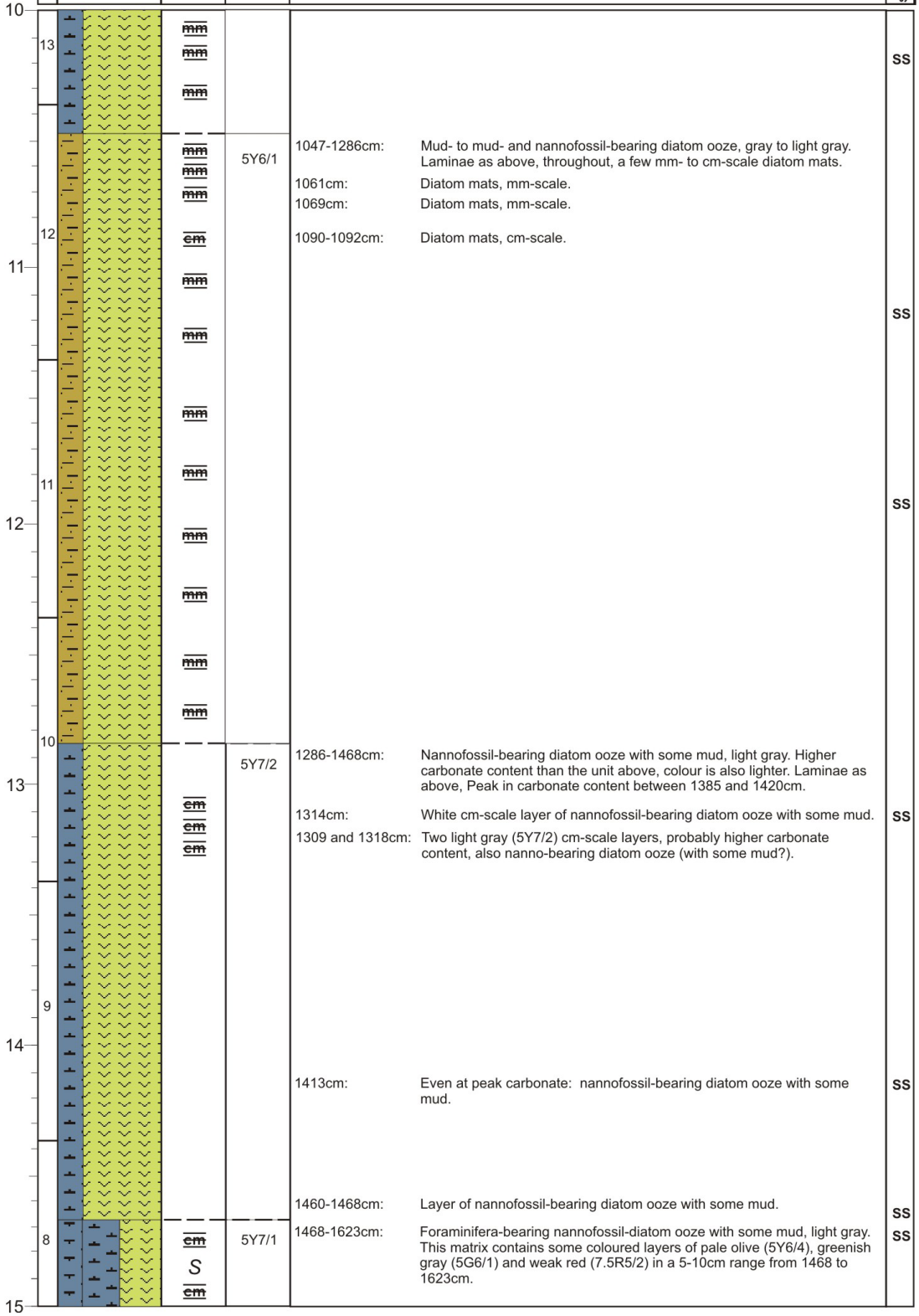

**PS75/054-1**
Recovery: 22.38 m

Latitude: 56° 09.11`S
Longitude: 115° 07.98`W
Transect 1: MAP-ETFZ (SAZ)

**ANT XXVI/2**
Water Depth: 4113m

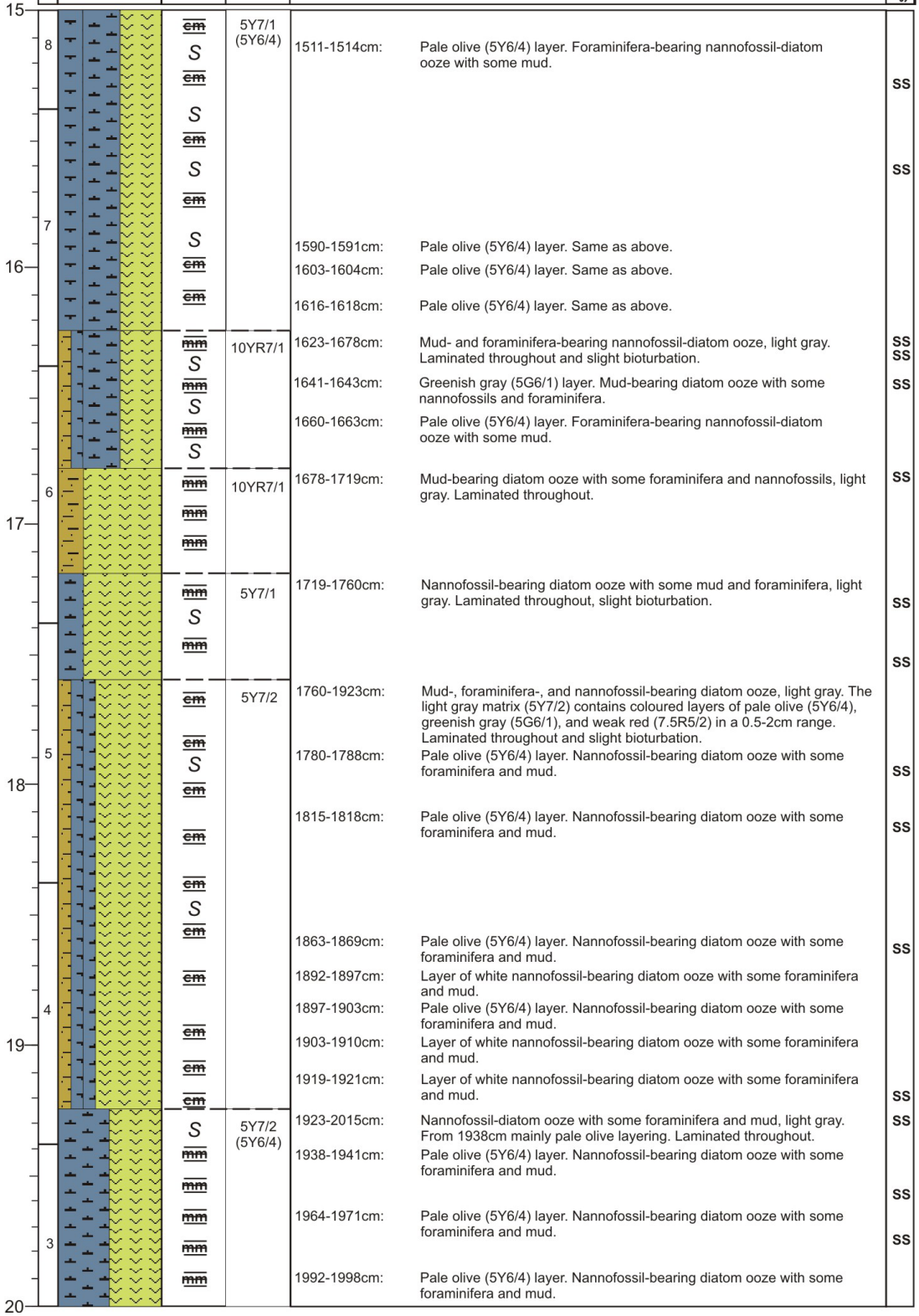


| Lithology | Struct. | Color | Description | Sample |
|---|---|---|---|---|
| | cm S cm S cm S cm S cm cm | 5Y7/1 (5Y6/4) | 1511-1514cm: Pale olive (5Y6/4) layer. Foraminifera-bearing nannofossil-diatom ooze with some mud. | SS |
| | | | 1590-1591cm: Pale olive (5Y6/4) layer. Same as above. | |
| | | | 1603-1604cm: Pale olive (5Y6/4) layer. Same as above. | |
| | | | 1616-1618cm: Pale olive (5Y6/4) layer. Same as above. | |
| | mm S mm S mm S | 10YR7/1 | 1623-1678cm: Mud- and foraminifera-bearing nannofossil-diatom ooze, light gray. Laminated throughout and slight bioturbation. | SS SS |
| | | | 1641-1643cm: Greenish gray (5G6/1) layer. Mud-bearing diatom ooze with some nannofossils and foraminifera. | SS |
| | | | 1660-1663cm: Pale olive (5Y6/4) layer. Foraminifera-bearing nannofossil-diatom ooze with some mud. | |
| | mm mm mm | 10YR7/1 | 1678-1719cm: Mud-bearing diatom ooze with some foraminifera and nannofossils, light gray. Laminated throughout. | SS |
| | mm S mm | 5Y7/1 | 1719-1760cm: Nannofossil-bearing diatom ooze with some mud and foraminifera, light gray. Laminated throughout, slight bioturbation. | SS |
| | | | | SS |
| | cm cm S cm cm cm cm S cm cm cm cm | 5Y7/2 | 1760-1923cm: Mud-, foraminifera-, and nannofossil-bearing diatom ooze, light gray. The light gray matrix (5Y7/2) contains coloured layers of pale olive (5Y6/4), greenish gray (5G6/1), and weak red (7.5R5/2) in a 0.5-2cm range. Laminated throughout and slight bioturbation. | |
| | | | 1780-1788cm: Pale olive (5Y6/4) layer. Nannofossil-bearing diatom ooze with some foraminifera and mud. | SS |
| | | | 1815-1818cm: Pale olive (5Y6/4) layer. Nannofossil-bearing diatom ooze with some foraminifera and mud. | SS |
| | | | 1863-1869cm: Pale olive (5Y6/4) layer. Nannofossil-bearing diatom ooze with some foraminifera and mud. | SS |
| | | | 1892-1897cm: Layer of white nannofossil-bearing diatom ooze with some foraminifera and mud. | |
| | | | 1897-1903cm: Pale olive (5Y6/4) layer. Nannofossil-bearing diatom ooze with some foraminifera and mud. | |
| | | | 1903-1910cm: Layer of white nannofossil-bearing diatom ooze with some foraminifera and mud. | |
| | | | 1919-1921cm: Layer of white nannofossil-bearing diatom ooze with some foraminifera and mud. | SS |
| | S mm mm mm mm mm | 5Y7/2 (5Y6/4) | 1923-2015cm: Nannofossil-diatom ooze with some foraminifera and mud, light gray. From 1938cm mainly pale olive layering. Laminated throughout. | SS |
| | | | 1938-1941cm: Pale olive (5Y6/4) layer. Nannofossil-bearing diatom ooze with some foraminifera and mud. | |
| | | | | SS |
| | | | 1964-1971cm: Pale olive (5Y6/4) layer. Nannofossil-bearing diatom ooze with some foraminifera and mud. | SS |
| | | | 1992-1998cm: Pale olive (5Y6/4) layer. Nannofossil-bearing diatom ooze with some foraminifera and mud. | |

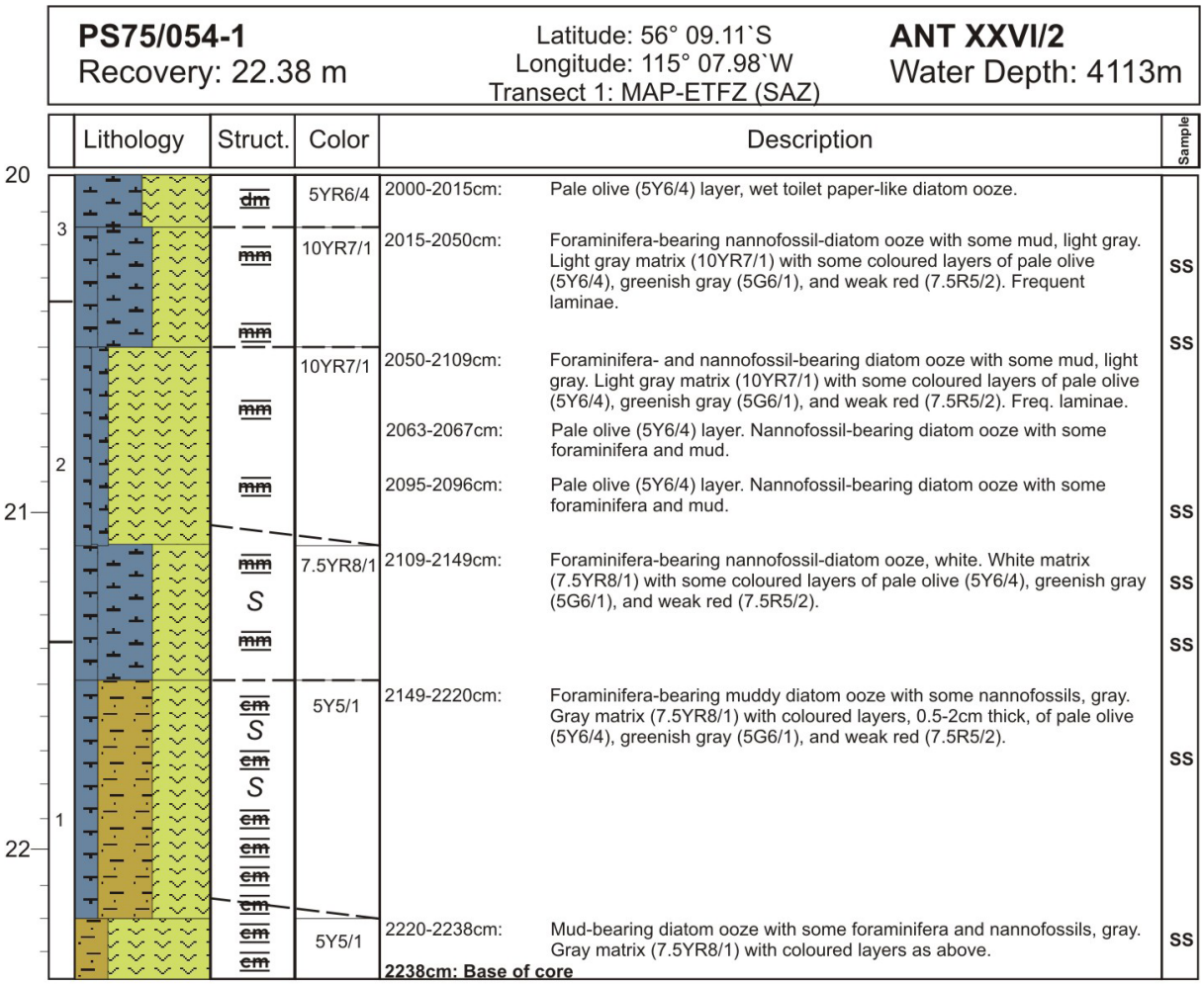
PS75/054-1
Recovery: 22.38 m
Latitude: 56° 09.11`S
Longitude: 115° 07.98`W
Transect 1: MAP-ETFZ (SAZ)
ANT XXVI/2
Water Depth: 4113m
Lithology
Struct.
Color
Description
Sample
20
21
22
3
2
1
dm
mm
S
cm
5YR6/4
10YR7/1
7.5YR8/1
5Y5/1
2000-2015cm: Pale olive (5Y6/4) layer, wet toilet paper-like diatom ooze.
2015-2050cm: Foraminifera-bearing nannofossil-diatom ooze with some mud, light gray. Light gray matrix (10YR7/1) with some coloured layers of pale olive (5Y6/4), greenish gray (5G6/1), and weak red (7.5R5/2). Frequent laminae.
2050-2109cm: Foraminifera- and nannofossil-bearing diatom ooze with some mud, light gray. Light gray matrix (10YR7/1) with some coloured layers of pale olive (5Y6/4), greenish gray (5G6/1), and weak red (7.5R5/2). Freq. laminae.
2063-2067cm: Pale olive (5Y6/4) layer. Nannofossil-bearing diatom ooze with some foraminifera and mud.
2095-2096cm: Pale olive (5Y6/4) layer. Nannofossil-bearing diatom ooze with some foraminifera and mud.
2109-2149cm: Foraminifera-bearing nannofossil-diatom ooze, white. White matrix (7.5YR8/1) with some coloured layers of pale olive (5Y6/4), greenish gray (5G6/1), and weak red (7.5R5/2).
2149-2220cm: Foraminifera-bearing muddy diatom ooze with some nannofossils, gray. Gray matrix (7.5YR8/1) with coloured layers, 0.5-2cm thick, of pale olive (5Y6/4), greenish gray (5G6/1), and weak red (7.5R5/2).
2220-2238cm: Mud-bearing diatom ooze with some foraminifera and nannofossils, gray. Gray matrix (7.5YR8/1) with coloured layers as above.
2238cm: Base of core
SS

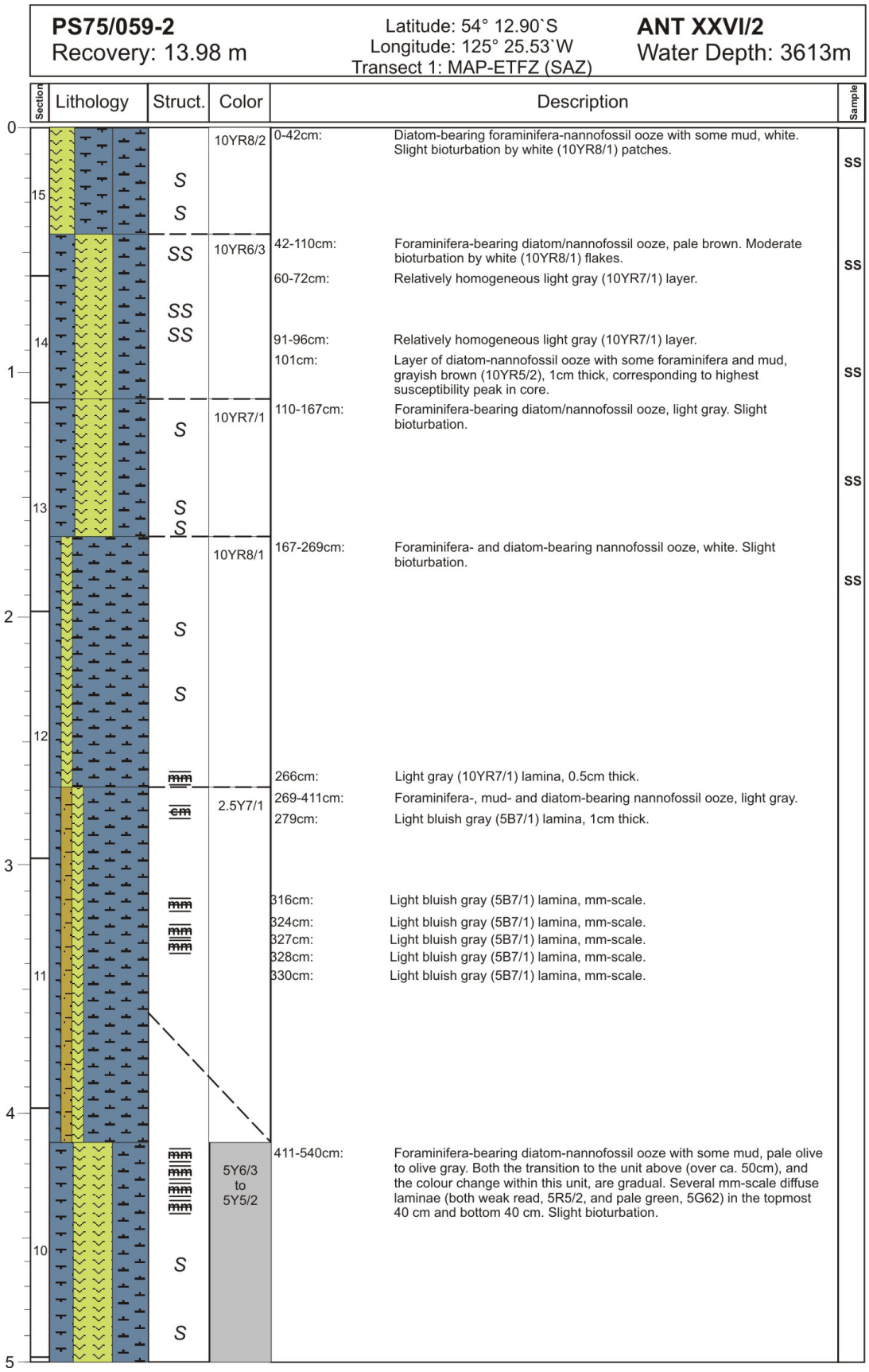
PS75/059-2
Recovery: 13.98 m
Latitude: 54° 12.90`S
Longitude: 125° 25.53`W
Transect 1: MAP-ETFZ (SAZ)
ANT XXVI/2
Water Depth: 3613m
Section
Lithology
Struct.
Color
Description
Sample
0
1
2
3
4
5
15
14
13
12
11
10
10YR8/2
0-42cm:
Diatom-bearing foraminifera-nannofossil ooze with some mud, white. Slight bioturbation by white (10YR8/1) patches.
SS
10YR6/3
42-110cm:
Foraminifera-bearing diatom/nannofossil ooze, pale brown. Moderate bioturbation by white (10YR8/1) flakes.
60-72cm:
Relatively homogeneous light gray (10YR7/1) layer.
91-96cm:
Relatively homogeneous light gray (10YR7/1) layer.
101cm:
Layer of diatom-nannofossil ooze with some foraminifera and mud, grayish brown (10YR5/2), 1cm thick, corresponding to highest susceptibility peak in core.
10YR7/1
110-167cm:
Foraminifera-bearing diatom/nannofossil ooze, light gray. Slight bioturbation.
10YR8/1
167-269cm:
Foraminifera- and diatom-bearing nannofossil ooze, white. Slight bioturbation.
266cm:
Light gray (10YR7/1) lamina, 0.5cm thick.
2.5Y7/1
269-411cm:
Foraminifera-, mud- and diatom-bearing nannofossil ooze, light gray.
279cm:
Light bluish gray (5B7/1) lamina, 1cm thick.
316cm:
Light bluish gray (5B7/1) lamina, mm-scale.
324cm:
Light bluish gray (5B7/1) lamina, mm-scale.
327cm:
Light bluish gray (5B7/1) lamina, mm-scale.
328cm:
Light bluish gray (5B7/1) lamina, mm-scale.
330cm:
Light bluish gray (5B7/1) lamina, mm-scale.
5Y6/3
to
5Y5/2
411-540cm:
Foraminifera-bearing diatom-nannofossil ooze with some mud, pale olive to olive gray. Both the transition to the unit above (over ca. 50cm), and the colour change within this unit, are gradual. Several mm-scale diffuse laminae (both weak read, 5R5/2, and pale green, 5G62) in the topmost 40 cm and bottom 40 cm. Slight bioturbation.

**PS75/059-2**
Recovery: 13.98 m

Latitude: 54° 12.90`S
Longitude: 125° 25.53`W
Transect 1: MAP-ETFZ (SAZ)

**ANT XXVI/2**
Water Depth: 3613m

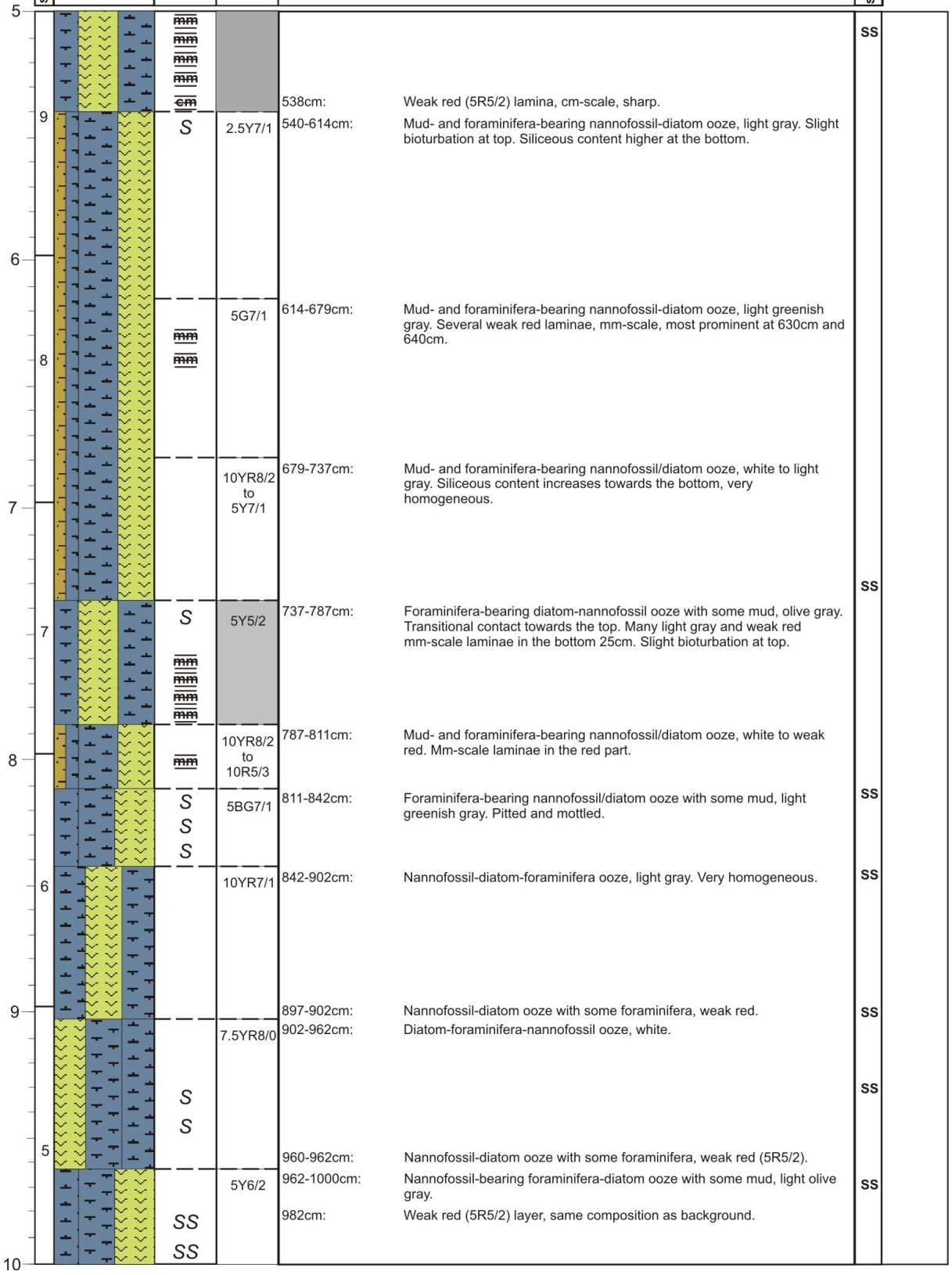

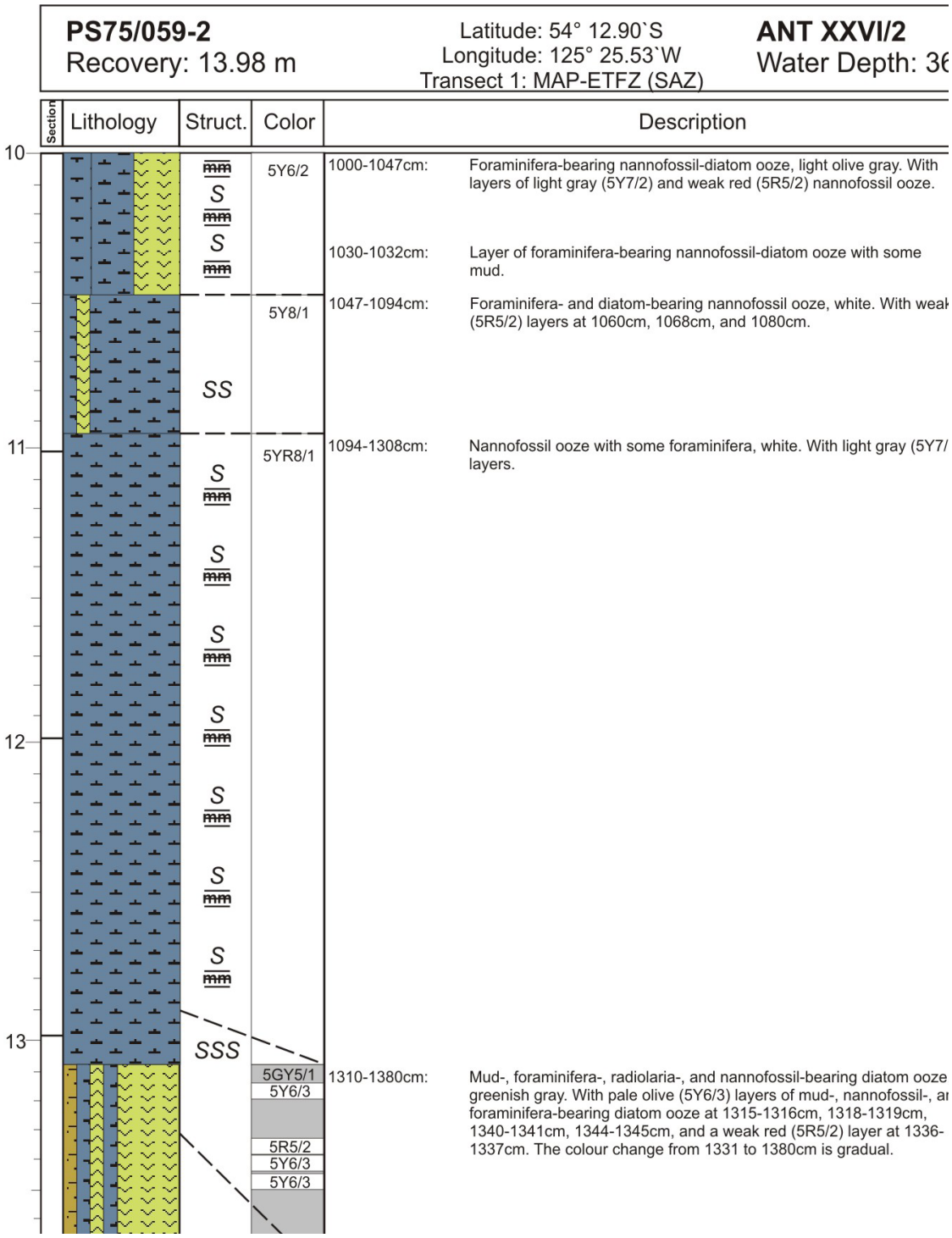
PS75/059-2
Recovery: 13.98 m
Latitude: 54° 12.90`S
Longitude: 125° 25.53`W
Transect 1: MAP-ETFZ (SAZ)
ANT XXVI/2
Water Depth: 36
Section
Lithology
Struct.
Color
Description
10
11
12
13
S
SS
SSS
5Y6/2
5Y8/1
5YR8/1
5GY5/1
5Y6/3
5R5/2
5Y6/3
5Y6/3
1000-1047cm: Foraminifera-bearing nannofossil-diatom ooze, light olive gray. With layers of light gray (5Y7/2) and weak red (5R5/2) nannofossil ooze.
1030-1032cm: Layer of foraminifera-bearing nannofossil-diatom ooze with some mud.
1047-1094cm: Foraminifera- and diatom-bearing nannofossil ooze, white. With weak (5R5/2) layers at 1060cm, 1068cm, and 1080cm.
1094-1308cm: Nannofossil ooze with some foraminifera, white. With light gray (5Y7/ layers.
1310-1380cm: Mud-, foraminifera-, radiolaria-, and nannofossil-bearing diatom ooze greenish gray. With pale olive (5Y6/3) layers of mud-, nannofossil-, ar foraminifera-bearing diatom ooze at 1315-1316cm, 1318-1319cm, 1340-1341cm, 1344-1345cm, and a weak red (5R5/2) layer at 1336-1337cm. The colour change from 1331 to 1380cm is gradual.

**PS75/062-2**
Recovery: 21.09 m

Latitude: 58° 16.60`S
Longitude: 135° 37.61`W
Transect 2: ETFZ-AAP (PFZ)

**ANT XXVI/2**
Water Depth: 4165m

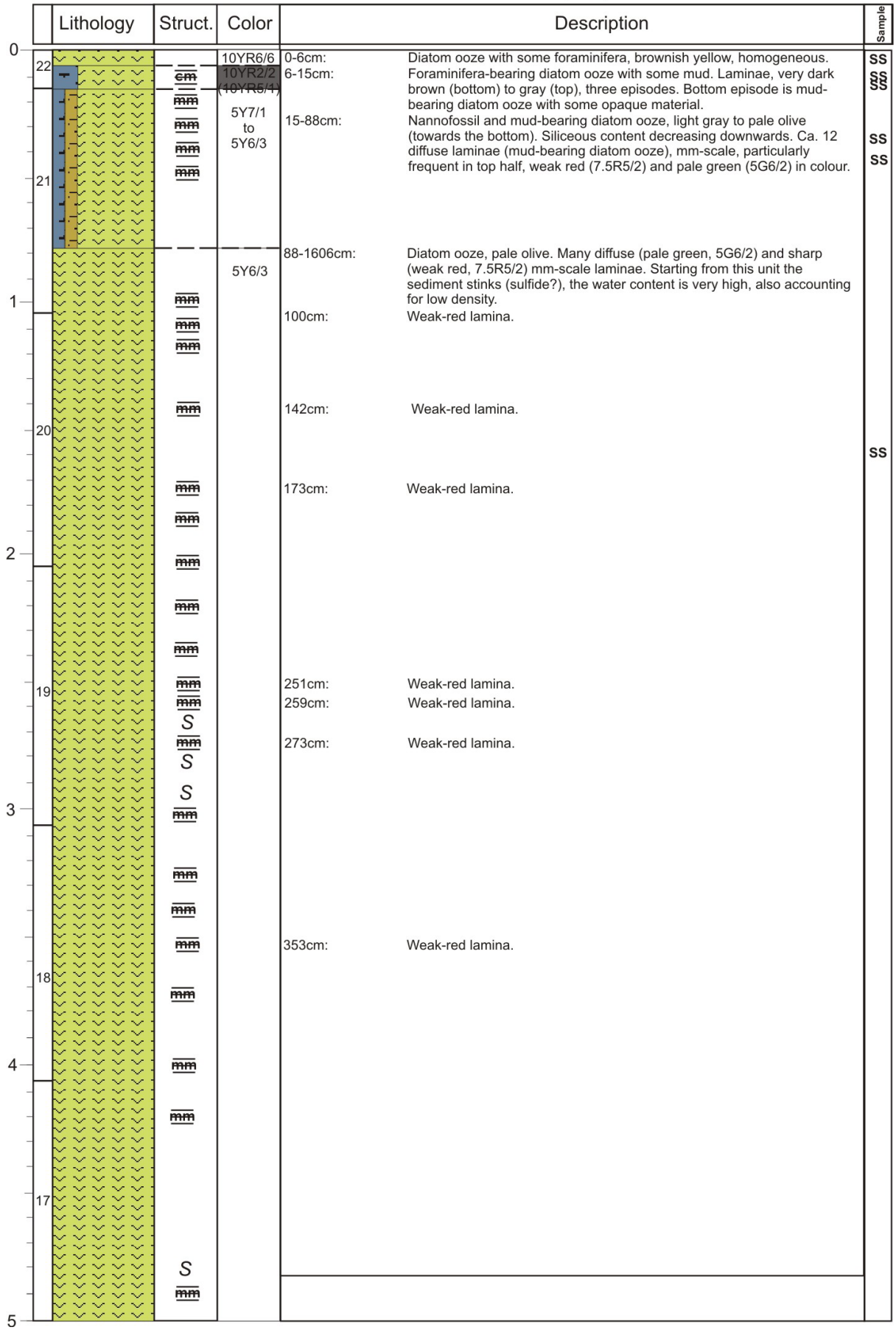

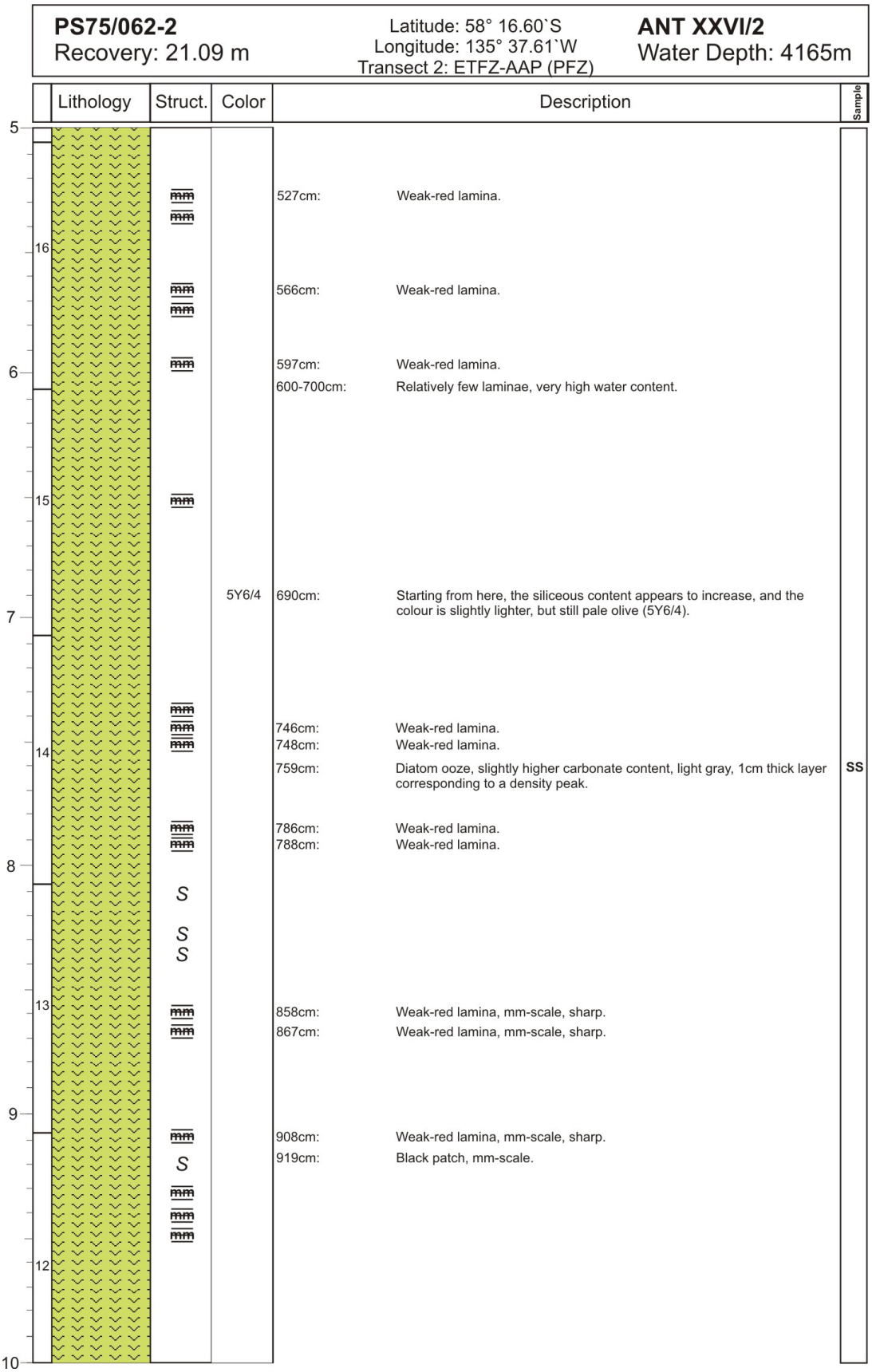
PS75/062-2
Recovery: 21.09 m
Latitude: 58° 16.60`S
Longitude: 135° 37.61`W
Transect 2: ETFZ-AAP (PFZ)
ANT XXVI/2
Water Depth: 4165m
Lithology
Struct.
Color
Description
Sample
5
6
7
8
9
10
16
15
14
13
12
5Y6/4
527cm: Weak-red lamina.
566cm: Weak-red lamina.
597cm: Weak-red lamina.
600-700cm: Relatively few laminae, very high water content.
690cm: Starting from here, the siliceous content appears to increase, and the colour is slightly lighter, but still pale olive (5Y6/4).
746cm: Weak-red lamina.
748cm: Weak-red lamina.
759cm: Diatom ooze, slightly higher carbonate content, light gray, 1cm thick layer corresponding to a density peak.
SS
786cm: Weak-red lamina.
788cm: Weak-red lamina.
858cm: Weak-red lamina, mm-scale, sharp.
867cm: Weak-red lamina, mm-scale, sharp.
908cm: Weak-red lamina, mm-scale, sharp.
919cm: Black patch, mm-scale.

**PS75/062-2**
Recovery: 21.09 m

Latitude: 58° 16.60`S
Longitude: 135° 37.61`W
Transect 2: ETFZ-AAP (PFZ)

**ANT XXVI/2**
Water Depth: 4165m

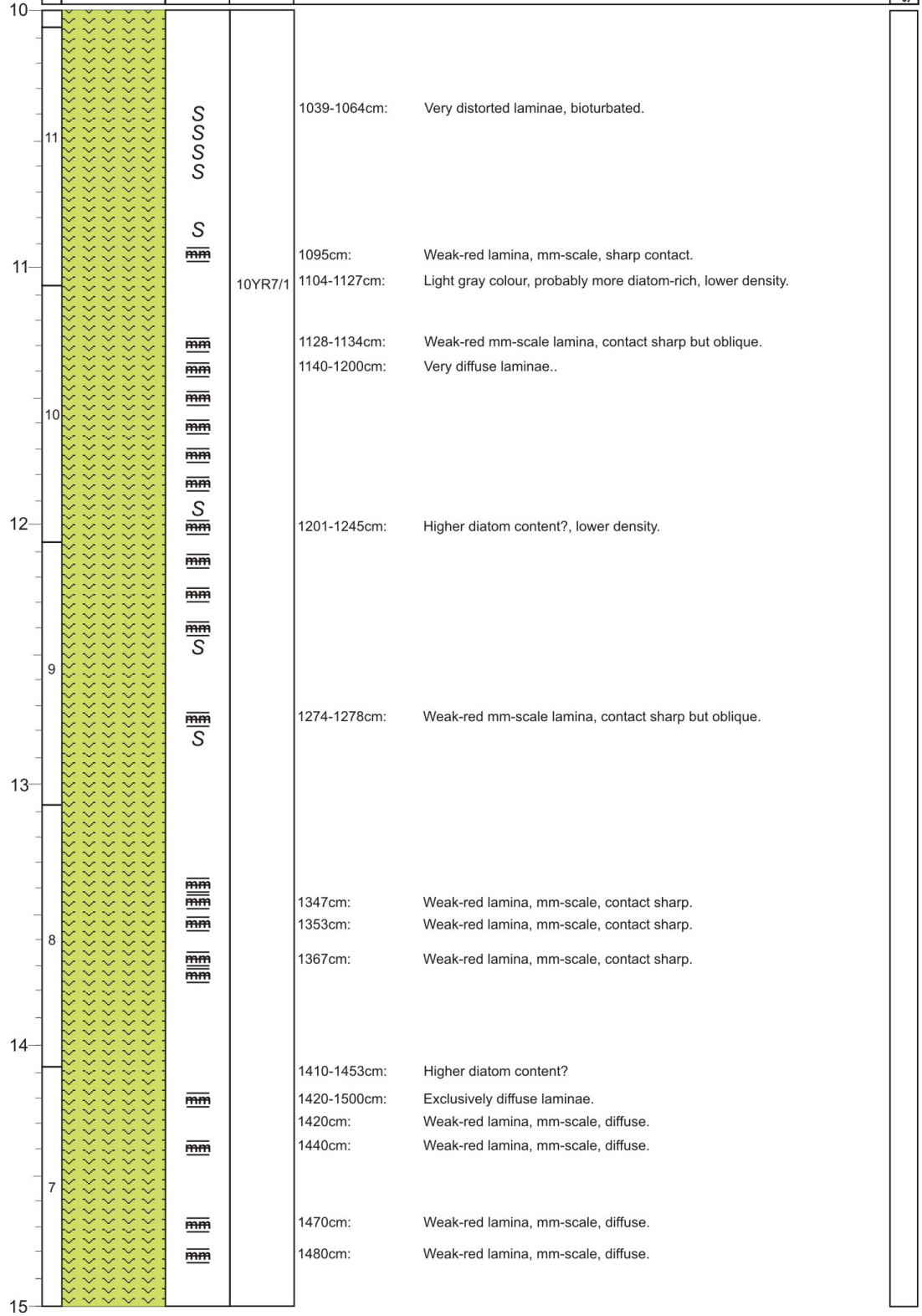

**PS75/062-2**
Recovery: 21.09 m

Latitude: 58° 16.60`S
Longitude: 135° 37.61`W
Transect 2: ETFZ-AAP (PFZ)

**ANT XXVI/2**
Water Depth: 4165m

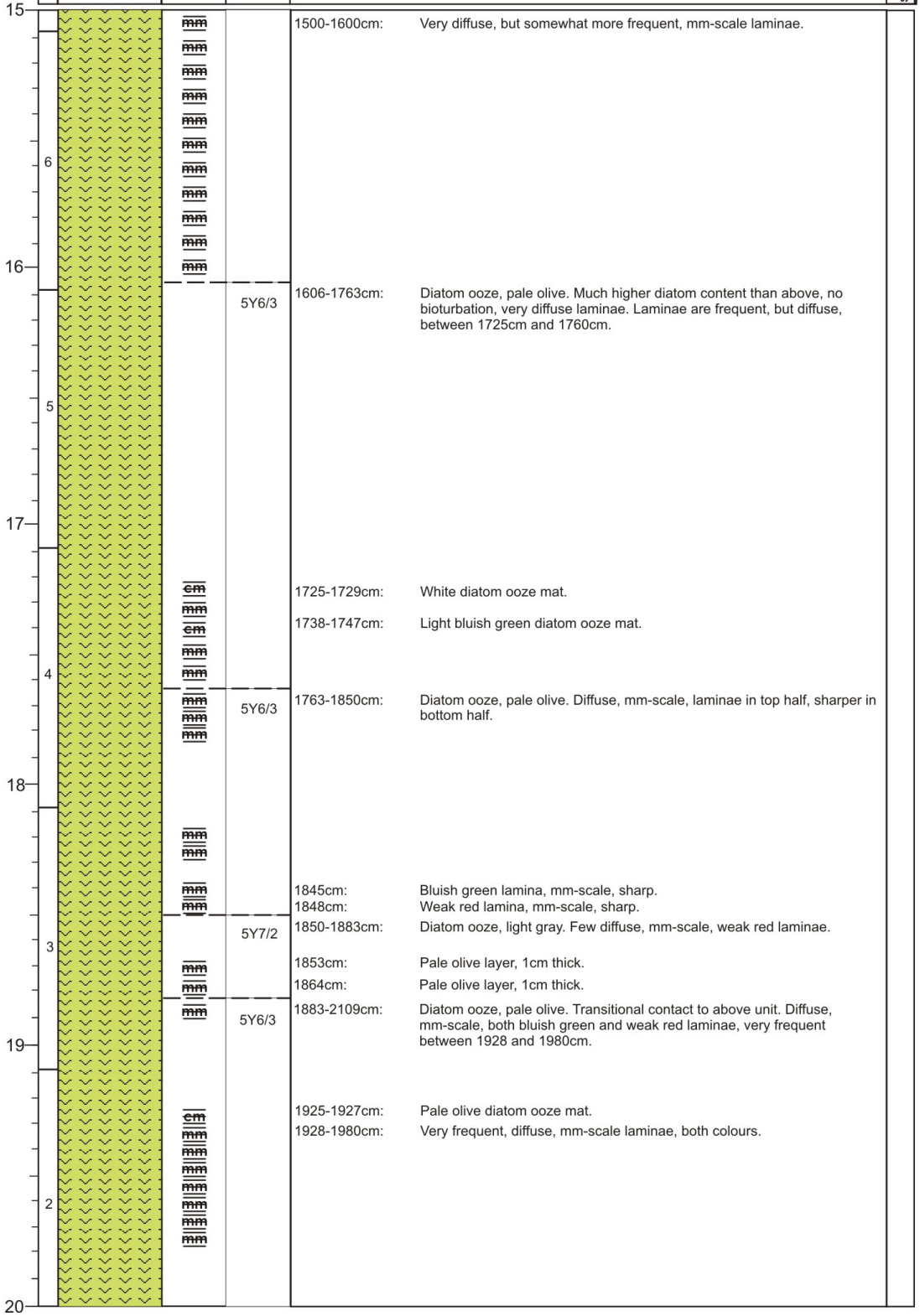

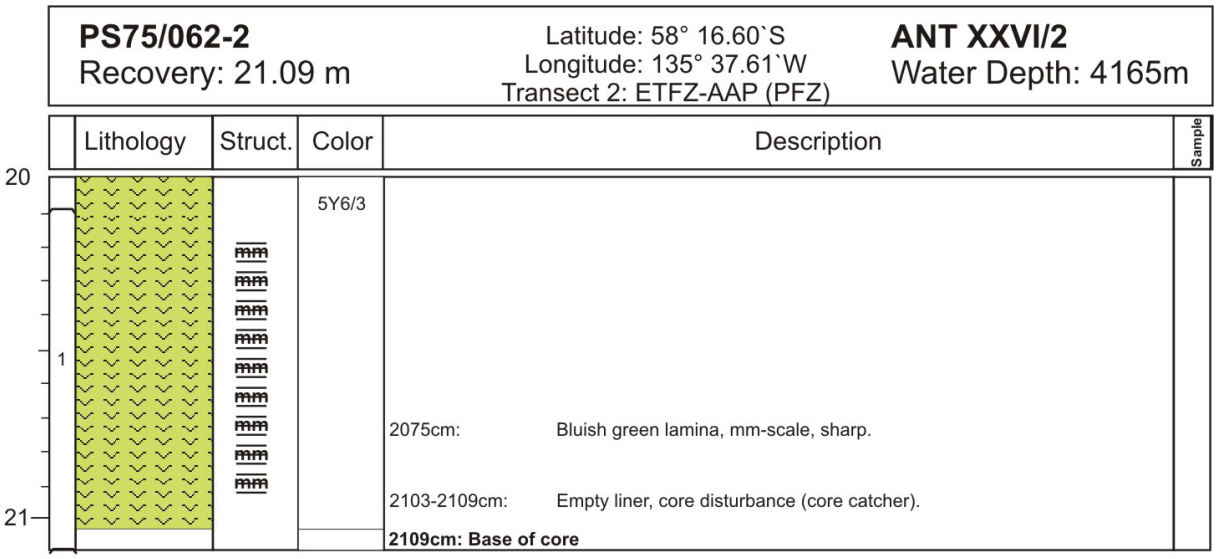
PS75/062-2
Recovery: 21.09 m
Latitude: 58° 16.60`S
Longitude: 135° 37.61`W
Transect 2: ETFZ-AAP (PFZ)
ANT XXVI/2
Water Depth: 4165m
Lithology
Struct.
Color
Description
Sample
20
21
1
5Y6/3
2075cm: Bluish green lamina, mm-scale, sharp.
2103-2109cm: Empty liner, core disturbance (core catcher).
2109cm: Base of core

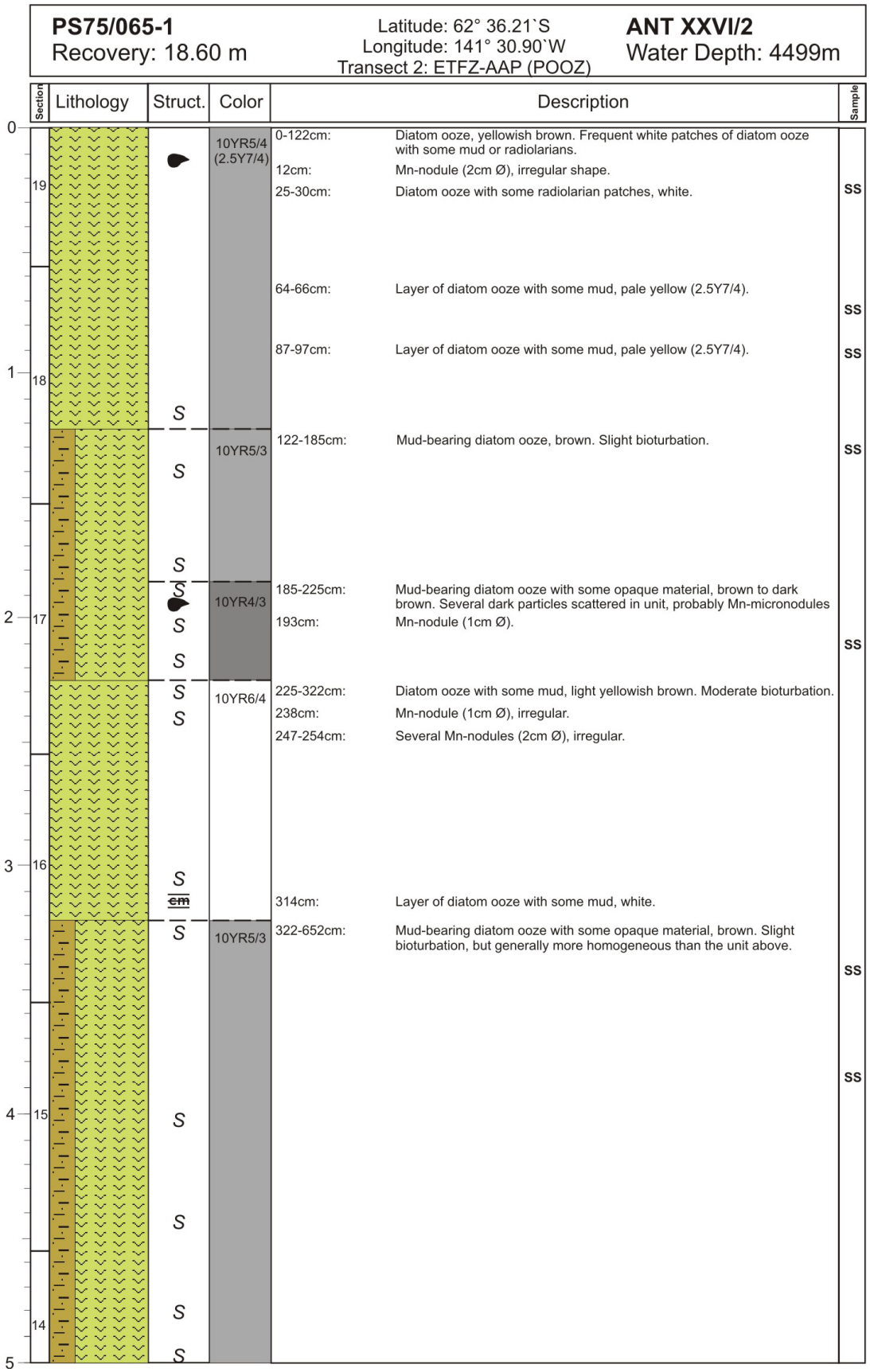
PS75/065-1
Recovery: 18.60 m
Latitude: 62° 36.21`S
Longitude: 141° 30.90`W
Transect 2: ETFZ-AAP (POOZ)
ANT XXVI/2
Water Depth: 4499m
Section
Lithology
Struct.
Color
Description
Sample
0
1
2
3
4
5
19
18
17
16
15
14
10YR5/4 (2.5Y7/4)
10YR5/3
10YR4/3
10YR6/4
10YR5/3
0-122cm: Diatom ooze, yellowish brown. Frequent white patches of diatom ooze with some mud or radiolarians.
12cm: Mn-nodule (2cm Ø), irregular shape.
25-30cm: Diatom ooze with some radiolarian patches, white.
64-66cm: Layer of diatom ooze with some mud, pale yellow (2.5Y7/4).
87-97cm: Layer of diatom ooze with some mud, pale yellow (2.5Y7/4).
122-185cm: Mud-bearing diatom ooze, brown. Slight bioturbation.
185-225cm: Mud-bearing diatom ooze with some opaque material, brown to dark brown. Several dark particles scattered in unit, probably Mn-micronodules
193cm: Mn-nodule (1cm Ø).
225-322cm: Diatom ooze with some mud, light yellowish brown. Moderate bioturbation.
238cm: Mn-nodule (1cm Ø), irregular.
247-254cm: Several Mn-nodules (2cm Ø), irregular.
314cm: Layer of diatom ooze with some mud, white.
322-652cm: Mud-bearing diatom ooze with some opaque material, brown. Slight bioturbation, but generally more homogeneous than the unit above.
SS
S
cm

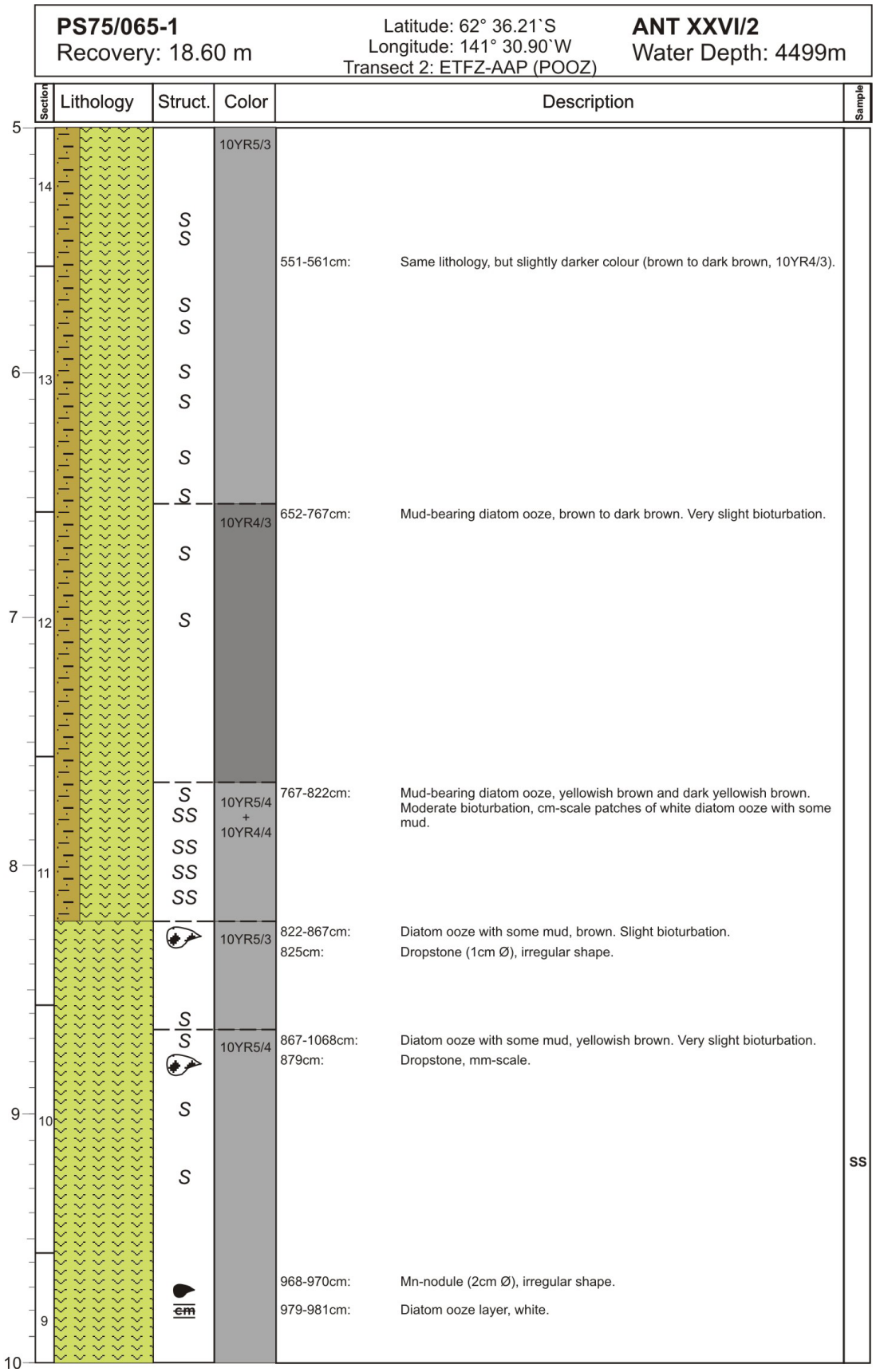
PS75/065-1
Recovery: 18.60 m
Latitude: 62° 36.21`S
Longitude: 141° 30.90`W
Transect 2: ETFZ-AAP (POOZ)
ANT XXVI/2
Water Depth: 4499m
Section
Lithology
Struct.
Color
Description
Sample
5
6
7
8
9
10
14
13
12
11
10
9
10YR5/3
10YR4/3
10YR5/4 + 10YR4/4
10YR5/3
10YR5/4
551-561cm: Same lithology, but slightly darker colour (brown to dark brown, 10YR4/3).
652-767cm: Mud-bearing diatom ooze, brown to dark brown. Very slight bioturbation.
767-822cm: Mud-bearing diatom ooze, yellowish brown and dark yellowish brown. Moderate bioturbation, cm-scale patches of white diatom ooze with some mud.
822-867cm: Diatom ooze with some mud, brown. Slight bioturbation.
825cm: Dropstone (1cm Ø), irregular shape.
867-1068cm: Diatom ooze with some mud, yellowish brown. Very slight bioturbation.
879cm: Dropstone, mm-scale.
968-970cm: Mn-nodule (2cm Ø), irregular shape.
979-981cm: Diatom ooze layer, white.
SS

**PS75/065-1**
Recovery: 18.60 m

Latitude: 62° 36.21`S
Longitude: 141° 30.90`W
Transect 2: ETFZ-AAP (POOZ)

**ANT XXVI/2**
Water Depth: 4499m

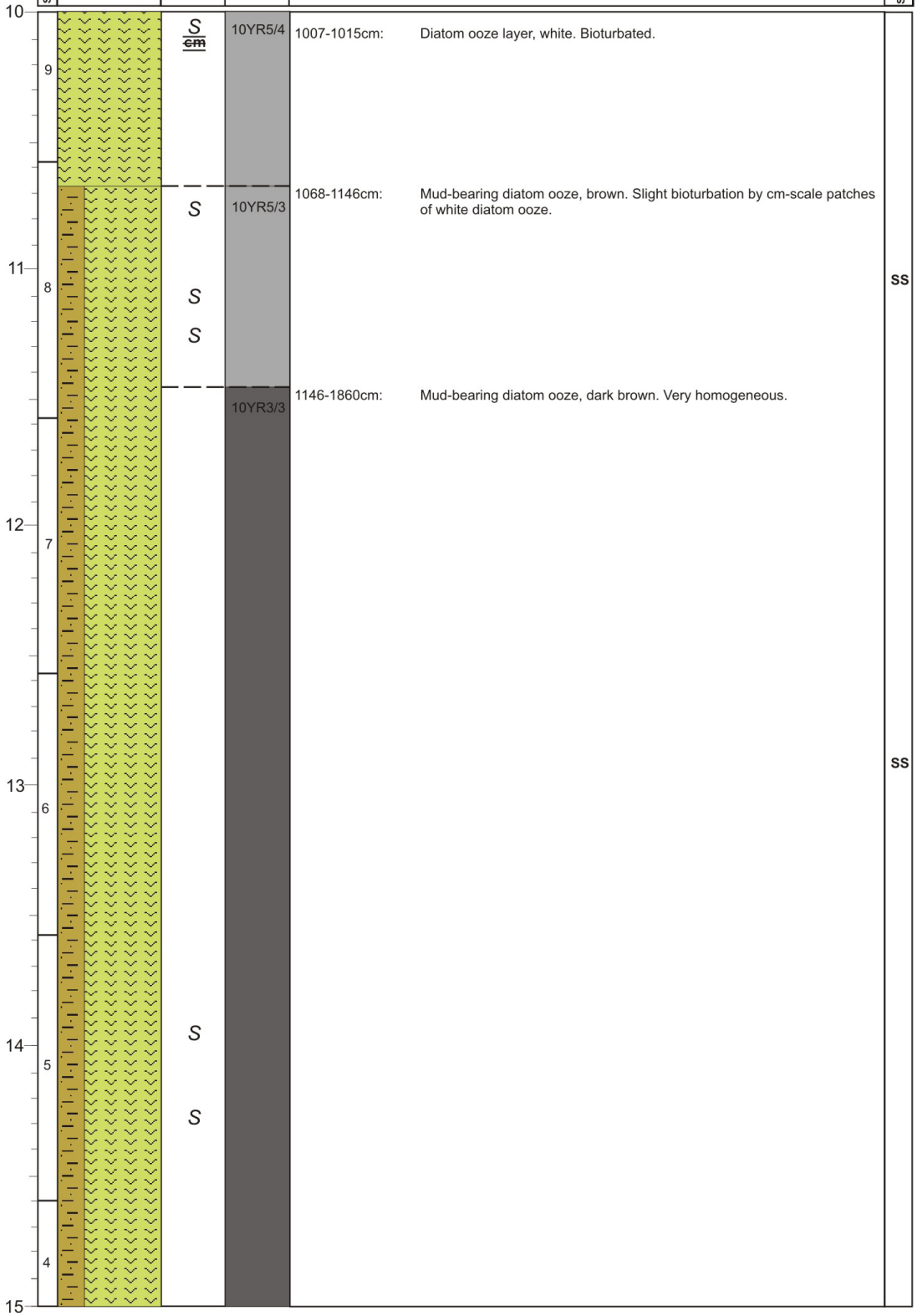

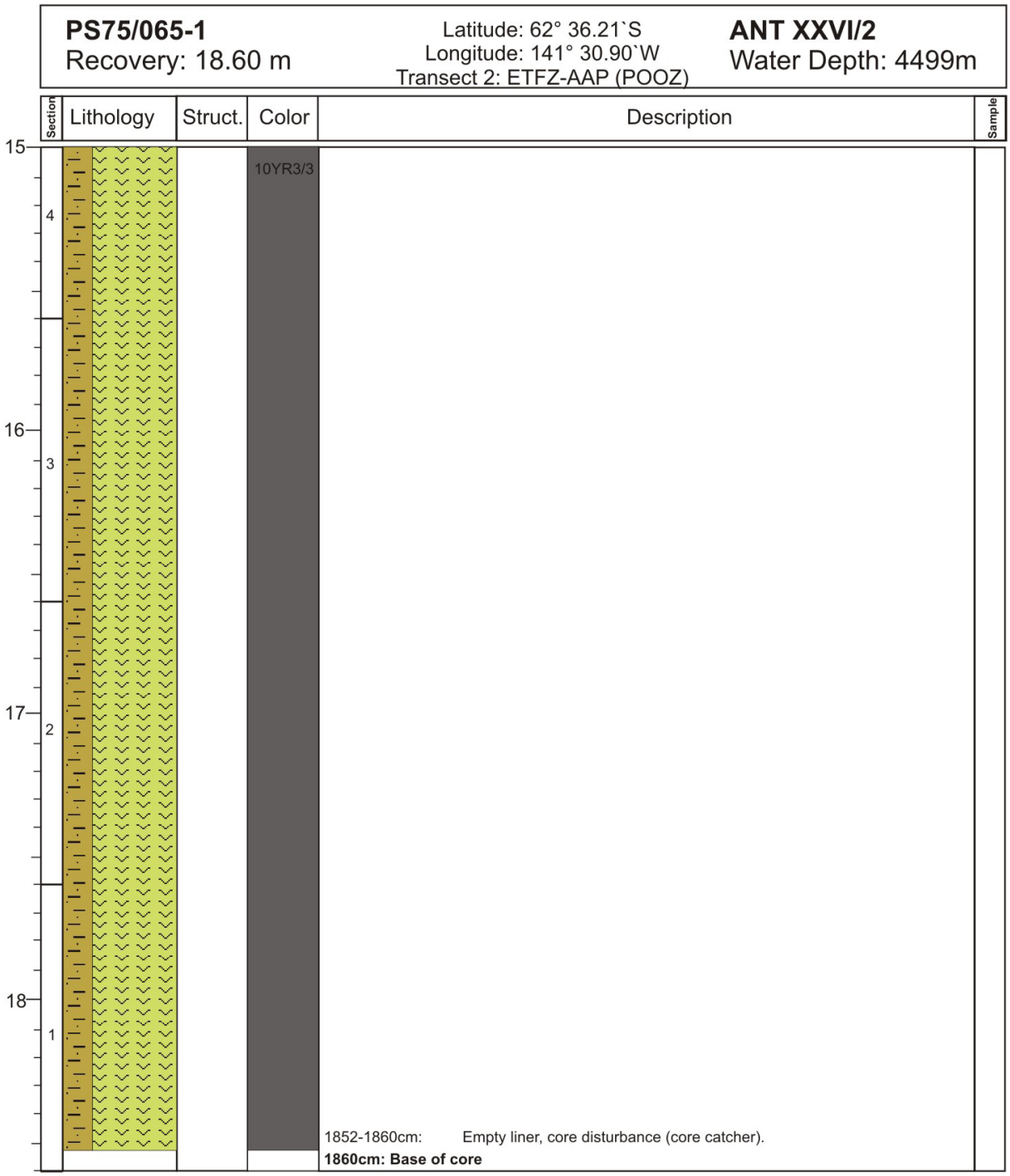
PS75/065-1
Recovery: 18.60 m
Latitude: 62° 36.21`S
Longitude: 141° 30.90`W
Transect 2: ETFZ-AAP (POOZ)
ANT XXVI/2
Water Depth: 4499m
Section
Lithology
Struct.
Color
Description
Sample
15
16
17
18
4
3
2
1
10YR3/3
1852-1860cm: Empty liner, core disturbance (core catcher).
1860cm: Base of core

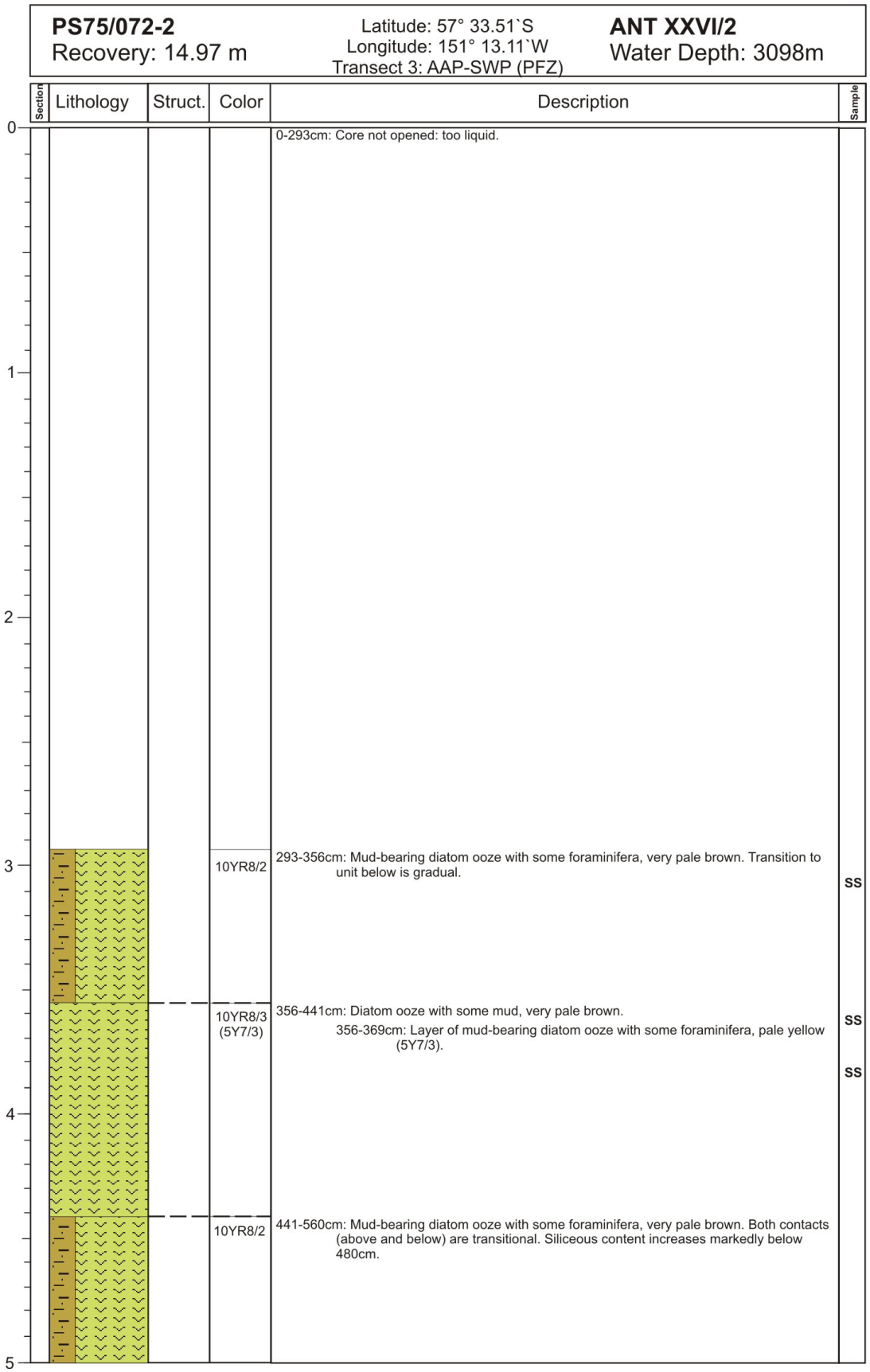
PS75/072-2
Recovery: 14.97 m
Latitude: 57° 33.51`S
Longitude: 151° 13.11`W
Transect 3: AAP-SWP (PFZ)
ANT XXVI/2
Water Depth: 3098m
Section
Lithology
Struct.
Color
Description
Sample
0
1
2
3
4
5
0-293cm: Core not opened: too liquid.
10YR8/2
293-356cm: Mud-bearing diatom ooze with some foraminifera, very pale brown. Transition to unit below is gradual.
SS
10YR8/3 (5Y7/3)
356-441cm: Diatom ooze with some mud, very pale brown.
356-369cm: Layer of mud-bearing diatom ooze with some foraminifera, pale yellow (5Y7/3).
SS
SS
10YR8/2
441-560cm: Mud-bearing diatom ooze with some foraminifera, very pale brown. Both contacts (above and below) are transitional. Siliceous content increases markedly below 480cm.

**PS75/072-2**
Recovery: 14.97 m

Latitude: 57° 33.51`S
Longitude: 151° 13.11`W
Transect 3: AAP-SWP (PFZ)

**ANT XXVI/2**
Water Depth: 3098m

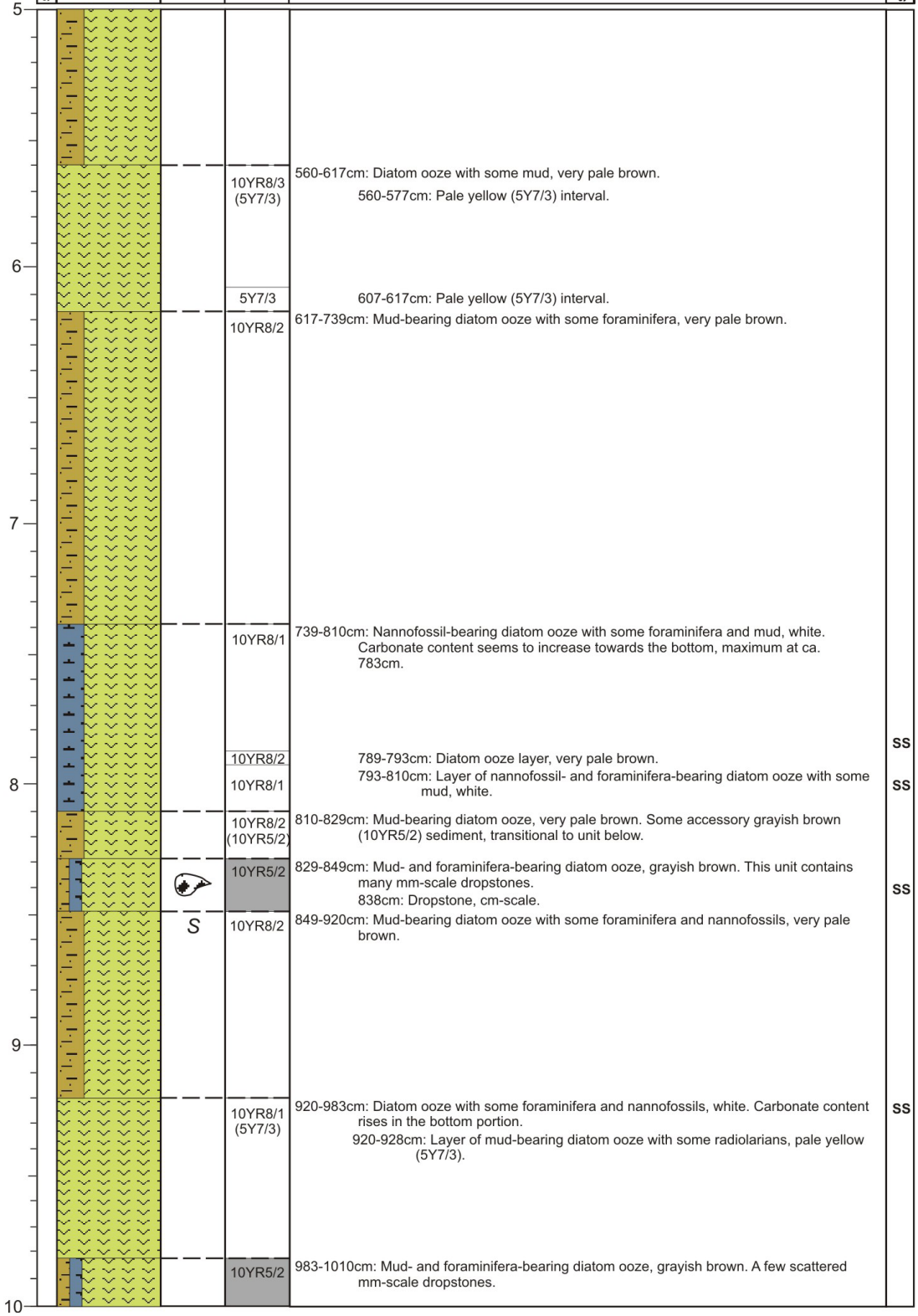

**PS75/072-2**
Recovery: 14.97 m

Latitude: 57° 33.51`S
Longitude: 151° 13.11`W
Transect 3: AAP-SWP (PFZ)

**ANT XXVI/2**
Water Depth: 3098m

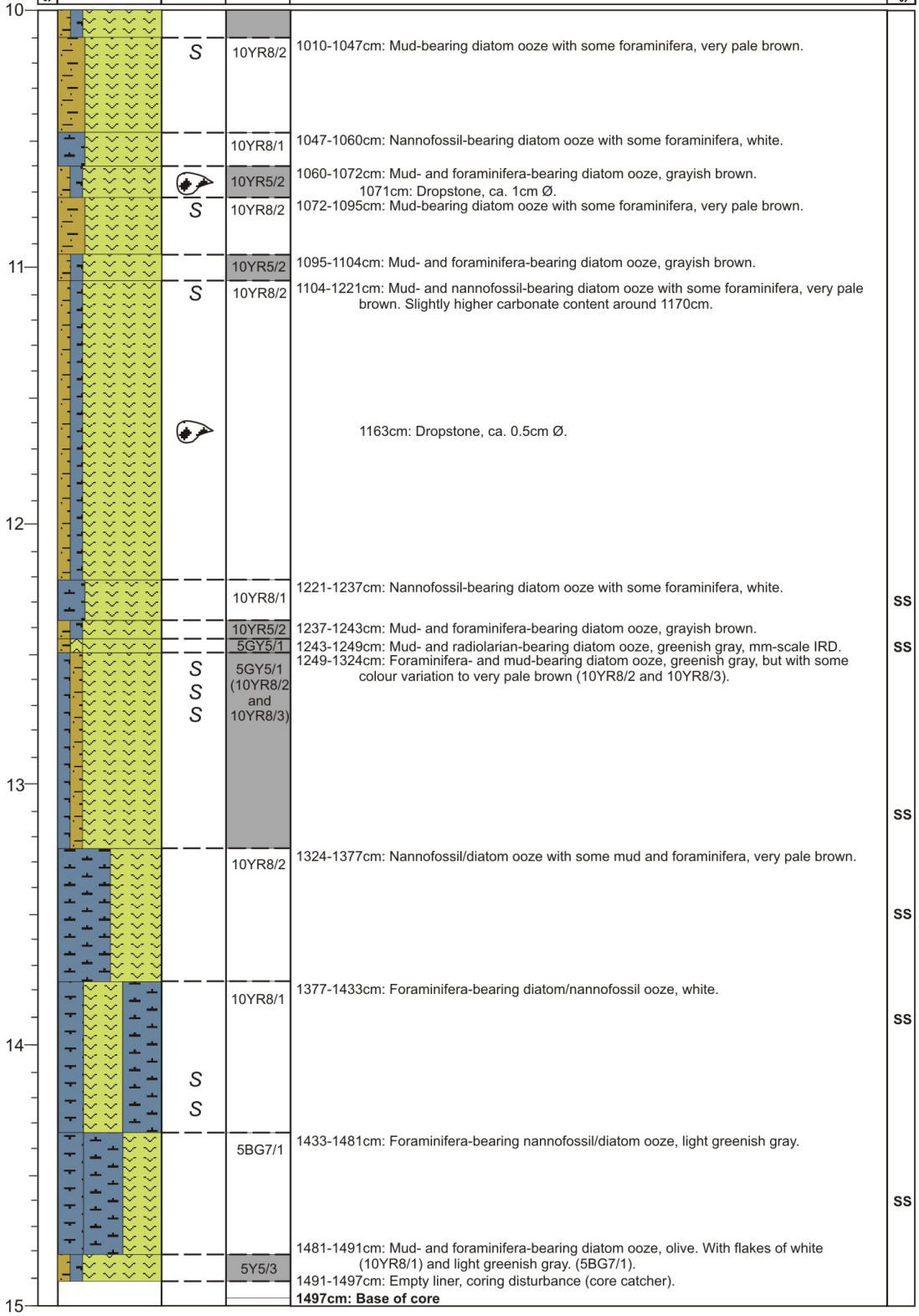

**PS75/073-2**
Recovery: 3.68 m

Latitude: 57° 12.26`S
Longitude: 151° 36.65`W
Transect 3: AAP-SWP (PFZ)

**ANT XXVI/2**
Water Depth: 3234m

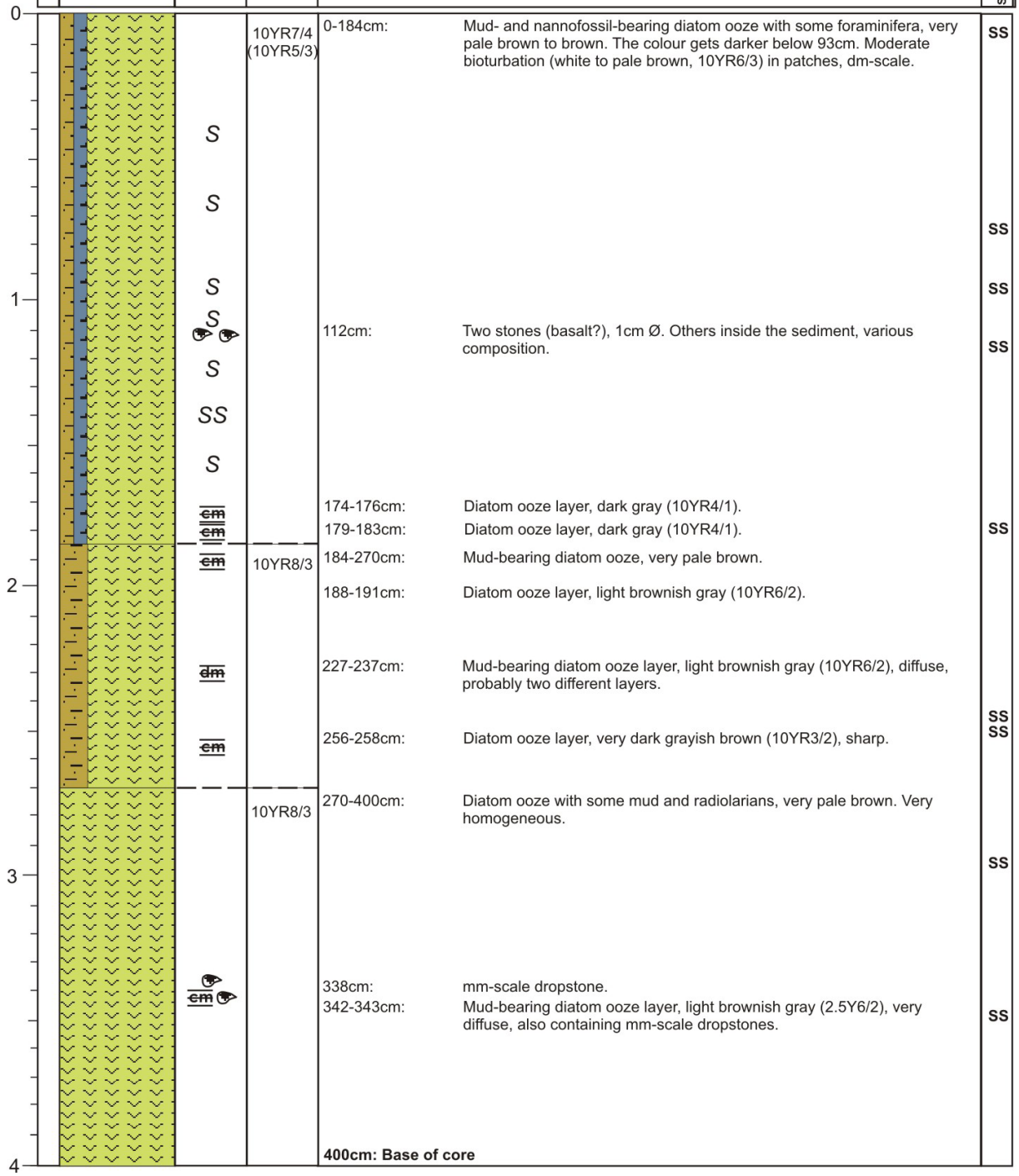


| | | | |
|---|---|---|---|
| 0-184cm: | Mud- and nannofossil-bearing diatom ooze with some foraminifera, very pale brown to brown. The colour gets darker below 93cm. Moderate bioturbation (white to pale brown, 10YR6/3) in patches, dm-scale. | | SS |
| | | | SS |
| | | | SS |
| 112cm: | Two stones (basalt?), 1cm Ø. Others inside the sediment, various composition. | | SS |
| 174-176cm: | Diatom ooze layer, dark gray (10YR4/1). | | |
| 179-183cm: | Diatom ooze layer, dark gray (10YR4/1). | | SS |
| 184-270cm: | Mud-bearing diatom ooze, very pale brown. | 10YR8/3 | |
| 188-191cm: | Diatom ooze layer, light brownish gray (10YR6/2). | | |
| 227-237cm: | Mud-bearing diatom ooze layer, light brownish gray (10YR6/2), diffuse, probably two different layers. | | SS |
| 256-258cm: | Diatom ooze layer, very dark grayish brown (10YR3/2), sharp. | | SS |
| 270-400cm: | Diatom ooze with some mud and radiolarians, very pale brown. Very homogeneous. | 10YR8/3 | SS |
| 338cm: | mm-scale dropstone. | | |
| 342-343cm: | Mud-bearing diatom ooze layer, light brownish gray (2.5Y6/2), very diffuse, also containing mm-scale dropstones. | | SS |
| **400cm: Base of core** | | | |

**PS75/076-2**
Recovery: 20.59 m

Latitude: 55° 31.71`S
Longitude: 156° 08.39`W
Transect 4: SWP-ROS (PFZ)

**ANT XXVI/2**
Water Depth: 3742m

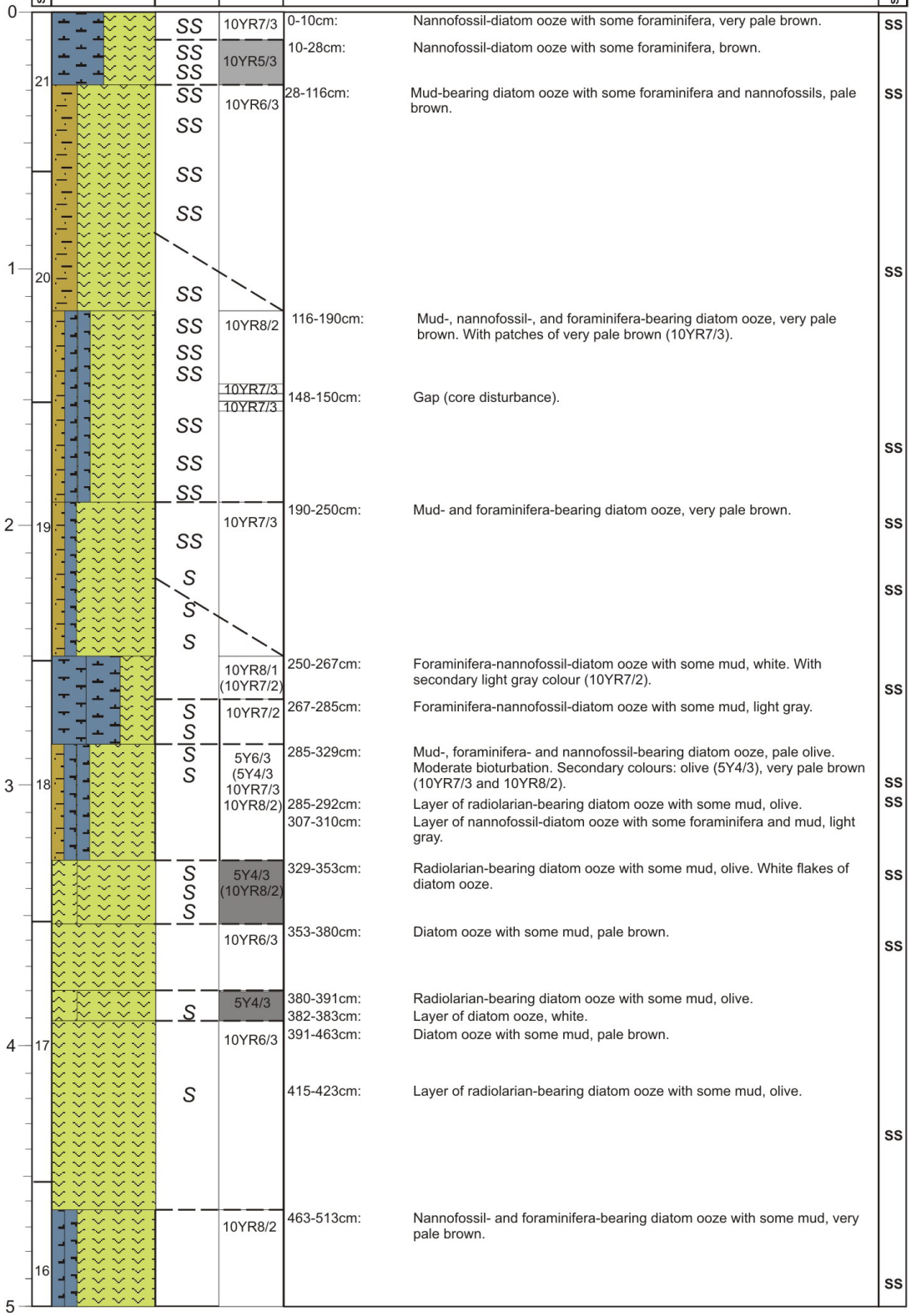

**PS75/076-2**
Recovery: 20.59 m

Latitude: 55° 31.71`S
Longitude: 156° 08.39`W
Transect 4: SWP-ROS (PFZ)

**ANT XXVI/2**
Water Depth: 3742m

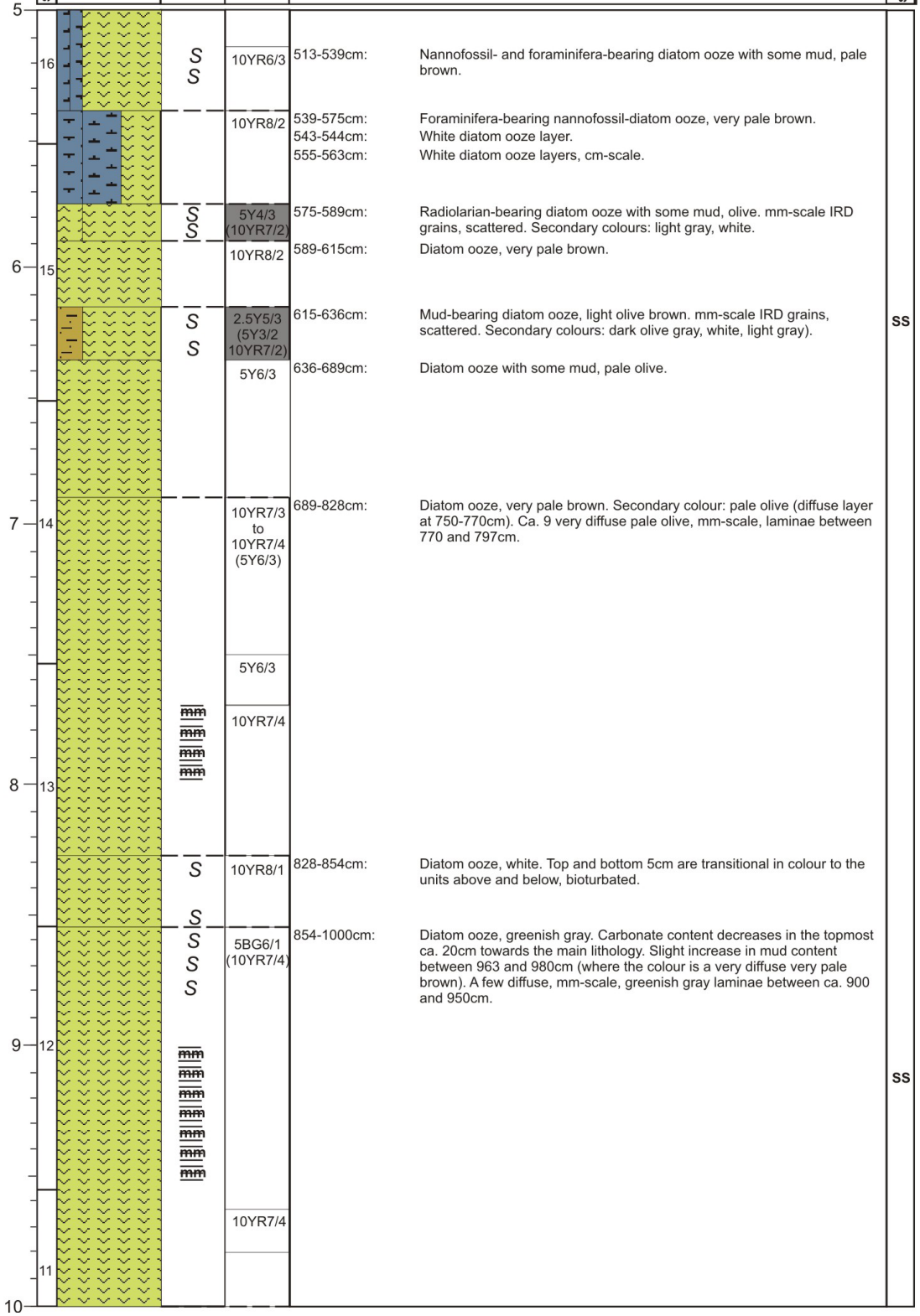

**PS75/076-2**
Recovery: 20.59 m

Latitude: 55° 31.71`S
Longitude: 156° 08.39`W
Transect 4: SWP-ROS (PFZ)

**ANT XXVI/2**
Water Depth: 3742m

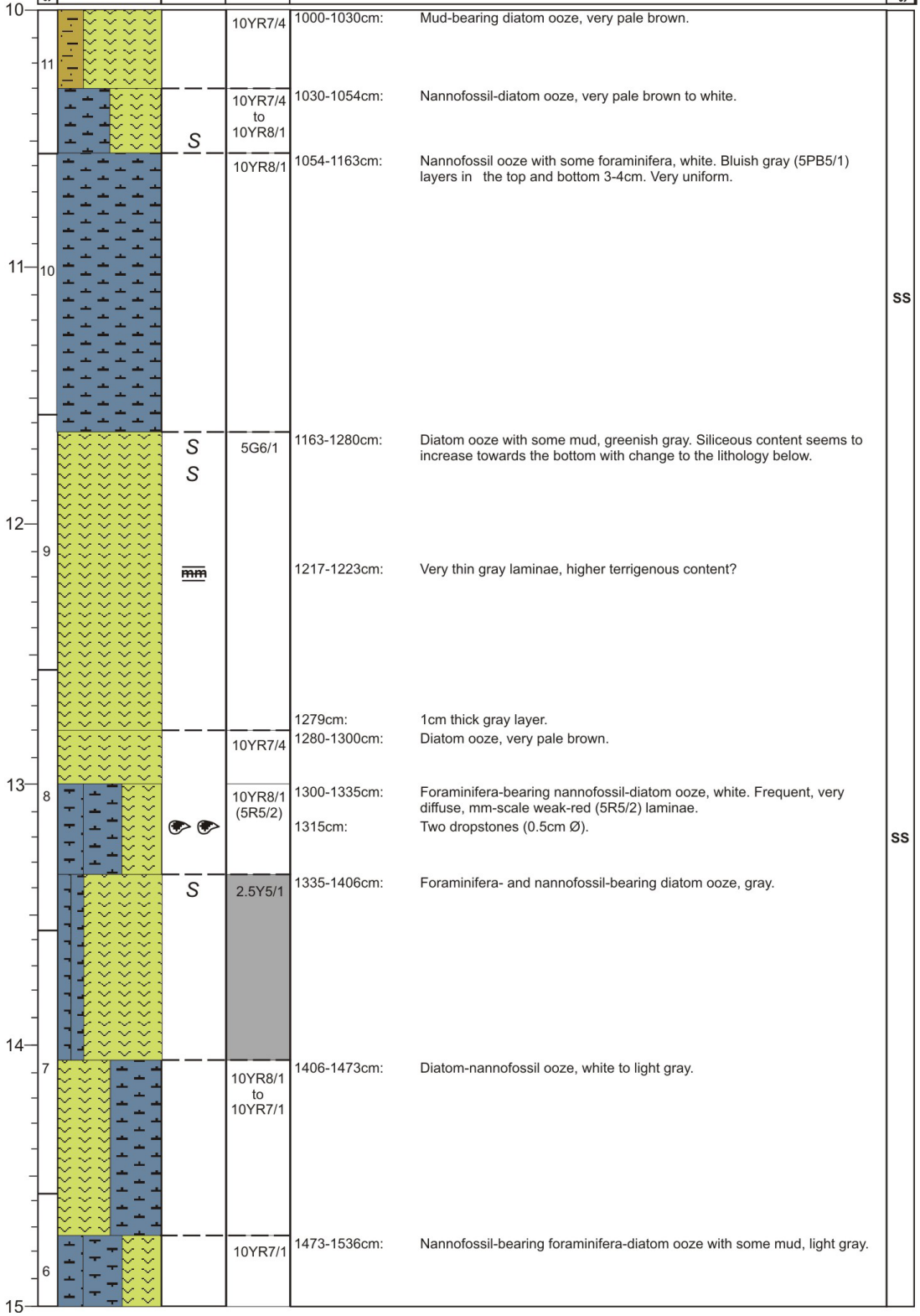

**PS75/076-2**
Recovery: 20.59 m

Latitude: 55° 31.71`S
Longitude: 156° 08.39`W
Transect 4: SWP-ROS (PFZ)

**ANT XXVI/2**
Water Depth: 3742m

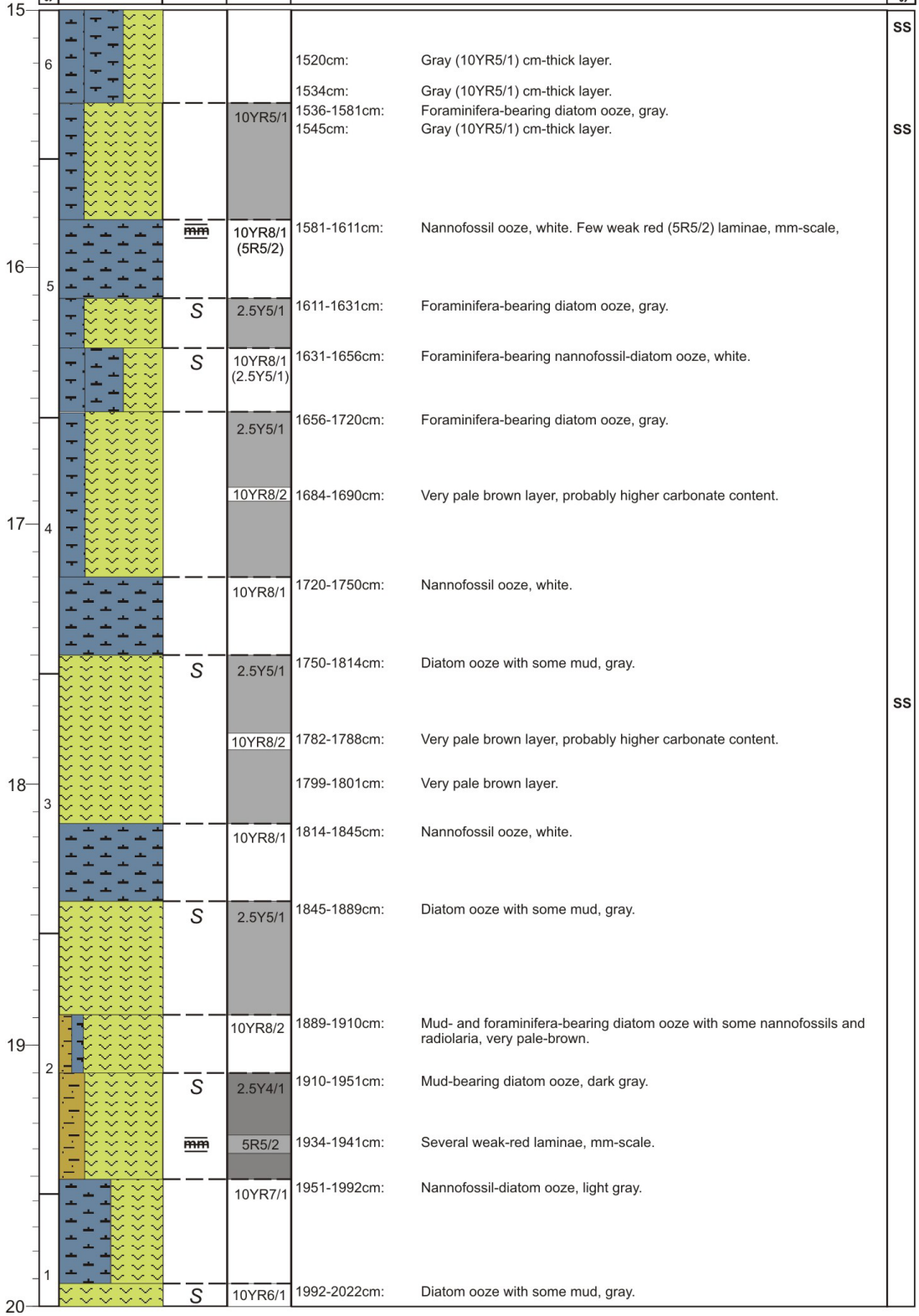

**PS75/076-2**
Recovery: 20.59 m

Latitude: 55° 31.71`S
Longitude: 156° 08.39`W
Transect 4: SWP-ROS (PFZ)

**ANT XXVI/2**
Water Depth: 3742m

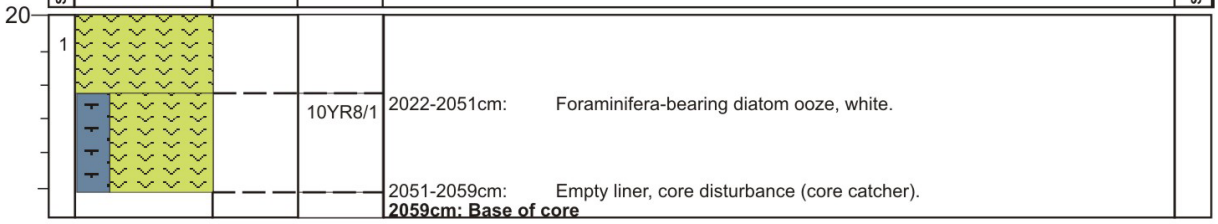

**PS75/079-2**
Recovery: 18.51 m

Latitude: 57° 30.16`S
Longitude: 157° 14.25`W
Transect 4: SWP-ROS (POOZ)

**ANT XXVI/2**
Water Depth: 3770m

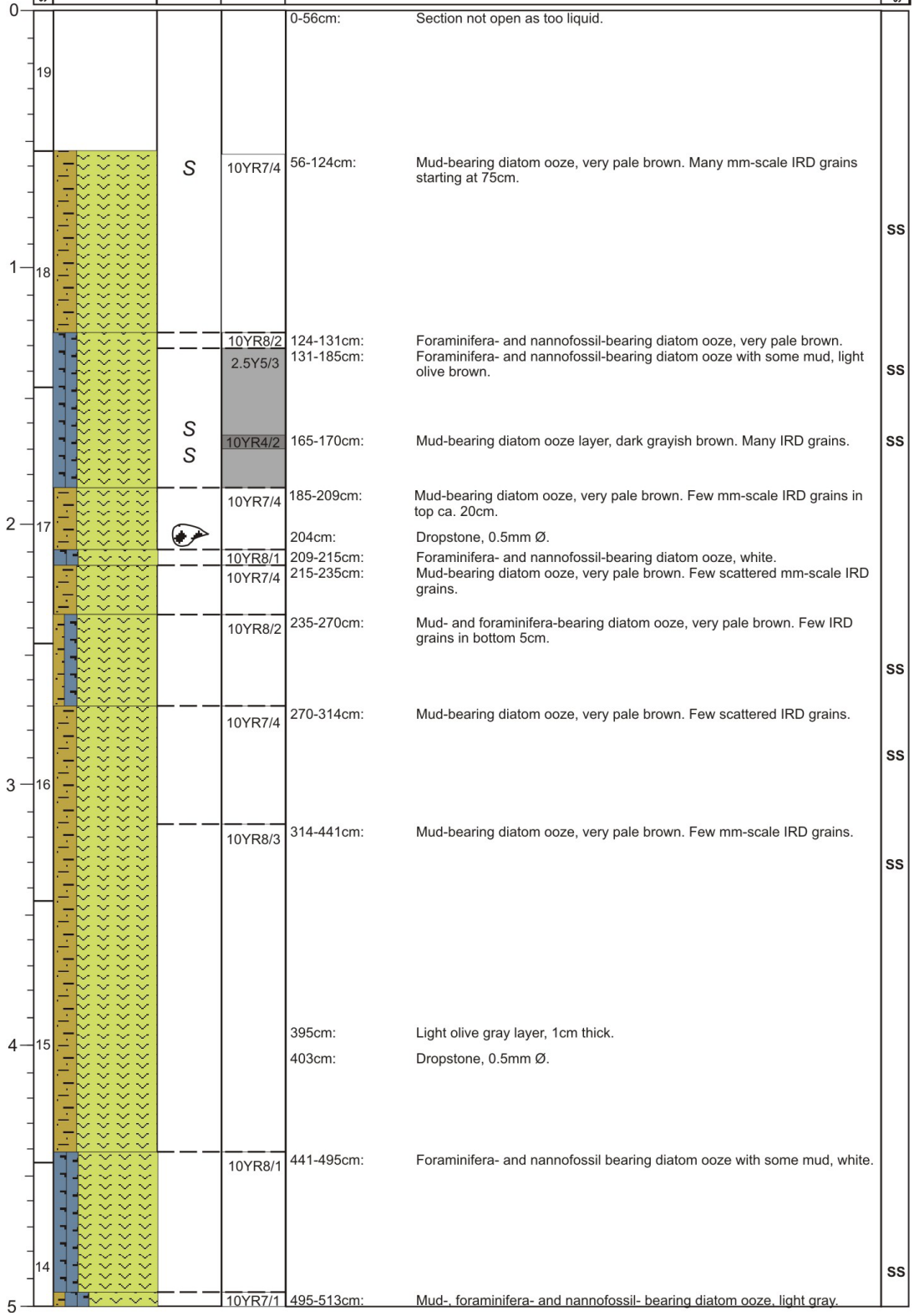

**PS75/079-2**
Recovery: 18.51 m

Latitude: 57° 30.16`S
Longitude: 157° 14.25`W
Transect 4: SWP-ROS (POOZ)

**ANT XXVI/2**
Water Depth: 3770m

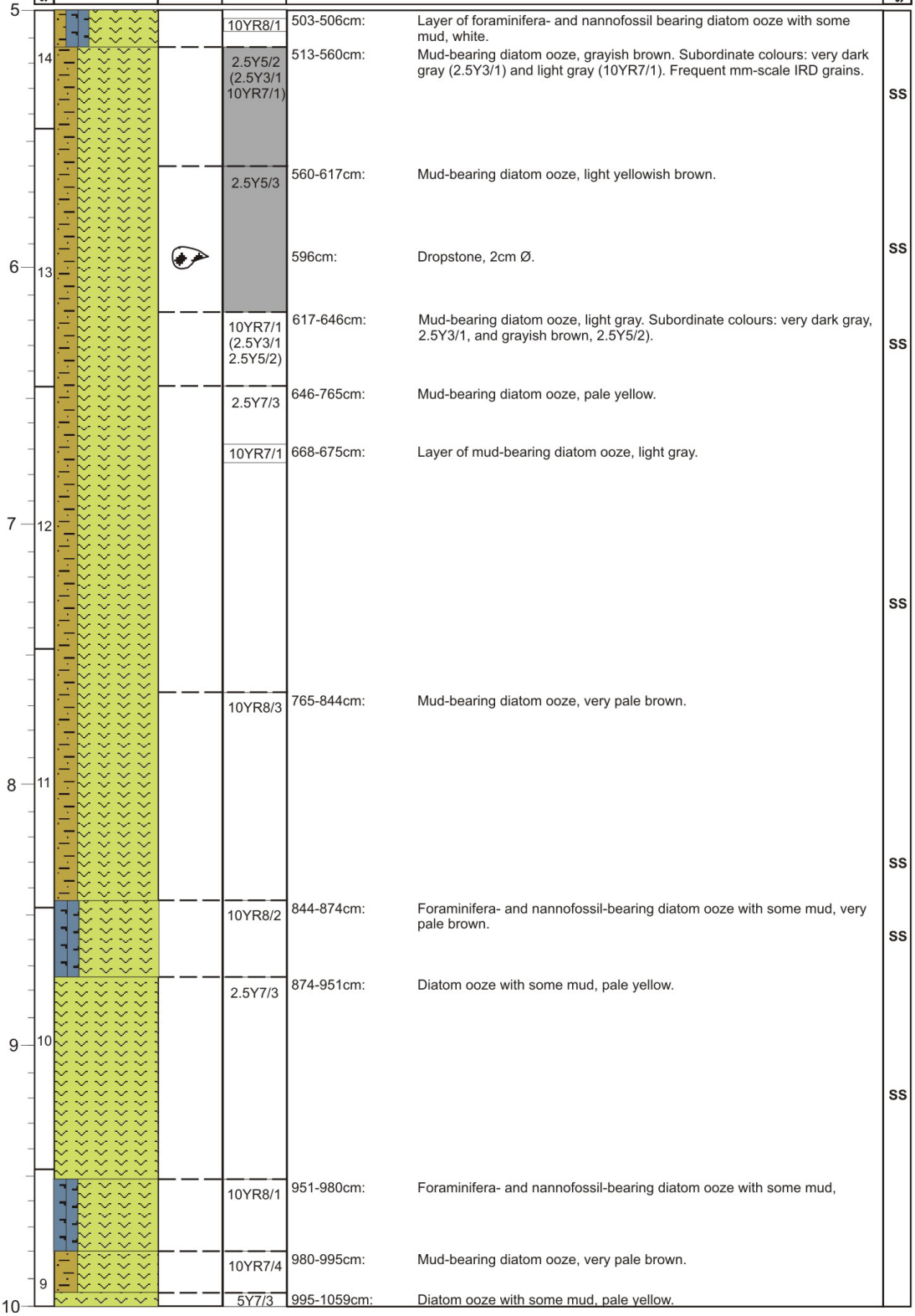

**PS75/079-2**
Recovery: 18.51 m

Latitude: 57° 30.16`S
Longitude: 157° 14.25`W
Transect 4: SWP-ROS (POOZ)

**ANT XXVI/2**
Water Depth: 3770m

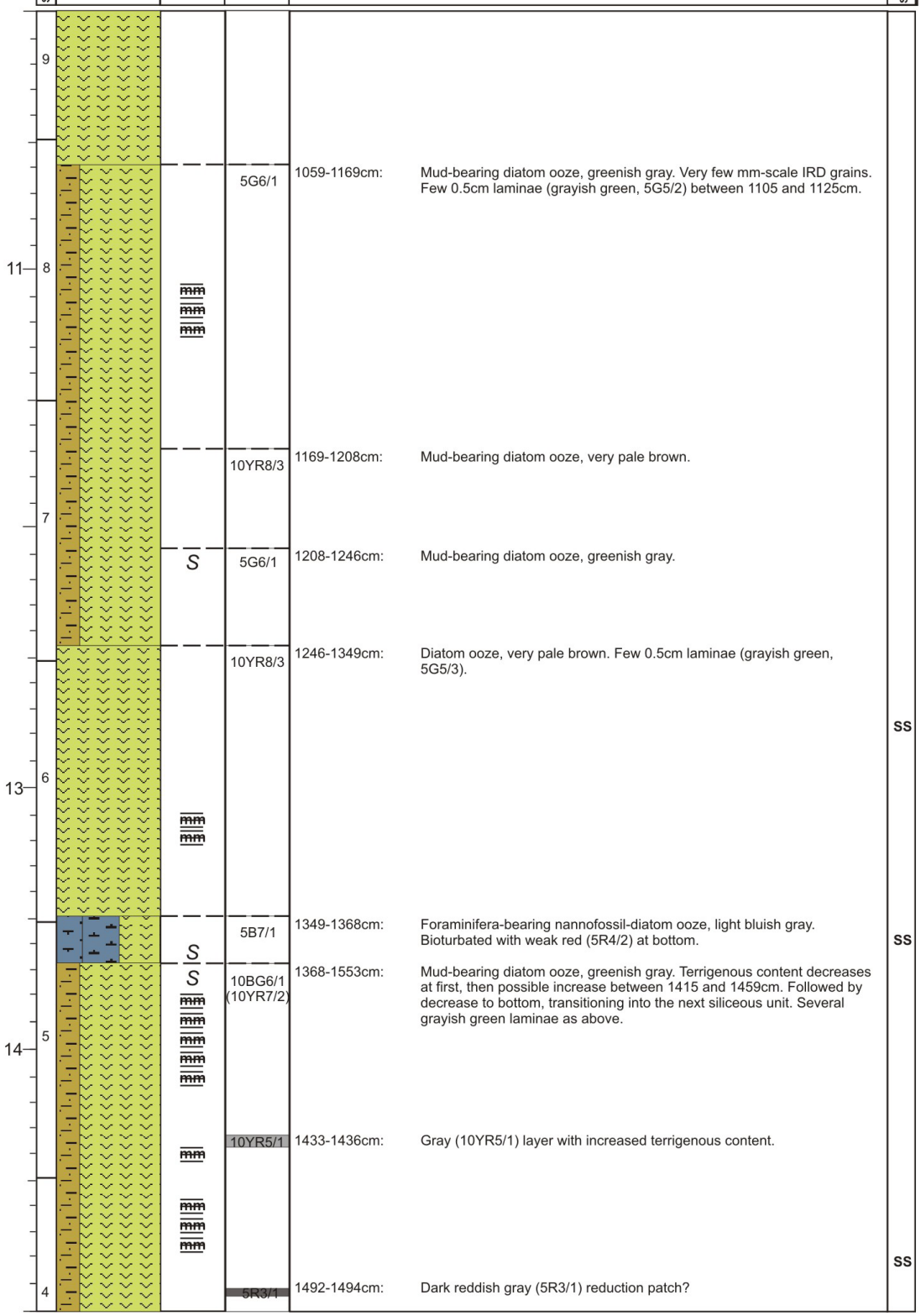

**PS75/079-2**
Recovery: 18.51 m

Latitude: 57° 30.16`S
Longitude: 157° 14.25`W
Transect 4: SWP-ROS (POOZ)

**ANT XXVI/2**
Water Depth: 3770m

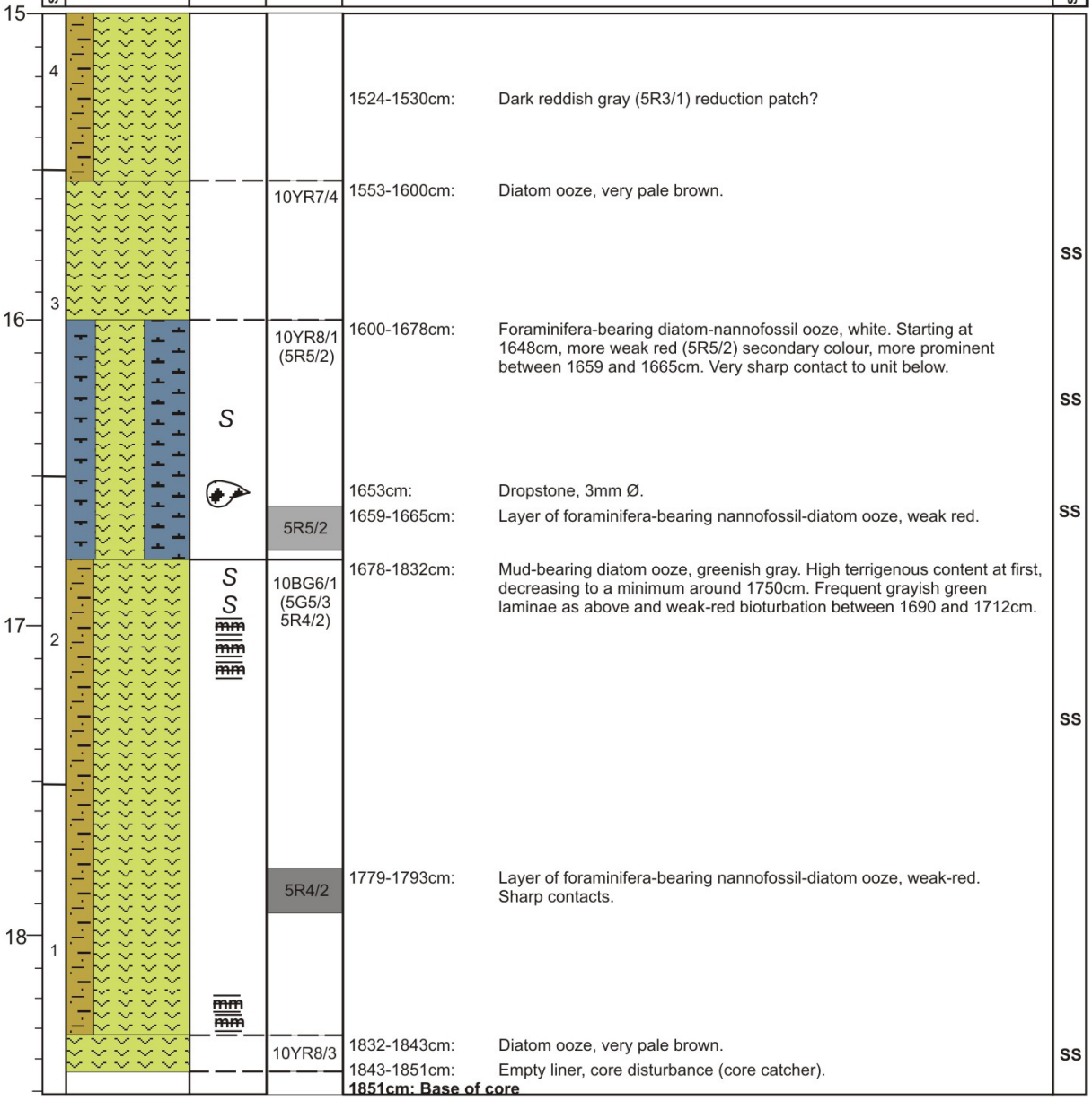

**PS75/083-1**
Recovery: 13.13 m

Latitude: 60° 16.13`S
Longitude: 159° 03.59`W
Transect 4: SWP-ROS (POOZ)

**ANT XXVI/2**
Water Depth: 3599m

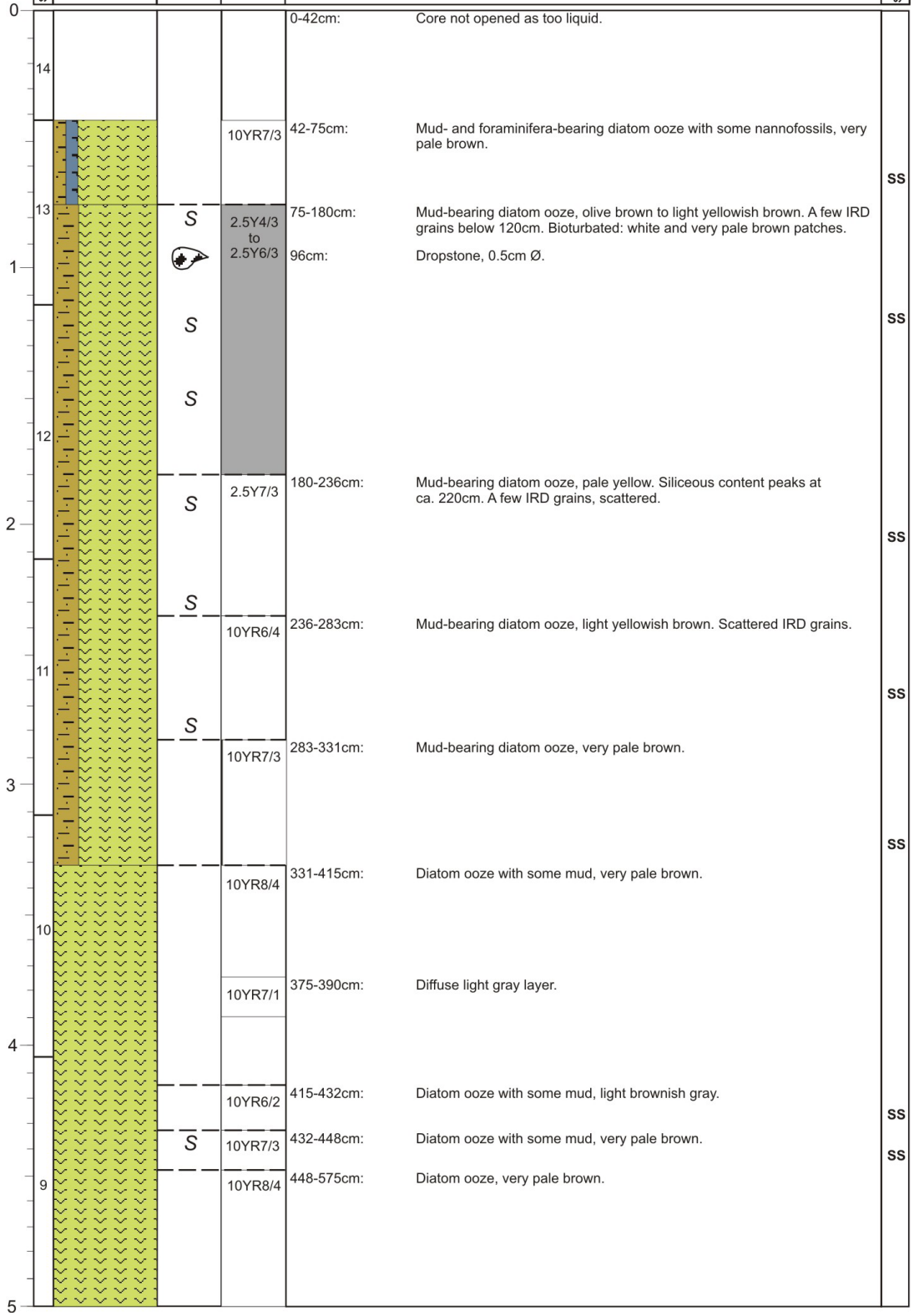

**PS75/083-1**
Recovery: 13.13 m

Latitude: 60° 16.13`S
Longitude: 159° 03.59`W
Transect 4: SWP-ROS (POOZ)

**ANT XXVI/2**
Water Depth: 3599m

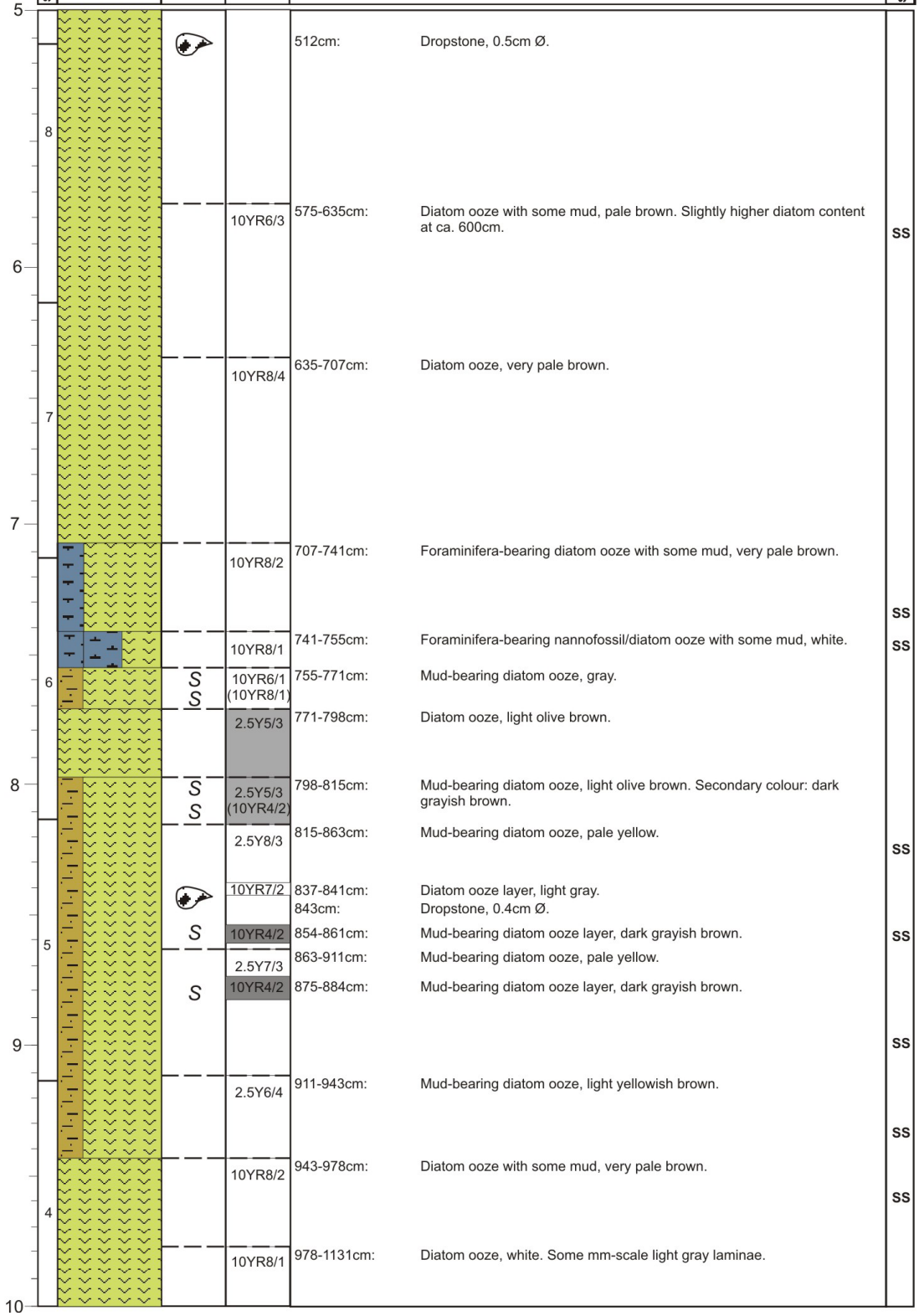

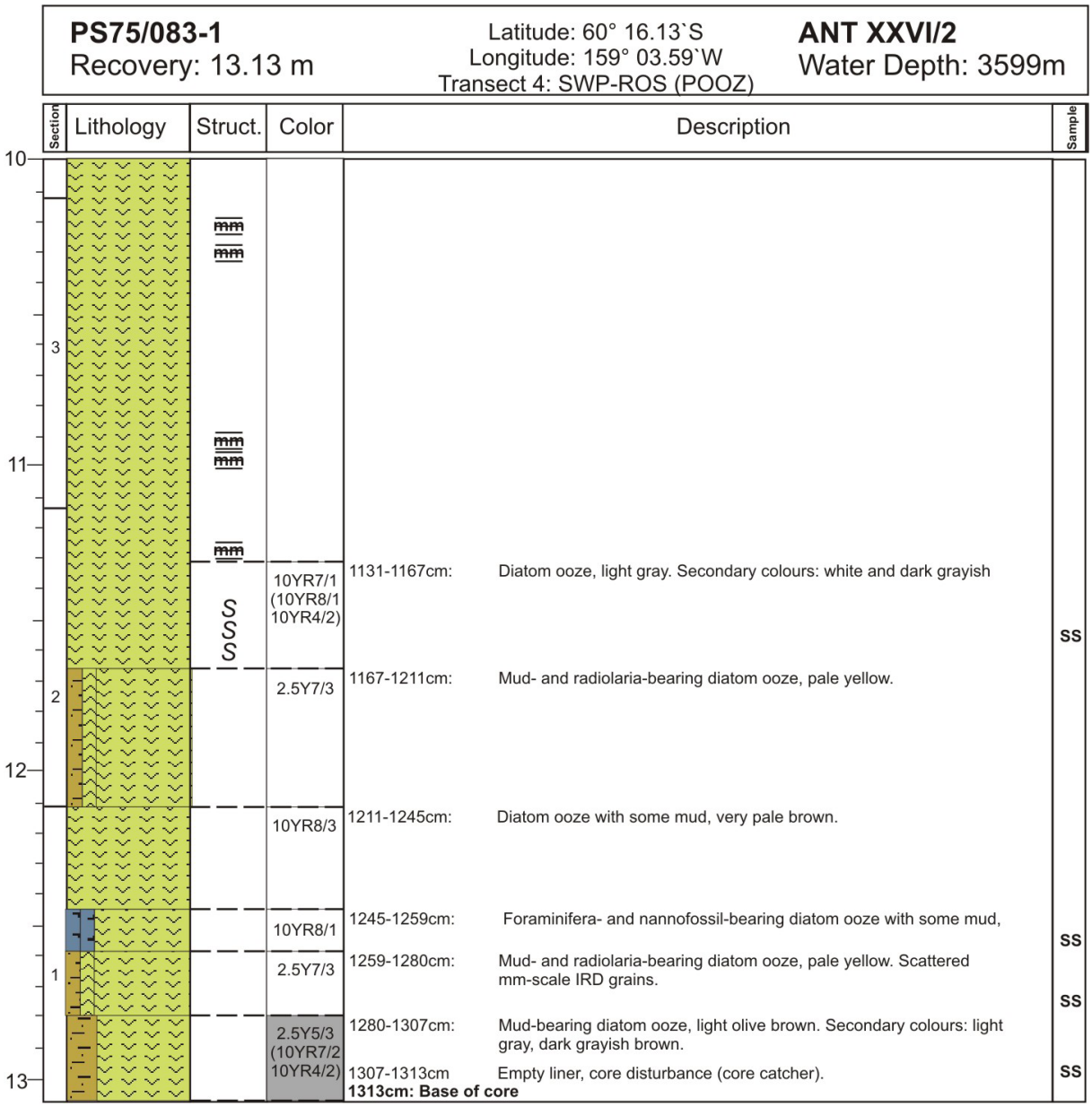
PS75/083-1
Recovery: 13.13 m
Latitude: 60° 16.13`S
Longitude: 159° 03.59`W
Transect 4: SWP-ROS (POOZ)
ANT XXVI/2
Water Depth: 3599m
Section
Lithology
Struct.
Color
Description
Sample
10
11
12
13
3
2
1
10YR7/1 (10YR8/1 10YR4/2)
1131-1167cm: Diatom ooze, light gray. Secondary colours: white and dark grayish
SS
2.5Y7/3
1167-1211cm: Mud- and radiolaria-bearing diatom ooze, pale yellow.
10YR8/3
1211-1245cm: Diatom ooze with some mud, very pale brown.
10YR8/1
1245-1259cm: Foraminifera- and nannofossil-bearing diatom ooze with some mud,
SS
2.5Y7/3
1259-1280cm: Mud- and radiolaria-bearing diatom ooze, pale yellow. Scattered mm-scale IRD grains.
SS
2.5Y5/3 (10YR7/2 10YR4/2)
1280-1307cm: Mud-bearing diatom ooze, light olive brown. Secondary colours: light gray, dark grayish brown.
1307-1313cm Empty liner, core disturbance (core catcher).
SS
1313cm: Base of core

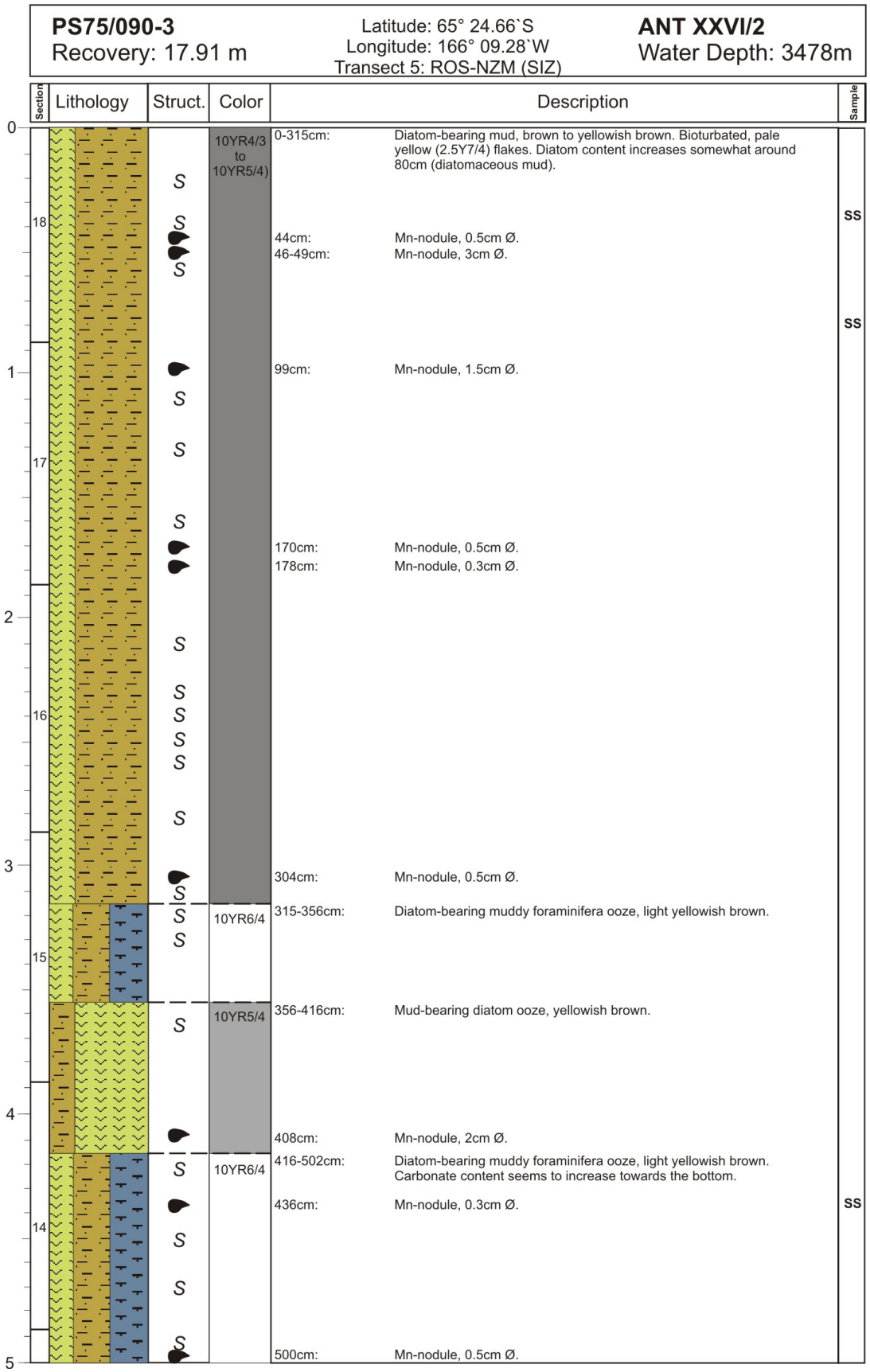
PS75/090-3
Recovery: 17.91 m
Latitude: 65° 24.66`S
Longitude: 166° 09.28`W
Transect 5: ROS-NZM (SIZ)
ANT XXVI/2
Water Depth: 3478m
Section
Lithology
Struct.
Color
Description
Sample
0
1
2
3
4
5
18
17
16
15
14
10YR4/3 to 10YR5/4)
10YR6/4
10YR5/4
10YR6/4
0-315cm: Diatom-bearing mud, brown to yellowish brown. Bioturbated, pale yellow (2.5Y7/4) flakes. Diatom content increases somewhat around 80cm (diatomaceous mud).
44cm: Mn-nodule, 0.5cm Ø.
46-49cm: Mn-nodule, 3cm Ø.
99cm: Mn-nodule, 1.5cm Ø.
170cm: Mn-nodule, 0.5cm Ø.
178cm: Mn-nodule, 0.3cm Ø.
304cm: Mn-nodule, 0.5cm Ø.
315-356cm: Diatom-bearing muddy foraminifera ooze, light yellowish brown.
356-416cm: Mud-bearing diatom ooze, yellowish brown.
408cm: Mn-nodule, 2cm Ø.
416-502cm: Diatom-bearing muddy foraminifera ooze, light yellowish brown. Carbonate content seems to increase towards the bottom.
436cm: Mn-nodule, 0.3cm Ø.
500cm: Mn-nodule, 0.5cm Ø.
SS
SS
SS

**PS75/090-3**
Recovery: 17.91 m

Latitude: 65° 24.66`S
Longitude: 166° 09.28`W
Transect 5: ROS-NZM (SIZ)

**ANT XXVI/2**
Water Depth: 3478m

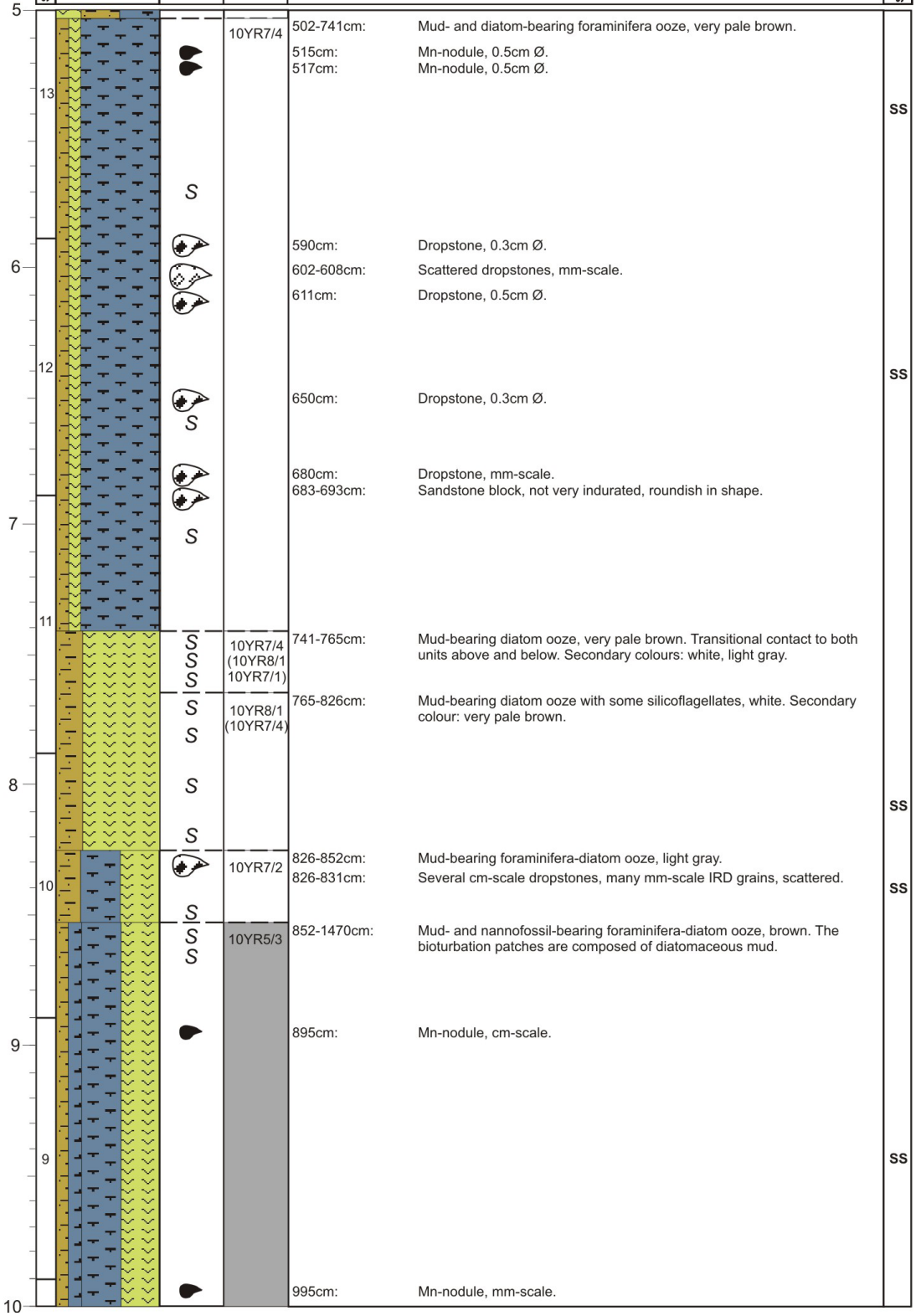

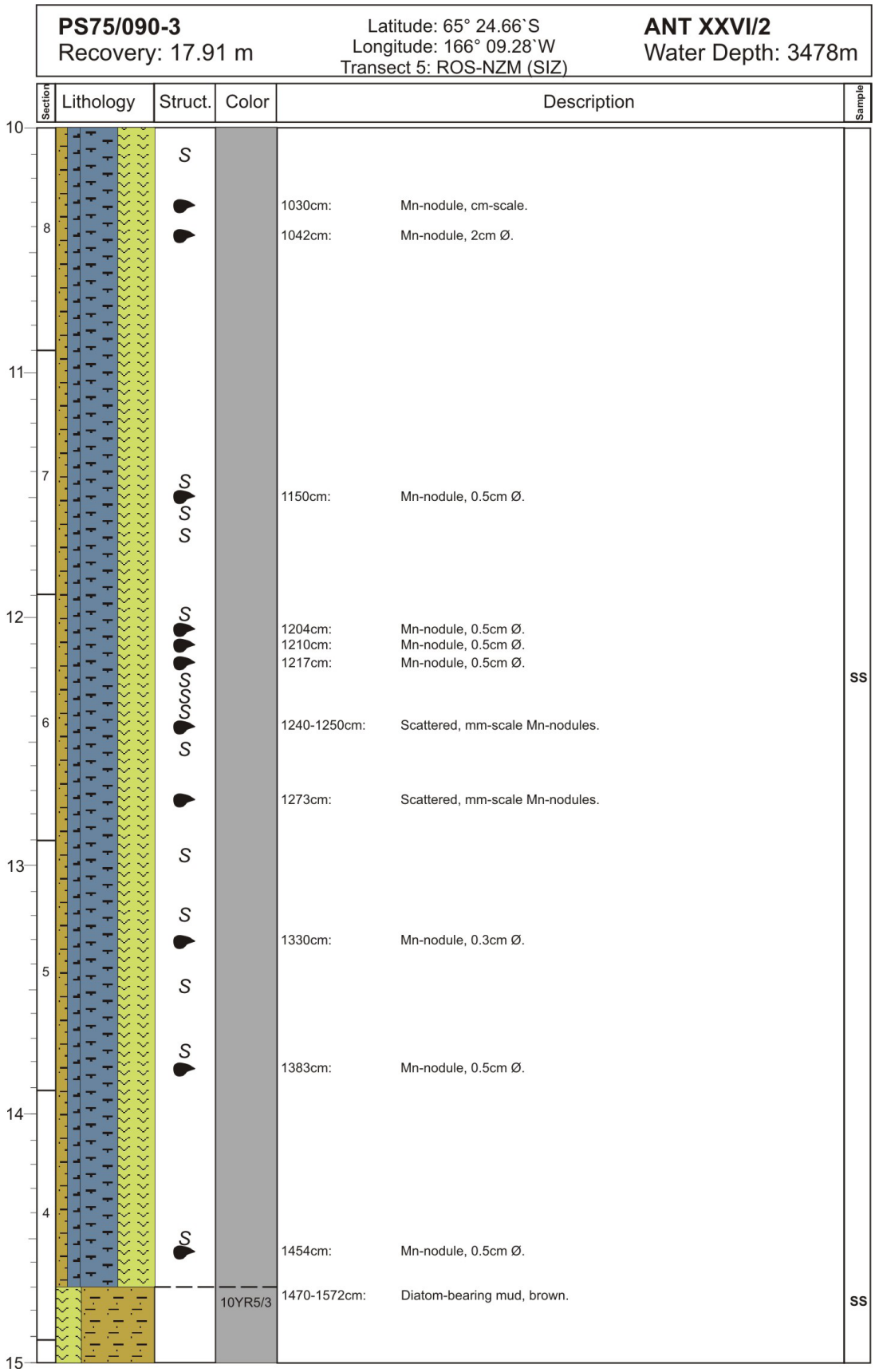
PS75/090-3
Recovery: 17.91 m
Latitude: 65° 24.66`S
Longitude: 166° 09.28`W
Transect 5: ROS-NZM (SIZ)
ANT XXVI/2
Water Depth: 3478m
Section
Lithology
Struct.
Color
Description
Sample
10
11
12
13
14
15
8
7
6
5
4
S
1030cm: Mn-nodule, cm-scale.
1042cm: Mn-nodule, 2cm Ø.
1150cm: Mn-nodule, 0.5cm Ø.
1204cm: Mn-nodule, 0.5cm Ø.
1210cm: Mn-nodule, 0.5cm Ø.
1217cm: Mn-nodule, 0.5cm Ø.
SS
1240-1250cm: Scattered, mm-scale Mn-nodules.
1273cm: Scattered, mm-scale Mn-nodules.
1330cm: Mn-nodule, 0.3cm Ø.
1383cm: Mn-nodule, 0.5cm Ø.
1454cm: Mn-nodule, 0.5cm Ø.
10YR5/3
1470-1572cm: Diatom-bearing mud, brown.
SS

**PS75/090-3**
Recovery: 17.91 m

Latitude: 65° 24.66`S
Longitude: 166° 09.28`W
Transect 5: ROS-NZM (SIZ)

**ANT XXVI/2**
Water Depth: 3478m

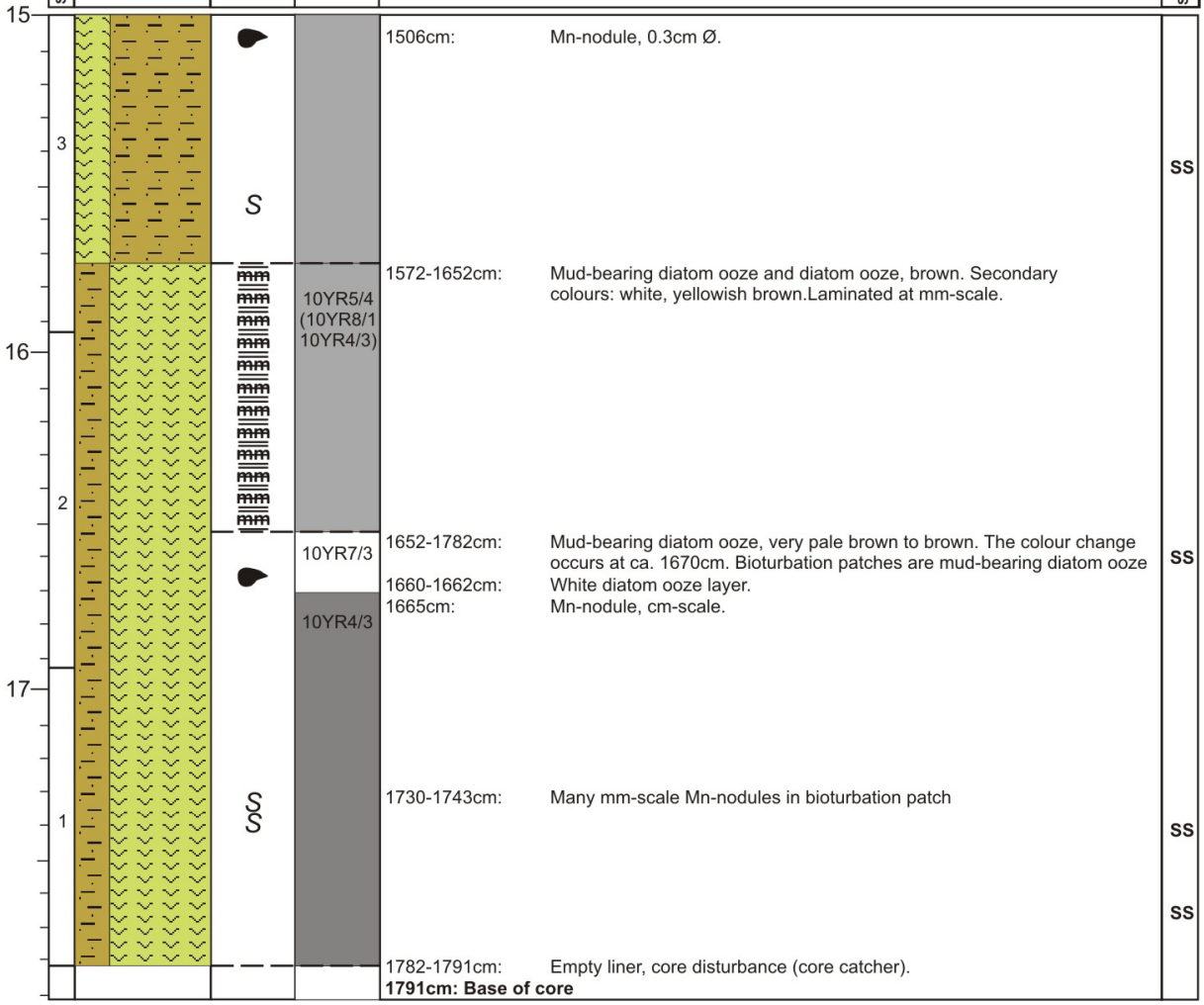

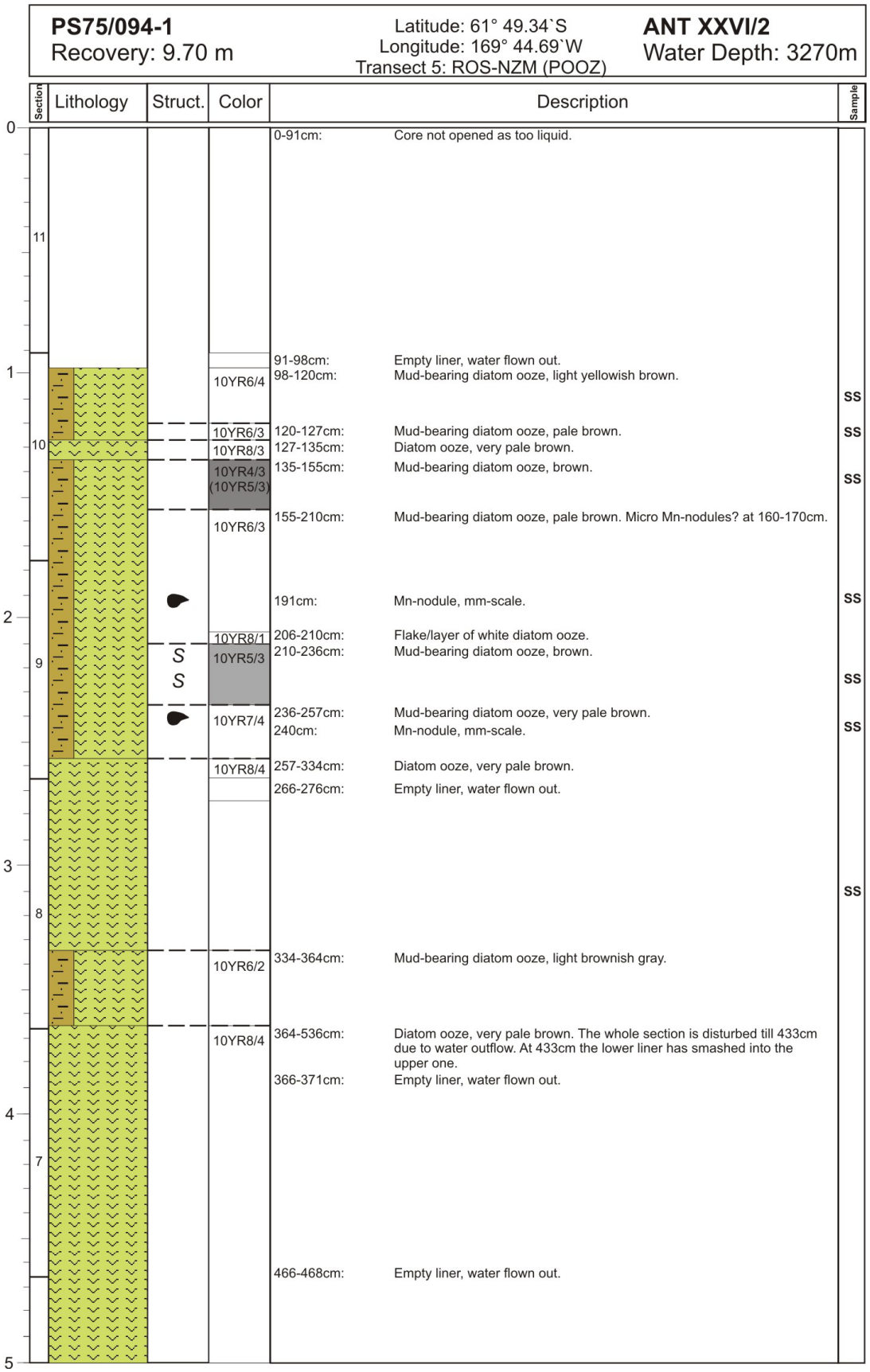
PS75/094-1
Recovery: 9.70 m
Latitude: 61° 49.34`S
Longitude: 169° 44.69`W
Transect 5: ROS-NZM (POOZ)
ANT XXVI/2
Water Depth: 3270m
Section
Lithology
Struct.
Color
Description
Sample
0-91cm: Core not opened as too liquid.
91-98cm: Empty liner, water flown out.
98-120cm: Mud-bearing diatom ooze, light yellowish brown.
10YR6/4
10YR6/3
120-127cm: Mud-bearing diatom ooze, pale brown.
10YR8/3
127-135cm: Diatom ooze, very pale brown.
10YR4/3
(10YR5/3)
135-155cm: Mud-bearing diatom ooze, brown.
10YR6/3
155-210cm: Mud-bearing diatom ooze, pale brown. Micro Mn-nodules? at 160-170cm.
191cm: Mn-nodule, mm-scale.
10YR8/1
206-210cm: Flake/layer of white diatom ooze.
S
S
10YR5/3
210-236cm: Mud-bearing diatom ooze, brown.
236-257cm: Mud-bearing diatom ooze, very pale brown.
10YR7/4
240cm: Mn-nodule, mm-scale.
10YR8/4
257-334cm: Diatom ooze, very pale brown.
266-276cm: Empty liner, water flown out.
10YR6/2
334-364cm: Mud-bearing diatom ooze, light brownish gray.
10YR8/4
364-536cm: Diatom ooze, very pale brown. The whole section is disturbed till 433cm due to water outflow. At 433cm the lower liner has smashed into the upper one.
366-371cm: Empty liner, water flown out.
466-468cm: Empty liner, water flown out.
SS
0
1
2
3
4
5
11
10
9
8
7

**PS75/094-1**
Recovery: 9.70 m

Latitude: 61° 49.34`S
Longitude: 169° 44.69`W
Transect 5: ROS-NZM (POOZ)

**ANT XXVI/2**
Water Depth: 3270m

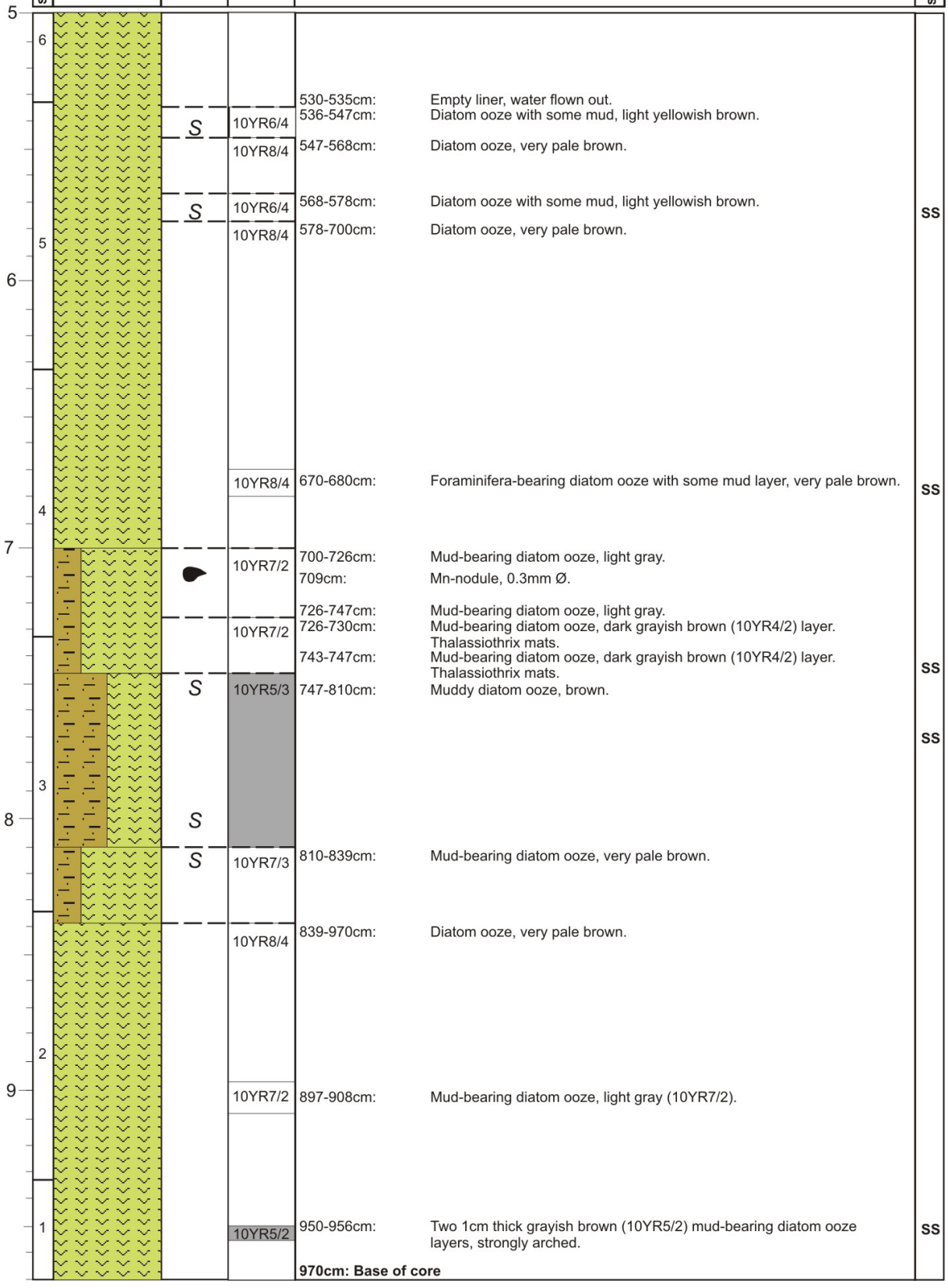

**PS75/095-5**
Recovery: 17.85 m

Latitude: 57° 01.18`S
Longitude: 174° 25.80`W
Transect 5: ROS-NZM

**ANT XXVI/2**
Water Depth: 4853m

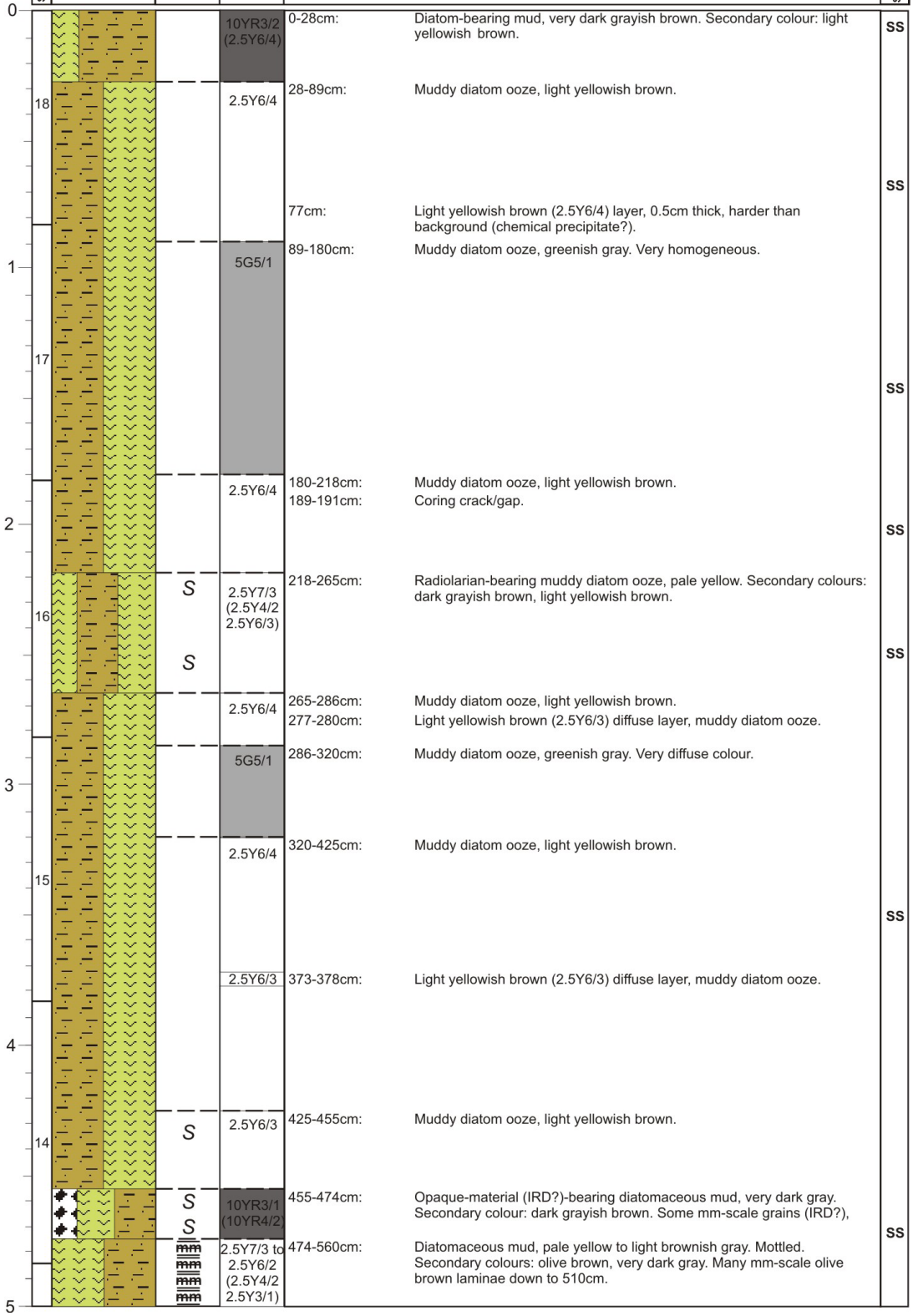

**PS75/095-5**
Recovery: 17.85 m

Latitude: 57° 01.18`S
Longitude: 174° 25.80`W
Transect 5: ROS-NZM

**ANT XXVI/2**
Water Depth: 4853m

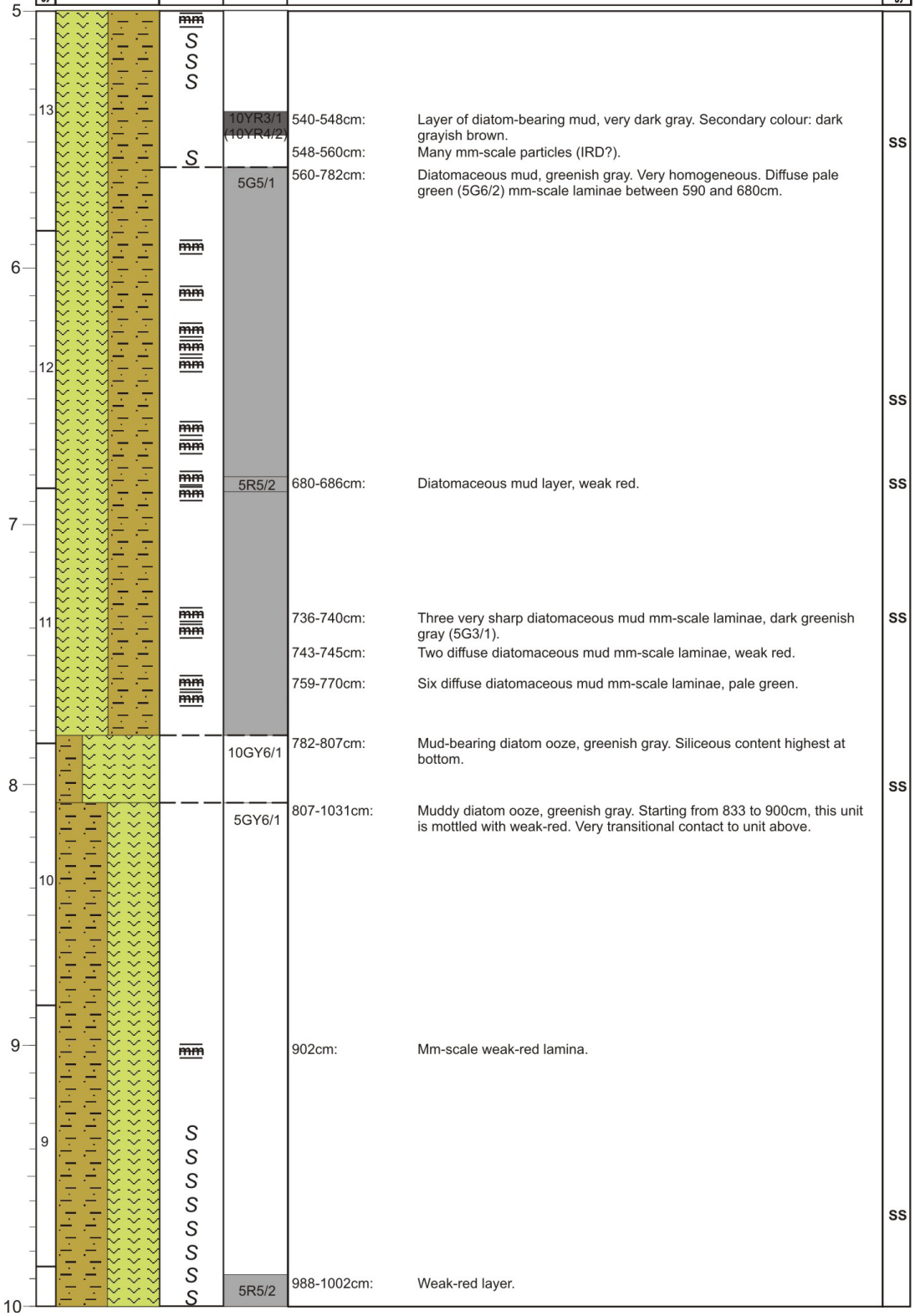

**PS75/095-5**
Recovery: 17.85 m

Latitude: 57° 01.18`S
Longitude: 174° 25.80`W
Transect 5: ROS-NZM

**ANT XXVI/2**
Water Depth: 4853m

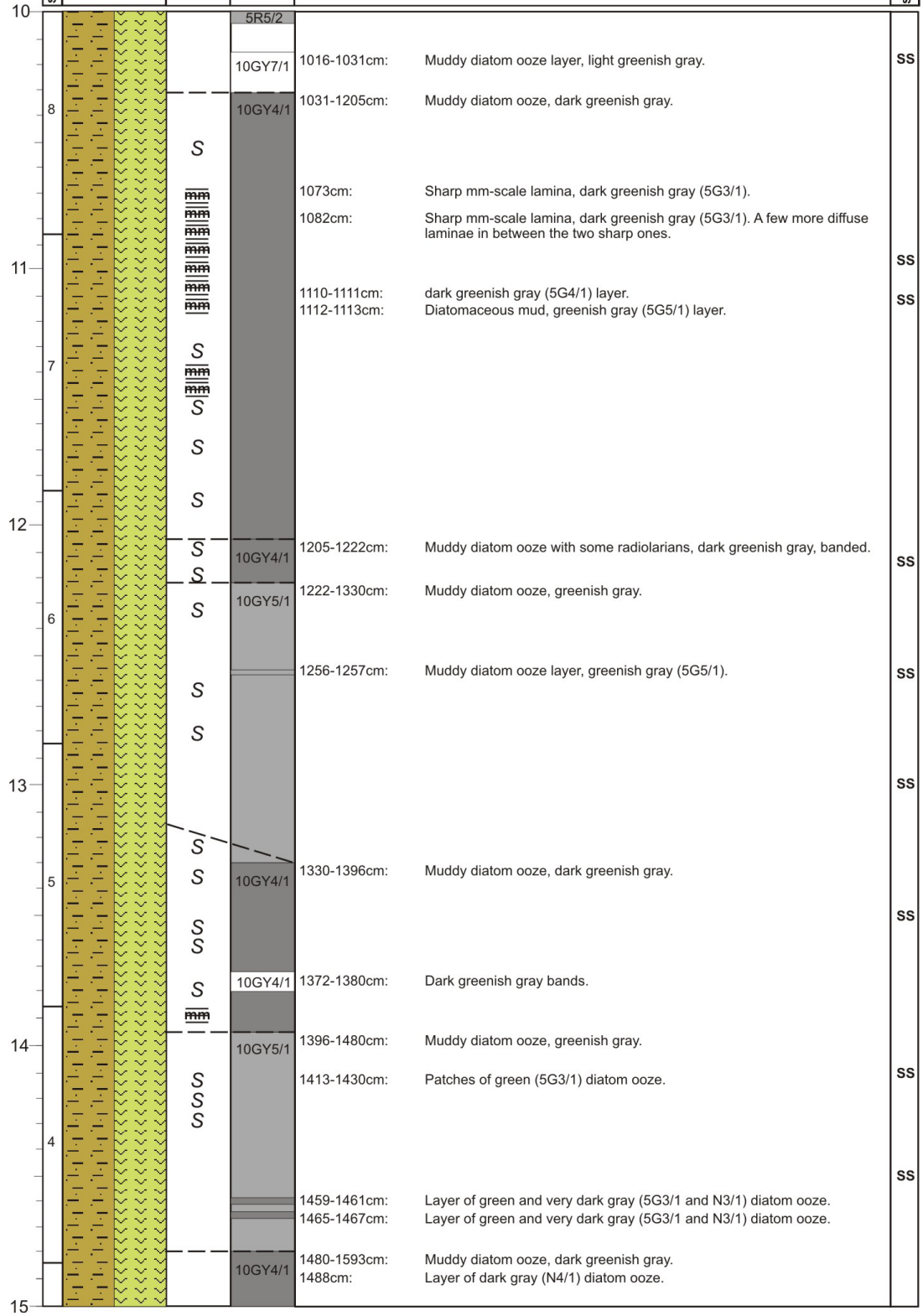

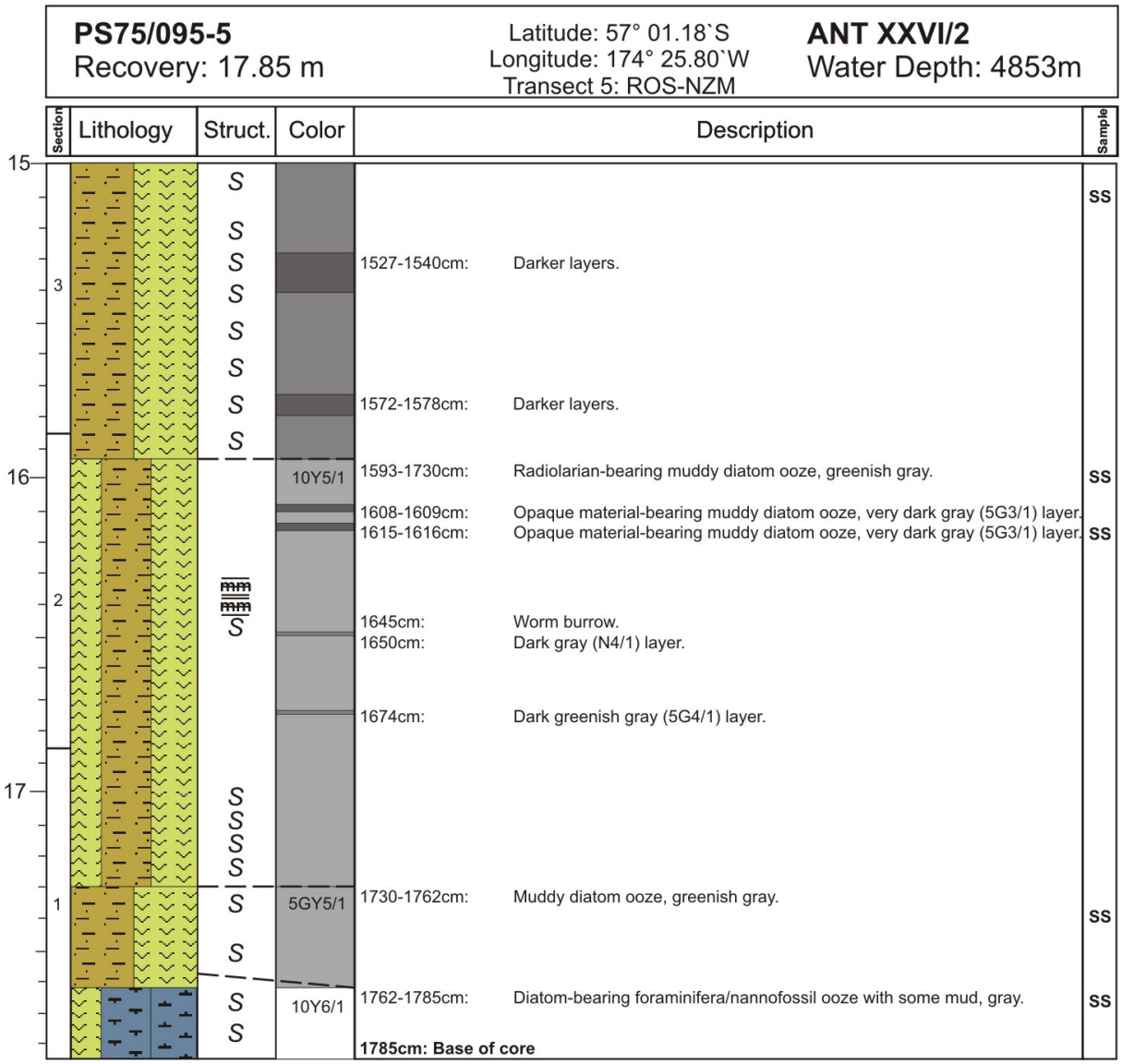
PS75/095-5
Recovery: 17.85 m
Latitude: 57° 01.18`S
Longitude: 174° 25.80`W
Transect 5: ROS-NZM
ANT XXVI/2
Water Depth: 4853m
Section
Lithology
Struct.
Color
Description
Sample
15
16
17
3
2
1
10Y5/1
5GY5/1
10Y6/1
1527-1540cm: Darker layers.
1572-1578cm: Darker layers.
1593-1730cm: Radiolarian-bearing muddy diatom ooze, greenish gray.
1608-1609cm: Opaque material-bearing muddy diatom ooze, very dark gray (5G3/1) layer.
1615-1616cm: Opaque material-bearing muddy diatom ooze, very dark gray (5G3/1) layer.
1645cm: Worm burrow.
1650cm: Dark gray (N4/1) layer.
1674cm: Dark greenish gray (5G4/1) layer.
1730-1762cm: Muddy diatom ooze, greenish gray.
1762-1785cm: Diatom-bearing foraminifera/nannofossil ooze with some mud, gray.
1785cm: Base of core
SS

# A.8 SEDIMENT CORE FOTOGRAPHIC DOCUMENTATION

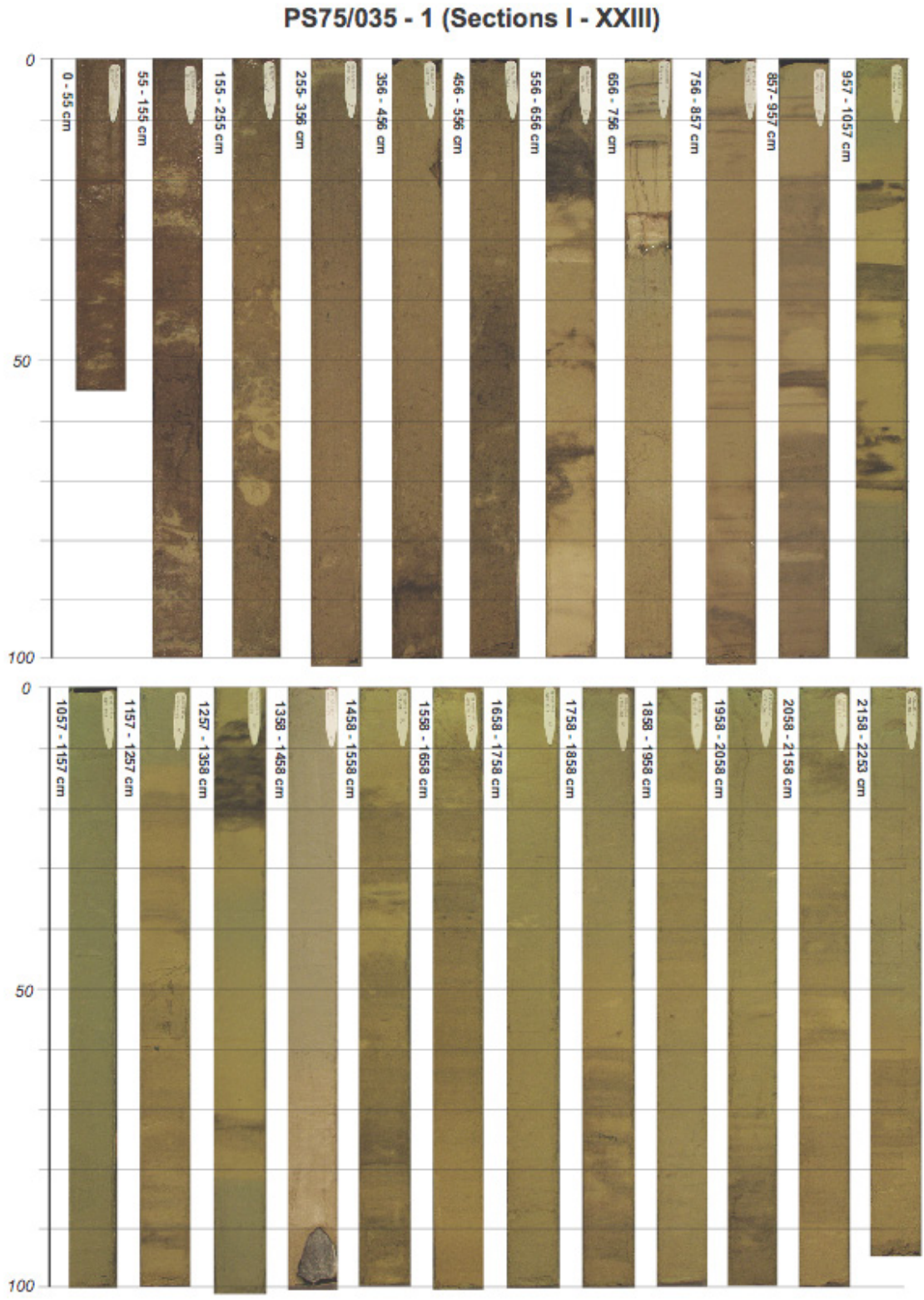

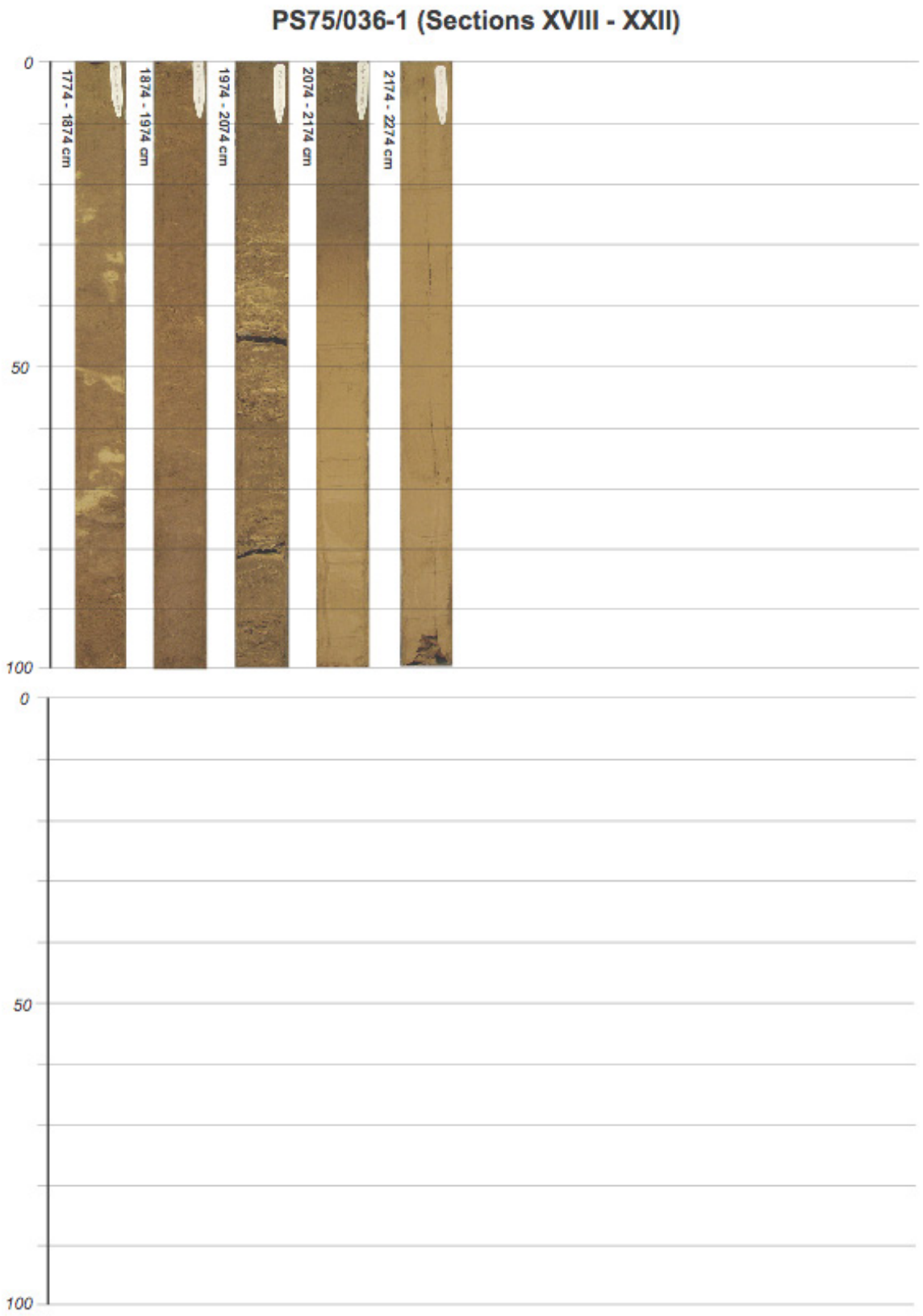
PS75/036-1 (Sections XVIII - XXII)
0
50
100
1774 - 1874 cm
1874 - 1974 cm
1974 - 2074 cm
2074 - 2174 cm
2174 - 2274 cm
0
50
100

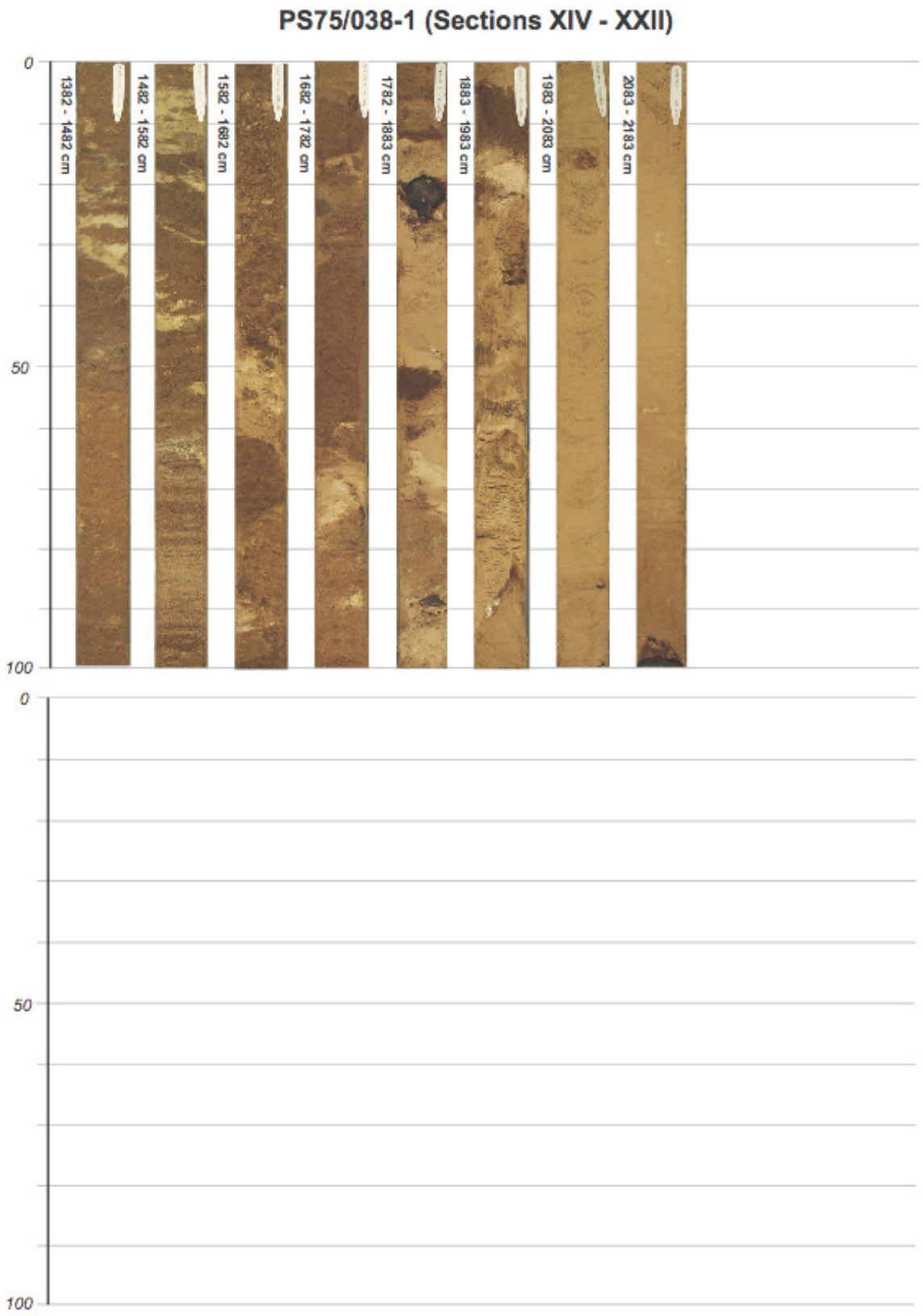
PS75/038-1 (Sections XIV - XXII)
0
50
100
1382 - 1482 cm
1482 - 1582 cm
1582 - 1682 cm
1682 - 1782 cm
1782 - 1883 cm
1883 - 1983 cm
1983 - 2083 cm
2083 - 2183 cm
0
50
100

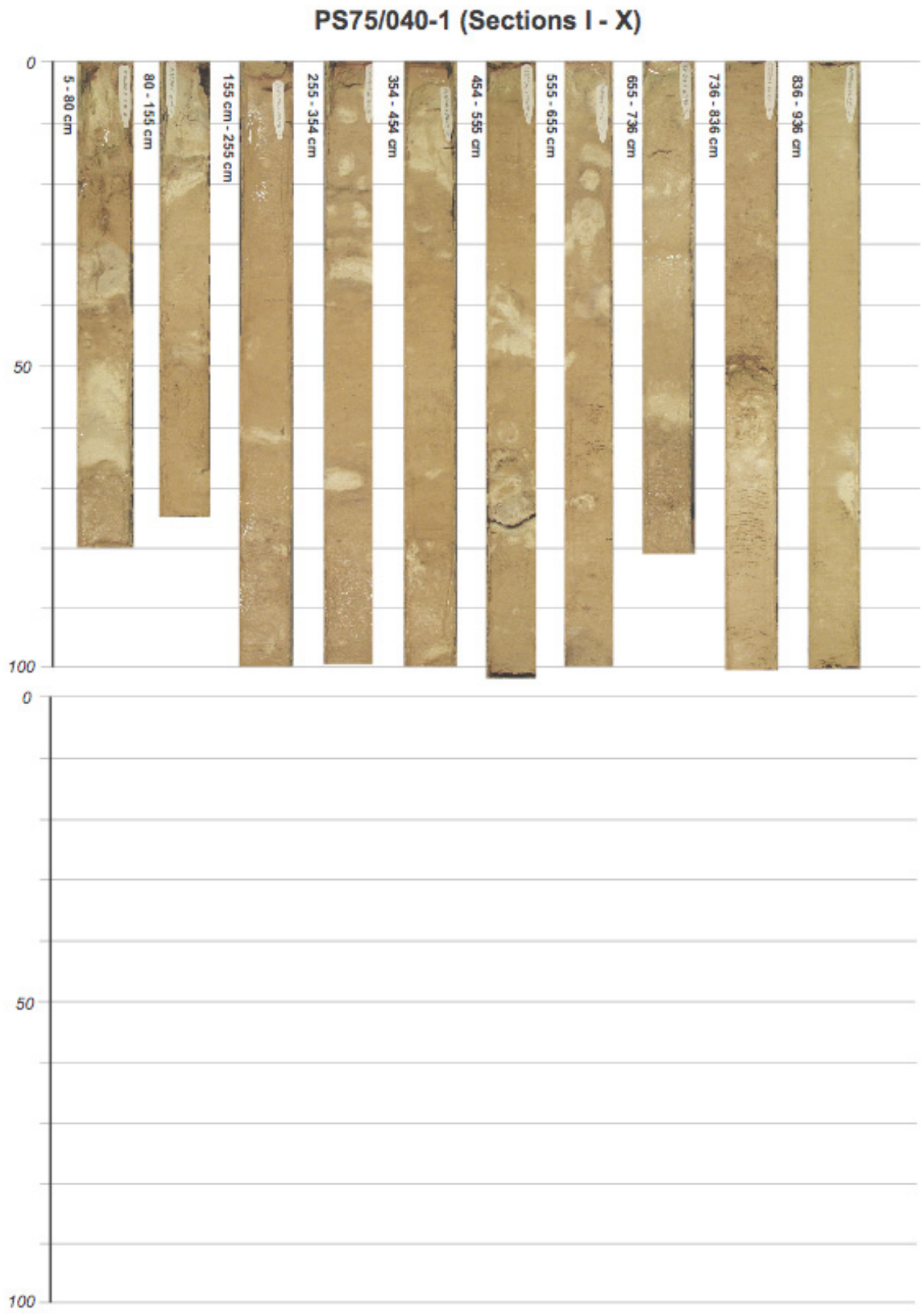
PS75/040-1 (Sections I - X)
0
50
100
5 - 80 cm
80 - 155 cm
155 cm - 255 cm
255 - 354 cm
354 - 454 cm
454 - 555 cm
555 - 655 cm
655 - 736 cm
736 - 836 cm
836 - 936 cm
0
50
100

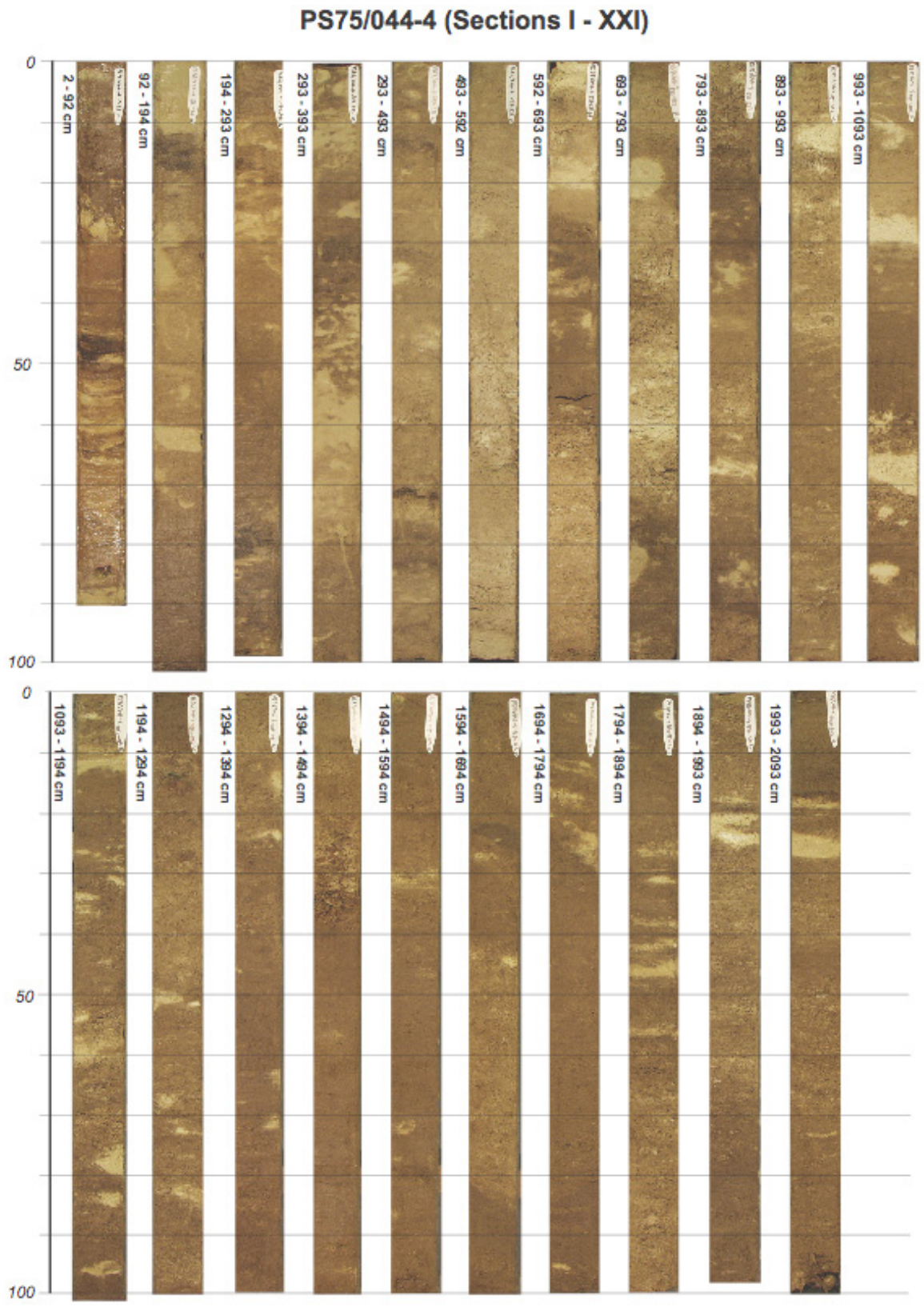
PS75/044-4 (Sections I - XXI)
0
50
100
2 - 92 cm
92 - 194 cm
194 - 293 cm
293 - 393 cm
293 - 493 cm
493 - 592 cm
592 - 693 cm
693 - 793 cm
793 - 893 cm
893 - 993 cm
993 - 1093 cm
0
50
100
1093 - 1194 cm
1194 - 1294 cm
1294 - 1394 cm
1394 - 1494 cm
1494 - 1594 cm
1594 - 1694 cm
1694 - 1794 cm
1794 - 1894 cm
1894 - 1993 cm
1993 - 2093 cm

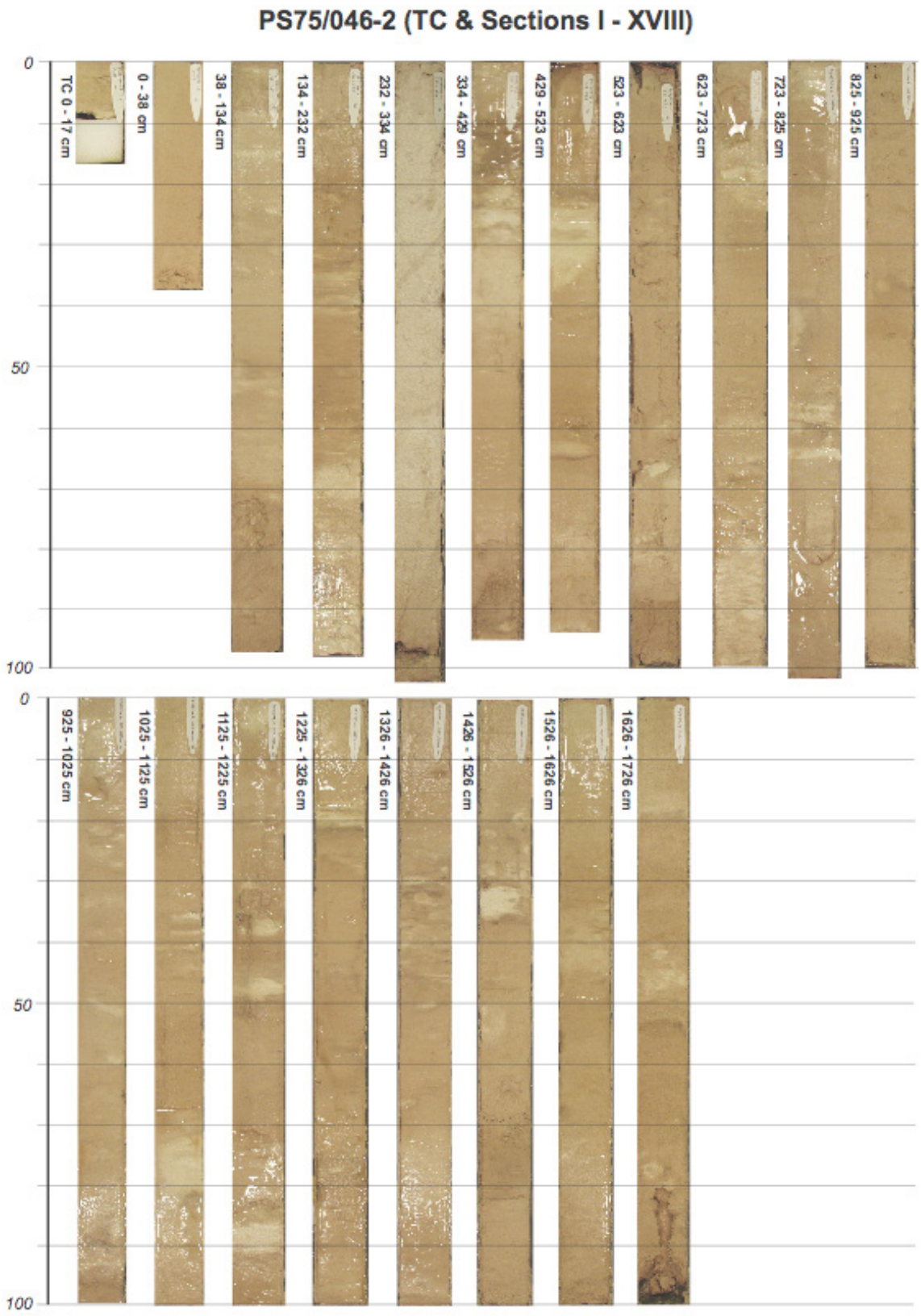
PS75/046-2 (TC & Sections I - XVIII)
0
50
100
TC 0 - 17 cm
0 - 38 cm
38 - 134 cm
134 - 232 cm
232 - 334 cm
334 - 429 cm
429 - 523 cm
523 - 623 cm
623 - 723 cm
723 - 825 cm
825 - 925 cm
0
50
100
925 - 1025 cm
1025 - 1125 cm
1125 - 1225 cm
1225 - 1326 cm
1326 - 1426 cm
1426 - 1526 cm
1526 - 1626 cm
1626 - 1726 cm

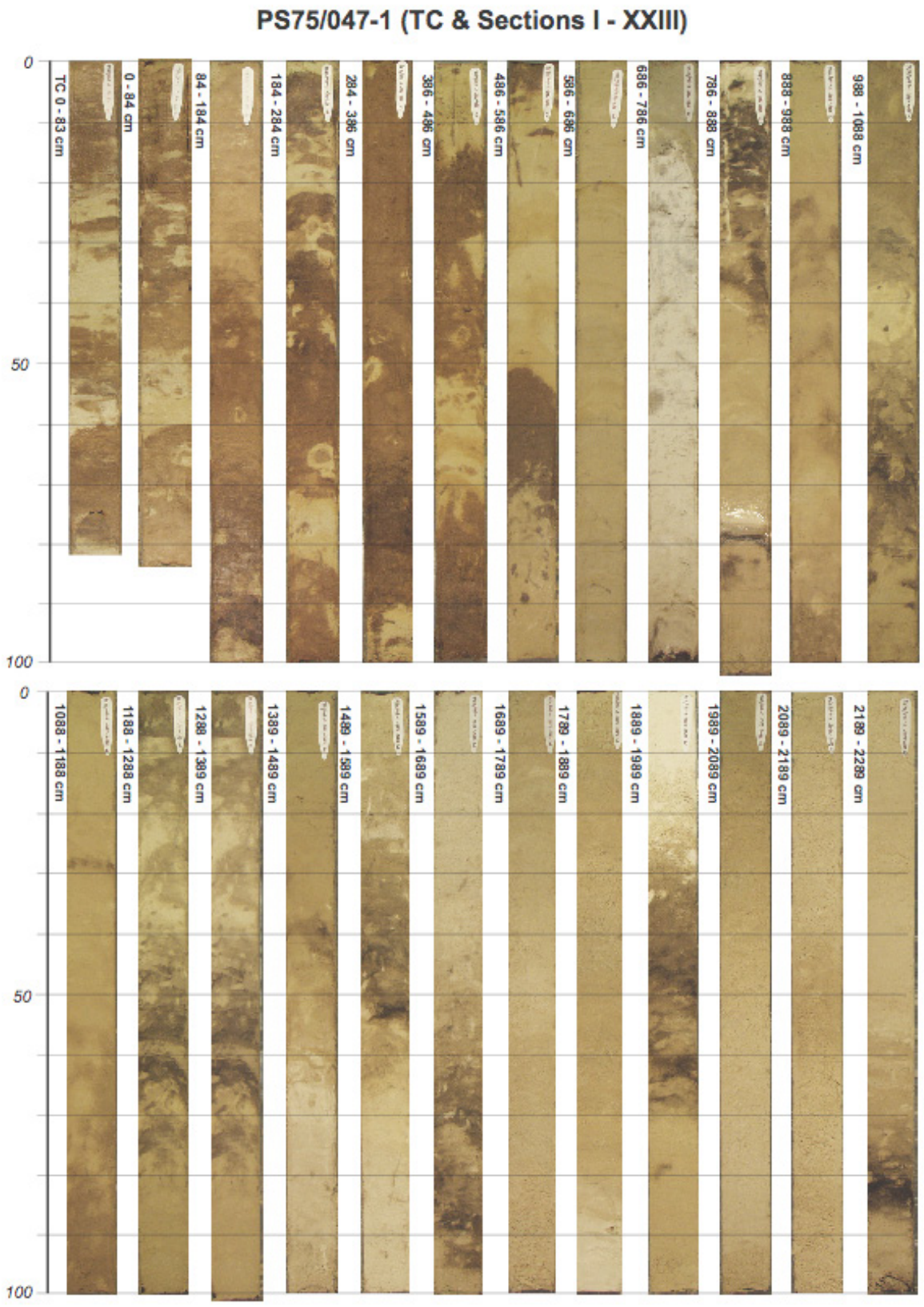
PS75/047-1 (TC & Sections I - XXIII)
0
50
100
TC 0 - 83 cm
0 - 84 cm
84 - 184 cm
184 - 284 cm
284 - 386 cm
386 - 486 cm
486 - 586 cm
586 - 686 cm
686 - 786 cm
786 - 888 cm
888 - 988 cm
988 - 1088 cm
1088 - 1188 cm
1188 - 1288 cm
1288 - 1389 cm
1389 - 1489 cm
1489 - 1589 cm
1589 - 1689 cm
1689 - 1789 cm
1789 - 1889 cm
1889 - 1989 cm
1989 - 2089 cm
2089 - 2189 cm
2189 - 2289 cm

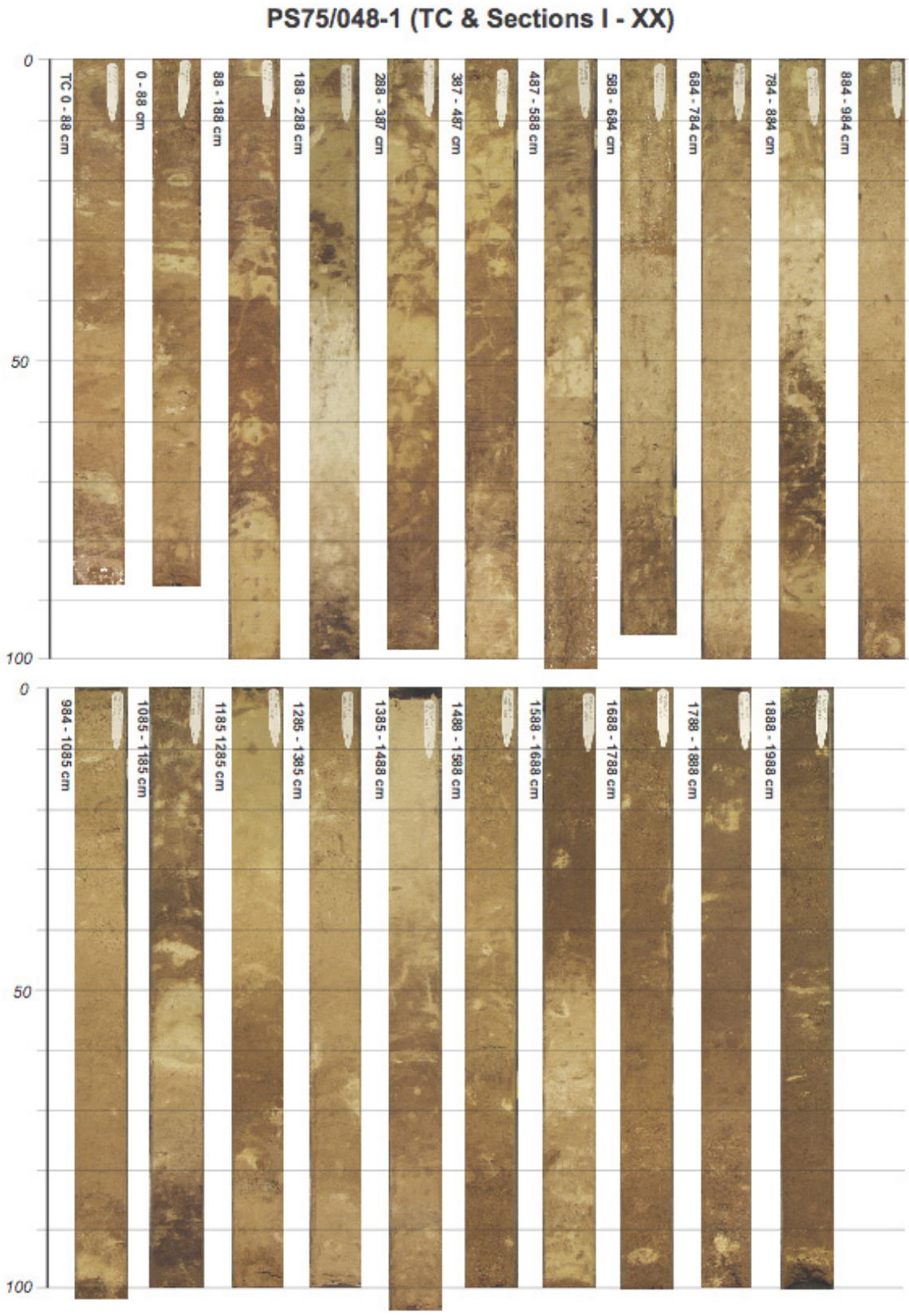
PS75/048-1 (TC & Sections I - XX)
0
50
100
TC 0 - 88 cm
0 - 88 cm
88 - 188 cm
188 - 288 cm
288 - 387 cm
387 - 487 cm
487 - 588 cm
588 - 684 cm
684 - 784 cm
784 - 884 cm
884 - 984 cm
984 - 1085 cm
1085 - 1185 cm
1185 1285 cm
1285 - 1385 cm
1385 - 1488 cm
1488 - 1588 cm
1588 - 1688 cm
1688 - 1788 cm
1788 - 1888 cm
1888 - 1988 cm

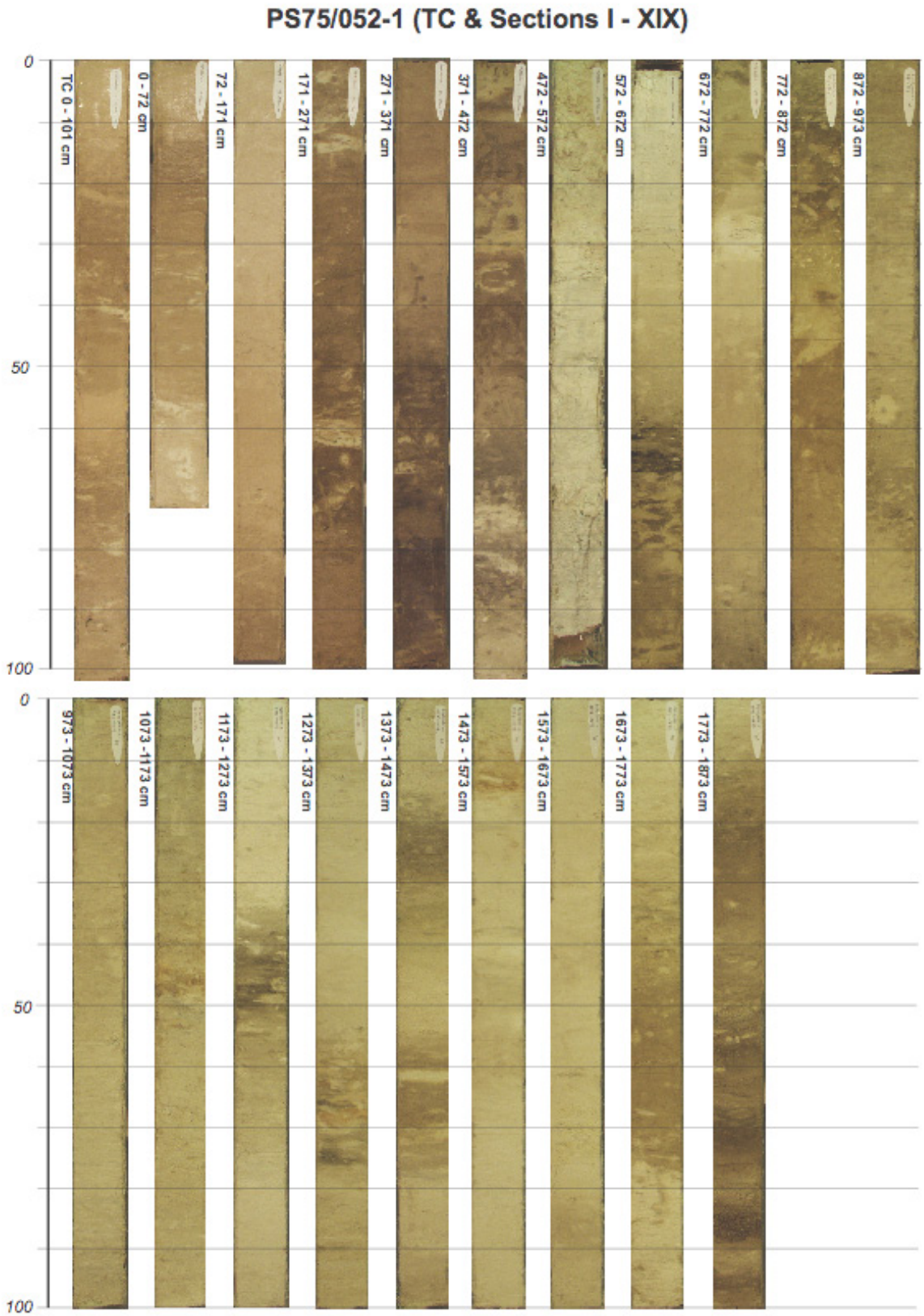
PS75/052-1 (TC & Sections I - XIX)
0
50
100
TC 0 - 101 cm
0 - 72 cm
72 - 171 cm
171 - 271 cm
271 - 371 cm
371 - 472 cm
472 - 572 cm
572 - 672 cm
672 - 772 cm
772 - 872 cm
872 - 973 cm
0
50
100
973 - 1073 cm
1073 - 1173 cm
1173 - 1273 cm
1273 - 1373 cm
1373 - 1473 cm
1473 - 1573 cm
1573 - 1673 cm
1673 - 1773 cm
1773 - 1873 cm

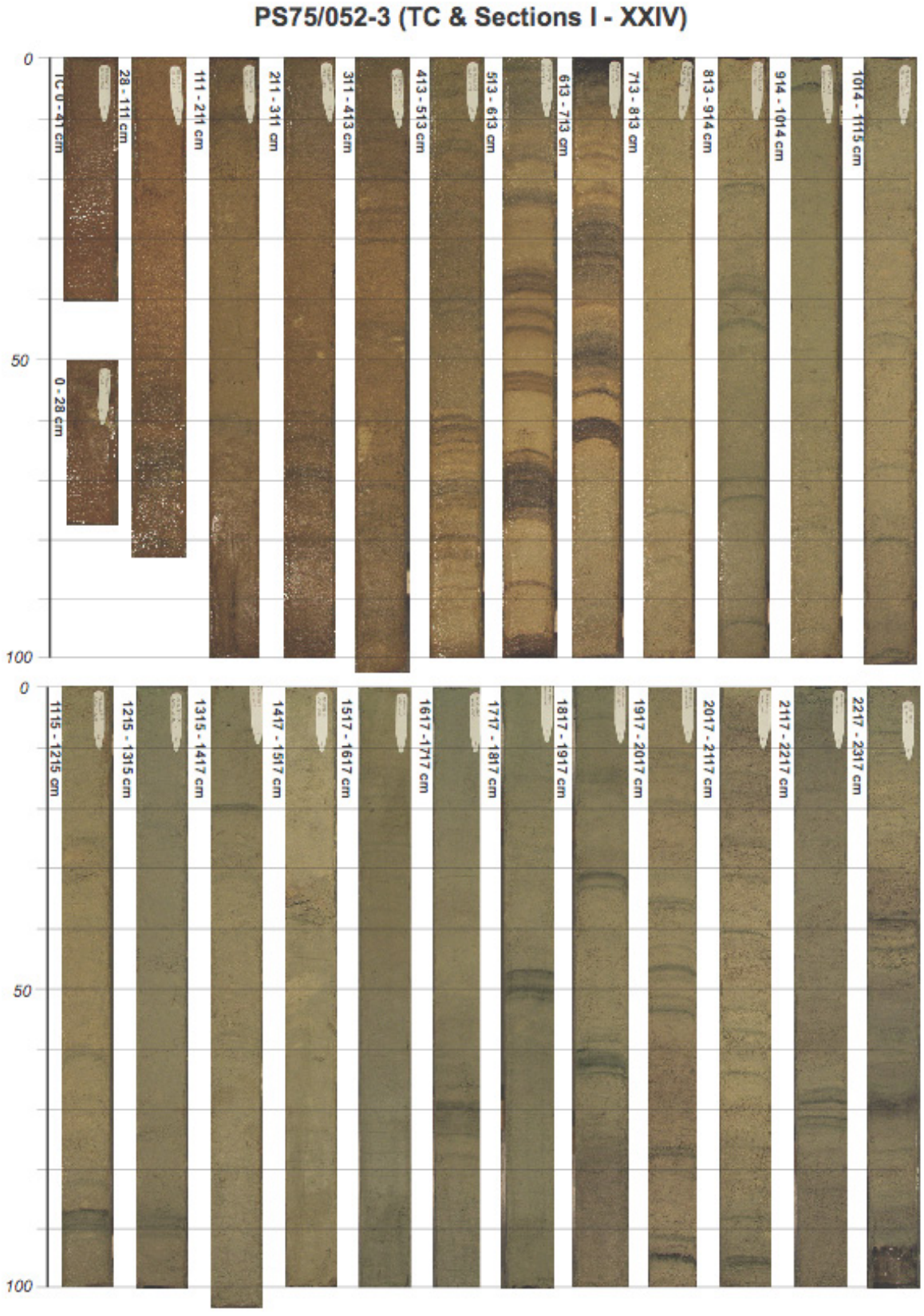
PS75/052-3 (TC & Sections I - XXIV)
0
50
100
TC 0 - 41 cm
0 - 28 cm
28 - 111 cm
111 - 211 cm
211 - 311 cm
311 - 413 cm
413 - 513 cm
513 - 613 cm
613 - 713 cm
713 - 813 cm
813 - 914 cm
914 - 1014 cm
1014 - 1115 cm
1115 - 1215 cm
1215 - 1315 cm
1315 - 1417 cm
1417 - 1517 cm
1517 - 1617 cm
1617 - 1717 cm
1717 - 1817 cm
1817 - 1917 cm
1917 - 2017 cm
2017 - 2117 cm
2117 - 2217 cm
2217 - 2317 cm

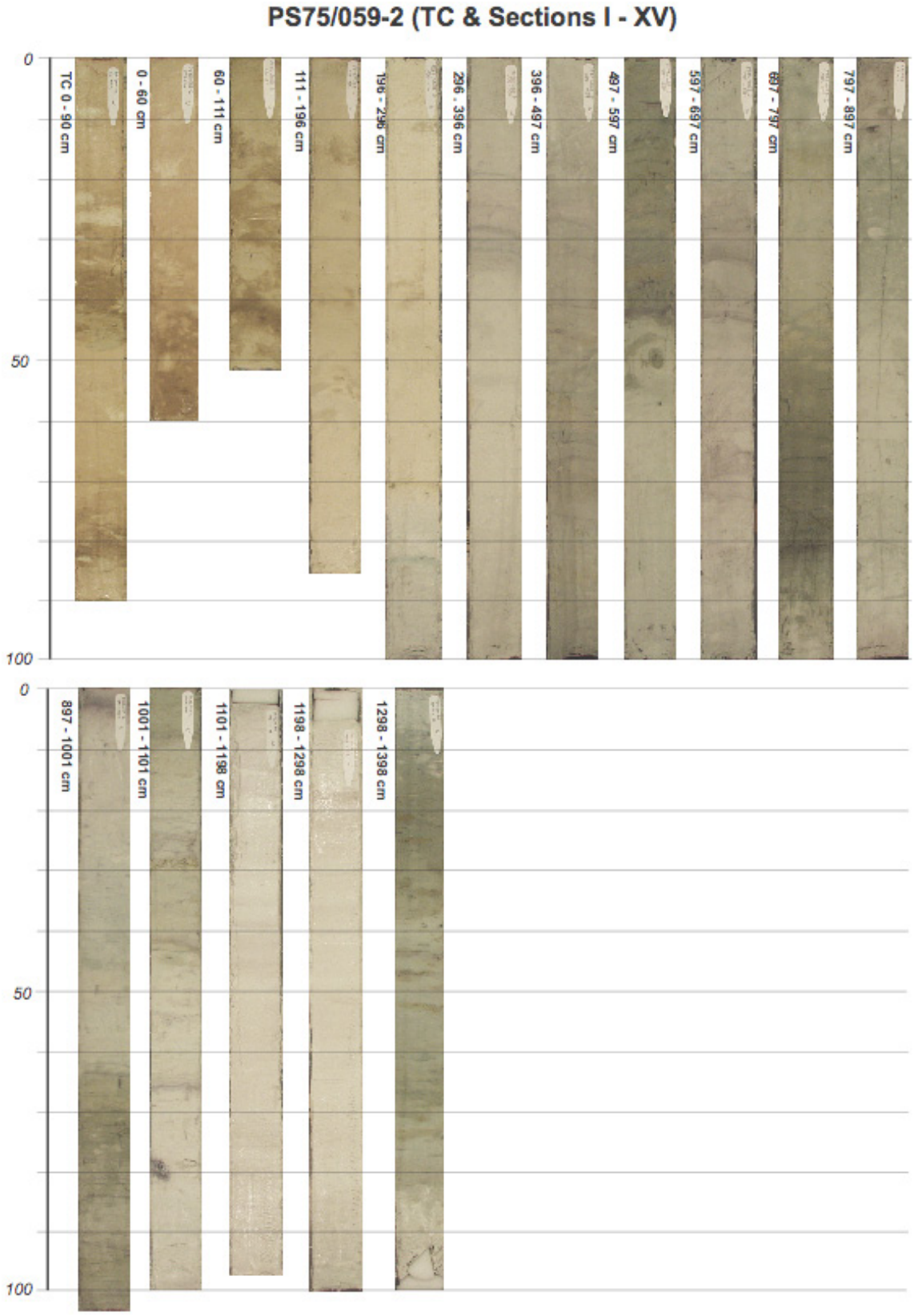
PS75/059-2 (TC & Sections I - XV)
0
50
100
TC 0 - 90 cm
0 - 60 cm
60 - 111 cm
111 - 196 cm
196 - 296 cm
296 - 396 cm
396 - 497 cm
497 - 597 cm
597 - 697 cm
697 - 797 cm
797 - 897 cm
897 - 1001 cm
1001 - 1101 cm
1101 - 1198 cm
1198 - 1298 cm
1298 - 1398 cm

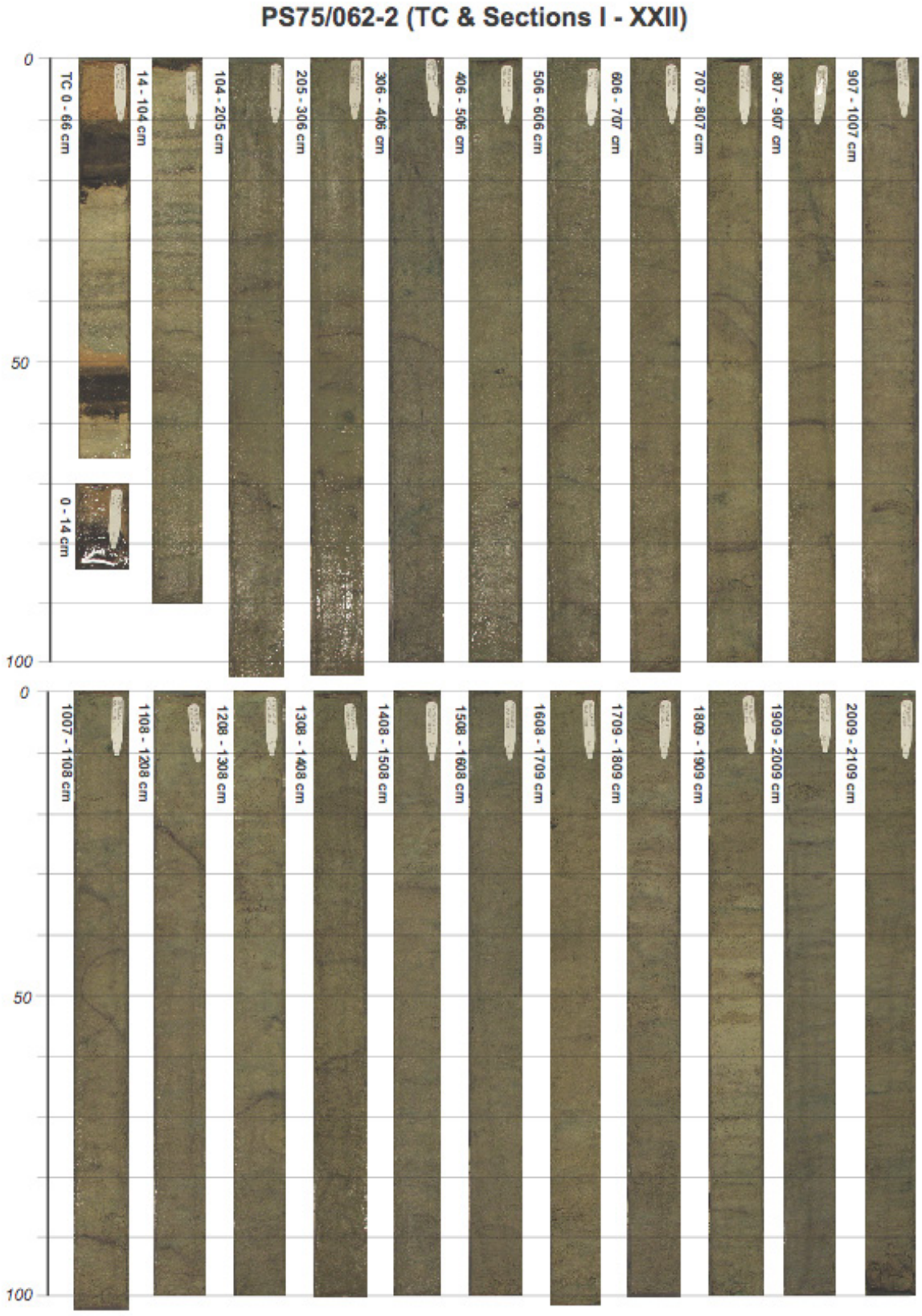
PS75/062-2 (TC & Sections I - XXII)
0
50
100
TC 0 - 66 cm
0 - 14 cm
14 - 104 cm
104 - 205 cm
205 - 306 cm
306 - 406 cm
406 - 506 cm
506 - 606 cm
606 - 707 cm
707 - 807 cm
807 - 907 cm
907 - 1007 cm
1007 - 1108 cm
1108 - 1208 cm
1208 - 1308 cm
1308 - 1408 cm
1408 - 1508 cm
1508 - 1608 cm
1608 - 1709 cm
1709 - 1809 cm
1809 - 1909 cm
1909 - 2009 cm
2009 - 2109 cm

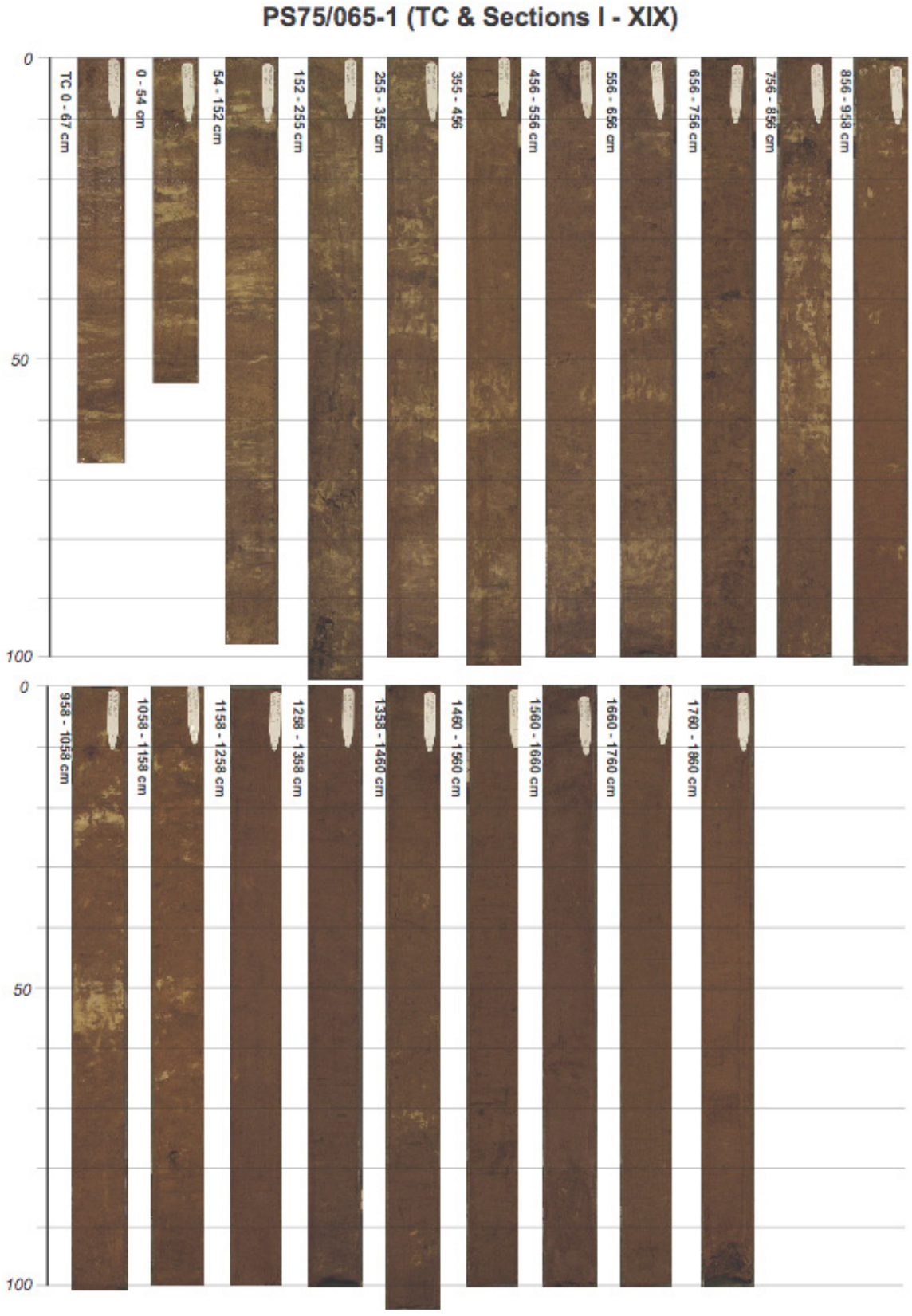
PS75/065-1 (TC & Sections I - XIX)
0
50
100
TC 0 - 67 cm
0 - 54 cm
54 - 152 cm
152 - 255 cm
255 - 355 cm
355 - 456
456 - 556 cm
556 - 656 cm
656 - 756 cm
756 - 856 cm
856 - 958 cm
0
50
100
958 - 1058 cm
1058 - 1158 cm
1158 - 1258 cm
1258 - 1358 cm
1358 - 1460 cm
1460 - 1560 cm
1560 - 1660 cm
1660 - 1760 cm
1760 - 1860 cm

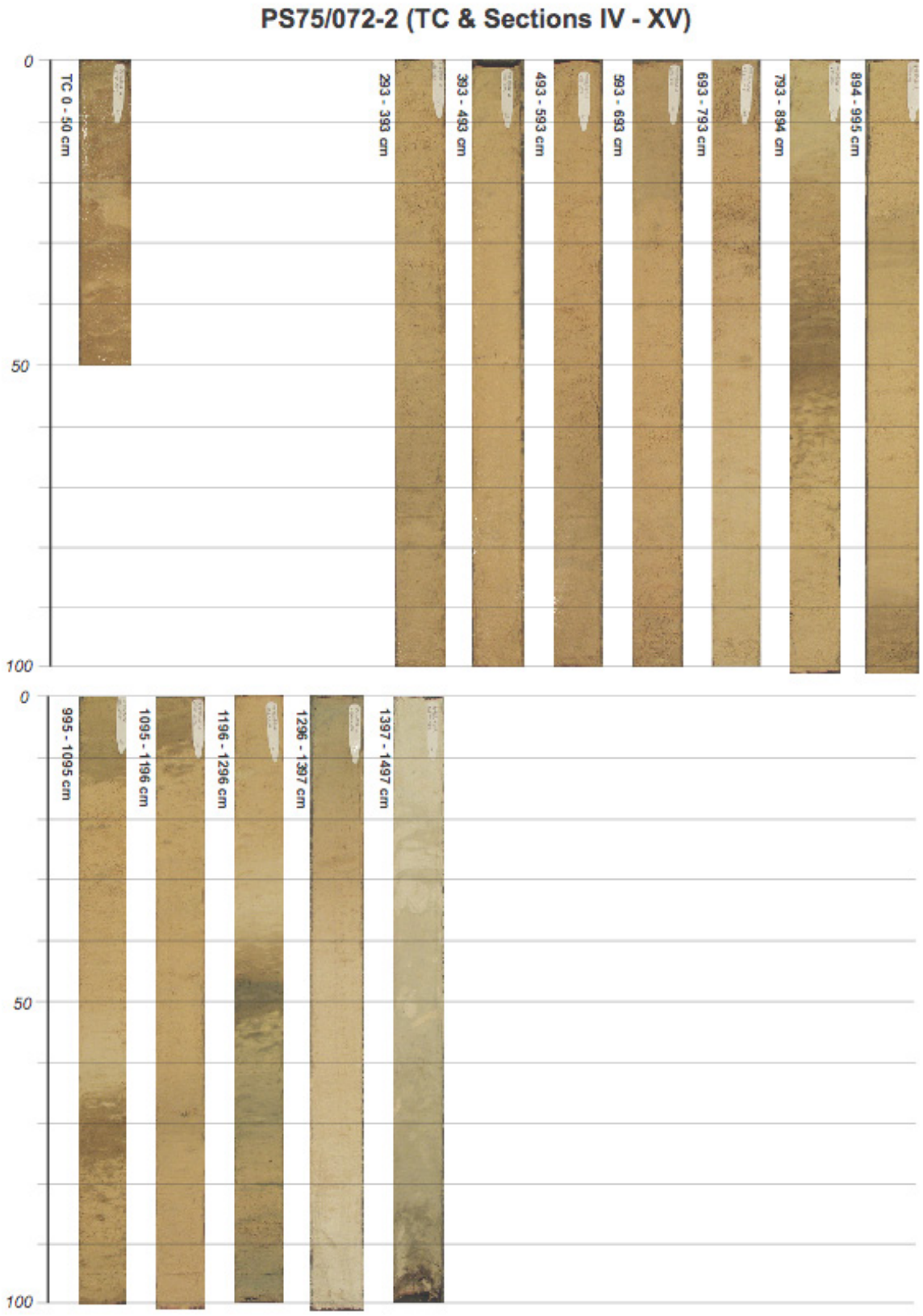
PS75/072-2 (TC & Sections IV - XV)
0
50
100
TC 0 - 50 cm
293 - 393 cm
393 - 493 cm
493 - 593 cm
593 - 693 cm
693 - 793 cm
793 - 894 cm
894 - 995 cm
0
50
100
995 - 1095 cm
1095 - 1196 cm
1196 - 1296 cm
1296 - 1397 cm
1397 - 1497 cm

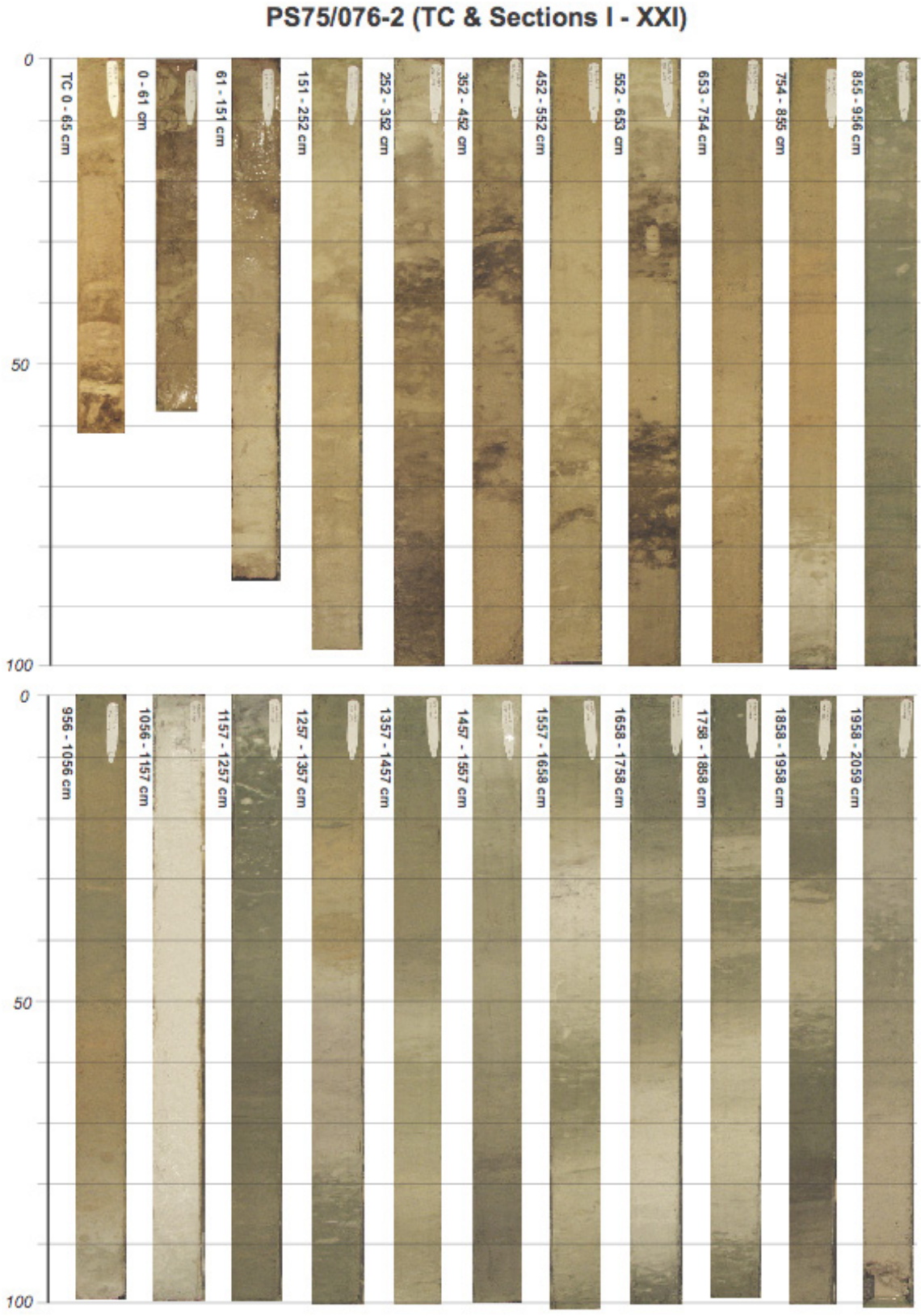
PS75/076-2 (TC & Sections I - XXI)
0
50
100
TC 0 - 65 cm
0 - 61 cm
61 - 151 cm
151 - 252 cm
252 - 352 cm
352 - 452 cm
452 - 552 cm
552 - 653 cm
653 - 754 cm
754 - 855 cm
855 - 956 cm
956 - 1056 cm
1056 - 1157 cm
1157 - 1257 cm
1257 - 1357 cm
1357 - 1457 cm
1457 - 1557 cm
1557 - 1658 cm
1658 - 1758 cm
1758 - 1858 cm
1858 - 1958 cm
1958 - 2059 cm

## PS75/079-2 (Sections II - XIX)

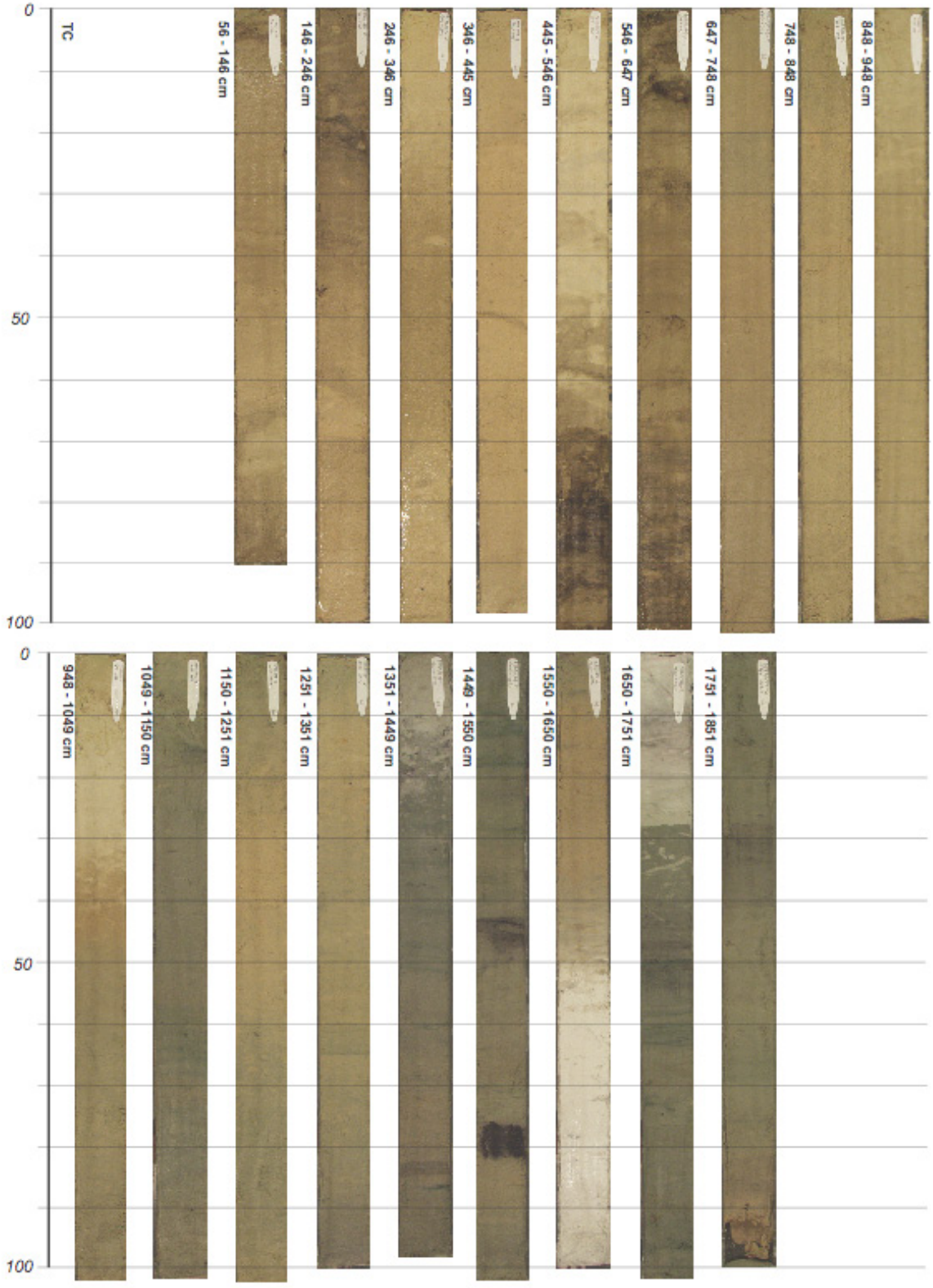

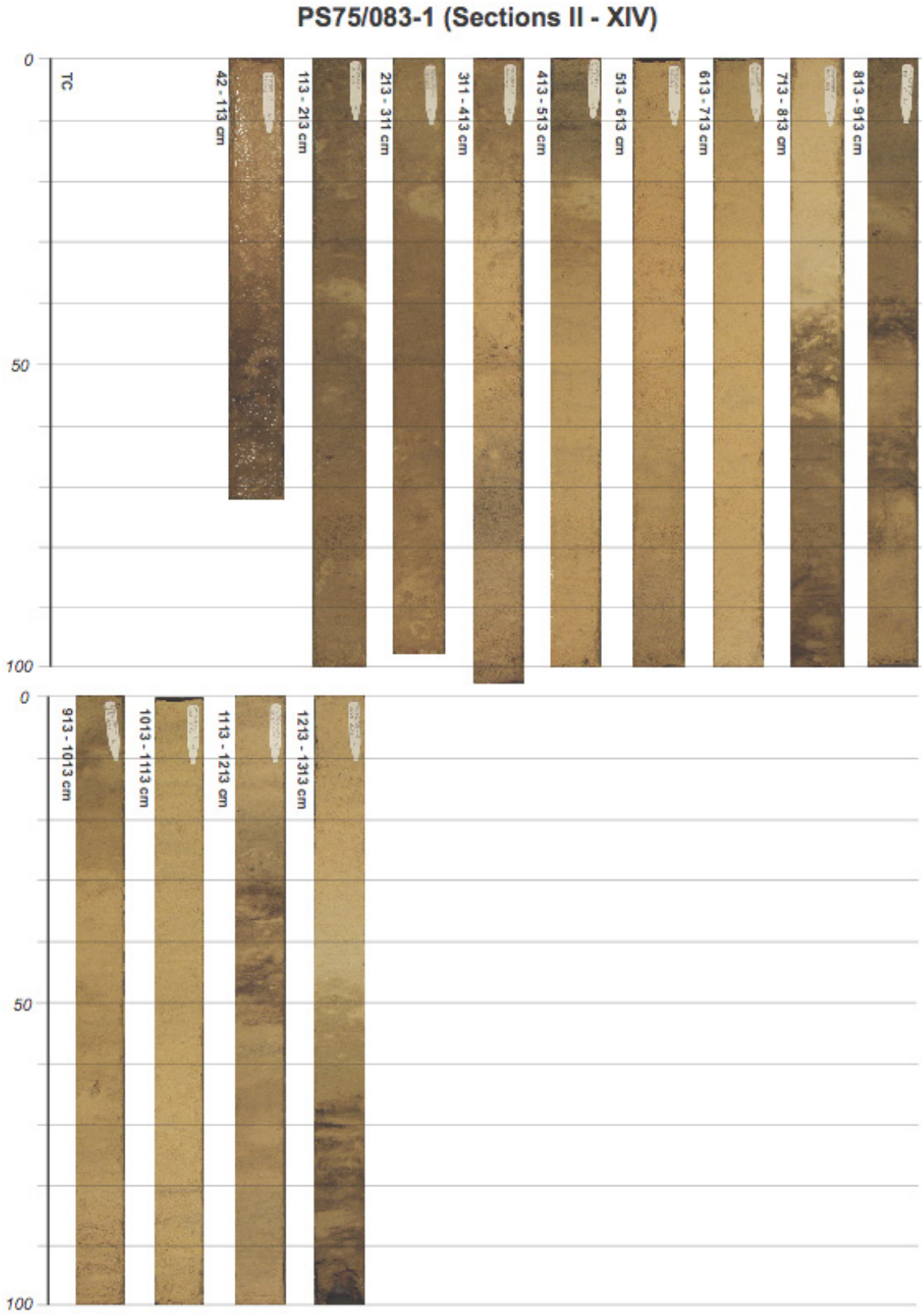
PS75/083-1 (Sections II - XIV)
0
50
100
TC
42 - 113 cm
113 - 213 cm
213 - 311 cm
311 - 413 cm
413 - 513 cm
513 - 613 cm
613 - 713 cm
713 - 813 cm
813 - 913 cm
0
50
100
913 - 1013 cm
1013 - 1113 cm
1113 - 1213 cm
1213 - 1313 cm

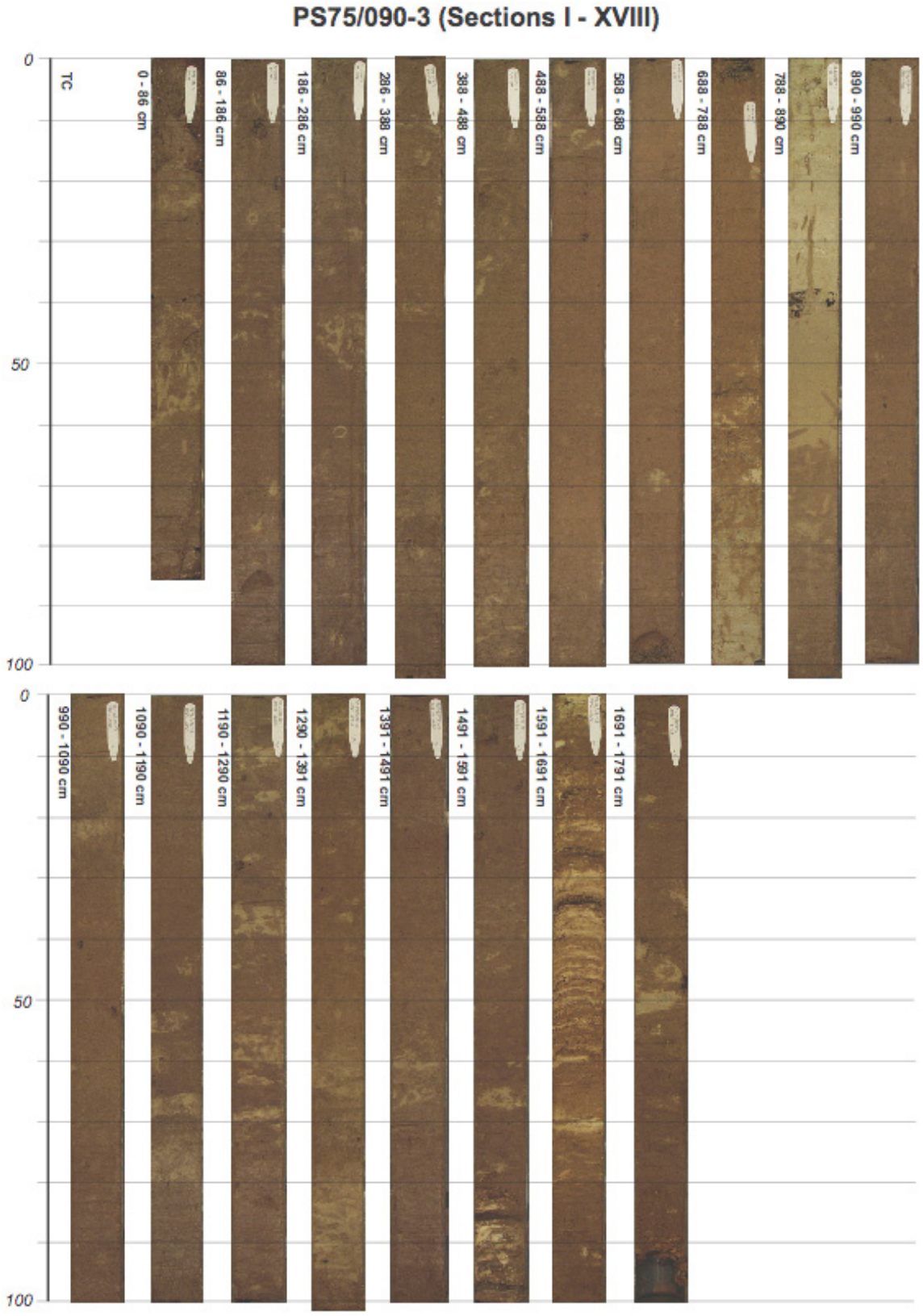
PS75/090-3 (Sections I - XVIII)
0
50
100
TC
0 - 86 cm
86 - 186 cm
186 - 286 cm
286 - 388 cm
388 - 488 cm
488 - 588 cm
588 - 688 cm
688 - 788 cm
788 - 890 cm
890 - 990 cm
990 - 1090 cm
1090 - 1190 cm
1190 - 1290 cm
1290 - 1391 cm
1391 - 1491 cm
1491 - 1591 cm
1591 - 1691 cm
1691 - 1791 cm

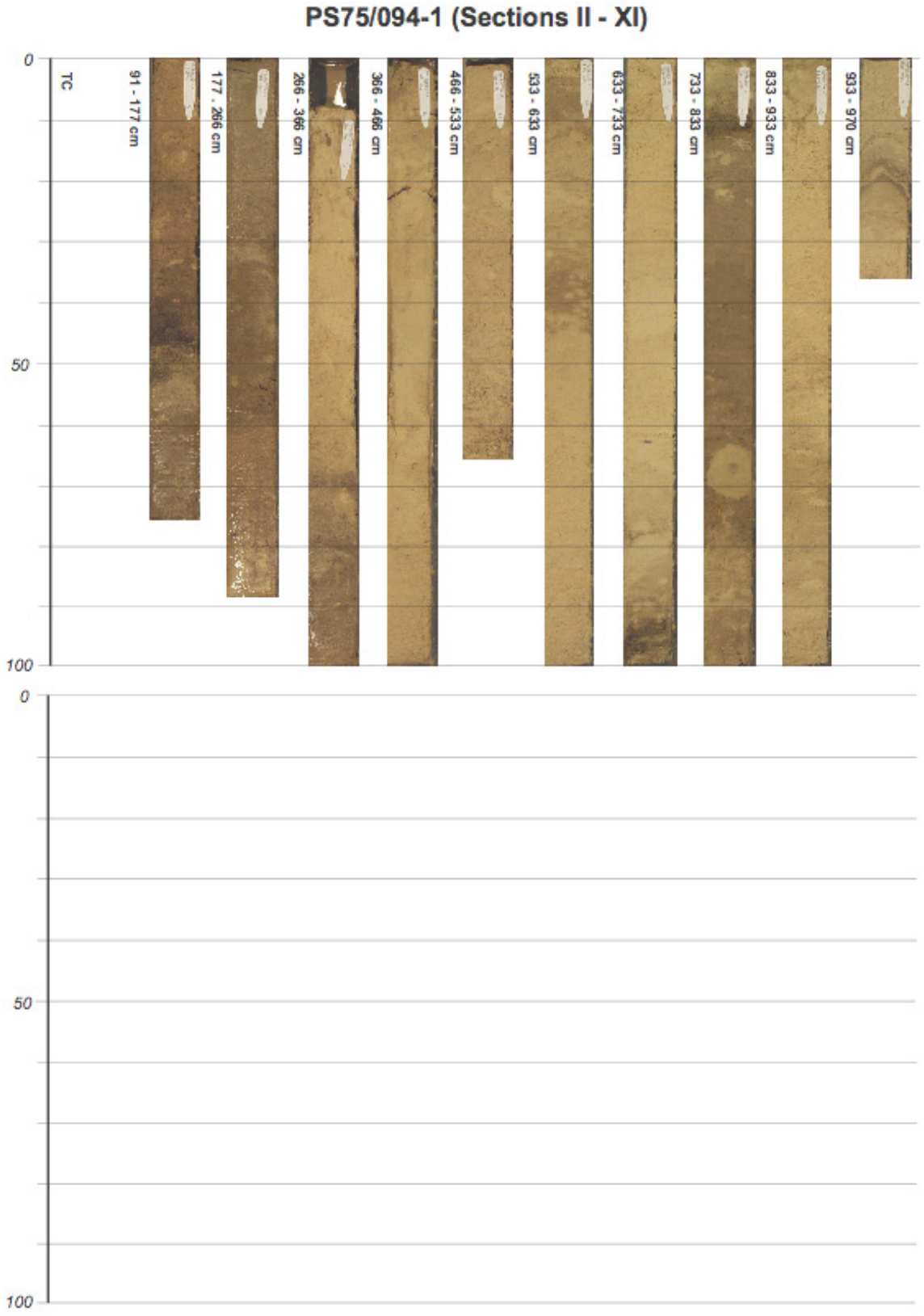
PS75/094-1 (Sections II - XI)
0
50
100
TC
91 - 177 cm
177 - 266 cm
266 - 366 cm
366 - 466 cm
466 - 533 cm
533 - 633 cm
633 - 733 cm
733 - 833 cm
833 - 933 cm
933 - 970 cm
0
50
100

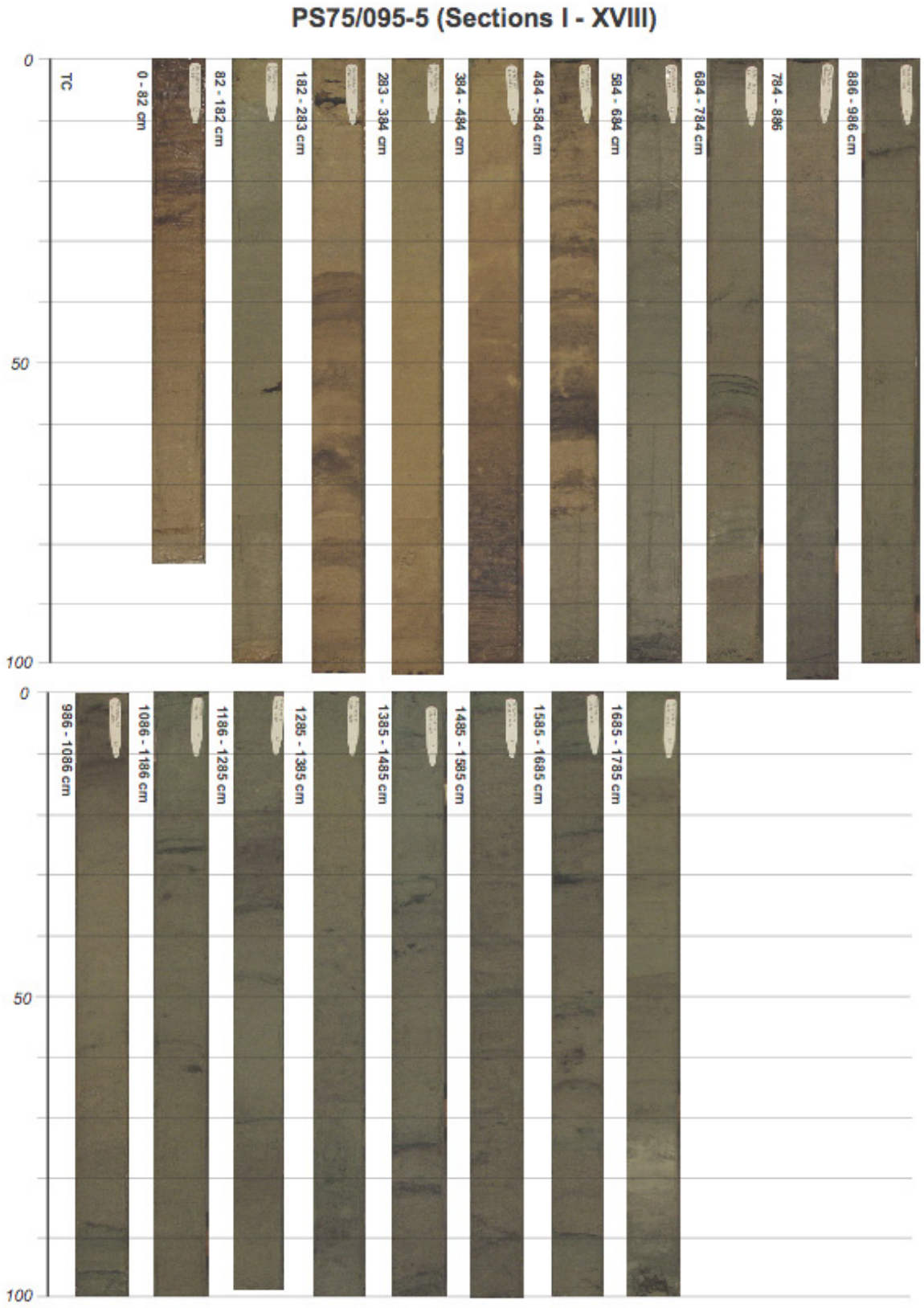
PS75/095-5 (Sections I - XVIII)
0
50
100
TC
0 - 82 cm
82 - 182 cm
182 - 283 cm
283 - 384 cm
384 - 484 cm
484 - 584 cm
584 - 684 cm
684 - 784 cm
784 - 886
886 - 986 cm
0
50
100
986 - 1086 cm
1086 - 1186 cm
1186 - 1285 cm
1285 - 1385 cm
1385 - 1485 cm
1485 - 1585 cm
1585 - 1685 cm
1685 - 1785 cm

**Die "Berichte zur Polar- und Meeresforschung"** (ISSN 1866-3192) werden beginnend mit dem Heft Nr. 569 (2008) ausschließlich elektronisch als Open-Access-Publikation herausgegeben. Ein Verzeichnis aller Hefte einschließlich der Druckausgaben (Heft 377-568) sowie der früheren **"Berichte zur Polarforschung** (Heft 1-376, von 1982 bis 2000) befindet sich im Internet in der Ablage des electronic Information Center des AWI (**ePIC**) unter der URL http://epic.awi.de. Durch Auswahl "Reports on Polar- and Marine Research" auf der rechten Seite des Fensters wird eine Liste der Publikationen in alphabetischer Reihenfolge (nach Autoren) innerhalb der absteigenden chronologischen Reihenfolge der Jahrgänge erzeugt.

*To generate a list of all Reports past issues, use the following URL: http://epic.awi.de and select the right frame to browse "Reports on Polar and Marine Research". A chronological list in declining order, author names alphabetical, will be produced, and pdf-icons shown for open access download.*

**Verzeichnis der zuletzt erschienenen Hefte:**

**Heft-Nr. 620/2010** — "Cool Libraries in a Melting World - Proceedings of the 23rd Polar Libraries Colloquy 2010, June 13-18, 2010, Bremerhaven, Germany", edited by Marcel Brannemann and Daria O. Carle

**Heft-Nr. 621/2010** — "The Expedition of the Research Vessel 'Polarstern' to the Arctic in 2010 (ARK-XXV/3)", edited by Volkmar Damm

**Heft-Nr. 622/2010** — "Environmentally induced responses of *Donax obesulus* and *Mesodesma donacium* (Bivalvia) inhabiting the Humboldt Current System", by Daniel Carstensen

**Heft-Nr. 623/2010** — "Research in the Laptev Sea region - Proceedings of the joint Russian-German workshop, November 8-11, 2010, St. Petersburg, Russia", edited by Sebastian Wetterich, Paul Pier Overduin and Irina Fedorova

**Heft-Nr. 624/2010** — "The Expedition of the Research Vessel 'Polarstern' to the Arctic in 2010 (ARK-XXV/2)", edited by Thomas Soltwedel

**Heft-Nr. 625/2011** — "The Expedition of the Research Vessel 'Polarstern' to the Arctic in 2010 (ARK-XXV/1)", edited by Gereon Budéus

**Heft-Nr. 626/2011** — "Towards data assimilation in ice-dynamic models: the (geo)physical basis", by Olaf Eisen

**Heft-Nr. 627/2011** — "The Expedition of the Research Vessel 'Polarstern' to the Arctic in 2007 (ARK-XXII/1a-c)", edited by Michael Klages & Jörn Thiede

**Heft-Nr. 628/2011** — "The Expedition of the Research Vessel 'Polarstern' to the Antarctic in 2010 (ANT-XXVII/1)", edited by Karl Bumke

**Heft-Nr. 629/2011** — "Russian-German Cooperation SYSTEM LAPTEV SEA: The expedition Eastern Laptev Sea - Buor Khaya Peninsula 2010" edited by Sebastian Wetterich, Pier Paul Overduin and Mikhail Grigoriev

**Heft-Nr. 630/2011** — "Comparative aerosol studies based on multi-wavelength Raman LIDAR at Ny-Ålesund, Spitsbergen", by Anne Hoffmann

**Heft-Nr. 631/2011** — "The Expedition of the Research Vessel 'Polarstern' to the Antarctic in 2010 (ANT-XXVI/4), edited by Arne Körtzinger

**Heft-Nr. 632/2011** — "The Expedition of the Research Vessel 'Polarstern' to the polar South Pacific in 2009/2010 (ANT-XXVI/2 - BIPOMAC), edited by Rainer Gersonde